

PALLADIUM-CATALYZED DECARBOXYLATIVE AND DECARBONYLATIVE
TRANSFORMATIONS IN THE SYNTHESIS OF FINE AND COMMODITY
CHEMICALS

Thesis by
Yiyang Liu

In Partial Fulfillment of the Requirements for the Degree of
Doctor of Philosophy

California Institute of Technology

Pasadena, California

2015

(Defended 14 May 2015)

© 2015

Yiyang Liu

All Rights Reserved

ACKNOWLEDGEMENTS

First, I would like to thank my advisor, Professor Brian M. Stoltz, for offering me the opportunity to pursue a Ph.D. degree in his group. Brian was very supportive of my research and always encouraged me to try out new ideas. Even when results were negative, he saw the positive side of them and guided me in my next steps. He has tremendous knowledge about chemistry and was always there to help whenever I had questions. Brian also took much time to edit every manuscript I wrote. I learned a lot from him, both in chemistry and in writing and presentation skills.

I would also like to thank other members of my thesis committee. Professor Robert H. Grubbs granted me an opportunity to collaborate with his group on projects related to green chemistry and sustainable development. Professor Sarah E. Reisman, my committee chair, and Professor Theodor Agapie, both provided insightful feedback on my research and maintained a high standard for my performance.

In addition, I would like to thank Dr. Scott C. Virgil of the Caltech Center for Catalysis and Chemical Synthesis. Scott helped me extensively with the experimental aspects of my chemistry. He also kept many analytical instruments running, which are critical to the success of not only myself but also the entire chemistry division.

The Resnick Sustainability Institute at Caltech deserves a special acknowledgement here for offering me a two-year graduate research fellowship. It is my great pleasure to know Dr. Neil Fromer, executive director of the Resnick Institute, and communications associate Heidi Rusina. They encouraged me to view my chemistry from the perspective of a general scientific audience and to evaluate the industrial, environmental, and social impacts of green, sustainable chemistry.

I would like to thank all of my collaborators, who have contributed enormously to my research projects and publications. Dr. Doug Behenna mentored me when I first joined the group

and taught me much about organic chemistry in general and catalytic asymmetric synthesis in particular while we were developing an enantioselective lactam alkylation method. Drs. Alexey Fedorov and Myles Herbert, both from the Grubbs group, and Kelly Kim from our group, collaborated with me on the fatty acid decarbonylation project. Dr. Marc Liniger and I worked together to complete the formal syntheses of several classical natural product molecules. Dr. Wen-Bo (Boger) Liu, Seo-Jung Han, and I co-authored an Accounts article on the enantioselective methods for quaternary center construction developed in our group.

I would like to thank all current and former members of the Stoltz group for making the lab a pleasant and hospitable place. In particular, I want to acknowledge the generous help from many labmates. Drs. Hosea Nelson, Alex Goldberg, and Jonny Gordon taught me experimental skills by demonstration when I first joined the group. I enjoyed discussions with them and others, including Dr. Yoshitaka Numajiri, Dr. Phil Kun-Liang Wu, Dr. Guillaume Lapointe, Dr. Jeffrey Holder, Dr. Max Klatté, Corey Reeves, Rob Craig, Doug Duquette, Christopher Haley, Chung Whan Lee, Nick O'Connor, Beau Pritchett, Katerina Korch, Sam Shockley, and my collaborators previously acknowledged. They shared with me their unique perspectives on chemistry and inspired me with fresh ideas. Many of them also took time to proofread my manuscripts and proposals.

In addition to the Stoltz group, I would like to acknowledge other chemistry graduate students and postdocs here at Caltech for their friendship and assistance. They include Dr. Lindsay Repka, Maddi Kieffer, Kangway Chuang, Haoxuan Wang, Alan Cherney, and Lauren Chapman from the Reisman group, Anton Toutov, Raymond Weitekamp, and Zach Wickens from the Grubbs group, Dr. Kuang Shen from the Shan group, Yufan Liang, Dr. Xin Mu, and Dr. Huan Cong from the Fu group, and Dr. Yichen Tan from the Peters group. The latter four often had lunch and dinner with me in the past three years.

I would like to thank Caltech staff for maintaining the institute in many ways. Dr. David VanderVelde, who directs the NMR laboratory, helped me extensively in setting up NMR

experiments and interpreting complex spectra. Dr. Mona Shahgholi and Naseem Torian collected mass spectrometry data for the new compounds I synthesized. Jeff Groseth and Rick Gerhart repaired our broken electronic instruments and glassware, respectively. I would also like to thank division chair Professor Jackie Barton, administrative assistants Agnes Tong, Anne Penney and Lynne Martinez, grant manager Yuhsien Wang, stockroom manager Joe Drew, and purchasing assistants Steve Gould and Elisa Brink for their contributions to the division as well as personal assistance.

Last but not least, I would like to thank those who have been supporting me since before my graduate career began. They include my undergraduate advisors Professors Jianbo Wang and Yan Zhang at Peking University, as well as Professors Brian P. Coppola and Zhan Chen at the University of Michigan who offered me an opportunity to participate in a summer undergraduate research exchange program. My family and friends who have been encouraging me throughout my graduate studies are gratefully acknowledged. Finally, I want to thank Professor Adam J. Matzger at the University of Michigan for offering me a postdoctoral position in his group, beginning in September 2015.

ABSTRACT

Decarboxylation and decarbonylation are important reactions in synthetic organic chemistry, transforming readily available carboxylic acids and their derivatives into various products through loss of carbon dioxide or carbon monoxide. In the past few decades, palladium-catalyzed decarboxylative and decarbonylative reactions experienced tremendous growth due to the excellent catalytic activity of palladium. Development of new reactions in this category for fine and commodity chemical synthesis continues to draw attention from the chemistry community.

The Stoltz laboratory has established a palladium-catalyzed enantioselective decarboxylative allylic alkylation of β -keto esters for the synthesis of α -quaternary ketones since 2005. Recently, we extended this chemistry to lactams due to the ubiquity and importance of nitrogen-containing heterocycles. A wide variety of α -quaternary and tetrasubstituted α -tertiary lactams were obtained in excellent yields and exceptional enantioselectivities using our palladium-catalyzed decarboxylative allylic alkylation chemistry. Enantioenriched α -quaternary carbonyl compounds are versatile building blocks that can be further elaborated to intercept synthetic intermediates en route to many classical natural products. Thus our chemistry enables catalytic asymmetric formal synthesis of these complex molecules.

In addition to fine chemicals, we became interested in commodity chemical synthesis using renewable feedstocks. In collaboration with the Grubbs group, we developed a palladium-catalyzed decarbonylative dehydration reaction that converts abundant and inexpensive fatty acids into value-added linear alpha olefins. The chemistry proceeds under relatively mild conditions, requires very low catalyst loading, tolerates a variety of functional groups, and is easily performed on a large scale. An additional advantage of this chemistry is that it provides access to expensive odd-numbered alpha olefins.

Finally, combining features of both projects, we applied a small-scale decarbonylative dehydration reaction to the synthesis of α -vinyl carbonyl compounds. Direct α -vinylation is challenging, and asymmetric vinylations are rare. Taking advantage of our decarbonylative dehydration chemistry, we were able to transform enantioenriched δ -oxocarboxylic acids into quaternary α -vinyl carbonyl compounds in good yields with complete retention of stereochemistry. Our explorations culminated in the catalytic enantioselective total synthesis of (-)-aspewentin B, a terpenoid natural product featuring a quaternary α -vinyl ketone. Both decarboxylative and decarbonylative chemistries found application in the late stage of the total synthesis.

TABLE OF CONTENTS

Acknowledgements.....	iii
Abstract.....	vi
Table of Contents.....	vii
List of Figures.....	xi
List of Schemes.....	xix
List of Tables.....	xxi
List of Abbreviations.....	xxiii

CHAPTER 1

<i>Palladium-Catalyzed Decarboxylative and Decarbonylative Transformations: Past, Present, and Future</i>	1
1.1 Introduction.....	1
1.2 Palladium-Catalyzed Decarboxylative Reactions.....	2
1.3 Palladium-Catalyzed Decarbonylative Reactions.....	6
1.4 Our Explorations in the Field of Palladium-Catalyzed Decarboxylative and Decarbonylative Reactions.....	9
1.4.1 Palladium-Catalyzed Enantioselective Decarboxylative Allylic Alkylation of Lactams.....	9
1.4.2 Formal Syntheses of Classical Natural Product Target Molecules via Palladium-Catalyzed Enantioselective Alkylation.....	10
1.4.3 Palladium-Catalyzed Decarbonylative Dehydration of Fatty Acids for the Synthesis of Linear Alpha Olefins.....	11
1.4.4 Palladium-Catalyzed Decarbonylative Dehydration for the Synthesis of α -Vinyl Carbonyl Compounds and Total Synthesis of (-)-Aspewentin B.....	12
1.5 Future Directions.....	15
1.6 Concluding Remarks.....	16
1.7 Notes and References.....	16

CHAPTER 2

<i>Palladium-Catalyzed Enantioselective Decarboxylative Allylic Alkylation of Lactam Enolates for the Construction of Quaternary N-Heterocycles</i>	19
2.1 Introduction.....	19
2.2 Reaction Development and Optimization.....	21
2.3 Study of Reaction Scope.....	23
2.4 Large-Scale Alkylation Reaction.....	26
2.5 Derivatization of Alkylated Lactam Products.....	26
2.6 Concluding Remarks.....	27
2.7 Experimental Section.....	27
2.7.1 Materials and Methods.....	27
2.7.2 Representative Procedures for the Preparation of Lactam Substrates.....	29
2.7.3 Characterization Data for Lactam Substrates Used in Table 2.1.....	34
2.7.4 General Procedure for Allylic Alkylation Screening Reactions.....	39
2.7.5 Results of Screening Various Reaction Parameters.....	40
2.7.6 Characterization Data for Lactam Products in Table 2.1.....	41
2.7.7 General Procedure for Preparative Allylic Alkylation Reactions.....	46
2.7.8 Characterization Data for Lactam Products in Table 2.2.....	46

2.7.9 Procedures for the Derivatization of Lactam 3	59
2.7.10 Methods for the Determination of Enantiomeric Excess	62
2.8 Notes and References	65
APPENDIX 1	
<i>Spectra Relevant to Chapter 2</i>	68
CHAPTER 3	
<i>Formal Synthesis of Classical Natural Product Target Molecules via Palladium-Catalyzed Enantioselective Alkylation</i>	154
3.1 Introduction	154
3.2 Thujopsene	155
3.3 Quinic Acid	158
3.4 Dysidiolide	160
3.5 Aspidospermine	162
3.6 Rhazinilam	164
3.7 Quebrachamine	166
3.8 Vincadifformine	167
3.9 Conclusions	169
3.10 Experimental Section	171
3.10.1 Materials and Methods	171
3.10.2 Syntheses of Compounds Related to Thujopsene	172
3.10.3 Syntheses of Compounds Related to Quinic Acid	178
3.10.4 Syntheses of Compounds Related to Dysidiolide	183
3.10.5 Syntheses of Compounds Related to Aspidospermine	185
3.10.6 Syntheses of Compounds Related to Rhazinilam	189
3.10.7 Syntheses of Compounds Related to Quebrachamine	190
3.10.8 Syntheses of Compounds Related to Vincadifformine	192
3.10.9 Methods for the Determination of Enantiomeric Excess	196
3.11 Notes and References	196
APPENDIX 2	
<i>Spectra Relevant to Chapter 3</i>	205
APPENDIX 3	
<i>X-Ray Crystallographic Data Relevant to Chapter 3</i>	248
APPENDIX 4	
<i>Catalytic Enantioselective Construction of Quaternary Stereocenters: Assembly of Key Building Blocks for the Synthesis of Biologically Active Molecules</i>	267
CONSPECTUS	267
A4.1 Introduction	269
A4.2 Enantioselective Syntheses of C(3) All Carbon Quaternary Centers on Oxindoles by Alkylation of 3-Bromooxindoles	272
A4.3 Palladium-Catalyzed Asymmetric Conjugate Addition of Arylboronic Acids to Cyclic Enones to Furnish Benzylic Quaternary Centers	276
A4.4 Palladium-Catalyzed Enantioselective Allylic Alkylation of Prochiral Enolates	280

A4.5 Iridium-Catalyzed Allylic Alkylation for the Construction of Vicinal Quaternary and Tertiary Stereocenters.....	290
A4.6 Conclusions.....	294
A4.7 Notes and References.....	294

CHAPTER 4

<i>Palladium-Catalyzed Decarbonylative Dehydration of Fatty Acids for the Synthesis of Linear Alpha Olefins</i>	300
4.1 Introduction	300
4.2 Optimization of Reaction Conditions.....	303
4.3 Study of Reaction Scope	305
4.4 Large Scale Reactions	308
4.5 Synthetic Utility of Alpha Olefin Products	308
4.6 Concluding Remarks.....	309
4.7 Experimental Section	310
4.7.1 Materials and Methods	310
4.7.2 General Procedure for Optimization Reactions (Route A).....	311
4.7.3 General Procedure for Optimization Reactions (Route B).....	312
4.7.4 General Procedure for Preparative Pd-Catalyzed Decarbonylative Dehydration	313
4.7.5 Spectroscopic Data for Acid Substrates.....	314
4.7.6 Spectroscopic Data for Olefin Products.....	315
4.7.7 General Procedure for Pheromone Synthesis by Ru-Catalyzed Cross Metathesis.	320
4.8 Notes and References	321

APPENDIX 5

<i>Spectra Relevant to Chapter 4</i>	325
--	-----

CHAPTER 5

<i>Palladium-Catalyzed Decarbonylative Dehydration for the Synthesis of α-Vinyl Carbonyl Compounds and Total Synthesis of (-)-Aspewentin B</i>	350
5.1 Introduction	350
5.2 Study of Reaction Scope	353
5.3 Total Synthesis of (-)-Aspewentin B	356
5.4 Concluding Remarks.....	358
5.5 Experimental Section	359
5.5.1 Materials and Methods	359
5.5.2 Preparation of Carboxylic Acid Substrates	360
5.5.3 Palladium-Catalyzed Decarbonylative Dehydration of Carboxylic Acids	373
5.5.4 Spectroscopic Data for Pd-Catalyzed Decarbonylative Dehydration Products	376
5.5.5 Total Synthesis of (-)-Aspewentin B and Related Compounds	380
5.5.6 Methods for the Determination of Enantiomeric Excess	395
5.6 Notes and References	396

APPENDIX 6

<i>Spectra Relevant to Chapter 5</i>	400
--	-----

APPENDIX 7

<i>Copper-Catalyzed Insertion of Carbenoids into Unactivated C(sp³)-H Bonds</i>	469
A7.1 Introduction.....	469
A7.2 Results and Discussions.....	470
A7.3 Concluding Remarks	476
A7.4 Experimental Section.....	477
A7.4.1 Materials and Methods.....	477
A7.4.2 Procedure for Screening Reactions.....	477
A7.4.3 Procedure for Preparative Scale Reactions	478
A7.5 Notes and References.....	478

APPENDIX 8

<i>Notebook Cross-Reference</i>	479
---------------------------------------	-----

APPENDIX 9

<i>Synthetic Route for (-)-Aspewentin B</i>	493
Comprehensive Bibliography.....	495
Index.....	503
About the Author	506

LIST OF FIGURES

CHAPTER 2

Figure 2.1 Natural products and pharmaceuticals containing chiral <i>N</i> -heterocycles ...	20
--	----

APPENDIX 1

Figure A1.1 ¹ H NMR (500 MHz, CDCl ₃) of compound 1a	69
Figure A1.2 Infrared spectrum (Thin Film, NaCl) of compound 1a	70
Figure A1.3 ¹³ C NMR (126 MHz, CDCl ₃) of compound 1a	70
Figure A1.4 ¹ H NMR (500 MHz, CDCl ₃) of compound 1b	71
Figure A1.5 Infrared spectrum (Thin Film, NaCl) of compound 1b	72
Figure A1.6 ¹³ C NMR (126 MHz, CDCl ₃) of compound 1b	72
Figure A1.7 ¹ H NMR (500 MHz, CDCl ₃) of compound 1c	73
Figure A1.8 Infrared spectrum (Thin Film, NaCl) of compound 1c	74
Figure A1.9 ¹³ C NMR (126 MHz, CDCl ₃) of compound 1c	74
Figure A1.10 ¹ H NMR (500 MHz, CDCl ₃) of compound 1d	75
Figure A1.11 Infrared spectrum (Thin Film, NaCl) of compound 1d	76
Figure A1.12 ¹³ C NMR (126 MHz, CDCl ₃) of compound 1d	76
Figure A1.13 ¹ H NMR (500 MHz, CDCl ₃) of compound 1e	77
Figure A1.14 Infrared spectrum (Thin Film, NaCl) of compound 1e	78
Figure A1.15 ¹³ C NMR (126 MHz, CDCl ₃) of compound 1e	78
Figure A1.16 ¹ H NMR (500 MHz, CDCl ₃) of compound 1f	79
Figure A1.17 Infrared spectrum (Thin Film, NaCl) of compound 1f	80
Figure A1.18 ¹³ C NMR (126 MHz, CDCl ₃) of compound 1f	80
Figure A1.19 ¹ H NMR (500 MHz, CDCl ₃) of compound 1g	81
Figure A1.20 Infrared spectrum (Thin Film, NaCl) of compound 1g	82
Figure A1.21 ¹³ C NMR (126 MHz, CDCl ₃) of compound 1g	82
Figure A1.22 ¹ H NMR (500 MHz, CDCl ₃) of compound 1h	83
Figure A1.23 Infrared spectrum (Thin Film, NaCl) of compound 1h	84
Figure A1.24 ¹³ C NMR (126 MHz, CDCl ₃) of compound 1h	84
Figure A1.25 ¹ H NMR (500 MHz, CDCl ₃) of compound 2a	85
Figure A1.26 Infrared spectrum (Thin Film, NaCl) of compound 2a	86
Figure A1.27 ¹³ C NMR (126 MHz, CDCl ₃) of compound 2a	86
Figure A1.28 ¹ H NMR (500 MHz, CDCl ₃) of compound 2a	87
Figure A1.29 Infrared spectrum (Thin Film, NaCl) of compound 2a	88
Figure A1.30 ¹³ C NMR (126 MHz, CDCl ₃) of compound 2a	88
Figure A1.31 ¹ H NMR (500 MHz, CDCl ₃) of compound 2b	89
Figure A1.32 Infrared spectrum (Thin Film, NaCl) of compound 2b	90
Figure A1.33 ¹³ C NMR (126 MHz, CDCl ₃) of compound 2b	90
Figure A1.34 ¹ H NMR (500 MHz, CDCl ₃) of compound 2c	91
Figure A1.35 Infrared spectrum (Thin Film, NaCl) of compound 2c	92
Figure A1.36 ¹³ C NMR (126 MHz, CDCl ₃) of compound 2c	92
Figure A1.37 ¹ H NMR (500 MHz, CDCl ₃) of compound 2d	93
Figure A1.38 Infrared spectrum (Thin Film, NaCl) of compound 2d	94
Figure A1.39 ¹³ C NMR (126 MHz, CDCl ₃) of compound 2d	94
Figure A1.40 ¹ H NMR (500 MHz, CDCl ₃) of compound 2e	95
Figure A1.41 Infrared spectrum (Thin Film, NaCl) of compound 2e	96

Figure A1.42	^{13}C NMR (126 MHz, CDCl_3) of compound 2e .	96
Figure A1.43	^1H NMR (500 MHz, CDCl_3) of compound 2f .	97
Figure A1.44	Infrared spectrum (Thin Film, NaCl) of compound 2f .	98
Figure A1.45	^{13}C NMR (126 MHz, CDCl_3) of compound 2f .	98
Figure A1.46	^1H NMR (500 MHz, CDCl_3) of compound 2g .	99
Figure A1.47	Infrared spectrum (Thin Film, NaCl) of compound 2g .	100
Figure A1.48	^{13}C NMR (126 MHz, CDCl_3) of compound 2g .	100
Figure A1.49	^1H NMR (500 MHz, CDCl_3) of compound 2h .	101
Figure A1.50	Infrared spectrum (Thin Film, NaCl) of compound 2h .	102
Figure A1.51	^{13}C NMR (126 MHz, CDCl_3) of compound 2h .	102
Figure A1.52	^1H NMR (500 MHz, CDCl_3) of compound 3 .	103
Figure A1.53	Infrared spectrum (Thin Film, NaCl) of compound 3 .	104
Figure A1.54	^{13}C NMR (126 MHz, CDCl_3) of compound 3 .	104
Figure A1.55	^1H NMR (500 MHz, CDCl_3) of compound 4 .	105
Figure A1.56	Infrared spectrum (Thin Film, NaCl) of compound 4 .	106
Figure A1.57	^{13}C NMR (126 MHz, CDCl_3) of compound 4 .	106
Figure A1.58	^1H NMR (500 MHz, CDCl_3) of compound 5 .	107
Figure A1.59	Infrared spectrum (Thin Film, NaCl) of compound 5 .	108
Figure A1.60	^{13}C NMR (126 MHz, CDCl_3) of compound 5 .	108
Figure A1.61	^1H NMR (500 MHz, CDCl_3) of compound 6 .	109
Figure A1.62	Infrared spectrum (Thin Film, NaCl) of compound 6 .	110
Figure A1.63	^{13}C NMR (126 MHz, CDCl_3) of compound 6 .	110
Figure A1.64	^1H NMR (500 MHz, CDCl_3) of compound 7 .	111
Figure A1.65	Infrared spectrum (Thin Film, NaCl) of compound 7 .	112
Figure A1.66	^{13}C NMR (126 MHz, CDCl_3) of compound 7 .	112
Figure A1.67	^1H NMR (500 MHz, CDCl_3) of compound 8 .	113
Figure A1.68	Infrared spectrum (Thin Film, NaCl) of compound 8 .	114
Figure A1.69	^{13}C NMR (126 MHz, CDCl_3) of compound 8 .	114
Figure A1.70	^1H NMR (500 MHz, CDCl_3) of compound 9 .	115
Figure A1.71	Infrared spectrum (Thin Film, NaCl) of compound 9 .	116
Figure A1.72	^{13}C NMR (126 MHz, CDCl_3) of compound 9 .	116
Figure A1.73	^1H NMR (500 MHz, CDCl_3) of compound 10 .	117
Figure A1.74	Infrared spectrum (Thin Film, NaCl) of compound 10 .	118
Figure A1.75	^{13}C NMR (126 MHz, CDCl_3) of compound 10 .	118
Figure A1.76	^1H NMR (500 MHz, CDCl_3) of compound 11 .	119
Figure A1.77	Infrared spectrum (Thin Film, NaCl) of compound 11 .	120
Figure A1.78	^{13}C NMR (126 MHz, CDCl_3) of compound 11 .	120
Figure A1.79	^1H NMR (500 MHz, CDCl_3) of compound 12 .	121
Figure A1.80	Infrared spectrum (Thin Film, NaCl) of compound 12 .	122
Figure A1.81	^{13}C NMR (126 MHz, CDCl_3) of compound 12 .	122
Figure A1.82	^1H NMR (500 MHz, CDCl_3) of compound 13 .	123
Figure A1.83	Infrared spectrum (Thin Film, NaCl) of compound 13 .	124
Figure A1.84	^{13}C NMR (126 MHz, CDCl_3) of compound 13 .	124
Figure A1.85	^1H NMR (500 MHz, CDCl_3) of compound 14 .	125
Figure A1.86	Infrared spectrum (Thin Film, NaCl) of compound 14 .	126
Figure A1.87	^{13}C NMR (126 MHz, CDCl_3) of compound 14 .	126
Figure A1.88	^1H NMR (500 MHz, CDCl_3) of compound 15 .	127
Figure A1.89	Infrared spectrum (Thin Film, NaCl) of compound 15 .	128

Figure A1.90	^{13}C NMR (126 MHz, CDCl_3) of compound 15	128
Figure A1.91	^1H NMR (500 MHz, CDCl_3) of compound 16	129
Figure A1.92	Infrared spectrum (Thin Film, NaCl) of compound 16	130
Figure A1.93	^{13}C NMR (126 MHz, CDCl_3) of compound 16	130
Figure A1.94	^1H NMR (500 MHz, CDCl_3) of compound 17	131
Figure A1.95	Infrared spectrum (Thin Film, NaCl) of compound 17	132
Figure A1.96	^{13}C NMR (126 MHz, CDCl_3) of compound 17	132
Figure A1.97	^1H NMR (500 MHz, CDCl_3) of compound 18	133
Figure A1.98	Infrared spectrum (Thin Film, NaCl) of compound 18	134
Figure A1.99	^{13}C NMR (126 MHz, CDCl_3) of compound 18	134
Figure A1.100	^1H NMR (500 MHz, CDCl_3) of compound 19	135
Figure A1.101	Infrared spectrum (Thin Film, NaCl) of compound 19	136
Figure A1.102	^{13}C NMR (126 MHz, CDCl_3) of compound 19	136
Figure A1.103	^1H NMR (500 MHz, CDCl_3) of compound 20	137
Figure A1.104	Infrared spectrum (Thin Film, NaCl) of compound 20	138
Figure A1.105	^{13}C NMR (126 MHz, CDCl_3) of compound 20	138
Figure A1.106	^1H NMR (500 MHz, CDCl_3) of compound 21	139
Figure A1.107	Infrared spectrum (Thin Film, NaCl) of compound 21	140
Figure A1.108	^{13}C NMR (126 MHz, CDCl_3) of compound 21	140
Figure A1.109	^1H NMR (500 MHz, CDCl_3) of compound 22	141
Figure A1.110	Infrared spectrum (Thin Film, NaCl) of compound 22	142
Figure A1.111	^{13}C NMR (126 MHz, CDCl_3) of compound 22	142
Figure A1.112	^1H NMR (500 MHz, CDCl_3) of compound 23	143
Figure A1.113	Infrared spectrum (Thin Film, NaCl) of compound 23	144
Figure A1.114	^{13}C NMR (126 MHz, CDCl_3) of compound 23	144
Figure A1.115	^1H NMR (300 MHz, CDCl_3) of compound 25	145
Figure A1.116	^1H NMR (500 MHz, CDCl_3) of compound 26	146
Figure A1.117	Infrared spectrum (Thin Film, NaCl) of compound 26	147
Figure A1.118	^{13}C NMR (126 MHz, CDCl_3) of compound 26	147
Figure A1.119	^1H NMR (300 MHz, CDCl_3) of compound 28	148
Figure A1.120	Infrared spectrum (Thin Film, NaCl) of compound 28	149
Figure A1.121	^{13}C NMR (75 MHz, CDCl_3) of compound 28	149
Figure A1.122	^1H NMR (300 MHz, CDCl_3) of compound 29	150
Figure A1.123	Infrared spectrum (Thin Film, NaCl) of compound 29	151
Figure A1.124	^{13}C NMR (75 MHz, CDCl_3) of compound 29	151
Figure A1.125	^1H NMR (300 MHz, CDCl_3) of compound 30	152
Figure A1.126	Infrared spectrum (Thin Film, NaCl) of compound 30	153
Figure A1.127	^{13}C NMR (75 MHz, CDCl_3) of compound 30	153

CHAPTER 3

Figure 3.1	Selected natural products from <i>Thujopsis dolabrata</i>	156
Figure 3.2	Two generations of building blocks	170
Figure 3.3	Crystal structure of 88 (ellipsoids, 50% probability level).....	194
Figure 3.4	Crystal structure of (\pm)- 84 (ellipsoids, 50% probability level)	195

APPENDIX 2

Figure A2.1	^1H NMR (300 MHz, CDCl_3) of compound 44	206
Figure A2.2	Infrared spectrum (Thin Film, NaCl) of compound 44	207

Figure A2.3	^{13}C NMR (75 MHz, CDCl_3) of compound 44	207
Figure A2.4	^1H NMR (300 MHz, CDCl_3) of compound 45	208
Figure A2.5	Infrared spectrum (Thin Film, NaCl) of compound 45	209
Figure A2.6	^{13}C NMR (75 MHz, CDCl_3) of compound 45	209
Figure A2.7	^1H NMR (300 MHz, CDCl_3) of compound 46A and 46B	210
Figure A2.8	Infrared spectrum (Thin Film, NaCl) of compound 46A and 46B	211
Figure A2.9	^{13}C NMR (75 MHz, CDCl_3) of compound 46A and 46B	211
Figure A2.10	^1H NMR (300 MHz, CDCl_3) of compound 47	212
Figure A2.11	Infrared spectrum (Thin Film, NaCl) of compound 47	213
Figure A2.12	^{13}C NMR (75 MHz, CDCl_3) of compound 47	213
Figure A2.13	^1H NMR (300 MHz, CDCl_3) of compound 42	214
Figure A2.14	Infrared spectrum (Thin Film, NaCl) of compound 42	215
Figure A2.15	^{13}C NMR (75 MHz, CDCl_3) of compound 42	215
Figure A2.16	^1H NMR (300 MHz, CDCl_3) of compound 89	216
Figure A2.17	Infrared spectrum (Thin Film, NaCl) of compound 89	217
Figure A2.18	^{13}C NMR (75 MHz, CDCl_3) of compound 89	217
Figure A2.19	^1H NMR (300 MHz, CDCl_3) of compound 53	218
Figure A2.20	Infrared spectrum (Thin Film, NaCl) of compound 53	219
Figure A2.21	^{13}C NMR (75 MHz, CDCl_3) of compound 53	219
Figure A2.22	^1H NMR (300 MHz, CDCl_3) of compound 54	220
Figure A2.23	Infrared spectrum (Thin Film, NaCl) of compound 54	221
Figure A2.24	^{13}C NMR (75 MHz, CDCl_3) of compound 54	221
Figure A2.25	^1H NMR (300 MHz, CDCl_3) of compound 55	222
Figure A2.26	Infrared spectrum (Thin Film, NaCl) of compound 55	223
Figure A2.27	^{13}C NMR (75 MHz, CDCl_3) of compound 55	223
Figure A2.28	^1H NMR (300 MHz, CDCl_3) of compound 50	224
Figure A2.29	Infrared spectrum (Thin Film, NaCl) of compound 50	225
Figure A2.30	^{13}C NMR (75 MHz, CDCl_3) of compound 50	225
Figure A2.31	^1H NMR (300 MHz, CDCl_3) of compound 61	226
Figure A2.32	Infrared spectrum (Thin Film, NaCl) of compound 61	227
Figure A2.33	^{13}C NMR (75 MHz, CDCl_3) of compound 61	227
Figure A2.34	^1H NMR (300 MHz, CDCl_3) of compound 62	228
Figure A2.35	Infrared spectrum (Thin Film, NaCl) of compound 62	229
Figure A2.36	^{13}C NMR (75 MHz, CDCl_3) of compound 62	229
Figure A2.37	^1H NMR (300 MHz, CDCl_3) of compound 59	230
Figure A2.38	Infrared spectrum (Thin Film, NaCl) of compound 59	231
Figure A2.39	^{13}C NMR (75 MHz, CDCl_3) of compound 59	231
Figure A2.40	^1H NMR (300 MHz, CDCl_3) of compound 69	232
Figure A2.14	Infrared spectrum (Thin Film, NaCl) of compound 69	233
Figure A2.42	^{13}C NMR (75 MHz, CDCl_3) of compound 69	233
Figure A2.43	^1H NMR (300 MHz, CDCl_3) of compound 70	234
Figure A2.44	Infrared spectrum (Thin Film, NaCl) of compound 70	235
Figure A2.45	^{13}C NMR (75 MHz, CDCl_3) of compound 70	235
Figure A2.46	^1H NMR (300 MHz, CDCl_3) of compound 65	236
Figure A2.47	Infrared spectrum (Thin Film, NaCl) of compound 65	237
Figure A2.48	^{13}C NMR (75 MHz, CDCl_3) of compound 65	237
Figure A2.49	^1H NMR (500 MHz, CDCl_3) of compound 80	238
Figure A2.50	Infrared spectrum (Thin Film, NaCl) of compound 80	239

Figure A2.51	¹³ C NMR (126 MHz, CDCl ₃) of compound 80	239
Figure A2.52	¹ H NMR (500 MHz, CDCl ₃) of compound 77	240
Figure A2.53	Infrared spectrum (Thin Film, NaCl) of compound 77	241
Figure A2.54	¹³ C NMR (126 MHz, CDCl ₃) of compound 77	241
Figure A2.55	¹ H NMR (500 MHz, CDCl ₃) of compound 87	242
Figure A2.56	Infrared spectrum (Thin Film, NaCl) of compound 87	243
Figure A2.57	¹³ C NMR (126 MHz, CDCl ₃) of compound 87	243
Figure A2.58	¹ H NMR (500 MHz, CDCl ₃) of compound 88	244
Figure A2.59	Infrared spectrum (Thin Film, NaCl) of compound 88	245
Figure A2.60	¹³ C NMR (126 MHz, CDCl ₃) of compound 88	245
Figure A2.61	¹ H NMR (500 MHz, CDCl ₃) of compound 84	246
Figure A2.62	Infrared spectrum (Thin Film, NaCl) of compound 84	247
Figure A2.63	¹³ C NMR (126 MHz, CDCl ₃) of compound 84	247

APPENDIX 4

Figure A4.1	Drug molecules containing quaternary stereocenters	271
Figure A4.2	Substrate possibilities for the enantioselective alkylation reaction	285
Figure A4.3	Enantioenriched building blocks accessible by our synthetic methods	294

APPENDIX 5

Figure A5.1	¹ H NMR (500 MHz, CDCl ₃) of compound 128h	326
Figure A5.2	Infrared spectrum (Thin Film, NaCl) of compound 128h	327
Figure A5.3	¹³ C NMR (126 MHz, CDCl ₃) of compound 128h	327
Figure A5.4	¹ H NMR (500 MHz, CDCl ₃) of compound 128o	328
Figure A5.5	Infrared spectrum (Thin Film, NaCl) of compound 128o	329
Figure A5.6	¹³ C NMR (126 MHz, CDCl ₃) of compound 128o	329
Figure A5.7	¹ H NMR (500 MHz, CDCl ₃) of compound 129a	330
Figure A5.8	¹ H NMR (500 MHz, CDCl ₃) of compound 129b	331
Figure A5.9	¹ H NMR (500 MHz, CDCl ₃) of compound 129c	332
Figure A5.10	¹ H NMR (500 MHz, CDCl ₃) of compound 129d	333
Figure A5.11	¹ H NMR (500 MHz, CDCl ₃) of compound 129e	334
Figure A5.12	¹ H NMR (500 MHz, CDCl ₃) of compound 129f	335
Figure A5.13	¹ H NMR (500 MHz, CDCl ₃) of compound 129g	336
Figure A5.14	¹ H NMR (500 MHz, CDCl ₃) of compound 129h	337
Figure A5.15	Infrared spectrum (Thin Film, NaCl) of compound 129h	338
Figure A5.16	¹³ C NMR (126 MHz, CDCl ₃) of compound 129h	338
Figure A5.17	¹ H NMR (500 MHz, CDCl ₃) of compound 129i	339
Figure A5.18	¹ H NMR (500 MHz, CDCl ₃) of compound 129j	340
Figure A5.19	¹ H NMR (500 MHz, CDCl ₃) of compound 129k	341
Figure A5.20	¹ H NMR (500 MHz, CDCl ₃) of compound 129l	342
Figure A5.21	¹ H NMR (500 MHz, CDCl ₃) of compound 129m	343
Figure A5.22	¹ H NMR (500 MHz, DMSO-d ₆ , 130 °C) of compound 129n	344
Figure A5.23	¹ H NMR (500 MHz, DMSO-d ₆ , 130 °C) of compound 130n	345
Figure A5.24	¹ H NMR (500 MHz, CDCl ₃) of compound 129o	346
Figure A5.25	¹ H NMR (500 MHz, CDCl ₃) of compound 130p	347
Figure A5.26	¹ H NMR (500 MHz, CDCl ₃) of compound 131a	348
Figure A5.27	¹ H NMR (500 MHz, CDCl ₃) of compound 131b	349

CHAPTER 5

Figure 5.1 Natural products with ethylene substituents.....	351
---	-----

APPENDIX 6

Figure A6.1 ¹ H NMR (500 MHz, CDCl ₃) of compound 140a	401
Figure A6.2 Infrared spectrum (Thin Film, NaCl) of compound 140a	402
Figure A6.3 ¹³ C NMR (126 MHz, CDCl ₃) of compound 140a	402
Figure A6.4 ¹ H NMR (500 MHz, CDCl ₃) of compound 152	403
Figure A6.5 Infrared spectrum (Thin Film, NaCl) of compound 152	404
Figure A6.6 ¹³ C NMR (126 MHz, CDCl ₃) of compound 152	404
Figure A6.7 ¹ H NMR (500 MHz, CDCl ₃) of compound 140b	405
Figure A6.8 Infrared spectrum (Thin Film, NaCl) of compound 140b	406
Figure A6.9 ¹³ C NMR (126 MHz, CDCl ₃) of compound 140b	406
Figure A6.10 ¹ H NMR (500 MHz, CDCl ₃) of compound 140c	407
Figure A6.11 Infrared spectrum (Thin Film, NaCl) of compound 140c	408
Figure A6.12 ¹³ C NMR (126 MHz, CDCl ₃) of compound 140c	408
Figure A6.13 ¹ H NMR (500 MHz, CDCl ₃) of compound 140d	409
Figure A6.14 Infrared spectrum (Thin Film, NaCl) of compound 140d	410
Figure A6.15 ¹³ C NMR (126 MHz, CDCl ₃) of compound 140d	410
Figure A6.16 ¹ H NMR (500 MHz, CDCl ₃) of compound 156	411
Figure A6.17 Infrared spectrum (Thin Film, NaCl) of compound 156	412
Figure A6.18 ¹³ C NMR (126 MHz, CDCl ₃) of compound 156	412
Figure A6.19 ¹ H NMR (500 MHz, CDCl ₃) of compound 157	413
Figure A6.20 Infrared spectrum (Thin Film, NaCl) of compound 157	414
Figure A6.21 ¹³ C NMR (126 MHz, CDCl ₃) of compound 157	414
Figure A6.22 ¹ H NMR (500 MHz, CDCl ₃) of compound 140e	415
Figure A6.23 Infrared spectrum (Thin Film, NaCl) of compound 140e	416
Figure A6.24 ¹³ C NMR (126 MHz, CDCl ₃) of compound 140e	416
Figure A6.25 ¹ H NMR (500 MHz, CDCl ₃) of compound 140f	417
Figure A6.26 Infrared spectrum (Thin Film, NaCl) of compound 140f	418
Figure A6.27 ¹³ C NMR (126 MHz, CDCl ₃) of compound 140f	418
Figure A6.28 ¹ H NMR (500 MHz, CDCl ₃) of compound 140g	419
Figure A6.29 Infrared spectrum (Thin Film, NaCl) of compound 140g	420
Figure A6.30 ¹³ C NMR (126 MHz, CDCl ₃) of compound 140g	420
Figure A6.31 ¹ H NMR (500 MHz, CDCl ₃) of compound 140h	421
Figure A6.32 Infrared spectrum (Thin Film, NaCl) of compound 140h	422
Figure A6.33 ¹³ C NMR (126 MHz, CDCl ₃) of compound 140h	422
Figure A6.34 ¹ H NMR (500 MHz, CDCl ₃) of compound 140i	423
Figure A6.35 Infrared spectrum (Thin Film, NaCl) of compound 140i	424
Figure A6.36 ¹³ C NMR (126 MHz, CDCl ₃) of compound 140i	424
Figure A6.37 ¹ H NMR (500 MHz, CDCl ₃) of compound 141a	425
Figure A6.38 Infrared spectrum (Thin Film, NaCl) of compound 141a	426
Figure A6.39 ¹³ C NMR (126 MHz, CDCl ₃) of compound 141a	426
Figure A6.40 ¹ H NMR (500 MHz, CDCl ₃) of compound 142	427
Figure A6.41 Infrared spectrum (Thin Film, NaCl) of compound 142	428
Figure A6.42 ¹³ C NMR (126 MHz, CDCl ₃) of compound 142	428
Figure A6.43 ¹ H NMR (500 MHz, CDCl ₃) of compound 139	429
Figure A6.44 Infrared spectrum (Thin Film, NaCl) of compound 139	430

Figure A6.45	^{13}C NMR (126 MHz, CDCl_3) of compound 139	430
Figure A6.46	^1H NMR (500 MHz, CDCl_3) of compound 141c	431
Figure A6.47	Infrared spectrum (Thin Film, NaCl) of compound 141c	432
Figure A6.48	^{13}C NMR (126 MHz, CDCl_3) of compound 141c	432
Figure A6.49	^1H NMR (500 MHz, CDCl_3) of compound 141d	433
Figure A6.50	Infrared spectrum (Thin Film, NaCl) of compound 141d	434
Figure A6.51	^{13}C NMR (126 MHz, CDCl_3) of compound 141d	434
Figure A6.52	^1H NMR (500 MHz, CDCl_3) of compound 141e	435
Figure A6.53	Infrared spectrum (Thin Film, NaCl) of compound 141e	436
Figure A6.54	^{13}C NMR (126 MHz, CDCl_3) of compound 141e	436
Figure A6.55	^1H NMR (500 MHz, CDCl_3) of compound 141f	437
Figure A6.56	Infrared spectrum (Thin Film, NaCl) of compound 141f	438
Figure A6.57	^{13}C NMR (126 MHz, CDCl_3) of compound 141f	438
Figure A6.58	^1H NMR (500 MHz, CDCl_3) of compound 141g	439
Figure A6.59	Infrared spectrum (Thin Film, NaCl) of compound 141g	440
Figure A6.60	^{13}C NMR (126 MHz, CDCl_3) of compound 141g	440
Figure A6.61	^1H NMR (500 MHz, CDCl_3) of compound 141h	441
Figure A6.62	Infrared spectrum (Thin Film, NaCl) of compound 141h	442
Figure A6.63	^{13}C NMR (126 MHz, CDCl_3) of compound 141h	442
Figure A6.64	^1H NMR (500 MHz, CDCl_3) of compound 141i	443
Figure A6.65	Infrared spectrum (Thin Film, NaCl) of compound 141i	444
Figure A6.66	^{13}C NMR (126 MHz, CDCl_3) of compound 141i	444
Figure A6.67	^1H NMR (500 MHz, CDCl_3) of compound 162	445
Figure A6.68	Infrared spectrum (Thin Film, NaCl) of compound 162	446
Figure A6.69	^{13}C NMR (126 MHz, CDCl_3) of compound 162	446
Figure A6.70	^1H NMR (500 MHz, CDCl_3) of compound 147	447
Figure A6.71	Infrared spectrum (Thin Film, NaCl) of compound 147	448
Figure A6.72	^{13}C NMR (126 MHz, CDCl_3) of compound 147	448
Figure A6.73	^1H NMR (500 MHz, CDCl_3) of compound 145	449
Figure A6.74	Infrared spectrum (Thin Film, NaCl) of compound 145	450
Figure A6.75	^{13}C NMR (126 MHz, CDCl_3) of compound 145	450
Figure A6.76	^1H NMR (500 MHz, CDCl_3) of compound 148	451
Figure A6.77	Infrared spectrum (Thin Film, NaCl) of compound 148	452
Figure A6.78	^{13}C NMR (126 MHz, CDCl_3) of compound 148	452
Figure A6.79	^1H NMR (500 MHz, CDCl_3) of compound 144	453
Figure A6.80	Infrared spectrum (Thin Film, NaCl) of compound 144	454
Figure A6.81	^{13}C NMR (126 MHz, CDCl_3) of compound 144	454
Figure A6.82	^1H NMR (500 MHz, CDCl_3) of compound 143	455
Figure A6.83	Infrared spectrum (Thin Film, NaCl) of compound 143	456
Figure A6.84	^{13}C NMR (126 MHz, CDCl_3) of compound 143	456
Figure A6.85	^1H NMR (500 MHz, CDCl_3) of compound 149	457
Figure A6.86	Infrared spectrum (Thin Film, NaCl) of compound 149	458
Figure A6.87	^{13}C NMR (126 MHz, CDCl_3) of compound 149	458
Figure A6.88	^1H NMR (500 MHz, CDCl_3) of compound 133	459
Figure A6.89	Infrared spectrum (Thin Film, NaCl) of compound 133	460
Figure A6.90	^{13}C NMR (126 MHz, CDCl_3) of compound 133	460
Figure A6.91	^1H NMR (500 MHz, CDCl_3) of compound 133A	461
Figure A6.92	Infrared spectrum (Thin Film, NaCl) of compound 133A	462

Figure A6.93	^{13}C NMR (126 MHz, CDCl_3) of compound 133A .	462
Figure A6.94	^1H NMR (500 MHz, CDCl_3) of compound 163 .	463
Figure A6.95	Infrared spectrum (Thin Film, NaCl) of compound 163 .	464
Figure A6.96	^{13}C NMR (126 MHz, CDCl_3) of compound 163 .	464
Figure A6.97	^1H NMR (500 MHz, CDCl_3) of compound 164 .	465
Figure A6.98	Infrared spectrum (Thin Film, NaCl) of compound 164 .	466
Figure A6.99	^{13}C NMR (126 MHz, CDCl_3) of compound 164 .	466
Figure A6.100	^1H NMR (500 MHz, CDCl_3) of compound 165 .	467
Figure A6.101	Infrared spectrum (Thin Film, NaCl) of compound 165 .	468
Figure A6.102	^{13}C NMR (126 MHz, CDCl_3) of compound 165 .	468

APPENDIX 7

Figure A7.1	Additives/ligands with $(\text{MeCN})_4\text{Cu}^+\text{PF}_6^-$.	474
Figure A7.2	Additives/ligands with $\text{Cu}^+(\text{OTf}) \bullet \text{toluene}$.	474

LIST OF SCHEMES

CHAPTER 1

Scheme 1.1	Decarboxylation/decarbonylation and subsequent transformations	2
Scheme 1.2	Palladium-catalyzed decarboxylative allylic alkylation reactions.....	3
Scheme 1.3	Decarboxylative reactions of other activated carboxylic acids	3
Scheme 1.4	Decarboxylative Heck-type olefination of aromatic carboxylic acids.....	4
Scheme 1.5	Palladium-catalyzed decarboxylative cross-coupling reactions.....	5
Scheme 1.6	Proposed reaction mechanism for decarboxylative cross-coupling	5
Scheme 1.7	Palladium-catalyzed decarboxylative allylic alkylation and benzylation of alkynyl carboxylic acids.....	6
Scheme 1.8	Palladium-catalyzed decarbonylation of aliphatic acyl chlorides.....	7
Scheme 1.9	Palladium-catalyzed decarboxylative Heck olefinations	8
Scheme 1.10	Palladium-catalyzed decarbonylation of aldehydes	8
Scheme 1.11	Palladium-catalyzed enantioselective decarboxylative allylic alkylation of lactams	10
Scheme 1.12	Formal synthesis of classical natural products via palladium-catalyzed enantioselective alkylation chemistry.....	11
Scheme 1.13	Palladium-catalyzed decarboxylative dehydration of fatty acids for the synthesis of linear alpha olefins.....	12
Scheme 1.14	Palladium-catalyzed decarboxylative dehydration for the synthesis of α -vinyl carbonyl compounds.....	14
Scheme 1.15	Total synthesis of (-)-aspewentin B: union of palladium-catalyzed allylic alkylation and decarboxylative dehydration reactions.....	15
Scheme 1.16	Challenges and opportunities in palladium-catalyzed decarboxylative and decarbonylative reactions	16

CHAPTER 2

Scheme 2.1	Gram-scale alkylation reactions	26
Scheme 2.2	Synthetic utility of lactam products	27

CHAPTER 3

Scheme 3.1	Three classes of Pd-catalyzed enantioselective allylic alkylations	155
Scheme 3.2	Srikrishna and Anebousevly's approach to thujopsene.....	157
Scheme 3.3	Formal total synthesis of (-)-thujopsene.....	158
Scheme 3.4	Renaud's formal total synthesis of quinic acid.....	159
Scheme 3.5	Formal total synthesis of (-)-quinic acid	160
Scheme 3.6	Danishesky's approach to (\pm)-dysidiolide	161
Scheme 3.7	Formal total synthesis of (-)-dysidiolide.....	162
Scheme 3.8	Meyers' approach to unnatural (+)-aspidospermine	163
Scheme 3.9	Formal total synthesis of (-)-aspidospermine	164
Scheme 3.10	Magnus' approach to rhazinilam.....	165
Scheme 3.11	Formal total synthesis of (+)-rhazinilam.....	166
Scheme 3.12	Amat's approach to quebrachamine.....	167
Scheme 3.13	Formal total synthesis of (+)-quebrachamine	167
Scheme 3.14	Pandey's approach to (+)-vincadifformine.....	168
Scheme 3.15	Formal total synthesis of (-)-vincadifformine	169

APPENDIX 4

Scheme A4.1 Alkylations of 3-haloindoles.....	274
Scheme A4.2 Alkylations of 3-haloindoles via reactive prochiral indolone 100	276
Scheme A4.3 Large-scale conjugate additions	279
Scheme A4.4 Mechanistic rationale for the asymmetric conjugate addition	280
Scheme A4.5 General mechanism of Pd-catalyzed Asymmetric Allylic Alkylation.....	281
Scheme A4.6 Challenges in alkylation of nonsymmetrical ketones.....	282
Scheme A4.7 The Tsuji allylic alkylation	283
Scheme A4.8 Discovery of an enantioselective catalyst system for the asymmetric Tsuji allylic alkylation.....	284
Scheme A4.9 Proposed mechanism for palladium-catalyzed allylic alkylation.....	288
Scheme A4.10 Generation of palladium enolate intermediates from other starting materials	289
Scheme A4.11 Asymmetric enolate alkylation cascade with different electrophiles	289
Scheme A4.12 Ir-catalyzed allylic alkylation of cyclic α -substituted β -ketoesters..	291

CHAPTER 4

Scheme 4.1 Palladium-catalyzed decarbonylative dehydration. (A) High temperature processes (Miller, Kraus). (B) Low temperature processes (Gooßen, Scott). (C) This research.....	302
Scheme 4.2 Large-scale decarbonylative dehydration of stearic acid and 10-acetoxydecanoic acid	308

CHAPTER 5

Scheme 5.1 Decarboxylative approach to vinylation.....	352
Scheme 5.2 Decarbonylative dehydration of δ -oxocarboxylic acid 140a	353
Scheme 5.3 Retrosynthetic analysis of (-)-aspewentin B	356
Scheme 5.4 Total synthesis of (-)-aspewentin B.....	358

APPENDIX 7

Scheme A7.1 Copper-tris(pyrazolyl)borate-catalyzed carbenoid C–H insertions ...	470
Scheme A7.2 Slow-addition experiments	476
Scheme A7.3 Methylcyclohexane as substrate	476

LIST OF TABLES

CHAPTER 2

Table 2.1	Solvent, protecting group, and ligand screen	23
Table 2.2	Palladium-catalyzed decarboxylative alkylation of lactams: reaction scope	25
Table 2.3	Influences of solvent, protecting group, and ligand.....	40
Table 2.4	Influence of temperature and concentration	40
Table 2.5	Analytical HPLC and SFC assays and retention times.....	62

CHAPTER 3

Table 3.1	Analytical GC and HPLC assays and retention times	196
-----------	---	-----

APPENDIX 3

Table A3.1	Crystal data and structure refinement for 88	250
Table A3.2	Atomic coordinates ($\times 10^4$) and equivalent isotropic displacement parameters ($\text{\AA}^2 \times 10^3$) for 88 . $U(\text{eq})$ is defined as one third of the trace of the orthogonalized U^{ij} tensor.	251
Table A3.3	Bond lengths [\AA] and angles [$^\circ$] for 88	252
Table A3.4	Anisotropic displacement parameters ($\text{\AA}^2 \times 10^3$) for 88 . The anisotropic displacement factor exponent takes the form: $-2p^2 [h^2 a^* U^{11} + \dots + 2 h k a^* b^* U^{12}]$	255
Table A3.5	Hydrogen coordinates ($\times 10^4$) and isotropic displacement parameters ($\text{\AA}^2 \times 10^3$) for 88	256
Table A3.6	Hydrogen bonds for 88 [\AA and $^\circ$].	257
Table A3.7	Crystal data and structure refinement for (\pm)- 84	258
Table A3.8	Atomic coordinates ($\times 10^4$) and equivalent isotropic displacement parameters ($\text{\AA}^2 \times 10^3$) for (\pm)- 84 . $U(\text{eq})$ is defined as one third of the trace of the orthogonalized U^{ij} tensor.....	260
Table A3.9	Bond lengths [\AA] and angles [$^\circ$] for (\pm)- 84	260
Table A3.10	Anisotropic displacement parameters ($\text{\AA}^2 \times 10^3$) for (\pm)- 84 . The anisotropic displacement factor exponent takes the form: $-2p^2 [h^2 a^* U^{11} + \dots + 2 h k a^* b^* U^{12}]$	264
Table A3.11	Hydrogen coordinates ($\times 10^4$) and isotropic displacement parameters ($\text{\AA}^2 \times 10^3$) for (\pm)- 84	265
Table A3.12	Hydrogen bonds for (\pm)- 84 [\AA and $^\circ$]......	266

APPENDIX 4

Table A4.1	Enantioselective alkylation of 3-haloindoles	275
Table A4.2	Asymmetric addition of arylboronic acids to 3-substituted cyclic enones.. ..	278
Table A4.3	Increased yields under new reaction conditions	279
Table A4.4	Enantioselective allylic alkylation of cyclic ketone enolates	286
Table A4.5	Enantioselective allylic alkylation of cyclobutanone and lactam enolates .	

.....	287
Table A4.6 Selected substrates of Ir-catalyzed allylic alkylation of cyclic α -substituted β -ketoesters.....	292
Table A4.7 Selected examples of Ir-catalyzed allylic alkylation of acyclic α -substituted β -ketoesters.....	292
Table A4.8 Sequential allylic alkylation catalyzed by iridium and palladium complexes	293

CHAPTER 4

Table 4.1 Effects of catalyst, ligand, and additive.....	304
Table 4.2 Portionwise addition of acetic anhydride.....	305
Table 4.3 Substrate scope study	307
Table 4.4 Synthesis of pheromones 131a and 131b from olefin 129f	309
Table 4.5 Additional ligand screen	312

CHAPTER 5

Table 5.1 Decarbonylative dehydration of δ -oxocarboxylic acids	355
Table 5.2 Comparison of Synthetic and Natural Aspewentin B.....	394
Table 5.3 Analytical HPLC and SFC assays and retention times.....	395

APPENDIX 7

Table A7.1 Screen of metal salts and ligands	471
Table A7.2 Screen of ligands with Cu(OTf) ₂	472
Table A7.3 Screen of other metal salts	473
Table A7.4 Top results from the additive/ligand screen with Cu ^I sources.....	475

APPENDIX 8

Table A8.1 Compounds from Chapter 2	480
Table A8.2 Compounds from Chapter 3	485
Table A8.3 Compounds from Chapter 4	487
Table A8.4 Compounds from Chapter 5	489

LIST OF ABBREVIATIONS

Å	Ångstrom
$[\alpha]_D$	specific rotation at wavelength of sodium D line
Ac	acetyl
APCI	atmospheric pressure chemical ionization
app	apparent
aq	aqueous
Ar	aryl
atm	atmosphere
BBN	borabicyclononane
BINAP	2,2'-bis(diphenylphosphino)-1,1'-binaphthyl
Bn	benzyl
Boc	<i>tert</i> -butyloxycarbonyl
br	broad
Bu	butyl
<i>i</i> -Bu	<i>iso</i> -butyl
<i>t</i> -Bu	<i>tert</i> -Butyl
Bz	benzoyl
<i>c</i>	concentration for specific rotation measurements
°C	degrees Celsius
calc'd	calculated
cat	catalytic
Cbz	carbobenzyloxy
CCDC	Cambridge Crystallographic Data Centre
CI	chemical ionization
Cy	cyclohexyl
d	doublet

D	deuterium
dba	dibenzylideneacetone
DBU	1,8-diazabicyclo[5.4.0]undec-7-ene
DIBAL	diisobutylaluminium hydride
DMAP	4-dimethylaminopyridine
DMF	<i>N,N</i> -dimethylformamide
DMSO	dimethyl sulfoxide
dppb	1,4-bis(diphenylphosphino)butane
dppf	1,1'-bis(diphenylphosphino)ferrocene
dr	diastereomeric ratio
ee	enantiomeric excess
EI	electron impact
e.g.	for example (Latin “ <i>exempli gratia</i> ”)
equiv	equivalent
ESI	electrospray ionization
Et	ethyl
FAB	fast atom bombardment
Fmoc	fluorenylmethyloxycarbonyl
g	gram(s)
GC	gas chromatography
h	hour(s)
HPLC	high-performance liquid chromatography
HRMS	high-resolution mass spectroscopy
Hz	hertz
i.e.	that is (Latin “ <i>id est</i> ”)
IR	infrared (spectroscopy)
<i>J</i>	coupling constant

λ	wavelength
L	liter
LDA	lithium diisopropylamide
LiHMDS	lithium hexamethyldisilazide
lit.	literature value
m	multiplet; milli
<i>m</i>	meta
<i>m/z</i>	mass to charge ratio
M	metal; molar; molecular ion
Me	methyl
MHz	megahertz
μ	micro
min	minute(s)
MM	mixed method
mol	mole(s)
mp	melting point
MS	molecular sieves
MTBE	methyl <i>tert</i> -butyl ether
N	normal
nbd	norbornadiene
NMP	<i>N</i> -methylpyrrolidone
NMR	nuclear magnetic resonance
[O]	oxidation
<i>o</i>	ortho
<i>p</i>	para
Ph	phenyl
pH	hydrogen ion concentration in aqueous solution

PHOX	phosphinooxazoline
pK_a	pK for association of an acid
pmdba	bis(4-methoxybenzylidene)acetone
ppm	parts per million
<i>i</i> -Pr	isopropyl
Py	pyridine
q	quartet
ref	reference
R_f	retention factor
s	singlet or strong or selectivity factor
sat.	saturated
SFC	supercritical fluid chromatography
t	triplet
TBAF	tetrabutylammonium fluoride
TBAT	tetrabutylammonium difluorotriphenylsilicate
TBS	<i>tert</i> -butyldimethylsilyl
TEMPO	2,2,6,6-Tetramethylpiperidin-1-yloxy
TFA	trifluoroacetic acid
THF	tetrahydrofuran
TLC	thin-layer chromatography
TMS	trimethylsilyl
TOF	time-of-flight
Tol	tolyl
TON	turnover number
t_R	retention time
Ts	<i>p</i> -toluenesulfonyl (tosyl)

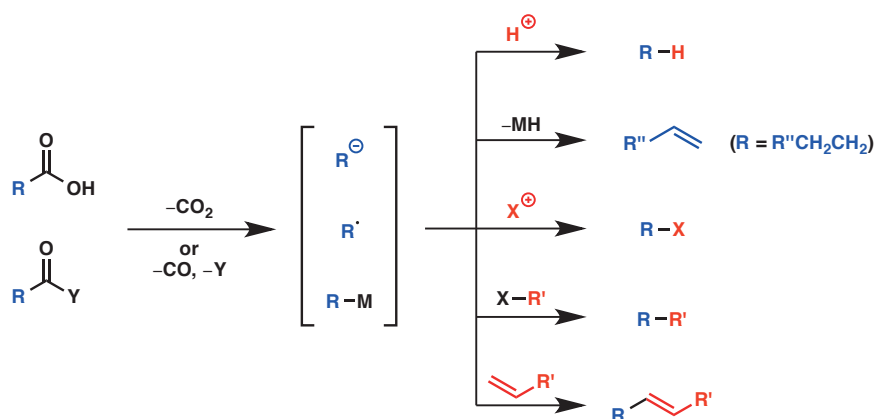
CHAPTER 1

Palladium-Catalyzed Decarboxylative and Decarbonylative Transformations: Past, Present, and Future

1.1 Introduction

Decarboxylation and decarbonylation are important transformations in synthetic organic chemistry. Loss of carbon dioxide or carbon monoxide from a carboxylic acid (R-COOH) or its derivatives (R-COY) generates a reactive intermediate (formally a carbocation, carbanion, radical, or organometallic species) of the R fragment, which may participate in a variety of subsequent transformations, including protonation, elimination, electrophilic halogenation, cross-coupling, and Heck-type reactions (Scheme 1.1). Since many carboxylic acids and their derivatives are readily available and inexpensive, using these compounds as starting materials in organic synthesis is an attractive option.

Scheme 1.1 Decarboxylation/decarbonylation and subsequent transformations

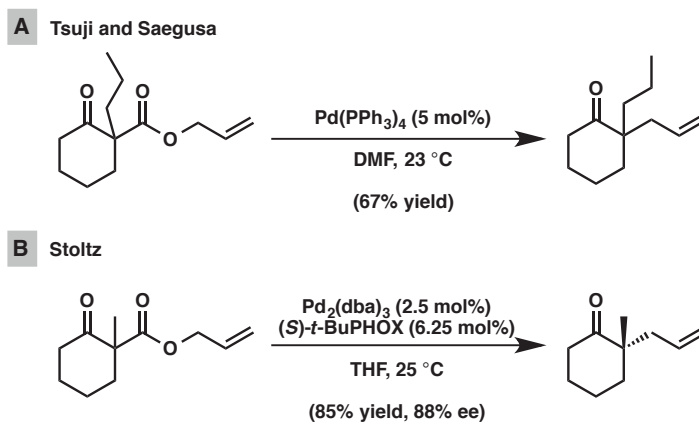


Since the 1980s, palladium-catalyzed decarboxylative and decarbonylative reactions have received significant attention from the synthetic community. Due to the excellent catalytic activity of palladium, a large number of synthetically useful decarboxylative and decarbonylative transformations using palladium catalysis have been developed. In this chapter, we will review past literature, then discuss our own adventure in this exciting field, and finally point out future directions for decarboxylative and decarbonylative chemistry.

1.2 Palladium-Catalyzed Decarboxylative Reactions

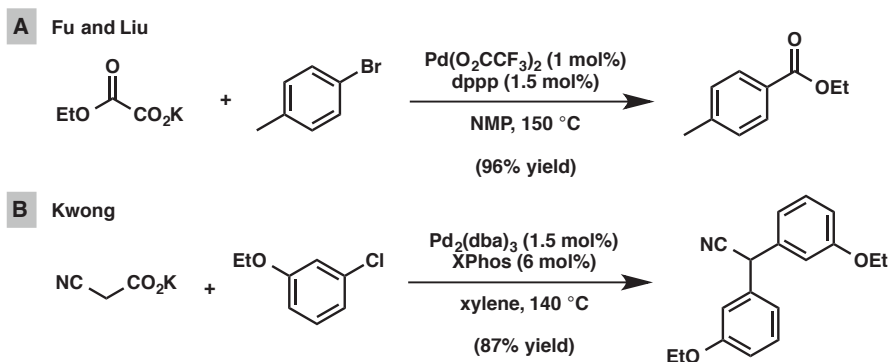
The earliest accounts of palladium-catalyzed decarboxylative reactions focused on carboxylates that readily undergo decarboxylation, e.g. β -keto carboxylates. Saegusa¹ and Tsuji² independently reported palladium-catalyzed decarboxylative allylic alkylation of β -keto esters in the early 1980s (Scheme 1.2A). Presumably, the Pd-carboxylate is generated upon deallylation of the ester. Two decades later, the Stoltz group developed enantioselective variants of this reaction (Scheme 1.2B).³

Scheme 1.2 Palladium-catalyzed decarboxylative allylic alkylation reactions



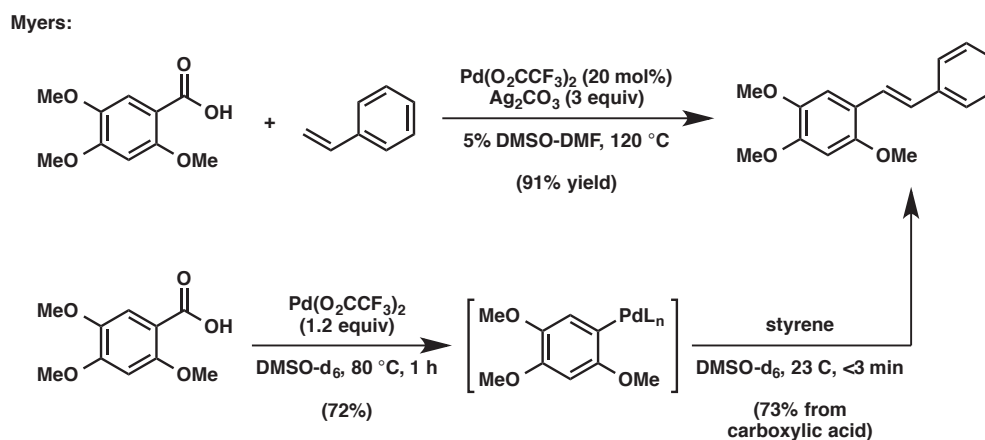
Besides β -keto carboxylates, other α - or β -activated carboxylic acids and derivatives have also been utilized in palladium-catalyzed reactions. For example, Fu and Liu jointly reported the decarboxylative coupling of potassium oxalate monoesters with aryl bromides and chlorides (Scheme 1.3A).⁴ Kwong and co-workers developed a palladium-catalyzed decarboxylative arylation of potassium cyanoacetate (Scheme 1.3B).⁵

Scheme 1.3 Decarboxylative reactions of other activated carboxylic acids



Another broad class of substrates for decarboxylation is aromatic carboxylic acids. A seminal publication from the Myers group describes the decarboxylative Heck-type olefination of aromatic carboxylic acids (Scheme 1.4).⁶ The reaction requires Ag_2CO_3 for catalyst turnover; however, decarboxylation is thought to be promoted by palladium alone as evidenced by the results of control experiments using 1.2 equiv $\text{Pd}(\text{O}_2\text{CCF}_3)_2$ in the absence of Ag_2CO_3 (Scheme 1.4).

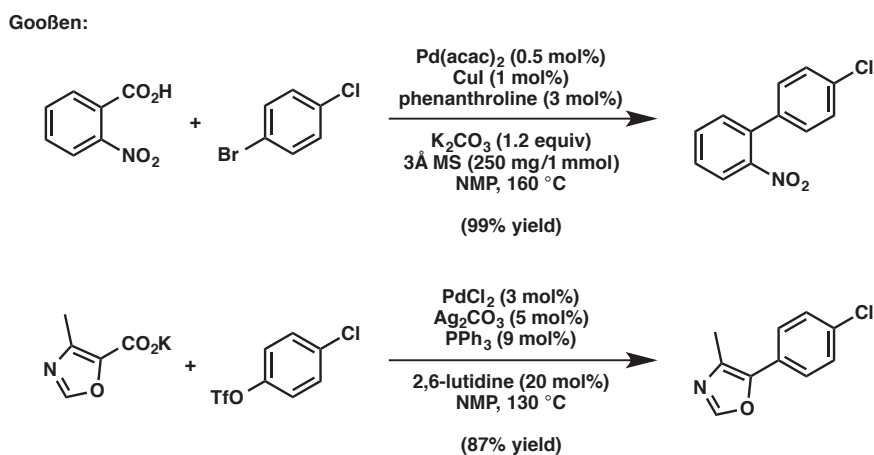
Scheme 1.4 Decarboxylative Heck-type olefination of aromatic carboxylic acids



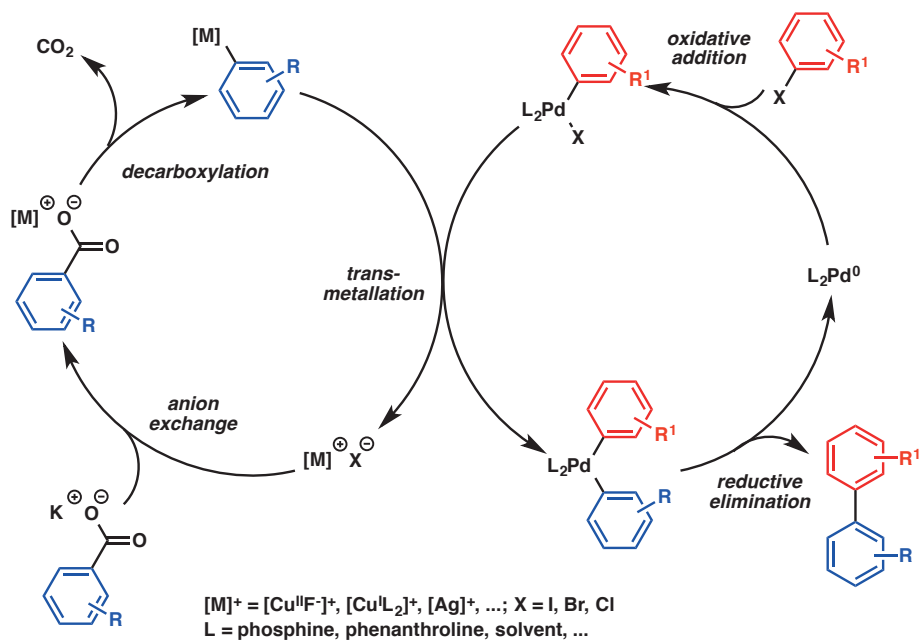
In the past decade, decarboxylative cross-coupling reactions have experienced a tremendous growth, in part because aromatic carboxylic acids can serve as the carbanion equivalent through decarboxylation and replace conventional but more expensive organometallic reagents (e.g. arylboronic acids).⁷ These reactions often involve another transition metal (catalytic or stoichiometric) such as copper or silver that facilitates decarboxylation.⁸ The Gooßen group has pioneered this field (Scheme 1.5).⁹ A proposed reaction mechanism is outlined in Scheme 1.6.⁷ In addition to aromatic carboxylic acids,

alkenyl carboxylic acids such as cinnamic acid have also been employed in palladium-catalyzed decarboxylative cross coupling reactions under similar conditions.¹⁰

Scheme 1.5 Palladium-catalyzed decarboxylative cross-coupling reactions

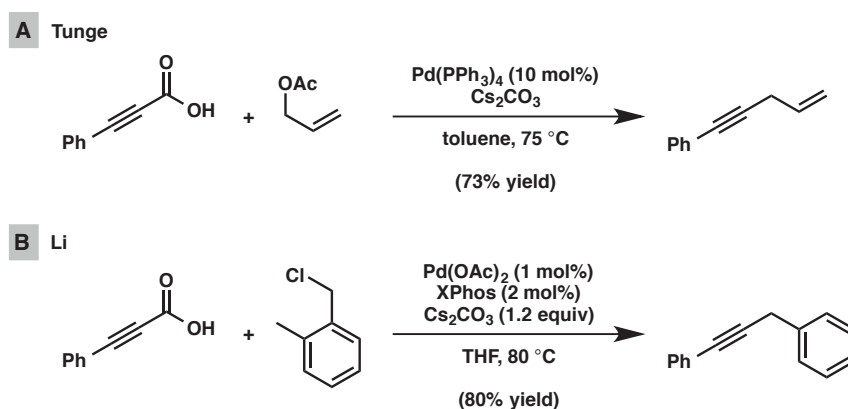


Scheme 1.6 Proposed reaction mechanism for decarboxylative cross-coupling



A third class of substrates are alkynyl carboxylic acids, which decarboxylate upon heating to produce an alkynylpalladium species that may be coupled with allylic or benzylic electrophiles (Scheme 1.7).¹¹

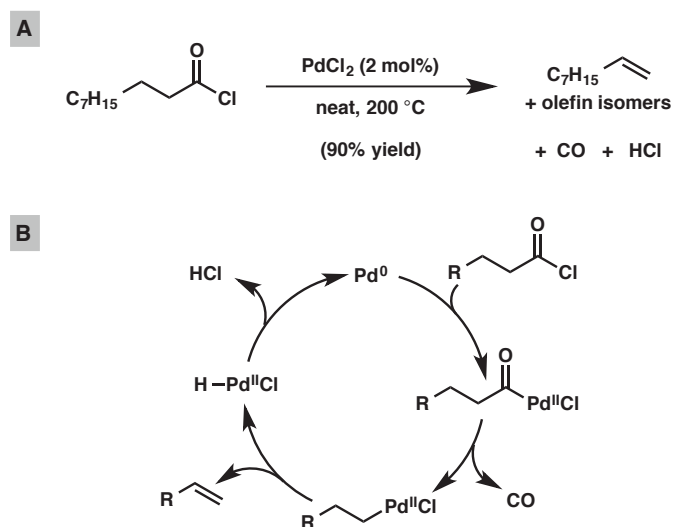
Scheme 1.7 Palladium-catalyzed decarboxylative allylic alkylation and benzylation of alkynyl carboxylic acids



1.3 Palladium-Catalyzed Decarbonylative Reactions

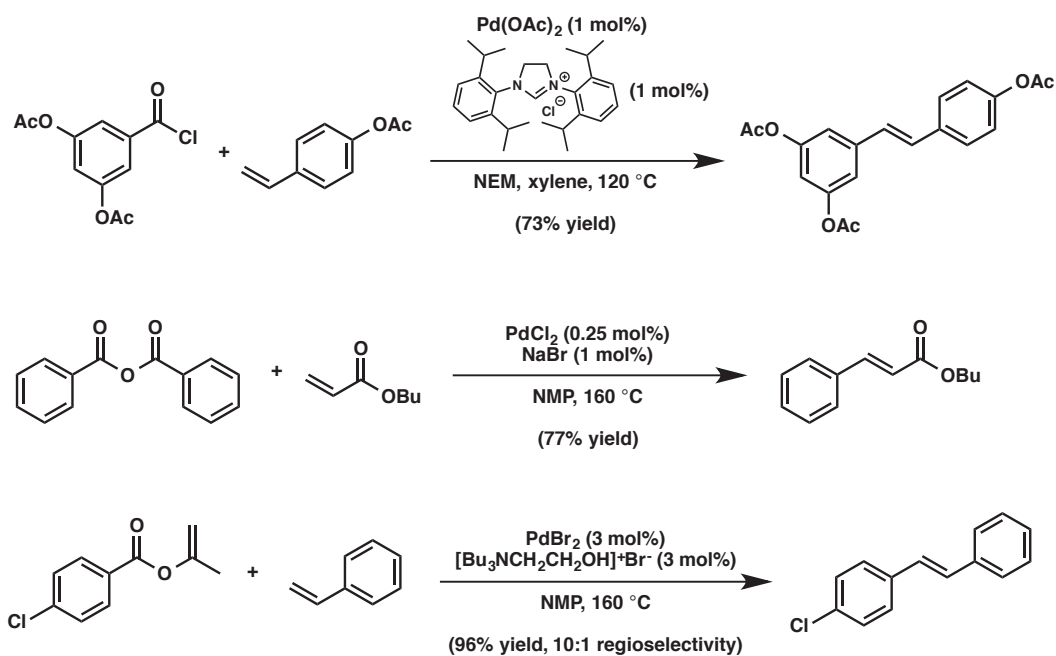
As an alternative to decarboxylation, decarbonylation represents another approach to cleaving the carbonyl group in a carboxylic acid derivative and generating an activated species for the remaining fragment. In 1965, Tsuji and co-workers reported the first example of palladium-catalyzed decarbonylation of aliphatic acyl chlorides to form alkenes along with CO and HCl (Scheme 1.8A). The reaction is thought to proceed via oxidative addition of the acyl chloride to Pd(0), forming an acylpalladium(II) species, which loses carbon monoxide to generate an alkylpalladium(II) species that undergoes β -hydride elimination to deliver the olefin product and regenerate the active Pd(0) catalyst (Scheme 1.8B). However, this reaction requires high temperature (200 °C) and the product is a mixture of double bond positional isomers.

Scheme 1.8 Palladium-catalyzed decarbonylation of aliphatic acyl chlorides



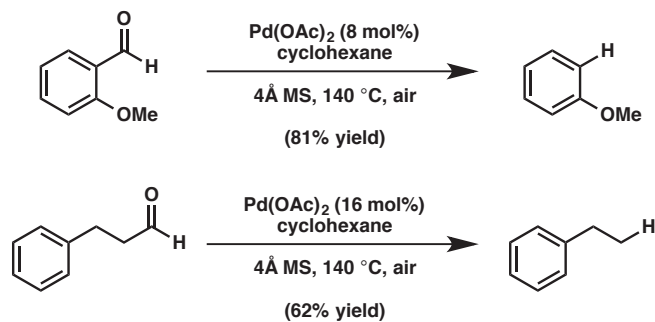
On the other hand, aromatic/alkenyl carboxylic acid derivatives have been extensively studied in the context of palladium-catalyzed decarbonylation. Since the corresponding aryl- or alkenylpalladium(II) species cannot undergo β -hydride elimination, they could be employed in further transformations, especially Heck-type olefination (Scheme 1.9). The starting material can be aryl chlorides,¹² anhydrides,¹³ or activated esters.¹⁴ These decarbonylative Heck reactions are particularly interesting because they avoid the use of base and thus the generation of stoichiometric salt byproducts.^{13,14}

Scheme 1.9 Palladium-catalyzed decarbonylative Heck olefinations



In addition to carboxylic acid derivatives, aldehydes have also been employed in decarbonylation reactions. Maiti and co-workers developed a decarbonylation process for converting aromatic and aliphatic aldehydes to arenes and alkanes, respectively (Scheme 1.10).

Scheme 1.10 Palladium-catalyzed decarbonylation of aldehydes

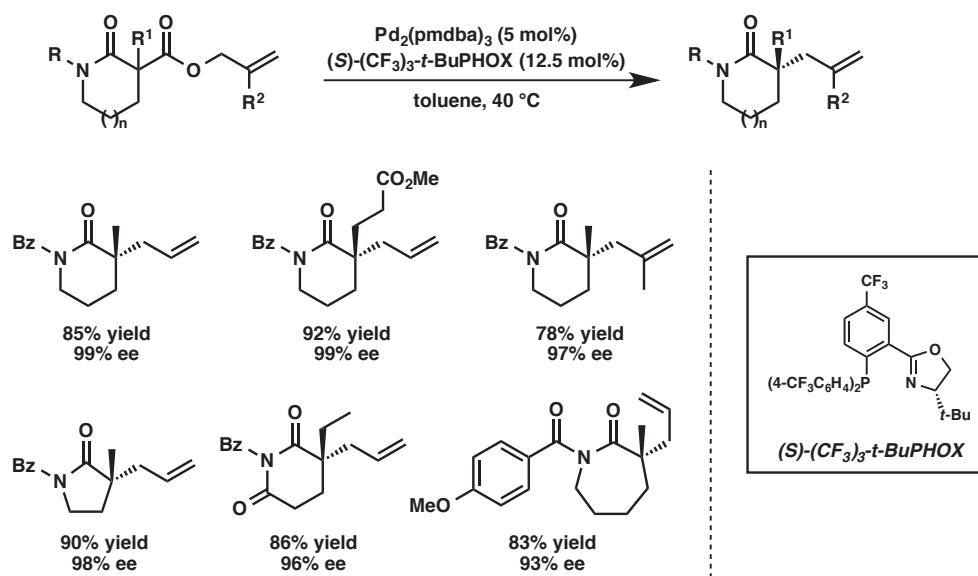


1.4 Our Explorations in the Field of Palladium-Catalyzed Decarboxylative and Decarbonylative Reactions

1.4.1 Palladium-Catalyzed Enantioselective Decarboxylative Allylic Alkylation of Lactams

At the outset of this study, our group had developed a palladium-catalyzed decarboxylative asymmetric allylic alkylation reaction that delivers α -quaternary ketones in high yield and enantioselectivity.³ Considering the ubiquity and medicinal importance of *N*-heterocycles, as well as the lack of direct, catalytic enantioselective methods for the synthesis of α -quaternary lactams, we became interested in extending our allylic alkylation methodology to this important class of substrates. A combinatorial screen of ligand, solvent, and lactam *N*-protecting group allowed us to identify a set of optimal reaction parameters. A wide range of α -quaternary lactams bearing various substituents, functional groups, and scaffolds were synthesized using our decarboxylative allylic alkylation reaction in high yield and exceptionally high enantioselectivity (Scheme 1.11, see Chapter 2 for details).¹⁵

Scheme 1.11 Palladium-catalyzed enantioselective decarboxylative allylic alkylation of lactams

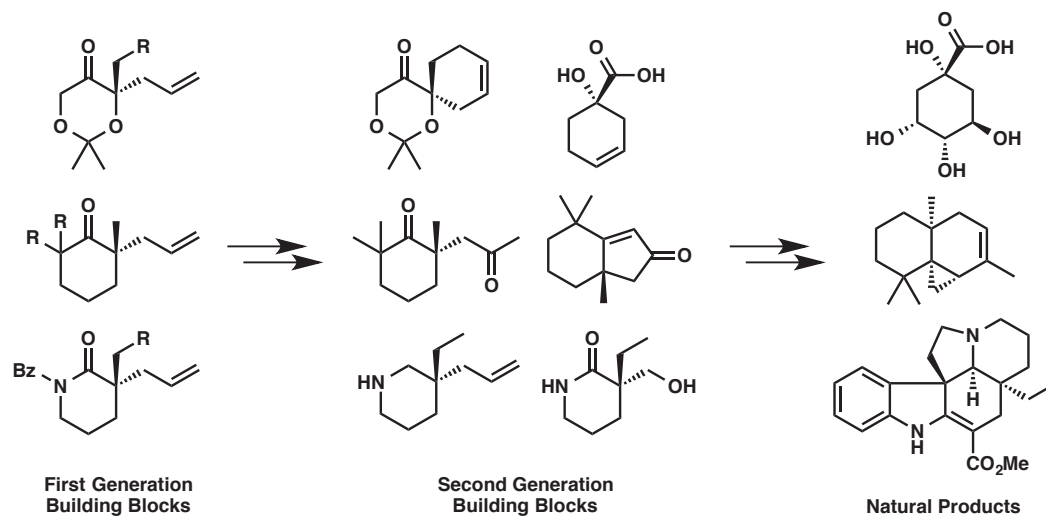


1.4.2 Formal Syntheses of Classical Natural Product Target Molecules via Palladium-Catalyzed Enantioselective Alkylation

Following the development of decarboxylative allylic alkylation chemistry of lactams, we became interested in the potential application of this chemistry in natural product synthesis. From a broader perspective, chiral α -quaternary carbonyl compounds represent an important class of building blocks that can be further elaborated into complex bioactive molecules. A brief literature survey reveals that many such building blocks are used as racemic compounds or require chiral auxiliaries for obtaining enantioenriched compounds en route to the target natural product. We envisioned that our palladium-catalyzed enantioselective alkylation chemistry presented a good opportunity to access these building blocks in enantioenriched form. In addition to the alkylation products (α -quaternary carbonyl compounds), which are the first generation of building blocks, we carried out chemical derivatization to produce a second generation of

building blocks that enable the catalytic asymmetric formal total synthesis of numerous classical natural products (Scheme 1.12, see Chapter 3 for details).¹⁶

Scheme 1.12 Formal synthesis of classical natural products via palladium-catalyzed enantioselective alkylation chemistry

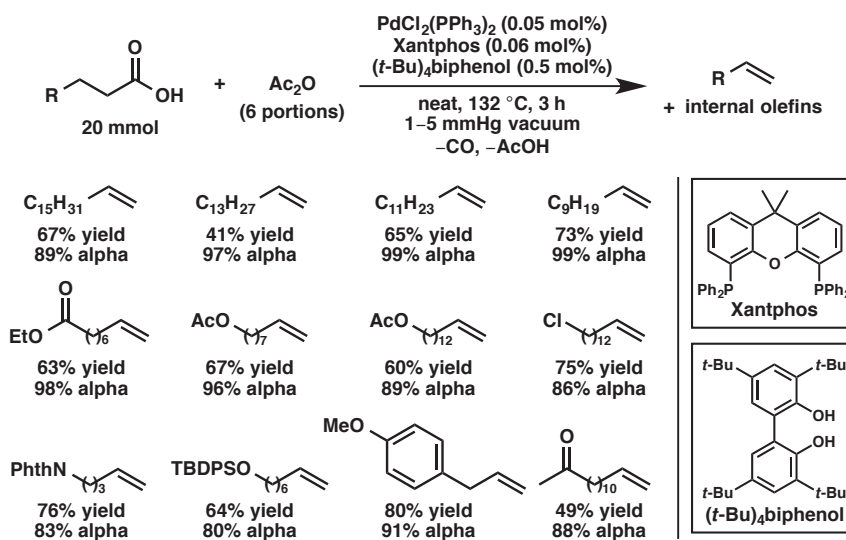


1.4.3 Palladium-Catalyzed Decarbonylative Dehydration of Fatty Acids for the Synthesis of Linear Alpha Olefins

The aforementioned projects focus primarily on fine chemical synthesis, i.e. natural products and pharmaceutical building blocks. As a synthetic organic chemistry group, we are also interested in commodity (bulk) chemical synthesis, especially in the context of green chemistry and sustainability. Linear alpha olefins represent an important class of commodity chemicals with a wide range of industrial applications. Currently, these olefins are mainly produced by oligomerization of ethylene derived from petroleum, a nonrenewable source. We envisioned that alpha olefins could also be obtained via either oxidative decarboxylation or decarbonylative dehydration of long

chain fatty acids, which are abundant, renewable, and inexpensive. However, existing methods for converting fatty acids to alpha olefins require either very high temperature or high loading of precious metal catalysts. To address these issues, we developed a new decarbonylative dehydration process that uses low catalyst loading and proceeds under relatively mild conditions. Alpha olefins of various chain lengths and bearing different functional groups are prepared, and the reaction can be easily scaled up (Scheme 1.13, see Chapter 4 for details).¹⁷

Scheme 1.13 Palladium-catalyzed decarbonylative dehydration of fatty acids for the synthesis of linear alpha olefins

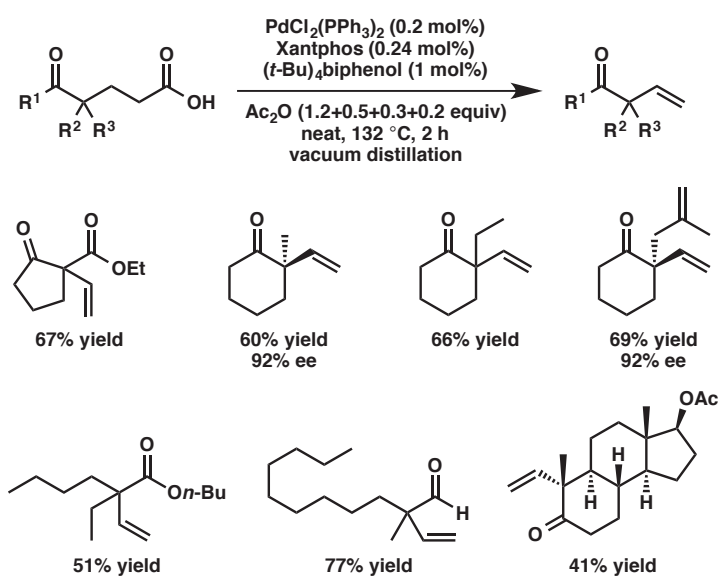


1.4.4 Palladium-Catalyzed Decarbonylative Dehydration for the Synthesis of α -Vinyl Carbonyl Compounds and Total Synthesis of (-)-Aspewentin B

Having established our decarbonylative dehydration process for commodity alpha olefin synthesis, we became interested in the application of this chemistry to the synthesis of fine chemicals containing a terminal olefin moiety. An all-carbon quaternary center

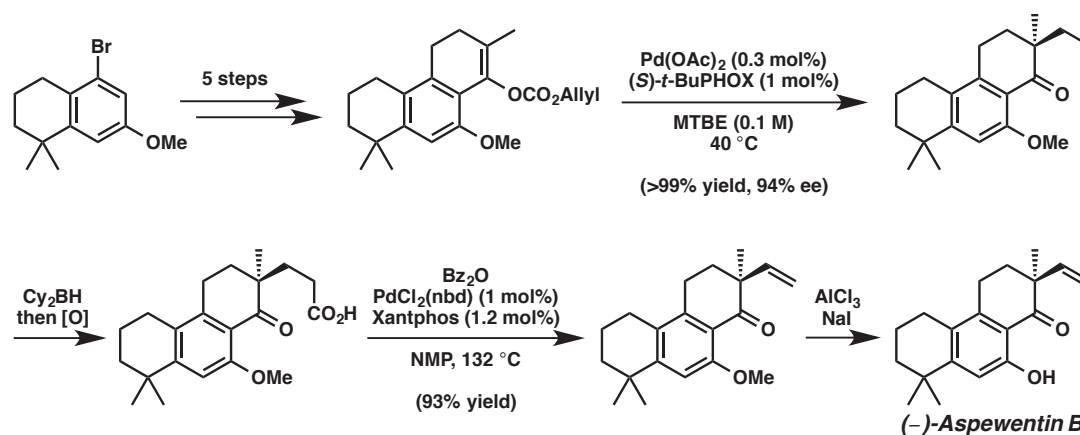
bearing an ethylene substituent is a common structural motif in many natural products. An important approach to the construction of this unit is the α -vinylation of carbonyl compounds. However, direct enolate vinylation is particularly challenging due to the unreactive nature of vinyl electrophiles. Current methods for installing a vinyl group α to a carbonyl often rely on an indirect alkylation-elimination strategy and are generally limited in substrate scope. Asymmetric vinylation reactions are rare and severely limited in scope. At the outset of our investigation, even the simple 2-methyl-2-vinylcyclohexanone was not known as a single enantiomer in the literature. We hypothesized that our decarbonylative dehydration chemistry would be a good method for obtaining enantioenriched α -vinyl carbonyl compounds since the quaternary stereocenter in the substrate carboxylic acid can be constructed in an asymmetric fashion using well-established chemistry. To test this hypothesis, we prepared a variety of γ -quaternary- δ -oxocarboxylic acids, subjected them to slightly modified decarbonylative dehydration conditions, and were pleased to obtain the corresponding α -vinyl carbonyl compounds in good yields (Scheme 1.14, see Chapter 5 for details).

Scheme 1.14 Palladium-catalyzed decarbonylative dehydration for the synthesis of α -vinyl carbonyl compounds



To further demonstrate the utility of this chemistry, we embarked on the total synthesis of (–)-aspewentin B. The quaternary carbon was built by palladium-catalyzed enantioselective allylic alkylation chemistry, and the vinyl substituent was revealed by palladium-catalyzed decarbonylative dehydration (Scheme 1.15, see Chapter 5 for details). This total synthesis represents a perfect union of the allylic alkylation and decarbonylative dehydration chemistries developed in our group.

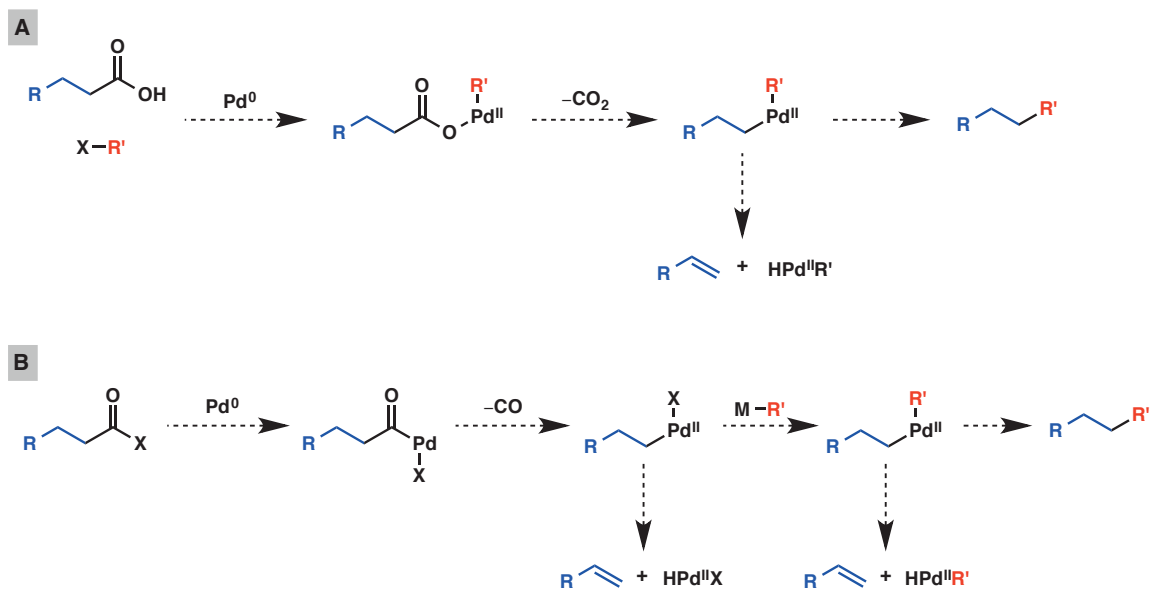
Scheme 1.15 Total synthesis of (–)-aspewentin B: union of palladium-catalyzed allylic alkylation and decarbonylative dehydration reactions



1.5 Future Directions

While we have made remarkable progress in palladium-catalyzed decarboxylative and decarbonylative transformations, there are several enduring challenges that have yet to be addressed. For example, palladium-catalyzed decarboxylative reactions have so far focused on carboxylic acids bearing sp^2 -, sp -, or activated sp^3 -hybridized substituents. Decarboxylative reactions of unactivated sp^3 -hybridized (aliphatic) carboxylic acids via palladium catalysis remains elusive (Scheme 1.16A). This reaction could potentially allow us to use fatty acids as alkyl Grignard equivalents in cross-coupling reactions. The challenge is twofold: first, decarboxylation of alkyl carboxylic acids has a high energy barrier; and second, the resulting alkylpalladium(II) species are prone to β -hydride elimination. The second issue is also present in palladium-catalyzed decarbonylation reactions, in which β -hydride elimination is currently the only pathway for the alkylpalladium(II) species. If this reaction pathway could be inhibited, we may be able to explore other chemistry such as cross coupling with a nucleophile (Scheme 1.16B).

Scheme 1.16 Challenges and opportunities in palladium-catalyzed decarboxylative and decarbonylative reactions



1.6 Concluding Remarks

Palladium-catalyzed decarboxylative and decarbonylative transformations are of great utility in organic synthesis. Research in the past three decades has led to a variety of synthetic methods. We contributed to this field through the development of a palladium-catalyzed enantioselective decarboxylative allylic alkylation reaction of lactams and a palladium-catalyzed decarbonylative dehydration reaction of carboxylic acids. These reactions address challenges in both commodity and fine chemical synthesis, and should find application in the context of both academic and industrial research.

1.7 Notes and References

-
- (1) Tsuda, T.; Chujo, Y.; Nishi, S.-i.; Tawara, K.; Saegusa, T. *J. Am. Chem. Soc.* **1980**, *102*, 6381–6384.
 - (2) Shimizu, I.; Yamada, T.; Tsuji, J. *Tetrahedron Lett.* **1980**, *21*, 3199–3202.
 - (3) Mohr, J. T.; Behenna, D. C.; Harned, A. M.; Stoltz, B. M. *Angew. Chem., Int. Ed.* **2005**, *44*, 6924–6927.
 - (4) Shang, R.; Fu, Y.; Li, J.-B.; Zhang, S.-L.; Guo, Q.-X.; Liu, L. *J. Am. Chem. Soc.* **2009**, *131*, 5738–5739.
 - (5) Yeung, P. Y.; Chung, K. H.; Kwong, F. Y. *Org. Lett.* **2011**, *13*, 2912–2915.
 - (6) Myers, A. G.; Tanaka, D.; Mannion, M. R. *J. Am. Chem. Soc.* **2002**, *124*, 11250–11251.
 - (7) For a review, see: Rodríguez, N.; Gooßen, L. J. *Chem. Soc. Rev.* **2011**, *40*, 5030–5048.
 - (8) (a) Voutchkova, A.; Coplin, A.; Leadbeater, N. E.; Crabtree, R. H. *Chem. Commun.* **2008**, 6312–6314. (b) Haley, C. K.; Gilmore, C. D.; Stoltz, B. M. *Tetrahedron* **2013**, *69*, 5732–5736.
 - (9) (a) Gooßen, L. J.; Deng, G.; Levy, L. M. *Science* **2006**, *313*, 662–664. (b) Gooßen, L. J.; Lange, P. P.; Rodríguez, N.; Linder, C. *Chem. Eur. J.* **2010**, *15*, 3906–3909.
 - (10) Wang, Z.; Ding, Q.; He, X.; Wu, J. *Org. Biomol. Chem.* **2009**, *7*, 863–865.
 - (11) (a) Rayabarapu, D. K.; Tunge, J. A. *J. Am. Chem. Soc.* **2005**, *127*, 13510–13511. (b) Zhang, W.-W.; Zhang, X.-G.; Li, J.-H. *J. Org. Chem.* **2010**, *75*, 5259–5264.
 - (12) (a) Blaser, H.-U.; Spencer, A. *J. Organomet. Chem.* **1982**, *233*, 267–274. (b) Obora, Y.; Tsuji, Y.; Kawamura, T. *J. Am. Chem. Soc.* **1993**, *115*, 10414–10415.

-
- (c) Andrus, M. B.; Liu, J.; Meredith, E. L.; Nartey, E. *Tetrahedron Lett.* **2003**, *44*, 4819–4822.
- (13) Stephan, M. S.; Teunissen, A. J. J. M.; Verzijl, G. J. M.; de Vries, J. G. *Angew. Chem., Int. Ed.* **1998**, *37*, 662–664.
- (14) (a) Gooßen, L. J.; Paetzold, J. *Angew. Chem., Int. Ed.* **2002**, *41*, 1237–1241. (b) Gooßen, L. J.; Paetzold, J. *Angew. Chem., Int. Ed.* **2004**, *43*, 1095–1098.
- (15) Behenna, D. C.; Liu, Y.; Yurino, T.; Kim, J.; White, D. E.; Virgil, S. C.; Stoltz, B. M. *Nature Chem.* **2012**, *4*, 130–133.
- (16) Liu, Y.; Liniger, M.; McFadden, R. M.; Roizen, J. L.; Malette, J.; Reeves, C. M.; Behenna, D. C.; Seto, M.; Kim, J.; Mohr, J. T.; Virgil, S. C.; Stoltz, B. M. *Beilstein J. Org. Chem.* **2014**, *10*, 2501–2512.
- (17) Liu, Y.; Kim, K. E.; Herbert, M. B.; Fedorov, A.; Grubbs, R. H.; Stoltz, B. M. *Adv. Synth. Catal.* **2014**, *356*, 130–136.

CHAPTER 2

Palladium-Catalyzed Enantioselective Decarboxylative Allylic Alkylation of Lactam Enolates for the Construction of Quaternary N-Heterocycles[†]

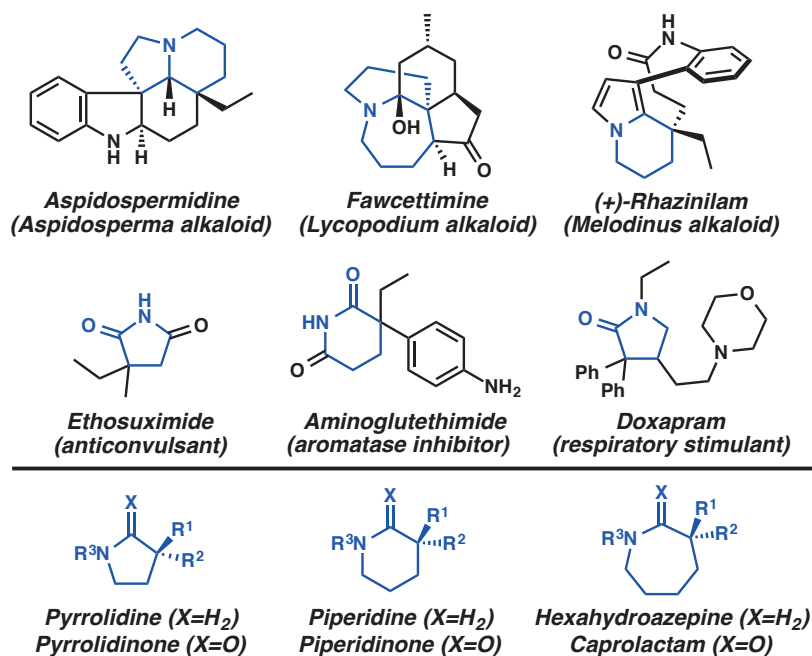
2.1 Introduction

Nitrogen-containing heterocycles are ubiquitous in natural products,¹ pharmaceuticals,² and materials science.^{3,4,5} Stereoselective methods for the synthesis of 3,3-disubstituted pyrrolidinones, piperidinones, and caprolactams, in addition to the corresponding amines, are valuable for the preparation of a wide array of important structures in these areas of research (Figure 2.1). Despite the prevalence of such architectures and the potential of lactam enolate alkylation as a direct method for their

[†] This work was performed in collaboration with Dr. Doug Behenna, Taiga Yurino, Dr. Jimin Kim, and Guillermo A. Guerrero-Vásquez, and was partially adapted from the publication: Behenna, D. C.; Liu, Y.; Yurino, T.; Kim, J.; White, D. E.; Virgil, S. C.; Stoltz, B. M. *Nature Chem.* **2012**, *4*, 130–133. Copyright 2011 Macmillan Publishers Limited.

synthesis, a paucity of enantioselective lactam alkylations leading to C(α)-quaternary centers are known. While most methods rely on chiral auxiliary chemistry,^{6,7,8} the few catalytic examples that exist are specific to the oxindole lactam nucleus^{9,10,11} or cyclic imides.¹² Importantly, enolate stabilization is critical for success in both of these catalytic systems, thereby limiting the scope of each transformation. To the best of our knowledge, there are no examples of catalytic asymmetric alkylations of simple piperidinone, pyrrolidinone, and caprolactam scaffolds for the formation of C(α)-quaternary or C(α)-tetrasubstituted tertiary centers. Herein, we describe the stereoselective synthesis of a wide range of structurally-diverse, functionalized lactams by palladium-catalyzed enantioselective enolate alkylation. The importance of this chemistry to the synthesis of bioactive alkaloids is specifically demonstrated, and the potential utility of this transformation for the construction of novel building blocks for medicinal and polymer chemistry can be readily inferred.

Figure 2.1 Natural products and pharmaceuticals containing chiral N-heterocycles



2.2 Reaction Development and Optimization

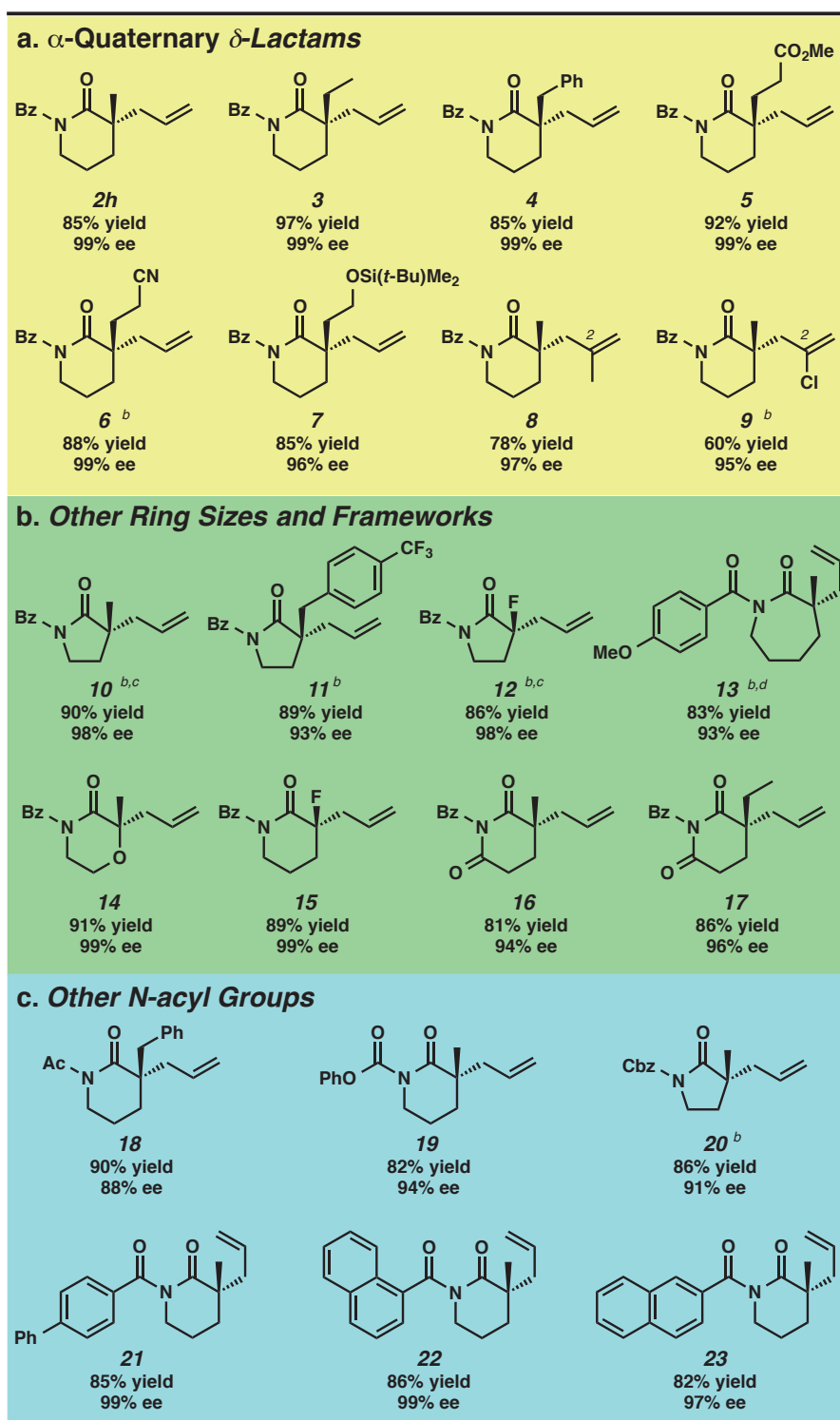
Transition metal-catalyzed allylic alkylation is a key method for the enantioselective preparation of chiral substances and ranks among the best general techniques for the catalytic alkylation of prochiral enolates.^{13,14,15,16} We sought to develop a general method for catalytic asymmetric α -alkylation, given the importance of α -quaternary lactams (vide supra). Over the past seven years, our laboratory has reported an array of methods for the synthesis of α -quaternary ketones^{17,18,19,20} and demonstrated the use of these methods in a number of complex molecule syntheses.^{21,22,23,24} In the course of our investigations of the ketone enolate allylic alkylation and other alkylation processes, we have often encountered interesting ligand electronic effects and, in certain cases, pronounced solvent effects.²⁵ In keeping with our ultimate goal of *N*-heterocycle alkylation, we set out to further probe these subtle effects by examining enolate reactivity in a lactam series that would be amenable to both steric and electronic fine-tuning.

We prepared a collection of racemic lactam substrates (i.e., **1a–h**) for palladium-catalyzed decarboxylative allylic alkylation and performed a reactivity and enantioselectivity screen across an array of solvents employing two chiral ligands, (*S*)-*t*-BuPHOX (**L1**) and (*S*)-(CF₃)₃-*t*-BuPHOX (**L2**).^{26,27,28} Preliminary data suggested that electron rich *N*-alkyl lactam derivatives were poor substrates for decarboxylative alkylation due to low reactivity. Thus, electron withdrawing *N*-protecting groups were chosen in our study. We screened these substrates across a series of four solvents (THF, MTBE, toluene, and 2:1 hexane–toluene) while employing two electronically distinct ligands on Pd. The results of this broad screen were highly encouraging (Table 2.1, see also Experimental Section). Reactivity across all substrates with either ligand was

uniformly good, as all of the compounds were completely converted to the desired product. Strikingly, as the *N*-substituent group was changed from sulfonyl to carbamoyl to acyl functionalities, the enantioselectivity rose from nearly zero to nearly perfect. There was also a substantial difference between the two ligands, and electron poor (*S*)-(CF₃)₃-*t*-BuPHOX was clearly the superior choice. As the solvent system became less polar, a distinct increase in enantiomeric excess was observed, however, this effect was substantially less pronounced for reactions employing the electron poor ligand and for reactions varying the *N*-substituent. Ultimately, with the *N*-benzoyl group (Bz) on the substrate (i.e., **1h**) and (*S*)-(CF₃)₃-*t*-BuPHOX as ligand, the reaction produced lactam **2h** in >96% ee in each of the four solvents.

CH₂CH₂CN) leads to high yields of lactams **3–6** in uniformly excellent enantioenrichment (99% ee). Common silyl protecting groups are tolerated in the transformation and lactam **7** is furnished in 85% yield and 96% ee. Substituted allyl groups can be incorporated, however only at C(2), leading to products such as methallyl lactam **8** and chloroallyl lactam **9** in good yield and outstanding enantioselectivity ($\geq 95\%$ ee).

Beyond piperidinones, we have demonstrated that pyrrolidinones and caprolactams are also exceptional substrate classes, leading to heterocycles **10–13** in excellent yield and ee (Table 2.2b). Additionally, morpholine-derived product **14**, which contains a C(α)-tetrasubstituted tertiary center, is produced in 91% yield and 99% ee. C(α)-Fluoro substitution is readily introduced into the 1,3-dicarbonyl starting material and is viable in the enantioselective reaction leading to fluoropyrrolidinone **12** (86% yield, 98% ee) and fluoropiperidinone **15** (89% yield, 99% ee). Moreover, *N*-Bz glutarimides serve as outstanding substrates, smoothly reacting to provide cyclic imides **16** and **17** in high yield and enantioselectivity. Finally, alteration of the *N*-Bz group is possible (Table 2.2c), leading to lactams with an *N*-acetyl group (**18**), *N*-carbamates (**19** and **20**), and a variety of *N*-aroyl derivatives (**21–23**).

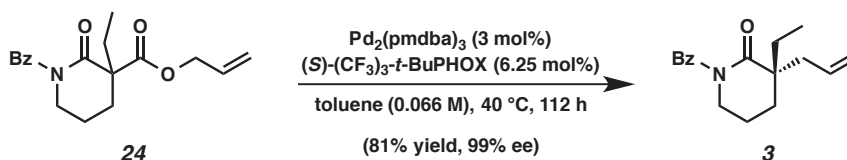
Table 2.2 Palladium-catalyzed decarboxylative alkylation of lactams: reaction scope^a

^a Conditions: Reactions were performed with lactam substrate (0.50 mmol), Pd₂(pmdba)₃ (5 mol%), and (*S*)-(CF₃)₃-*t*-BuPHOX (12.5 mol%) in toluene (15 mL) at 40 °C for 11–172 h. In all cases, complete consumption of starting material and product formation was observed by thin layer chromatography on silica gel. Isolated yields are reported. Enantiomeric excess (ee) was determined by chiral GC, SFC, or HPLC. See Supplementary Information for details. ^b Pd₂(dba)₃ was employed. ^c Reaction performed at 50 °C. ^d Reaction performed in MTBE as solvent.

2.4 Large-Scale Alkylation Reaction

To test the scalability of our palladium-catalyzed enantioselective alkylation reaction, we conducted gram-scale experiments (Scheme 2.1). Using 4.73 g (15 mmol) of starting material **24**, the reaction proceeded smoothly to afford the desired quaternary lactam **3** in 81% isolated yield (3.87 g) and 99% ee. This result establishes the practical utility of our chemistry in organic synthesis.

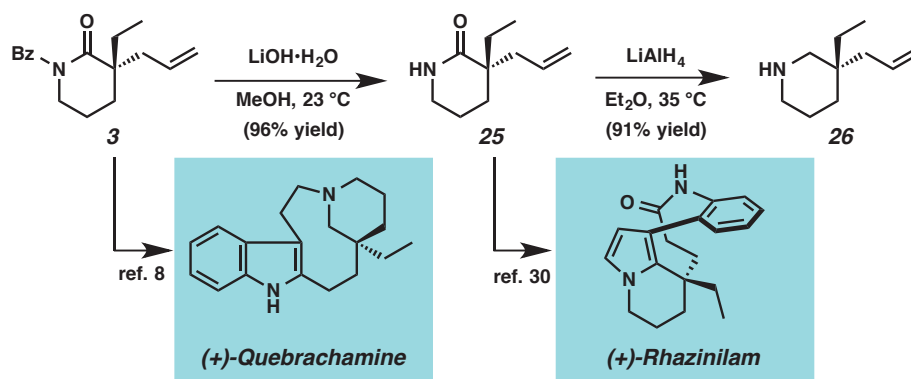
Scheme 2.1 Gram-scale alkylation reactions



2.5 Derivatization of Alkylated Lactam Products

The enantioenriched lactam products formed by our catalytic asymmetric alkylation chemistry are envisioned to be of broad utility in synthetic chemistry. To illustrate this point, lactam **3** can be transformed into the *Aspidosperma* alkaloid (+)-quebrachamine by modification of a previous route that employed a chiral auxiliary.⁸ Additionally, cleavage of the *N*-Bz group of lactam **3** produces chiral lactam **25**, a compound previously used as a racemate in the synthesis of rhazinilam, a microtubule-disrupting agent that displays similar cellular characteristics to paclitaxel (Scheme 2.2).^{29,30} Finally, reduction of lactam **25** produces the C(3)-quaternary piperidine (**26**) and demonstrates access to the corresponding amine building blocks.

Scheme 2.2 Synthetic utility of lactam products



2.6 Concluding Remarks

In summary, we have reported the first method for catalytic enantioselective alkylation of monocyclic 5-, 6-, and 7-membered lactam enolate derivatives to form α -quaternary and α -tetrasubstituted tertiary lactams. The reaction discovery process was enabled by parallel screening of reaction parameters and led to the identification of a sterically and electronically tuned system for highly enantioselective alkylation. We have applied this method to the catalytic asymmetric synthesis of key intermediates previously employed for the construction of *Aspidosperma* alkaloids. Finally, the asymmetric products formed in this investigation are envisioned to be widely useful as building blocks for the preparation of range of nitrogen containing heterocycles in materials science, medicinal chemistry and natural products synthesis.

2.7 Experimental Section

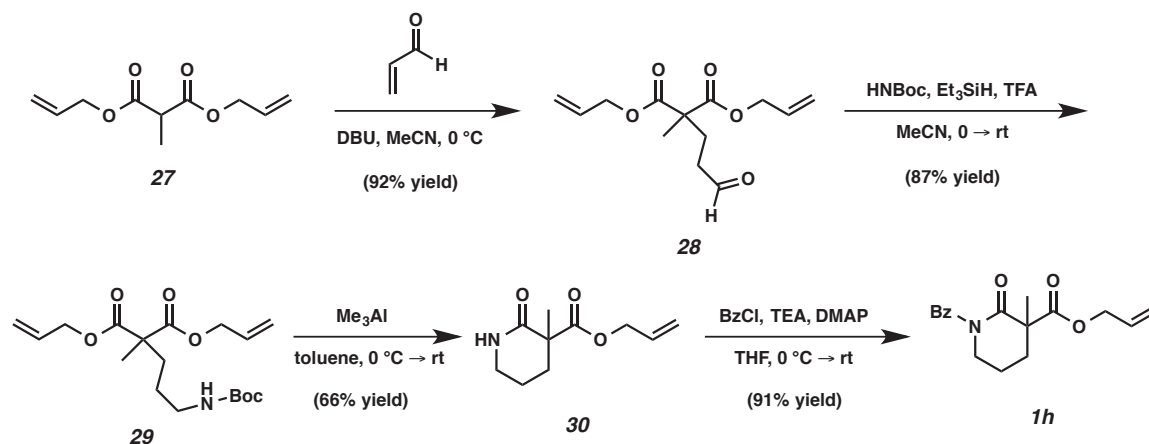
2.7.1 Materials and Methods

Unless otherwise stated, reactions were performed in flame-dried glassware under an argon or nitrogen atmosphere using dry, deoxygenated solvents. Solvents were dried

by passage through an activated alumina column under argon. Brine solutions are saturated aqueous sodium chloride solutions. Tris(dibenzylideneacetone)dipalladium(0) ($\text{Pd}_2(\text{dba})_3$) was purchased from Strem and stored in a glove box. Lithium bis(trimethylsilyl)amide was purchased from Aldrich and stored in a glove box. Tris[bis(*p*-methoxybenzylidene)-acetone]dipalladium(0) ($\text{Pd}_2(\text{pmdba})_3$) was prepared by known methods and stored in a glovebox.¹ (*S*)-*t*-BuPHOX, (*S*)-(CF₃)₃-*t*-BuPHOX, and allyl cyanofornate were prepared by known methods.^{2,3,4} Selectfluor, methyl iodide, and ethyl iodide were purchased from Aldrich, Acros Organics, Strem, or Alfa Aesar and used as received unless otherwise stated. Sodium hydride (NaH) was purchased as a 60% dispersion in mineral oil from Acros and used as such unless otherwise stated. Triethylamine was distilled from CaH₂ prior to use. Acrolein, acrylonitrile, methyl acrylate, and benzoyl chloride were distilled prior to use. Reaction temperatures were controlled by an IKAmag temperature modulator. Thin-layer chromatography (TLC) was performed using E. Merck silica gel 60 F254 pre-coated plates (0.25 mm) and visualized by UV fluorescence quenching, anisaldehyde, KMnO₄, or CAM staining. ICN Silica gel (particle size 0.032-0.063 mm) was used for flash chromatography. Analytical chiral HPLC was performed with an Agilent 1100 Series HPLC utilizing a Chiralpak (AD-H or AS) or Chiralcel (OD-H, OJ-H, or OB-H) columns (4.6 mm x 25 cm) obtained from Daicel Chemical Industries, Ltd. with visualization at 220 or 254 nm. Analytical chiral SFC was performed with a JACSO 2000 series instrument utilizing Chiralpak (AD-H or AS-H) or Chiralcel (OD-H, OJ-H, or OB-H) columns (4.6 mm x 25 cm), or a Chiralpak IC column (4.6 mm x 10 cm) obtained from Daicel Chemical Industries, Ltd with visualization at 210 or 254 nm. Optical rotations were measured with a Jasco P-

2000 polarimeter at 589 nm. ^1H and ^{13}C NMR spectra were recorded on a Varian Inova 500 (at 500 MHz and 126 MHz, respectively) or a Mercury 300 (at 300 MHz and 75 MHz, respectively), and are reported relative to residual protio solvent ($\text{CDCl}_3 = 7.26$ and 77.0 ppm and $\text{C}_6\text{D}_6 = 7.16$ and 128.0 ppm, respectively). Data for ^1H NMR spectra are reported as follows: chemical shift (d ppm) (multiplicity, coupling constant (Hz), integration). IR spectra were recorded on a Perkin Elmer Paragon 1000 spectrometer and are reported in frequency of absorption (cm^{-1}). High resolution mass spectra were obtained using an Agilent 6200 Series TOF with an Agilent G1978A Multimode source in electrospray ionization (ESI), atmospheric pressure chemical ionization (APCI) or mixed (MM) ionization mode or from the Caltech Mass Spectral Facility.

2.7.2 Representative Procedures for the Preparation of Lactam Substrates



Aldehyde 28: To a cooled (0 °C) solution of diallyl 2-methylmalonate (**27**)³¹ (17.0 g, 84.7 mmol, 1.00 equiv) and acrolein (6.23 mL, 93.2 mmol, 1.10 equiv) in MeCN (282 mL) was added DBU (253 mL, 1.70 mmol, 0.02 equiv). After 15 min, the reaction mixture was diluted with saturated aqueous NH_4Cl (200 mL) and EtOAc (100 mL) and the phases were separated. The aqueous phase was extracted with EtOAc (3 x 200 mL)

and the combined organic phases were dried (Na_2SO_4), filtered, and concentrated under reduced pressure. The resulting oil was purified by flash chromatography (8 x 16 cm SiO_2 , 10 to 20% EtOAc in hexanes) to afford aldehyde **28** as a colorless oil (19.7 g, 92% yield). $R_f = 0.32$ (20% EtOAc in hexanes); ^1H NMR (300 MHz, CDCl_3) δ 9.71 (t, $J = 1.2$ Hz, 1H), 5.83 (ddt, $J = 17.2, 10.5, 5.7$ Hz, 2H), 5.26 (dq, $J = 17.2, 1.5$ Hz, 2H), 5.19 (dq, $J = 10.4, 1.3$ Hz, 2H), 4.57 (dt, $J = 5.6, 1.4$ Hz, 4H), 2.55–2.45 (m, 2H), 2.20–2.10 (m, 2H), 1.41 (s, 3H); ^{13}C NMR (75 MHz, CDCl_3) δ 200.6, 171.2, 131.3, 118.5, 65.9, 52.8, 39.2, 27.7, 20.3; IR (Neat Film NaCl) 2988, 2945, 1732, 1230, 1186, 1116, 984, 935 cm^{-1} ; HRMS (MM: ESI-APCI) m/z calc'd for $\text{C}_{13}\text{H}_{19}\text{O}_5$ $[\text{M}+\text{H}]^+$: 255.1227, found 255.1223.

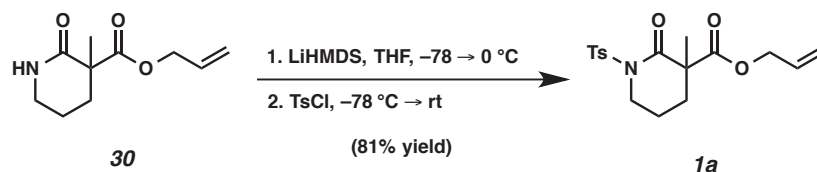
Carbamate 29: To a cooled (0 °C) solution of aldehyde **28** (19.7 g, 77.5 mmol, 1.00 equiv), BocNH_2 ³² (22.7 g, 194 mmol, 2.50 equiv), and Et_3SiH (31.0 mL, 194 mmol, 2.50 equiv) in MeCN (310 mL) was added trifluoroacetic acid (12.1 mL, 163 mmol, 2.10 equiv) dropwise over 5 min. The reaction mixture was stirred at 0° C for 2 h and at ambient temperature for an additional 18 h, at which point the reaction mixture was cooled (0 °C), treated with saturated aqueous NaHCO_3 (150 mL), stirred for 40 min, and concentrated under reduced pressure to remove MeCN (~250 mL). The remaining material was diluted with Et_2O (200 mL) and the phases were separated. The aqueous phase was extracted with Et_2O (4 x 100 mL) and EtOAc (1 x 150 mL), and the combined organic phases were washed with brine (2 x 150 mL), dried over Na_2SO_4 , filtered, and concentrated under reduced pressure. The resulting oil was purified by flash chromatography (8 x 25 cm SiO_2 , 5 to 15% EtOAc in hexanes) to afford carbamate **29** as a colorless oil (23.0 g, 87% yield). $R_f = 0.32$ (20% EtOAc in hexanes); ^1H NMR (300

MHz, CDCl₃) δ 5.88 (ddt, $J = 17.3, 10.4, 5.7$ Hz, 2H), 5.30 (dq, $J = 17.2, 1.6, 1.5$ Hz, 2H), 5.23 (dq, $J = 10.4, 1.3, 1.3$ Hz, 2H), 4.61 (dt, $J = 5.6, 1.4$ Hz, 4H), 4.55 (br s, 1H), 3.12 (q, $J = 6.7$ Hz, 2H), 2.00–1.75 (m, 2H), 1.44 (m, 14H); ¹³C NMR (75 MHz, CDCl₃) δ 171.6, 155.8, 131.5, 118.4, 79.0, 65.7, 53.4, 40.4, 32.7, 28.3, 24.9, 19.9; IR (Neat Film NaCl) 3403, 2977, 2939, 1734, 1517, 1366, 1250, 1173, 985, 934 cm⁻¹; HRMS (MM: ESI-APCI) m/z calc'd for C₁₈H₂₉NO₆Na [M+Na]⁺: 378.1887, found 378.1892.

Lactam 30: To a cooled (0 °C) solution of carbamate **29** (10.4 g, 30.6 mmol, 1.00 equiv) in toluene (306 mL) was added trimethylaluminum (11.7 mL, 61.1 mmol, 2.00 equiv) dropwise over 10 min. After 5 h the reaction was allowed to warm to ambient temperature and stirred for an additional 17 h. The reaction was cooled (0 °C), treated with brine (100 mL, *CAUTION: Gas evolution and exotherm*) in a dropwise manner over 30 min, and stirred until gas evolution ceased. The reaction mixture was then treated with saturated aqueous sodium potassium tartrate (200 mL) and stirred for 4 h. The phases were separated and the aqueous phase was extracted with EtOAc (5 x 150 mL). The combined organic phases were dried over Na₂SO₄, filtered, and concentrated under reduced pressure. The resulting oil was purified by flash chromatography (5 x 16 cm SiO₂, 45 to 65% EtOAc in hexanes) to afford lactam **30** as a colorless oil (3.99 g, 66% yield). $R_f = 0.41$ (100% EtOAc); ¹H NMR (300 MHz, CDCl₃) δ 6.85 (s, 1H), 6.00–5.75 (m, 1H), 5.30 (d, $J = 17.1$ Hz, 1H), 5.20 (d, $J = 10.4$ Hz, 1H), 4.70–4.50 (m, 2H), 3.40–3.20 (m, 2H), 2.30–2.15 (m, 1H), 1.94–1.59 (m, 3H), 1.48 (s, 3H); ¹³C NMR (75 MHz, CDCl₃) δ 173.1, 172.0, 131.7, 118.1, 65.7, 50.1, 42.3, 33.0, 22.4, 19.3; IR (Neat Film

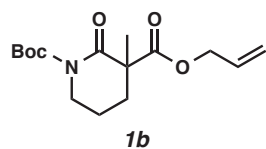
NaCl) 3207, 3083, 2942, 2873, 1737, 1668, 1254, 1194, 1132 cm^{-1} ; HRMS (MM: ESI-APCI) m/z calc'd for $\text{C}_{10}\text{H}_{16}\text{NO}_3$ $[\text{M}+\text{H}]^+$: 198.1125, found 198.1117.

Benzoyl Lactam 1h: To a cooled (0 °C) solution of lactam **30** (394 mg, 2.00 mmol, 1.00 equiv), triethylamine (840 mL, 6.00 mmol, 3.00 equiv), and DMAP (25.0 mg, 205 μmol , 0.102 equiv) in THF (8.00 mL) was added benzoyl chloride (470 mL, 4.00 mmol, 2.00 equiv) dropwise over 5 min. The reaction mixture was allowed to warm to ambient temperature and stirred for 14 h. The reaction mixture was then diluted with brine (10 mL) and EtOAc (10 mL), and the phases were separated. The aqueous phase was extracted with EtOAc (3 x 15 mL), and the combined organic phases were washed with brine (2 x 30 mL), dried over Na_2SO_4 , filtered, and concentrated under reduced pressure. The resulting oil was purified by flash chromatography (3 x 25 cm SiO_2 , 15 to 25% Et₂O in hexanes) to afford benzoyl lactam **1h** as an amorphous solid (550 mg, 91% yield). R_f = 0.38 (25% EtOAc in hexanes); ^1H NMR (500 MHz, CDCl_3) δ 7.78–7.63 (m, 2H), 7.52–7.42 (m, 1H), 7.42–7.32 (m, 2H), 5.98 (ddt, J = 17.2, 10.4, 5.9 Hz, 1H), 5.40 (dq, J = 17.2, 1.4 Hz, 1H), 5.33 (dq, J = 10.4, 1.2 Hz, 1H), 4.72 (dt, J = 6.0, 1.3 Hz, 2H), 3.93–3.82 (m, 1H), 3.83–3.73 (m, 1H), 2.56–2.43 (m, 1H), 2.13–1.90 (m, 2H), 1.87–1.76 (m, 1H), 1.49 (s, 3H); ^{13}C NMR (126 MHz, CDCl_3) δ 174.9, 172.8, 172.4, 135.9, 131.6, 131.4, 128.0, 127.9, 119.5, 66.5, 52.9, 46.8, 33.8, 22.5, 20.2; IR (Neat Film NaCl) 3063, 2941, 2873, 1735, 1681, 1449, 1276, 1040, 942, 724 cm^{-1} ; HRMS (MM: ESI-APCI) m/z calc'd for $\text{C}_{17}\text{H}_{20}\text{NO}_4$ $[\text{M}+\text{H}]^+$: 302.1387, found 302.1388.

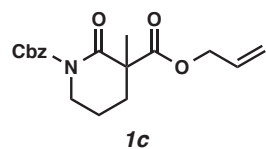


Tosyl Lactam 1a: To a cooled ($-78\text{ }^\circ\text{C}$) solution of LiHMDS (385 mg, 2.30 mmol, 1.15 equiv) in THF (8.0 mL) was added lactam **30** (394 mg, 2.00 mmol, 1.00 equiv). The reaction mixture warmed to $0\text{ }^\circ\text{C}$ and stirred for 30 min, then cooled to $-78\text{ }^\circ\text{C}$ and treated with TsCl (572 mg, 3.00 mmol, 1.50 equiv). After 5 min, the reaction mixture was allowed to warm to ambient temperature for 30 min and treated with saturated aqueous NH_4Cl (10 mL). The phases were separated, and the aqueous phase was extracted with EtOAc (3 x 20 mL). The combined organic phases were washed with saturated aqueous NaHCO_3 (20 mL) and brine (20 mL), dried over Na_2SO_4 , filtered, and concentrated under reduced pressure. The resulting oil was purified by flash chromatography (3 x 30 cm SiO_2 , 4:1:1 hexanes-EtOAc-DCM) to afford tosyl lactam **1a** as a colorless oil (571 mg, 81% yield). $R_f = 0.58$ (33% EtOAc in hexanes); $^1\text{H NMR}$ (500 MHz, CDCl_3) δ 7.93–7.83 (m, 2H), 7.35–7.27 (m, 2H), 5.68 (ddt, $J = 17.2, 10.5, 5.6$ Hz, 1H), 5.17 (dq, $J = 9.1, 1.4$ Hz, 1H), 5.14 (q, $J = 1.4$ Hz, 1H), 4.47 (qdt, $J = 13.2, 5.6, 1.4$ Hz, 2H), 3.98 (ddd, $J = 12.8, 6.9, 6.1$ Hz, 1H), 3.90 (ddt, $J = 12.4, 6.0, 0.8$ Hz, 1H), 2.42 (s, 3H), 2.34–2.26 (m, 1H), 1.95 (tt, $J = 6.5, 5.5$ Hz, 2H), 1.71 (ddd, $J = 14.2, 8.1, 6.6$ Hz, 1H), 1.41 (s, 3H); $^{13}\text{C NMR}$ (126 MHz, CDCl_3) δ 171.8, 169.9, 144.6, 135.7, 131.1, 129.2, 128.6, 118.7, 66.1, 52.8, 46.4, 32.4, 22.3, 21.6, 20.4; IR (Neat Film NaCl) 2942, 1740, 1691, 1353, 1284, 1167, 1090 cm^{-1} ; HRMS (MM: ESI-APCI) m/z calc'd for $\text{C}_{17}\text{H}_{21}\text{NO}_5\text{SNa}$ $[\text{M}+\text{Na}]^+$: 374.1033, found 374.1042.

2.7.3 Characterization Data for Lactam Substrates Used in Table 2.1

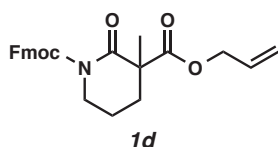


Boc Lactam 1b: Prepared in a manner analogous to tosyl lactam **1a** using lactam **30** (394 mg, 2.00 mmol, 1.00 equiv) and Boc_2O (873 mg, 4.00 mmol, 2.00 equiv). Boc lactam **1b** (407 mg, 68% yield) was isolated as an amorphous solid by flash chromatography (SiO_2 , 9 to 11% Et_2O in hexanes). $R_f = 0.54$ (25% EtOAc in hexanes); ^1H NMR (500 MHz, CDCl_3) δ 5.95–5.81 (m, 1H), 5.33 (dq, $J = 17.2, 1.5$ Hz, 1H), 5.22 (dq, $J = 10.5, 1.5$ Hz, 1H), 4.64 (m, 2H), 3.80–3.70 (m, 1H), 3.63–3.49 (m, 1H), 2.43–2.33 (m, 1H), 1.98–1.77 (m, 2H), 1.75–1.66 (m, 1H), 1.52 (s, 9H), 1.50 (s, 3H); ^{13}C NMR (126 MHz, CDCl_3) δ 172.5, 170.9, 153.1, 131.5, 118.4, 83.0, 65.9, 53.1, 46.0, 32.6, 28.0, 22.9, 20.1; IR (Neat Film NaCl) 2981, 2939, 1772, 1719, 1457, 1393, 1294, 1282, 1254, 1152, 988, 945, 852 cm^{-1} ; HRMS (MM: ESI-APCI) m/z calc'd for $\text{C}_{15}\text{H}_{23}\text{NO}_5\text{Na}$ $[\text{M}+\text{Na}]^+$: 320.1468, found 320.1470.



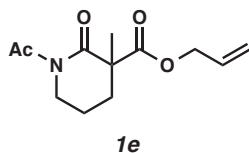
Cbz Lactam 1c: Prepared in a manner analogous to tosyl lactam **1a** using lactam **30** (394 mg, 2.00 mmol, 1.00 equiv) and CbzCl (682 mg, 4.00 mmol, 2.00 equiv). Cbz lactam **1c** (325 mg, 49% yield) was isolated as a colorless oil by flash chromatography (SiO_2 , 14 to 17% Et_2O in hexanes). $R_f = 0.34$ (25% EtOAc in hexanes); ^1H NMR (500 MHz, CDCl_3) δ 7.47–7.40 (m, 2H), 7.39–7.28 (m, 3H), 5.85 (ddt, $J = 17.1, 10.5, 5.6$ Hz,

1H), 5.30 (dq, $J = 10.5, 1.3$ Hz, 1H), 5.29 (s, 2H), 5.19 (dq, $J = 10.5, 1.3$ Hz, 1H), 4.69–4.54 (m, 2H), 3.86–3.79 (m, 1H), 3.71–3.60 (m, 1H), 2.44–2.37 (m, 1H), 1.98–1.78 (m, 2H), 1.73 (ddd, $J = 14.0, 9.1, 5.1$ Hz, 1H), 1.52 (s, 3H); ^{13}C NMR (126 MHz, CDCl_3) δ 172.3, 170.9, 154.4, 135.4, 131.3, 128.5, 128.2, 128.0, 118.7, 68.6, 66.1, 53.3, 46.4, 32.5, 22.8, 20.0; IR (Neat Film NaCl) 2943, 2876, 1776, 1721, 1456, 1378, 1270, 1191, 1167, 1125, 1002, 941, 739, 698 cm^{-1} ; HRMS (MM: ESI-APCI) m/z calc'd for $\text{C}_{18}\text{H}_{21}\text{NO}_5\text{Na}$ $[\text{M}+\text{Na}]^+$: 354.1312, found 354.1310.

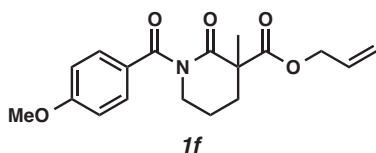


Fmoc Lactam 1d: Prepared in a manner analogous to tosyl lactam **1a** using lactam **30** (394 mg, 2.00 mmol, 1.00 equiv) and FmocCl (621 mg, 2.40 mmol, 1.20 equiv). Fmoc lactam **1d** (352 mg, 42% yield) was isolated as a colorless oil by flash chromatography (SiO_2 , 2 to 12% Et_2O in hexanes). $R_f = 0.28$ (25% EtOAc in hexanes); ^1H NMR (500 MHz, CDCl_3) δ 7.77 (dt, $J = 7.6, 0.9$ Hz, 2H), 7.73 (ddd, $J = 7.5, 5.0, 1.0$ Hz, 2H), 7.43–7.38 (m, 2H), 7.32 (tdd, $J = 7.4, 4.8, 1.2$ Hz, 2H), 5.91 (ddt, $J = 17.2, 10.5, 5.6$ Hz, 1H), 5.36 (dq, $J = 17.2, 1.5$ Hz, 1H), 5.25 (dq, $J = 10.5, 1.3$ Hz, 1H), 4.69 (ddt, $J = 5.6, 2.8, 1.4$ Hz, 2H), 4.56–4.43 (m, 2H), 4.33 (t, $J = 7.5$ Hz, 1H), 3.86–3.79 (m, 1H), 3.73–3.61 (m, 1H), 2.44 (dddd, $J = 13.8, 6.8, 5.0, 0.9$ Hz, 1H), 2.00–1.83 (m, 2H), 1.78 (ddd, $J = 14.0, 9.1, 5.0$ Hz, 1H), 1.59 (s, 3H); ^{13}C NMR (126 MHz, CDCl_3) δ 172.3, 170.9, 154.5, 143.6, 141.2, 131.4, 127.8, 127.1, 125.4, 119.9, 118.7, 69.3, 66.1, 53.4, 46.6, 46.4, 32.6, 22.9, 20.0; IR (Neat Film NaCl) 2948, 2892, 1776, 1721, 1451, 1378, 1269, 1191, 997, 759,

742 cm^{-1} ; HRMS (MM: ESI-APCI) m/z calc'd for $\text{C}_{25}\text{H}_{25}\text{NO}_5\text{Na}$ $[\text{M}+\text{Na}]^+$: 442.1625, found 442.1610.

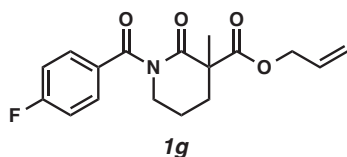


Acetyl Lactam 1e: Prepared in a manner analogous to benzoyl lactam **1h** using lactam **30** (394 mg, 2.00 mmol, 1.00 equiv), acetic anhydride (940 mL, 10.0 mmol, 5.00 equiv), and triethylamine (2.80 mL, 20.0 mmol, 10.0 equiv). Acetyl lactam **1e** (347 mg, 72% yield) was isolated as a colorless oil by flash chromatography (SiO_2 , 12 to 25% Et_2O in hexanes). $R_f = 0.44$ (25% EtOAc in hexanes); ^1H NMR (500 MHz, CDCl_3) δ 5.88 (ddt, $J = 17.1, 10.4, 5.7$ Hz, 1H), 5.31 (dq, $J = 17.2, 1.5$ Hz, 1H), 5.25 (dq, $J = 10.5, 1.2$ Hz, 1H), 4.66–4.60 (m, 2H), 3.78 (ddd, $J = 13.1, 7.6, 5.3$ Hz, 1H), 3.71–3.62 (m, 1H), 2.49 (s, 3H), 2.44–2.37 (m, 1H), 1.93–1.77 (m, 2H), 1.78–1.70 (m, 1H), 1.52 (s, 3H); ^{13}C NMR (126 MHz, CDCl_3) δ 174.0, 173.5, 172.4, 131.3, 119.1, 66.2, 53.2, 44.0, 32.9, 27.0, 22.7, 19.9; IR (Neat Film NaCl) 2985, 2942, 1739, 1699, 1457, 1368, 1301, 1261, 1190, 1132, 1048, 990, 959, 936 cm^{-1} ; HRMS (MM: ESI-APCI) m/z calc'd for $\text{C}_{12}\text{H}_{18}\text{NO}_4$ $[\text{M}+\text{H}]^+$: 240.1230, found 240.1237.



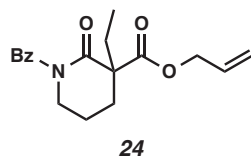
4-Methoxybenzoyl Lactam 1f: Prepared in a manner analogous to benzoyl lactam **1h** using lactam **30** (394 mg, 2.00 mmol, 1.00 equiv), 4-methoxybenzoyl chloride (682 mg,

4.00 mmol, 2.00 equiv), and triethylamine (840 mL, 6.00 mmol, 3.00 equiv). 4-Methoxybenzoyl lactam **1f** (425 mg, 64% yield) was isolated as a colorless oil by flash chromatography (SiO₂, CHCl₃-hexanes-Et₂O 6.5:5:1). $R_f = 0.76$ (50% EtOAc in hexanes); ¹H NMR (500 MHz, CDCl₃) δ 7.81–7.67 (m, 2H), 6.93–6.79 (m, 2H), 6.05–5.88 (m, 1H), 5.39 (dq, $J = 17.2, 1.4$ Hz, 1H), 5.31 (dq, $J = 10.4, 1.2$ Hz, 1H), 4.71 (dt, $J = 6.0, 1.3$ Hz, 2H), 3.90–3.77 (m, 1H), 3.82 (s, 3H), 3.76–3.63 (m, 1H), 2.48 (ddd, $J = 13.7, 5.7, 4.3$ Hz, 1H), 2.06–1.89 (m, 2H), 1.80 (ddd, $J = 13.5, 10.0, 5.0$ Hz, 1H), 1.49 (s, 3H); ¹³C NMR (126 MHz, CDCl₃) δ 174.3, 172.6, 172.6, 162.7, 131.4, 130.7, 127.7, 119.3, 113.3, 66.3, 55.3, 52.8, 46.9, 33.7, 22.5, 20.2; IR (Neat Film NaCl) 3080, 2941, 1732, 1682, 1604, 1512, 1456, 1390, 1257, 1173, 1139, 1029, 939, 844, 770 cm⁻¹; HRMS (MM: ESI-APCI) m/z calc'd for C₁₈H₂₂NO₅ [M+H]⁺: 332.1492, found 332.1501.



4-Fluorobenzoyl Lactam 1g: Prepared in a manner analogous to benzoyl lactam **1h** using lactam **30** (394 mg, 2.00 mmol, 1.00 equiv), 4-fluorobenzoyl chloride (470 mL, 4.00 mmol, 2.00 equiv), and triethylamine (840 mL, 6.00 mmol, 3.00 equiv). 4-Fluorobenzoyl lactam **1g** (557 mg, 87% yield) was isolated as an amorphous white solid by flash chromatography (SiO₂, 15 to 25% Et₂O in hexanes). $R_f = 0.37$ (25% EtOAc in hexanes); ¹H NMR (500 MHz, CDCl₃) δ 7.84–7.72 (m, 2H), 7.12–6.97 (m, 2H), 5.99 (ddt, $J = 17.2, 10.4, 5.9$ Hz, 1H), 5.41 (dq, $J = 17.2, 1.4$ Hz, 1H), 5.35 (dq, $J = 10.4, 1.2$ Hz, 1H), 4.73 (dt, $J = 6.0, 1.3$ Hz, 2H), 3.89–3.82 (m, 1H), 3.81–3.75 (m, 1H), 2.57–2.42 (m, 1H), 2.09–1.91 (m, 2H), 1.89–1.75 (m, 1H), 1.50 (s, 3H); ¹³C NMR (126 MHz,

CDCl₃) δ 173.8, 172.9, 172.5, 164.8 (d, J_{C-F} = 252.5 Hz), 131.8 (d, J_{C-F} = 3.3 Hz), 131.3, 130.7 (d, J_{C-F} = 9.0 Hz), 119.5, 115.2 (d, J_{C-F} = 22.0 Hz), 66.5, 52.9, 47.0, 33.8, 22.4, 20.2; IR (Neat Film NaCl) 3079, 2943, 2874, 1734, 1684, 1602, 1508, 1277, 1240, 1193, 1140, 939, 849, 770 cm⁻¹; HRMS (MM: ESI-APCI) m/z calc'd for C₁₇H₁₉NO₄F [M+H]⁺: 320.1293, found 320.1297.



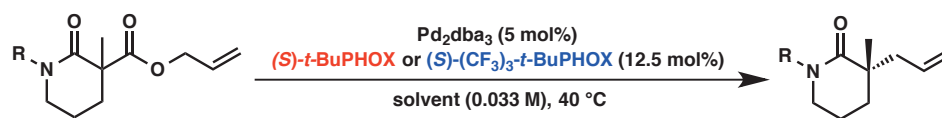
Benzoyl Lactam 24: Prepared in a manner analogous to benzoyl lactam **1h** using diallyl 2-ethylmalonate as a starting material. Benzoyl lactam **24** was isolated by flash chromatography (SiO₂, 15 to 25% Et₂O in hexanes) as a colorless oil. R_f = 0.38 (35% Et₂O in hexanes); ¹H NMR (500 MHz, CDCl₃) δ 7.72–7.67 (m, 2H), 7.51–7.43 (m, 1H), 7.37 (dd, J = 8.3, 7.1 Hz, 2H), 5.99 (ddt, J = 17.3, 10.4, 5.9 Hz, 1H), 5.40 (dq, J = 17.2, 1.4 Hz, 1H), 5.33 (dq, J = 10.4, 1.2 Hz, 1H), 4.73 (dt, J = 6.0, 1.3 Hz, 2H), 3.93–3.63 (m, 2H), 2.43 (ddt, J = 13.7, 4.4, 1.4 Hz, 1H), 2.17–1.65 (m, 5H), 0.91 (t, J = 7.4 Hz, 3H); ¹³C NMR (126 MHz, CDCl₃) δ 175.0, 172.0, 171.8, 135.9, 131.6, 131.4, 128.0, 128.0, 119.5, 66.4, 56.9, 46.4, 29.8, 28.6, 20.3, 9.0; IR (Neat Film NaCl) 3062, 2943, 2882, 1732, 1678, 1449, 1385, 1268, 1188, 1137, 980, 937, 723, 693, 660 cm⁻¹; HRMS (MM: ESI-APCI) m/z calc'd for C₁₈H₂₂NO₄ [M+H]⁺: 316.1543, found 316.1545.

2.7.4 General Procedure for Allylic Alkylation Screening Reactions

All reagents were dispensed as solutions using a Symyx Core Module within a nitrogen-filled glovebox. Oven-dried half-dram vials were charged with a solution of the palladium source (Pd_2dba_3 or $\text{Pd}_2\text{pmdba}_3$, 1.68 μmol , 0.05 equiv) in THF (368 μL). The palladium solutions were evaporated to dryness under reduced pressure using a Genevac centrifugal evaporator within the glovebox, and stirbars were added to the vials. The reaction vials were then charged with the desired reaction solvent (500 mL) and a solution of the PHOX ligand (4.20 μmol , 0.125 equiv) in the reaction solvent (250 μL) and stirred at ambient glovebox temperature ($\sim 28^\circ\text{C}$). After 30 min, solutions of the lactam substrate (33.6 μmol , 1.0 equiv) in the reaction solvent (250 μL) were added. The reaction vials were tightly capped and heated to the desired temperature. When complete consumption of the starting material was observed by colorimetric change (from light green to red-orange) and confirmed by thin-layer chromatography on SiO_2 (typically less than 72 h), the reaction mixtures were removed from the glovebox, concentrated under reduced pressure, resuspended in an appropriate solvent for analysis (e.g., hexanes), filtered, and analyzed for enantiomeric excess (see Methods for the Determination of Enantiomeric Excess).

2.7.5 Results of Screening Various Reaction Parameters

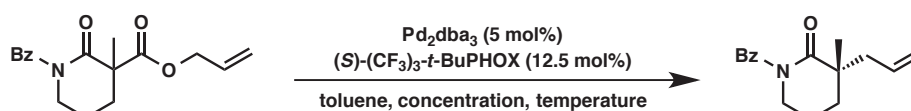
Table 2.3 Influences of solvent, protecting group, and ligand



	% ee			
	THF	MTBE	Toluene	Hex:Tol 2:1
R = Ts ^a	4.1 35.2	25.9 57.2	6.5 37.2	31.4 44.2
R = Boc ^a	57.3 70.3	74.5 72.1	73.6 73.0	76.7 71.0
R = Cbz	36.3 79.9	75.2 83.5	75.1 87.3	71.5 83.2
R = Fmoc	45.7 78.9	64.9 84.6	38.3 87.1	44.9 84.6
R = Ac	20.0 75.1	64.1 90.6 ^b	61.6 90.2 ^b	83.2 90.9 ^b
R = 4-MeO-Bz	59.5 97.1	90.7 98.3	87.4 99.0	96.8 98.5
R = 4-F-Bz	42.3 95.3	85.8 99.0	83.2 99.3	96.4 99.4
R = Bz	52.2 96.2	88.3 99.2	85.8 99.0	96.4 98.8

^a Reactions performed at 50 °C. ^b Reaction performed at 60 °C.

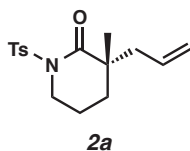
Table 2.4 Influence of temperature and concentration



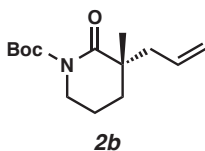
0.1 mmol

entry	temperature (°C)	concentration (M)	time (h)	% ee
1	40	0.033	43	99.2
2	45	0.033	22	98.9
3	50	0.033	12	98.7
4	55	0.033	6	98.2
5	40	0.10	43	98.9
6	40	0.20	43	97.4

2.7.6 Characterization Data for Lactam Products in Table 2.1

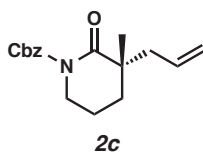


Tosyl Lactam 2a: Reaction performed in MTBE at 40 °C. Tosyl lactam **2a** was isolated by flash chromatography (SiO₂, 3 to 15% Et₂O in hexanes) as a light yellow solid. 90.0% yield. $R_f = 0.29$ (35% Et₂O in hexanes); ¹H NMR (500 MHz, CDCl₃) δ 7.89–7.84 (m, 2H), 7.33–7.27 (m, 2H), 5.41 (dddd, $J = 16.9, 10.2, 8.1, 6.7$ Hz, 1H), 4.99–4.86 (m, 2H), 3.99 (dddd, $J = 11.9, 5.9, 4.9, 1.3$ Hz, 1H), 3.82–3.71 (m, 1H), 2.42 (s, 3H), 2.41–2.34 (m, 1H), 2.07 (ddt, $J = 13.6, 8.1, 1.0$ Hz, 1H), 1.98–1.83 (m, 2H), 1.83–1.75 (m, 1H), 1.55–1.48 (m, 1H), 1.12 (s, 3H); ¹³C NMR (126 MHz, CDCl₃) δ 175.7, 144.4, 136.2, 132.9, 129.2, 128.5, 118.9, 47.6, 44.2, 44.0, 32.1, 25.5, 21.6, 20.1; IR (Neat Film NaCl) 3074, 2938, 1689, 1597, 1454, 1351, 1283, 1171, 1103, 1089, 1039, 921, 814, 748 cm⁻¹; HRMS (MM: ESI-APCI) m/z calc'd for C₁₆H₂₁NO₃SNa [M+Na]⁺: 330.1134, found 330.1141; $[\alpha]_D^{25} -69.2^\circ$ (c 1.16, CHCl₃, 75% ee).

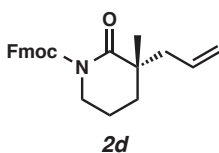


Boc Lactam 2b: Reaction performed in toluene at 40 °C. Boc lactam **2b** was isolated by flash chromatography (SiO₂, 8 to 9% Et₂O in hexanes) as a colorless oil. 87.1% yield. $R_f = 0.57$ (35% Et₂O in hexanes); ¹H NMR (500 MHz, CDCl₃) δ 5.74 (dddd, $J = 17.1, 10.4, 7.8, 7.0$ Hz, 1H), 5.14–5.02 (m, 2H), 3.71–3.61 (m, 1H), 3.58–3.48 (m, 1H), 2.48 (dd, $J = 13.6, 7.0$ Hz, 1H), 2.26 (dd, $J = 13.6, 7.9$ Hz, 1H), 1.87–1.76 (m, 3H), 1.61–1.52

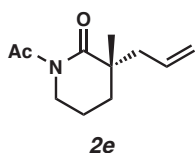
(m, 1H), 1.50 (s, 9H), 1.22 (s, 3H); ^{13}C NMR (126 MHz, CDCl_3) δ 177.1, 153.7, 133.7, 118.5, 82.5, 47.4, 44.5, 44.2, 33.0, 28.0, 25.4, 19.7; IR (Neat Film NaCl) 3076, 2978, 2936, 1768, 1715, 1457, 1392, 1368, 1298, 1280, 1252, 1149, 999, 917, 854 cm^{-1} ; HRMS (MM: ESI-APCI) m/z calc'd for $\text{C}_{14}\text{H}_{23}\text{NO}_3\text{Na}$ $[\text{M}+\text{Na}]^+$: 276.1570, found 276.1574; $[\alpha]_{\text{D}}^{25}$ -73.6° (c 1.025, CHCl_3 , 81% ee).



Cbz Lactam 2c: Reaction performed in toluene at 40 °C. Cbz lactam **2c** was isolated by flash chromatography (SiO_2 , 8 to 10% Et_2O in hexanes) as a colorless oil. 84.6% yield. R_f = 0.49 (25% EtOAc in hexanes); ^1H NMR (500 MHz, CDCl_3) δ 7.44–7.40 (m, 2H), 7.36 (ddd, J = 7.9, 7.0, 1.0 Hz, 2H), 7.33–7.29 (m, 1H), 5.74 (dddd, J = 16.6, 10.5, 7.8, 6.9 Hz, 1H), 5.26 (s, 2H), 5.13–5.02 (m, 2H), 3.80–3.72 (m, 1H), 3.67–3.58 (m, 1H), 2.51 (dd, J = 13.6, 7.0 Hz, 1H), 2.26 (dd, J = 13.6, 7.9 Hz, 1H), 1.90–1.77 (m, 3H), 1.62–1.53 (m, 1H), 1.25 (s, 3H); ^{13}C NMR (126 MHz, CDCl_3) δ 177.0, 154.8, 135.6, 133.4, 128.5, 128.2, 128.0, 118.8, 68.3, 47.8, 44.8, 44.2, 32.8, 25.5, 19.6; IR (Neat Film NaCl) 2940, 1772, 1712, 1456, 1377, 1296, 1270, 1218, 1161, 1001, 918 cm^{-1} ; HRMS (MM: ESI-APCI) m/z calc'd for $\text{C}_{17}\text{H}_{20}\text{NO}_3\text{Na}$ $[\text{M}+\text{Na}]^+$: 310.1414, found 310.1414; $[\alpha]_{\text{D}}^{25}$ -65.8° (c 1.48, CHCl_3 , 86% ee).

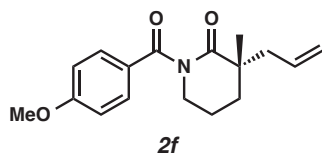


Fmoc Lactam 2d: Reaction performed in toluene at 40 °C. Fmoc lactam **2d** was isolated by flash chromatography (SiO₂, 6 to 8% Et₂O in hexanes) as a colorless oil. 82.4% yield. $R_f = 0.45$ (25% EtOAc in hexanes); ¹H NMR (500 MHz, CDCl₃) δ 7.77 (dt, $J = 7.6, 1.0$ Hz, 2H), 7.71 (ddd, $J = 7.5, 3.6, 1.0$ Hz, 2H), 7.41 (tt, $J = 7.5, 0.9$ Hz, 2H), 7.33 (ddt, $J = 7.5, 2.0, 1.2$ Hz, 2H), 5.80 (dddd, $J = 17.9, 8.7, 7.9, 6.9$ Hz, 1H), 5.18–5.10 (m, 2H), 4.53–4.42 (m, 2H), 4.33 (t, $J = 7.4$ Hz, 1H), 3.80–3.71 (m, 1H), 3.65–3.57 (m, 1H), 2.58 (dd, $J = 13.6, 7.0$ Hz, 1H), 2.32 (ddt, $J = 13.6, 7.8, 1.1$ Hz, 1H), 1.93–1.79 (m, 3H), 1.64–1.57 (m, 1H), 1.31 (s, 3H); ¹³C NMR (126 MHz, CDCl₃) δ 177.0, 154.9, 143.7, 141.2, 133.5, 127.7, 127.1, 125.4, 119.9, 118.8, 68.9, 47.7, 46.7, 44.8, 44.2, 32.8, 25.5, 19.6; IR (Neat Film NaCl) 3067, 2945, 1770, 1712, 1478, 1451, 1377, 1297, 1269, 1161, 1000, 759, 740 cm⁻¹; HRMS (MM: ESI-APCI) m/z calc'd for C₂₄H₂₆NO₃ [M+H]⁺: 376.1907, found 376.1914; $[\alpha]_D^{25} -38.5^\circ$ (c 2.17, CHCl₃, 89% ee).

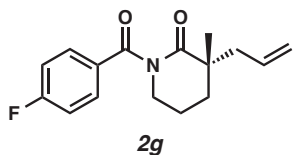


Acetyl Lactam 2e: Reaction performed in toluene at 40 °C. Acetyl lactam **2e** was isolated by flash chromatography (SiO₂, 8 to 10% Et₂O in hexanes) as a colorless oil. 47.2% yield. $R_f = 0.38$ (25% EtOAc in hexanes); ¹H NMR (500 MHz, CDCl₃) δ 5.73 (dddd, $J = 16.6, 10.4, 7.8, 7.0$ Hz, 1H), 5.14–5.04 (m, 2H), 3.82–3.72 (m, 1H), 3.60–3.49 (m, 1H), 2.50 (ddt, $J = 13.6, 7.0, 1.2$ Hz, 1H), 2.44 (s, 3H), 2.25 (ddt, $J = 13.6, 7.7, 1.1$ Hz, 1H), 1.91–1.71 (m, 3H), 1.64–1.52 (m, 1H), 1.25 (s, 3H); ¹³C NMR (126 MHz, CDCl₃) δ 179.3, 174.4, 133.3, 118.9, 45.4, 44.8, 44.4, 32.8, 27.2, 25.7, 19.4; IR (Neat Film NaCl) 2941, 1694, 1387, 1367, 1293, 1248, 1177, 1114, 1046, 920 cm⁻¹; HRMS

(MM: ESI-APCI) m/z calc'd for $C_{11}H_{18}NO_2$ $[M+H]^+$: 196.1332, found 196.1329; $[\alpha]_D^{25} -100.9^\circ$ (c 0.99, $CHCl_3$, 91% ee).

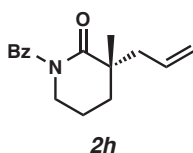


4-Methoxybenzoyl Lactam 2f: Reaction performed in toluene at 40 °C. 4-Methoxybenzoyl lactam **2f** was isolated by flash chromatography (SiO_2 , 15% EtOAc in hexanes) as a colorless oil. 92.7% yield. $R_f = 0.36$ (25% EtOAc in hexanes); 1H NMR (500 MHz, $CDCl_3$) δ 7.60–7.48 (m, 2H), 6.92–6.82 (m, 2H), 5.76 (dddd, $J = 17.2, 10.3, 7.7, 7.0$ Hz, 1H), 5.19–5.03 (m, 2H), 3.83 (s, 3H), 3.80 (ddd, $J = 12.1, 5.3, 1.4$ Hz, 1H), 3.73–3.64 (m, 1H), 2.57 (ddt, $J = 13.6, 7.1, 1.2$ Hz, 1H), 2.29 (ddt, $J = 13.7, 7.6, 1.1$ Hz, 1H), 2.05–1.91 (m, 3H), 1.72–1.63 (m, 1H), 1.32 (s, 3H); ^{13}C NMR (126 MHz, $CDCl_3$) δ 179.0, 174.9, 162.4, 133.4, 130.1, 128.4, 118.9, 113.5, 55.4, 47.3, 43.9, 43.4, 33.3, 25.3, 19.6; IR (Neat Film NaCl) 2937, 1675, 1604, 1511, 1254, 1164, 1029, 922, 840, 770 cm^{-1} ; HRMS (MM: ESI-APCI) m/z calc'd for $C_{17}H_{22}NO_3$ $[M+H]^+$: 288.1594, found 288.1595; $[\alpha]_D^{25} -94.2^\circ$ (c 1.00, $CHCl_3$, 99% ee).



4-Fluorobenzoyl Lactam 2g: Reaction performed in toluene at 40 °C. 4-Fluorobenzoyl lactam **2g** was isolated by flash chromatography (SiO_2 , 9% Et_2O in hexanes) as a colorless oil. 89.4% yield. $R_f = 0.41$ (17% EtOAc in hexanes); 1H NMR (500 MHz,

CDCl₃) δ 7.59–7.47 (m, 2H), 7.12–6.99 (m, 2H), 5.74 (ddt, $J = 17.0, 10.4, 7.3$ Hz, 1H), 5.18–5.05 (m, 2H), 3.89–3.77 (m, 1H), 3.77–3.63 (m, 1H), 2.55 (dd, $J = 13.7, 7.0$ Hz, 1H), 2.28 (dd, $J = 13.7, 7.6$ Hz, 1H), 2.07–1.88 (m, 3H), 1.76–1.62 (m, 1H), 1.31 (s, 3H); ¹³C NMR (126 MHz, CDCl₃) δ 179.1, 174.2, 164.6 (d, $J_{C-F} = 252.4$ Hz), 133.2, 132.5 (d, $J_{C-F} = 3.4$ Hz), 123.0 (d, $J_{C-F} = 8.9$ Hz), 119.1, 115.3 (d, $J_{C-F} = 22.1$ Hz), 47.3, 44.0, 43.3, 33.3, 25.2, 19.5; IR (Neat Film NaCl) 3076, 2940, 1679, 1602, 1507, 1384, 1280, 1145, 922, 844, 769 cm⁻¹; HRMS (MM: ESI-APCI) m/z calc'd for C₁₆H₁₉NO₂F [M+H]⁺: 276.1394, found 276.1392; [α]_D²⁵ -85.5° (c 1.02, CHCl₃, 99% ee).

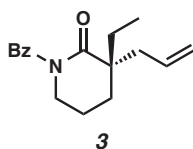


Benzoyl Lactam 2h: Reaction performed in toluene at 40 °C. Benzoyl lactam **2h** was isolated by flash chromatography (SiO₂, 5 to 9% Et₂O in pentane) as a colorless oil. 84.7% yield. $R_f = 0.55$ (25% EtOAc in hexanes); ¹H NMR (500 MHz, CDCl₃) δ 7.54–7.50 (m, 2H), 7.49–7.43 (m, 1H), 7.40–7.35 (m, 2H), 5.75 (dddd, $J = 17.1, 10.2, 7.7, 7.0$ Hz, 1H), 5.19–5.03 (m, 2H), 3.92–3.78 (m, 1H), 3.72 (ddt, $J = 12.6, 6.4, 6.0, 1.2$ Hz, 1H), 2.55 (ddt, $J = 13.7, 7.0, 1.2$ Hz, 1H), 2.29 (ddt, $J = 13.7, 7.7, 1.1$ Hz, 1H), 2.07–1.87 (m, 3H), 1.75–1.60 (m, 1H), 1.31 (s, 3H); ¹³C NMR (126 MHz, CDCl₃) δ 179.0, 175.3, 136.5, 133.3, 131.3, 128.1, 127.4, 118.9, 47.1, 44.0, 43.3, 33.3, 25.1, 19.5; IR (Neat Film NaCl) 3074, 2939, 2870, 1683, 1478, 1449, 1386, 1282, 1151, 919, 726, 695 cm⁻¹; HRMS (MM: ESI-APCI) m/z calc'd for C₁₆H₂₀NO₂ [M+H]⁺: 258.1489, found 258.1491; [α]_D²⁵ -91.2° (c 1.07, CHCl₃, 99% ee).

2.7.7 General Procedure for Preparative Allylic Alkylation Reactions

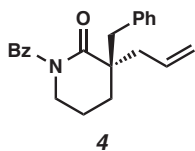
In a nitrogen-filled glovebox, an oven-dried 20 mL vial was charged with Pd₂pmdba₃ (27.4 mg, 0.025 mmol, 0.05 equiv) or Pd₂dba₃ (22.9 mg, 0.025 mmol, 0.05 equiv),³³ (*S*)-(CF₃)₃-*t*-BuPHOX (37.0 mg, 0.0625 mmol, 0.125 equiv), toluene (15 mL or 13 mL if the substrate is an oil), and a magnetic stir bar. The vial was stirred at ambient glovebox temperature (~28 °C) for 30 min and the substrate (0.50 mmol, 1.00 equiv) was added either as a solid or as a solution of an oil dissolved in toluene (2 mL). The vial was sealed and heated to 40 °C. When complete consumption of the starting material was observed by colorimetric change (from light green to red-orange) and confirmed by thin layer chromatography on SiO₂, the reaction mixtures were removed from the glovebox, concentrated under reduced pressure, and purified by flash chromatography to afford the desired alkylated product.

2.7.8 Characterization Data for Lactam Products in Table 2.2

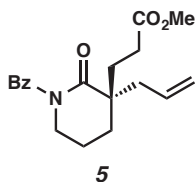


Benzoyl Lactam 3: Benzoyl lactam **3** was isolated by flash chromatography (SiO₂, 15 to 20% Et₂O in hexanes) as a colorless oil. 97.2% yield. $R_f = 0.39$ (20% Et₂O in hexanes); ¹H NMR (500 MHz, CDCl₃) δ 7.53–7.49 (m, 2H), 7.48–7.43 (m, 1H), 7.41–7.34 (m, 2H), 5.74 (dddd, $J = 16.7, 10.4, 7.6, 7.0$ Hz, 1H), 5.19–5.02 (m, 2H), 3.84–3.70 (m, 2H), 2.51 (ddt, $J = 13.8, 7.0, 1.3$ Hz, 1H), 2.28 (ddt, $J = 13.8, 7.6, 1.2$ Hz, 1H), 2.06–1.91 (m, 2H), 1.91–1.74 (m, 3H), 1.74–1.63 (m, 1H), 0.91 (t, $J = 7.4$ Hz, 3H); ¹³C NMR (126 MHz, CDCl₃) δ 178.0, 175.6, 136.7, 133.6, 131.2, 128.1, 127.4, 118.6, 47.4, 46.9, 41.3, 30.3,

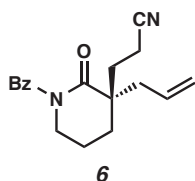
30.3, 19.6, 8.3; IR (Neat Film NaCl) 3072, 2970, 2941, 2880, 1678, 1448, 1384, 1283, 1147, 916, 725, 694 cm^{-1} ; HRMS (MM: ESI-APCI) m/z calc'd for $\text{C}_{17}\text{H}_{22}\text{NO}_2$ $[\text{M}+\text{H}]^+$: 272.1645, found 272.1649; $[\alpha]_{\text{D}}^{25}$ -28.6° (c 1.15, CHCl_3 , 99% ee).



Benzoyl Lactam 4: Benzoyl lactam **4** was isolated by flash chromatography (SiO_2 , 10% Et_2O in hexanes) as a white solid. 84.8% yield. $R_f = 0.48$ (35% Et_2O in hexanes); ^1H NMR (500 MHz, CDCl_3) δ 7.54 (dd, $J = 8.1, 1.4$ Hz, 2H), 7.52–7.46 (m, 1H), 7.43–7.37 (m, 2H), 7.32–7.22 (m, 3H), 7.18–7.11 (m, 2H), 5.80 (dddd, $J = 16.8, 10.1, 7.6, 6.8$ Hz, 1H), 5.21–5.06 (m, 2H), 3.70 (ddd, $J = 12.2, 7.0, 4.8$ Hz, 1H), 3.63 (ddd, $J = 12.5, 7.7, 4.4$ Hz, 1H), 3.34 (d, $J = 13.4$ Hz, 1H), 2.73–2.64 (m, 1H), 2.68 (d, $J = 13.3$ Hz, 1H), 2.25 (ddt, $J = 13.8, 7.7, 1.1$ Hz, 1H), 2.03–1.91 (m, 1H), 1.91–1.83 (m, 1H), 1.81 (dd, $J = 6.7, 5.3$ Hz, 2H); ^{13}C NMR (126 MHz, CDCl_3) δ 177.4, 175.5, 136.9, 136.6, 133.2, 131.4, 130.8, 128.2, 128.1, 127.6, 126.7, 119.3, 48.8, 46.8, 43.0, 42.9, 28.9, 19.6; IR (Neat Film NaCl) 3061, 3028, 2942, 1679, 1449, 1286, 1149, 919, 724, 704, 695 cm^{-1} ; HRMS (MM: ESI-APCI) m/z calc'd for $\text{C}_{22}\text{H}_{24}\text{NO}_2$ $[\text{M}+\text{H}]^+$: 334.1802, found 334.1800; $[\alpha]_{\text{D}}^{25}$ $+48.1^\circ$ (c 0.825, CHCl_3 , 99% ee).

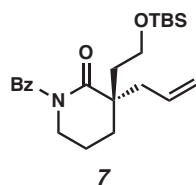


Benzoyl Lactam 5: Benzoyl lactam **5** was isolated by flash chromatography (SiO₂, 25% Et₂O in hexanes) as a light yellow oil. 91.8% yield. $R_f = 0.39$ (35% Et₂O in hexanes); ¹H NMR (500 MHz, CDCl₃) δ 7.53–7.49 (m, 2H), 7.49–7.44 (m, 1H), 7.41–7.31 (m, 2H), 5.72 (ddt, $J = 17.4, 10.3, 7.3$ Hz, 1H), 5.23–5.05 (m, 2H), 3.78 (t, $J = 6.0$ Hz, 2H), 3.67 (s, 3H), 2.58–2.47 (m, 1H), 2.42–2.24 (m, 3H), 2.08–1.97 (m, 4H), 1.93 (ddd, $J = 14.0, 7.8, 4.6$ Hz, 1H), 1.78 (ddd, $J = 13.9, 7.1, 4.9$ Hz, 1H); ¹³C NMR (126 MHz, CDCl₃) δ 177.4, 175.5, 173.7, 136.5, 132.6, 131.4, 128.2, 127.4, 119.4, 51.7, 47.0, 46.6, 41.2, 32.2, 31.2, 29.0, 19.4; IR (Neat Film NaCl) 3073, 2950, 2874, 1736, 1679, 1448, 1281, 1150, 920, 727, 696, 665 cm⁻¹; HRMS (MM: ESI-APCI) m/z calc'd for C₁₉H₂₄NO₄ [M+H]⁺: 330.1700, found 330.1704; $[\alpha]_D^{25} +14.0^\circ$ (c 0.72, CHCl₃, 99% ee).

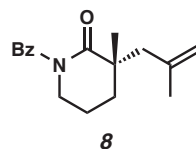


Benzoyl Lactam 6: Benzoyl lactam **6** was isolated by flash chromatography (SiO₂, 15 to 25% EtOAc in hexanes) as a colorless oil. 88.2% yield. $R_f = 0.43$ (35% EtOAc in hexanes); ¹H NMR (500 MHz, CDCl₃) δ 7.52–7.47 (m, 3H), 7.41 (ddt, $J = 8.7, 6.6, 1.0$ Hz, 2H), 5.71 (ddt, $J = 17.4, 10.1, 7.3$ Hz, 1H), 5.28–5.15 (m, 2H), 3.88–3.79 (m, 1H), 3.76 (ddd, $J = 12.9, 8.7, 4.2$ Hz, 1H), 2.57 (ddt, $J = 14.1, 7.3, 1.2$ Hz, 1H), 2.44–2.29 (m, 3H), 2.13–2.04 (m, 2H), 2.03–1.89 (m, 3H), 1.87–1.78 (m, 1H); ¹³C NMR (126 MHz, CDCl₃) δ 176.8, 175.2, 136.2, 131.7, 131.5, 128.3, 127.3, 120.3, 119.5, 47.0, 46.5, 41.1, 32.7, 30.8, 19.2, 12.5; IR (Neat Film NaCl) 3074, 2945, 2876, 1678, 1448, 1389, 1282,

1151, 922, 727, 696 cm^{-1} ; HRMS (MM: ESI-APCI) m/z calc'd for $\text{C}_{18}\text{H}_{21}\text{N}_2\text{O}_2$ $[\text{M}+\text{H}]^+$: 297.1598, found 297.1603; $[\alpha]_{\text{D}}^{25} +46.9^\circ$ (c 0.83, CHCl_3 , 99% ee).

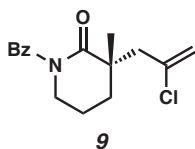


Benzoyl Lactam 7: Benzoyl lactam **7** was isolated by flash chromatography (SiO_2 , 5 to 15% Et_2O in hexanes) as a colorless oil. 85.4% yield. $R_f = 0.32$ (10% Et_2O in hexanes); ^1H NMR (500 MHz, CDCl_3) δ 7.54–7.48 (m, 2H), 7.48–7.42 (m, 1H), 7.41–7.33 (m, 2H), 5.76 (ddt, $J = 17.3, 10.2, 7.3$ Hz, 1H), 5.18–5.06 (m, 2H), 3.81–3.75 (m, 2H), 3.75–3.64 (m, 2H), 2.55 (ddt, $J = 13.8, 7.1, 1.2$ Hz, 1H), 2.33 (ddt, $J = 13.8, 7.5, 1.1$ Hz, 1H), 2.10–1.94 (m, 4H), 1.94–1.85 (m, 1H), 1.81 (ddd, $J = 13.9, 7.3, 5.6$ Hz, 1H), 0.88 (s, 9H), 0.04 (s, 6H); ^{13}C NMR (126 MHz, CDCl_3) δ 177.6, 175.5, 136.8, 133.4, 131.2, 128.1, 127.4, 118.9, 59.2, 46.9, 46.3, 42.2, 39.7, 30.8, 25.9, 19.6, 18.2, –5.4; IR (Neat Film NaCl) 2953, 2928, 2884, 2856, 1681, 1280, 1257, 1151, 1093, 836, 776, 725, 694 cm^{-1} ; HRMS (MM: ESI-APCI) m/z calc'd for $\text{C}_{23}\text{H}_{36}\text{NO}_3\text{Si}$ $[\text{M}+\text{H}]^+$: 402.2459, found 402.2467; $[\alpha]_{\text{D}}^{25} -3.71^\circ$ (c 1.40, CHCl_3 , 96% ee).

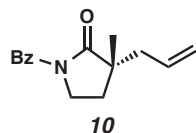


Benzoyl Lactam 8: Benzoyl lactam **8** was isolated by flash chromatography (SiO_2 , 5 to 9% EtOAc in hexanes) as a colorless oil. 78.0% yield. $R_f = 0.54$ (25% EtOAc in hexanes); ^1H NMR (500 MHz, CDCl_3) δ 7.54–7.50 (m, 2H), 7.48–7.43 (m, 1H), 7.41–

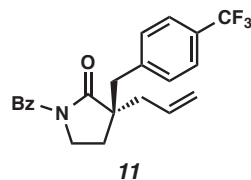
7.35 (m, 2H), 4.89 (t, $J = 1.8$ Hz, 1H), 4.70 (dt, $J = 2.1, 1.0$ Hz, 1H), 3.94–3.84 (m, 1H), 3.74–3.63 (m, 1H), 2.75 (dd, $J = 13.8, 1.3$ Hz, 1H), 2.13 (dd, $J = 13.8, 0.8$ Hz, 1H), 2.08–1.94 (m, 3H), 1.69 (s, 3H), 1.68–1.61 (m, 1H), 1.37 (s, 3H); ^{13}C NMR (126 MHz, CDCl_3) δ 178.8, 175.5, 141.9, 136.5, 131.3, 128.1, 127.4, 115.5, 47.2, 46.2, 44.0, 32.9, 26.9, 24.7, 19.8; IR (Neat Film NaCl) 3070, 2940, 1678, 1448, 1274, 1144, 726 cm^{-1} ; HRMS (MM: ESI-APCI) m/z calc'd for $\text{C}_{17}\text{H}_{22}\text{NO}_2$ $[\text{M}+\text{H}]^+$: 272.1645, found 272.1655; $[\alpha]_{\text{D}}^{25} -105.6^\circ$ (c 0.99, CHCl_3 , 97% ee).



Benzoyl Lactam 9: Benzoyl lactam **9** was isolated by flash chromatography (SiO_2 , 8 to 10% Et_2O in hexanes) as a colorless oil. 60.3% yield. $R_f = 0.39$ (25% EtOAc in hexanes); ^1H NMR (500 MHz, CDCl_3) δ 7.55–7.49 (m, 2H), 7.49–7.43 (m, 1H), 7.42–7.34 (m, 2H), 5.32 (d, $J = 1.7$ Hz, 1H), 5.18 (s, 1H), 3.92 (ddt, $J = 12.7, 4.8, 1.7$ Hz, 1H), 3.75–3.66 (m, 1H), 3.04 (dd, $J = 14.5, 1.0$ Hz, 1H), 2.50 (d, $J = 14.5$ Hz, 1H), 2.16 (ddd, $J = 13.4, 10.2, 4.4$ Hz, 1H), 2.12–1.98 (m, 2H), 1.86–1.77 (m, 1H), 1.43 (s, 3H); ^{13}C NMR (126 MHz, CDCl_3) δ 177.9, 175.3, 138.3, 136.4, 131.4, 128.1, 127.4, 117.1, 47.0, 47.0, 44.2, 32.8, 26.3, 19.7; IR (Neat Film NaCl) 2944, 2872, 1679, 1628, 1448, 1386, 1277, 1151, 894, 726 cm^{-1} ; HRMS (MM: ESI-APCI) m/z calc'd for $\text{C}_{16}\text{H}_{19}\text{NO}_2\text{Cl}$ $[\text{M}+\text{H}]^+$: 292.1099, found 292.1102; $[\alpha]_{\text{D}}^{25} -91.4^\circ$ (c 0.94, CHCl_3 , 95% ee).

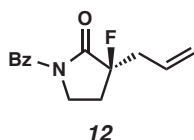


Benzoyl Lactam 10: Benzoyl lactam **10** was isolated by flash chromatography (SiO₂, 5 to 10% Et₂O in hexanes) as a colorless oil. 90.3% yield. $R_f = 0.35$ (35% Et₂O in hexanes); ¹H NMR (500 MHz, CDCl₃) δ 7.58–7.54 (m, 2H), 7.53–7.48 (m, 1H), 7.43–7.38 (m, 2H), 5.78 (dddd, $J = 17.1, 10.2, 7.8, 7.0$ Hz, 1H), 5.22–5.09 (m, 2H), 3.87 (dd, $J = 7.7, 6.7$ Hz, 2H), 2.36 (dd, $J = 13.8, 7.0$ Hz, 1H), 2.24 (dd, $J = 13.7, 7.8$ Hz, 1H), 2.15 (dt, $J = 12.9, 7.6$ Hz, 1H), 1.85 (dt, $J = 13.1, 6.7$ Hz, 1H), 1.22 (s, 3H); ¹³C NMR (126 MHz, CDCl₃) δ 178.6, 170.8, 134.4, 133.0, 131.8, 128.8, 127.7, 119.3, 46.2, 42.8, 41.8, 29.3, 22.8; IR (Neat Film NaCl) 3075, 2974, 2902, 1742, 1674, 1448, 1377, 1357, 1306, 1243, 1156, 921, 860, 731, 694, 656 cm⁻¹; HRMS (MM: ESI-APCI) m/z calc'd for C₁₅H₁₈NO₂ [M+H]⁺: 244.1332, found 244.1336; $[\alpha]_D^{25} -31.6^\circ$ (c 1.04, CHCl₃, 98% ee).

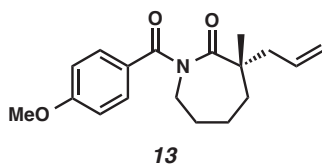


Benzoyl Lactam 11: Benzoyl lactam **11** was isolated by flash chromatography (SiO₂, 10 to 20% Et₂O in hexanes) as a colorless oil. 89.3% yield. $R_f = 0.24$ (20% Et₂O in hexanes); ¹H NMR (500 MHz, CDCl₃) δ 7.60–7.56 (m, 2H), 7.56–7.51 (m, 1H), 7.49–7.45 (m, 2H), 7.42 (ddt, $J = 7.8, 6.7, 1.0$ Hz, 2H), 7.31 (d, $J = 7.7$ Hz, 2H), 5.83 (dddd, $J = 17.1, 10.1, 7.8, 6.9$ Hz, 1H), 5.28–5.10 (m, 2H), 3.70 (dt, $J = 11.4, 7.5$ Hz, 1H), 3.39 (dt, $J = 11.4, 6.9$ Hz, 1H), 3.10 (d, $J = 13.4$ Hz, 1H), 2.76 (d, $J = 13.5$ Hz, 1H), 2.48 (dd, $J = 13.8, 7.0$ Hz, 1H), 2.32 (dd, $J = 13.8, 7.8$ Hz, 1H), 2.05 (t, $J = 7.3$ Hz, 2H); ¹³C NMR

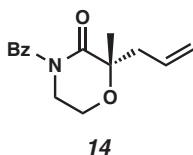
(126 MHz, CDCl₃) δ 177.1, 170.5, 140.9, 134.2, 132.3, 131.9, 130.7, 129.4 (q, J_{C-F} = 32.5 Hz), 128.7, 127.7, 125.3 (q, J_{C-F} = 3.7 Hz), 124.1 (q, J_{C-F} = 272.2 Hz), 120.1, 51.3, 43.0, 41.9, 41.9, 25.2; IR (Neat Film NaCl) 3080, 2977, 2913, 1738, 1677, 1325, 1294, 1244, 1164, 1121, 1067, 859, 728, 701, 665 cm⁻¹; HRMS (FAB) m/z calc'd for C₂₂H₂₁NO₂F₃ [M+H]⁺: 388.1524, found 388.1525; [α]_D²⁵ +78.3° (c 1.90, CHCl₃, 93% ee).



Benzoyl Lactam 12: Benzoyl lactam **12** was isolated by flash chromatography (SiO₂, 10 to 20% Et₂O in hexanes) as a white solid. 85.7% yield. R_f = 0.35 (35% Et₂O in hexanes); ¹H NMR (500 MHz, CDCl₃) δ 7.63–7.58 (m, 2H), 7.58–7.52 (m, 1H), 7.49–7.40 (m, 2H), 5.87–5.73 (m, 1H), 5.32–5.20 (m, 2H), 4.00 (ddd, J = 11.5, 7.7, 6.5 Hz, 1H), 3.90–3.80 (m, 1H), 2.81–2.70 (m, 1H), 2.62–2.48 (m, 1H), 2.46–2.27 (m, 2H); ¹³C NMR (126 MHz, CDCl₃) δ 170.3, 169.7 (d, J_{C-F} = 23.1 Hz), 133.4, 132.4, 129.7 (d, J_{C-F} = 7.1 Hz), 129.0, 127.9, 121.0, 97.0 (d, J_{C-F} = 185.4 Hz), 42.0 (d, J_{C-F} = 2.3 Hz), 38.4 (d, J_{C-F} = 25.2 Hz), 28.5 (d, J_{C-F} = 22.6 Hz); IR (Neat Film NaCl) 3076, 1760, 1676, 1365, 1314, 1253, 1132, 1058, 1008, 980, 920, 863, 791, 729 cm⁻¹; HRMS (MM: ESI-APCI) m/z calc'd for C₁₄H₁₅NO₂F [M+H]⁺: 248.1081, found 248.1092; [α]_D²⁵ -120.5° (c 1.11, CHCl₃, 98% ee).

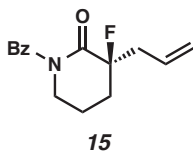


4-Methoxybenzoyl Lactam 13: Reaction performed in MTBE at 40 °C. 4-Methoxybenzoyl lactam **13** was isolated by flash chromatography (SiO₂, 8% Et₂O in hexanes) as a colorless oil. 83.2% yield. $R_f = 0.48$ (25% EtOAc in hexanes); ¹H NMR (500 MHz, CDCl₃) δ 7.56–7.48 (m, 2H), 6.91–6.82 (m, 2H), 5.86–5.66 (m, 1H), 5.18–5.02 (m, 2H), 4.03 (ddd, $J = 15.0, 8.0, 2.4$ Hz, 1H), 3.88 (ddd, $J = 15.1, 8.5, 2.1$ Hz, 1H), 3.83 (s, 3H), 2.50 (ddt, $J = 13.6, 7.0, 1.2$ Hz, 1H), 2.35 (ddt, $J = 13.7, 7.6, 1.1$ Hz, 1H), 1.92–1.77 (m, 4H), 1.77–1.62 (m, 2H), 1.31 (s, 3H); ¹³C NMR (126 MHz, CDCl₃) δ 182.3, 174.7, 162.2, 133.9, 130.0, 128.9, 118.6, 113.5, 55.4, 47.7, 44.7, 43.0, 35.1, 28.2, 25.0, 23.4; IR (Neat Film NaCl) 3074, 2932, 1673, 1605, 1511, 1279, 1255, 1168, 1112, 1025, 837 cm⁻¹; HRMS (MM: ESI-APCI) m/z calc'd for C₁₈H₂₄NO₃ [M+H]⁺: 302.1751, found 302.1744; $[\alpha]_D^{25} -34.7^\circ$ (c 0.75, CHCl₃, 93% ee).

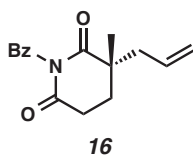


Benzoyl Lactam 14: Benzoyl lactam **14** was isolated by flash chromatography (SiO₂, 10 to 20% Et₂O in hexanes) as a colorless oil. 91.4% yield. $R_f = 0.36$ (35% Et₂O in hexanes); ¹H NMR (500 MHz, CDCl₃) δ 7.55–7.52 (m, 2H), 7.52–7.47 (m, 1H), 7.42–7.37 (m, 2H), 5.90 (ddt, $J = 17.3, 10.3, 7.2$ Hz, 1H), 5.26–5.10 (m, 2H), 4.12–3.95 (m, 3H), 3.94–3.81 (m, 1H), 2.71 (ddt, $J = 14.1, 7.3, 1.2$ Hz, 1H), 2.47 (ddt, $J = 14.1, 7.0, 1.3$ Hz, 1H), 1.48 (s, 3H); ¹³C NMR (126 MHz, CDCl₃) δ 174.3, 173.1, 135.7, 132.1, 131.7, 128.1, 127.7, 119.3, 80.3, 59.4, 45.7, 43.1, 23.3; IR (Neat Film NaCl) 3075, 2978, 2894, 1685, 1448, 1373, 1283, 1227, 1111, 1092, 921, 726, 694 cm⁻¹; HRMS (FAB) m/z calc'd

for $C_{15}H_{18}NO_3$ $[M+H]^+$: 260.1287, found 260.1277; $[\alpha]_D^{25}$ -72.1° (c 0.97, $CHCl_3$, 99% ee).

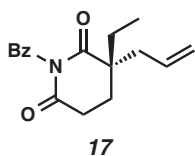


Benzoyl Lactam 15: Benzoyl lactam **15** was isolated by flash chromatography (SiO_2 , 5 to 10% EtOAc in hexanes) as a colorless oil. 88.8% yield. $R_f = 0.35$ (35% Et_2O in hexanes); 1H NMR (500 MHz, $CDCl_3$) δ 7.62–7.57 (m, 2H), 7.53–7.47 (m, 1H), 7.44–7.37 (m, 2H), 5.87–5.70 (m, 1H), 5.28–5.15 (m, 2H), 3.91 (dddd, $J = 12.8, 6.0, 4.7, 1.4$ Hz, 1H), 3.74 (dddd, $J = 13.6, 9.2, 4.5, 2.4$ Hz, 1H), 2.86–2.60 (m, 2H), 2.33–2.14 (m, 2H), 2.13–1.89 (m, 2H); ^{13}C NMR (126 MHz, $CDCl_3$) δ 174.5, 170.8 (d, $J_{C-F} = 23.5$ Hz), 135.0, 132.0, 130.6 (d, $J_{C-F} = 6.5$ Hz), 128.3, 128.0, 120.4, 93.9 (d, $J_{C-F} = 179.3$ Hz), 46.4, 40.0 (d, $J_{C-F} = 23.6$ Hz), 32.1 (d, $J_{C-F} = 22.5$ Hz), 19.1 (d, $J_{C-F} = 4.6$ Hz); IR (Neat Film NaCl) 3078, 2956, 1715, 1687, 1478, 1449, 1435, 1390, 1288, 1273, 1175, 1152, 1000, 930, 725, 694, 662 cm^{-1} ; HRMS (MM: ESI-APCI) m/z calc'd for $C_{15}H_{16}NO_2F$ $[M+H]^+$: 262.1238, found 262.1244; $[\alpha]_D^{25}$ -120.6° (c 1.09, $CHCl_3$, 99% ee).

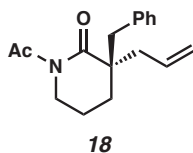


Benzoyl Glutarimide 16: Benzoyl glutarimide **16** was isolated by flash chromatography (SiO_2 , 17 to 25% EtOAc in hexanes) as a colorless oil. 81% yield. $R_f = 0.21$ (25% EtOAc in hexanes); 1H NMR (500 MHz, $CDCl_3$) δ 7.83 (d, $J = 8.29$ Hz, 2H), 7.63 (t, $J = 7.45$

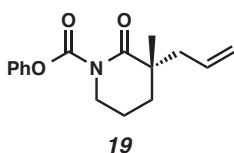
Hz, 1H), 7.48 (dd, $J = 8.29, 7.45$ Hz, 2H), 5.77 (dddd, $J = 17.4, 10.2, 7.4, 7.0$ Hz, 1H), 5.22–5.16 (m, 2H), 2.87–2.77 (m, 2H), 2.59 (ddt, $J = 13.8, 7.0, 1.0$ Hz, 1H), 2.40 (ddt, $J = 13.8, 7.4, 1.0$ Hz, 1H), 2.12 (ddd, $J = 14.2, 7.73, 6.81$ Hz, 1H), 1.85 (ddd, $J = 14.2, 6.5, 6.1$ Hz, 1H), 1.37 (s, 3H); ^{13}C NMR (126 MHz, CDCl_3) δ 176.6, 171.6, 170.9, 134.8, 132.0, 131.9, 130.0, 129.1, 120.0, 41.9, 41.7, 29.2, 28.2, 22.8; IR (Neat Film NaCl) 3077, 2975, 2935, 1750, 1713, 1683, 1450, 1340, 1239, 1198, 981, 776 cm^{-1} ; HRMS (MM: ESI-APCI) m/z calc'd for $\text{C}_{16}\text{H}_{18}\text{NO}_3[\text{M}+\text{H}]^+$: 272.1281, found 272.1281; $[\alpha]_{\text{D}}^{25} -31.3^\circ$ (c 1.00, CHCl_3 , 94% ee).



Benzoyl Glutarimide 17: Benzoyl glutarimide **17** was isolated by flash chromatography (SiO_2 , 17 to 25% EtOAc in hexanes) as a colorless oil. 86% yield. $R_f = 0.24$ (25% EtOAc in hexanes); ^1H NMR (500 MHz, CDCl_3) δ 7.83 (d, $J = 8.38$ Hz, 2H), 7.64 (t, $J = 7.46$ Hz, 1H), 7.48 (dd, $J = 8.38, 7.46$ Hz, 2H), 5.75 (dddd, $J = 17.2, 10.2, 7.7, 7.0$ Hz, 1H), 5.20–5.15 (m, 2H), 2.86–2.76 (m, 2H), 2.60 (ddt, $J = 14.0, 7.0, 1.1$ Hz, 1H), 2.37 (ddt, $J = 14.0, 7.7, 1.1$ Hz, 1H), 2.05 (ddd, $J = 14.3, 7.85, 6.81$ Hz, 1H), 1.97 (ddd, $J = 14.3, 6.56, 6.24$ Hz, 1H), 1.87–1.75 (m, 2H), 0.97 (t, $J = 7.46$, 3H); ^{13}C NMR (126 MHz, CDCl_3) δ 175.9, 171.6, 171.0, 134.8, 132.4, 131.9, 130.0, 129.0, 119.8, 45.4, 39.3, 29.0, 28.1, 25.4, 8.1; IR (Neat Film NaCl) 3076, 2974, 2940, 2882, 1750, 1713, 1683, 1450, 1340, 1239, 1195, 1001, 923, 778 cm^{-1} ; HRMS (MM: ESI-APCI) m/z calc'd for $\text{C}_{17}\text{H}_{20}\text{NO}_3[\text{M}+\text{H}]^+$: 286.1438, found 286.1432; $[\alpha]_{\text{D}}^{25} -16.2^\circ$ (c 1.00, CHCl_3 , 96% ee).

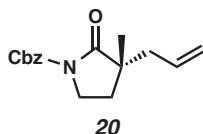


Acyl Lactam 18: Acyl lactam **18** was isolated by flash chromatography (SiO₂, 10 to 20% Et₂O in hexanes) as a colorless oil. 88.4% yield. $R_f = 0.40$ (35% Et₂O in hexanes); ¹H NMR (500 MHz, CDCl₃) δ 7.32–7.17 (m, 3H), 7.17–7.09 (m, 2H), 5.77 (dddd, $J = 17.0, 10.3, 7.9, 6.8$ Hz, 1H), 5.19–5.05 (m, 2H), 3.60–3.48 (m, 1H), 3.44 (dddd, $J = 13.0, 7.0, 4.6, 1.0$ Hz, 1H), 3.27 (d, $J = 13.3$ Hz, 1H), 2.68 (d, $J = 13.2$ Hz, 1H), 2.66–2.62 (m, 1H), 2.51 (s, 3H), 2.23 (ddt, $J = 13.5, 7.9, 1.1$ Hz, 1H), 1.90–1.61 (m, 3H), 1.57–1.38 (m, 1H); ¹³C NMR (126 MHz, CDCl₃) δ 178.0, 174.2, 137.1, 133.2, 130.4, 128.3, 126.8, 119.2, 49.7, 45.1, 44.8, 44.5, 29.0, 27.6, 19.6; IR (Neat Film NaCl) 3028, 2941, 1691, 1367, 1291, 1247, 111178, 1131, 1031, 923 cm⁻¹; HRMS (MM: ESI-APCI) m/z calc'd for C₁₇H₂₂NO₂ [M+H]⁺: 272.1645, found 272.1646; $[\alpha]_D^{25} +11.4^\circ$ (c 1.03, CHCl₃, 88% ee).

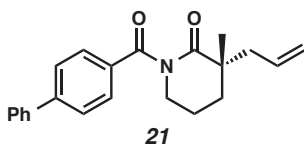


Phenyl Carbamate Lactam 19: Phenyl Carbamate lactam **19** was isolated by flash chromatography (SiO₂, 10 to 20% Et₂O in hexanes) as a colorless oil. 82.2% yield. $R_f = 0.39$ (35% Et₂O in hexanes); ¹H NMR (500 MHz, CDCl₃) δ 7.40–7.35 (m, 2H), 7.25–7.21 (m, 1H), 7.20–7.15 (m, 2H), 5.79 (dddd, $J = 16.7, 10.4, 7.8, 7.0$ Hz, 1H), 5.18–5.08 (m, 2H), 3.89–3.82 (m, 1H), 3.78–3.70 (m, 1H), 2.55 (ddt, $J = 13.6, 7.0, 1.2$ Hz, 1H), 2.33 (ddt, $J = 13.6, 7.8, 1.1$ Hz, 1H), 2.00–1.85 (m, 3H), 1.70–1.59 (m, 1H), 1.30 (s, 3H); ¹³C NMR (126 MHz, CDCl₃) δ 177.3, 153.8, 150.8, 133.3, 129.3, 125.9, 121.5, 118.9,

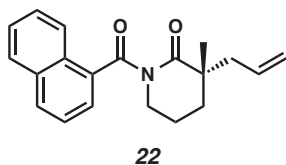
48.2, 45.0, 44.1, 33.0, 25.3, 19.6; IR (Neat Film NaCl) 3074, 2939, 2870, 1783, 1733, 1718, 1494, 1299, 1265, 1203, 1153, 991, 920 cm^{-1} ; HRMS (MM: ESI-APCI) m/z calc'd for $\text{C}_{16}\text{H}_{20}\text{NO}_3$ $[\text{M}+\text{H}]^+$: 274.1438, found 274.1444; $[\alpha]_{\text{D}}^{25}$ -81.6° (c 1.11, CHCl_3 , 94% ee).



Benzyl Carbamate Lactam 20: Benzyl carbamate lactam **20** was isolated by flash chromatography (SiO_2 , 10 to 30% Et_2O in hexanes) as a colorless oil. 85.9% yield. $R_f = 0.41$ (35% Et_2O in hexanes); ^1H NMR (500 MHz, CDCl_3) δ 7.46–7.42 (m, 2H), 7.37 (ddd, $J = 7.4, 6.3, 1.5$ Hz, 2H), 7.35–7.30 (m, 1H), 5.74 (dddd, $J = 15.9, 11.0, 7.9, 6.9$ Hz, 1H), 5.28 (s, 2H), 5.18–5.06 (m, 2H), 3.77–3.63 (m, 2H), 2.33 (ddt, $J = 13.8, 6.9, 1.2$ Hz, 1H), 2.24 (ddt, $J = 13.8, 7.9, 1.0$ Hz, 1H), 2.03 (ddd, $J = 12.9, 8.1, 6.9$ Hz, 1H), 1.74 (ddd, $J = 13.2, 7.7, 5.9$ Hz, 1H), 1.19 (s, 3H); ^{13}C NMR (126 MHz, CDCl_3) δ 178.0, 151.7, 135.3, 133.0, 128.6, 128.3, 128.1, 119.1, 68.0, 45.5, 42.9, 41.7, 29.5, 22.6; IR (Neat Film NaCl) 3066, 2973, 2930, 2903, 1789, 1750, 1719, 1456, 1380, 1363, 1301, 1217, 1001, 919, 776, 736 cm^{-1} ; HRMS (MM: ESI-APCI) m/z calc'd for $\text{C}_{16}\text{H}_{20}\text{NO}_3$ $[\text{M}+\text{H}]^+$: 274.1438, found 274.1438; $[\alpha]_{\text{D}}^{25}$ -41.4° (c 1.02, CHCl_3 , 91% ee).

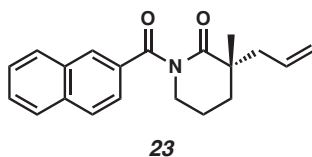


4-Phenylbenzoyl Lactam 21: 4-Phenylbenzoyl lactam **21** was isolated by flash chromatography (SiO₂, 10 to 15% Et₂O in pentane) as a colorless oil. 84.6% yield. $R_f = 0.43$ (35% Et₂O in hexanes); ¹H NMR (500 MHz, CDCl₃) δ 7.64–7.57 (m, 6H), 7.45 (ddd, $J = 7.8, 6.7, 1.1$ Hz, 2H), 7.40–7.34 (m, 1H), 5.84–5.70 (m, 1H), 5.20–5.09 (m, 2H), 3.91–3.82 (m, 1H), 3.74 (ddd, $J = 12.1, 7.4, 5.7$ Hz, 1H), 2.59 (ddd, $J = 13.7, 7.0, 1.3$ Hz, 1H), 2.32 (ddt, $J = 13.7, 7.7, 1.2$ Hz, 1H), 2.10–1.91 (m, 3H), 1.77–1.64 (m, 1H), 1.34 (s, 3H); ¹³C NMR (126 MHz, CDCl₃) δ 179.1, 175.1, 144.2, 140.2, 135.1, 133.3, 128.8, 128.1, 127.8, 127.2, 126.9, 119.0, 47.2, 44.0, 43.3, 33.3, 25.2, 19.5; IR (Neat Film NaCl) 3073, 2938, 2869, 1677, 1607, 1478, 1383, 1295, 1279, 1145, 922, 849, 743, 698 cm⁻¹; HRMS (MM: ESI-APCI) m/z calc'd for C₂₂H₂₄NO₂ [M+H]⁺: 334.1802, found 334.1812; $[\alpha]_D^{25} -82.6^\circ$ (c 0.75, CHCl₃, 99% ee).



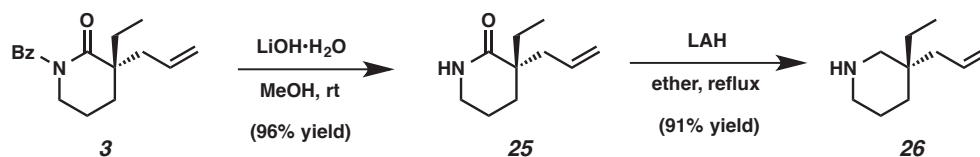
1-Naphthoyl Lactam 22: 1-Naphthoyl lactam **22** was isolated by flash chromatography (SiO₂, 10 to 20% Et₂O in hexanes) as a white solid. 86.3% yield. $R_f = 0.42$ (35% Et₂O in hexanes); ¹H NMR (500 MHz, CDCl₃) δ 8.03–7.97 (m, 1H), 7.90–7.83 (m, 2H), 7.55–7.46 (m, 2H), 7.42 (dd, $J = 8.1, 7.1$ Hz, 1H), 7.37 (dd, $J = 7.1, 1.3$ Hz, 1H), 5.64 (dddd, $J = 17.2, 10.2, 7.6, 7.1$ Hz, 1H), 5.16–4.97 (m, 2H), 4.05 (dddd, $J = 12.8, 6.3, 5.2, 1.3$ Hz, 1H), 3.95–3.82 (m, 1H), 2.43 (ddt, $J = 13.7, 7.1, 1.2$ Hz, 1H), 2.19 (ddt, $J = 13.7, 7.6, 1.1$ Hz, 1H), 2.11–1.99 (m, 2H), 1.99–1.91 (m, 1H), 1.73–1.64 (m, 1H), 1.18 (s, 3H); ¹³C NMR (126 MHz, CDCl₃) δ 178.5, 174.3, 135.8, 133.6, 133.1, 130.0, 129.8, 128.4, 126.9, 126.2, 124.9, 124.5, 123.3, 118.9, 46.4, 44.1, 43.3, 33.2, 24.8, 19.5; IR (Neat Film NaCl)

3062, 2937, 2869, 1702, 1677, 1381, 1295, 1251, 1147, 923, 781 cm^{-1} ; HRMS (MM: ESI-APCI) m/z calc'd for $\text{C}_{20}\text{H}_{22}\text{NO}_2$ $[\text{M}+\text{H}]^+$: 308.1645, found 308.1648; $[\alpha]_{\text{D}}^{25} -102.3^\circ$ (c 1.12, CHCl_3 , 99% ee).



2-Naphthoyl Lactam 23: 2-Naphthoyl lactam **23** was isolated by flash chromatography (SiO_2 , 10 to 20% Et_2O in hexanes) as a colorless oil. 82.1% yield. $R_f = 0.42$ (35% Et_2O in hexanes); ^1H NMR (500 MHz, CDCl_3) δ 8.10 (dd, $J = 1.8, 0.8$ Hz, 1H), 7.93–7.76 (m, 3H), 7.63–7.43 (m, 3H), 5.87–5.67 (m, 1H), 5.21–5.06 (m, 2H), 3.95–3.84 (m, 1H), 3.84–3.72 (m, 1H), 2.58 (ddt, $J = 13.8, 7.1, 1.2$ Hz, 1H), 2.33 (ddt, $J = 13.7, 7.6, 1.1$ Hz, 1H), 2.12–1.89 (m, 3H), 1.71 (ddt, $J = 10.9, 4.9, 4.3, 2.4$ Hz, 1H), 1.34 (s, 3H); ^{13}C NMR (126 MHz, CDCl_3) δ 179.0, 175.3, 134.6, 133.7, 133.3, 132.5, 128.9, 128.1, 127.7, 127.7, 127.5, 126.4, 124.1, 118.9, 47.2, 44.0, 43.3, 33.3, 25.1, 19.5; IR (Neat Film NaCl) 3059, 2938, 2869, 1677, 1467, 1383, 1293, 1234, 1165, 1139, 923, 862, 822, 780, 762 cm^{-1} ; HRMS (FAB) m/z calc'd for $\text{C}_{20}\text{H}_{22}\text{NO}_2$ $[\text{M}+\text{H}]^+$: 308.1650, found 308.1638; $[\alpha]_{\text{D}}^{25} -257.4^\circ$ (c 0.92, CHCl_3 , 97% ee).

2.7.9 Procedures for the Derivatization of Lactam **3**



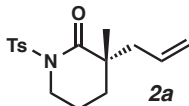
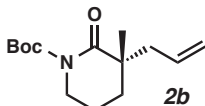
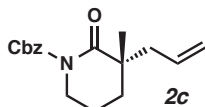
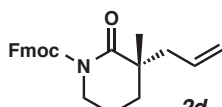
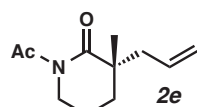
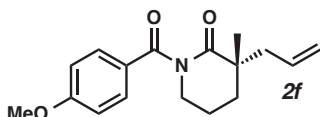
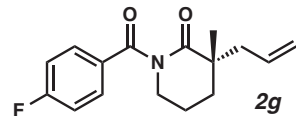
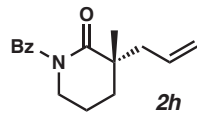
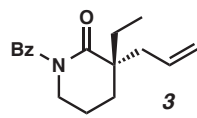
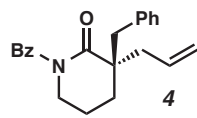
Piperidin-2-one 25: To a solution of lactam **3** (2.00 g, 7.37 mmol, 1.00 equiv) in MeOH (188 mL) was added a solution of LiOH•H₂O (464 mg, 11.1 mmol, 1.50 equiv) in H₂O (75 mL). After 20 h, the reaction mixture was concentrated under reduced pressure and diluted with saturated aqueous NaHCO₃ (100 mL) and EtOAc (75 mL). The phases were separated, and the aqueous phase was extracted with EtOAc (4 x 75 mL). The combined organic phases were washed with brine (2 x 30 mL), dried (Na₂SO₄), filtered, and concentrated under reduced pressure. The resulting oil was purified by flash chromatography (3 x 25 cm SiO₂, 40 to 60% EtOAc in hexanes) to afford known³⁰ lactam **25** as a colorless oil (1.18 g, 96% yield). $R_f = 0.21$ (50% EtOAc in hexanes); ¹H NMR (300 MHz, CDCl₃) δ 6.05 (br s, 1H), 5.88–5.66 (m, 1H), 5.12–4.95 (m, 2H), 3.25 (td, $J = 5.8, 1.9$ Hz, 2H), 2.48 (ddt, $J = 13.6, 6.7, 1.3$ Hz, 1H), 2.18 (ddt, $J = 13.6, 8.1, 1.0$ Hz, 1H), 1.87–1.62 (m, 5H), 1.49 (dq, $J = 13.5, 7.4$ Hz, 1H), 0.89 (t, $J = 7.5$ Hz, 3H); $[\alpha]_D^{25} - 13.7^\circ$ (c 0.57, CHCl₃, 99% ee).

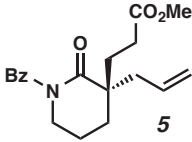
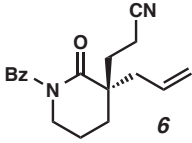
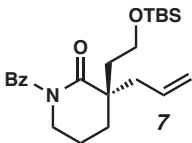
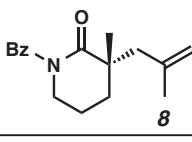
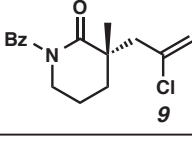
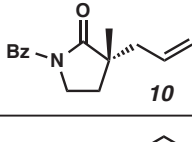
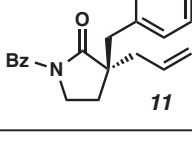
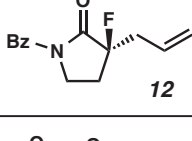
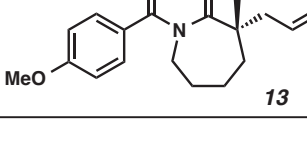
Piperidine 26: To a solution of piperidin-2-one **25** (250 mg, 1.49 mmol, 1.00 equiv) in ether (14.9 mL) was added lithium aluminum hydride (170 mg, 4.48 mmol, 3.0 equiv) (*Caution: Gas evolution and exotherm*). After stirring at ambient temperature for 5 min, the reaction mixture was heated to reflux for 36 h, cooled (0 °C), and quenched with saturated aqueous K₂CO₃ (20 mL, *Caution: Gas evolution and exotherm*). The phases were separated, and the aqueous phase was extracted with Et₂O (4 x 75 mL). The combined organic phases were washed with brine (2 x 30 mL), dried (Na₂SO₄), filtered, and concentrated under reduced pressure to provide piperidine **26** (206 mg, 90% yield) as a colorless oil. $R_f = 0.29$ (20% MeOH in DCM); ¹H NMR (500 MHz, CDCl₃) δ 5.76 (ddt,

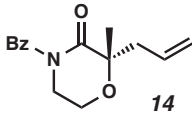
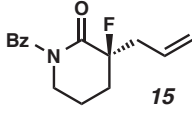
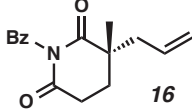
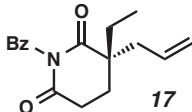
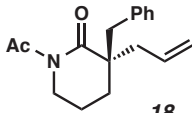
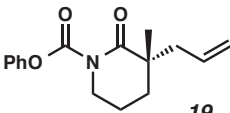
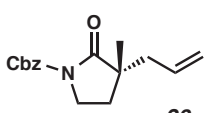
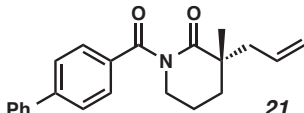
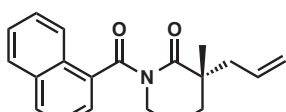
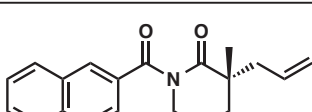
$J = 16.4, 10.6, 7.5$ Hz, 1H), 5.10–4.96 (m, 2H), 2.81–2.68 (m, 2H), 2.53 (dd, $J = 13.0, 20.0$ Hz, 2H), 2.06 (d, $J = 7.5$ Hz, 2H), 2.02 (br s, 1H), 1.55–1.42 (m, 2H), 1.40–1.30 (m, 2H), 1.32 (q, $J = 7.5$ Hz, 2H), 0.80 (t, $J = 7.6$ Hz, 3H); ^{13}C NMR (126 MHz, CDCl_3) δ 134.6, 116.9, 55.1, 47.0, 39.2, 34.9, 33.6, 27.7, 22.4, 7.1; IR (Neat Film NaCl) 3298, 3073, 2963, 2931, 2853, 2799, 1638, 1462, 1125, 996, 911 cm^{-1} ; HRMS (MM: ESI-APCI) m/z calc'd for $\text{C}_{10}\text{H}_{20}\text{N}$ $[\text{M}+\text{H}]^+$: 154.1590, found 154.1590; $[\alpha]_{\text{D}}^{25} -7.5^\circ$ (c 0.80, MeOH, 96% ee).

2.7.10 Methods for the Determination of Enantiomeric Excess

Table 2.5 Analytical HPLC and SFC assays and retention times

entry	product	assay conditions	retention time of major isomer (min)	retention time of minor isomer (min)	% ee
1	 2a	HPLC Chiralpak AD-H 5% EtOH in hexanes isocratic, 1.0 mL/min 254 nm	19.10	15.77	75
2	 2b	HPLC Chiralcel OJ-H 0.1% IPA in hexanes isocratic, 1.0 mL/min 220 nm	15.22	18.10	81
3	 2c	HPLC Chiralcel OJ-H 3% EtOH in hexanes isocratic, 1.0 mL/min 220 nm	18.68	17.60	86
4	 2d	HPLC Chiralcel OD 3% EtOH in hexanes isocratic, 1.0 mL/min 254 nm	28.89	21.47	89
5	 2e	HPLC Chiralcel OJ 1% IPA in hexanes isocratic, 1.0 mL/min 254 nm	10.15	9.71	91
6	 2f	HPLC Chiralcel OD-H 3% IPA in hexanes isocratic, 1.0 mL/min 254 nm	15.73	18.12	99
7	 2g	HPLC Chiralcel OJ-H 2% IPA in hexanes isocratic, 1.0 mL/min 254 nm	29.12	19.74	99
8	 2h	HPLC Chiralcel OJ-H 5% IPA in hexanes isocratic, 1.0 mL/min 254 nm	32.97	31.16	99
9	 3	SFC Chiralcel OJ-H 3% MeOH in CO ₂ isocratic, 5.0 mL/min 254 nm	3.85	2.49	99
10	 4	SFC Chiralcel OD-H 10% MeOH in CO ₂ isocratic, 5.0 mL/min 254 nm	3.84	3.20	99

entry	product	assay conditions	retention time of major isomer (min)	retention time of minor isomer (min)	% ee
11	 5	HPLC Chiralpak AD-H 3% EtOH in hexane isocratic, 1.0 mL/min 254 nm	32.69	27.83	99
12	 6	SFC Chiralpak IC 10% MeOH in CO ₂ isocratic, 5.0 mL/min 254 nm	2.67	3.84	99
13	 7	HPLC Chiralcel OJ-H 3% IPA in hexane isocratic, 1.0 mL/min 254 nm	7.75	5.95	96
14	 8	HPLC Chiralcel OJ-H 8% IPA in hexane isocratic, 1.0 mL/min 254 nm	25.94	19.12	97
15	 9	HPLC Chiralpak AD 2% IPA in hexane isocratic, 1.0 mL/min 254 nm	18.72	27.05	95
16	 10	SFC Chiralcel OJ-H 10% MeOH in CO ₂ isocratic, 5.0 mL/min 254 nm	2.93	1.84	98
17	 11	SFC Chiralcel OJ-H 5% MeOH in CO ₂ isocratic, 5.0 mL/min 254 nm	2.31	3.73	93
18	 12	SFC Chiralpak AD-H 15% MeOH in CO ₂ isocratic, 5.0 mL/min 254 nm	4.16	5.05	99
19	 13	HPLC Chiralcel OJ-H 5% IPA in hexane isocratic, 1.0 mL/min 254 nm	29.16	24.82	93

entry	product	assay conditions	retention time of major isomer (min)	retention time of minor isomer (min)	% ee
20	 14	SFC Chiralpak AD-H 10% MeOH in CO ₂ isocratic, 5.0 mL/min 254 nm	1.96	1.41	99
21	 15	SFC Chiralcel OJ-H 5% MeOH in CO ₂ isocratic, 5.0 mL/min 254 nm	2.55	2.25	99
22	 16	SFC Chiralcel OJ-H 3% MeOH in CO ₂ isocratic, 5.0 mL/min 254 nm	3.05	2.72	94
23	 17	SFC Chiralcel OJ-H 3% MeOH in CO ₂ isocratic, 5.0 mL/min 254 nm	3.28	2.87	96
24	 18	SFC Chiralpak AD-H 3% MeOH in CO ₂ isocratic, 3.0 mL/min 235 nm	4.03	4.69	88
25	 19	SFC Chiralcel OB-H 10% MeOH in CO ₂ isocratic, 5.0 mL/min 210 nm	2.65	2.39	94
26	 20	SFC Chiralpak AD-H 15% MeOH in CO ₂ isocratic, 5.0 mL/min 210 nm	4.23	2.51	91
27	 21	SFC Chiralcel OJ-H 10% MeOH in CO ₂ isocratic, 5.0 mL/min 254 nm	4.53	3.80	99
28	 22	SFC Chiralcel OB-H 10% MeOH in CO ₂ isocratic, 5.0 mL/min 210 nm	4.05	4.60	99
29	 23	SFC Chiralpak AD-H 20% MeOH in CO ₂ isocratic, 5.0 mL/min 254 nm	3.73	2.93	97

2.8 Notes and References

- (1) Cordell, G. A., Ed. *The Alkaloids: Chemistry And Biology*. In *Alkaloids*; Elsevier: San Diego, 2010; Vol. 69, p. 609.
- (2) Joule, J. A.; Mills, K. *Heterocycles in Medicine*. In *Heterocyclic Chemistry*, 5th Ed; Wiley: Chichester, 2010.
- (3) Anton, A.; Baird, B. R. *Polyamides, fibers*. *Kirk-Othmer Encyclopedia of Chemical Technology* (5th Ed.) **2006**, 19, 739–772.
- (4) Schlack, P. *Pure Appl. Chem.* **1967**, 15, 507–523.
- (5) Kohan, M. I., Ed. *Nylon*. In *Plastics*; Interscience: New York, 1973.
- (6) Groaning, M. D.; Meyers, A. I. *Tetrahedron* **2000**, 56, 9843–9873.
- (7) Enders, D.; Teschner, P.; Raabe, G.; Runsink, J. *Eur. J. Org. Chem.* **2001**, 4463–4477.
- (8) Amat, M.; Lozano, O.; Escolano, C.; Molins, E.; Bosch, J. *J. Org. Chem.* **2007**, 72, 4431–4439.
- (9) Trost, B. M.; Brennan, M. K. *Synthesis* **2009**, 3003–3025.
- (10) Badillo, J. J.; Hanhan, N. V.; Franz, A. K. *Curr. Opin. Drug Disc. Dev.* **2010**, 13, 758–776.
- (11) Zhou, F.; Liu, Y.-L.; Zhou, J. *Adv. Synth. Catal.* **2010**, 352, 1381–1407.
- (12) Moss, T. A.; Alonso, B.; Fenwick, D. R.; Dixon, D. J. *Angew. Chem., Int. Ed.* **2010**, 49, 568–571.
- (13) Trost, B. M. *J. Org. Chem.* **2004**, 69, 5813–5837.
- (14) Lu, Z.; Ma, S. *Angew. Chem., Int. Ed.* **2008**, 47, 258–297.
- (15) Mohr, J. T.; Stoltz, B. M. *Chem. Asian J.* **2007**, 2, 1476–1491.

-
- (16) Weaver, J. D.; Recio, A., III.; Grenning, A. J.; Tunge, J. A. *Chem. Rev.* **2011**, *111*, 1846–1913.
- (17) Behenna, D. C.; Stoltz, B. M. *J. Am. Chem. Soc.* **2004**, *126*, 15044–15045.
- (18) Mohr, J. T.; Behenna, D. C.; Harned, A. M.; Stoltz, B. M. *Angew. Chem., Int. Ed.* **2005**, *44*, 6924–6927.
- (19) Seto, M.; Roizen, J. L.; Stoltz, B. M. *Angew. Chem., Int. Ed.* **2008**, *47*, 6873–6876.
- (20) Streuff, J.; White, D. E.; Virgil, S. C.; Stoltz, B. M. *Nature Chem.* **2010**, *2*, 192–196.
- (21) McFadden, R. M.; Stoltz, B. M. *J. Am. Chem. Soc.* **2006**, *128*, 7738–7739.
- (22) White, D. E.; Stewart, I. C.; Grubbs, R. H.; Stoltz, B. M. *J. Am. Chem. Soc.* **2008**, *130*, 810–811.
- (23) Enquist, J. A., Jr.; Stoltz, B. M. *Nature* **2008**, *453*, 1228–1231.
- (24) Day, J. J.; McFadden, R. M.; Virgil, S. C.; Kolding, H.; Alleva, J. L.; Stoltz, B. M. *Angew. Chem., Int. Ed.* **2011**, *50*, 6814–6818.
- (25) McDougal, N. T.; Virgil, S. C.; Stoltz, B. M. *Synlett* **2010**, 1712–1716.
- (26) Helmchen, G.; Pfaltz, A. *Acc. Chem. Res.* **2000**, *33*, 336–345.
- (27) Tani, K.; Behenna, D. C.; McFadden, R. M.; Stoltz, B. M. *Org. Lett.* **2007**, *9*, 2529–2531.
- (28) McDougal, N. T.; Streuff, J.; Mukherjee, H.; Virgil, S. C.; Stoltz, B. M. *Tetrahedron Lett.* **2010**, *51*, 5550–5554.
- (29) Edler, M. C.; Yang, G.; Jung, M. K.; Bai, R.; Bornmann, W. G.; Hamel, E. *Arch. Biochem. Biophys.* **2009**, *487*, 98–104.
- (30) Magnus, P.; Rainey, T. *Tetrahedron* **2001**, *57*, 8647–8651.

-
- (31) Compound **27** can be prepared by methylation of diallyl malonate in a manner analogous to dimethyl 2-methylmalonate or by esterification of 2-methyl malonic acid, see: (a) Hosokawa, T.; Yamanaka, T.; Itotani, M.; Murahashi, S.-I. *J. Org. Chem.* **1995**, *60*, 6159–6167. (b) Imao, D.; Itoi, A.; Yamazaki, A.; Shirakura, M.; Ohtoshi, R.; Ogata, K.; Ohmori, Y.; Ohta, T.; Ito, Y. *J. Org. Chem.* **2007**, *72*, 1652–1658.
- (32) Tsuzuki, Y.; Chiba, K.; Mizuno, K.; Tomita, K.; Suzuki, K. *Tetrahedron: Asymmetry* **2001**, *12*, 2989–2997.
- (33) The palladium source was chosen solely to simplify the chromatographic separation of the dba from the lactam product.

APPENDIX 1

Spectra Relevant to Chapter 2

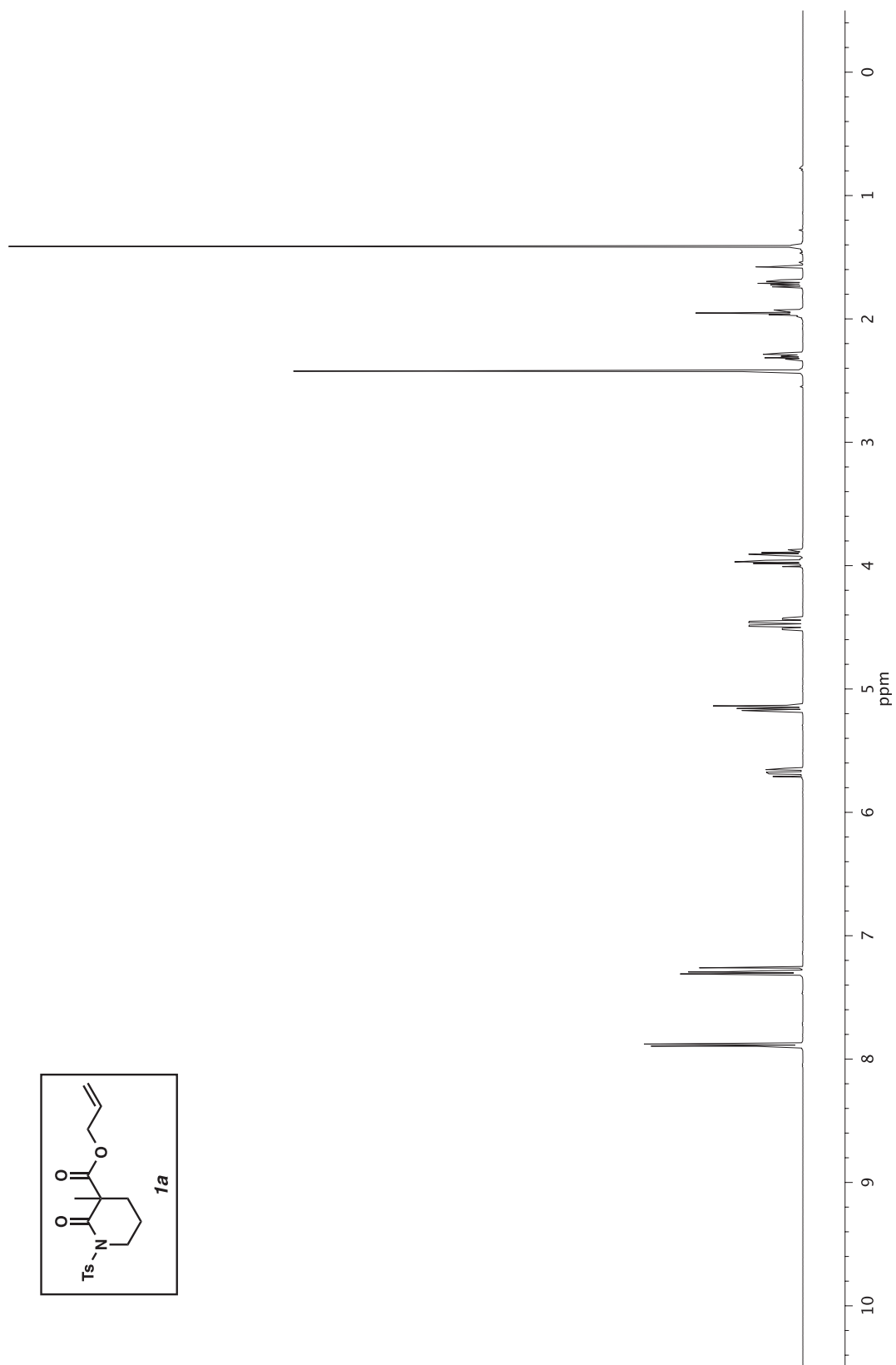


Figure A1.1 ¹H NMR (500 MHz, CDCl₃) of compound **1a**.

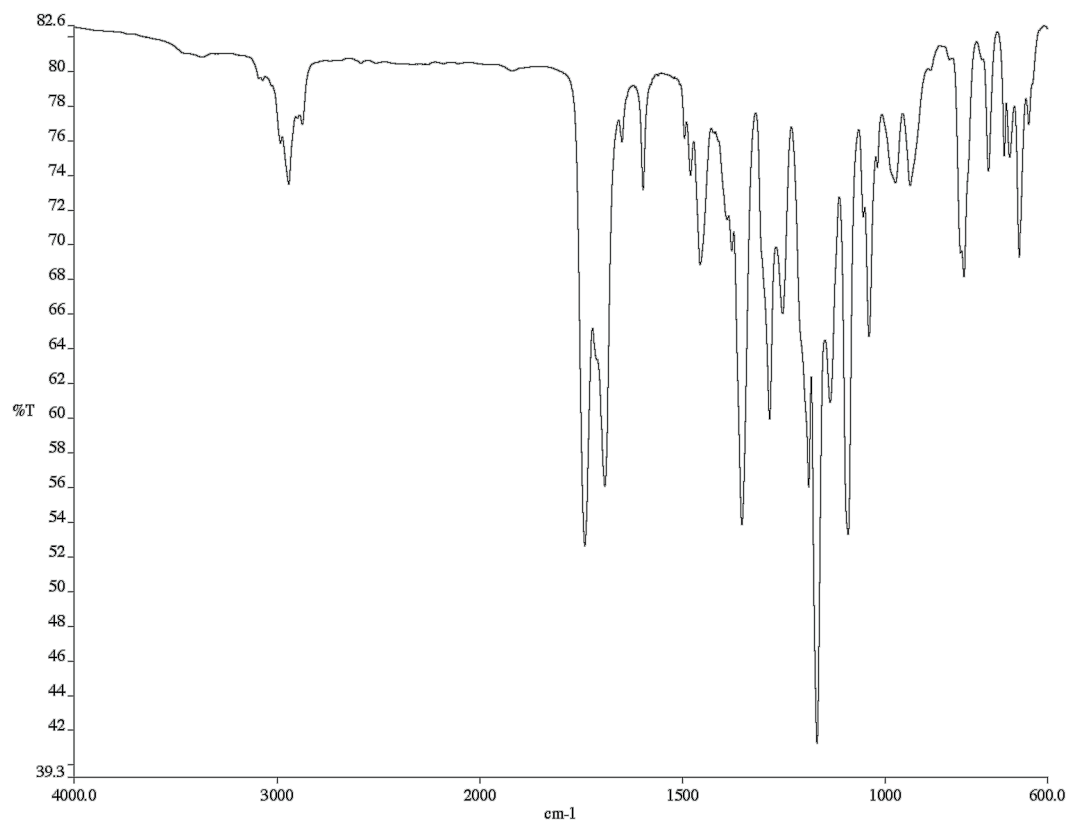


Figure A1.2 Infrared spectrum (Thin Film, NaCl) of compound **1a**.

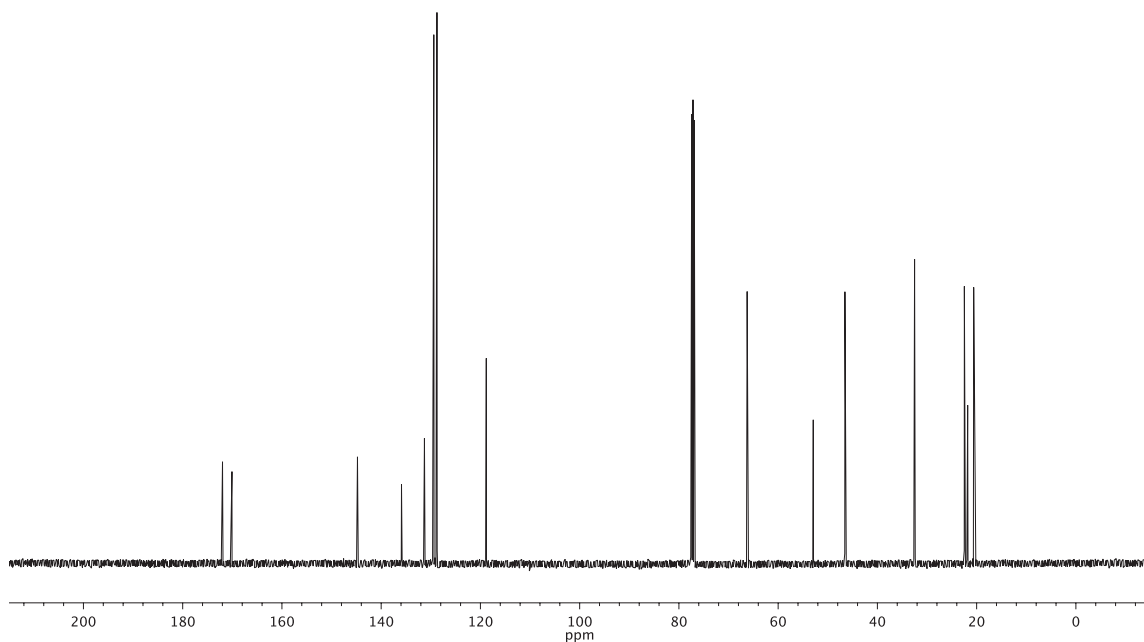


Figure A1.3 ¹³C NMR (126 MHz, CDCl₃) of compound **1a**.

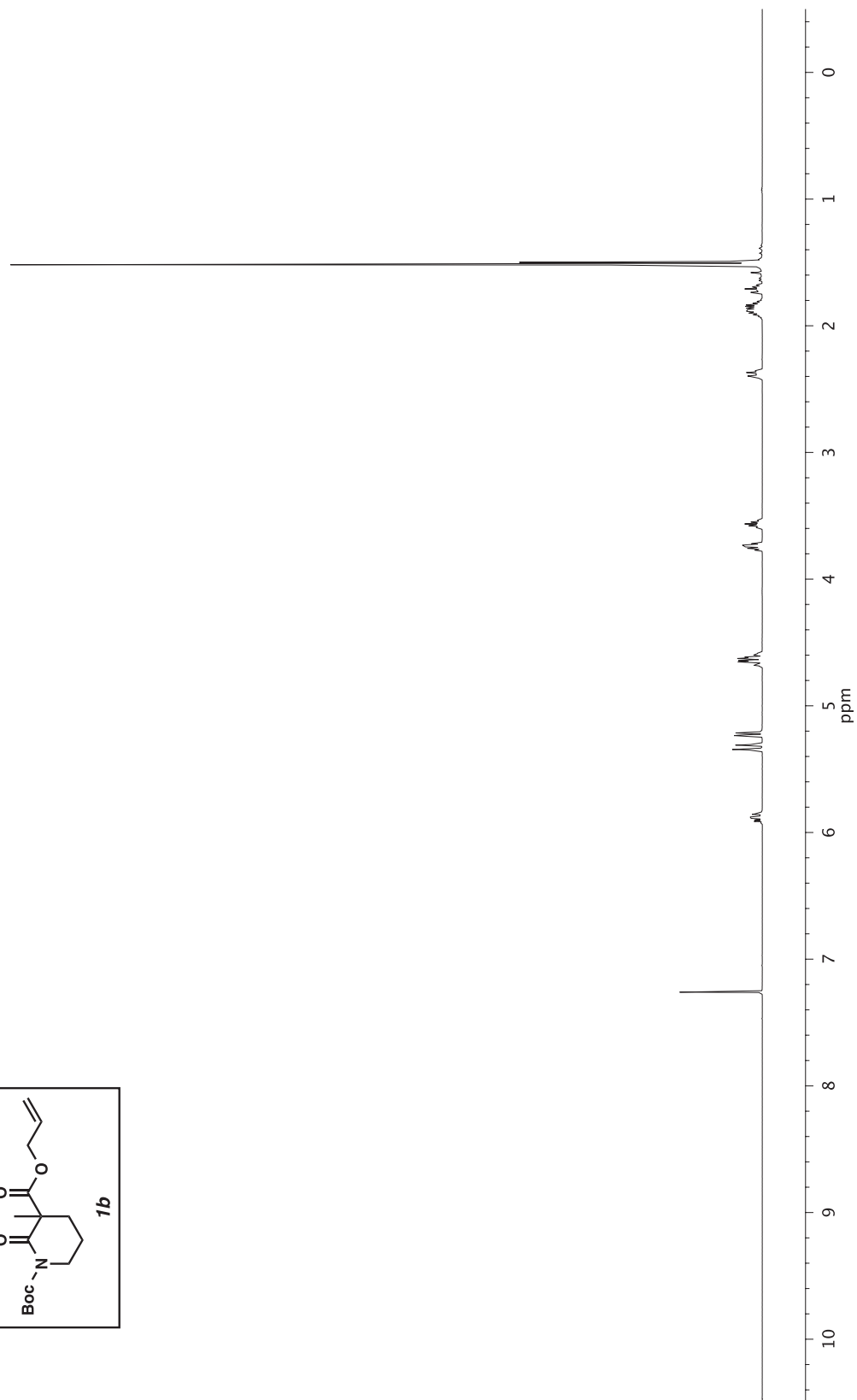
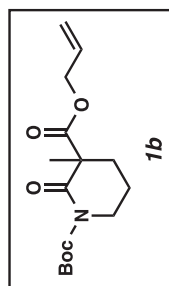


Figure A1.4 ^1H NMR (500 MHz, CDCl_3) of compound **1b**.

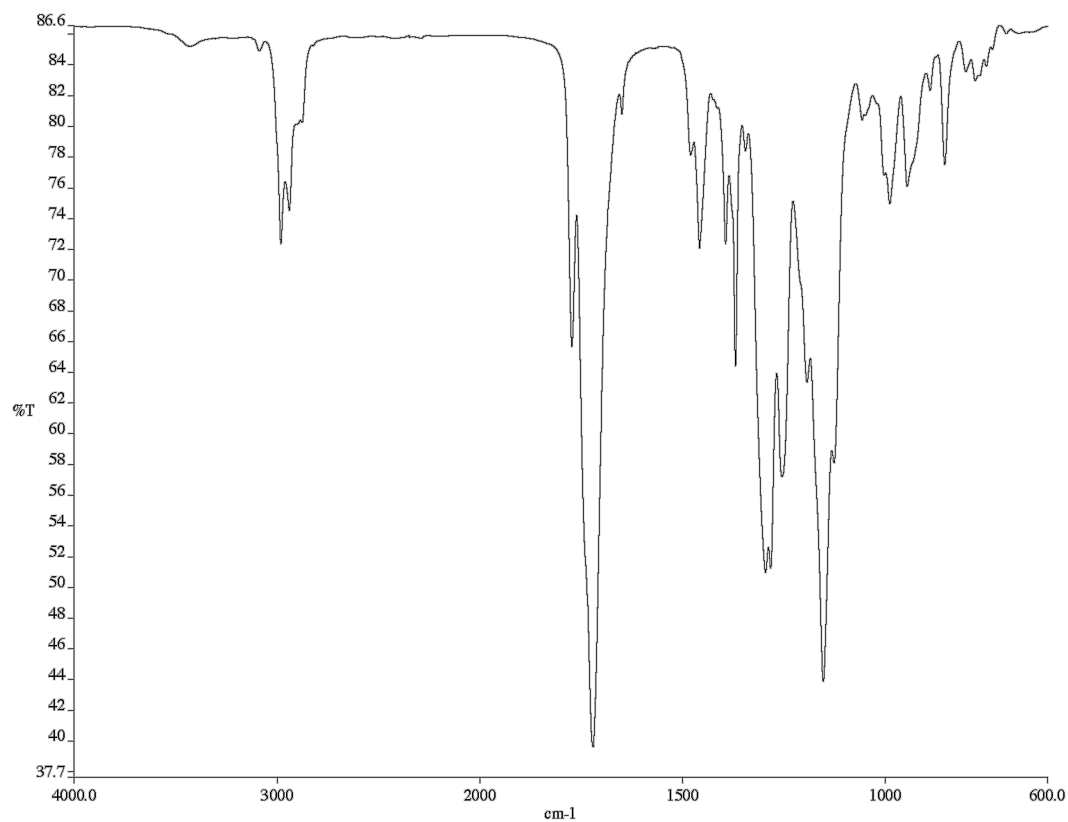


Figure A1.5 Infrared spectrum (Thin Film, NaCl) of compound **1b**.

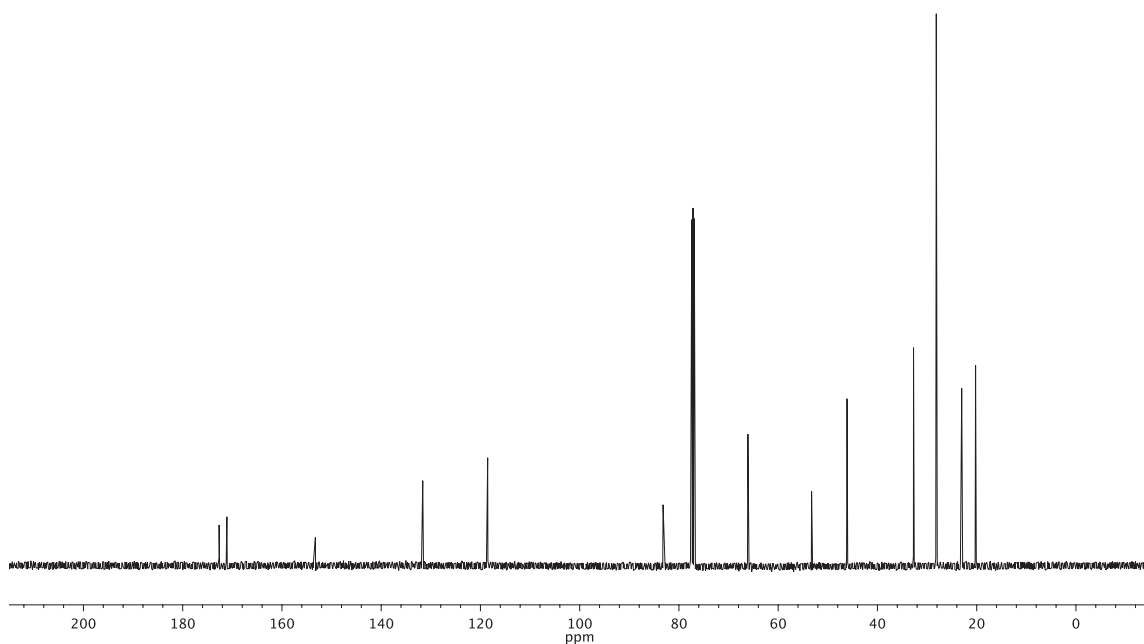


Figure A1.6 ¹³C NMR (126 MHz, CDCl₃) of compound **1b**.

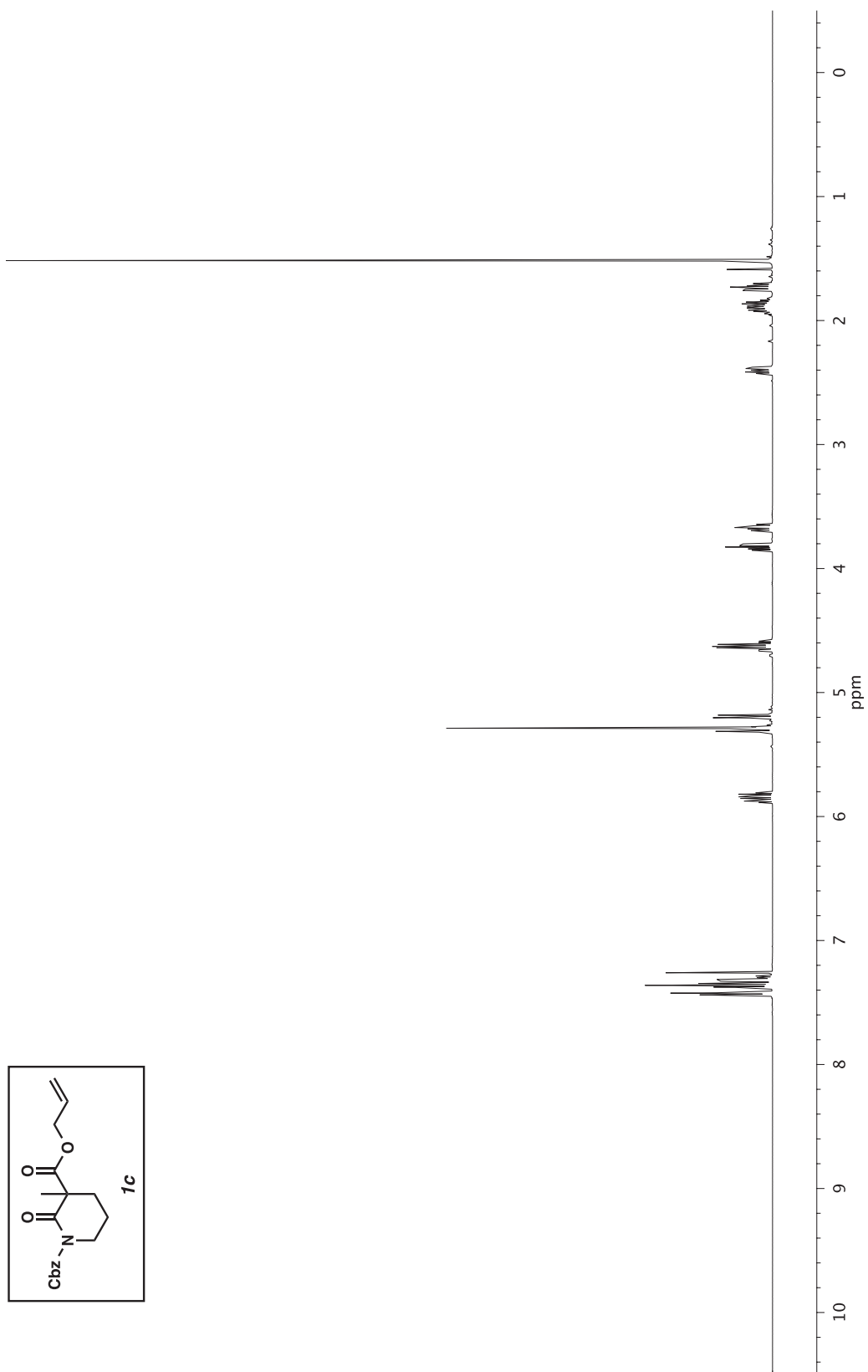


Figure A1.7 ¹H NMR (500 MHz, CDCl₃) of compound **1c**.

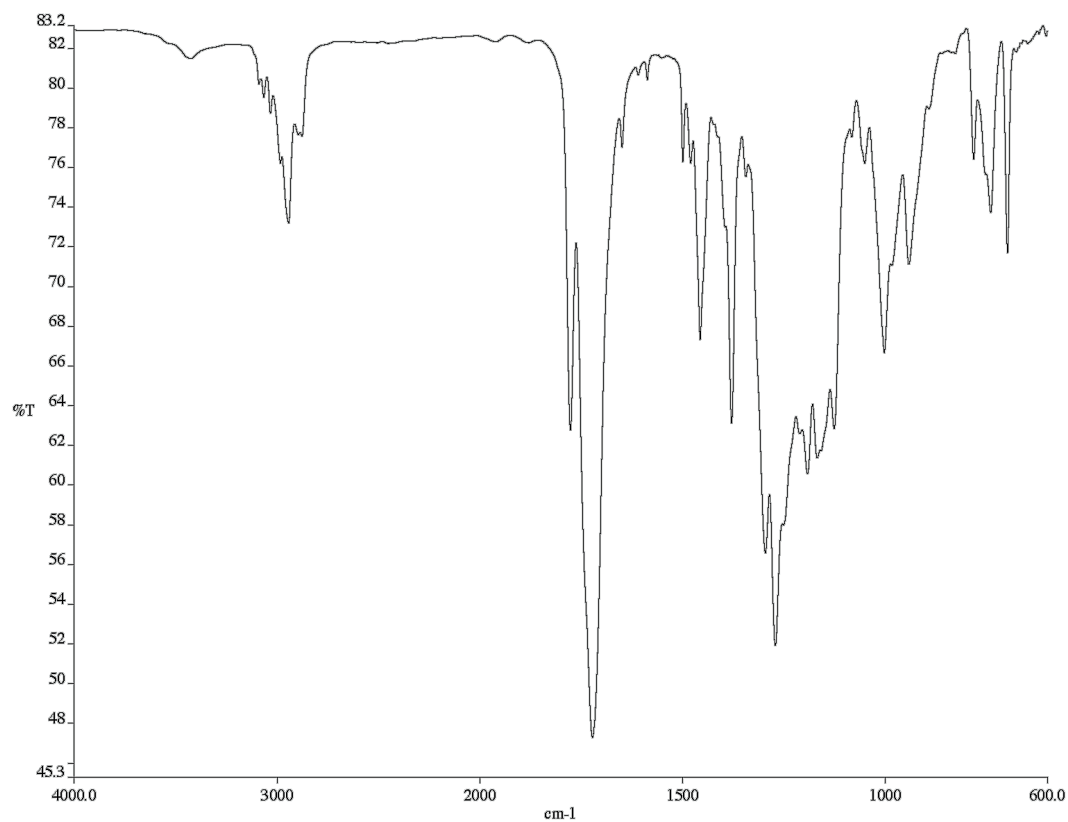


Figure A1.8 Infrared spectrum (Thin Film, NaCl) of compound **1c**.

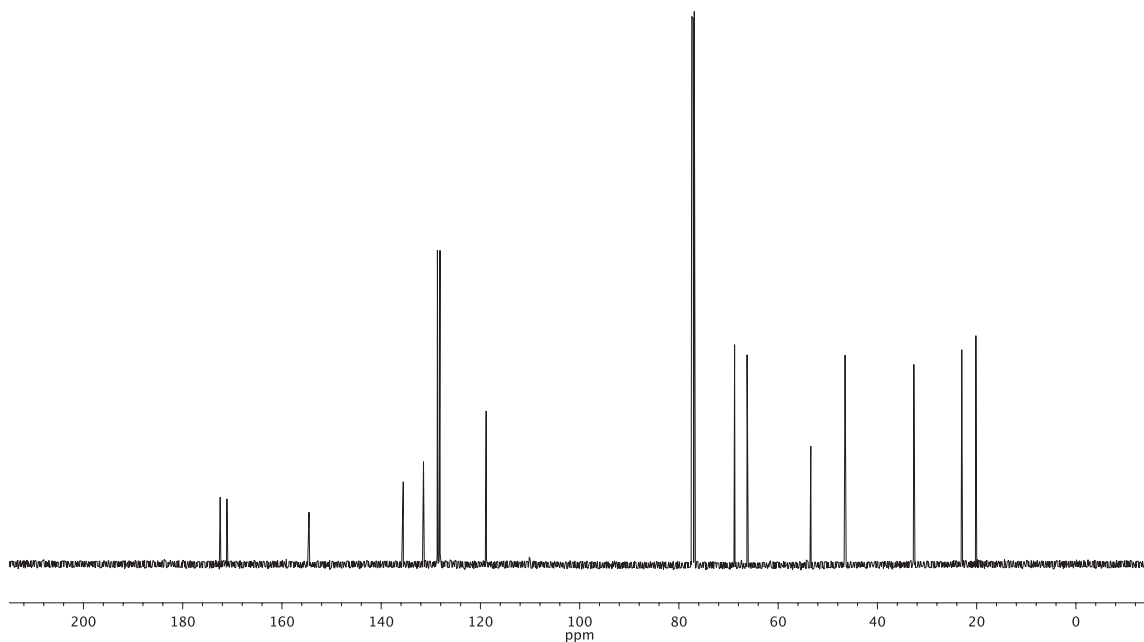


Figure A1.9 ¹³C NMR (126 MHz, CDCl₃) of compound **1c**.

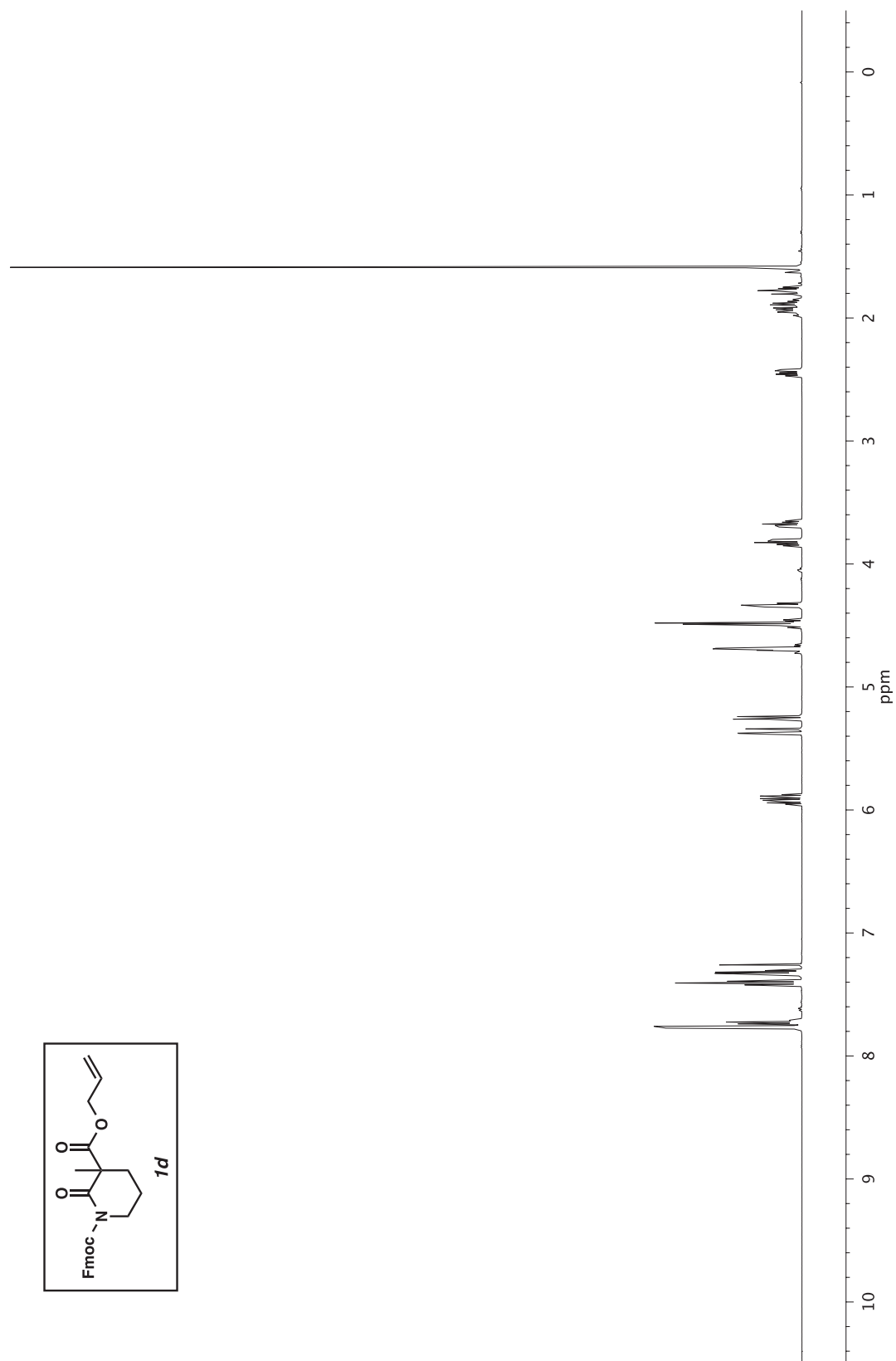


Figure A1.10 ¹H NMR (500 MHz, CDCl₃) of compound **1d**.

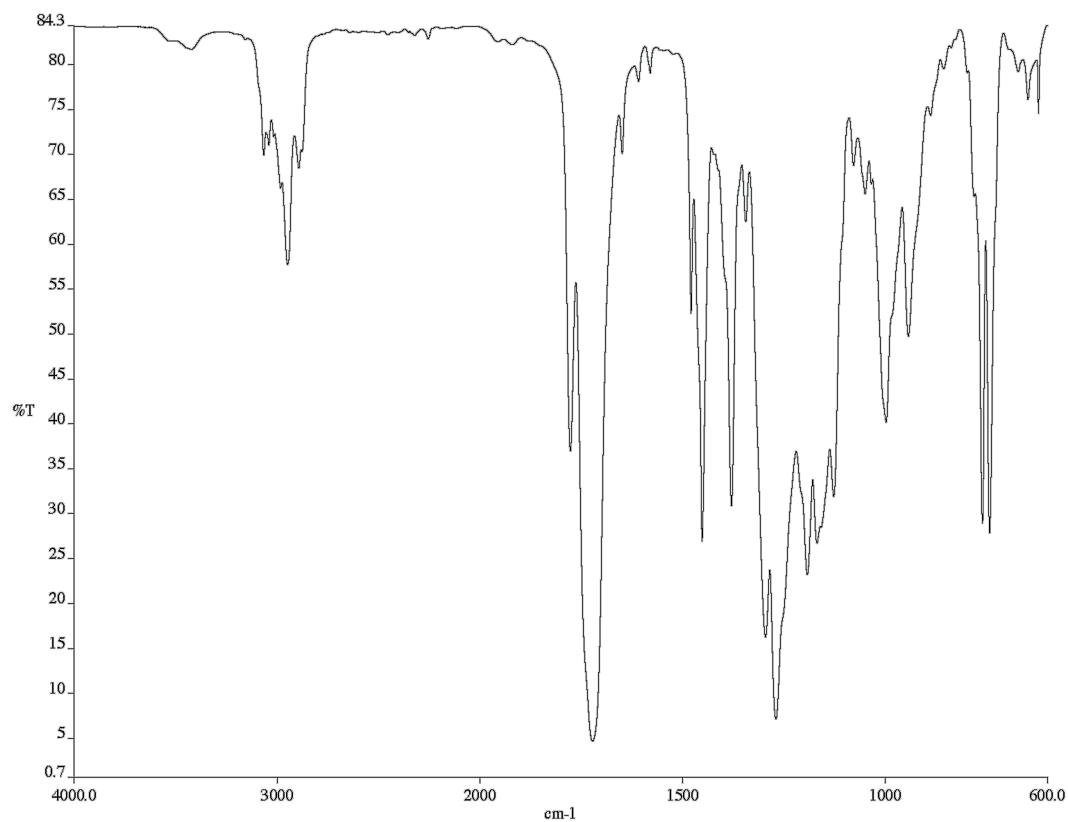


Figure A1.11 Infrared spectrum (Thin Film, NaCl) of compound **1d**.

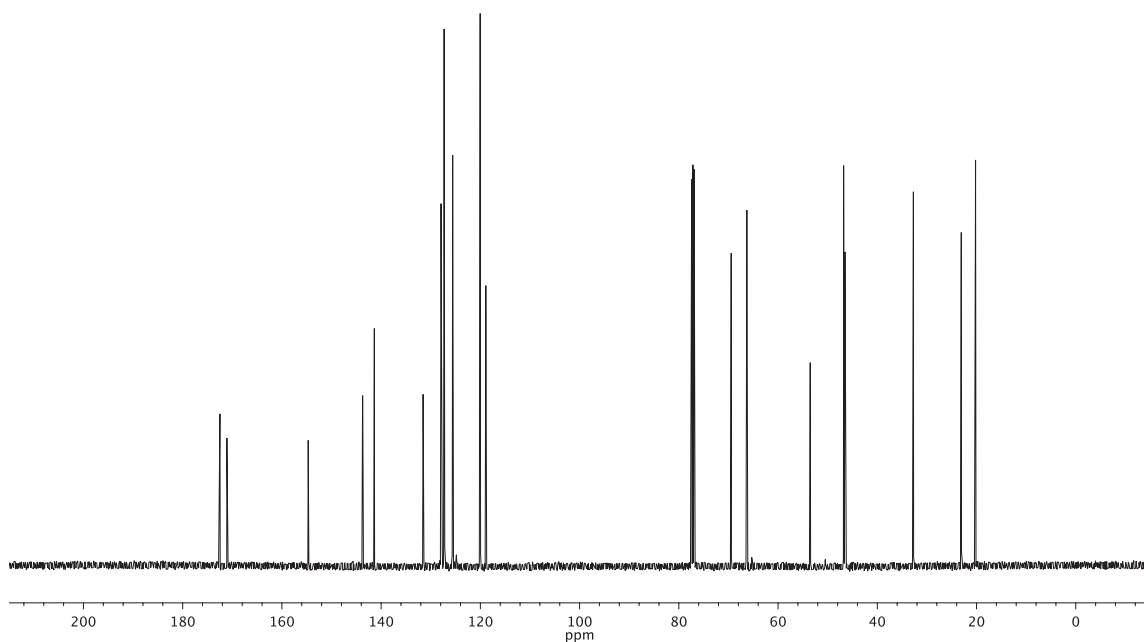


Figure A1.12 ¹³C NMR (126 MHz, CDCl₃) of compound **1d**.

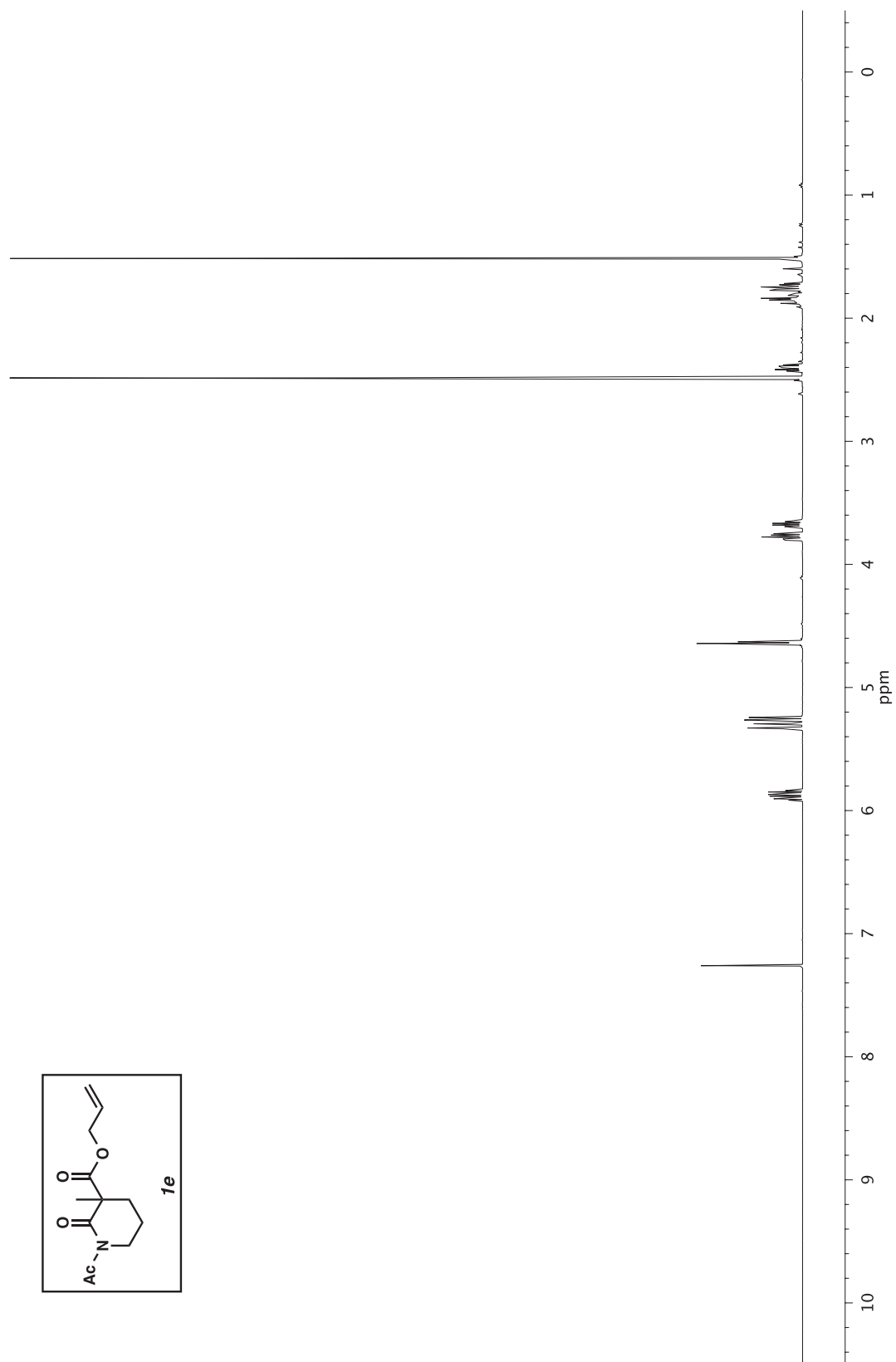


Figure A1.13 ^1H NMR (500 MHz, CDCl_3) of compound **1e**.

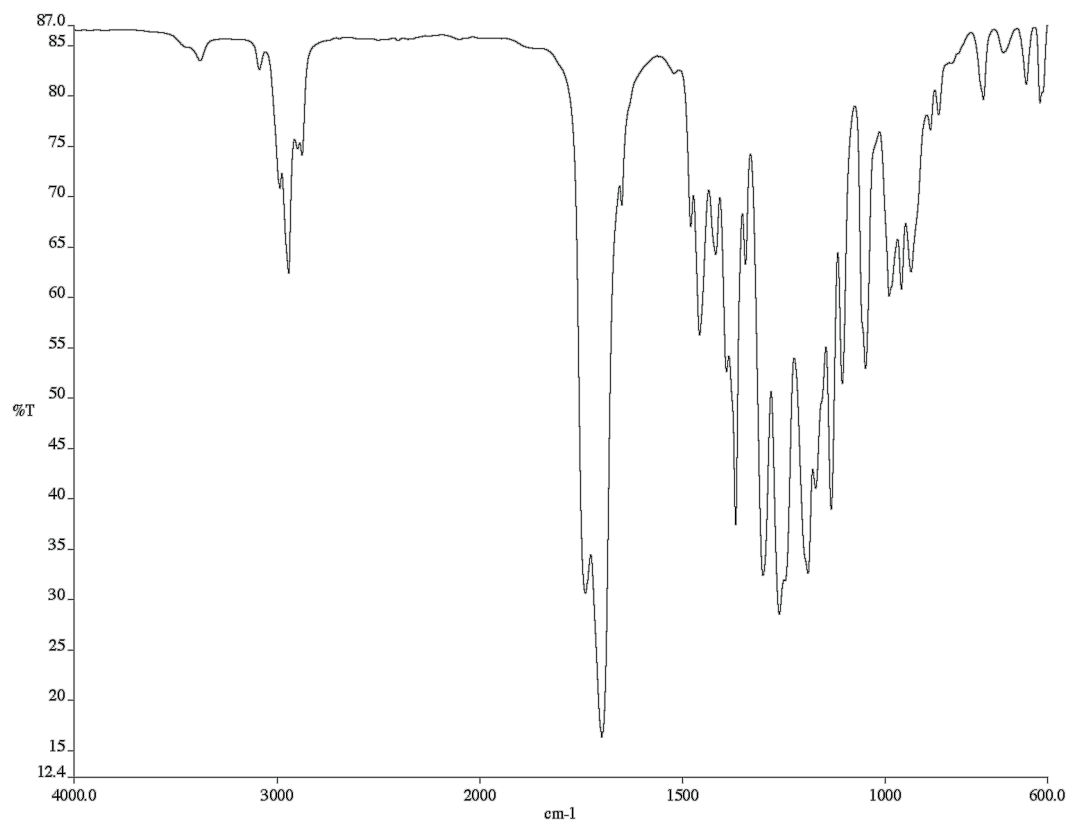


Figure A1.14 Infrared spectrum (Thin Film, NaCl) of compound **1e**.

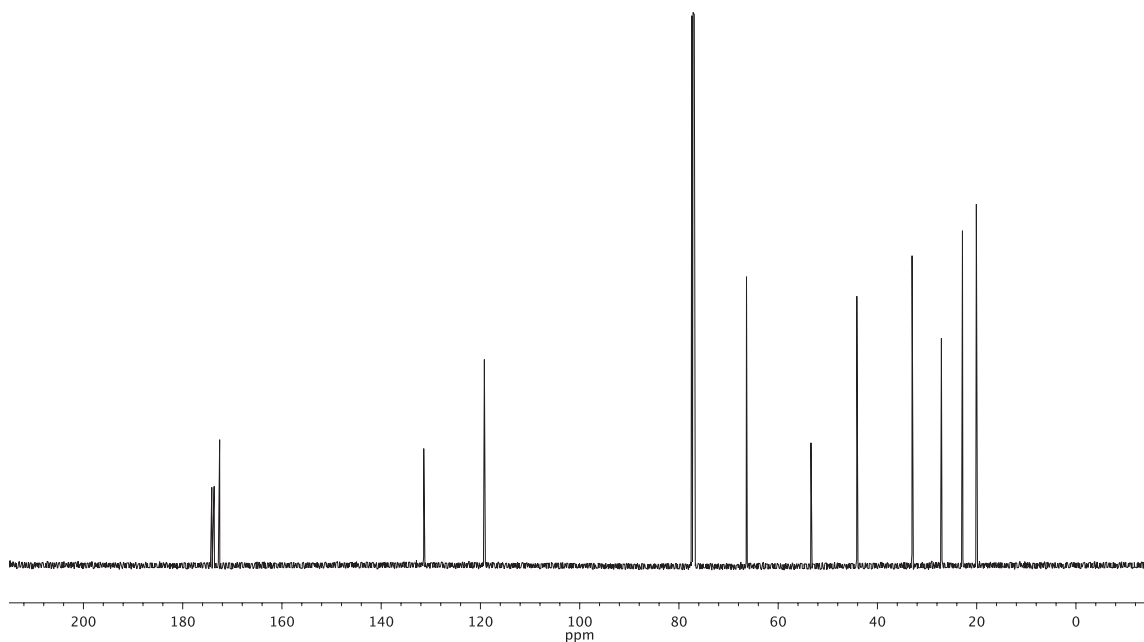


Figure A1.15 ¹³C NMR (126 MHz, CDCl₃) of compound **1e**.

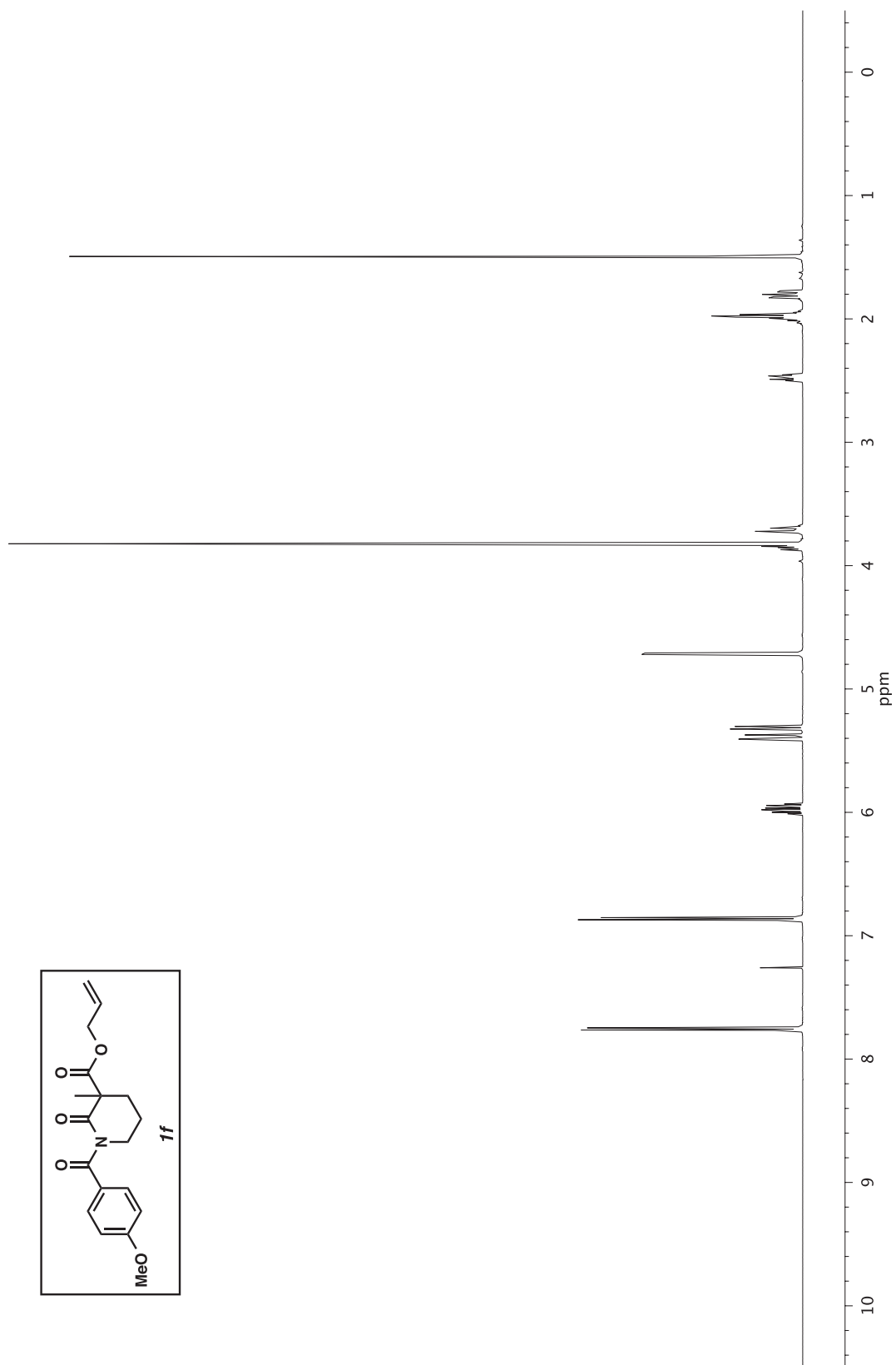


Figure A1.16 ^1H NMR (500 MHz, CDCl_3) of compound **1f**.

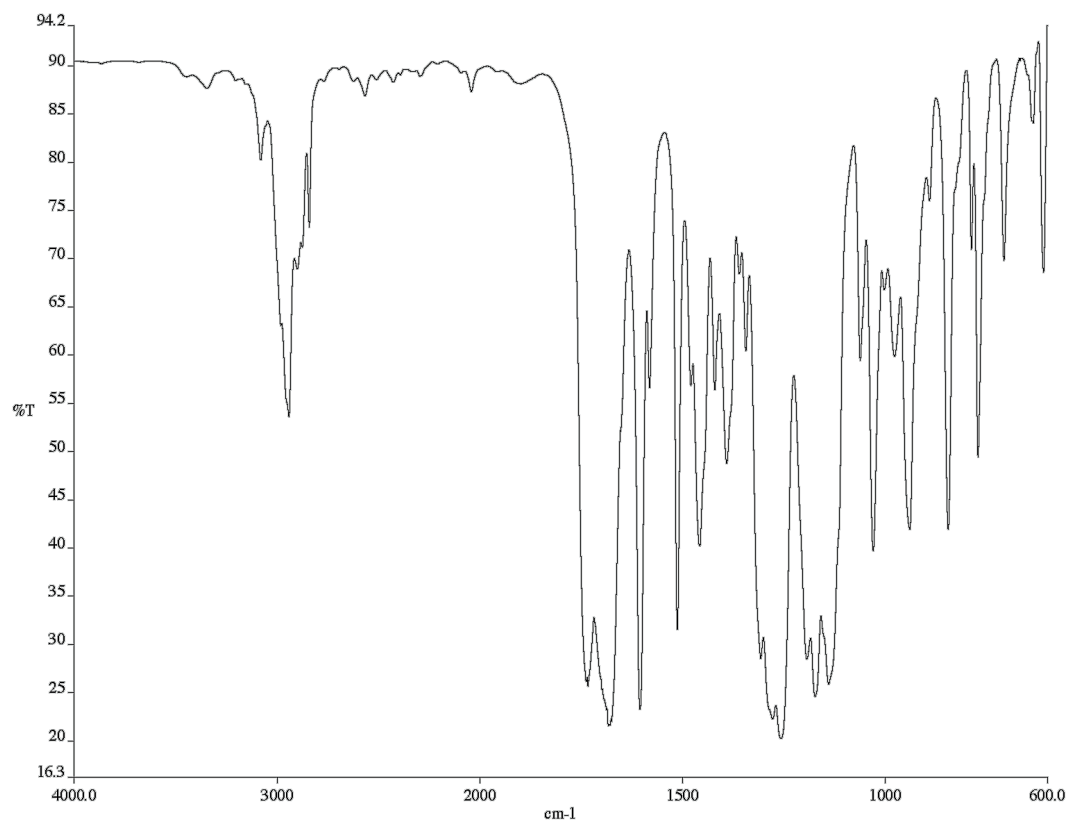


Figure A1.17 Infrared spectrum (Thin Film, NaCl) of compound **1f**.

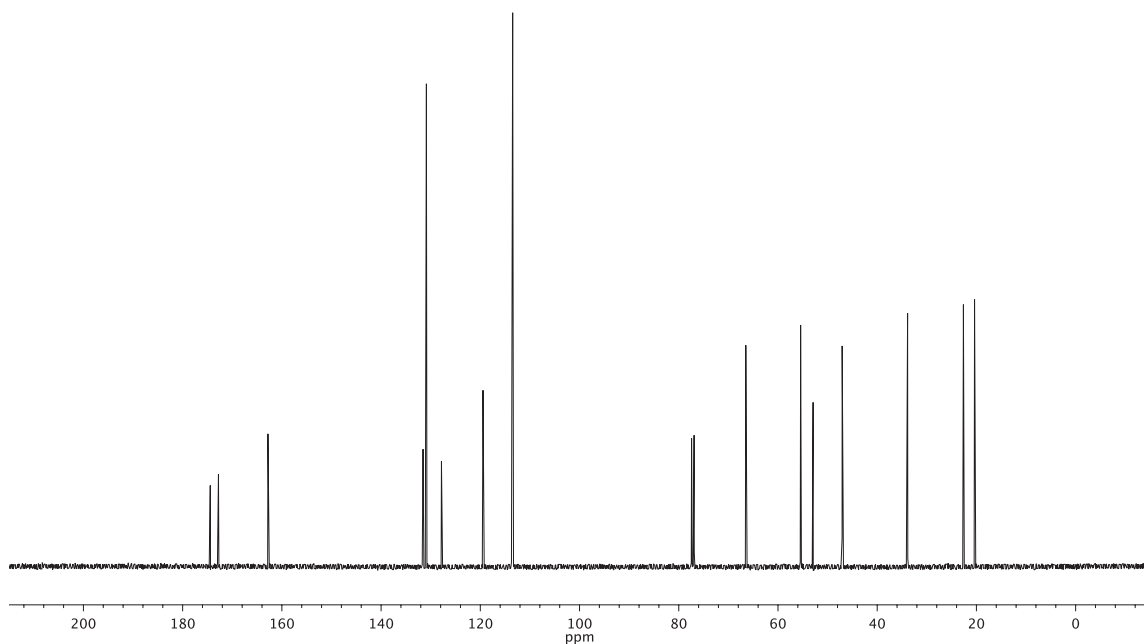


Figure A1.18 ¹³C NMR (126 MHz, CDCl₃) of compound **1f**.

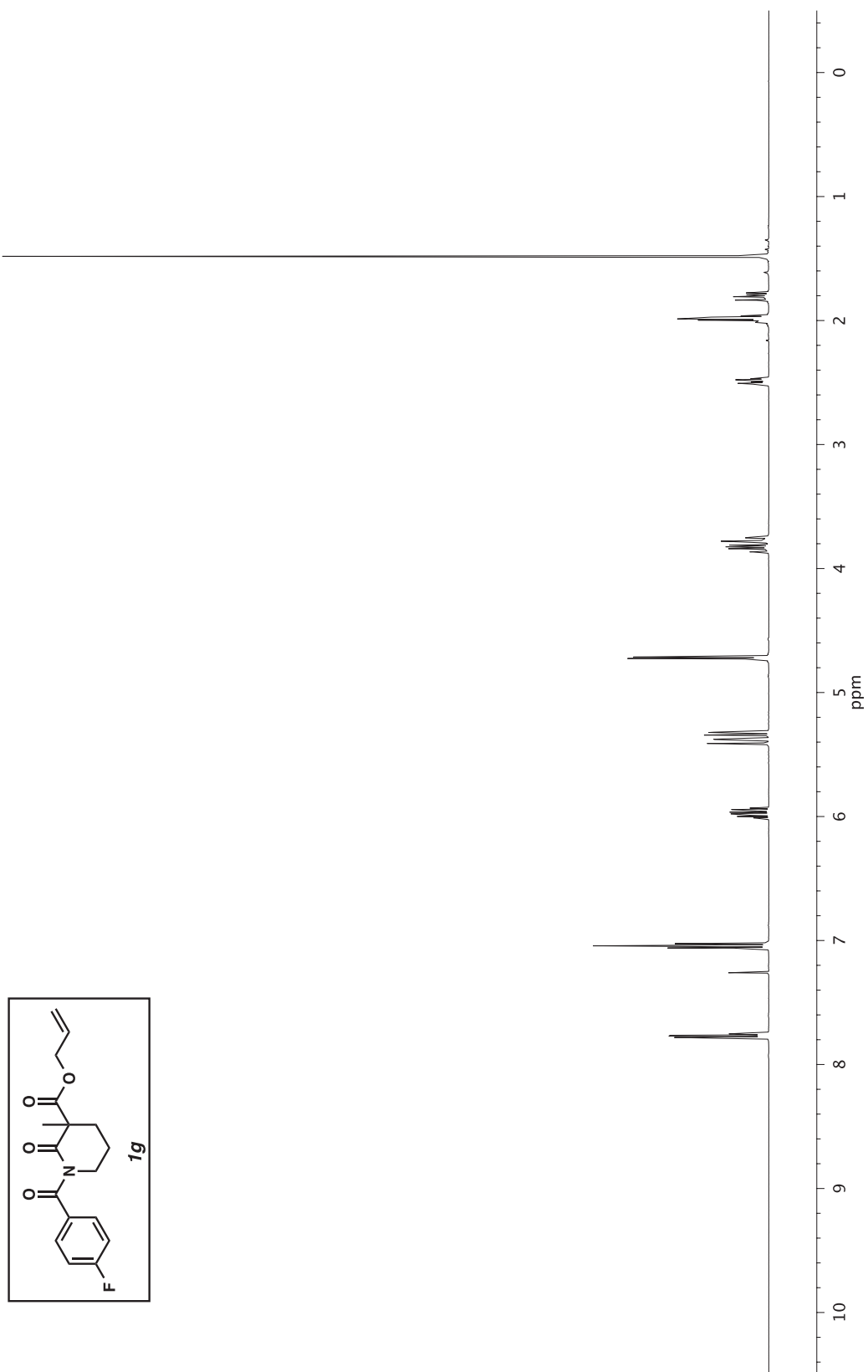


Figure A1.19 ¹H NMR (500 MHz, CDCl₃) of compound **1g**.

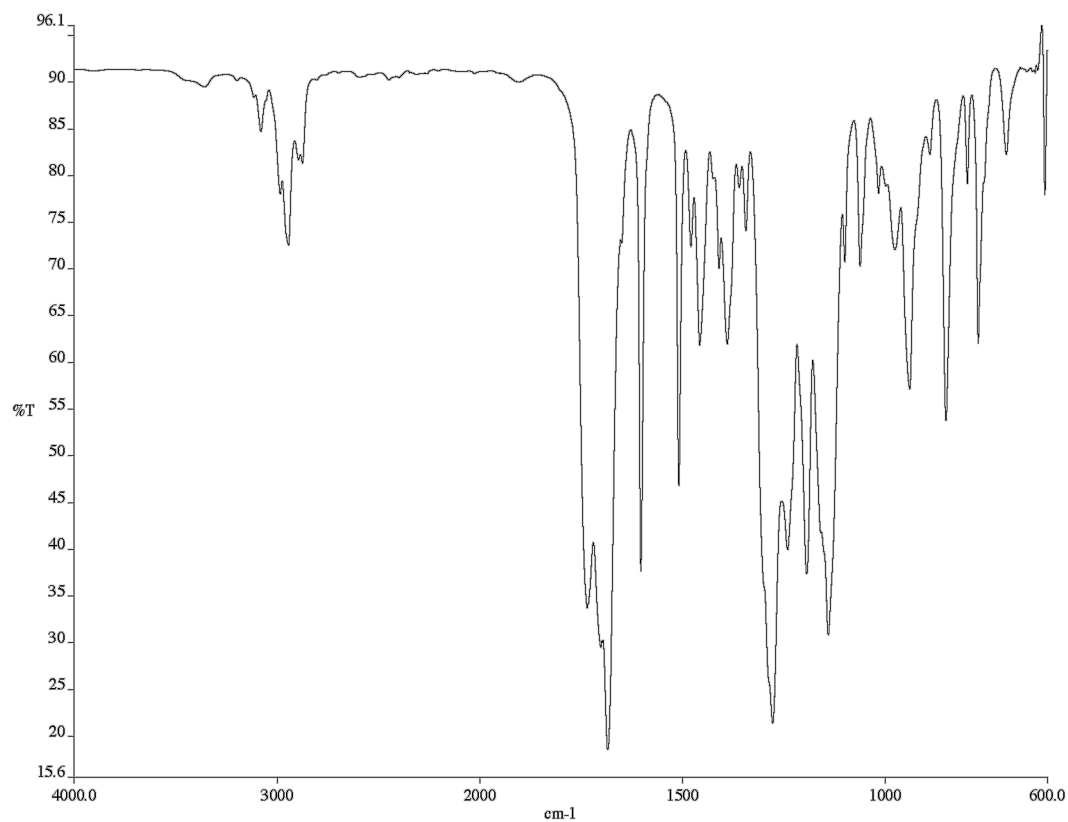


Figure A1.20 Infrared spectrum (Thin Film, NaCl) of compound **1g**.

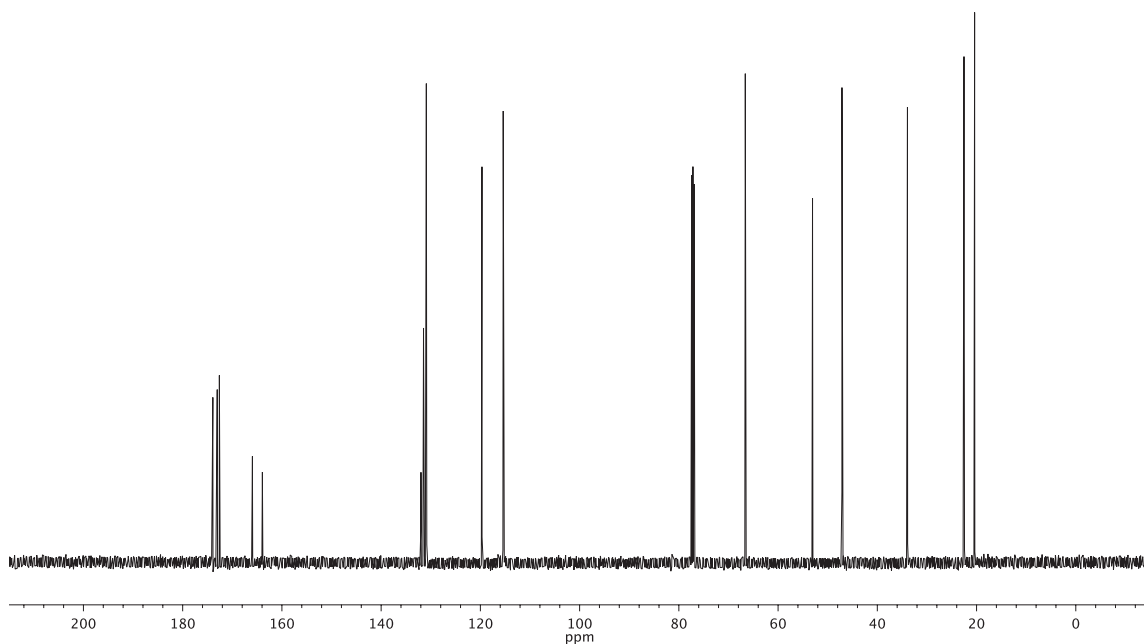


Figure A1.21 ^{13}C NMR (126 MHz, CDCl_3) of compound **1g**.

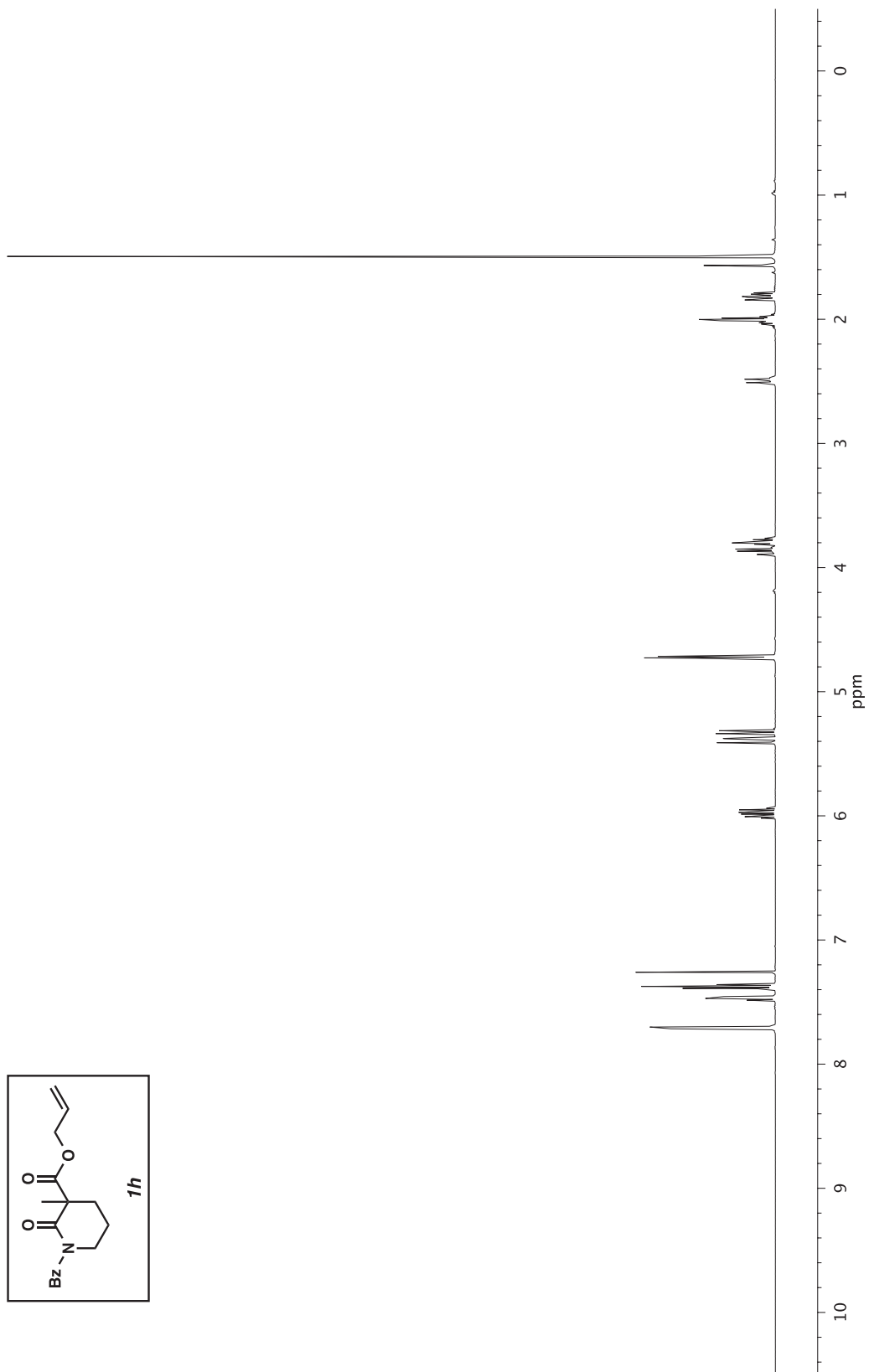


Figure A1.22 ¹H NMR (500 MHz, CDCl₃) of compound **1h**.

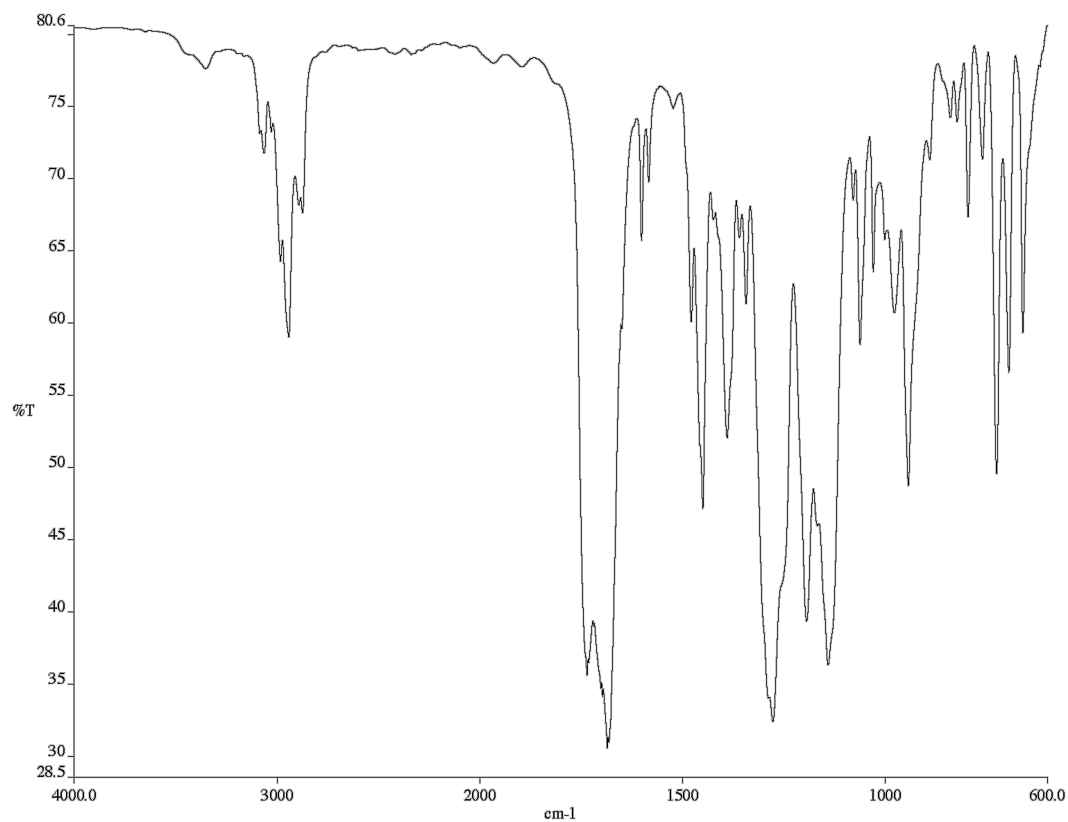


Figure A1.23 Infrared spectrum (Thin Film, NaCl) of compound **1h**.

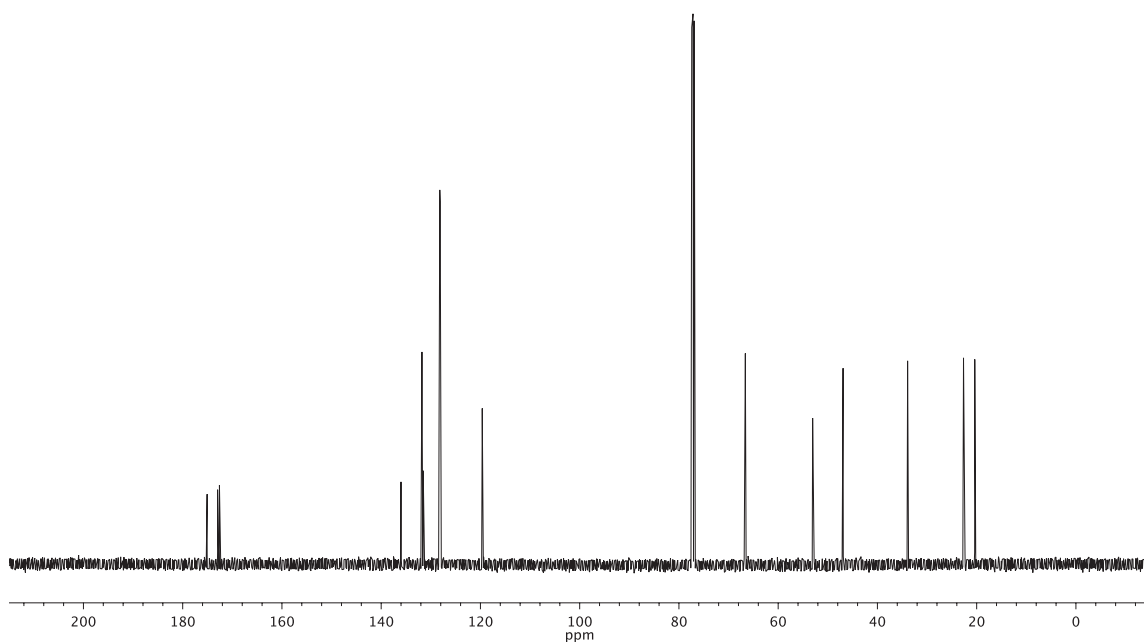


Figure A1.24 ¹³C NMR (126 MHz, CDCl₃) of compound **1h**.

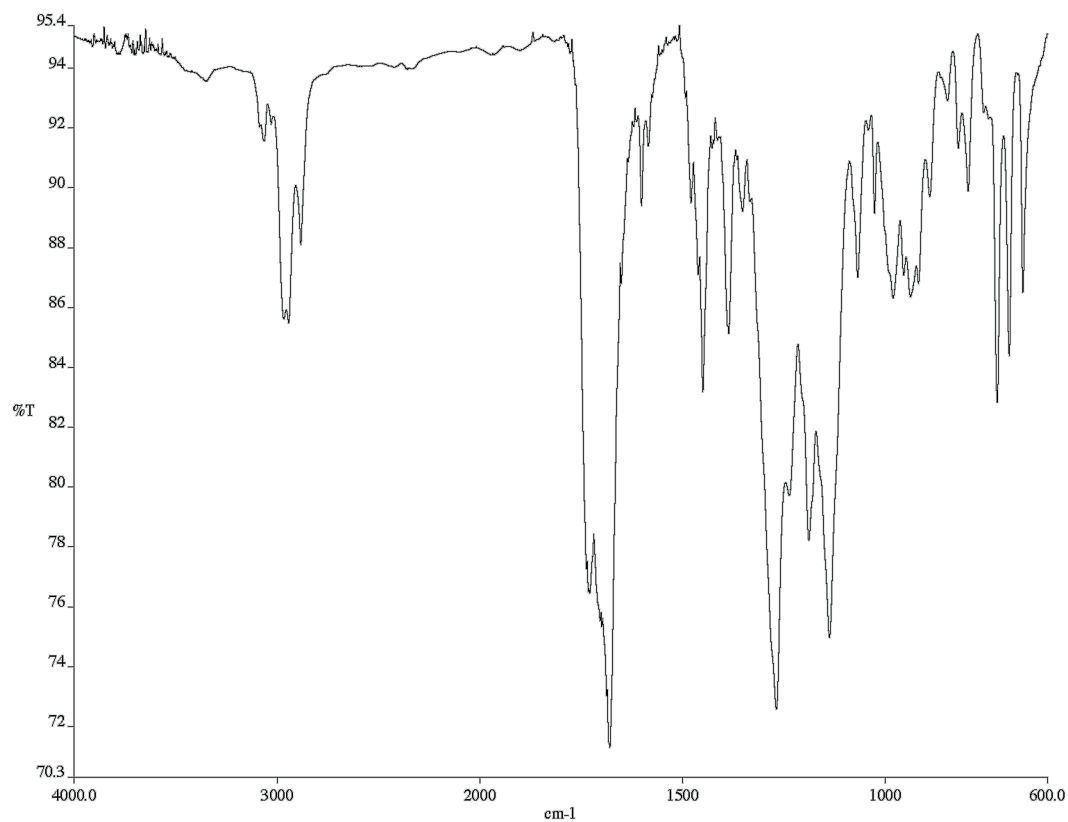


Figure A1.26 Infrared spectrum (Thin Film, NaCl) of compound **24**.

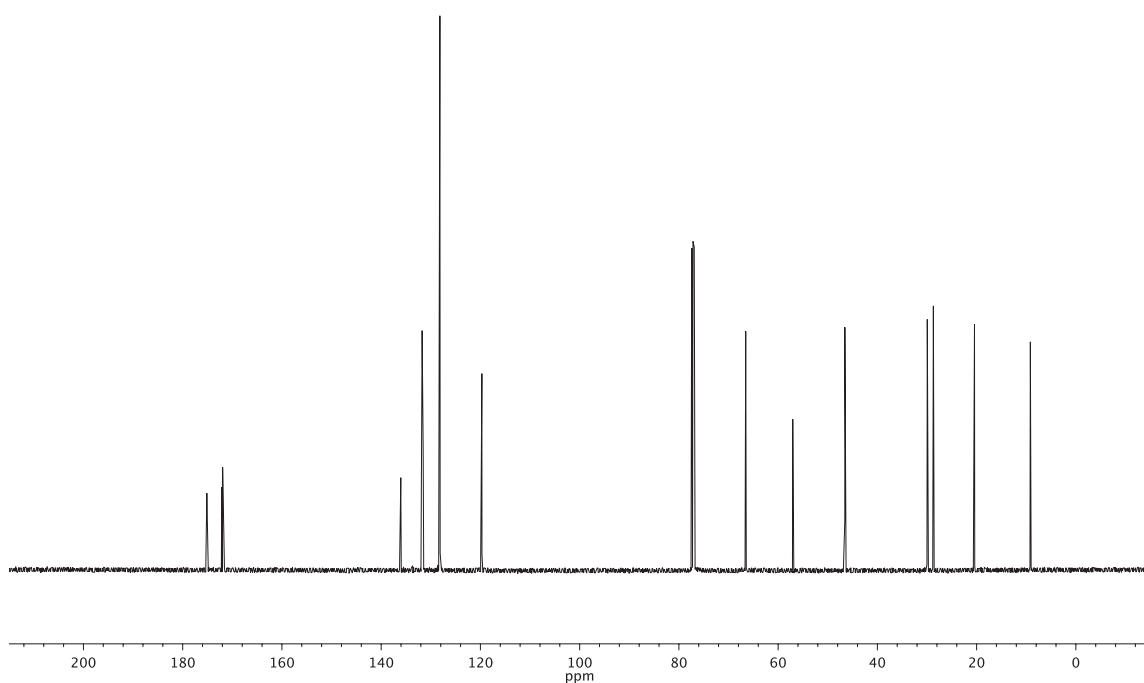


Figure A1.27 ¹³C NMR (126 MHz, CDCl₃) of compound **24**.

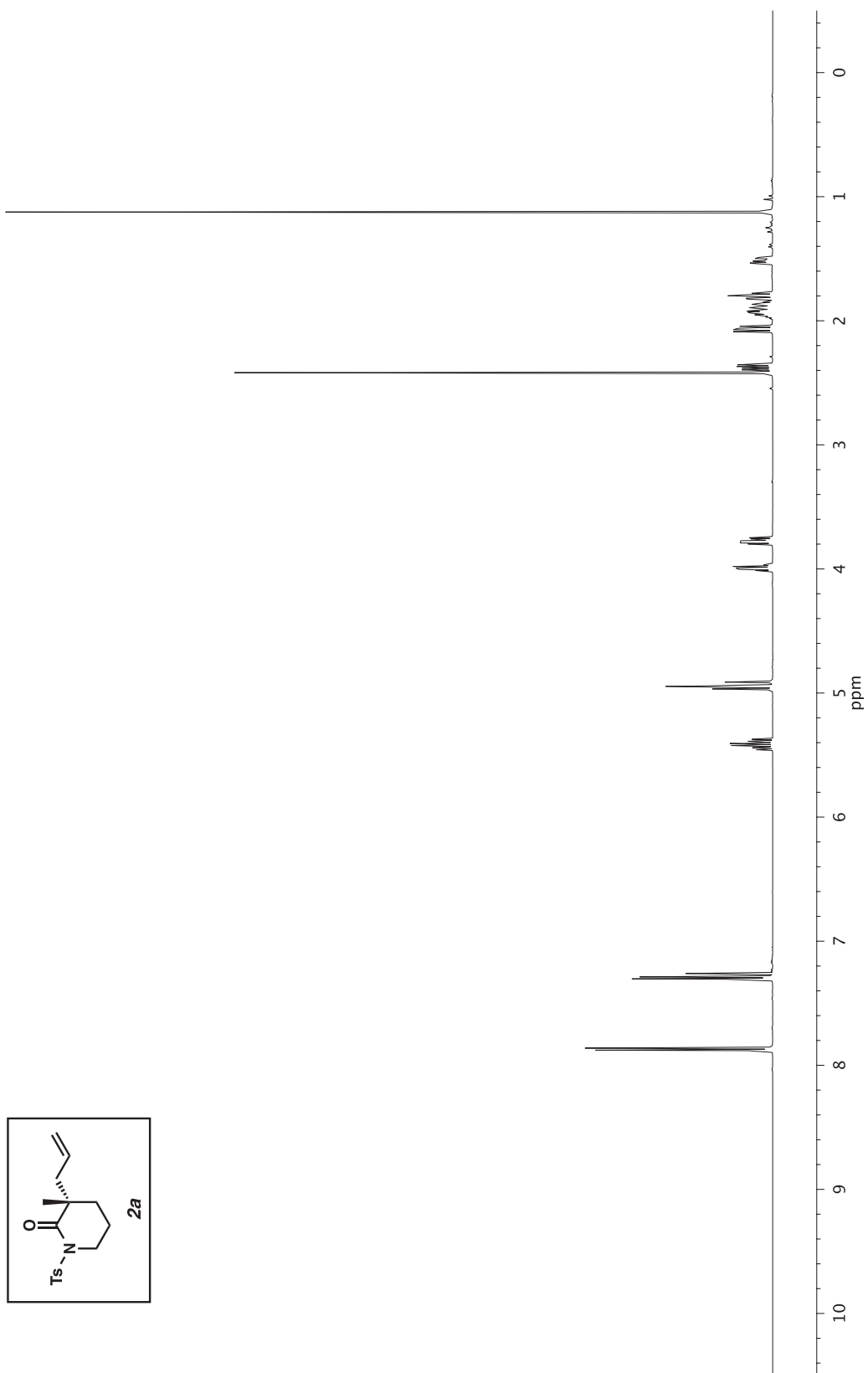


Figure A1.28 ^1H NMR (500 MHz, CDCl_3) of compound **2a**.

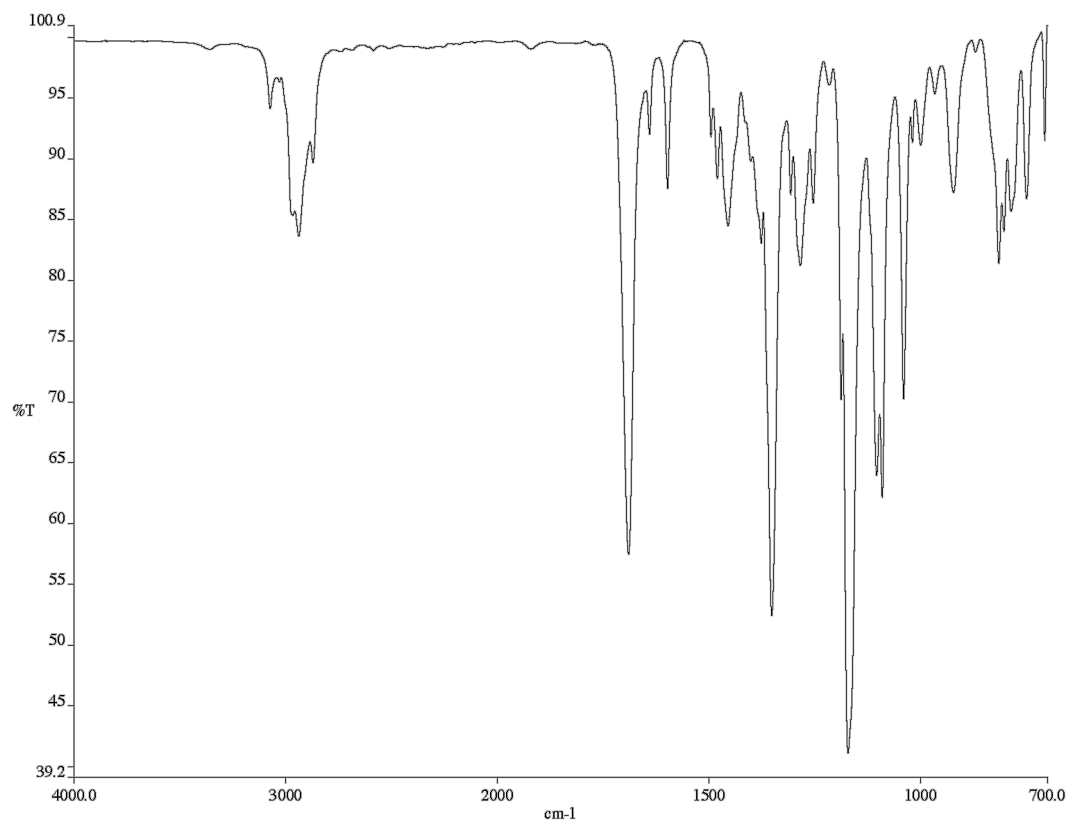


Figure A1.29 Infrared spectrum (Thin Film, NaCl) of compound **2a**.

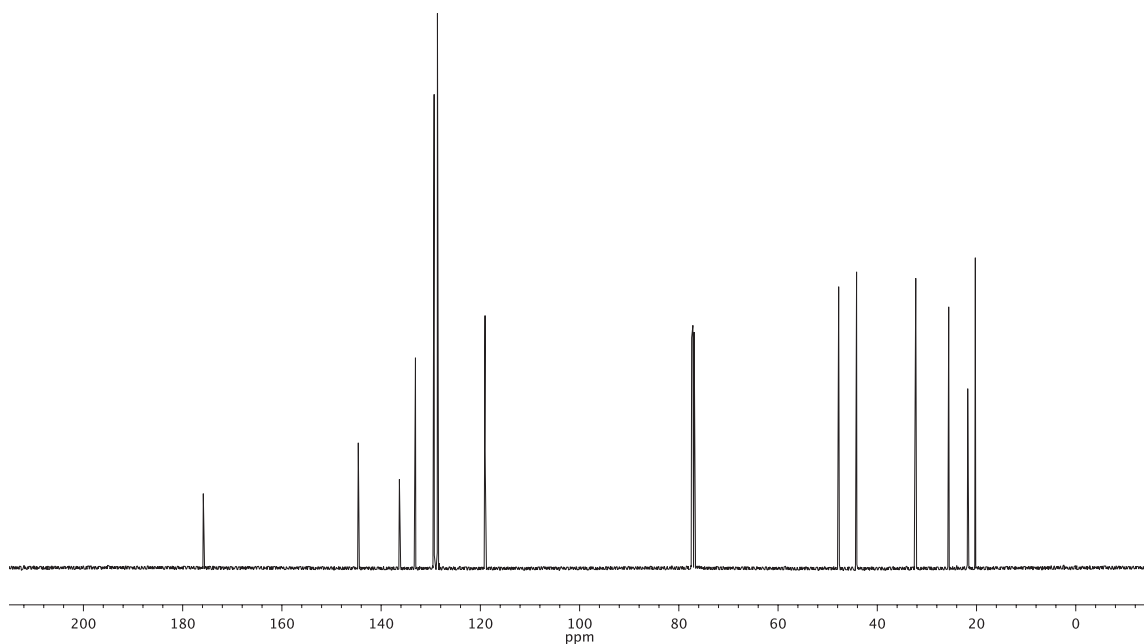


Figure A1.30 ¹³C NMR (126 MHz, CDCl₃) of compound **2a**.

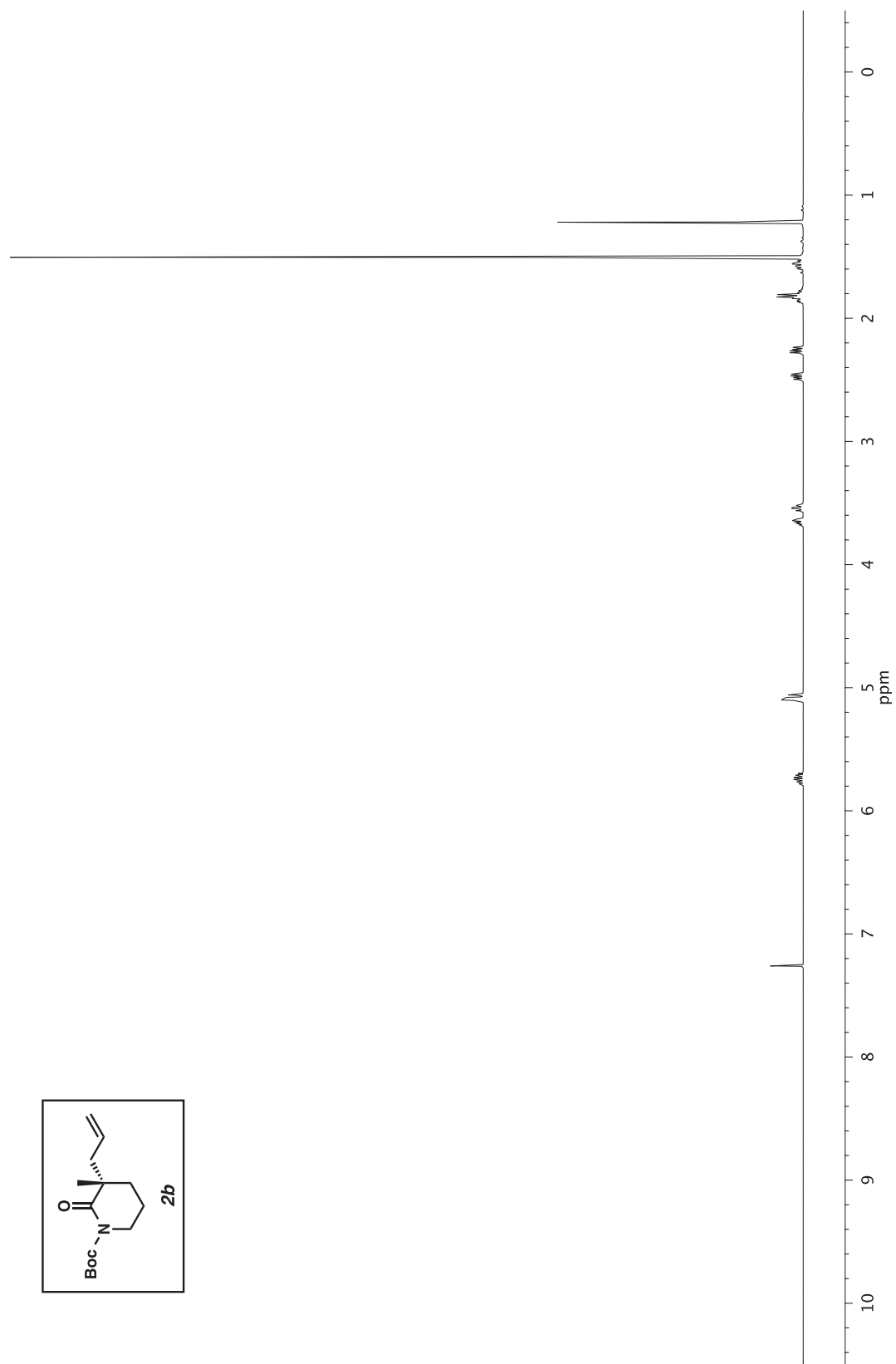


Figure A1.31 ^1H NMR (500 MHz, CDCl₃) of compound **2b**.

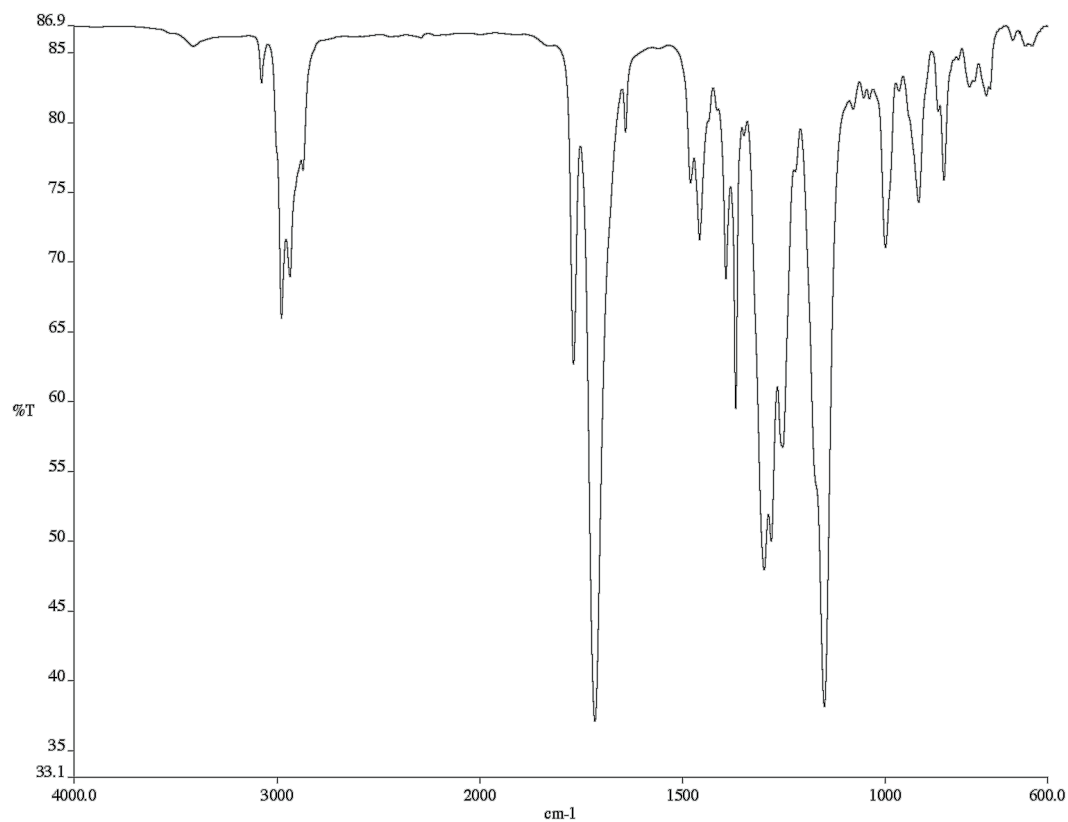


Figure A1.32 Infrared spectrum (Thin Film, NaCl) of compound **2b**.

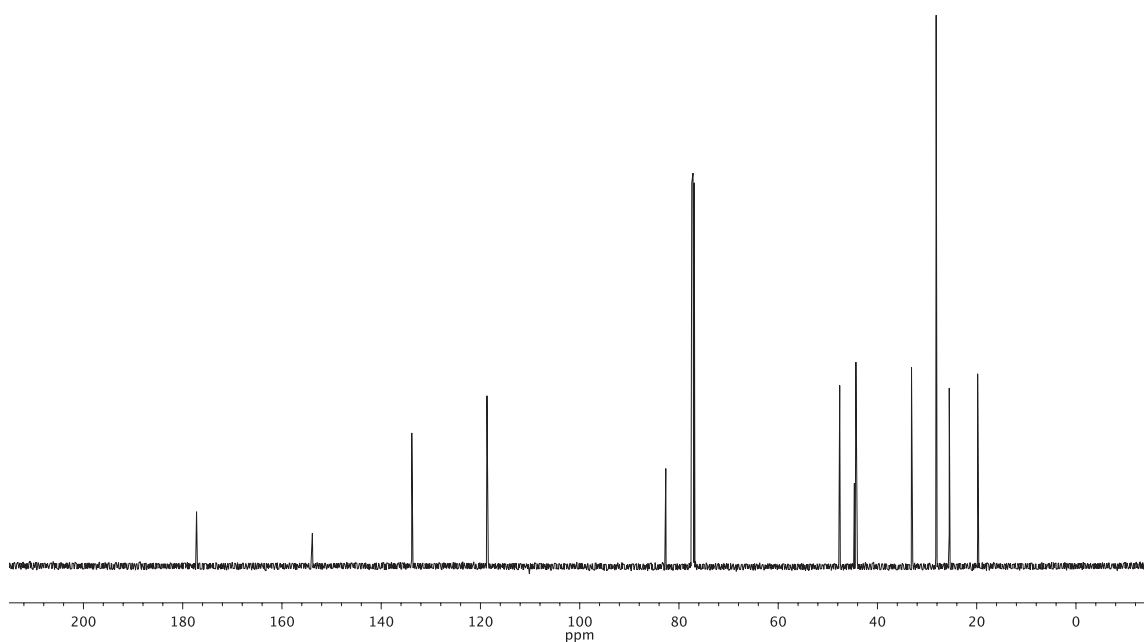


Figure A1.33 ¹³C NMR (126 MHz, CDCl₃) of compound **2b**.

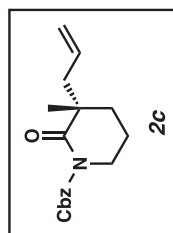
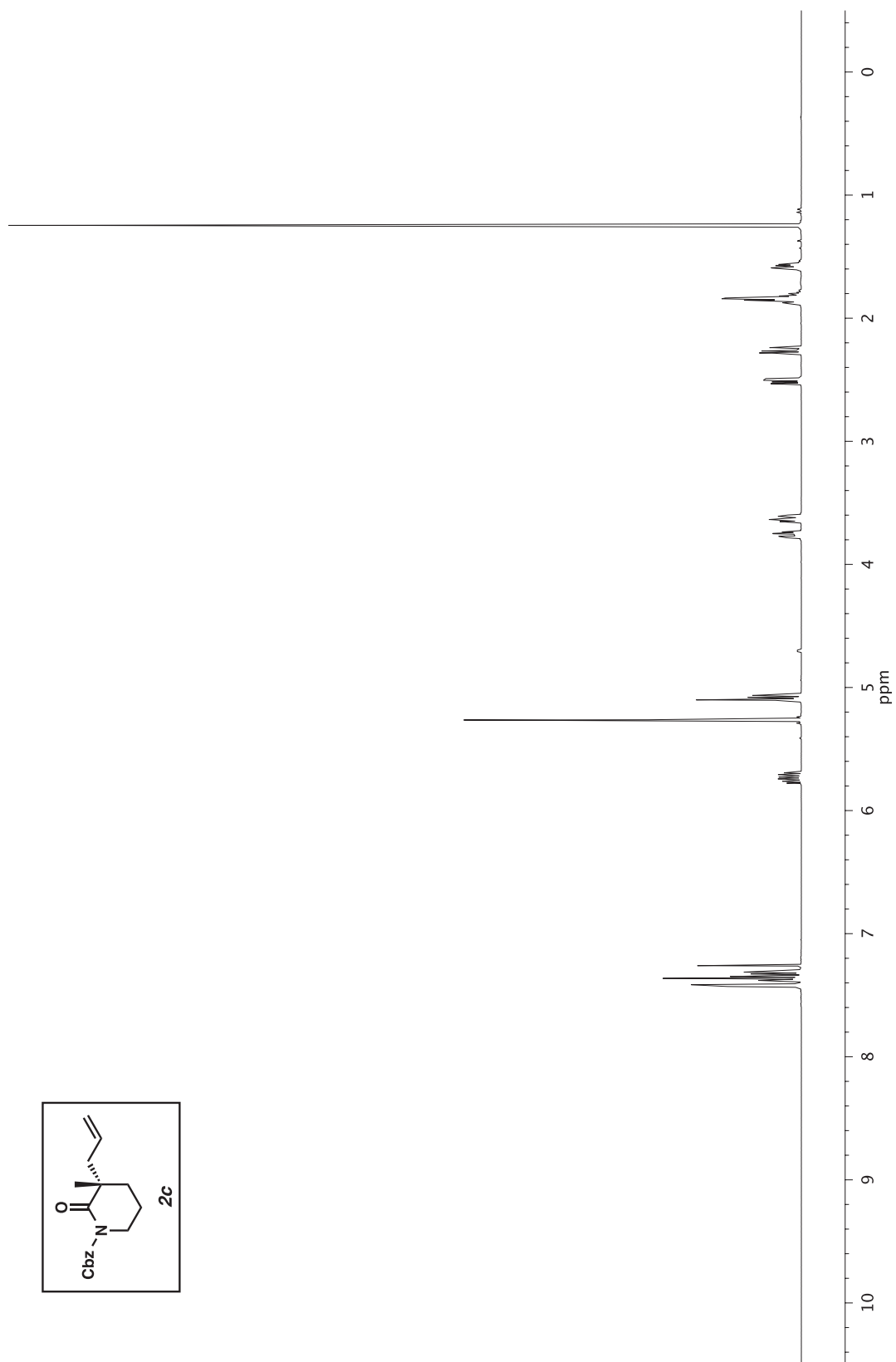


Figure A1.34 ^1H NMR (500 MHz, CDCl_3) of compound **2c**.

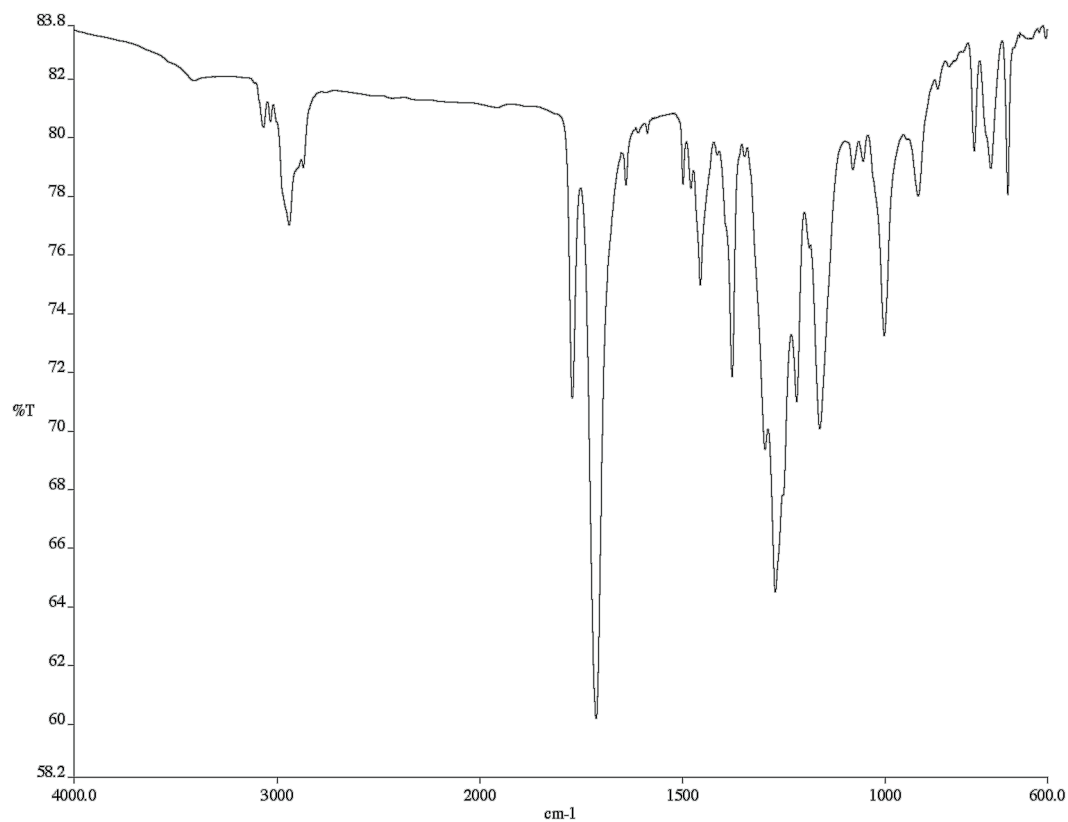


Figure A1.35 Infrared spectrum (Thin Film, NaCl) of compound **2c**.

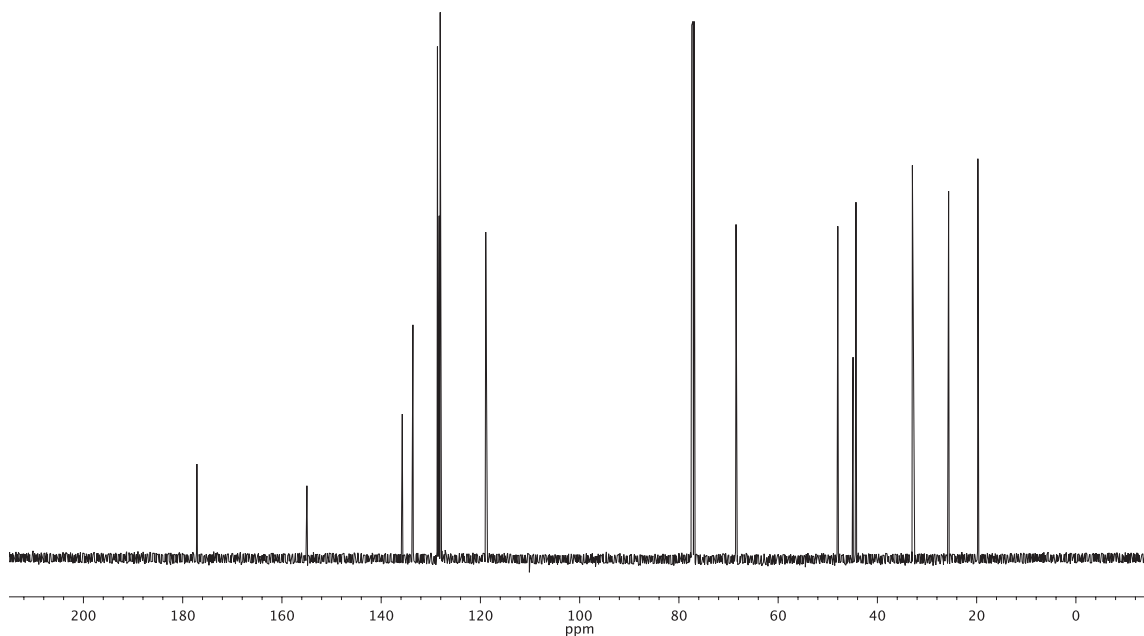


Figure A1.36 ¹³C NMR (126 MHz, CDCl₃) of compound **2c**.

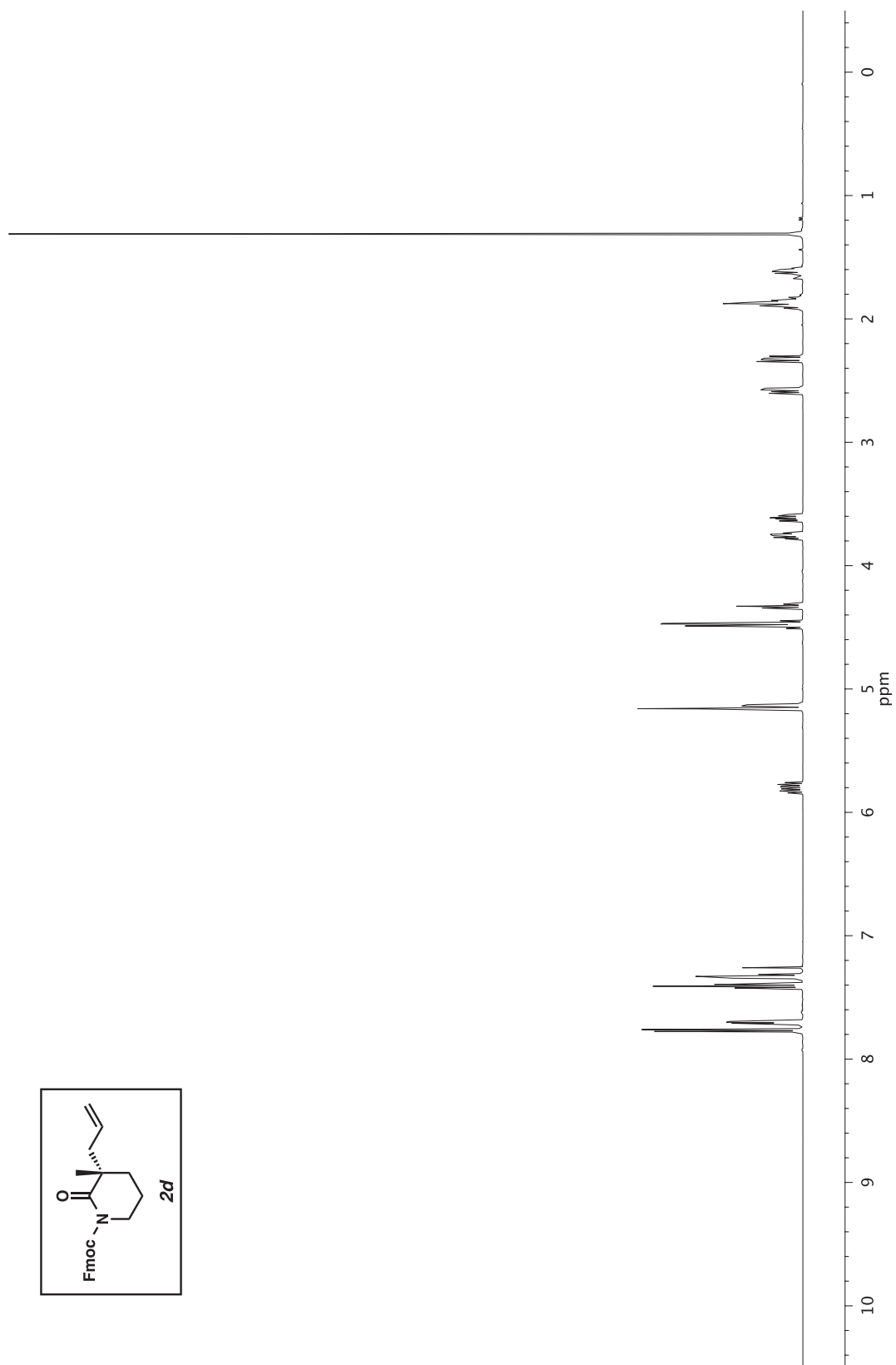


Figure A1.37 ¹H NMR (500 MHz, CDCl₃) of compound **2d**.

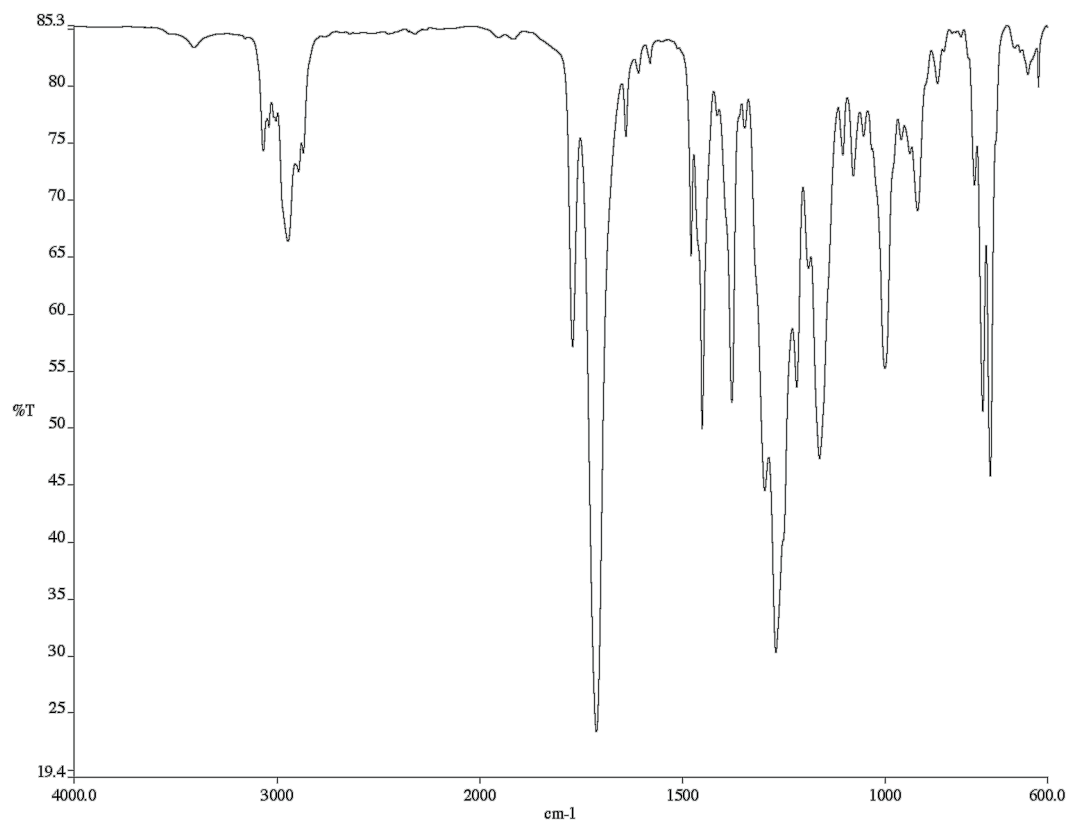


Figure A1.38 Infrared spectrum (Thin Film, NaCl) of compound **2d**.

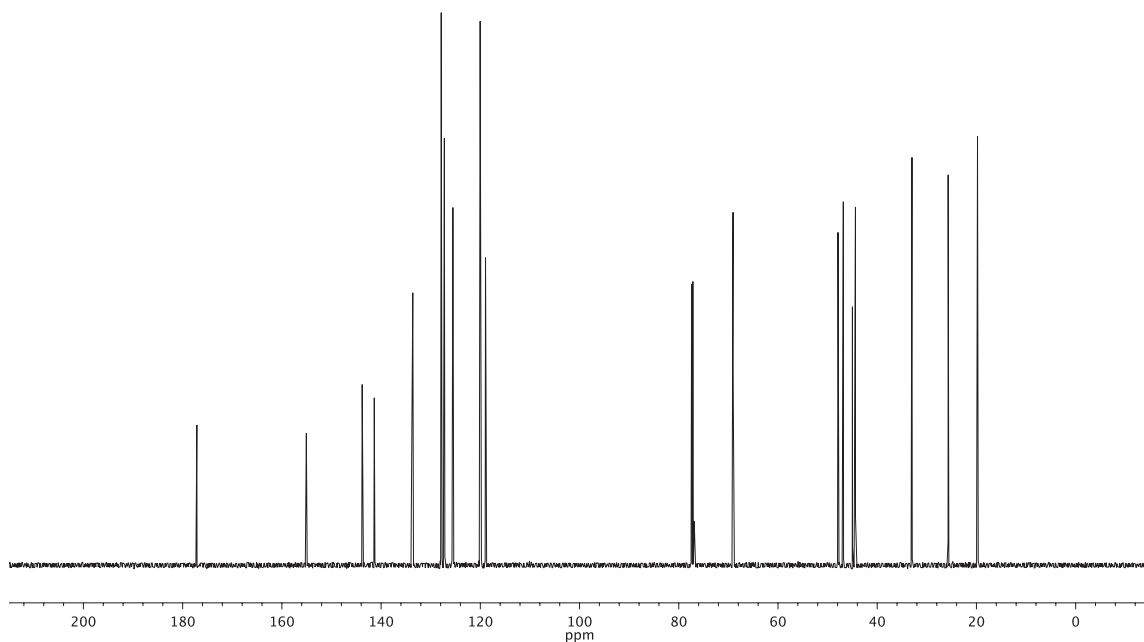


Figure A1.39 ¹³C NMR (126 MHz, CDCl₃) of compound **2d**.

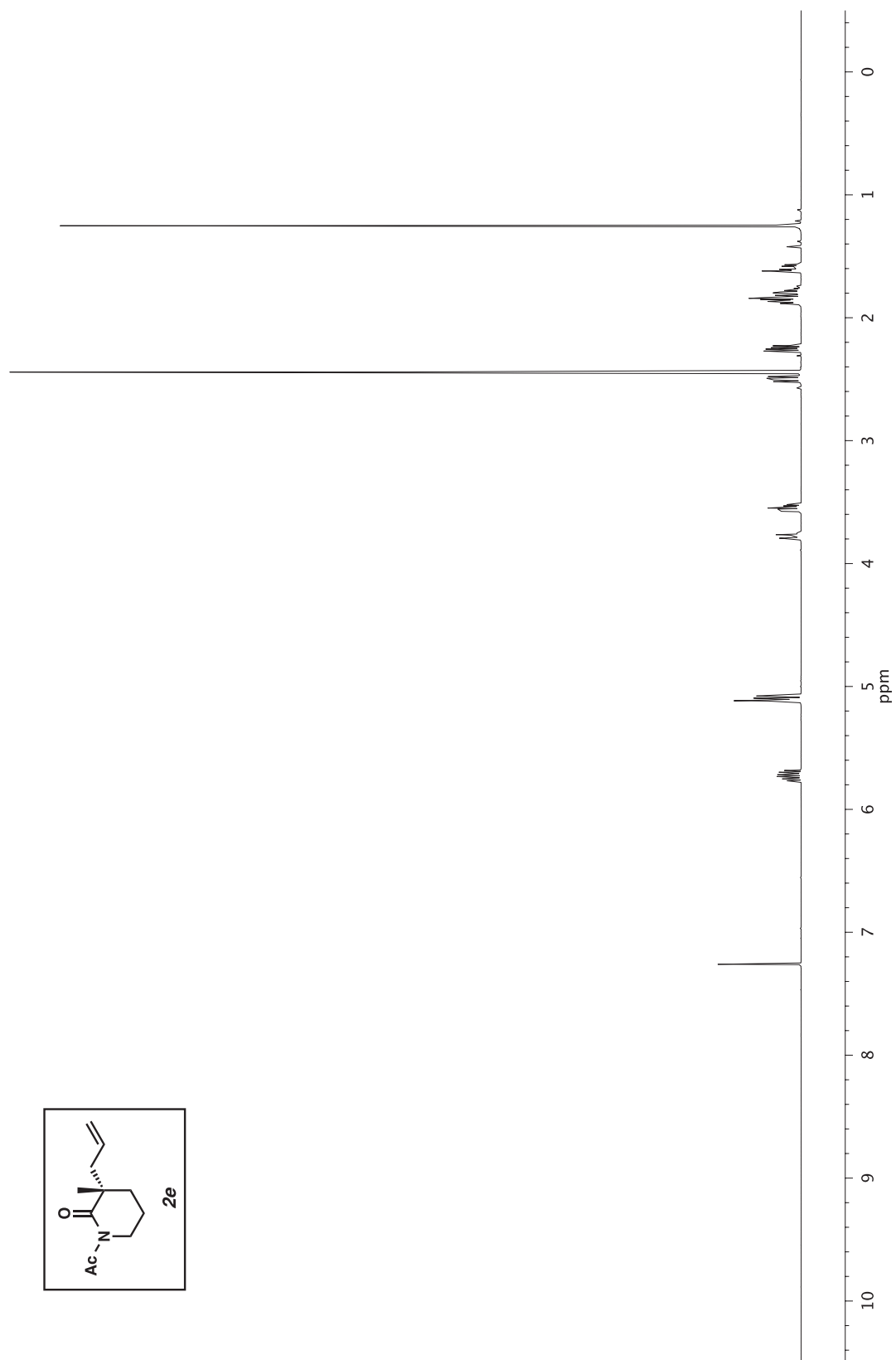


Figure A1.40 ^1H NMR (500 MHz, CDCl_3) of compound **2e**.

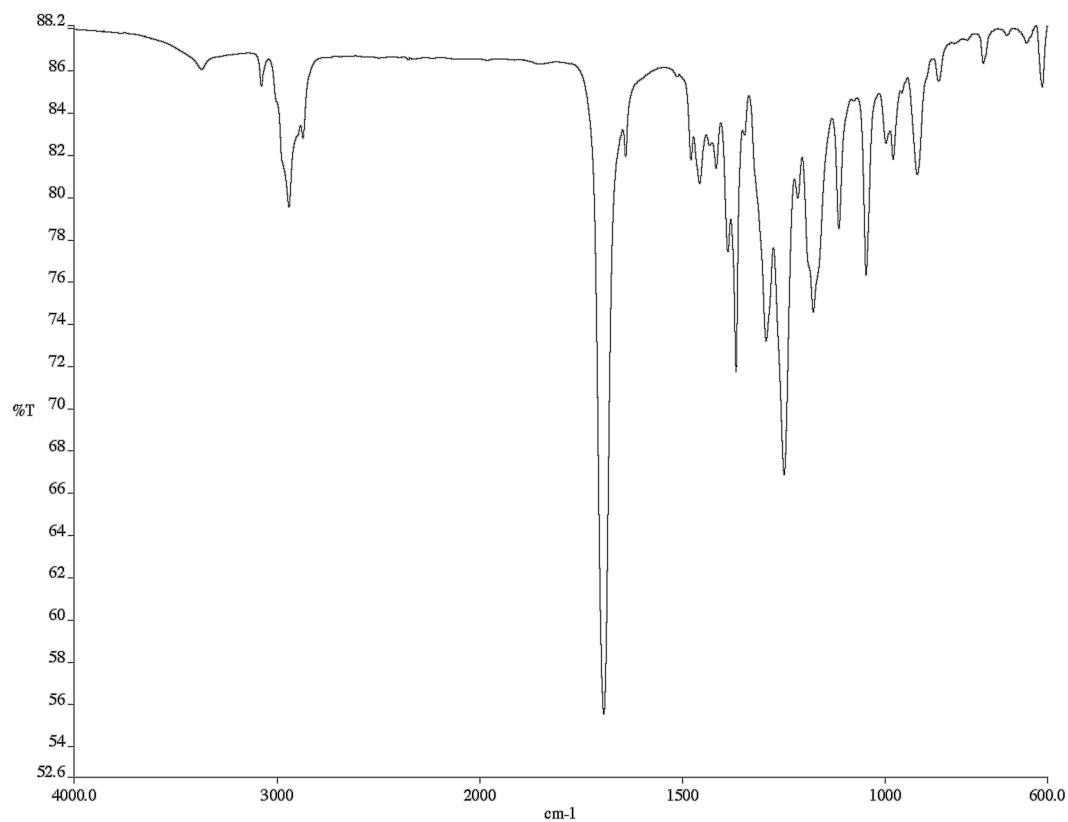


Figure A1.41 Infrared spectrum (Thin Film, NaCl) of compound **2e**.

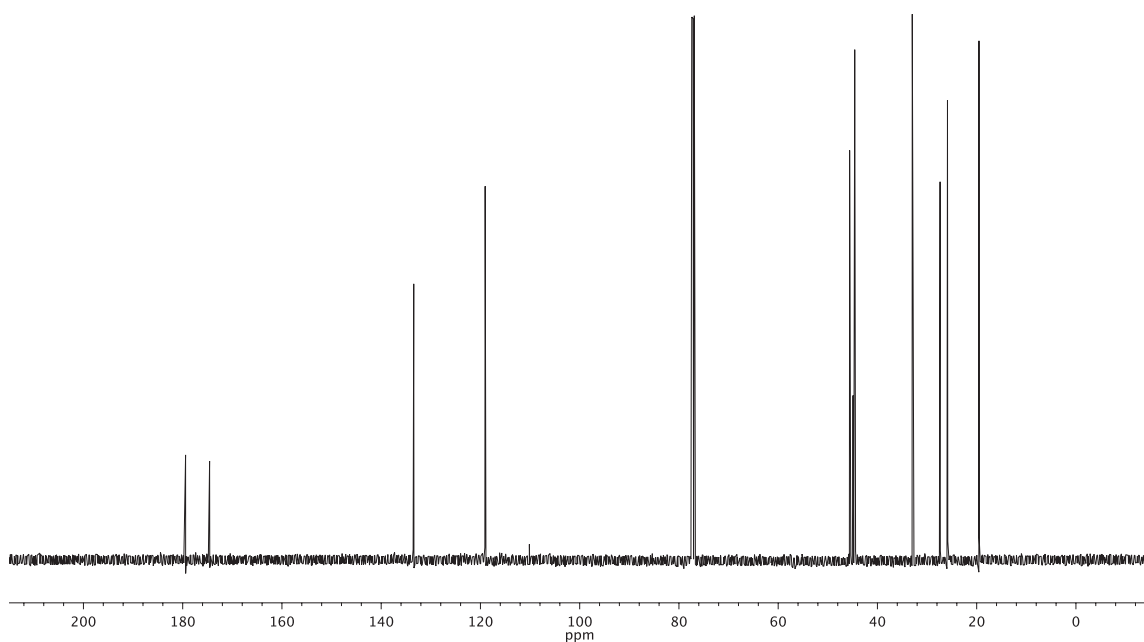
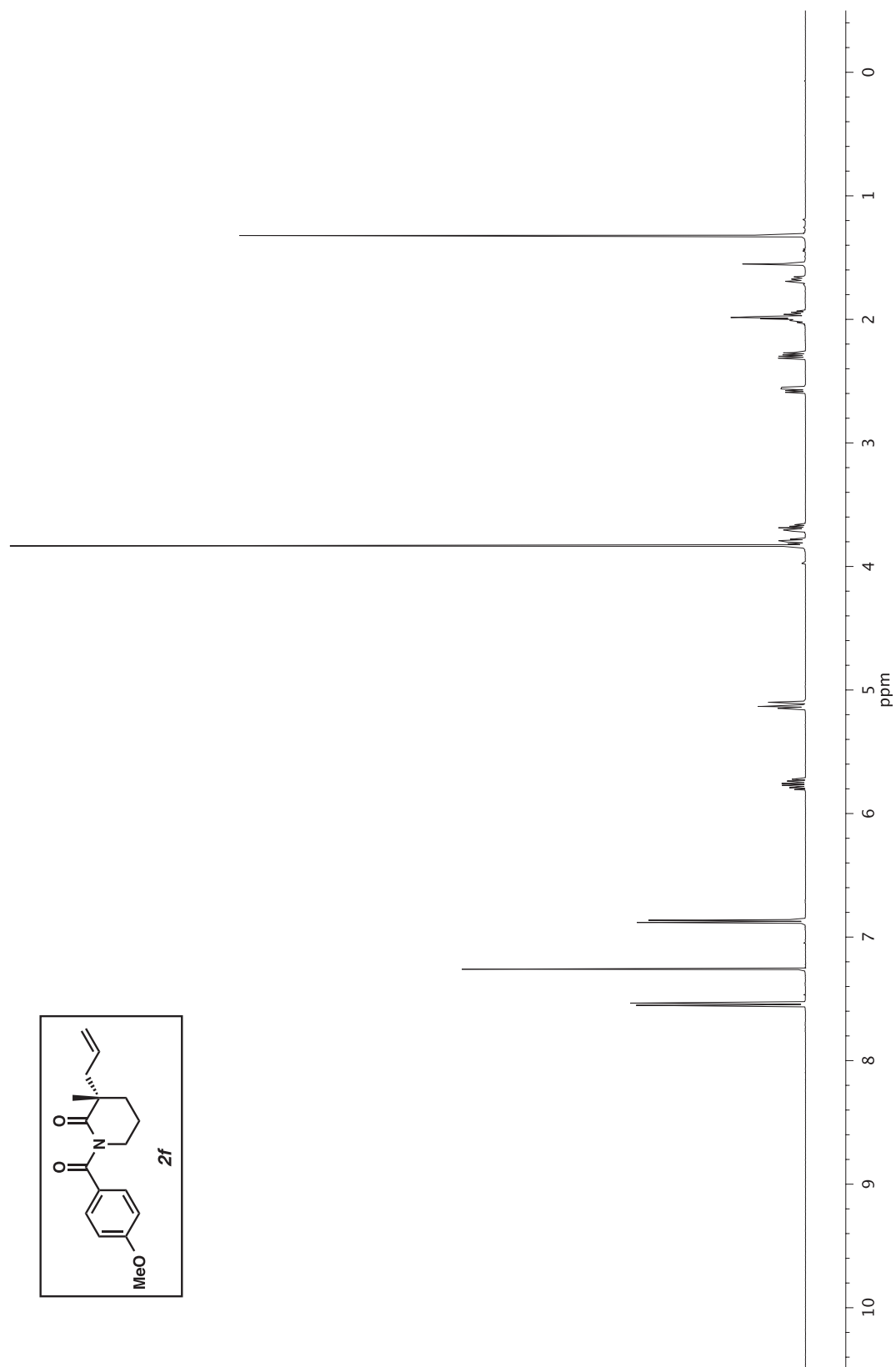


Figure A1.42 ¹³C NMR (126 MHz, CDCl₃) of compound **2e**.

Figure A1.43 ^1H NMR (500 MHz, CDCl_3) of compound **2f**.

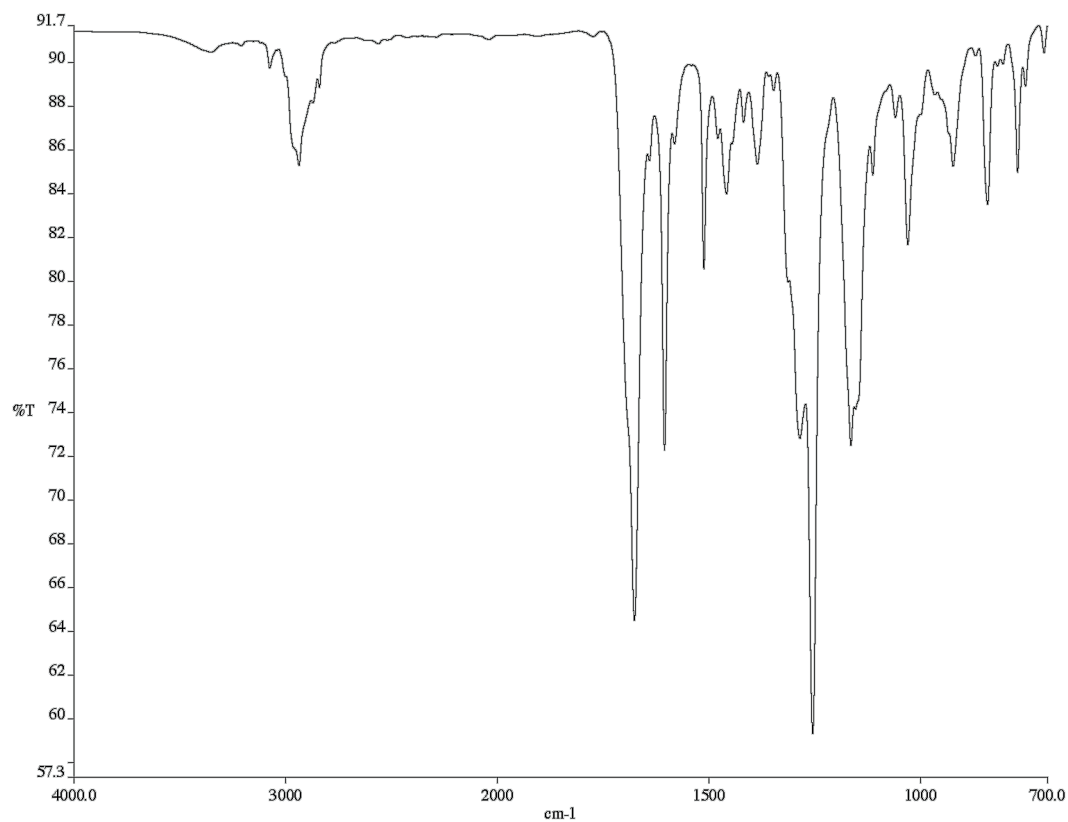


Figure A1.44 Infrared spectrum (Thin Film, NaCl) of compound **2f**.

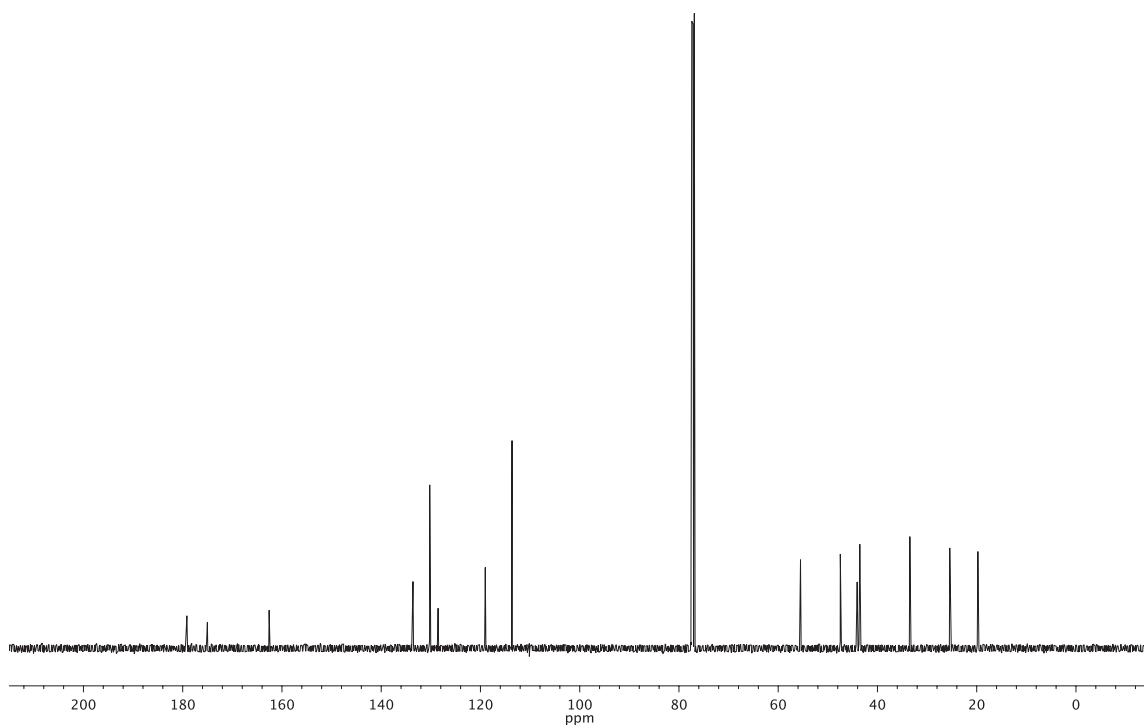


Figure A1.45 ¹³C NMR (126 MHz, CDCl₃) of compound **2f**.

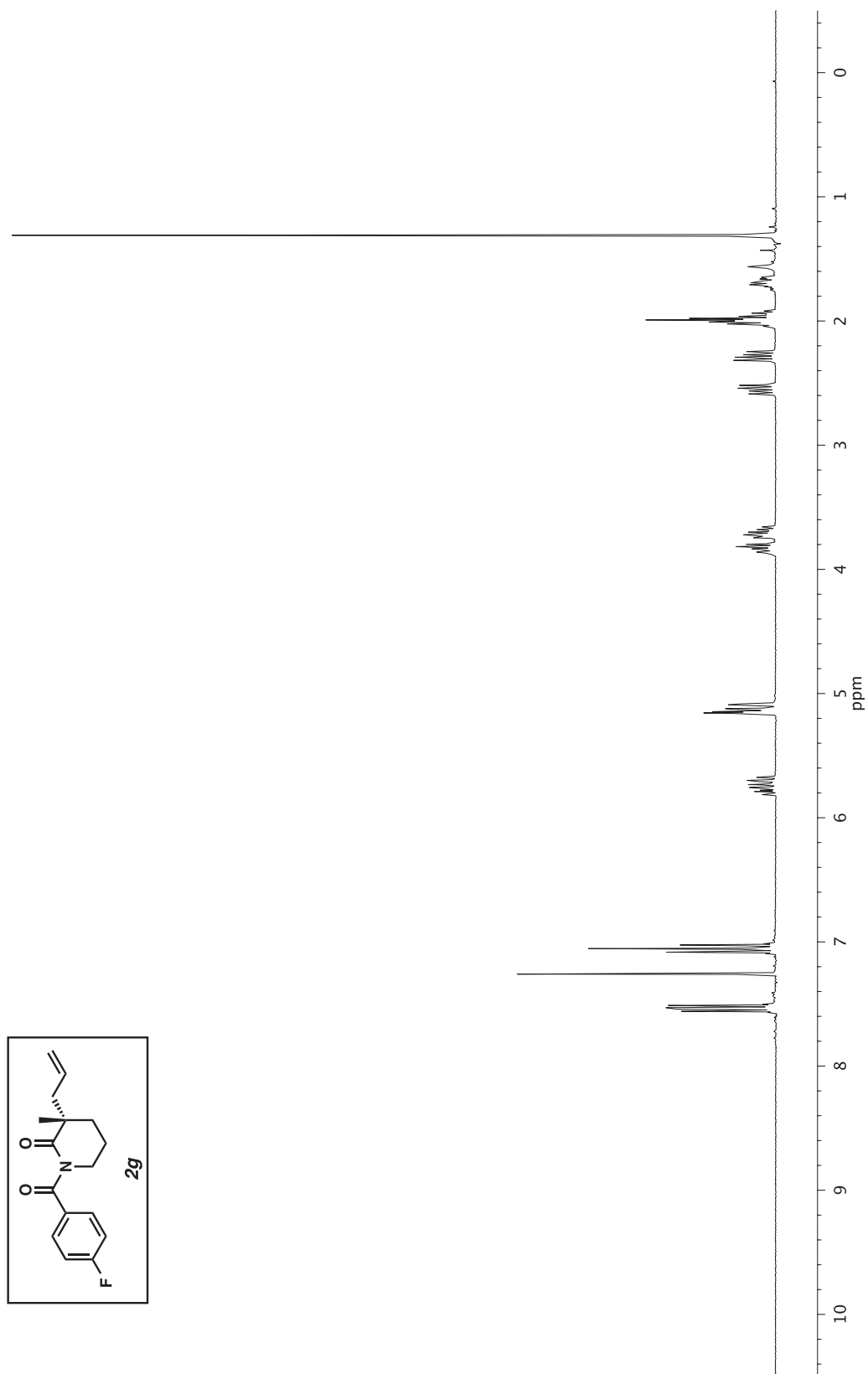


Figure A1.46 ¹H NMR (500 MHz, CDCl₃) of compound **2g**.

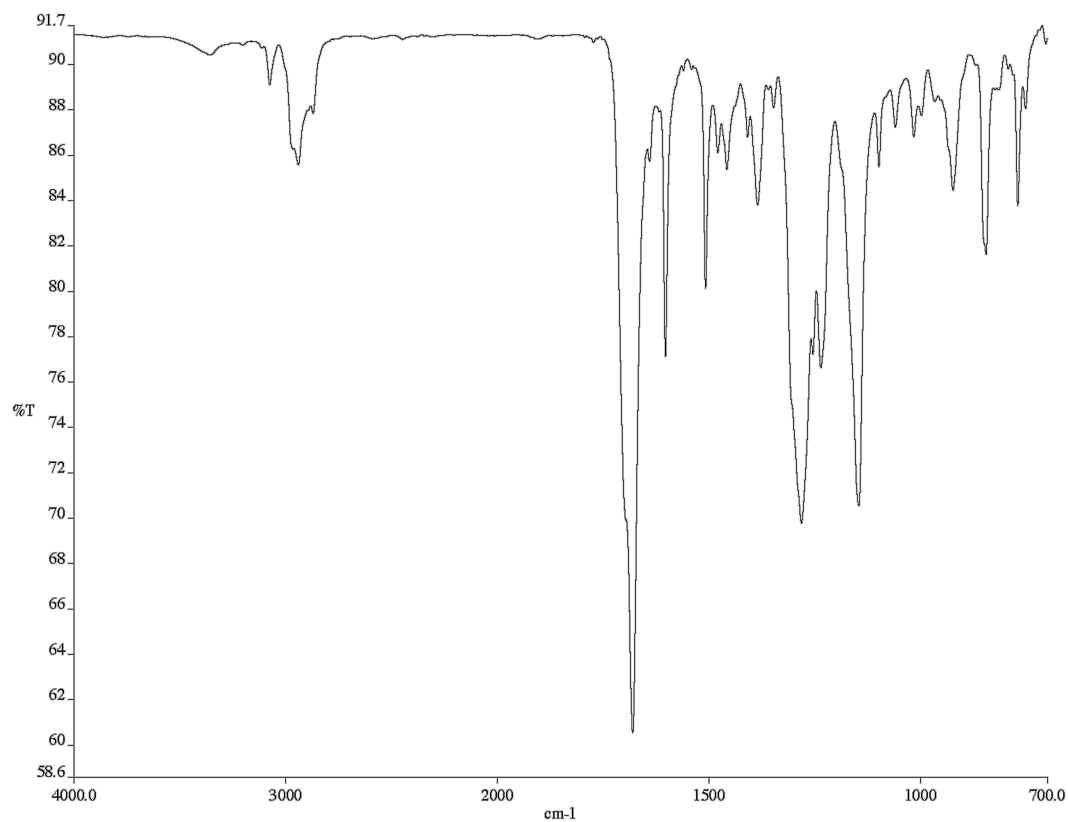


Figure A1.47 Infrared spectrum (Thin Film, NaCl) of compound **2g**.

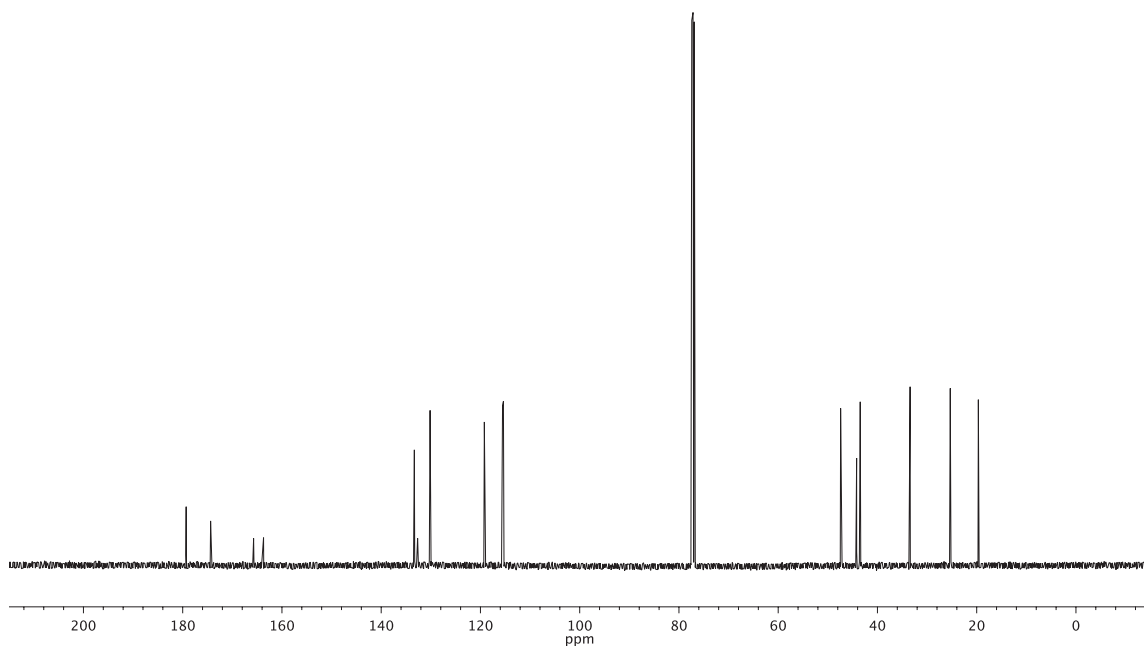


Figure A1.48 ¹³C NMR (126 MHz, CDCl₃) of compound **2g**.

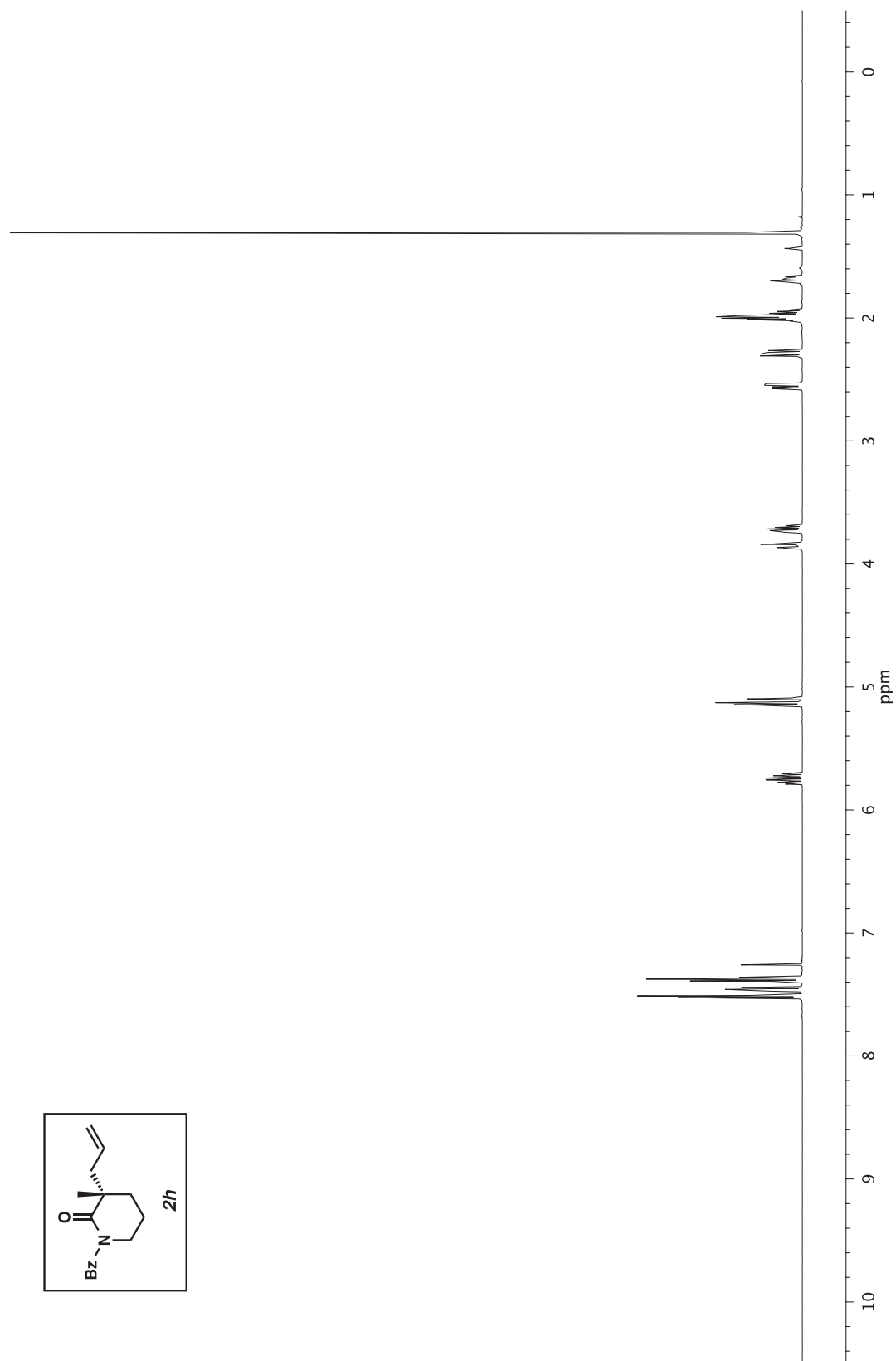


Figure A1.49 ¹H NMR (500 MHz, CDCl₃) of compound **2h**.

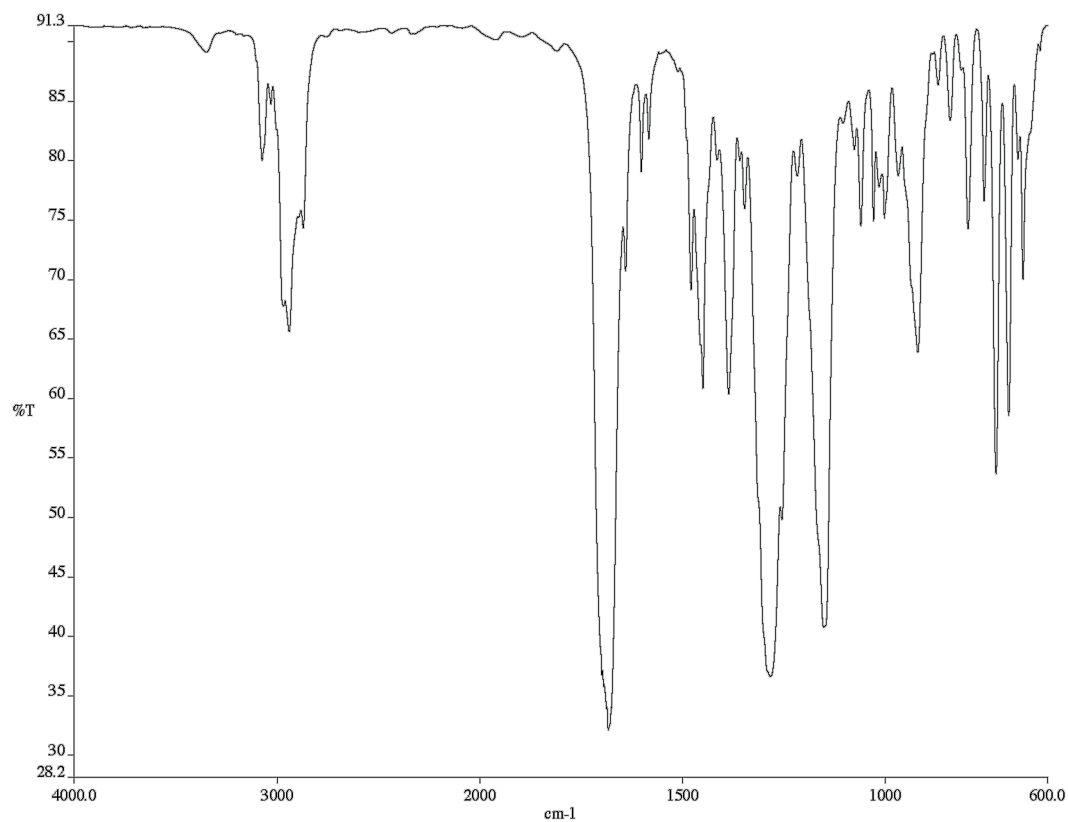


Figure A1.50 Infrared spectrum (Thin Film, NaCl) of compound **2h**.

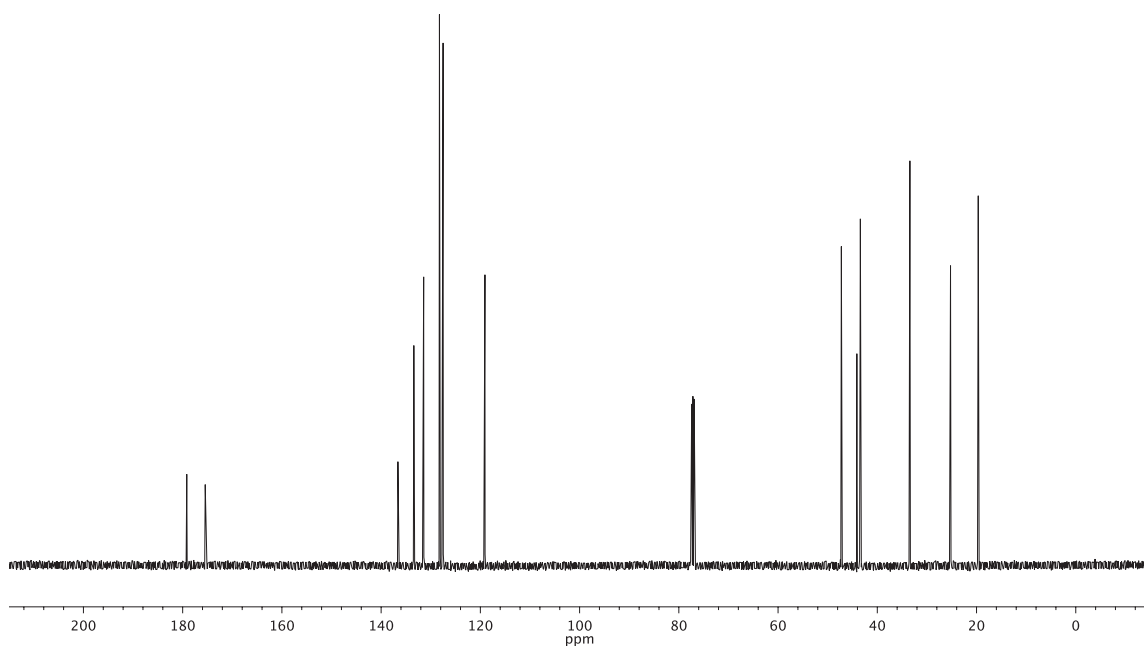


Figure A1.51 ¹³C NMR (126 MHz, CDCl₃) of compound **2h**.

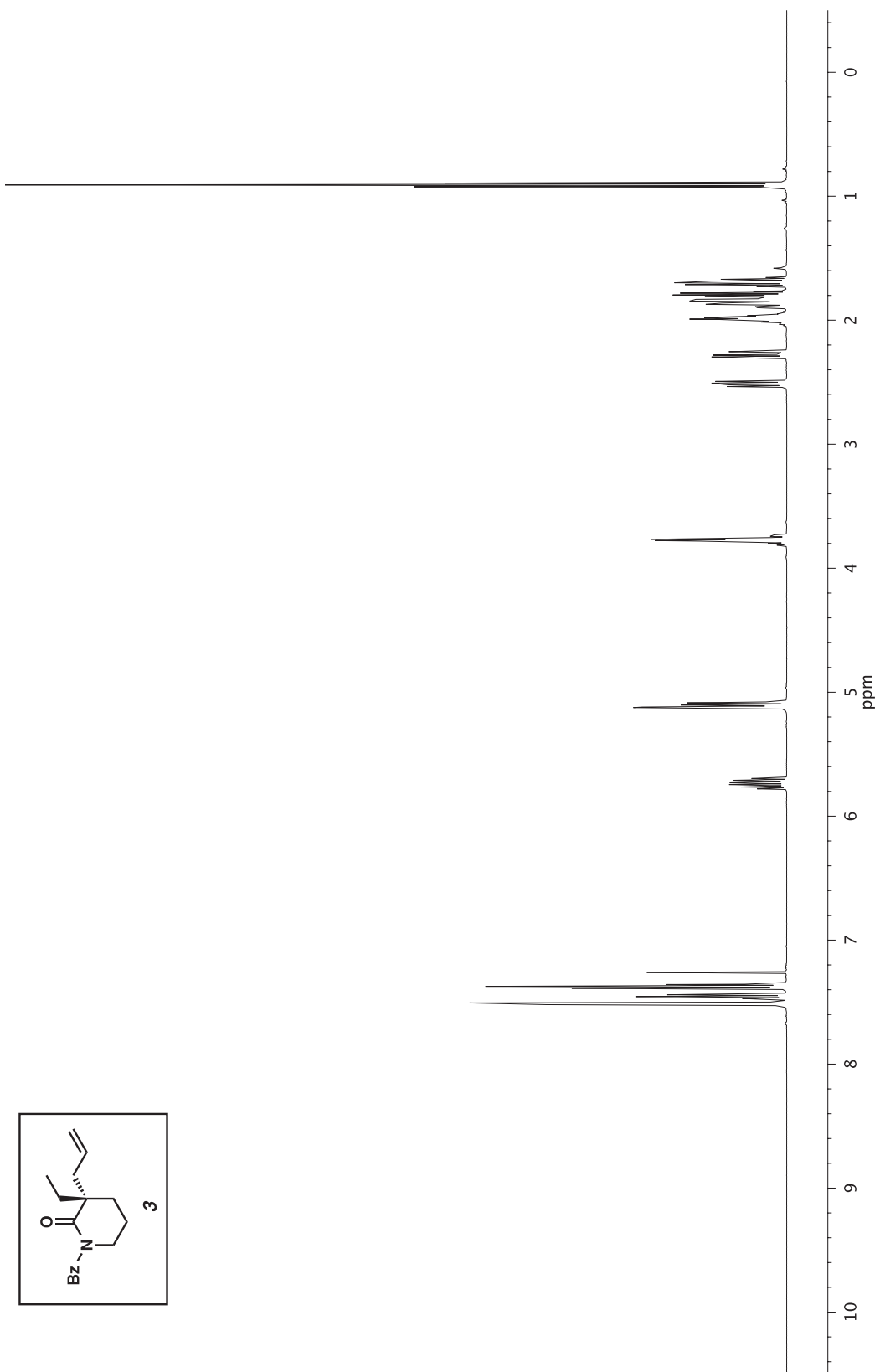


Figure A1.52 ^1H NMR (500 MHz, CDCl_3) of compound **3**.

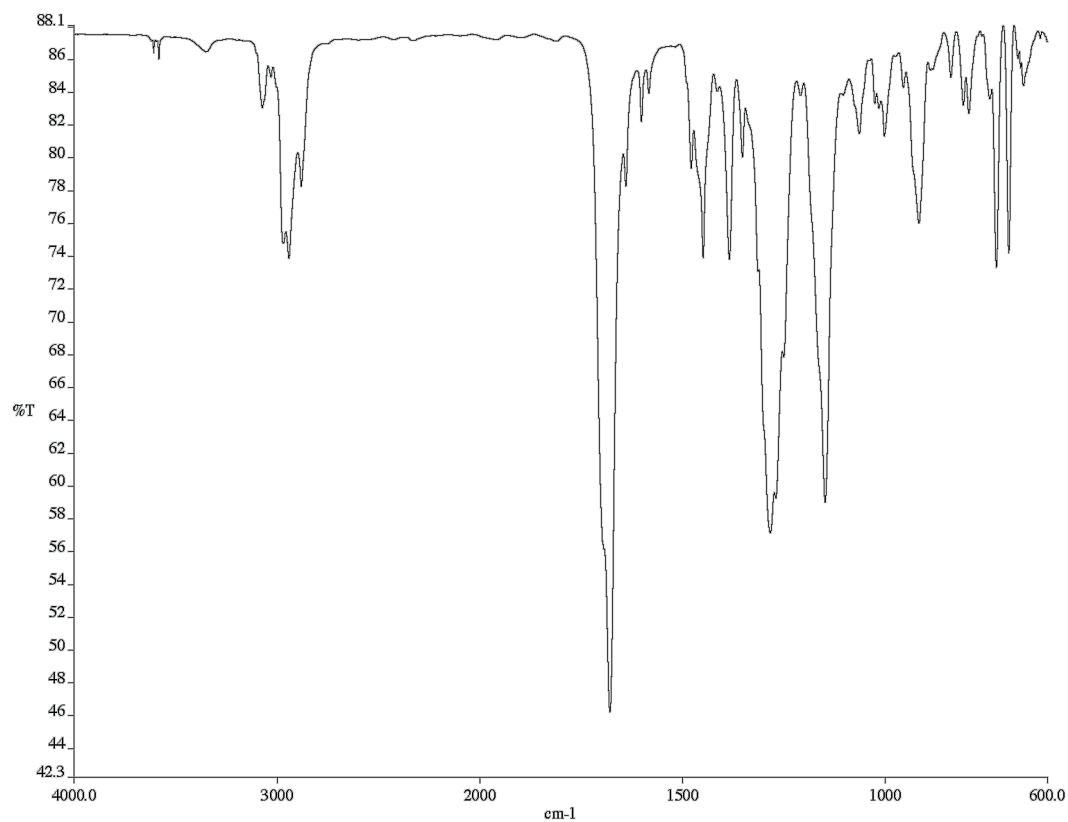


Figure A1.53 Infrared spectrum (Thin Film, NaCl) of compound 3.

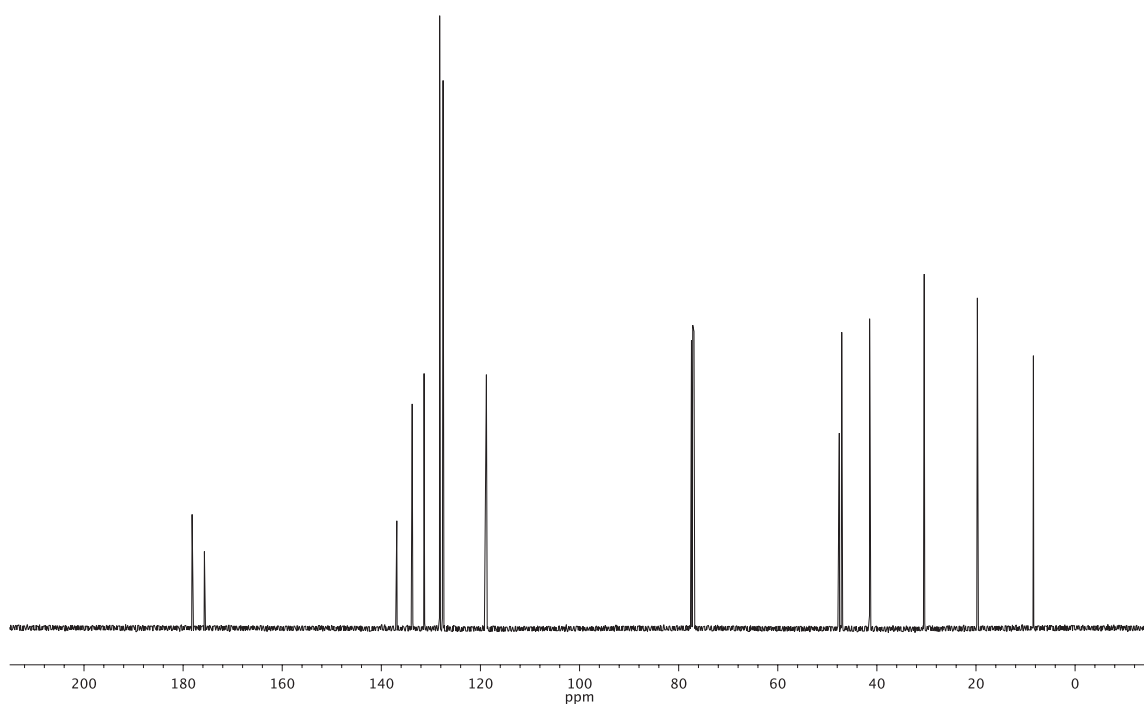


Figure A1.54 ¹³C NMR (126 MHz, CDCl₃) of compound 3.

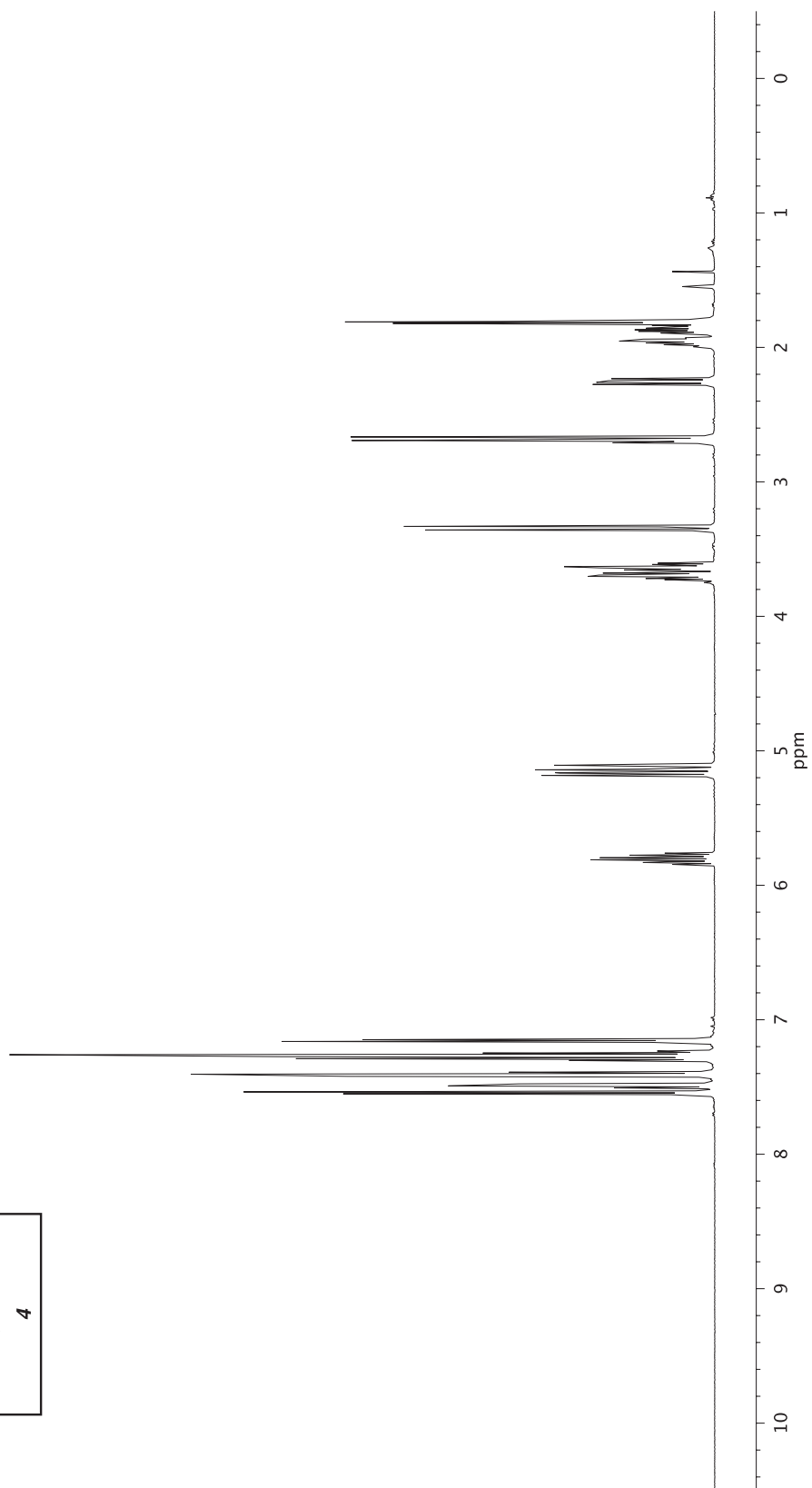
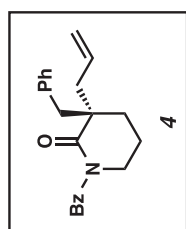


Figure A1.55 $^1\text{H NMR}$ (500 MHz, CDCl_3) of compound 4.

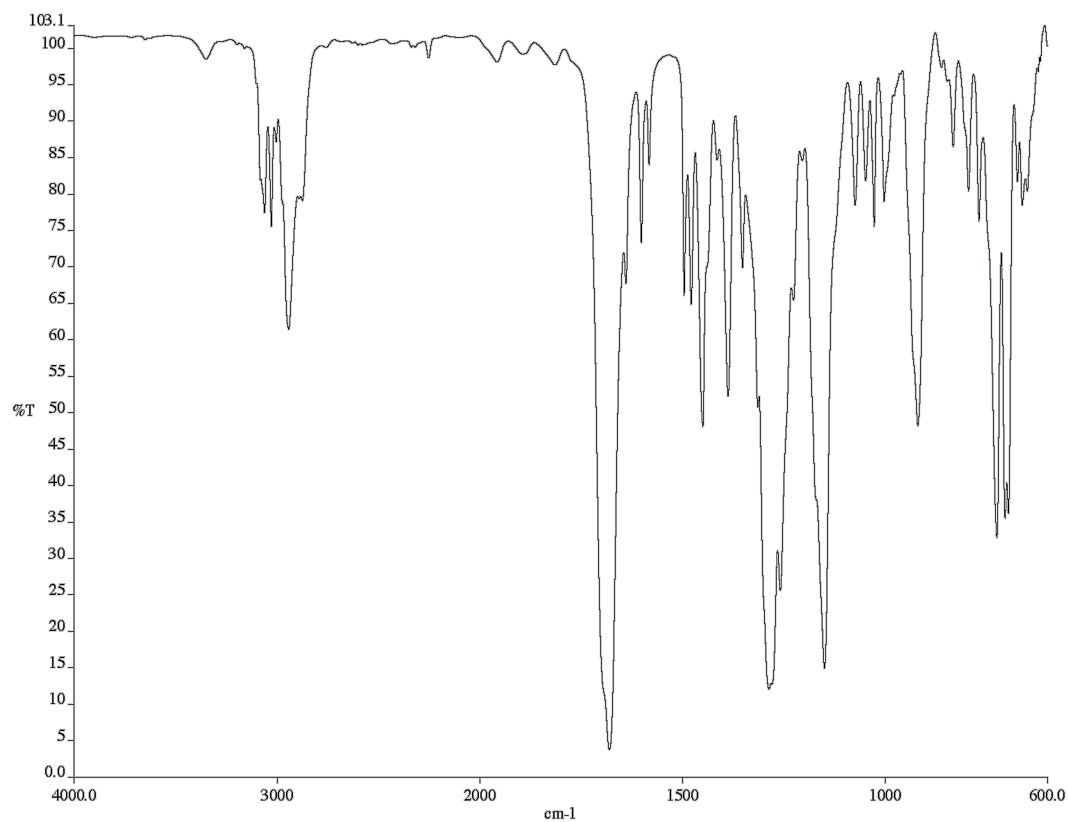


Figure A1.56 Infrared spectrum (Thin Film, NaCl) of compound 4.

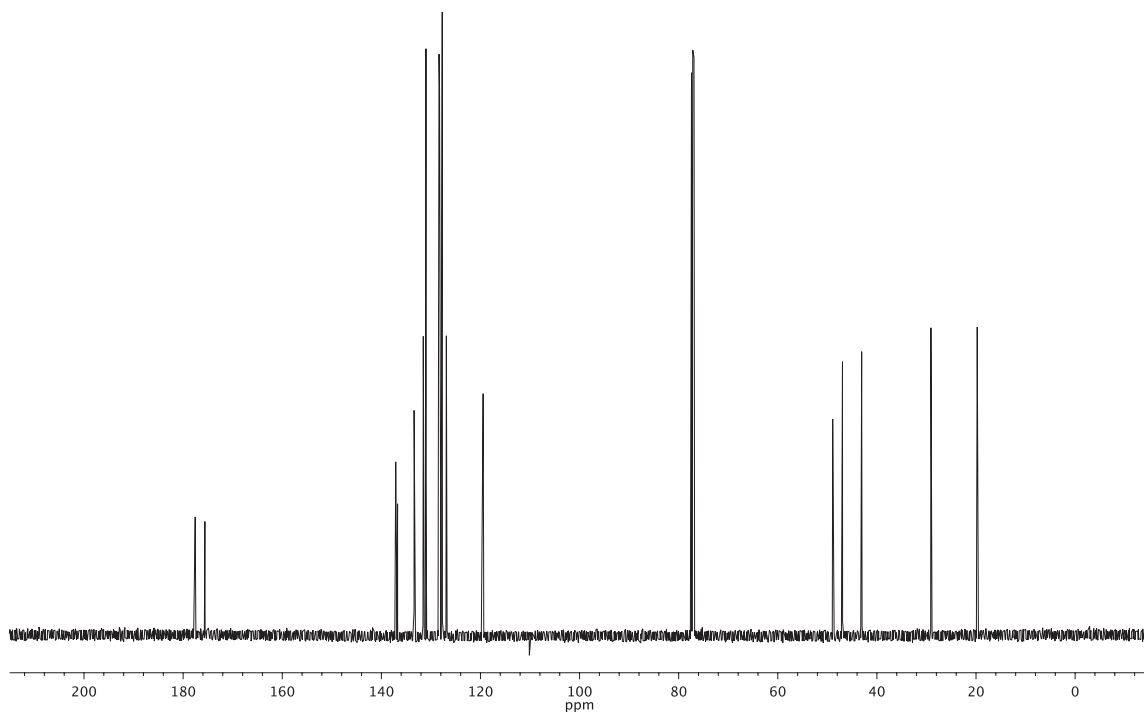


Figure A1.57 ¹³C NMR (126 MHz, CDCl₃) of compound 4.

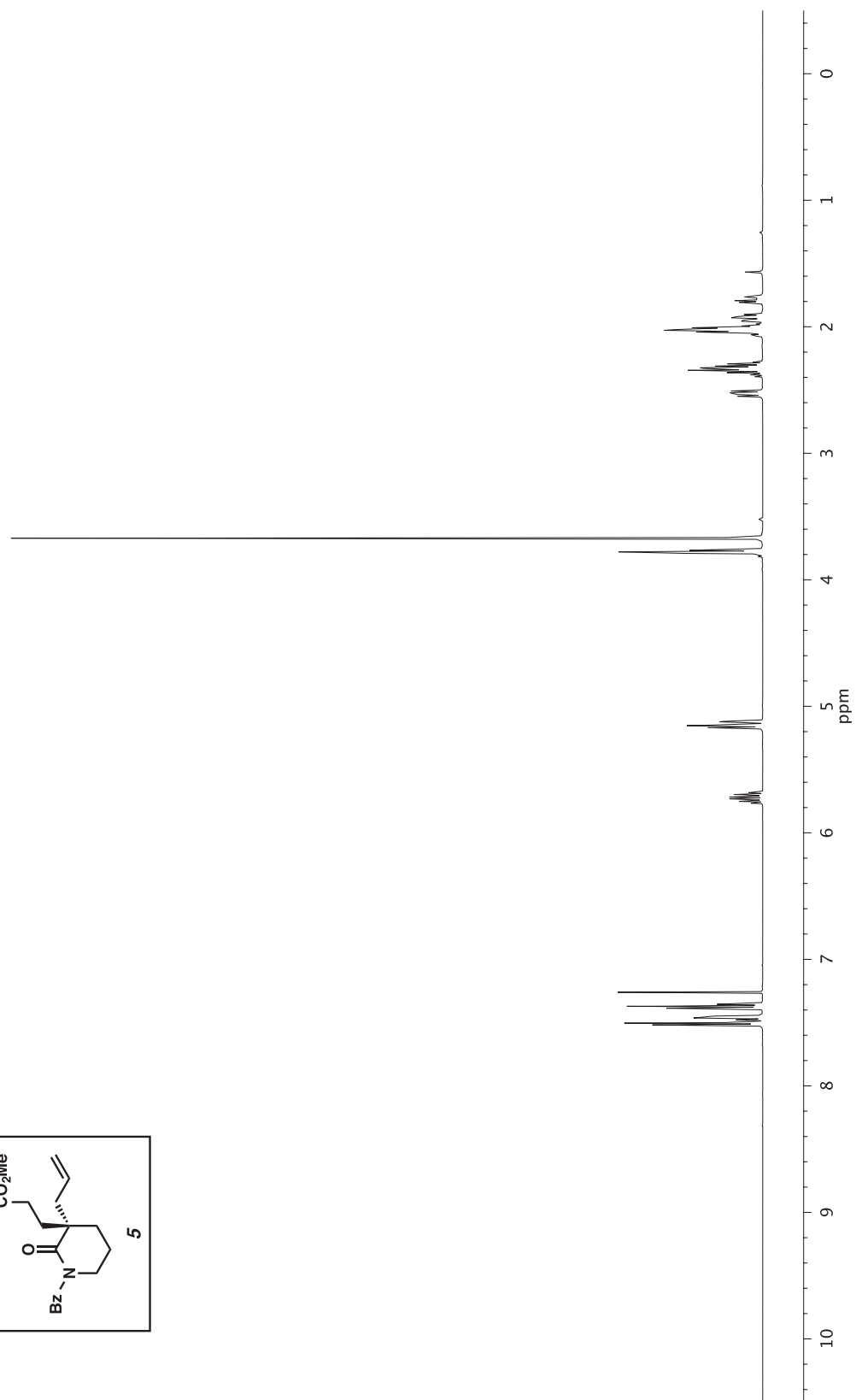
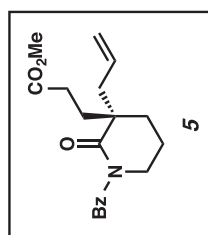


Figure A1.58 ¹H NMR (500 MHz, CDCl₃) of compound **5**.

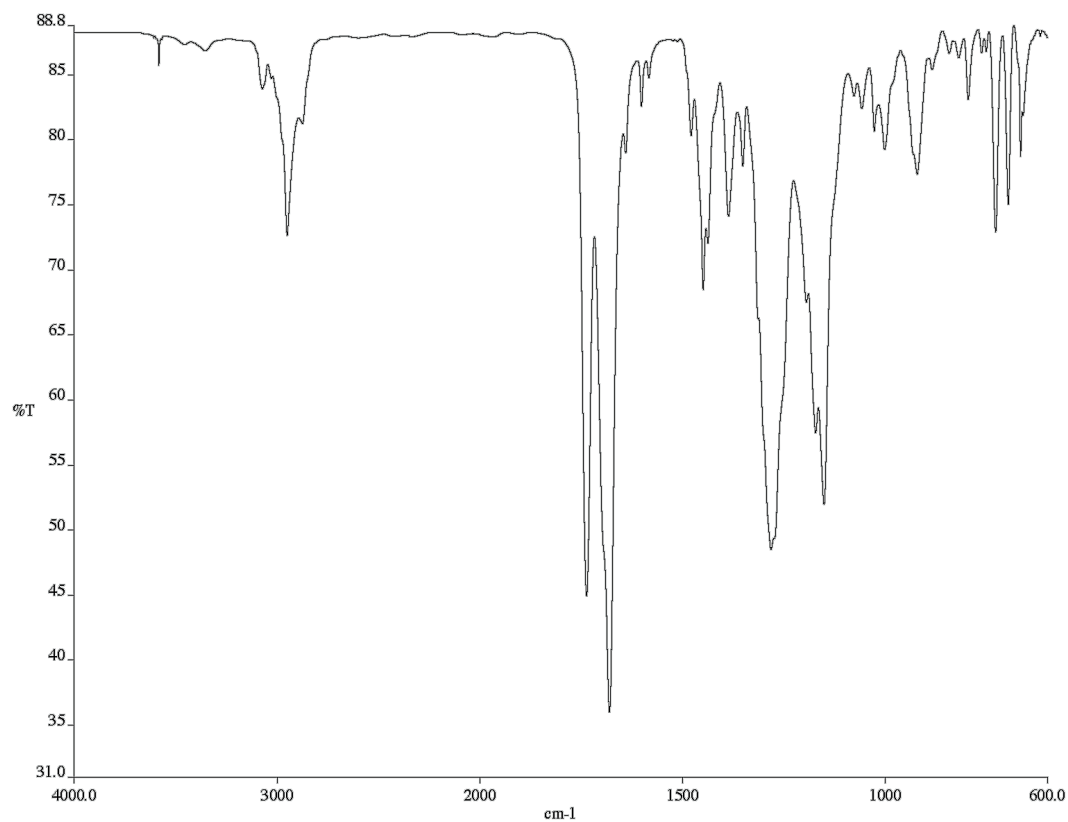


Figure A1.59 Infrared spectrum (Thin Film, NaCl) of compound **5**.

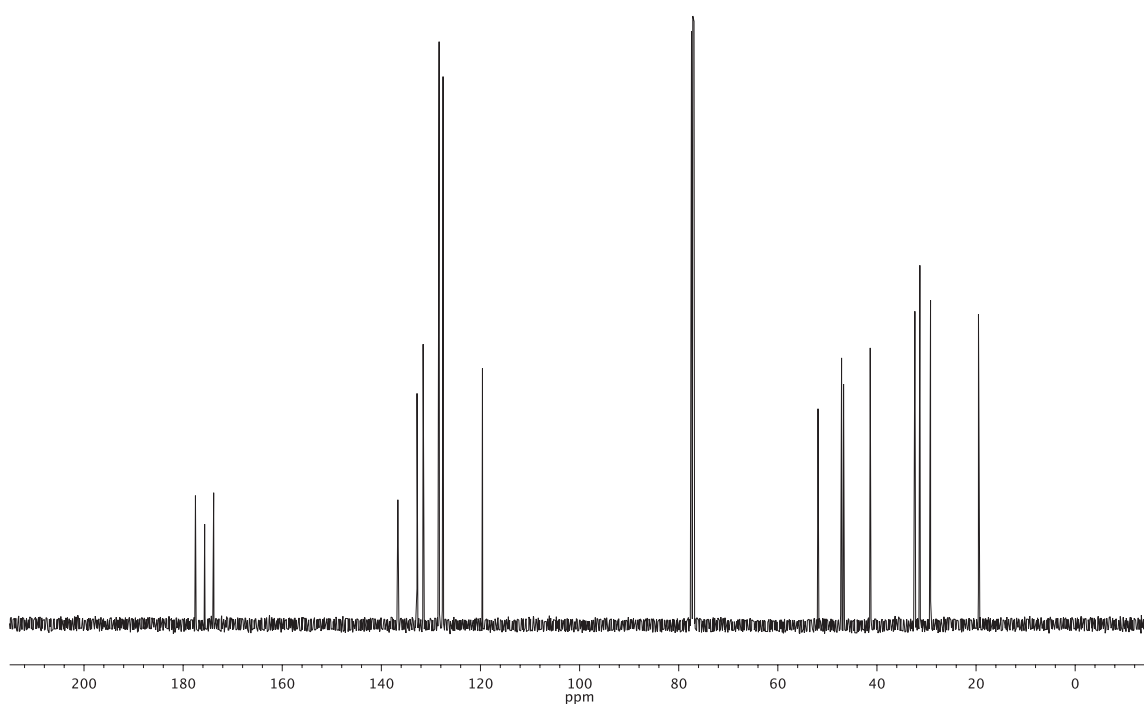


Figure A1.60 ¹³C NMR (126 MHz, CDCl₃) of compound **5**.

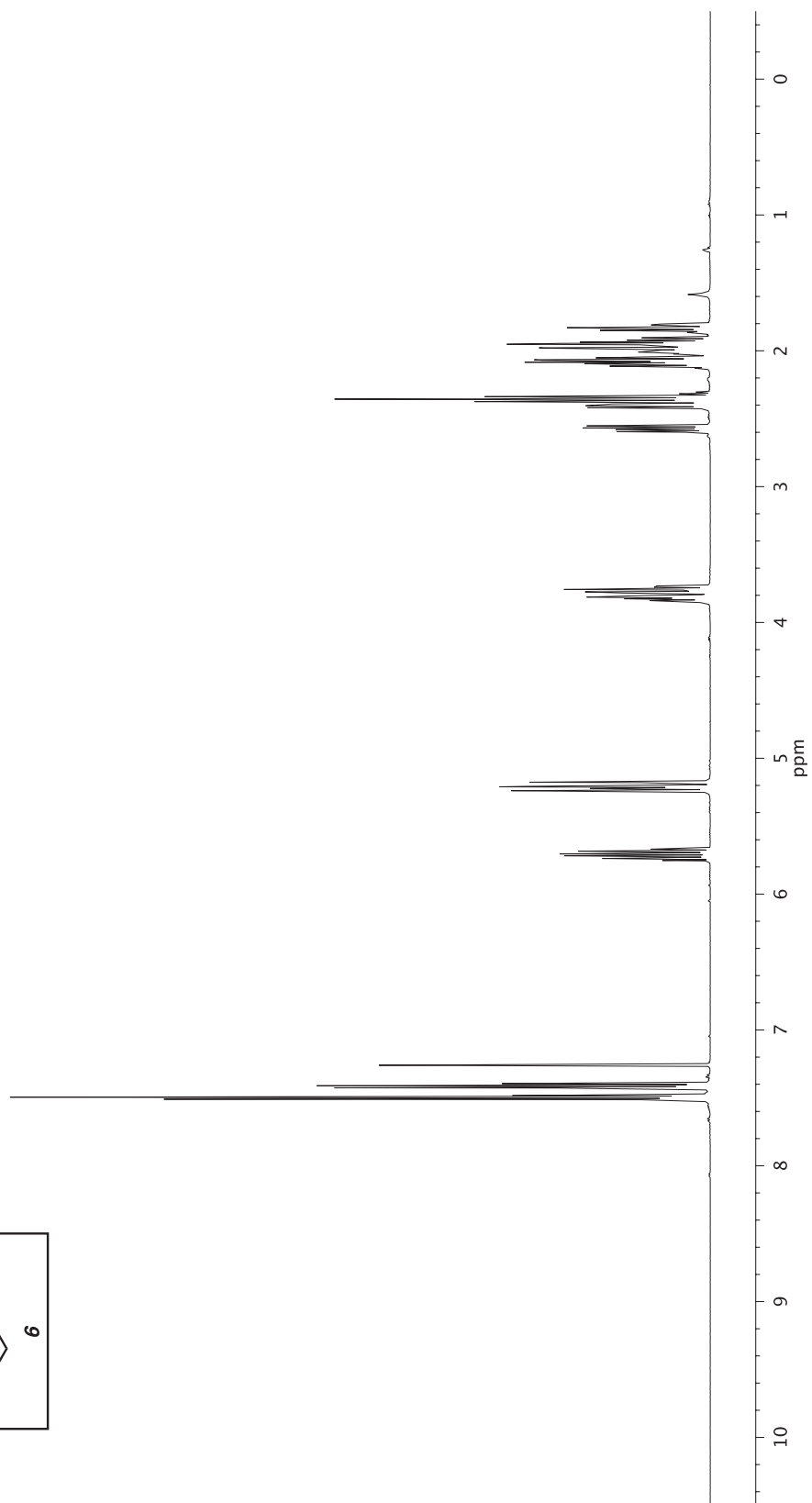
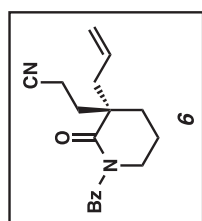


Figure A1.61 ¹H NMR (500 MHz, CDCl₃) of compound **6**.

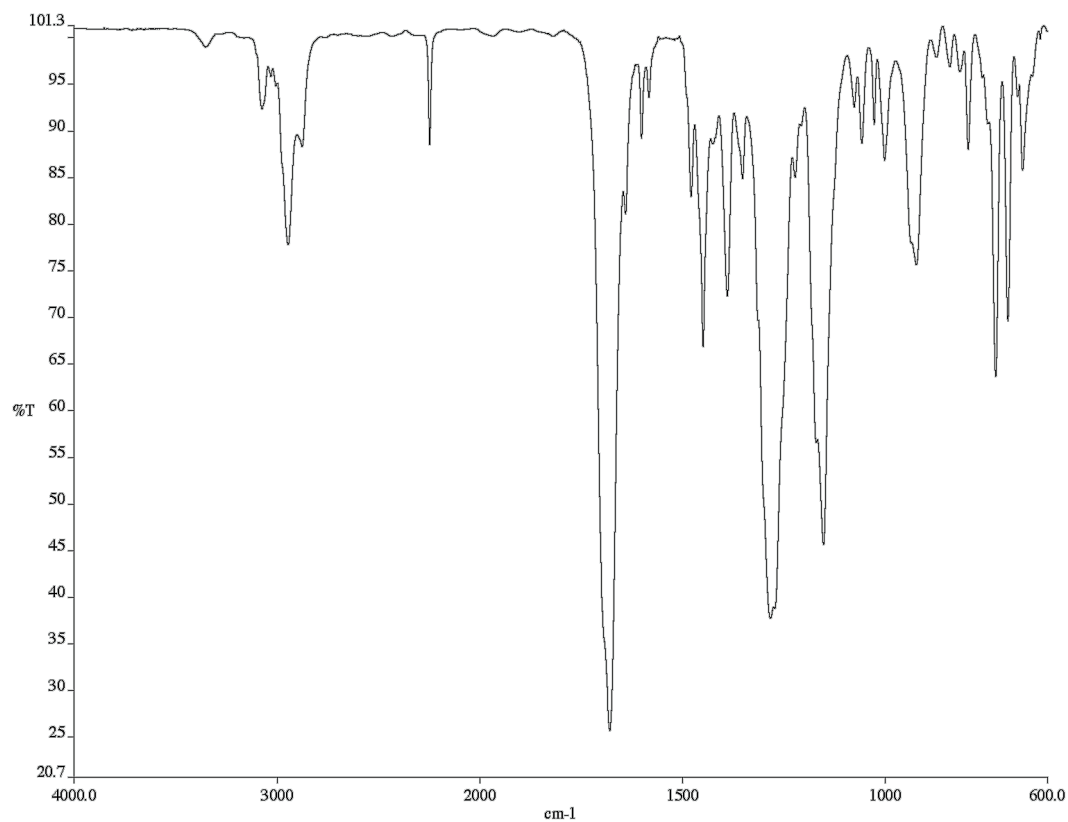


Figure A1.62 Infrared spectrum (Thin Film, NaCl) of compound 6.

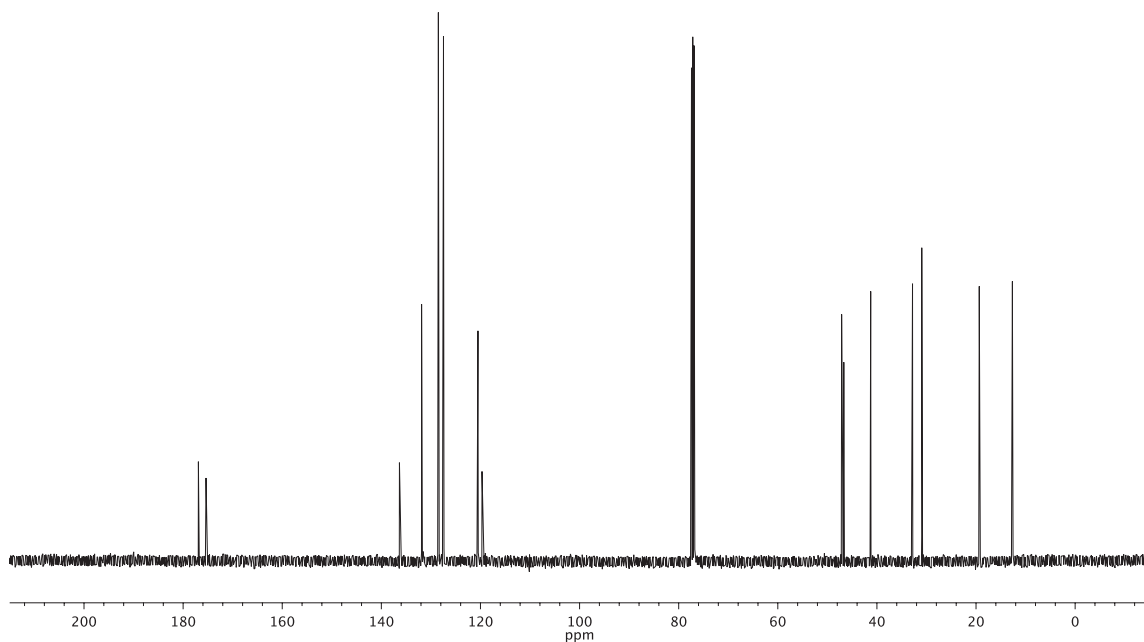


Figure A1.63 ¹³C NMR (126 MHz, CDCl₃) of compound 6.

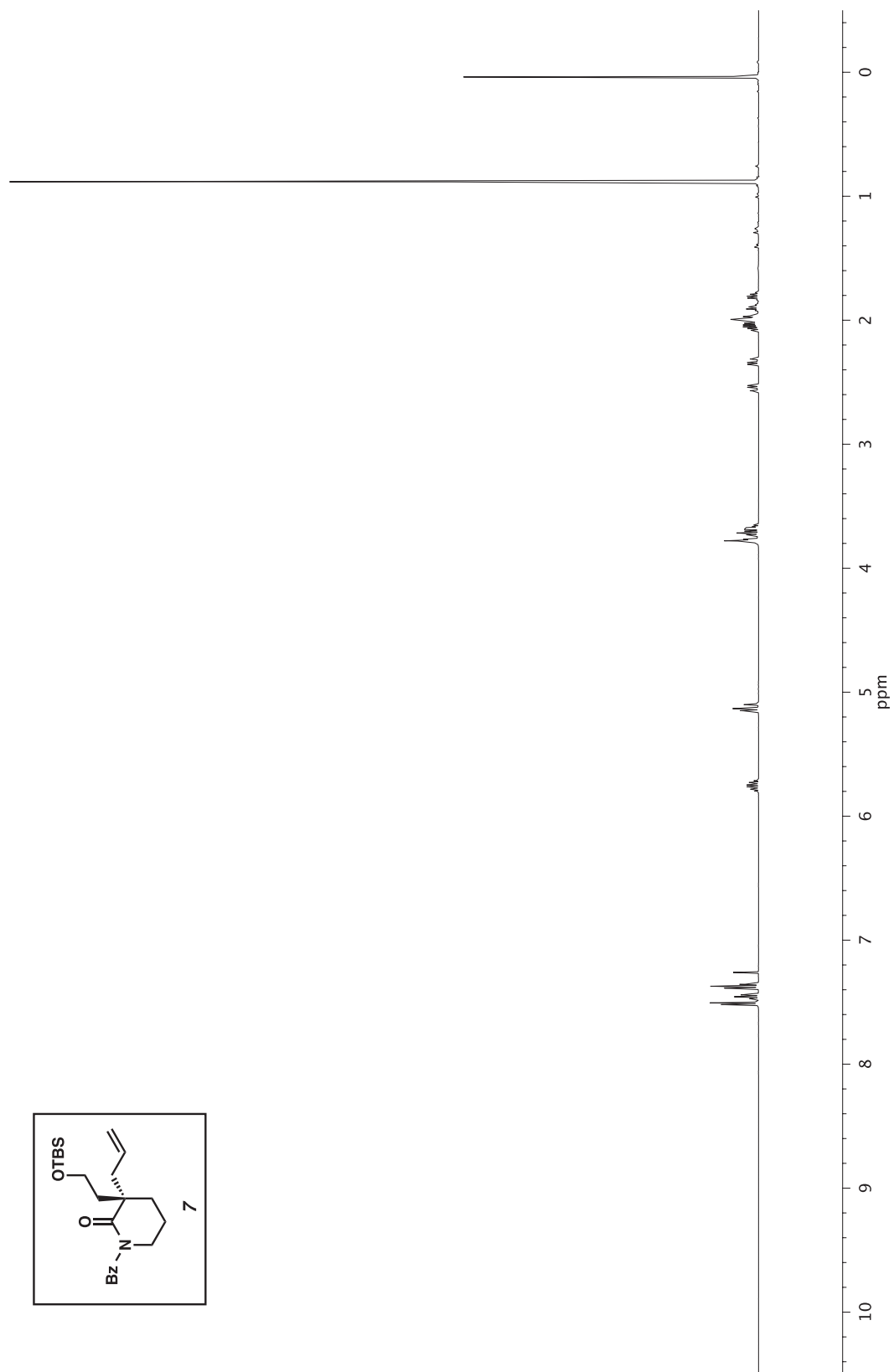


Figure A1.64 ^1H NMR (500 MHz, CDCl_3) of compound 7.

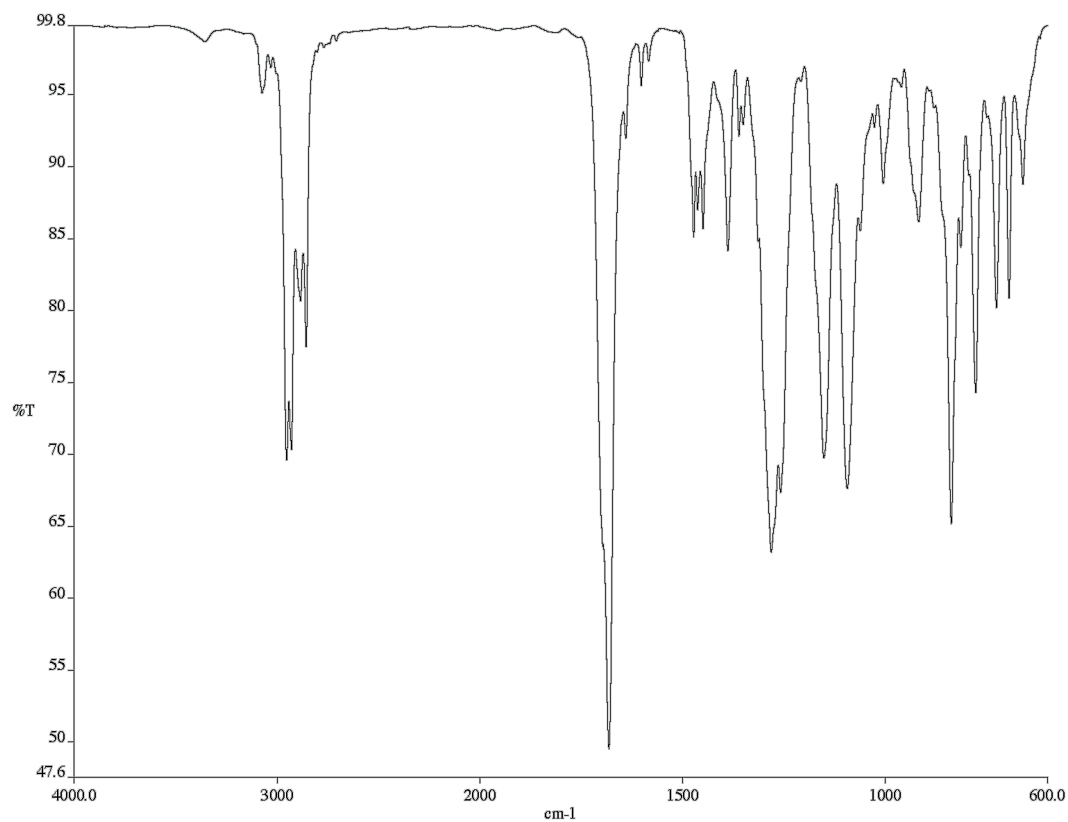


Figure A1.65 Infrared spectrum (Thin Film, NaCl) of compound 7.

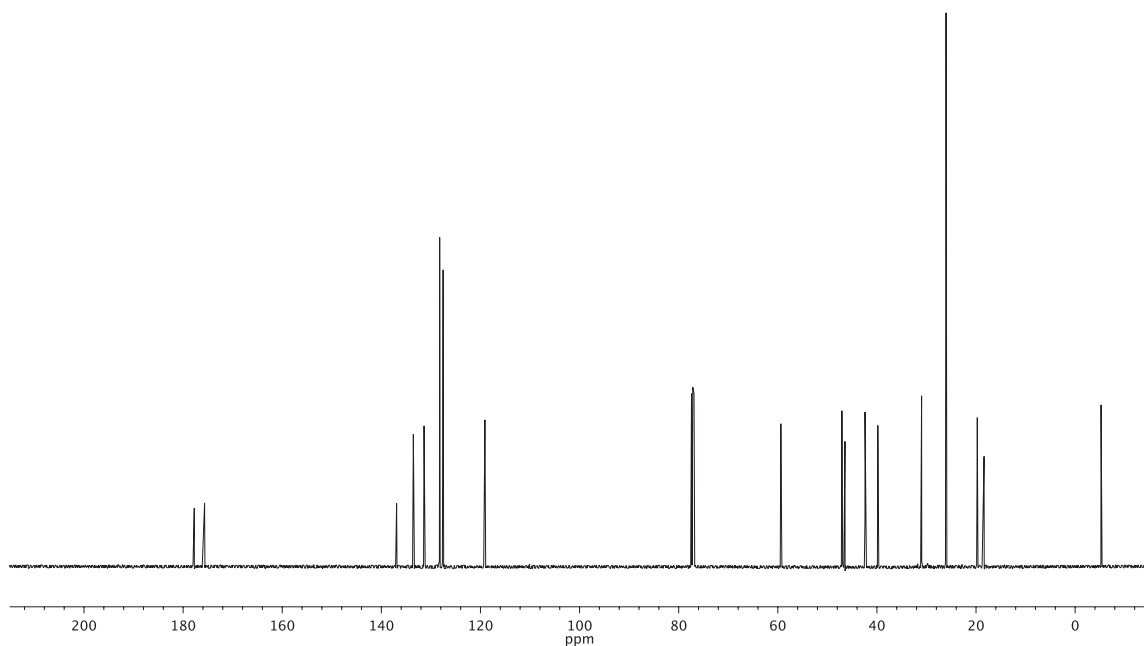


Figure A1.66 ¹³C NMR (126 MHz, CDCl₃) of compound 7.

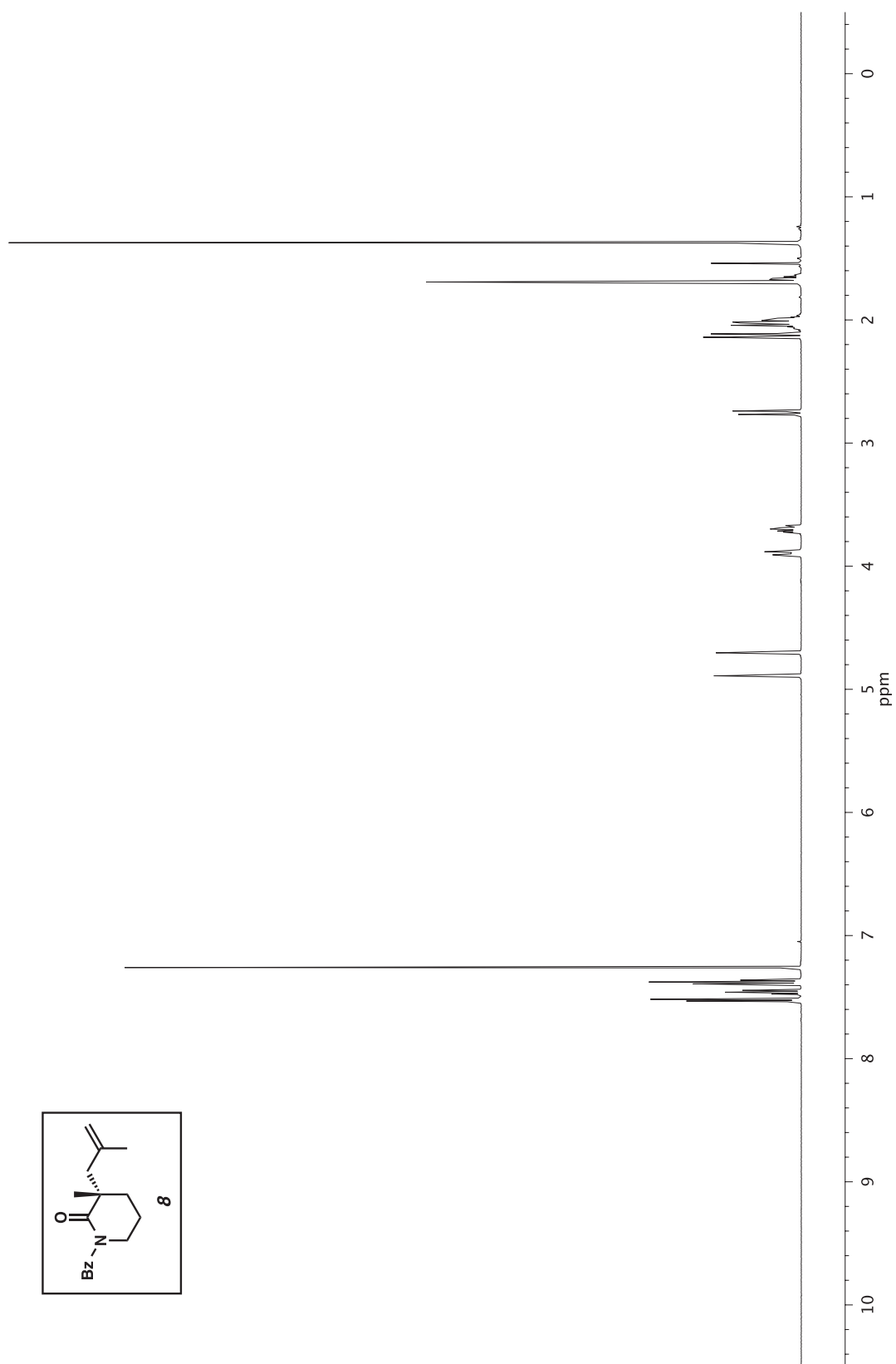


Figure A1.67 ^1H NMR (500 MHz, CDCl_3) of compound **8**.

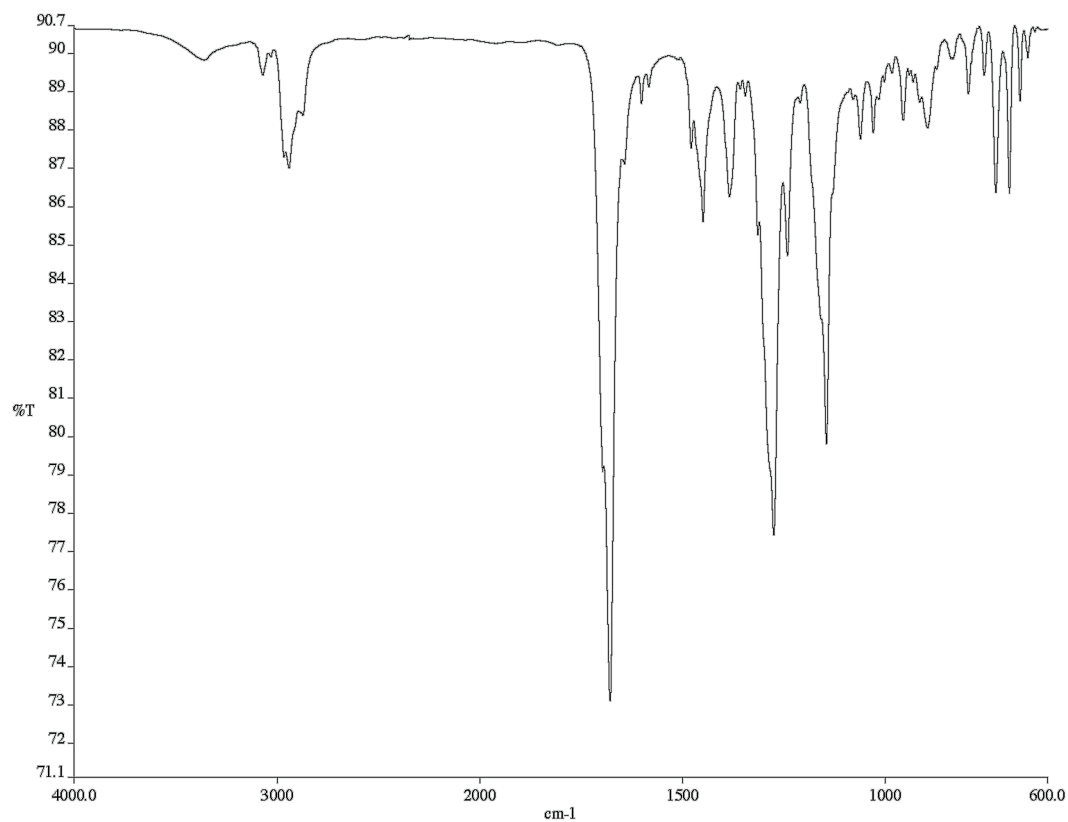


Figure A1.68 Infrared spectrum (Thin Film, NaCl) of compound **8**.

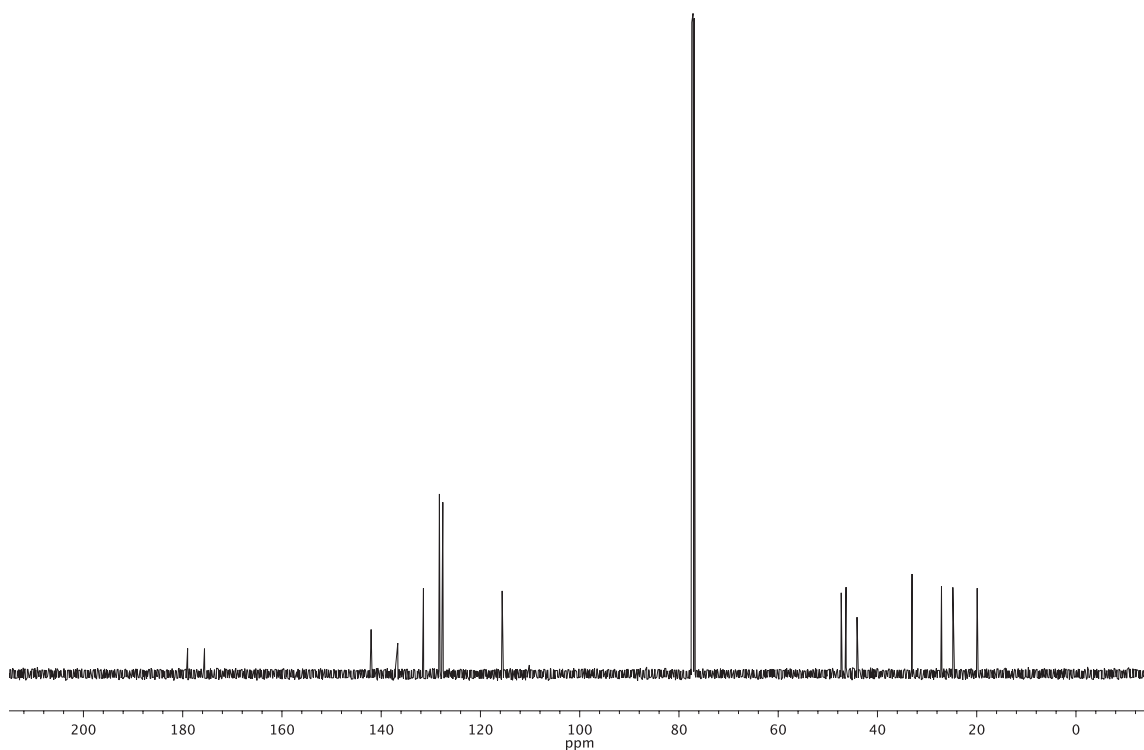


Figure A1.69 ¹³C NMR (126 MHz, CDCl₃) of compound **8**.

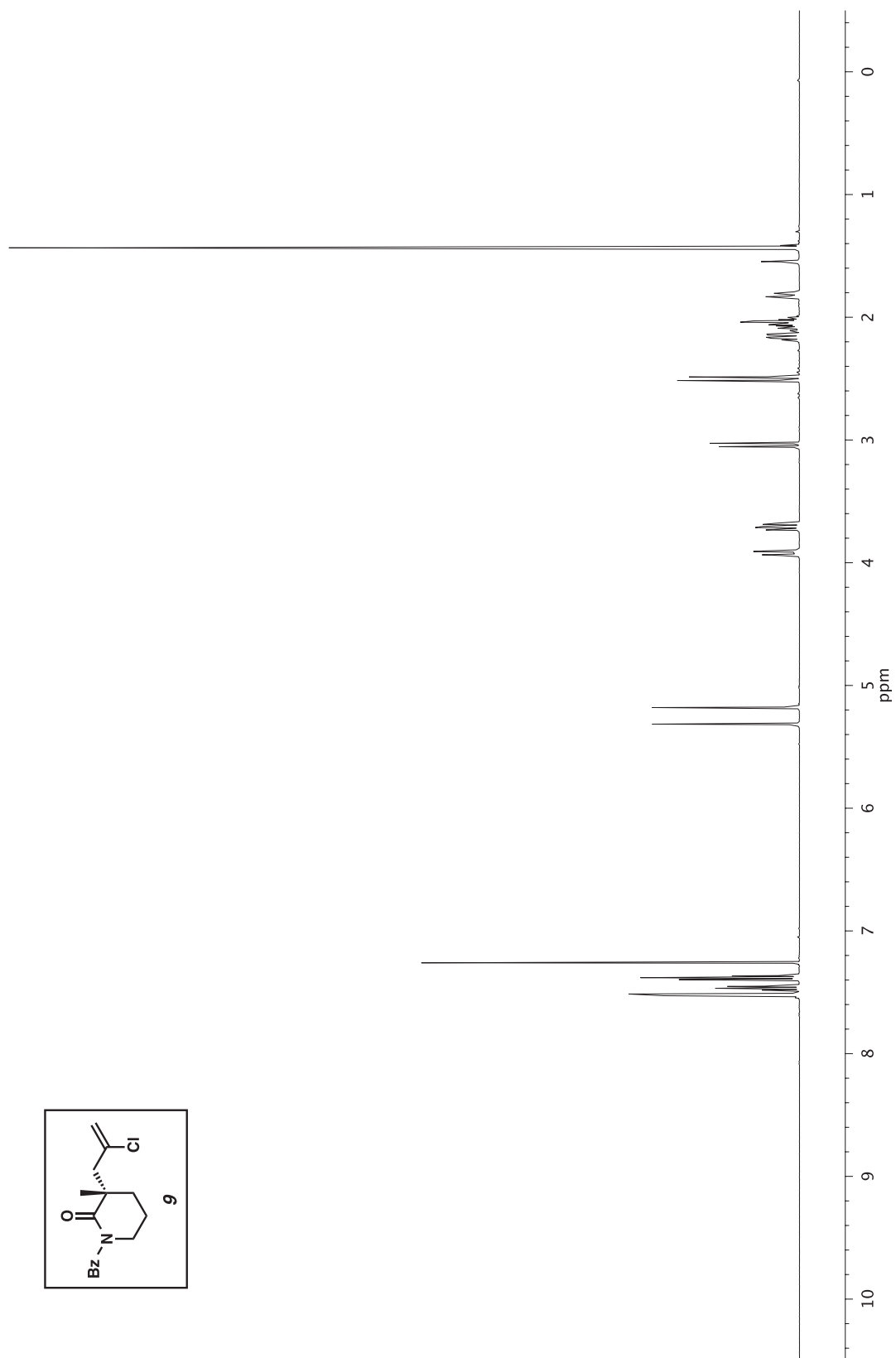


Figure A1.70 ^1H NMR (500 MHz, CDCl_3) of compound **9**.

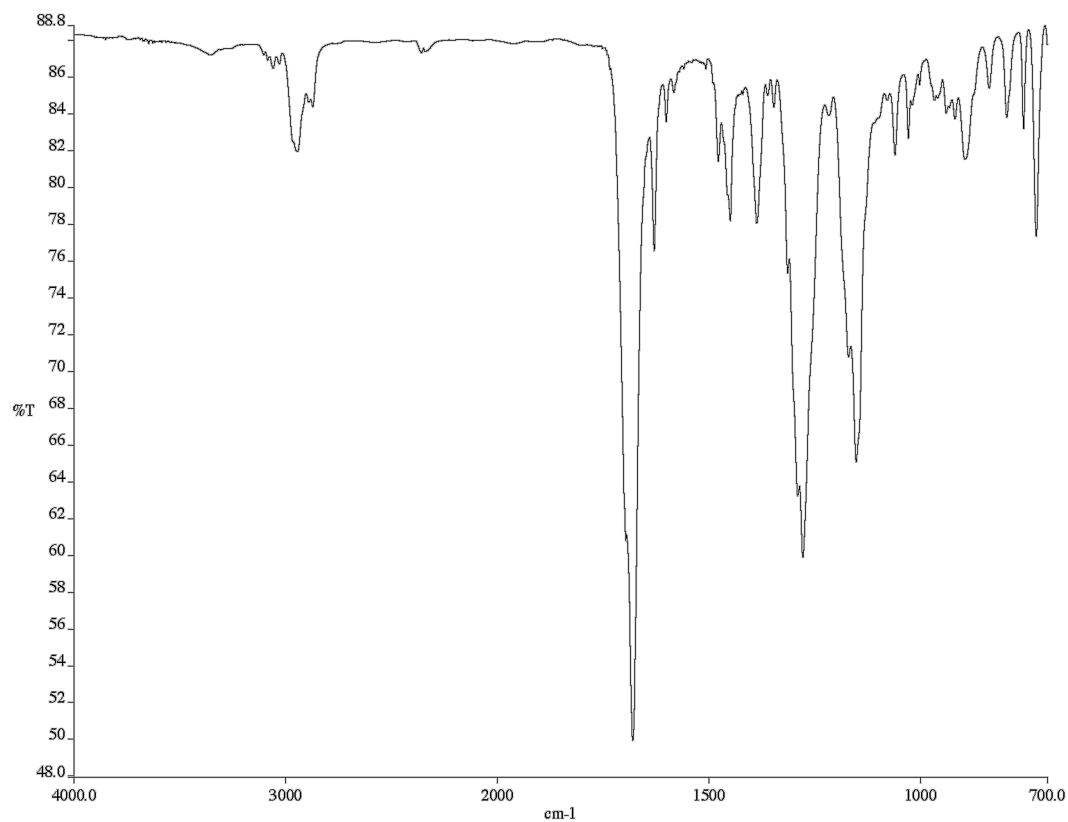


Figure A1.71 Infrared spectrum (Thin Film, NaCl) of compound **9**.

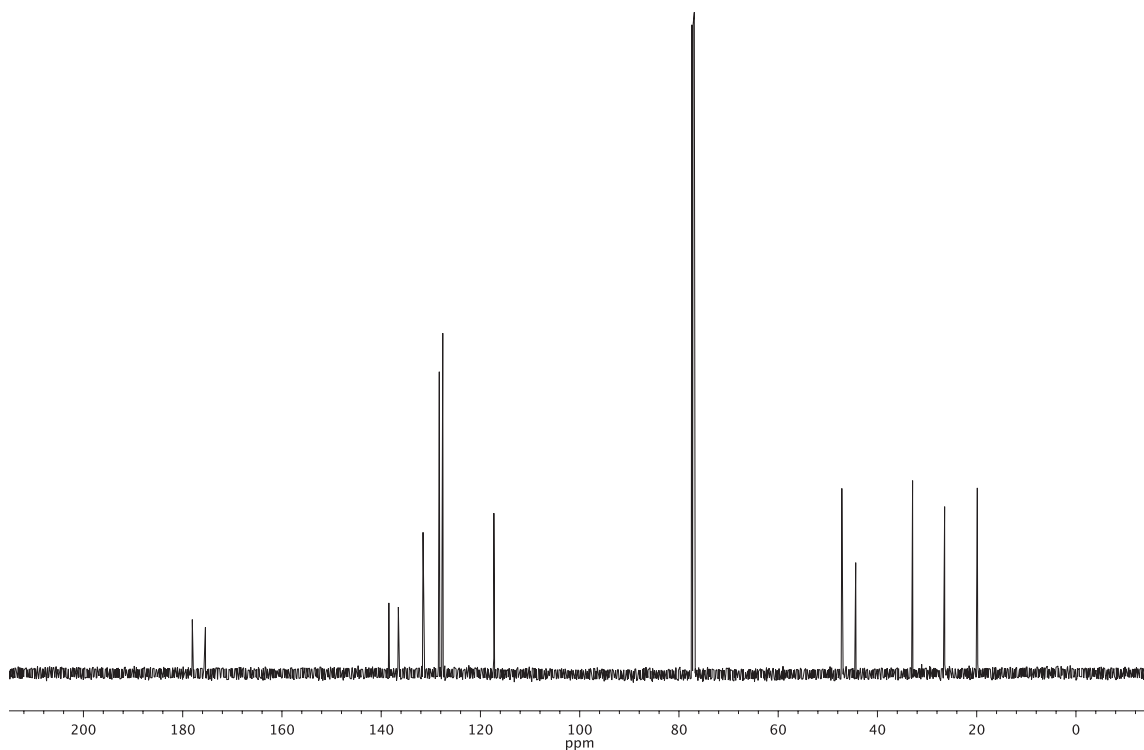


Figure A1.72 ¹³C NMR (126 MHz, CDCl₃) of compound **9**.

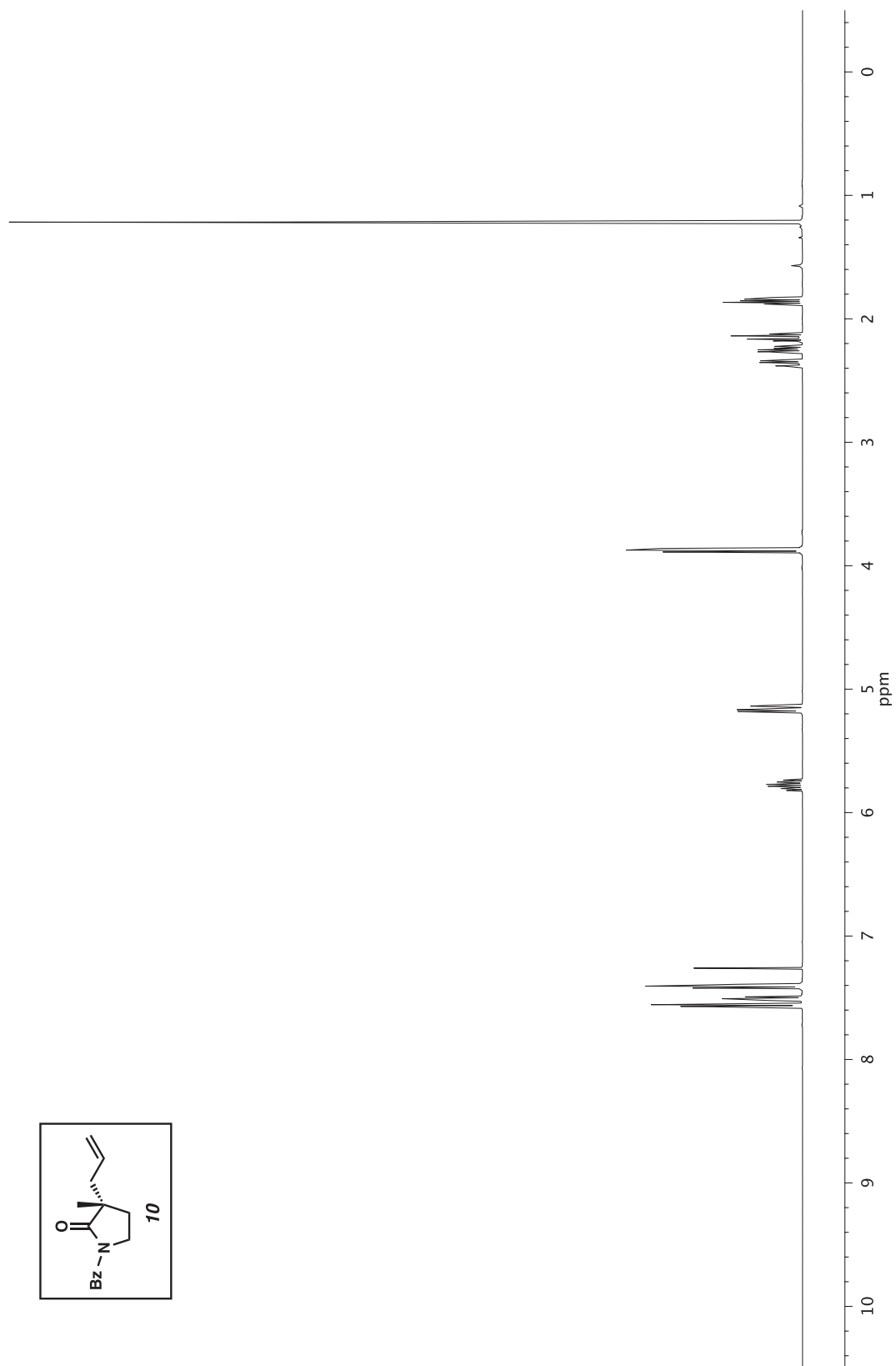


Figure A1.73 ^1H NMR (500 MHz, CDCl_3) of compound **10**.

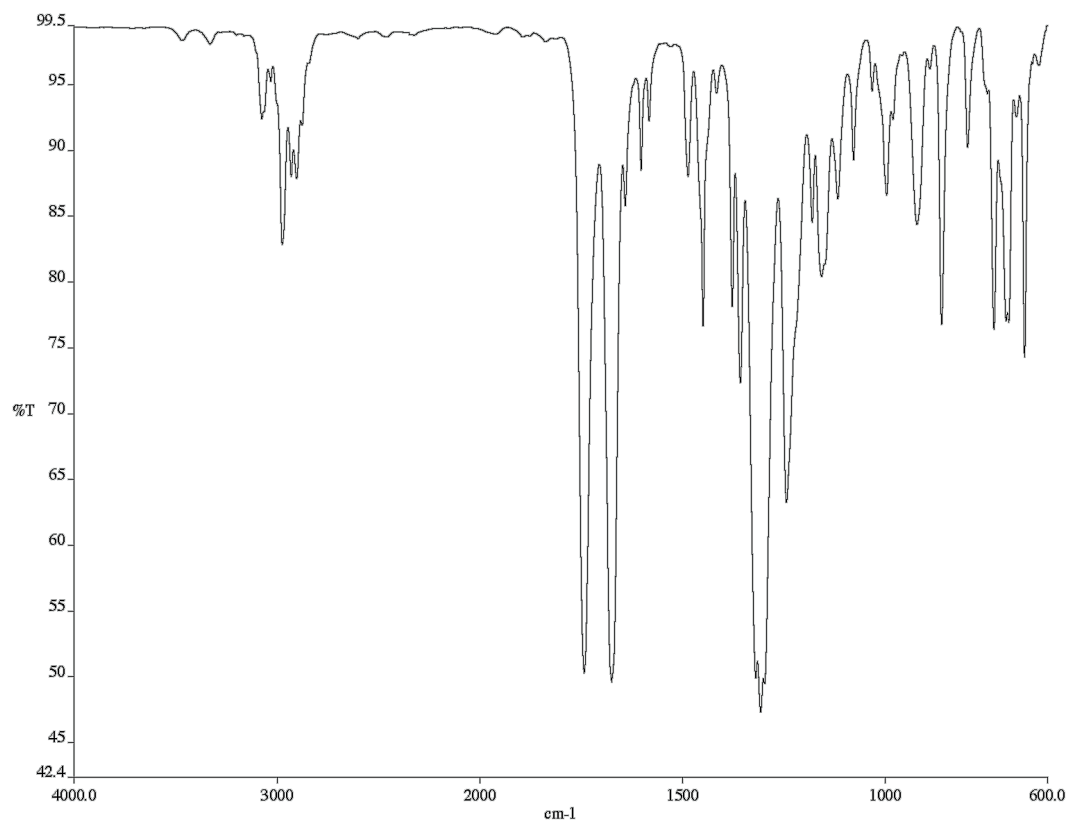


Figure A1.74 Infrared spectrum (Thin Film, NaCl) of compound **10**.

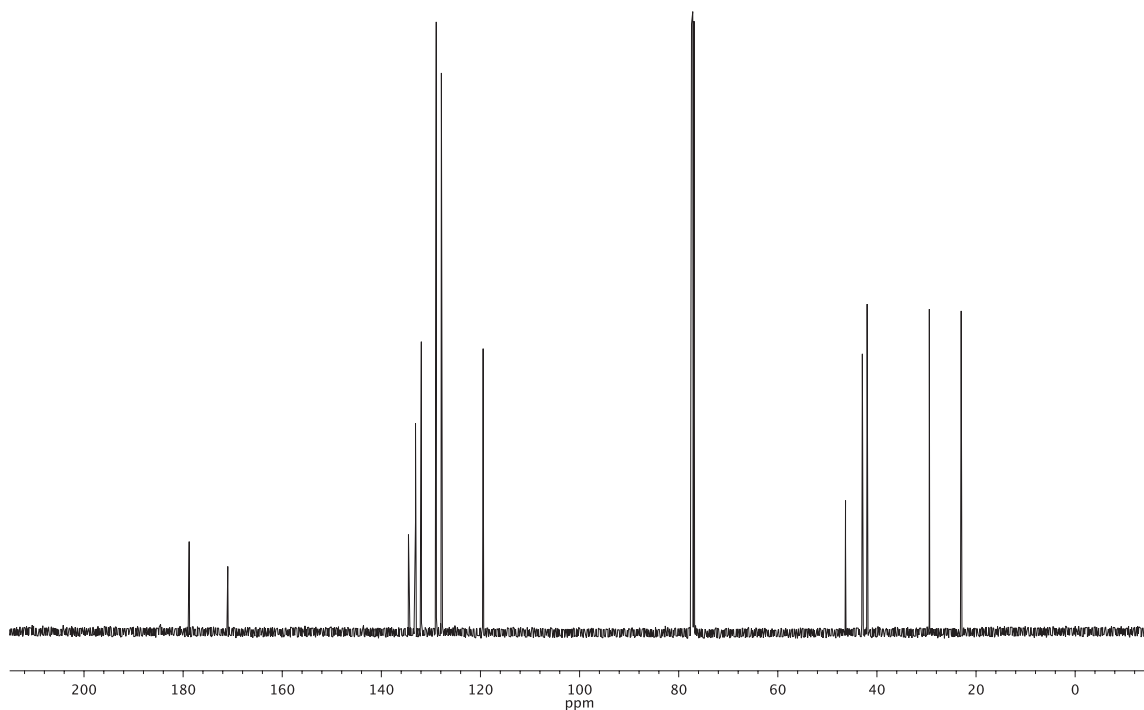


Figure A1.75 ¹³C NMR (126 MHz, CDCl₃) of compound **10**.

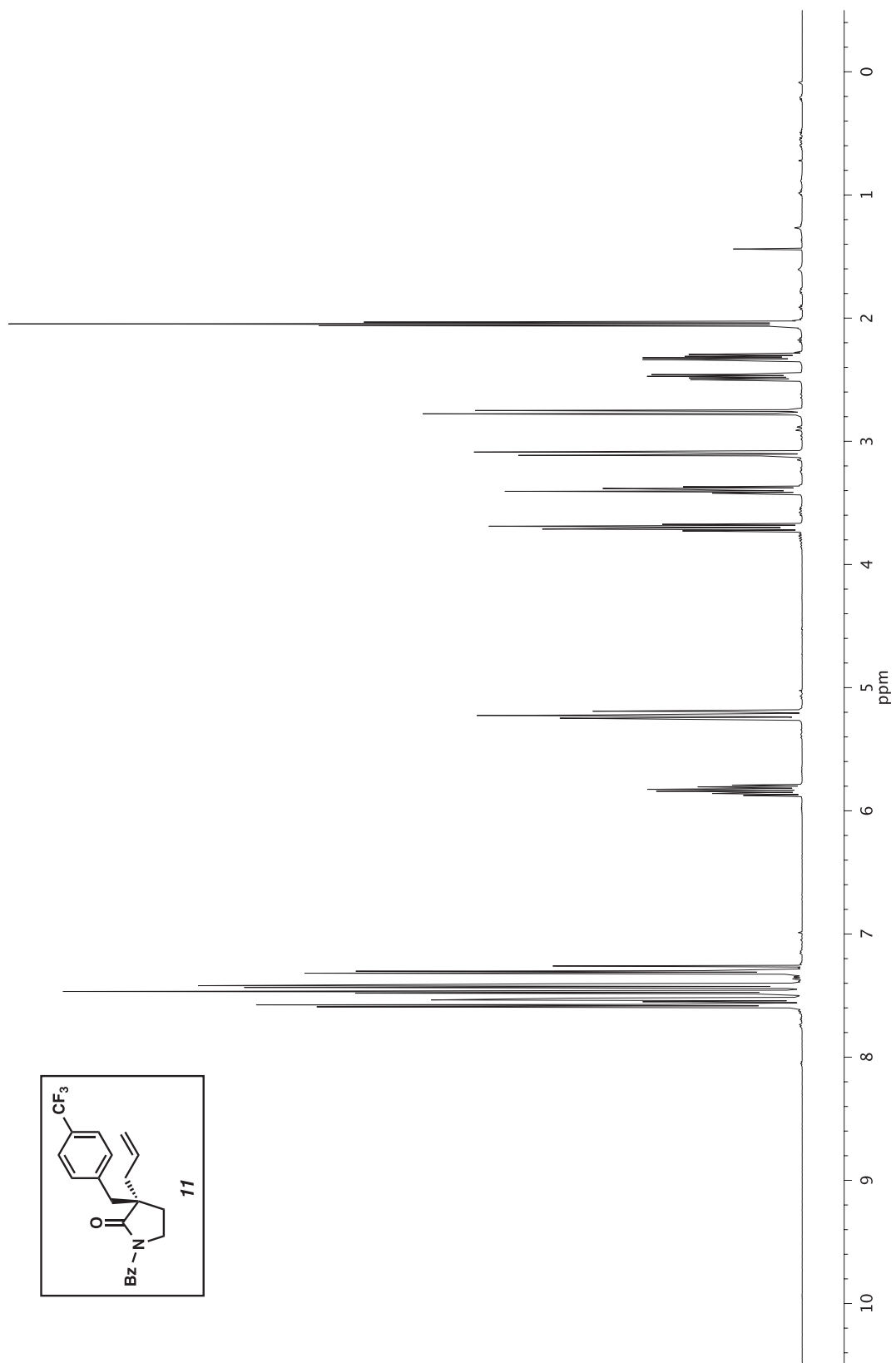


Figure A1.76 ^1H NMR (500 MHz, CDCl_3) of compound **11**.

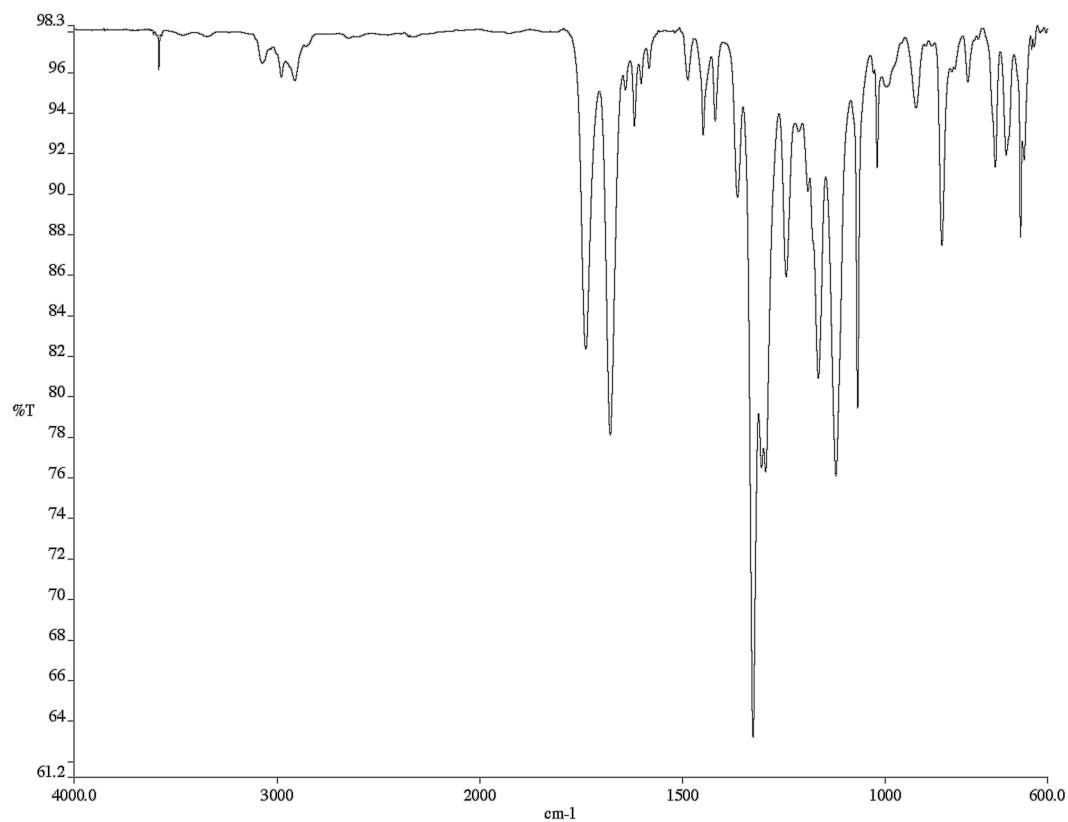


Figure A1.77 Infrared spectrum (Thin Film, NaCl) of compound **11**.

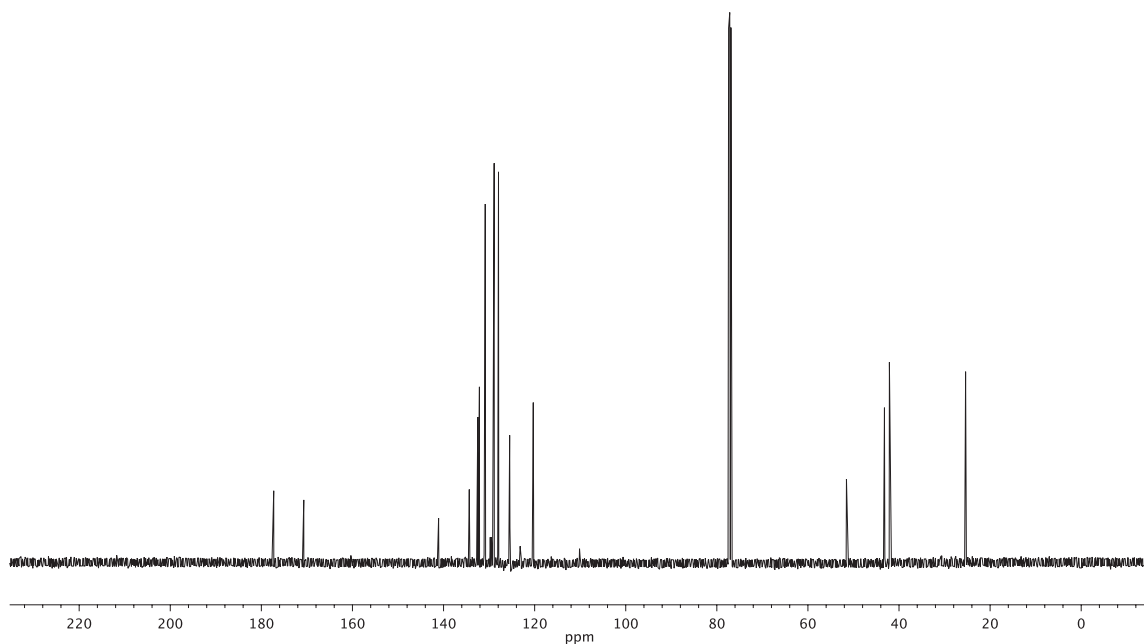


Figure A1.78 ¹³C NMR (126 MHz, CDCl₃) of compound **11**.

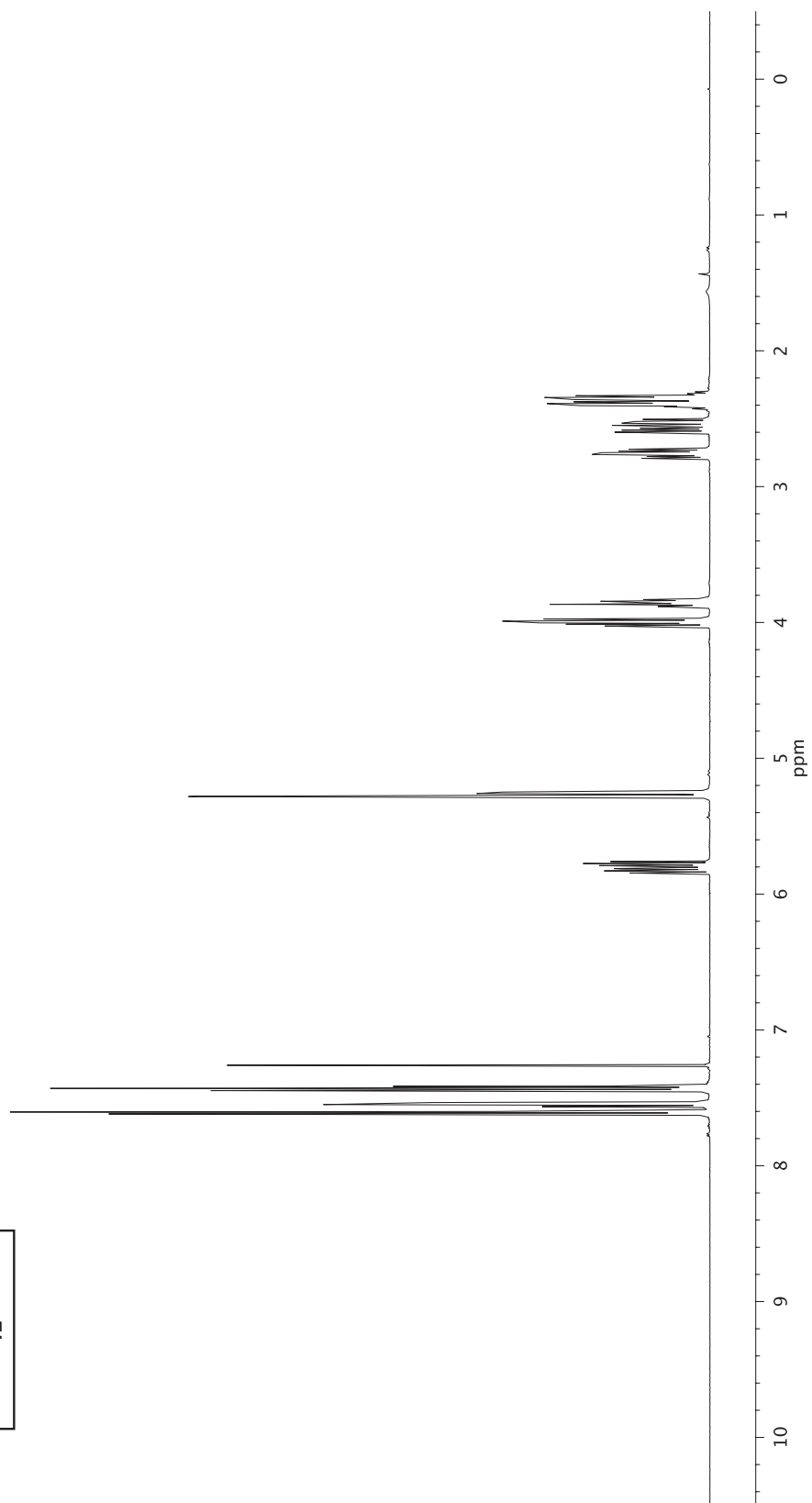
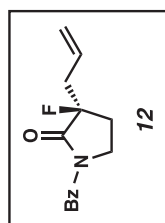


Figure A1.79 ¹H NMR (500 MHz, CDCl₃) of compound **12**.

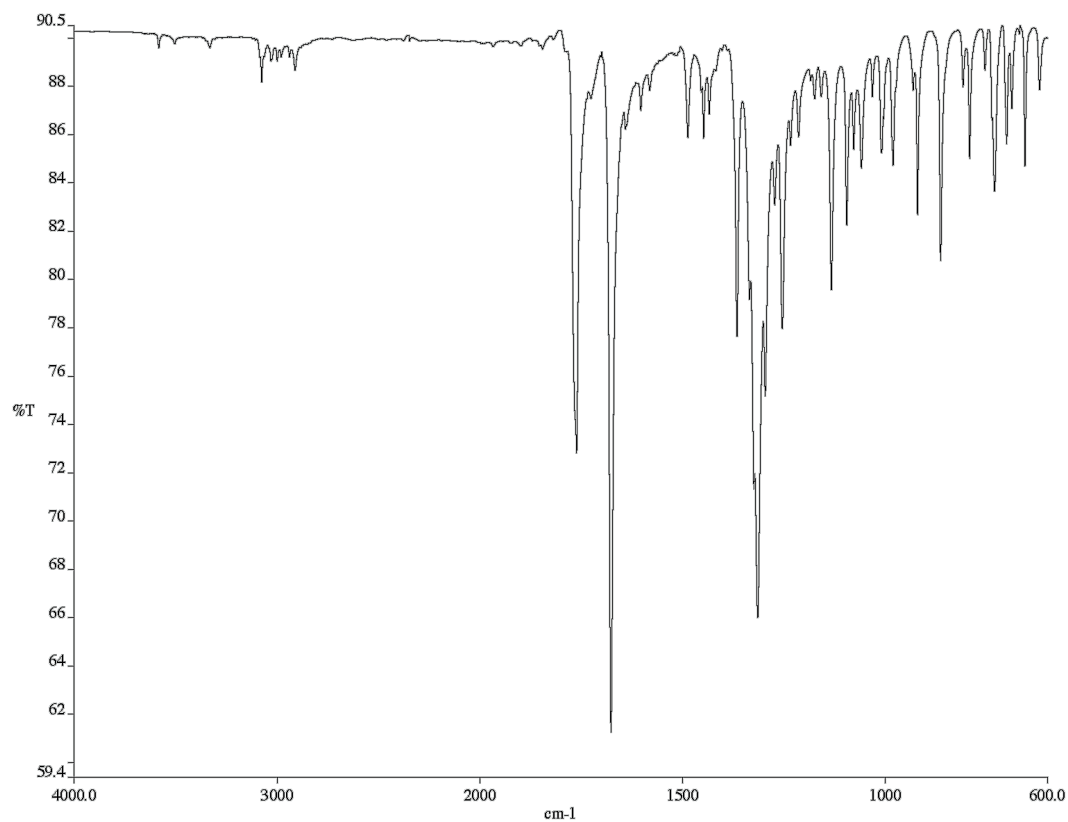


Figure A1.80 Infrared spectrum (Thin Film, NaCl) of compound **12**.

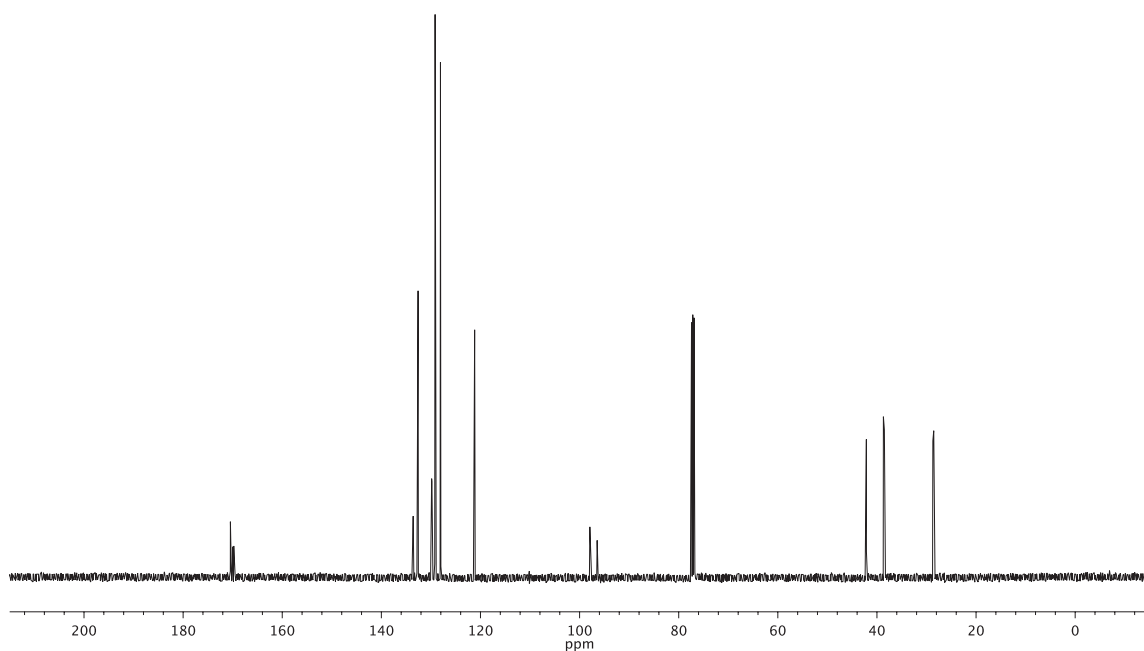


Figure A1.81 ¹³C NMR (126 MHz, CDCl₃) of compound **12**.

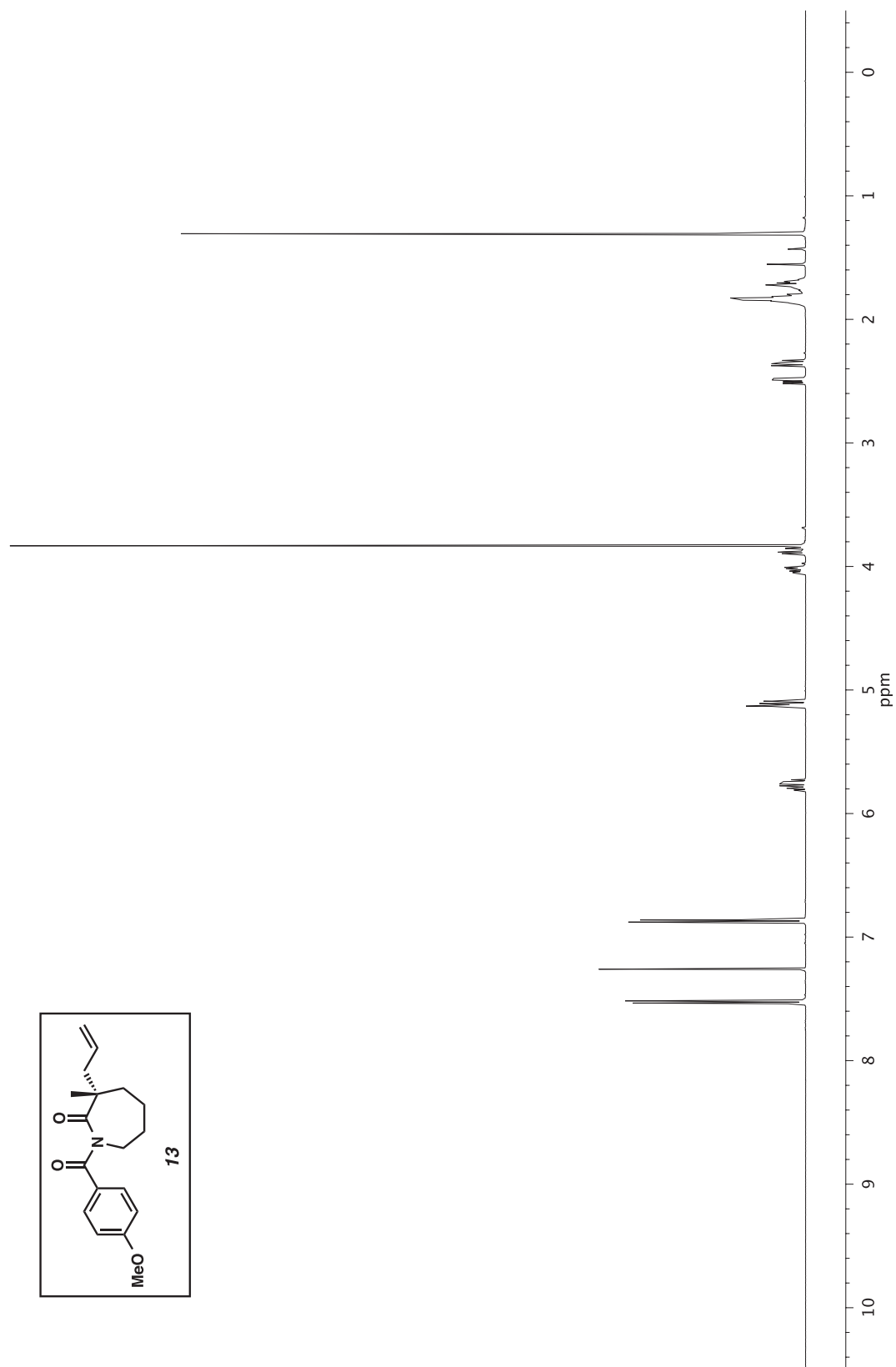


Figure A1.82 ^1H NMR (500 MHz, CDCl_3) of compound **13**.

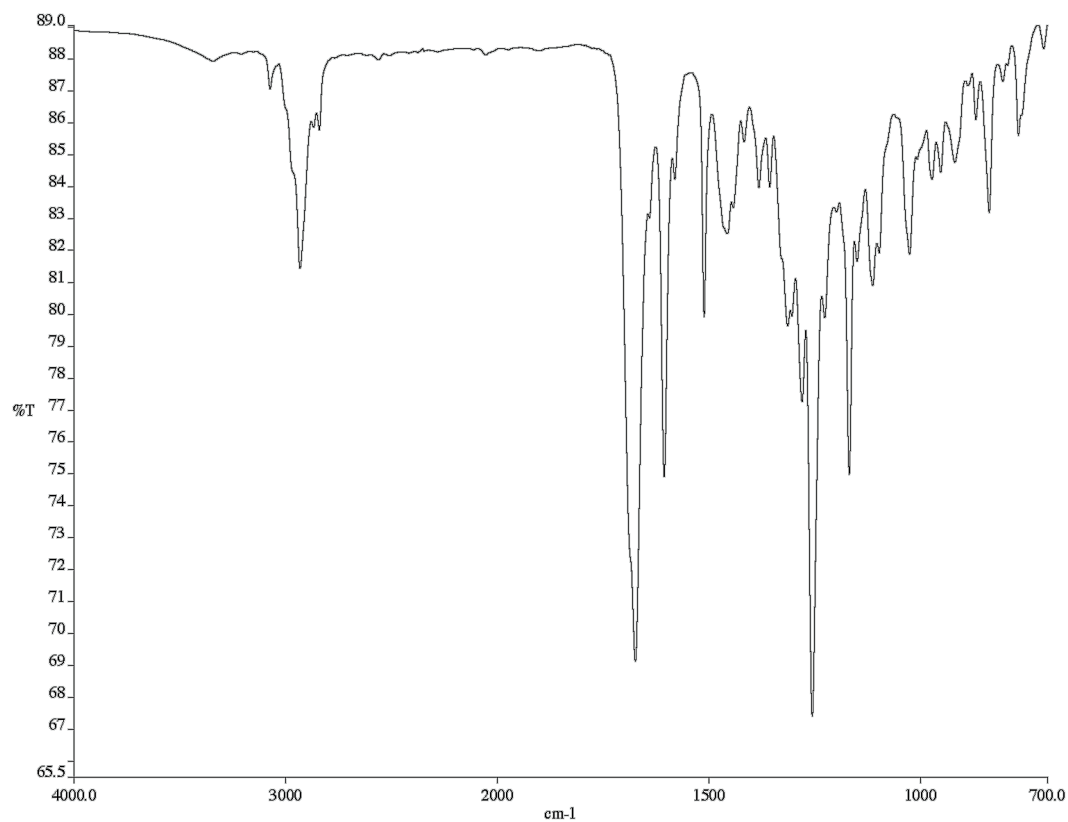


Figure A1.83 Infrared spectrum (Thin Film, NaCl) of compound **13**.

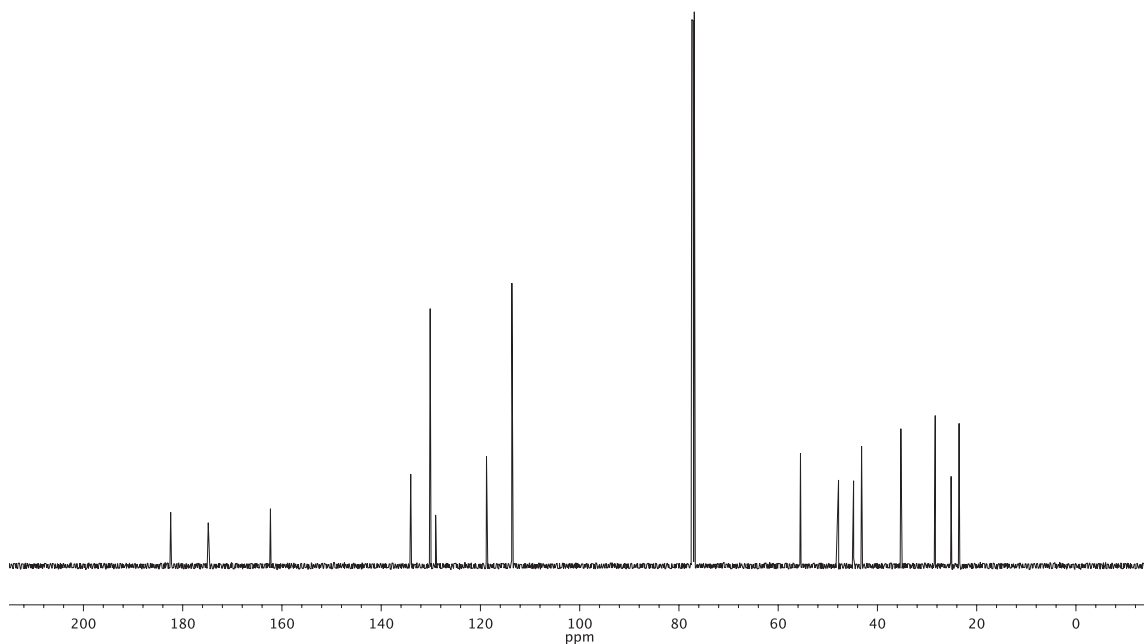


Figure A1.84 ¹³C NMR (126 MHz, CDCl₃) of compound **13**.

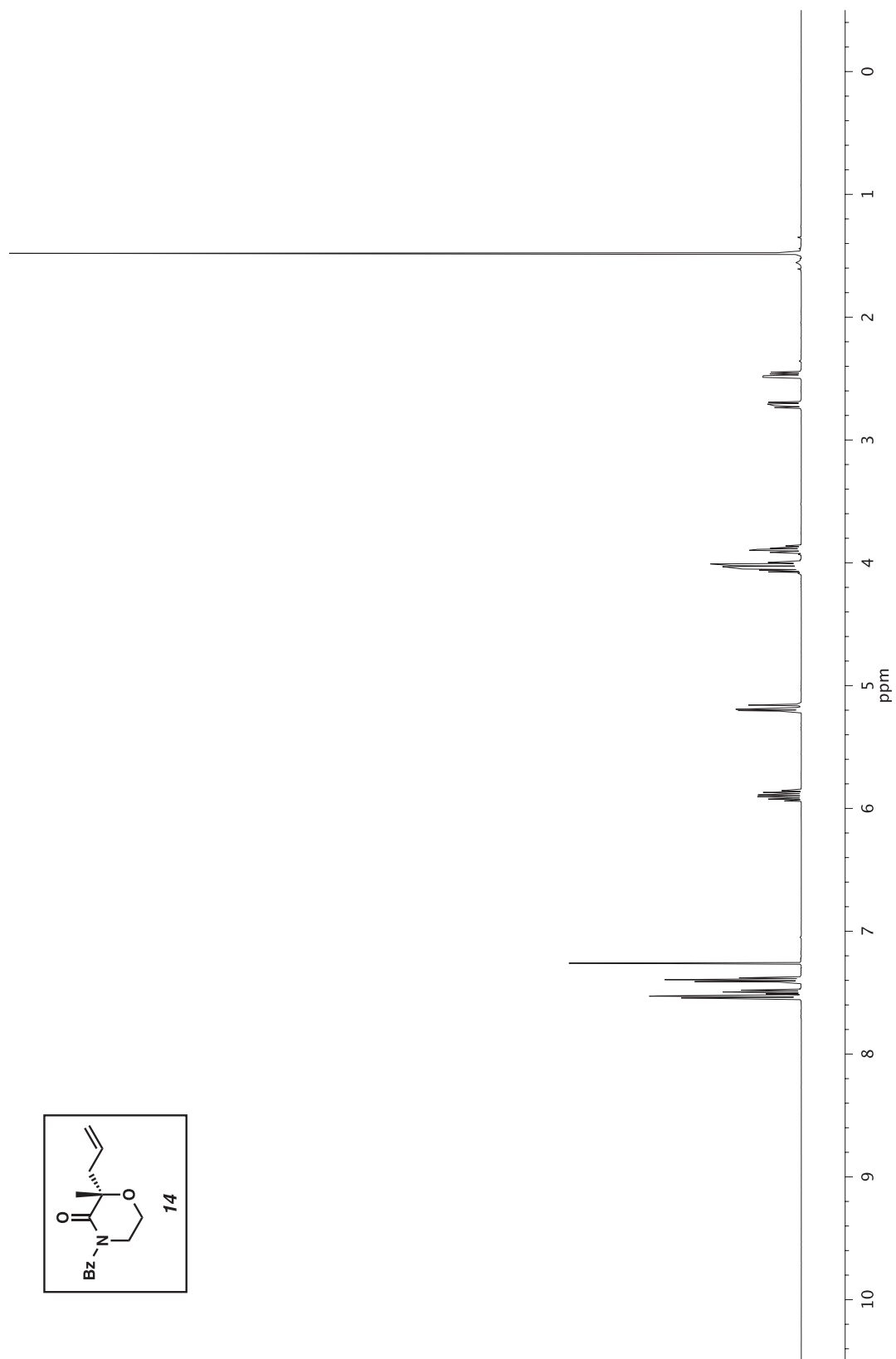


Figure A1.85 ^1H NMR (500 MHz, CDCl_3) of compound **14**.

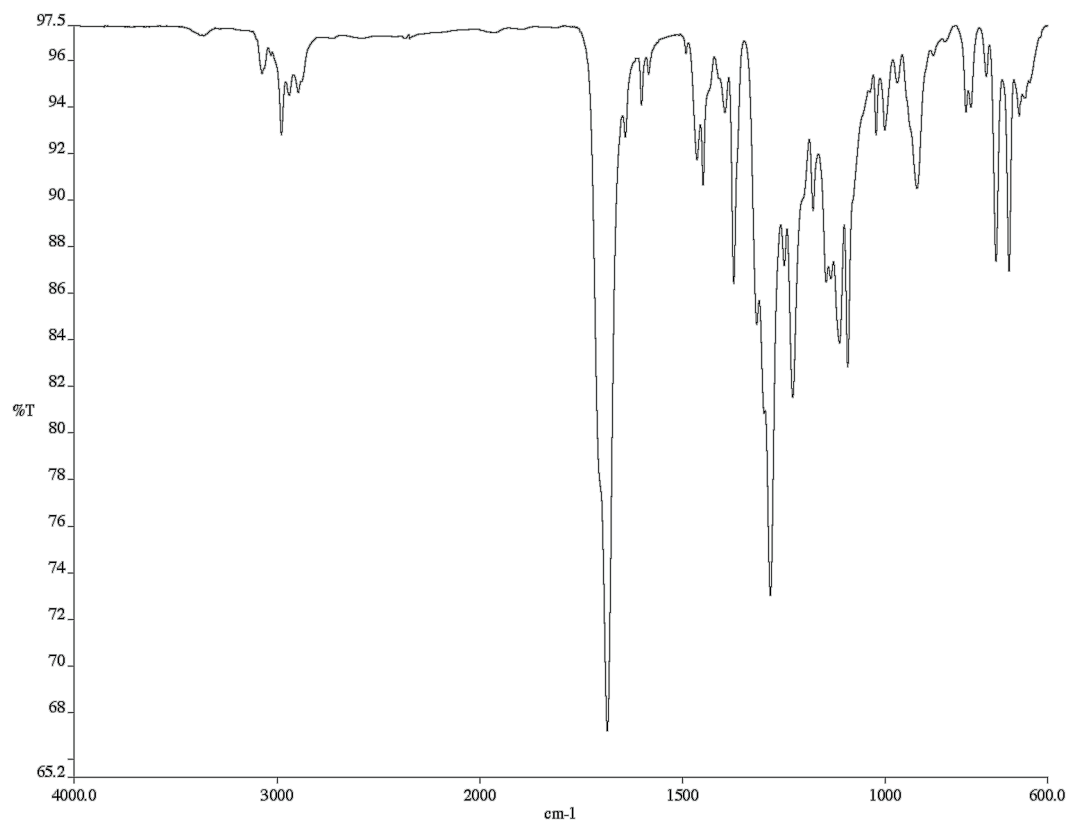


Figure A1.86 Infrared spectrum (Thin Film, NaCl) of compound **14**.

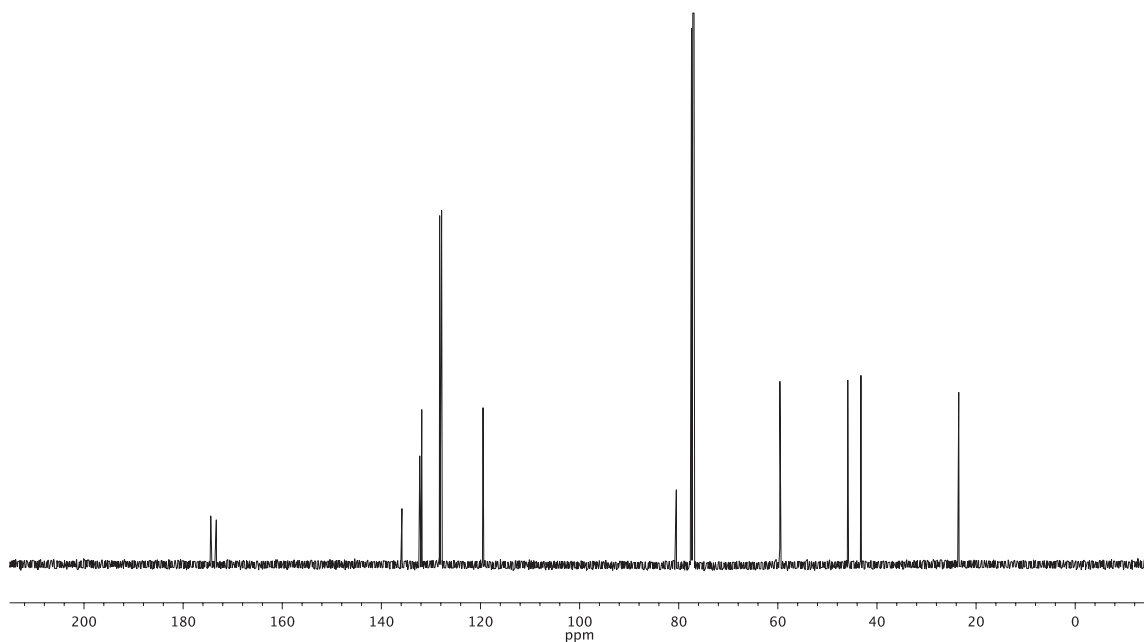
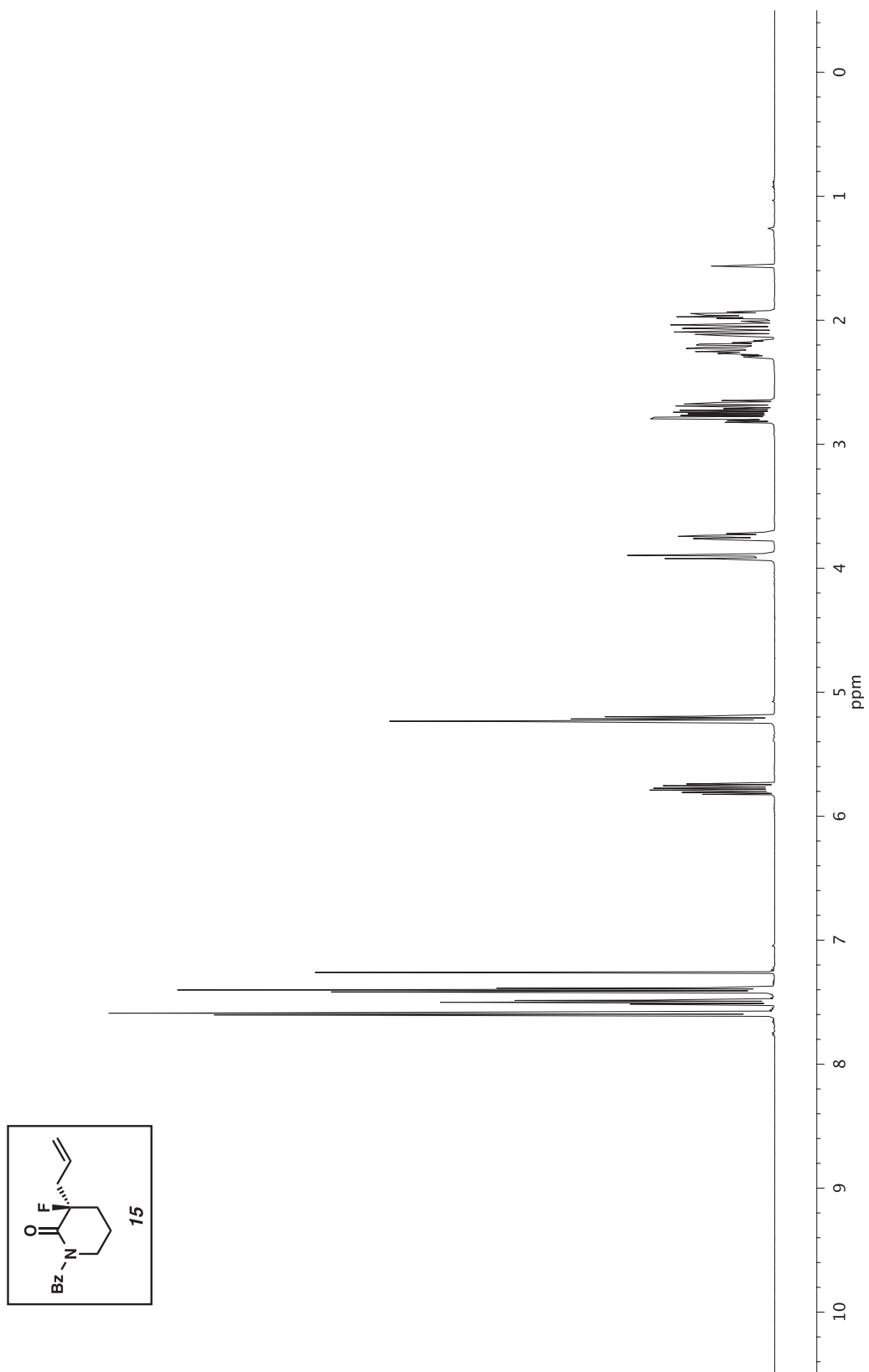


Figure A1.87 ¹³C NMR (126 MHz, CDCl₃) of compound **14**.

Figure A1.88 ^1H NMR (500 MHz, CDCl_3) of compound **15**.

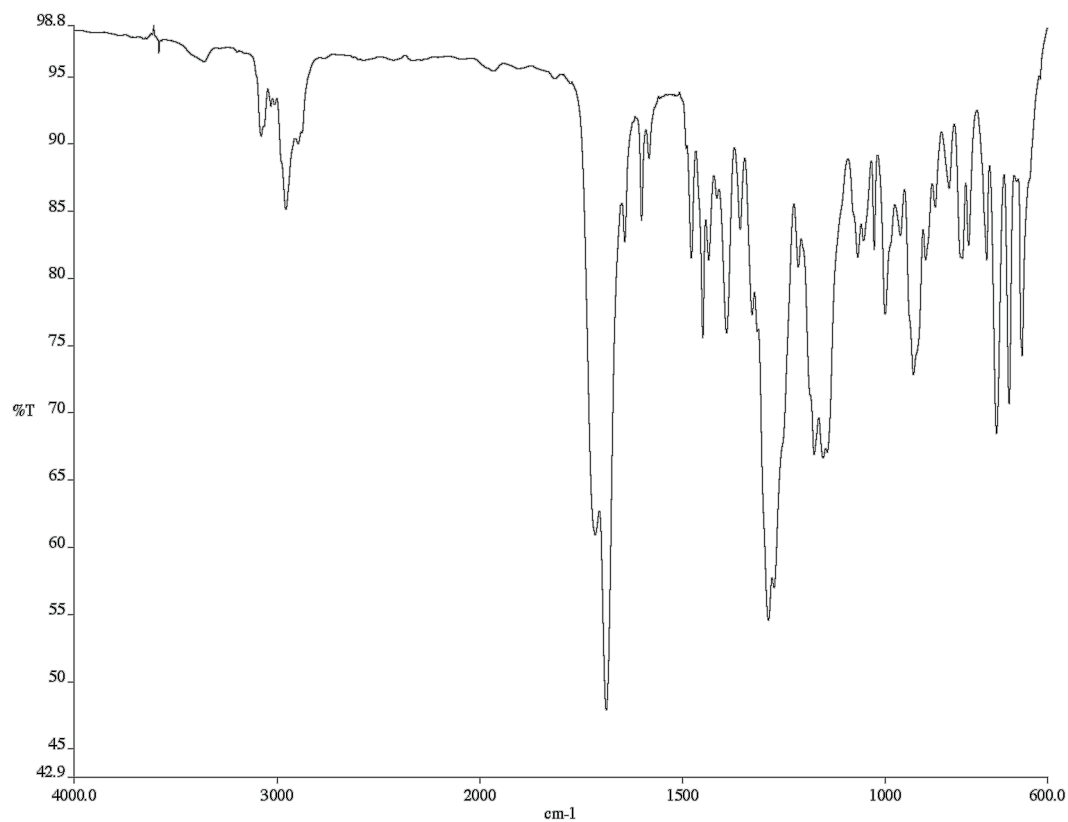


Figure A1.89 Infrared spectrum (Thin Film, NaCl) of compound **15**.

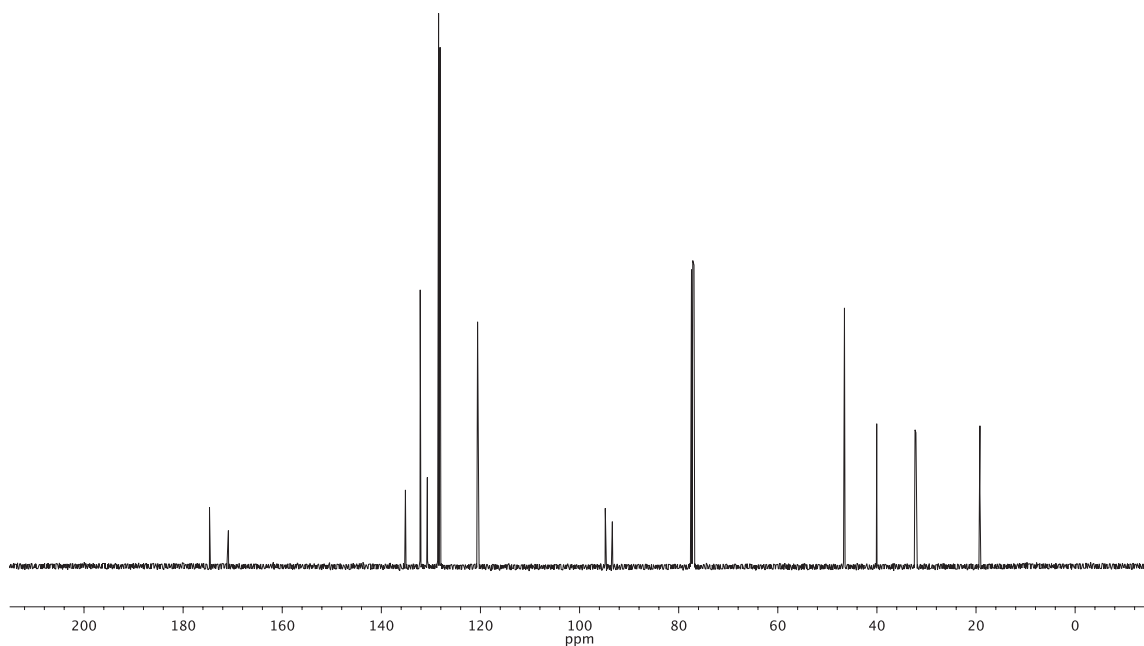


Figure A1.90 ¹³C NMR (126 MHz, CDCl₃) of compound **15**.

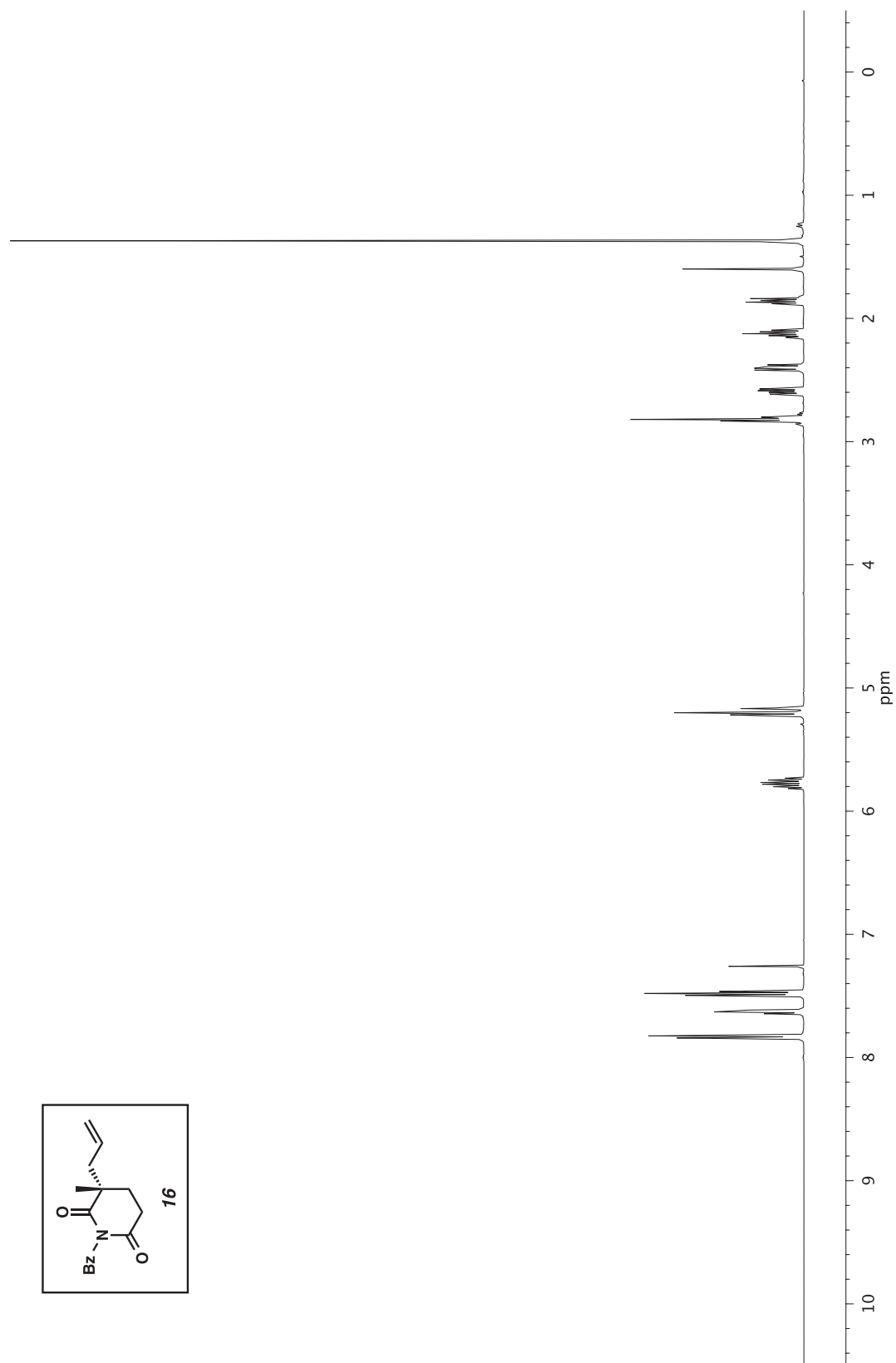
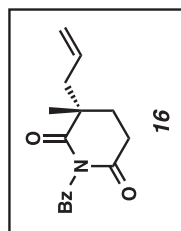


Figure A1.91 ¹H NMR (500 MHz, CDCl₃) of compound **16**.

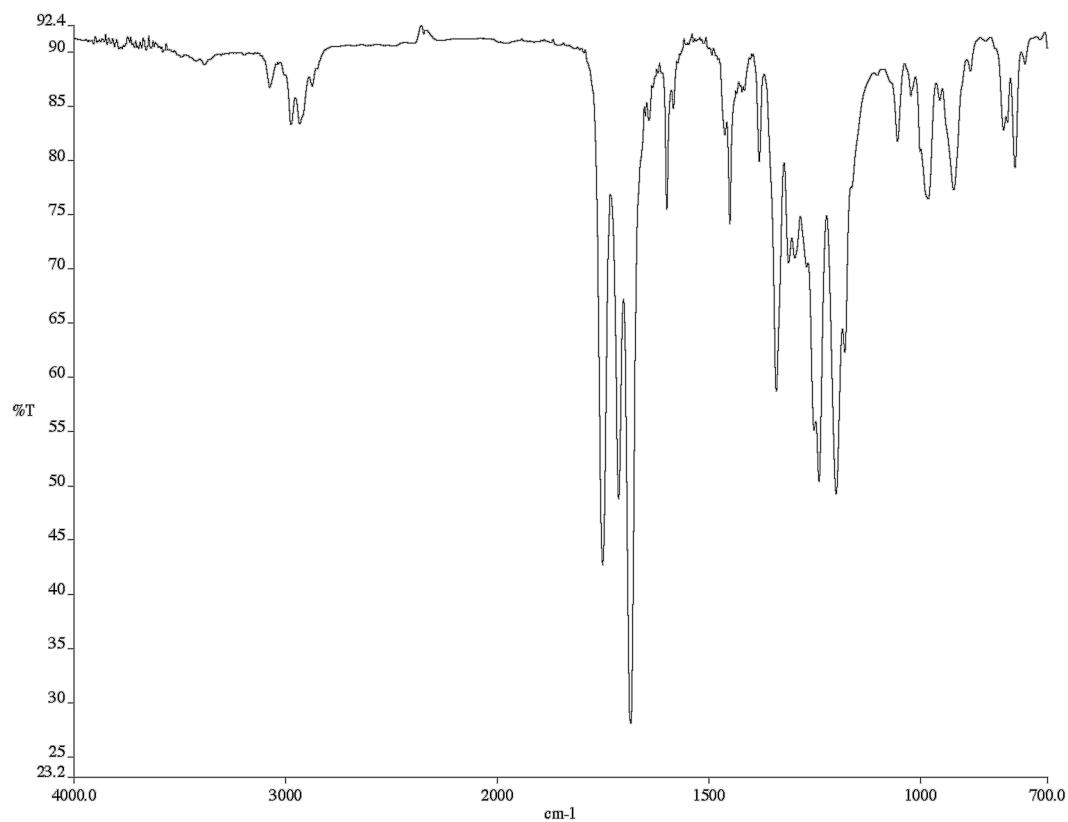


Figure A1.92 Infrared spectrum (Thin Film, NaCl) of compound **16**.

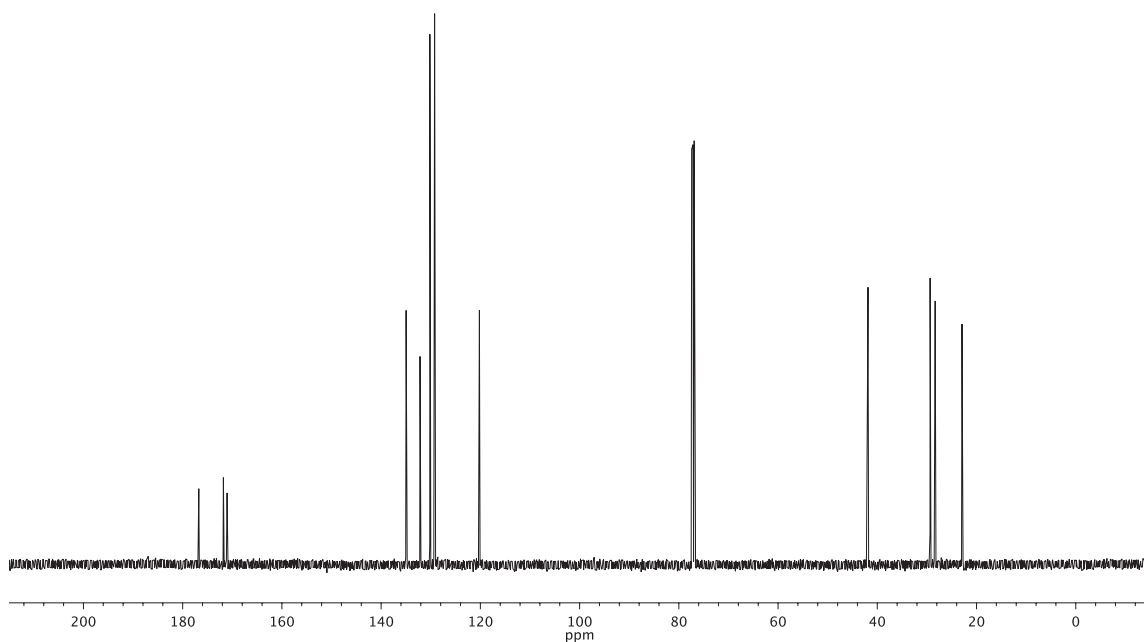


Figure A1.93 ¹³C NMR (126 MHz, CDCl₃) of compound **16**.

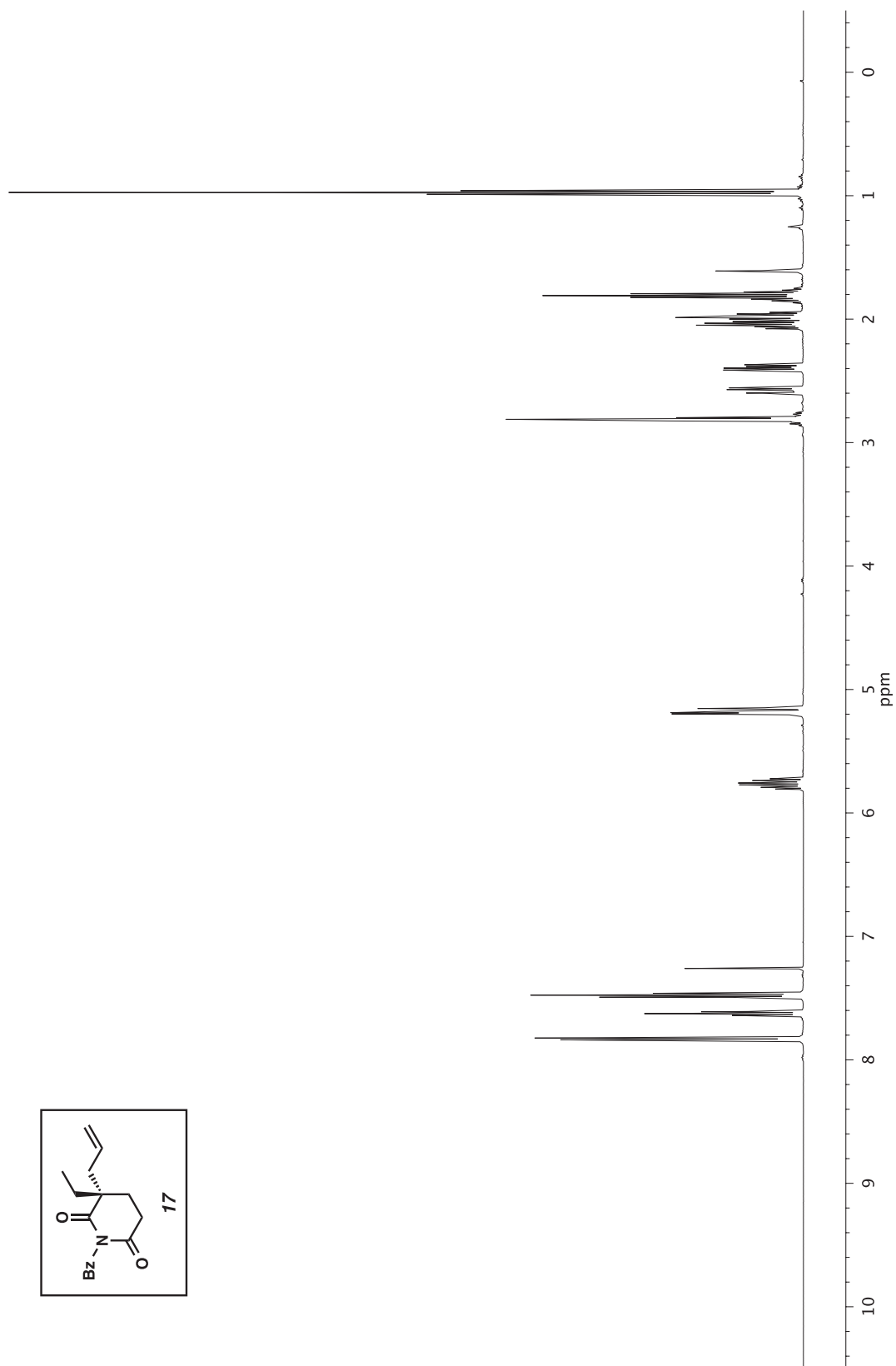


Figure A1.94 ^1H NMR (500 MHz, CDCl_3) of compound 17.

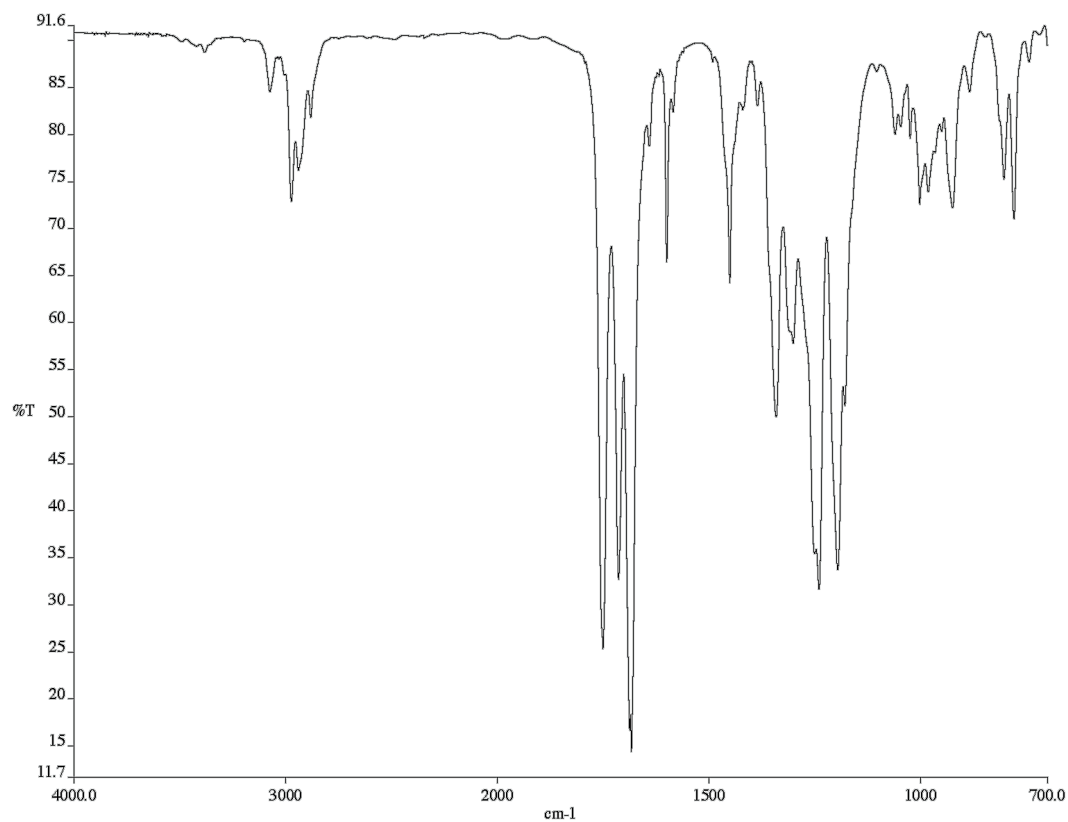


Figure A1.95 Infrared spectrum (Thin Film, NaCl) of compound 17.

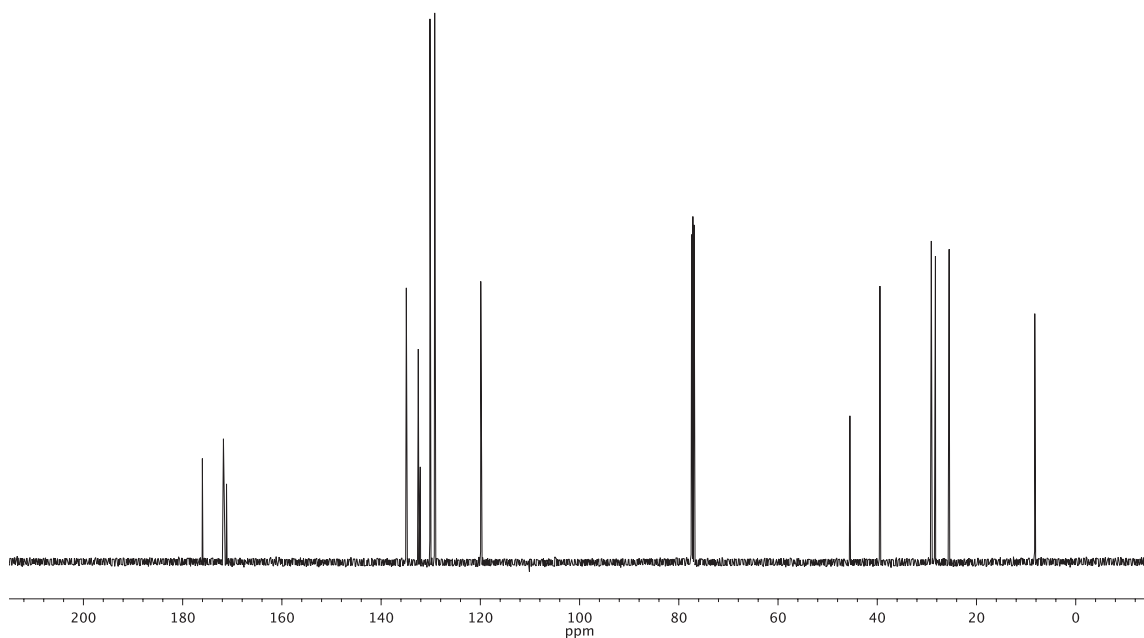
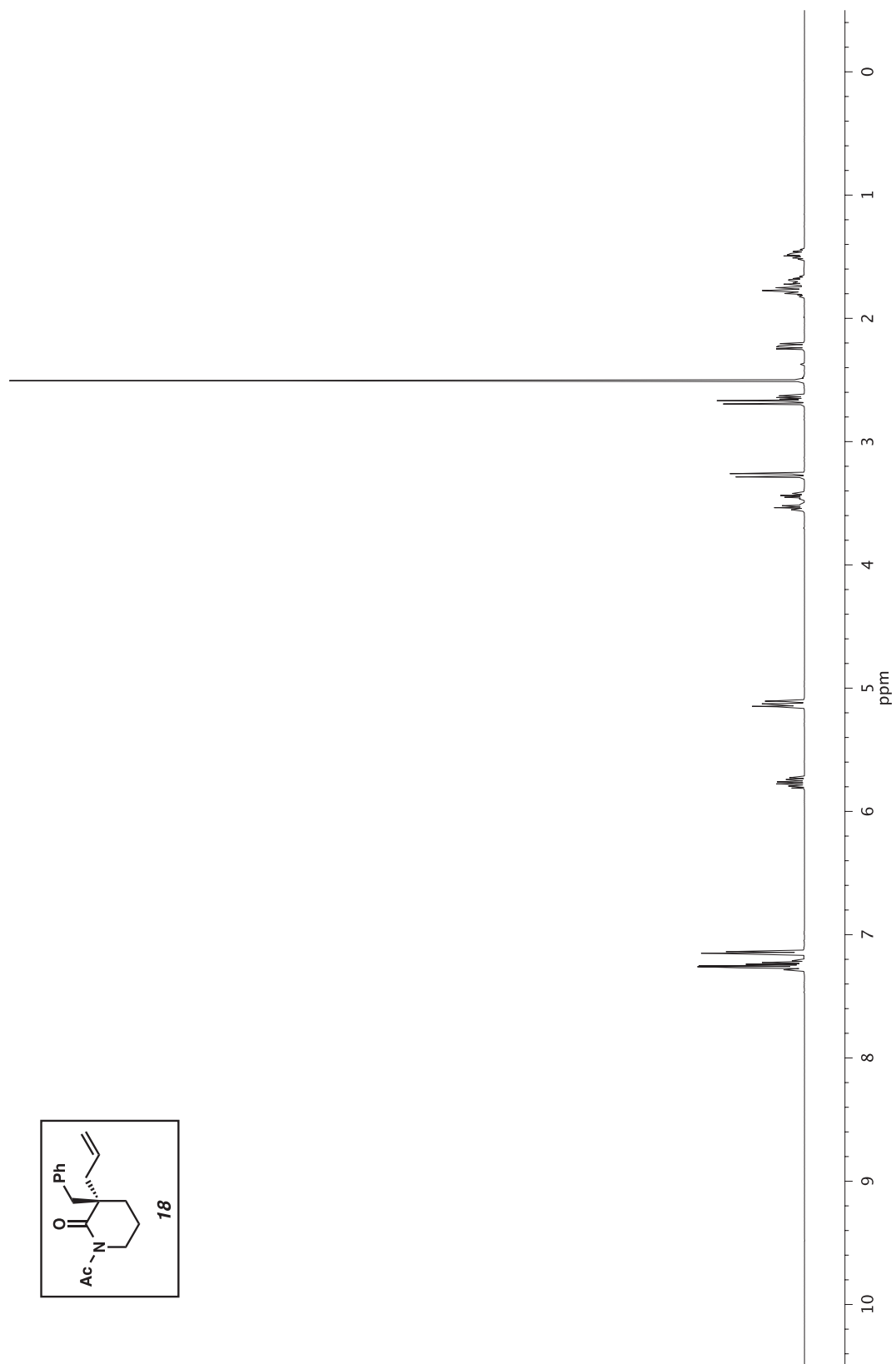


Figure A1.96 ¹³C NMR (126 MHz, CDCl₃) of compound 17.



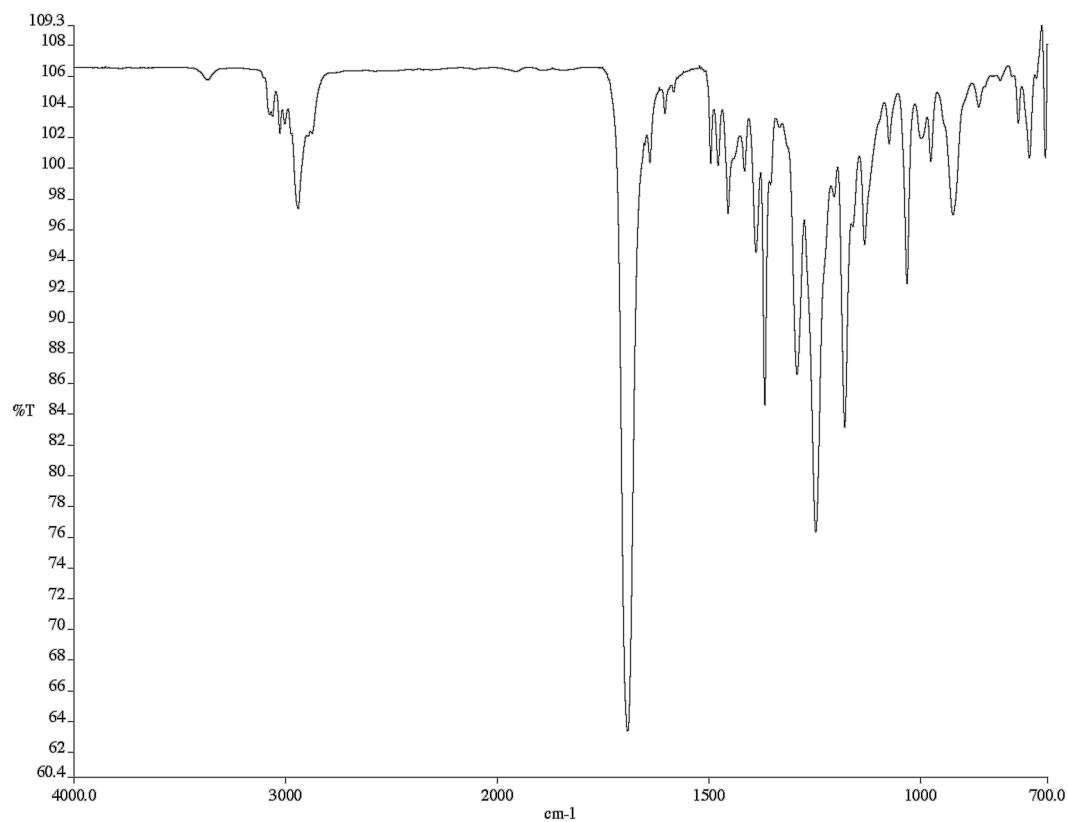


Figure A1.98 Infrared spectrum (Thin Film, NaCl) of compound **18**.

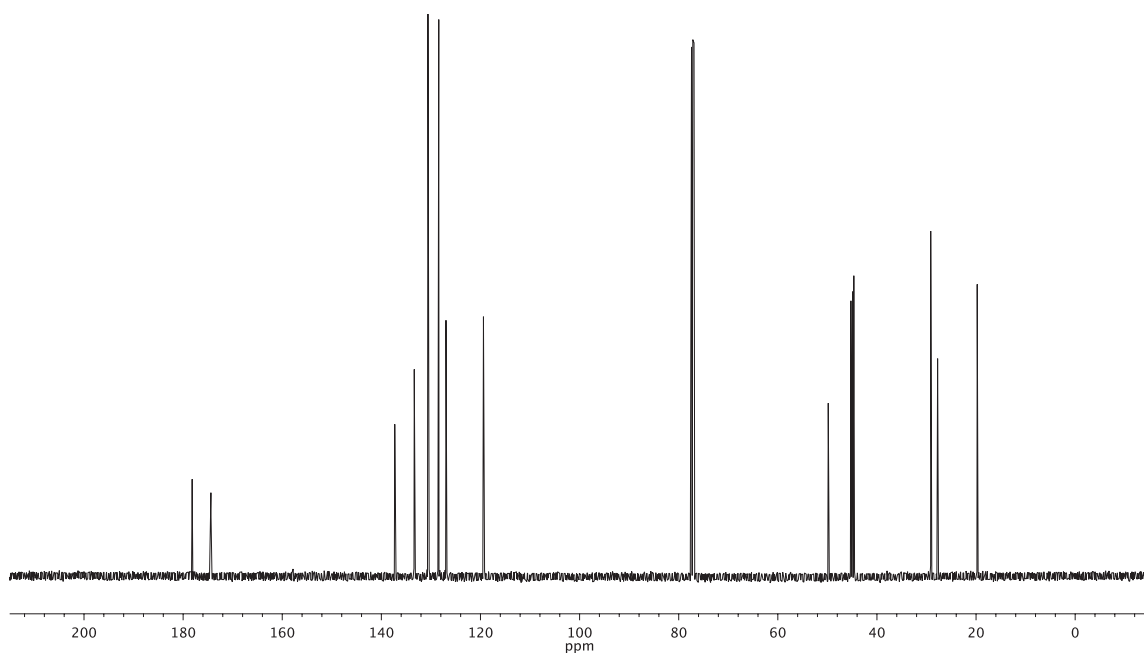


Figure A1.99 ¹³C NMR (126 MHz, CDCl₃) of compound **18**.

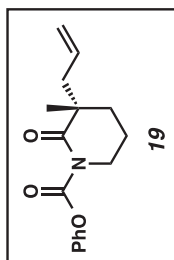
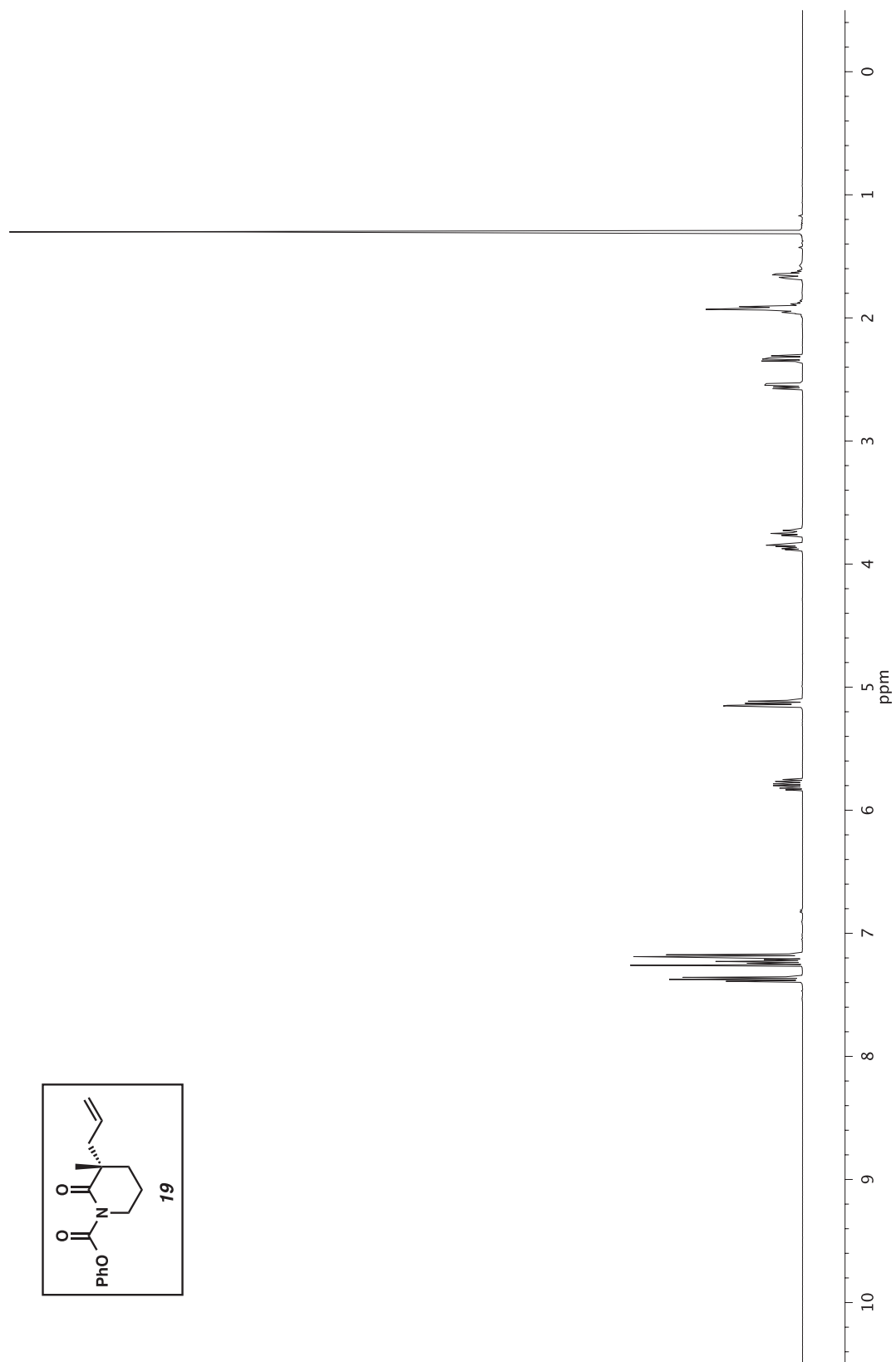


Figure A1.100 ^1H NMR (500 MHz, CDCl_3) of compound **19**.

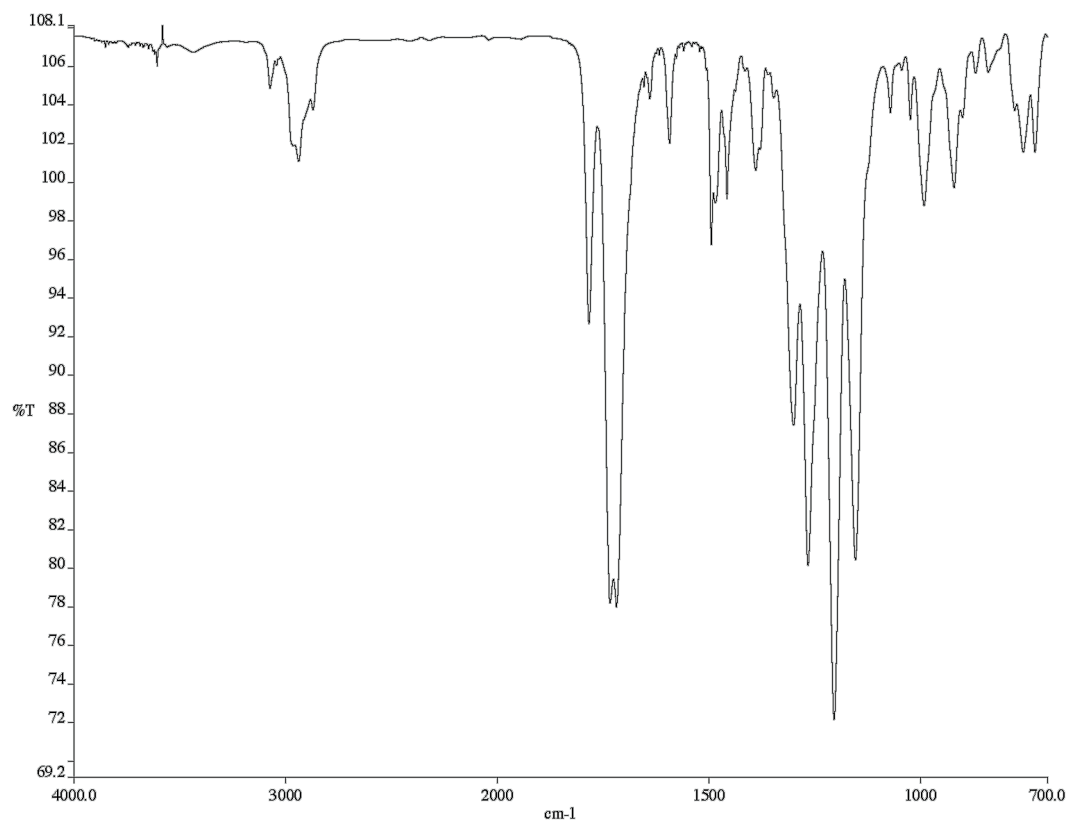


Figure A1.101 Infrared spectrum (Thin Film, NaCl) of compound **19**.

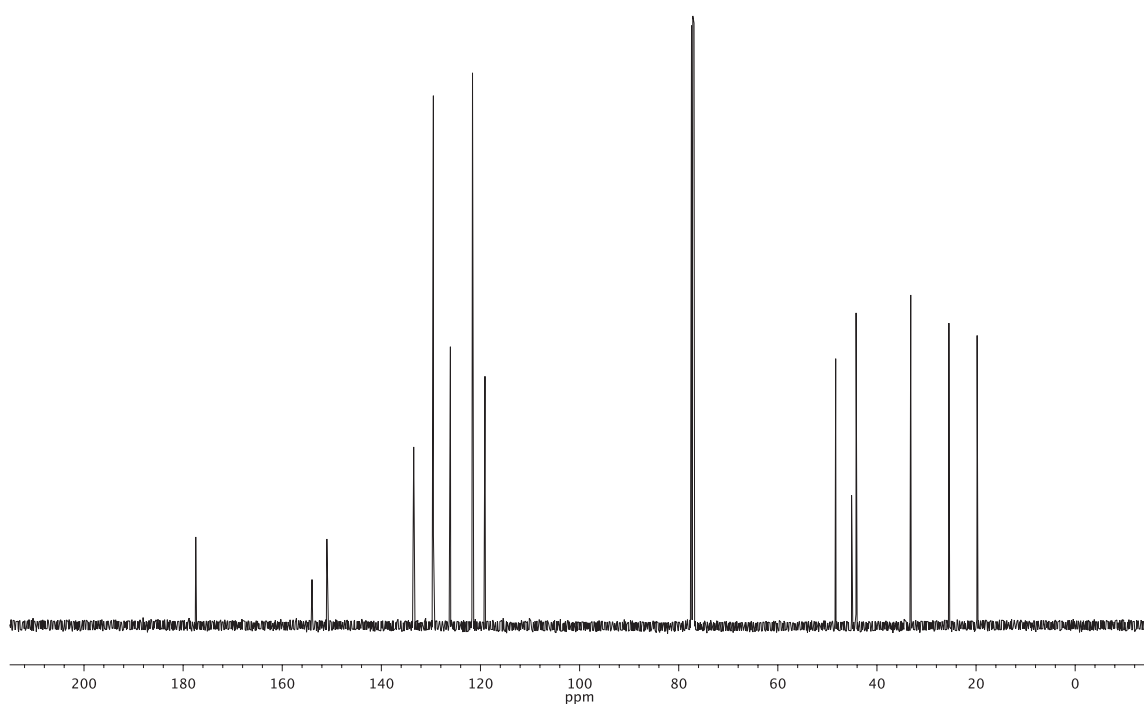


Figure A1.102 ¹³C NMR (126 MHz, CDCl₃) of compound **19**.

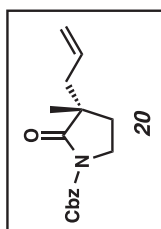
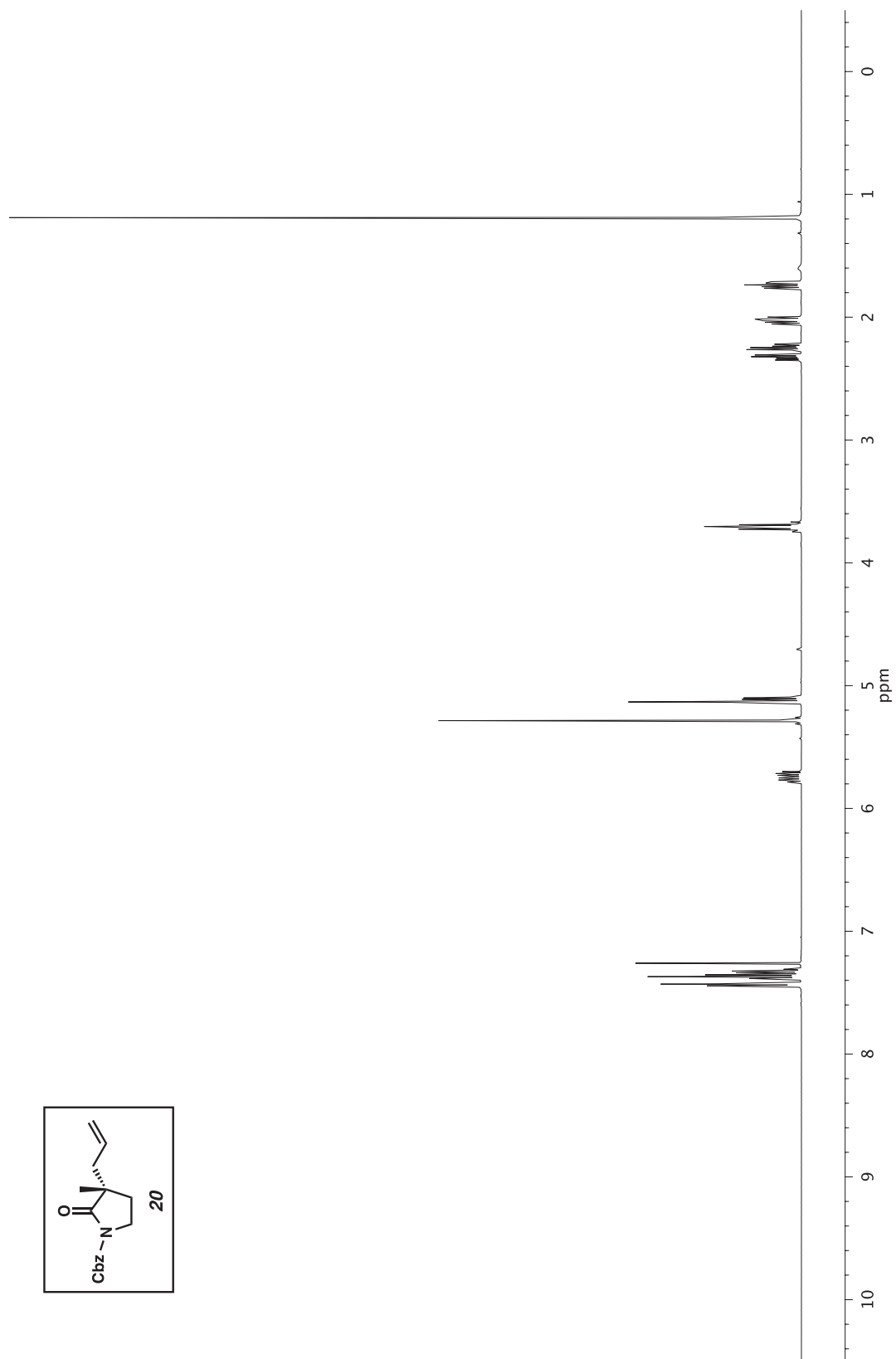


Figure A1.103 ^1H NMR (500 MHz, CDCl_3) of compound **20**.

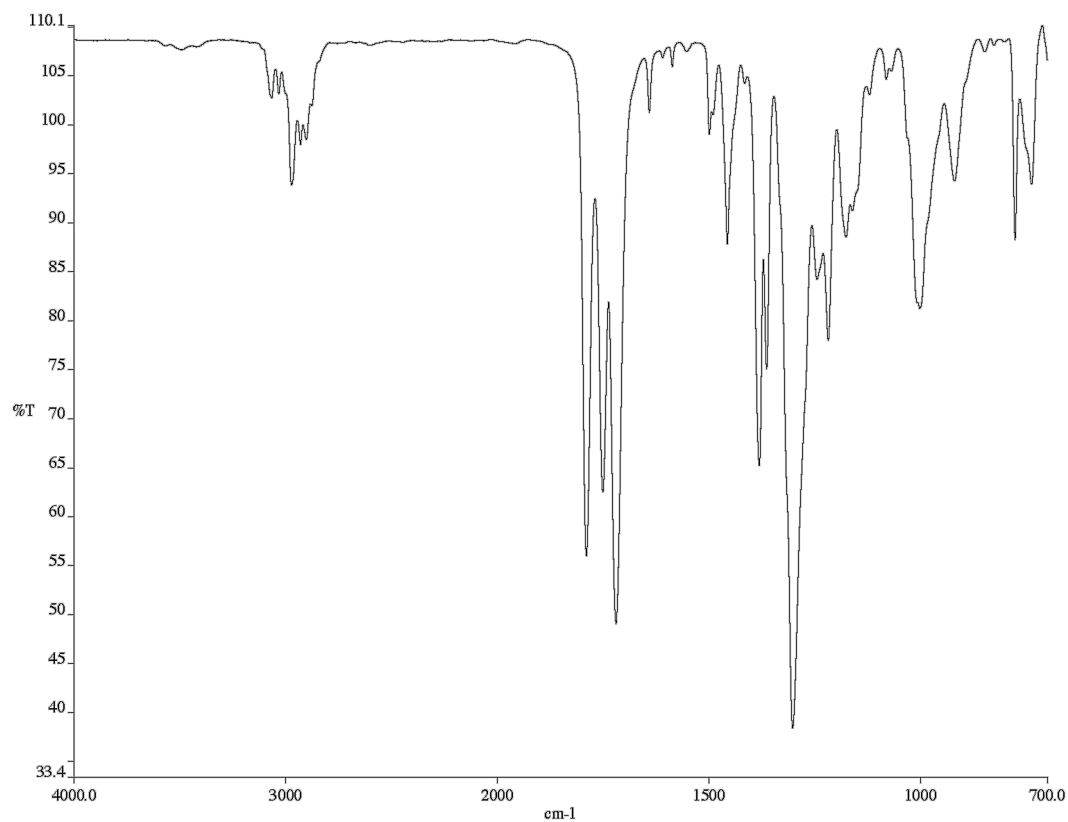


Figure A1.104 Infrared spectrum (Thin Film, NaCl) of compound **20**.

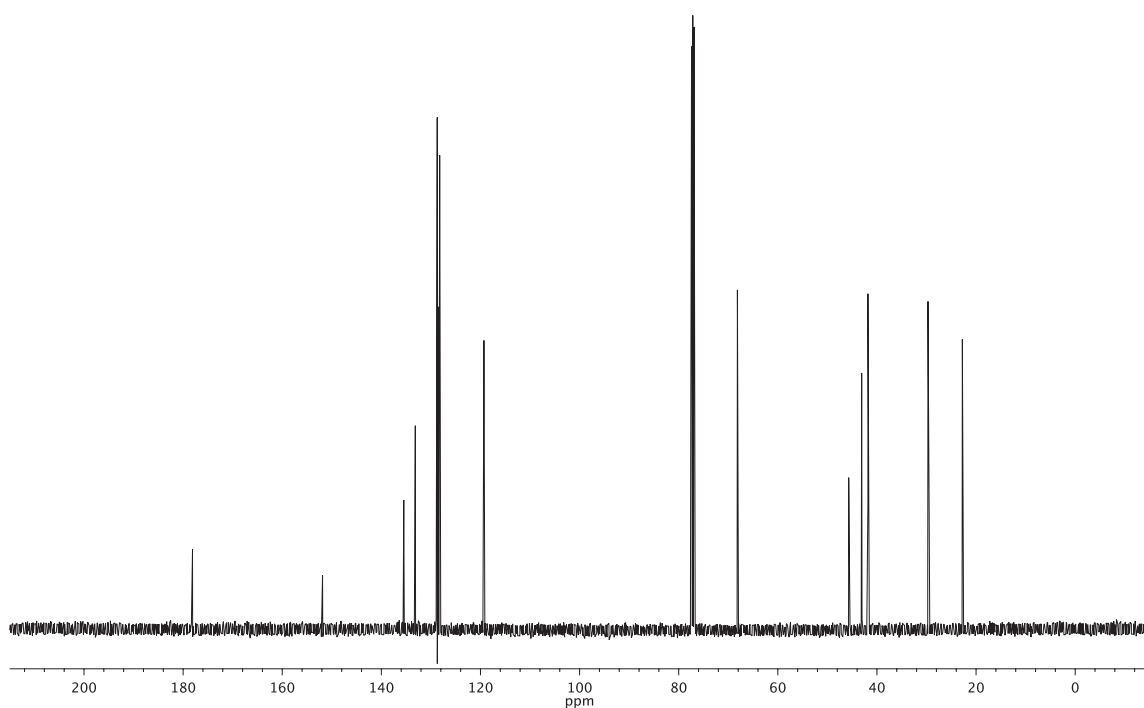


Figure A1.105 ¹³C NMR (126 MHz, CDCl₃) of compound **20**.

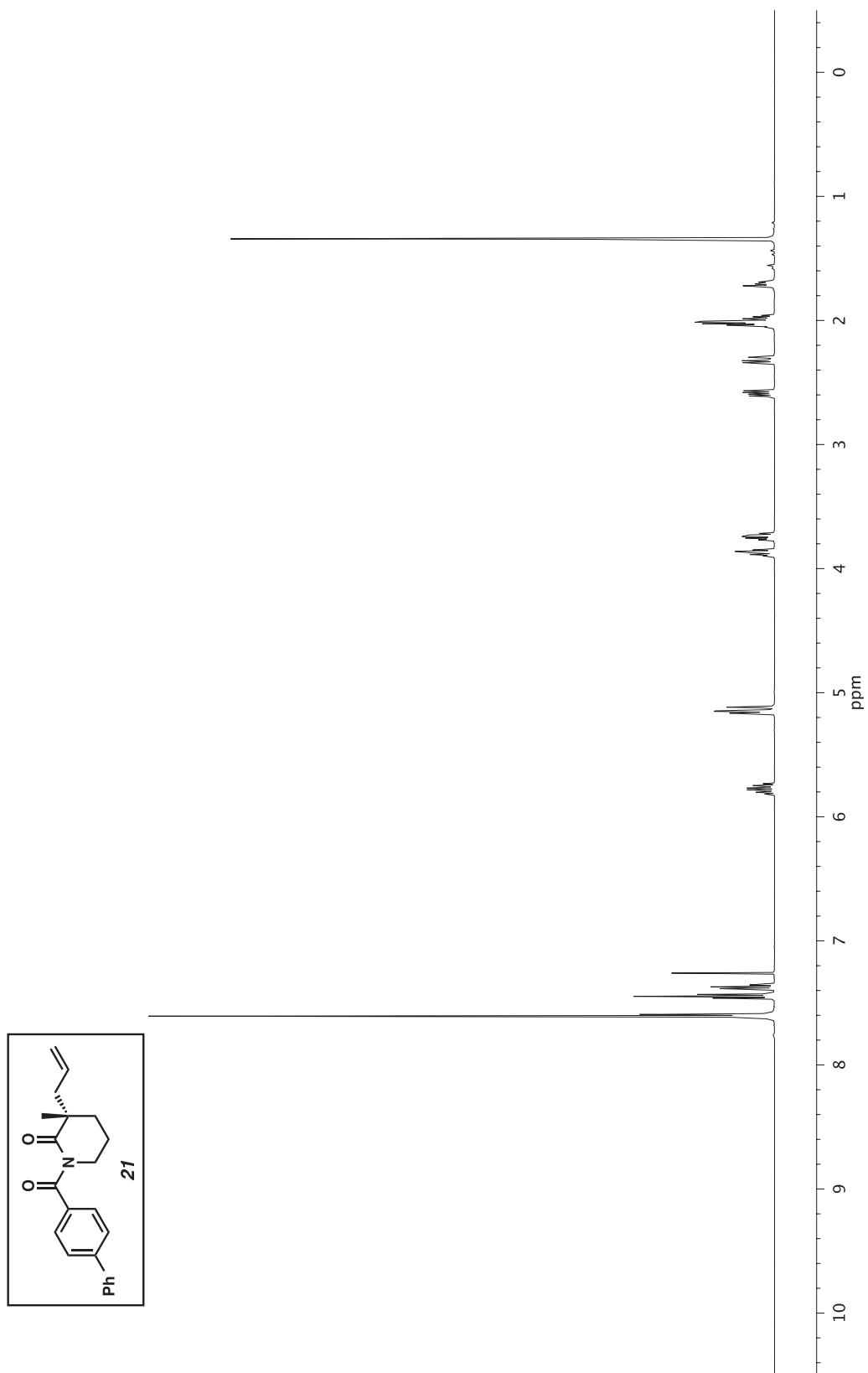


Figure A1.106 ^1H NMR (500 MHz, CDCl_3) of compound **21**.

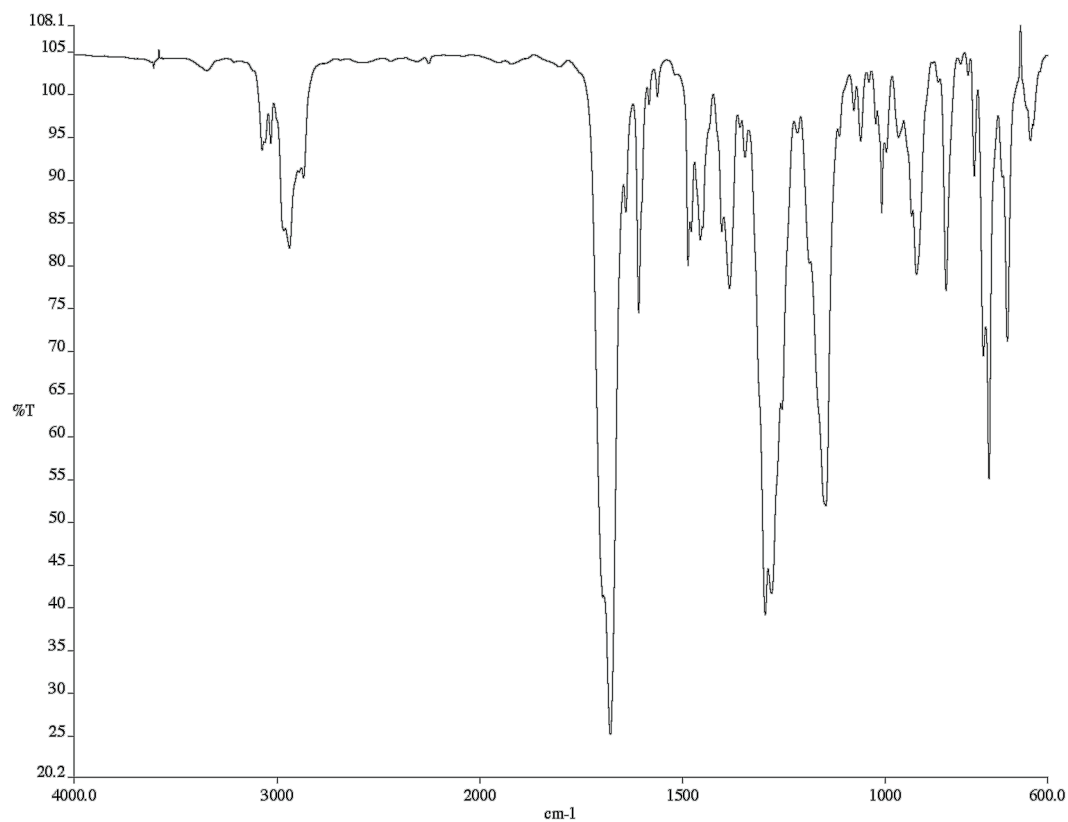


Figure A1.107 Infrared spectrum (Thin Film, NaCl) of compound **21**.

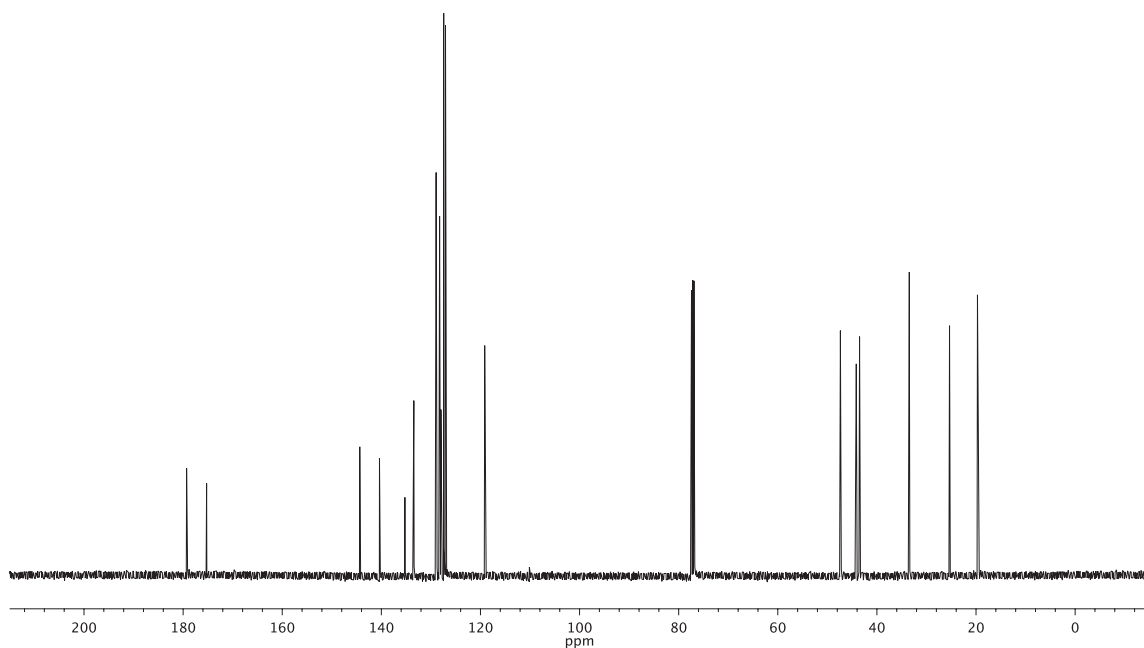


Figure A1.108 ¹³C NMR (126 MHz, CDCl₃) of compound **21**.

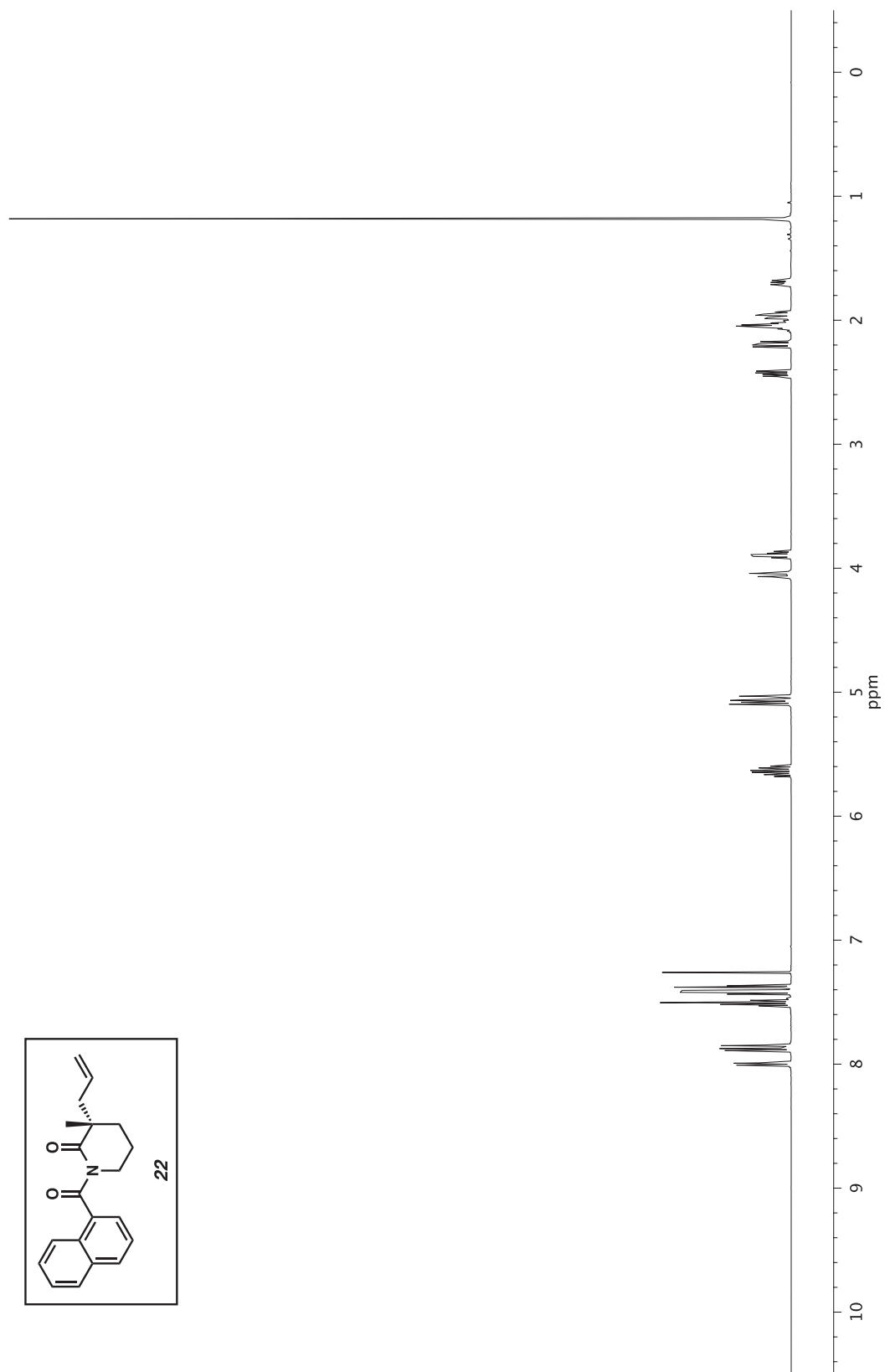


Figure A1.109 $^1\text{H NMR}$ (500 MHz, CDCl_3) of compound **22**.

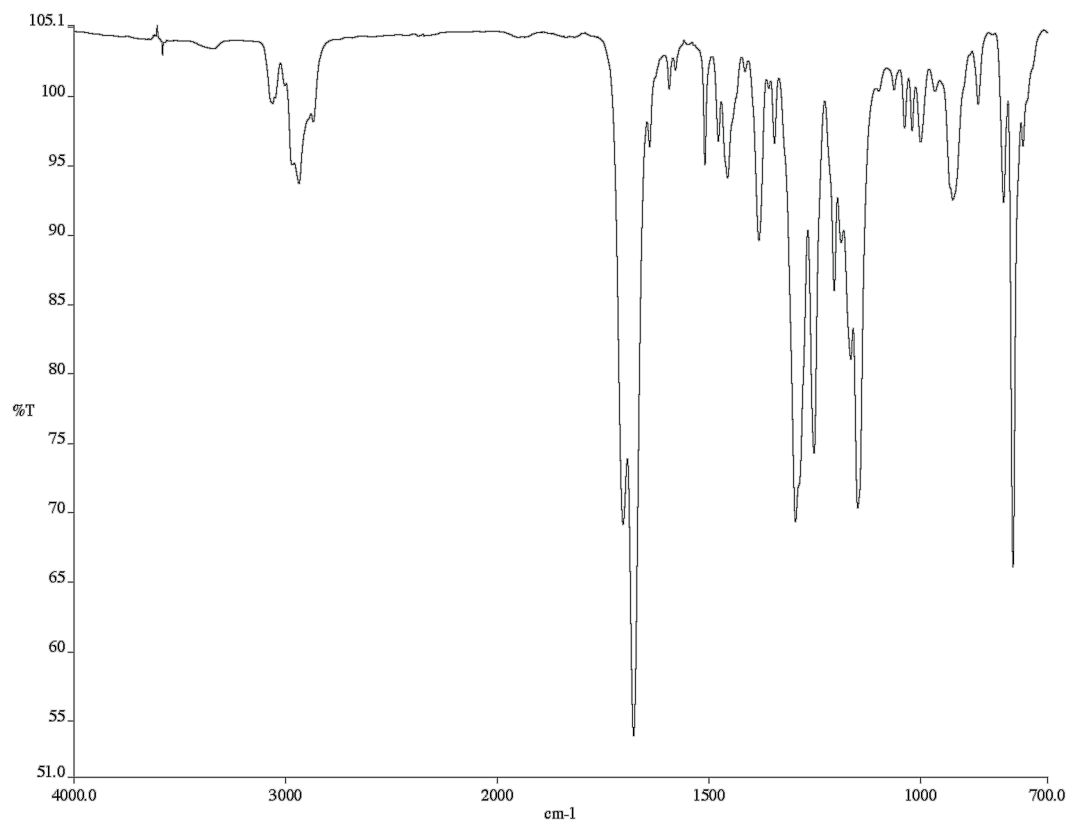


Figure A1.110 Infrared spectrum (Thin Film, NaCl) of compound **22**.

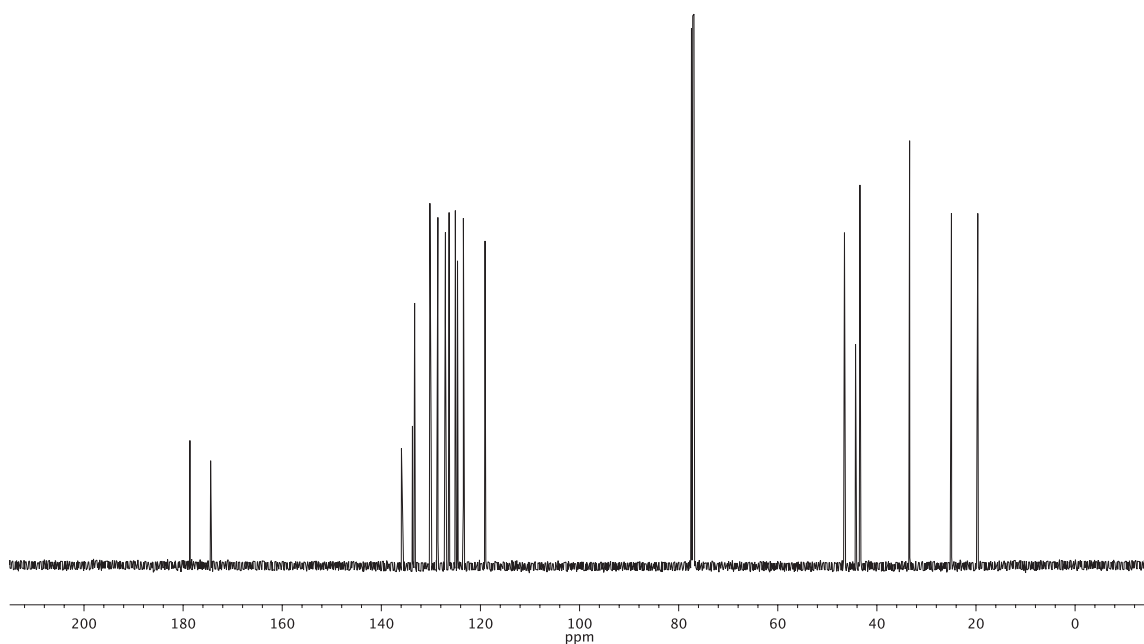


Figure A1.111 ¹³C NMR (126 MHz, CDCl₃) of compound **22**.

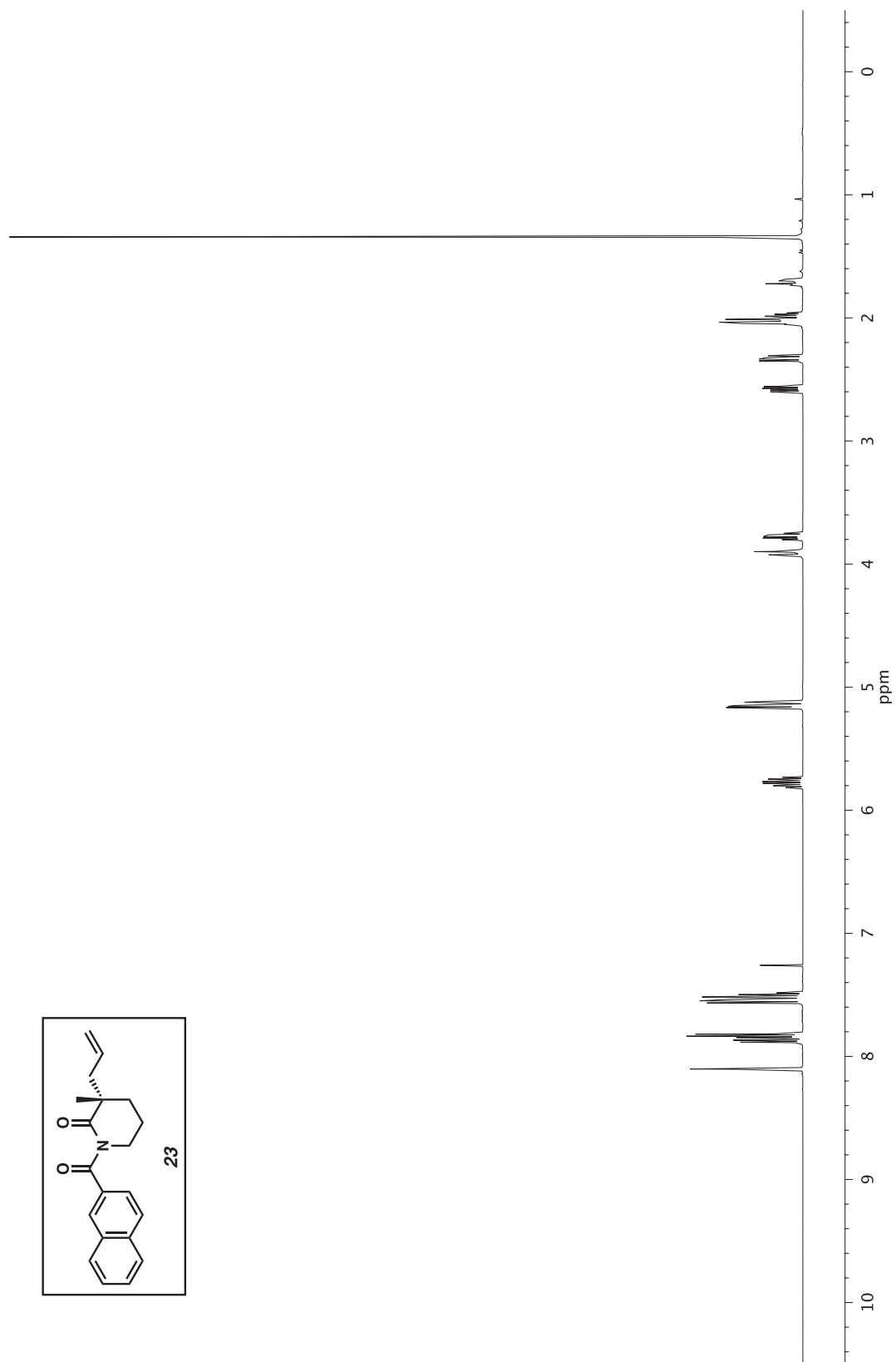


Figure A1.112 ^1H NMR (500 MHz, CDCl_3) of compound **23**.

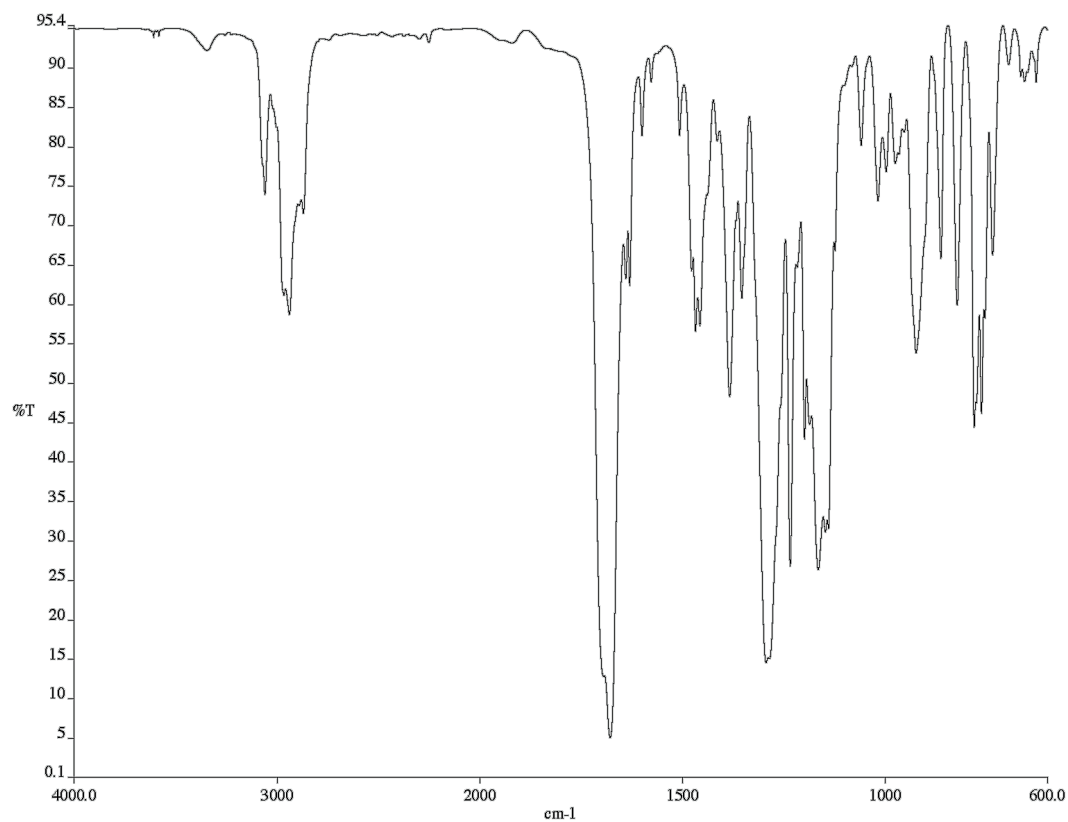


Figure A1.113 Infrared spectrum (Thin Film, NaCl) of compound **23**.

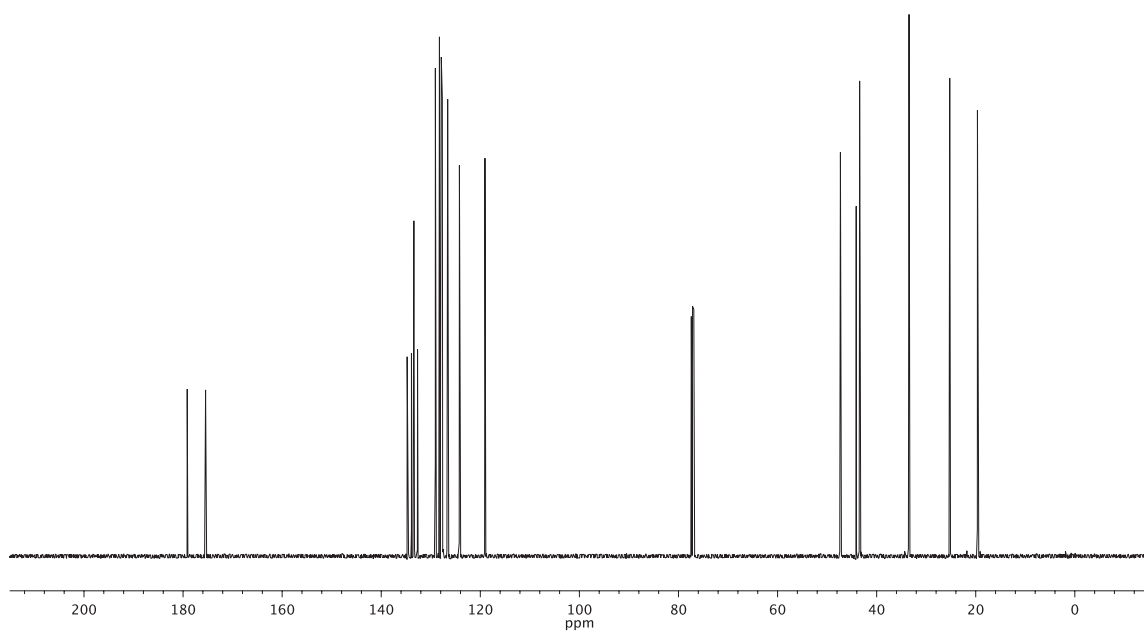


Figure A1.114 ¹³C NMR (126 MHz, CDCl₃) of compound **23**.

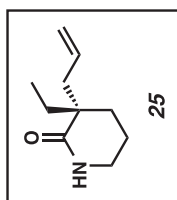
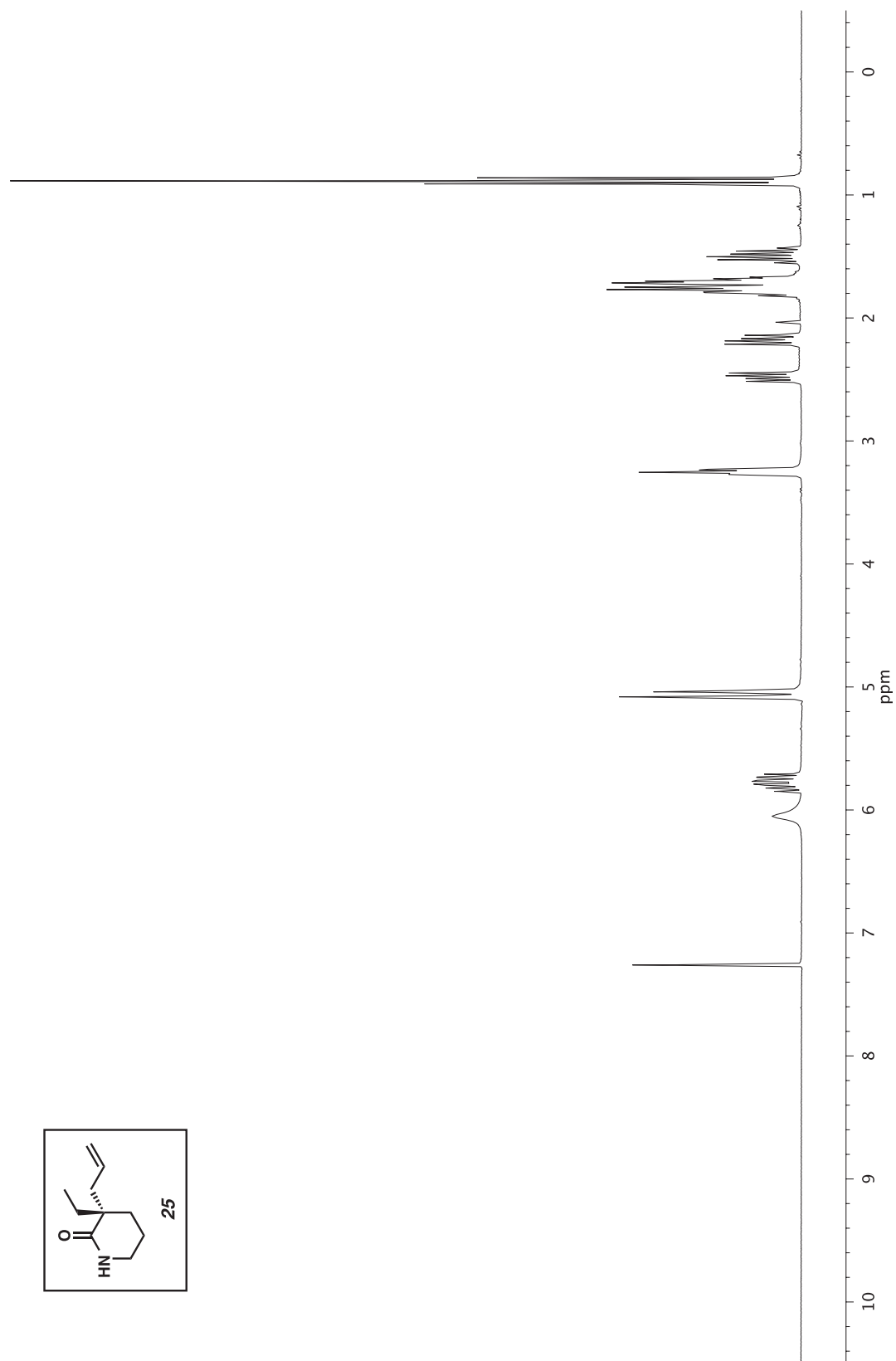


Figure A1.115 ^1H NMR (300 MHz, CDCl_3) of compound **25**.

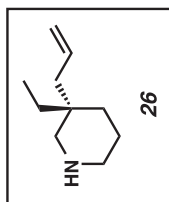
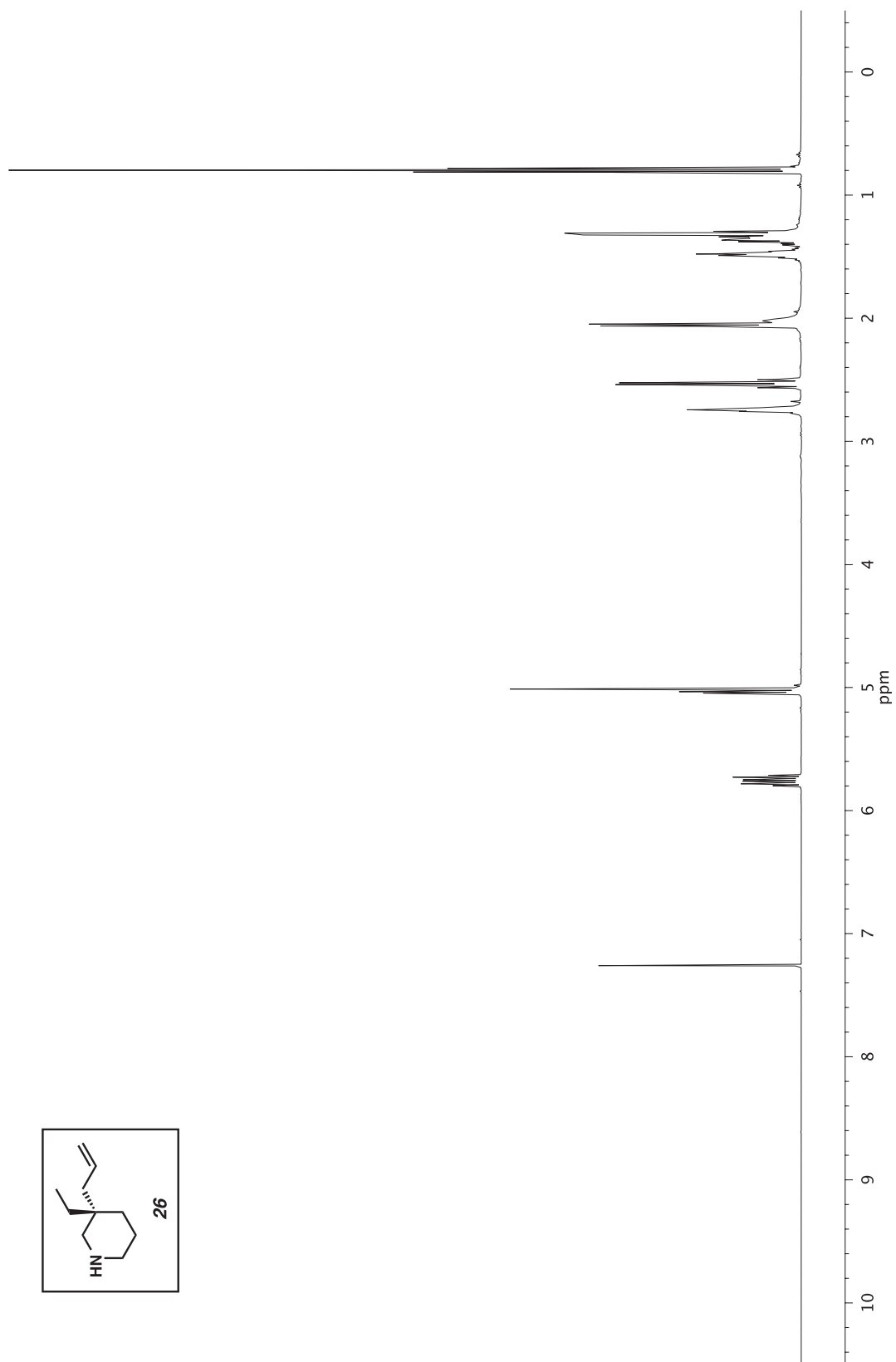


Figure A1.116 ^1H NMR (500 MHz, CDCl_3) of compound **26**.

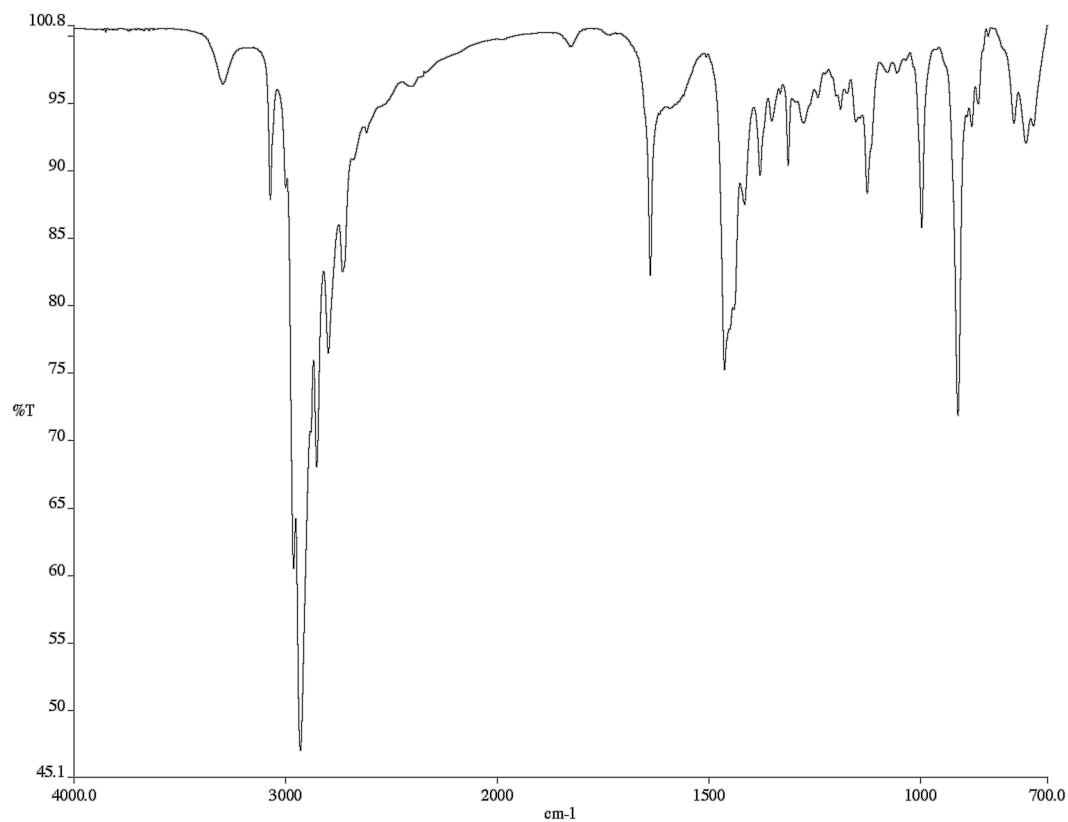


Figure A1.117 Infrared spectrum (Thin Film, NaCl) of compound **26**.

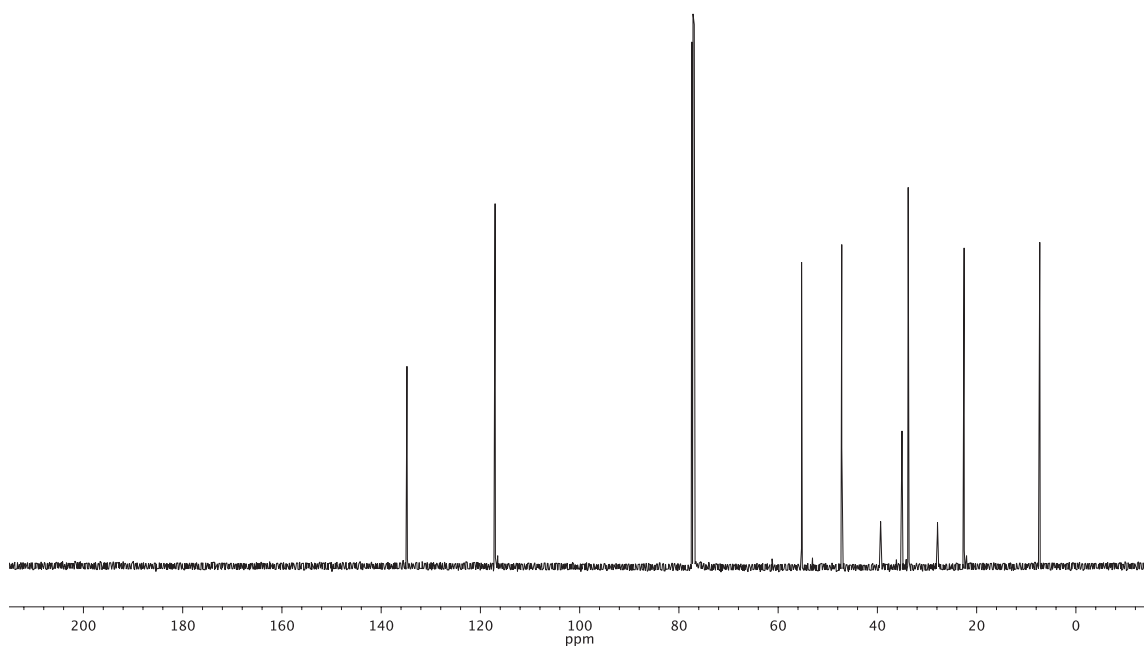


Figure A1.118 ¹³C NMR (126 MHz, CDCl₃) of compound **26**.

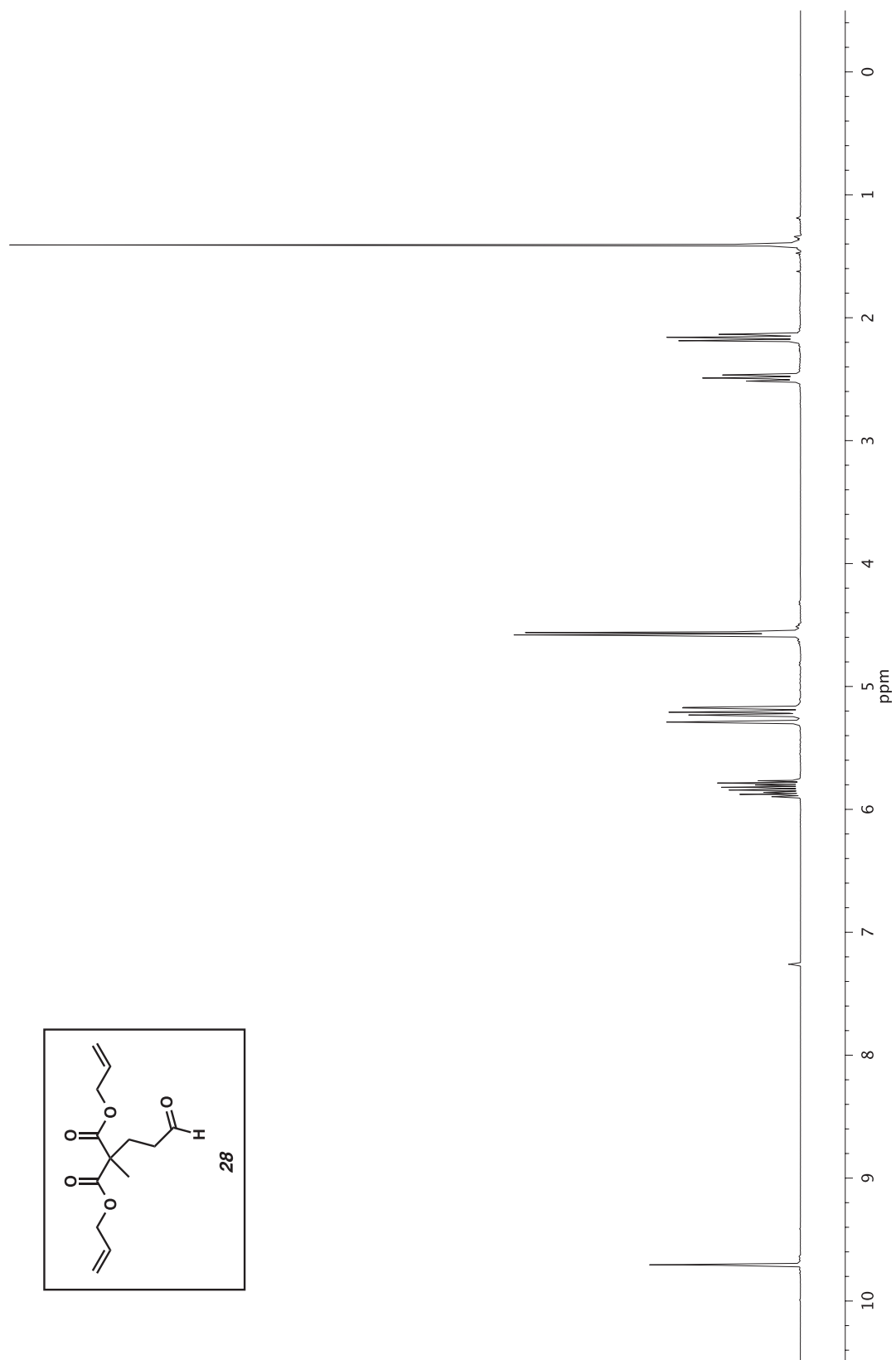


Figure A1.119 ^1H NMR (300 MHz, CDCl_3) of compound **28**.

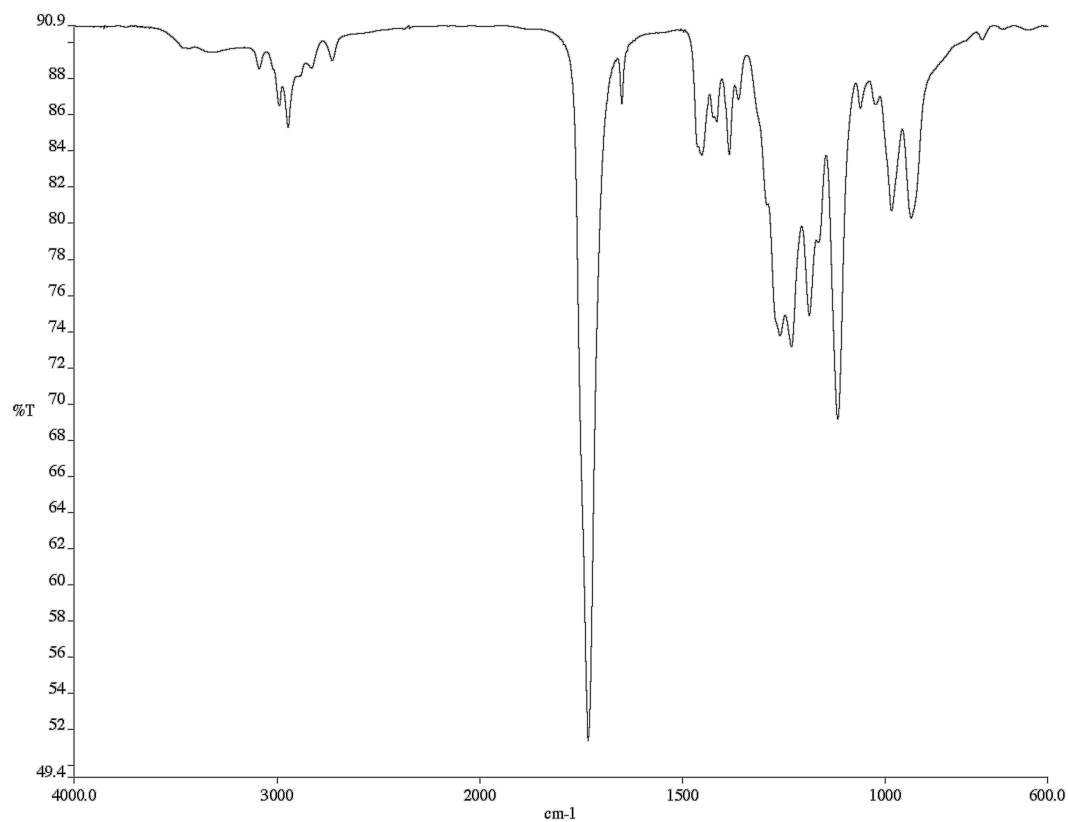


Figure A1.120 Infrared spectrum (Thin Film, NaCl) of compound **28**.

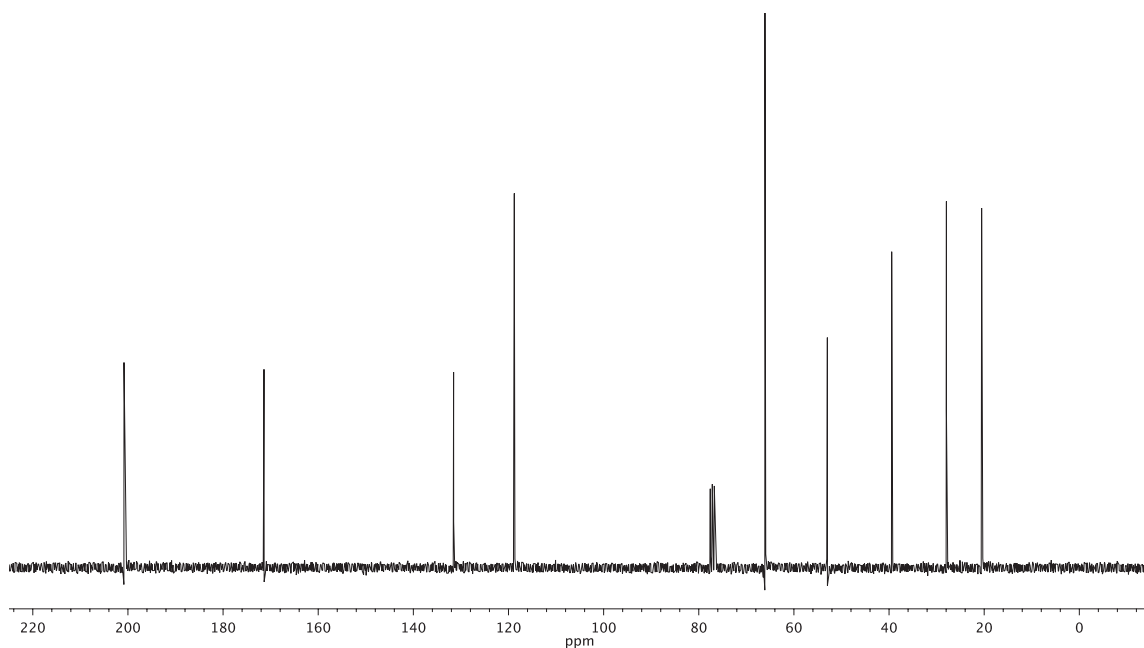


Figure A1.121 ¹³C NMR (75 MHz, CDCl₃) of compound **28**.

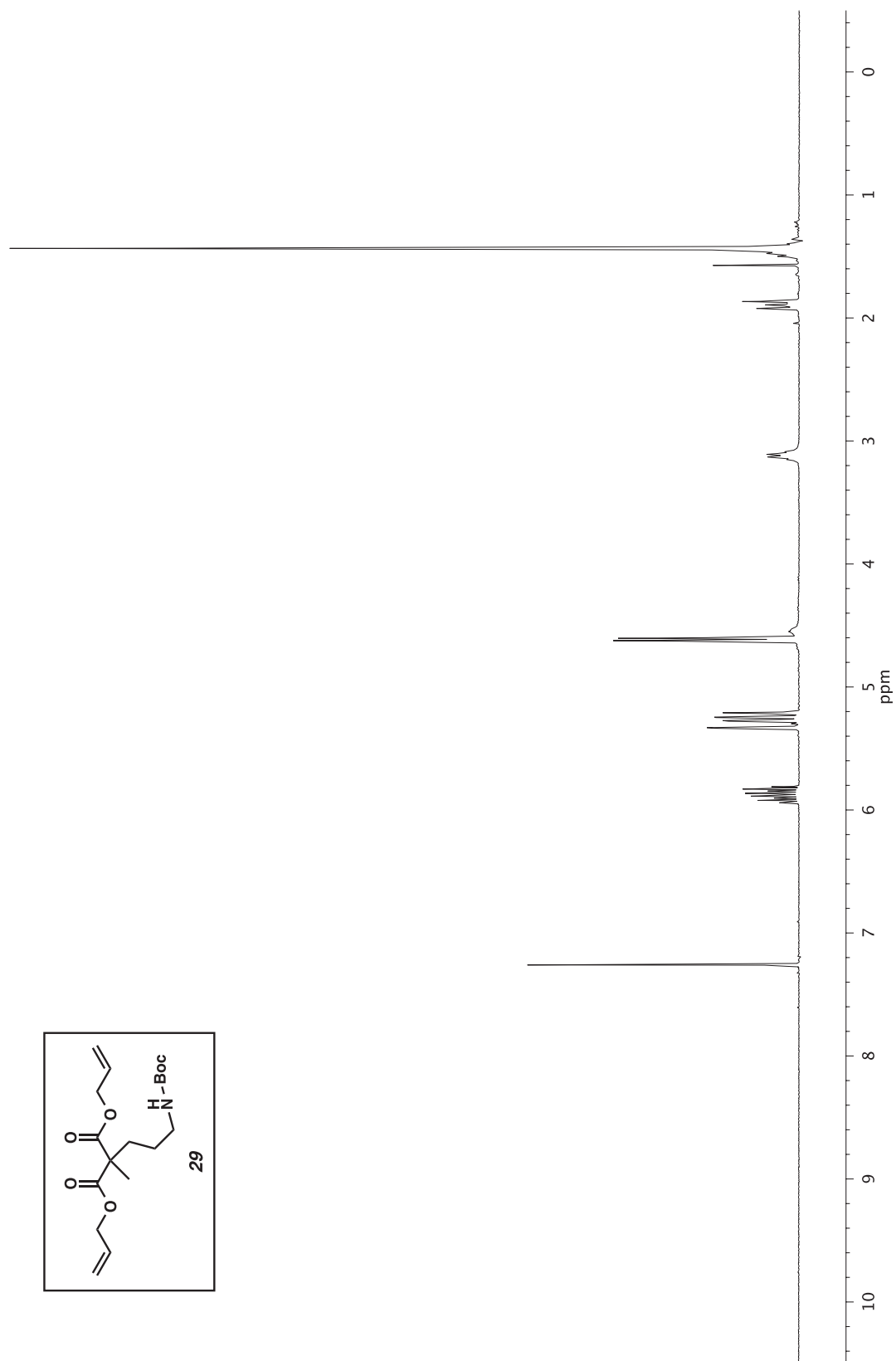


Figure A1.122 ^1H NMR (300 MHz, CDCl_3) of compound **29**.

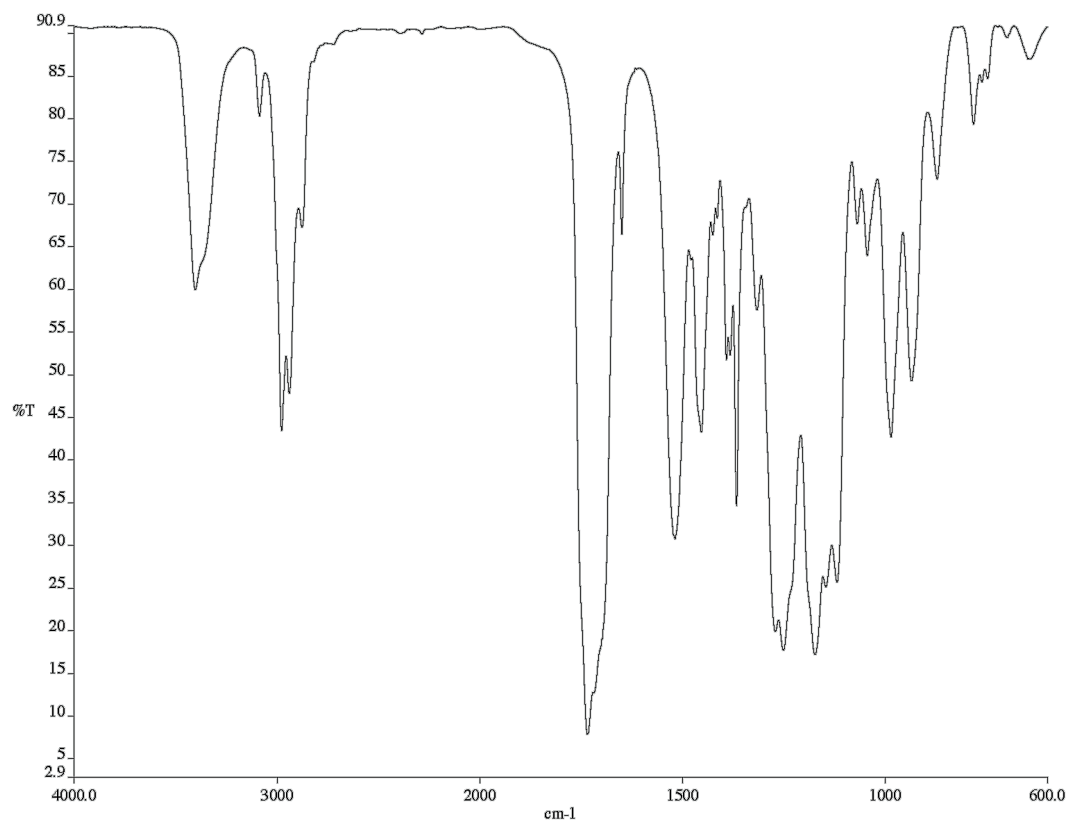


Figure A1.123 Infrared spectrum (Thin Film, NaCl) of compound **29**.

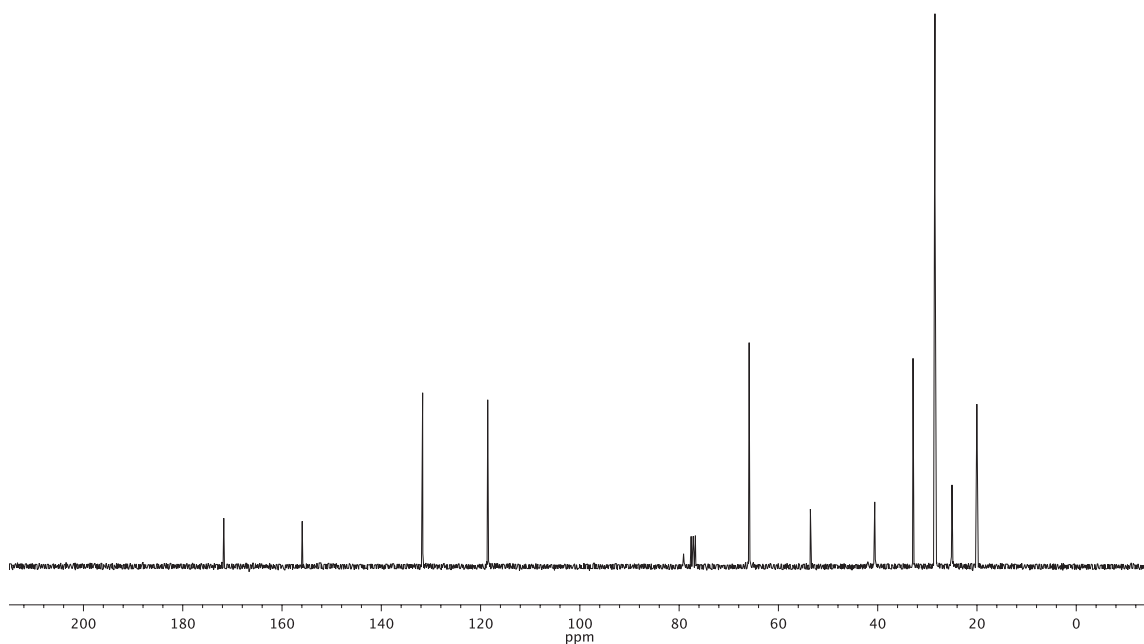


Figure A1.124 ¹³C NMR (75 MHz, CDCl₃) of compound **29**.

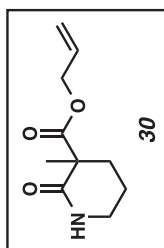
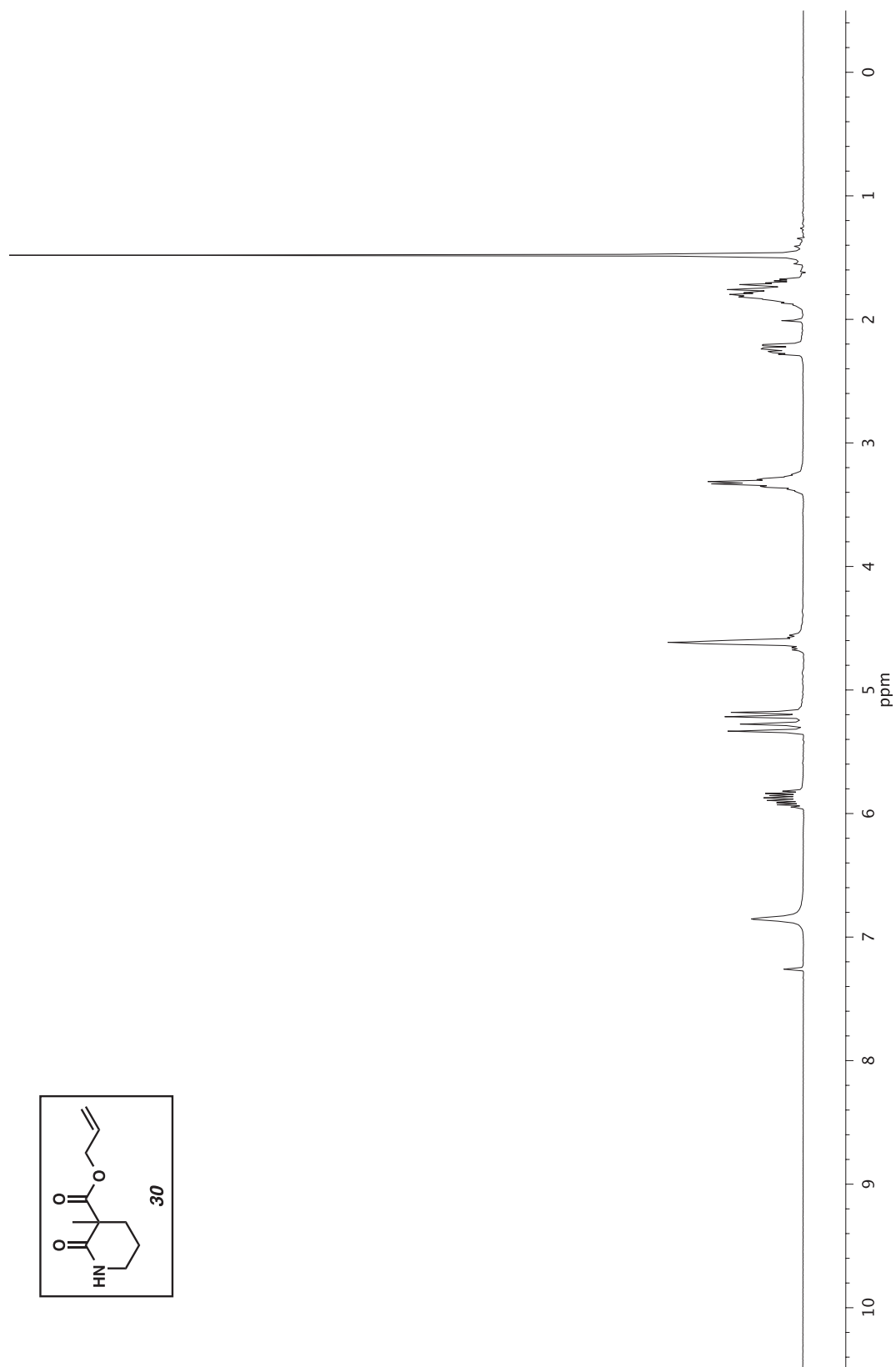


Figure A1.125 ^1H NMR (300 MHz, CDCl_3) of compound **30**.

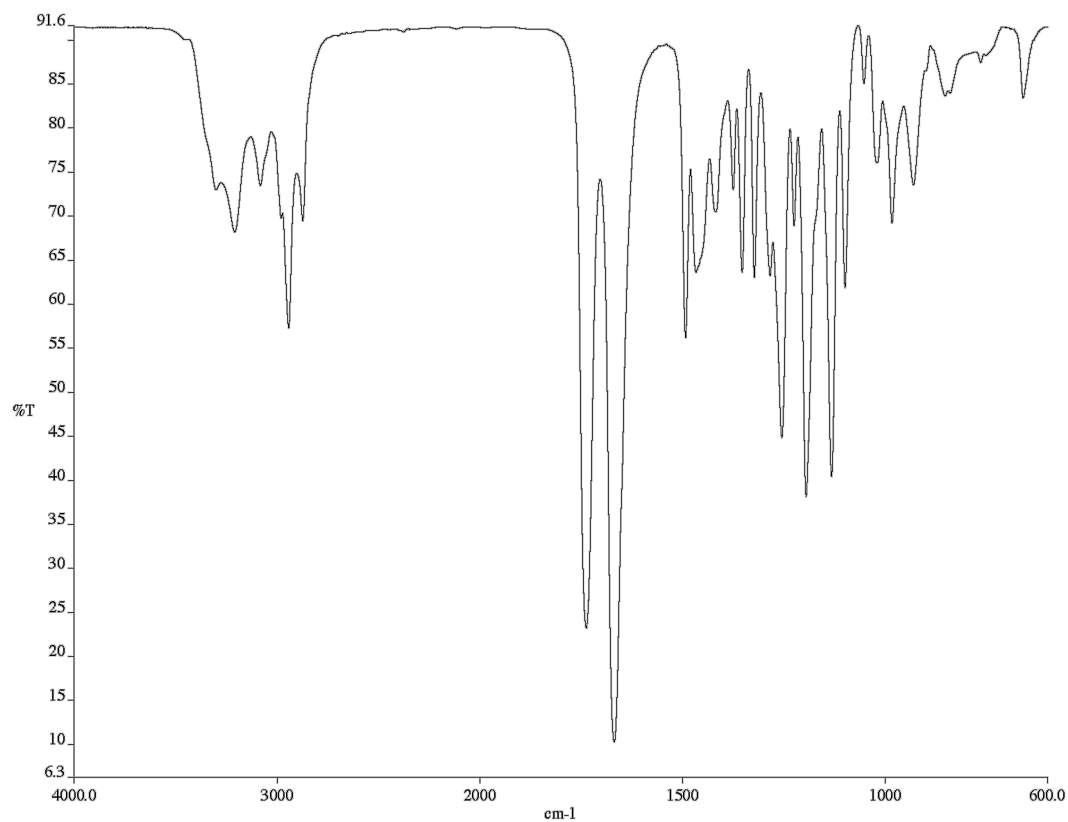


Figure A1.126 Infrared spectrum (Thin Film, NaCl) of compound **30**.

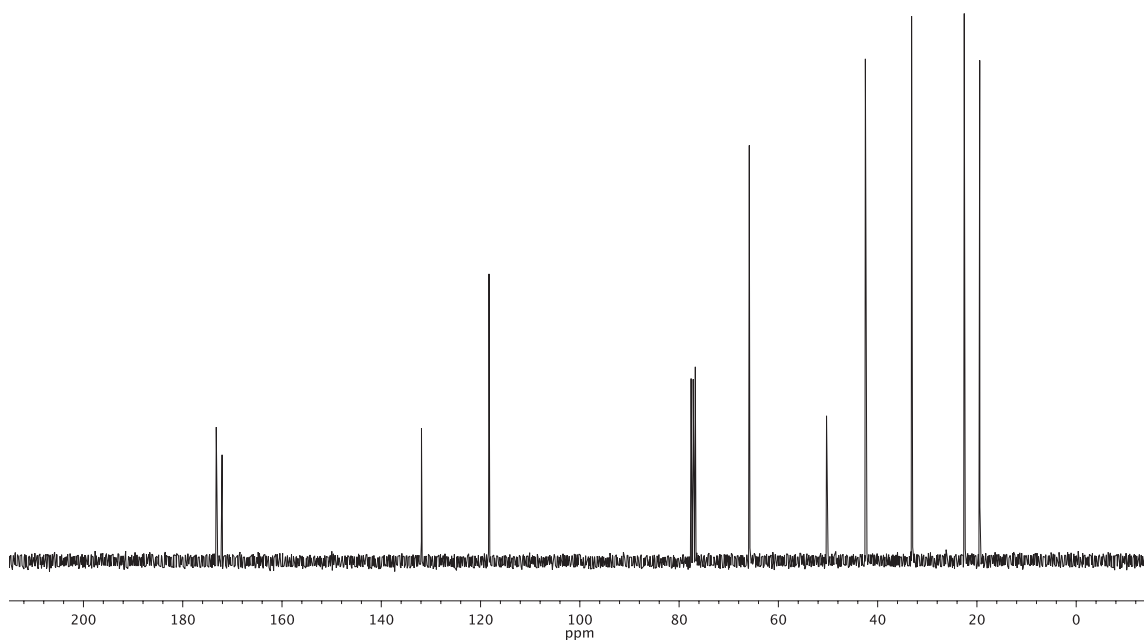


Figure A1.127 ¹³C NMR (75 MHz, CDCl₃) of compound **30**.

CHAPTER 3

Formal Synthesis of Classical Natural Product Target Molecules via Palladium-Catalyzed Enantioselective Alkylation[†]

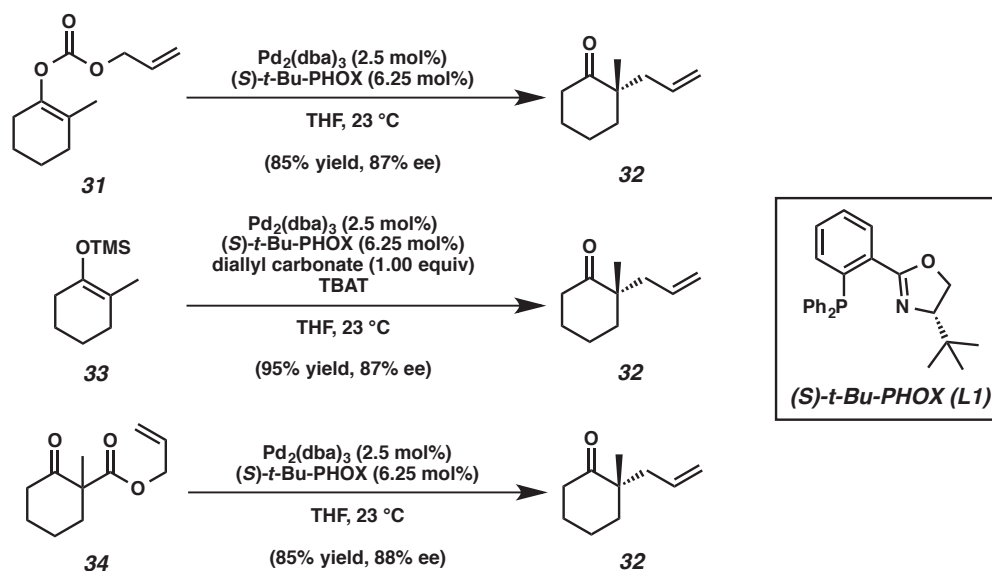
3.1 Introduction

Catalytic enantioselective allylic alkylation has emerged as a powerful method for the construction of building blocks bearing quaternary carbon and fully substituted tertiary centers.^{1,2} A recent addition developed by our laboratory is the allylic alkylation of nonstabilized enolate precursors to form α -quaternary carbonyl compounds (Scheme 3.1).³ Once the key stereocenter is set by this chemistry, further elaboration allows access to many bioactive small molecules. In our lab alone, this palladium-catalyzed

[†] This work was performed in collaboration with Dr. Marc Liniger. Drs. Ryan M. McFadden and Jenny L. Roizen also contributed significantly to this work. This chapter was partially adapted from the publication: Liu, Y.; Liniger, M.; McFadden, R. M.; Roizen, J. L.; Malette, J.; Reeves, C. M.; Behenna, D. C.; Seto, M.; Kim, J.; Mohr, J. T.; Virgil, S. C.; Stoltz, B. M. *Beilstein J. Org. Chem.* **2014**, *10*, 2501–2512. Open Access 2014 Beilstein-Institut.

alkylation has enabled the enantioselective total syntheses of dichroanone,⁴ elatol,⁵ cyanthiwiggins,^{6,7,8} carissone,⁹ cassiol,¹⁰ chamigrenes,¹¹ and liphagal.¹² Other labs have also utilized our method in natural products total synthesis.^{13,14} Often, it is the case that a new technology that allows the synthesis of building blocks will open up new avenues to complex structures of long standing interest.^{15,16} Herein we detail the application of this asymmetric chemistry in formal total syntheses of “classic” natural product targets across a range of compound families by strategic selection of allylic alkylation substrates and subsequent product transformations.

Scheme 3.1 Three classes of Pd-catalyzed enantioselective allylic alkylations

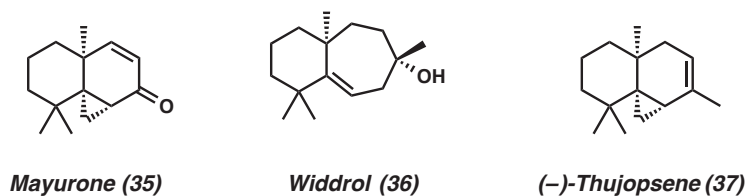


3.2 Thujopsene

The Japanese hiba tree, *Thujopsis dolabrata* has been used for centuries as decoration and within traditional architecture.¹⁷ The plant is a member of the order *Cupressaceae*, and its fragrant wood oil contains numerous sesquiterpenes including

mayurone (**35**),^{18,19} widdrol (**36**),²⁰ and (-)-thujopsene (**37**) (Figure 3.1).^{21,22} The wood oil is a potent dust mite deterrent; thus, in addition to its ornamental value, the hiba tree also provides an environmentally benign means of pest control.^{23,24}

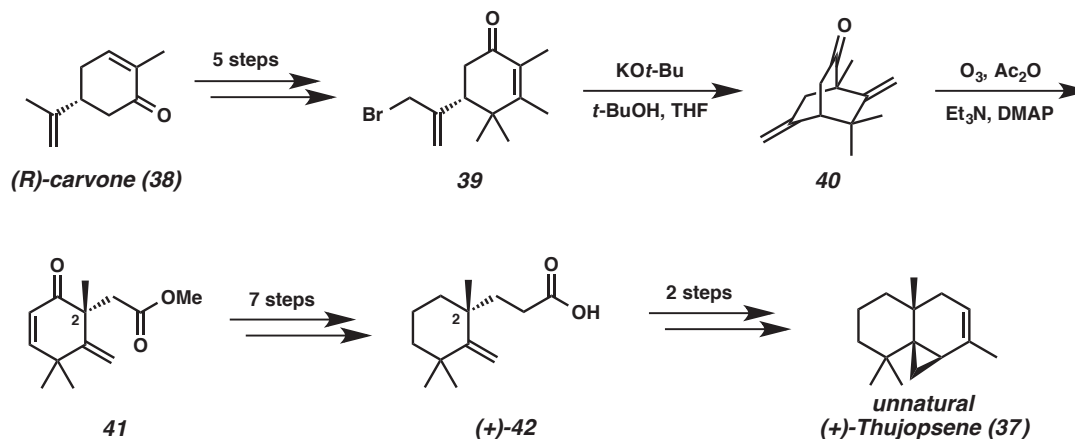
Figure 3.1 Selected natural products from *Thuja dolabrata*



(-)-Thujopsene (**37**) has attractive features to the synthetic chemist. Its tricyclo[5.4.0.0^{1,3}]undecane skeleton contains three contiguous all-carbon quaternary centers, two of which are stereogenic. Being a hydrocarbon, (-)-thujopsene (**37**) has few natural handles for retrosynthetic analysis. Inspired by the complexity of this relatively small natural product, several total syntheses of racemic **37** have been reported^{25,26,27,28,29} along with at least two enantioselective routes.^{30,31,32}

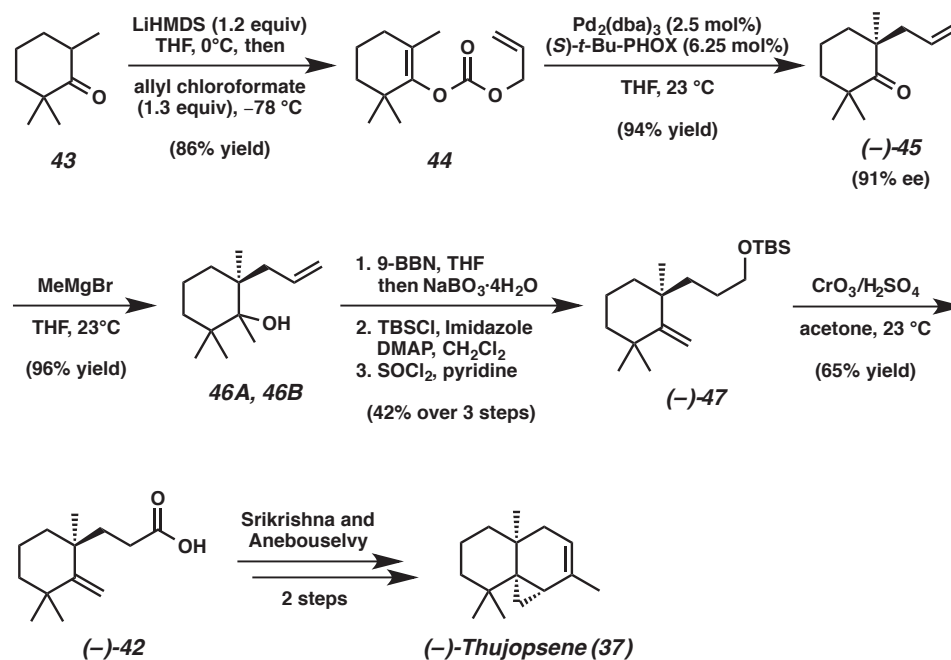
One enantiospecific total synthesis of (+)-thujopsene (**37**) by Srikrishna and Anebousely began with (*R*)-carvone (**38**) (Scheme 3.2).³³ During the total synthesis, the authors prepared carboxylic acid (+)-**42** over a 14-step sequence. We planned to intercept the antipode of (+)-**42** using the palladium-catalyzed enantioselective alkylation chemistry described above.

Scheme 3.2 Srikrishna and Anebousevly's approach to thujopsene



We commenced a formal total synthesis of (–)-Thujopsene (37) with the goal of improved efficiency compared to the Srikrishna/Anebousevly route and to use enantioselective palladium catalysis to install the initial stereocenters (Scheme 3.3). Treatment of 43 with LiHMDS in THF, followed by allyl chloroformate, furnished the known carbonate 44 in high yield.³⁴ This substrate smoothly undergoes palladium-catalyzed enantioselective decarboxylative allylation in the presence of (*S*)-*t*-Bu-PHOX (L1), giving allyl ketone (–)-45 in 94% yield and 91% ee.³⁴ Treatment of the ketone (–)-45 with MeMgBr at 23 °C provided a mixture of two diastereomeric alcohols 46A and 46B in 96% yield. Without separation, the diastereomers were rapidly carried through a three-step sequence of hydroboration/oxidation, terminal alcohol silylation, and tertiary alcohol dehydration, affording methylene cyclohexane (–)-47. Treatment of this silyl ether with Jones reagent simultaneously cleaved the silyl group and oxidized the resulting alcohol, furnishing carboxylic acid (–)-42 in 65% yield. With this enantioenriched acid in hand, the formal total synthesis of (–)-thujopsene (37) is completed in only 9 steps from trimethylcyclohexanone (43).

Scheme 3.3 Formal total synthesis of (-)-thujopsene

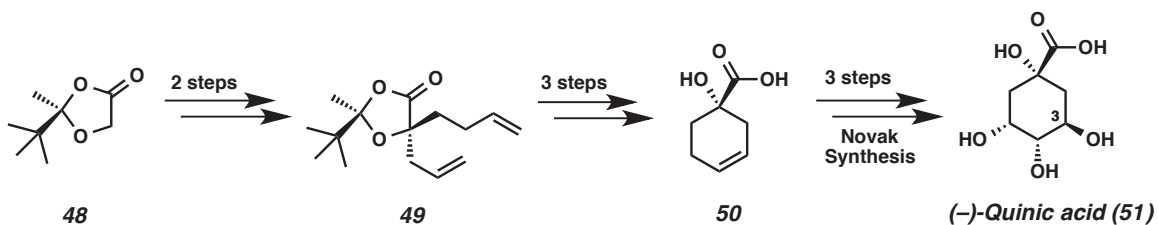


3.3 Quinic Acid

(-)-Quinic acid (**51**)^{35,36} serves as a useful chiral building block that has been employed in numerous syntheses,³⁷ including our own syntheses of (+)- and (-)-drugmacidin F,^{38,39,40,41} and the initial commercial-scale synthesis of Tamiflu.⁴² In Renaud's formal total synthesis of (-)-quinic acid (**51**),³⁵ a key carboxylic acid **50** was accessed, intercepting Novak's older synthesis of the natural product (Scheme 3.4).³⁶ To begin, Renaud transformed the chiral glycolic acid ketal **48** (enantioenriched to 80% ee) to the more elaborate diene **49** via two diastereoselective alkylations. After a sequence of three reactions including removal of the pinacolone portion of the auxiliary, carboxylic acid **50** could be accessed. Novak's synthesis applied a bromolactonization of **50** to build

in the requisite syn relationship between the carboxylate group and the 3-hydroxyl group, ultimately leading to quinic acid.

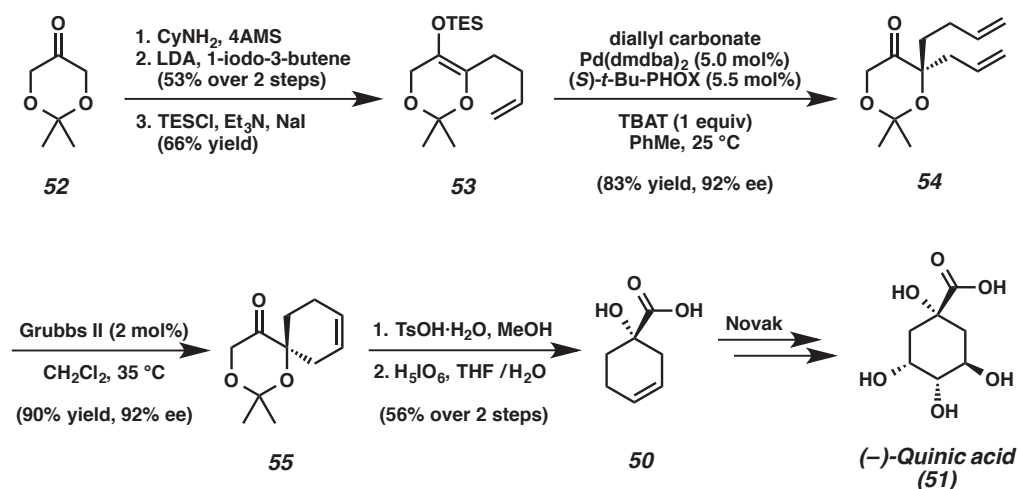
Scheme 3.4 Renaud's formal total synthesis of quinic acid



Unlike the allylic alkylations in Scheme 3.1, which form all-carbon stereocenters, we envisioned a unique modification of the silyl enol ether version to access nonracemic tertiary alcohols (Scheme 3.5).⁴³ The planned modification would involve the use of dioxanone-derived substrates instead of the prototypical cycloalkanone-derived ones. To demonstrate this new technology in the context of formal total synthesis, we chose to intercept the acid **50** in the Renaud and Novak routes to quinic acid (**51**). Conversion of dioxanone **52** to a cyclohexylimine enabled alkylation via a metalloenamine. On acidic work-up, imine hydrolysis furnished an alkylated dioxanone in good yield. The targeted silyl enol ether **53** was prepared by thermodynamic silylation in 66% yield.⁴³ Optimal conversions and enantioselectivities were achieved from triethylsilyl enol ether **53** on exposure to Pd(dmdba)₂ (5 mol%), (*S*)-*t*-BuPHOX (**L1**, 5.5 mol%), and diallyl carbonate (1.05 equiv) at 25 °C, in PhMe with an equivalent of Bu₄NPh₃SiF₂ (TBAT).⁴³ Recognizing that enantioenriched α,ω -dienes could be transformed into cycloalkenes with a stereocenter remote to the olefin,⁴⁴ chiral diene **54** was submitted to ring closing metathesis to generate **55** in 90% yield and 92% ee.⁴³ Cyclohexene **55** readily undergoes

acetonide cleavage and periodic acid oxidation to provide carboxylic acid (*S*)-**50**,⁴³ completing the formal synthesis of (–)-quinic acid (**51**). Additionally, one could in principle also access the less commercially abundant antipode (+)-quinic acid (**51**) using the catalyst (*R*)-*t*-Bu-PHOX.

Scheme 3.5 Formal total synthesis of (–)-quinic acid

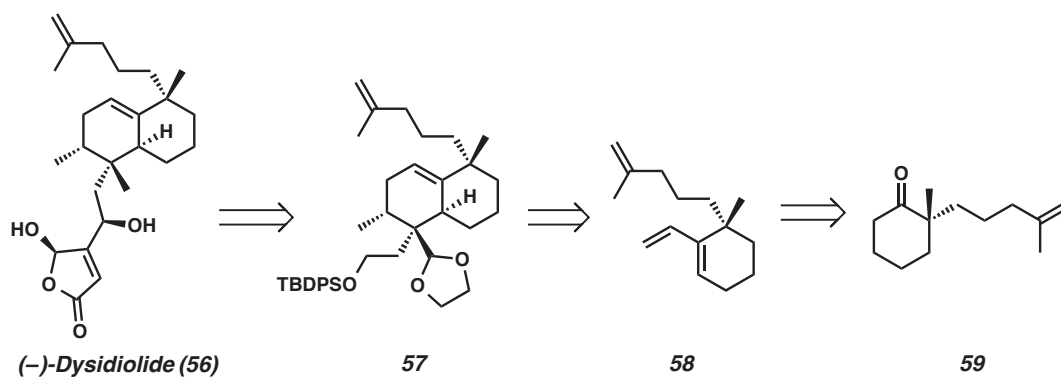


3.4 Dysidiolide

Dysidiolide (**56**, Scheme 3.6) was isolated from the marine sponge *Dysidea etheria* and found to have inhibitory activity toward protein phosphatase cdc25, with an IC_{50} value of 9.4 μM .⁴⁵ This enzyme is a member of the protein family responsible for dephosphorylation of cyclin-dependent kinases.⁴⁶ Thus, inhibitors of cdc25 might allow for targeted cell-cycle disruption.⁴⁵ The relative stereochemistry of dysidiolide (**56**) was determined via single-crystal X-ray diffraction analysis, revealing a molecule with six stereocenters, one of which is a quaternary carbon.⁴⁵ Several groups have reported total syntheses of this natural product,^{47,48,49,50,51,52,53} three of which are enantioselective.^{54,55,56}

In Danishefsky's approach to racemic dysidiolide, the cyclohexene ring of **57** was installed via diastereoselective Diels-Alder reaction of a transient dioxolenium dienophile and chiral vinylcyclohexene **58**.⁴⁸ Triene **58** was prepared from α -quaternary ketone (\pm)-**59** in racemic form. We anticipated the interception of (-)-**59** in Danishefsky's route using enantioselective palladium-catalyzed allylic alkylation to set the quaternary stereocenter.

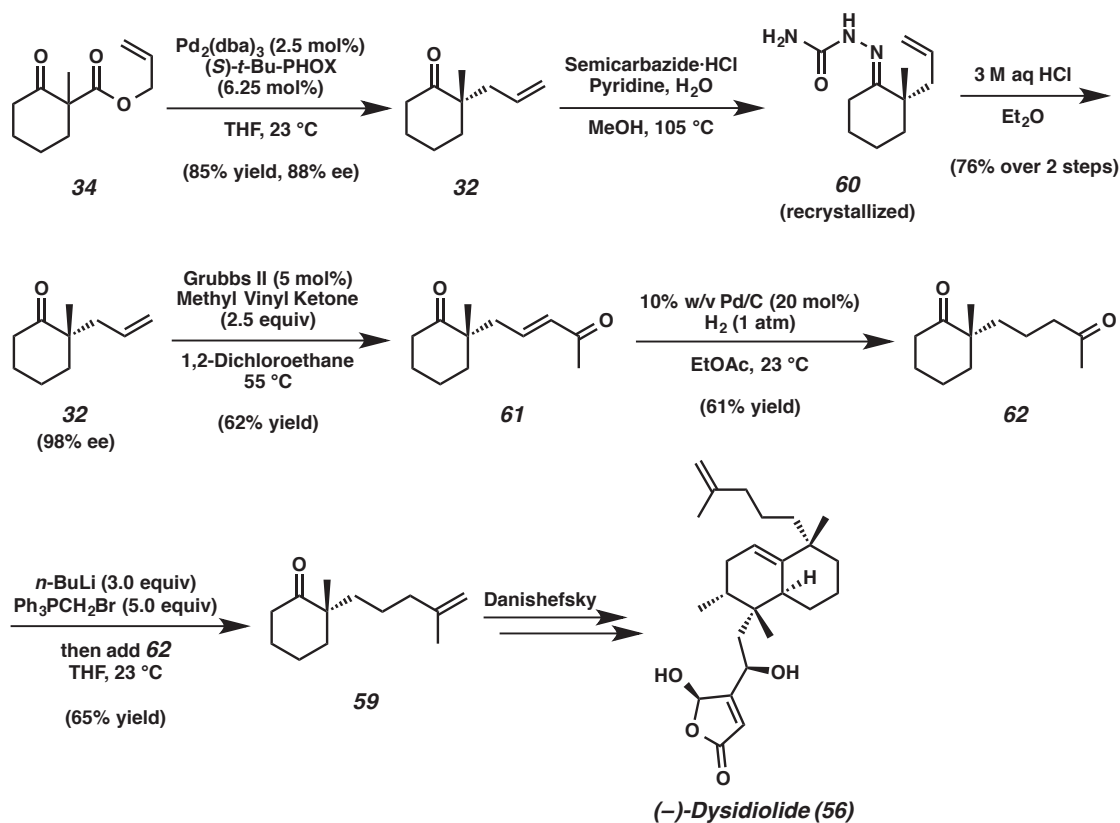
Scheme 3.6 Danishefsky's approach to (\pm)-dysidiolide



The formal total synthesis of (-)-Dysidiolide (**56**) commenced with known allyl β -ketoester **34** (Scheme 3.7), which was converted to 2-allyl-2-methylcyclohexanone (**32**) in 85% yield and 88% ee⁵⁷ with a catalytic amount of Pd₂dba₃ and (*S*)-*t*-BuPHOX (**L1**, Scheme 3.1). The allyl ketone was enriched to 98% ee via the semicarbazone **60**.⁵⁸ Using the Grubbs 2nd generation metathesis catalyst, allyl ketone (-)-**32** was crossed with methyl vinyl ketone in 62% yield.³⁴ Reduction of enone **61** was achieved in the presence of Pd/C with H₂ in EtOAc to furnish diketone **62**.³⁴ Chemoselective Wittig mono-olefination of **62** provided ω -enone (-)-**59**, spectroscopically identical to the material in Danishefsky's racemic synthesis. This formal synthesis shows the power of the

enantioselective allylic alkylation to access formerly racemic constructs as single enantiomers; Danishefsky's synthesis is now rendered enantioselective.

Scheme 3.7 Formal total synthesis of (-)-dysidiolide



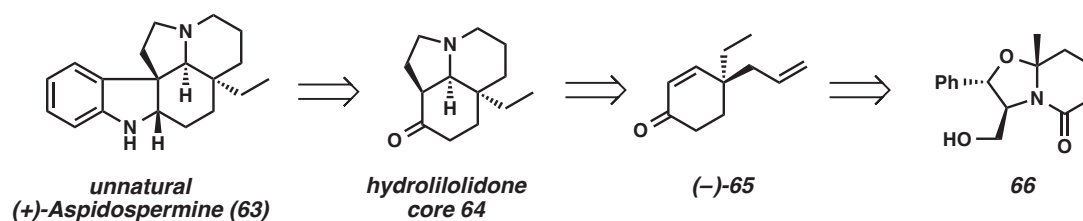
3.5 Aspidospermine

The aspidosperma alkaloids have garnered much attention as beautiful targets for the synthetic chemist. Most of the 250-plus compounds in this class share a pentacyclic core, from the clinical anti-cancer therapeutics vincristine and vinblastine to the simpler aspidospermidine.⁵⁹ To address the challenging synthetic features of the aspidosperma alkaloids, many clever synthetic approaches have been reported.^{60,61} One popular target in this family is aspidospermine (**63**, Scheme 3.8). Although its medicinal potency is

inferior to other members of the class, this alkaloid has served as a proving ground for many synthetic chemists.

In 1989, Meyers reported an enantioselective synthesis of the (4*aS*,8*aR*,8*S*)-hydrolilolidone core **64**^{60,62} present in aspidospermine (**63**), and thus a formal total synthesis of the alkaloid itself,⁶³ intercepting Stork's classic route.⁶⁴ One precursor described in the core synthesis is enone (–)-**65**, which bears the quaternary stereocenter of the natural product. Contrasting Meyers' approach, which employed a chiral auxiliary as part of **66**, we thought a catalytic enantioselective alkylation strategy would be ideal for a formal total synthesis of natural (–)-aspidospermine (**63**) via the antipode of (–)-**65**.

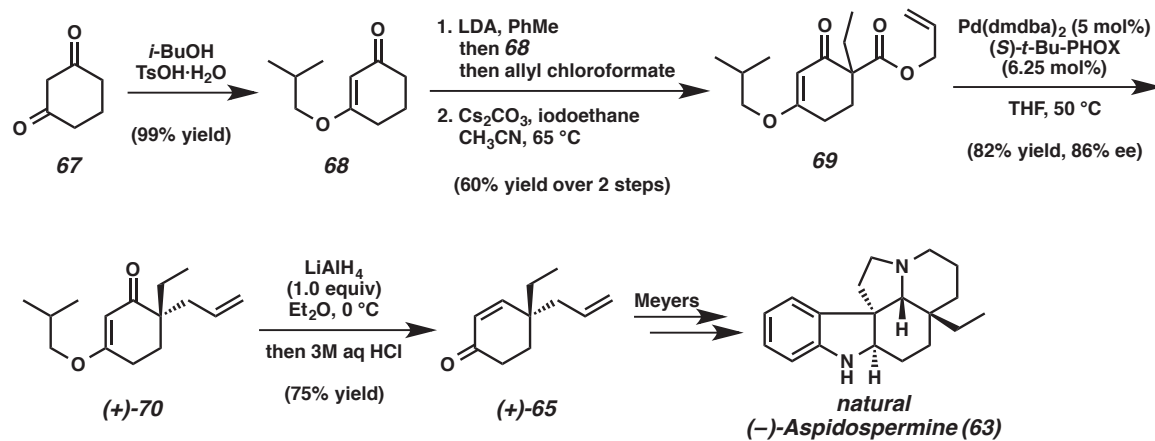
Scheme 3.8 Meyers' approach to unnatural (+)-aspidospermine



The formal synthesis began with 1,3-cyclohexanedione (**67**), which was converted to isobutyl vinylogous ether **68** under acid promotion (Scheme 3.9).⁶⁵ The β -ketoester **69** was prepared using a two-step sequence of acylation and alkylation, then treated with the (*S*)-*t*-Bu-PHOX catalyst system (with Pd(dmdba)₂) to generate (+)-**70** in 86% ee. The challenge of installing the γ -stereocenter of the target (+)-**65** was addressed as follows: LiAlH₄ treatment of (+)-**70** gave exclusive 1,2-reduction. When the crude product was hydrolyzed, β -elimination gave the desired enone (+)-**65**. The overall formal synthesis

represents a previously rare but now readily accessible example of enantioselective Stork-Danheiser chemistry.^{66,67}

Scheme 3.9 Formal total synthesis of (-)-aspidospermine



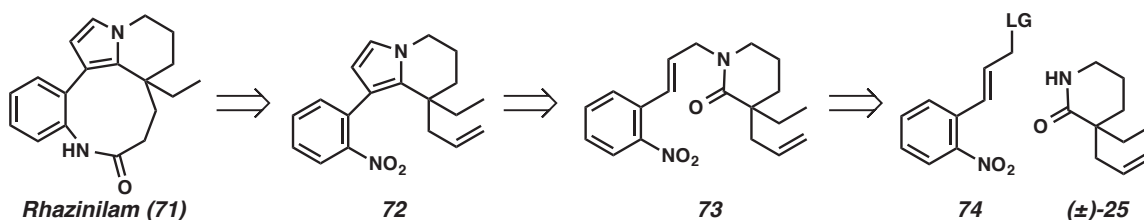
3.6 Rhazinilam

(-)-Rhazinilam (71) has been isolated from various plants including *Rhazya strica decaisne*,⁶⁸ *Melodinus australis*,⁶⁹ and *Kopsia singaporensis*.⁷⁰ Shortly after the first isolation, its structure was elucidated by single crystal X-ray diffraction analysis.⁷¹ It features a tetracyclic scaffold with a nine-membered ring and an all-carbon quaternary stereocenter. This alkaloid is a microtubule-disrupting agent that displays similar cellular effects to paclitaxel.^{72,73} Because of its biological activities and potential pharmaceutical use, many groups have pursued its total synthesis,^{74,75,76,77} including a number of enantioselective syntheses.^{78,79,80,81,82}

In 2001, Magnus and Rainey reported a total synthesis of rhazinilam in racemic form (Scheme 3.10).⁸³ In their approach, the first retrosynthetic disconnection of the amide C–N bond in the nine-membered ring led to tricyclic compound **72**. The pyrrole

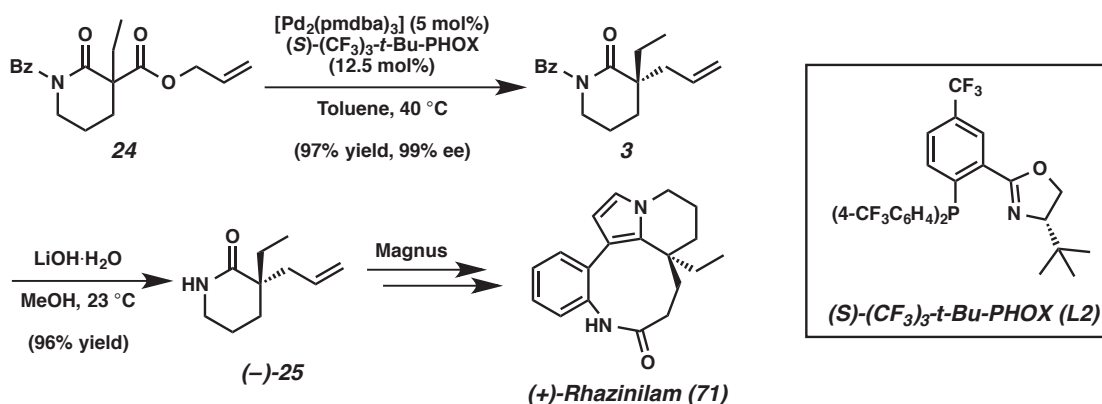
ring of **72** was formed by intramolecular condensation of cinnamyl amide **73**, which is prepared via union of quaternary piperidinone **25** and cinnamyl electrophile **74**. We envisioned that our allylic alkylation of lactam enolates would furnish enantioenriched piperidinone **25**, and thus a single enantiomer of rhazinilam may be prepared.

Scheme 3.10 Magnus' approach to rhazinilam



The formal synthesis of (+)-rhazinilam commenced with palladium-catalyzed decarboxylative allylic alkylation of known carboxy-lactam **24** to afford benzoyl-protected piperidinone **3** in 97% yield and 99% ee (Scheme 3.11).⁸⁴ Cleavage of the benzoyl group under basic conditions furnished piperidinone (–)-**25**,⁸⁴ which can be advanced to (+)-rhazinilam via Magnus' route. This formal synthesis demonstrates the utility of our recently developed asymmetric lactam alkylation chemistry.

Scheme 3.11 Formal total synthesis of (+)-rhazinilam

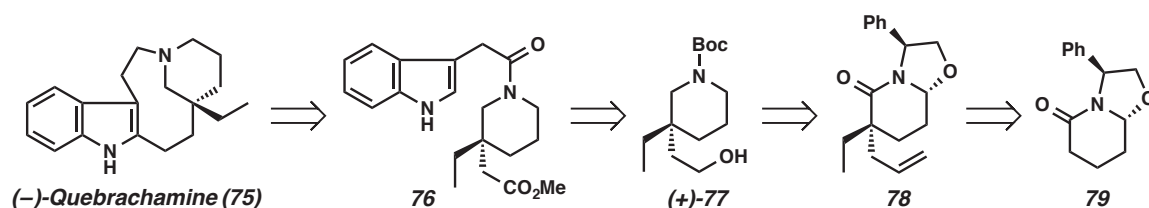


3.7 Quebrachamine

Quebrachamine (**75**) is an indole alkaloid isolated from the *Aspidosperma quebracho* tree bark.⁸⁵ It has been found to possess adrenergic blocking activities for a variety of urogenital tissues.⁸⁶ Structurally, it features a tetracycle including an indole nucleus, a 9-membered macrocycle, and an all-carbon quaternary stereocenter. Due to its structural complexity and biological activities, quebrachamine has received considerable attention from the chemistry community. A number of total syntheses have been reported,^{87,88,89} with several examples of asymmetric syntheses.^{90,91,92}

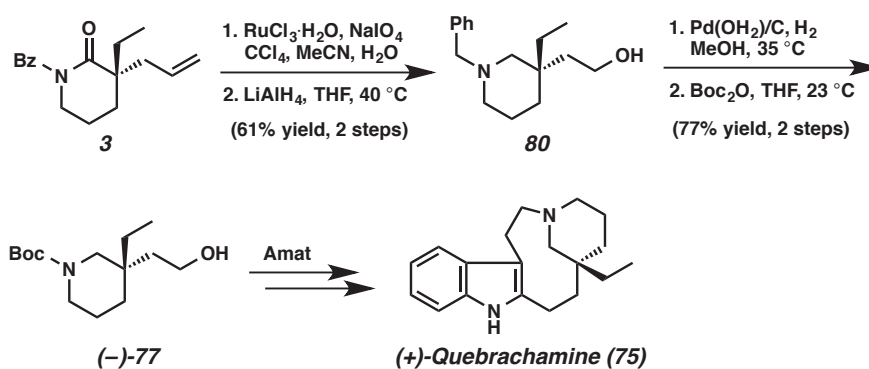
In 2007, Amat reported an enantioselective total synthesis of quebrachamine (Scheme 3.12).⁹³ In their planning, disconnection at the macrocycle led to amide **76**, which was prepared from 3,3-disubstituted piperidine (+)-**77**. The all-carbon quaternary stereocenter in **78** was installed by double alkylation of lactam **79**, using an auxiliary to control the stereoselectivity. We envisioned that an alternative way of constructing this motif would again make use of our recently developed palladium-catalyzed asymmetric alkylation of lactam enolates.

Scheme 3.12 Amat's approach to quebrachamine



The formal synthesis of (+)-quebrachamine commenced with benzoyl lactam **3** (Scheme 3.13), which was prepared in excellent yield and ee by alkylation of carboxylactam **24** (see Scheme 3.11).⁸⁴ Oxidative cleavage of the terminal double bond and subsequent reduction with LiAlH_4 afforded *N*-benzyl piperidine-alcohol **80**.⁸⁴ Hydrogenolysis of the *N*-benzyl group and re-protection with di-*tert*-butyl dicarbonate furnished *N*-boc piperidine-alcohol (-)-77,⁸⁴ thus intercepting an intermediate in Amat's synthesis of quebrachamine.

Scheme 3.13 Formal total synthesis of (+)-quebrachamine



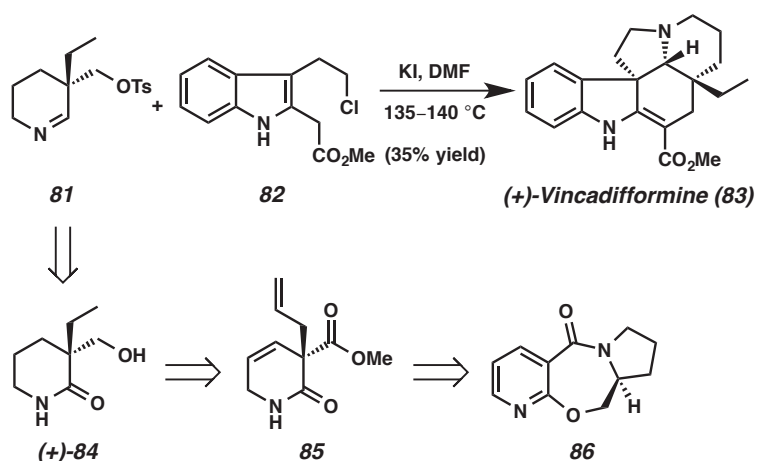
3.8 Vincadifformine

Vincadifformine (**83**) was isolated in both enantioenriched and racemic forms from the leaves and roots of *Rhazya stricta* in 1963.⁹⁴ Not only is it a representative

member of the *Aspidosperma* alkaloid family, but it also holds particular significance as a valuable precursor to pharmaceutically important vincamine, vincamone, and cavinton.^{95,96,97,98} The molecule has a fused pentacyclic framework with three contiguous stereocenters, two of which are all-carbon quaternary centers. The medicinal relevance and structural complexity of vincadifformine have led to a large number of total syntheses,^{99,100,101,102,103,104,105} including several enantioselective examples.^{106,107,108,109}

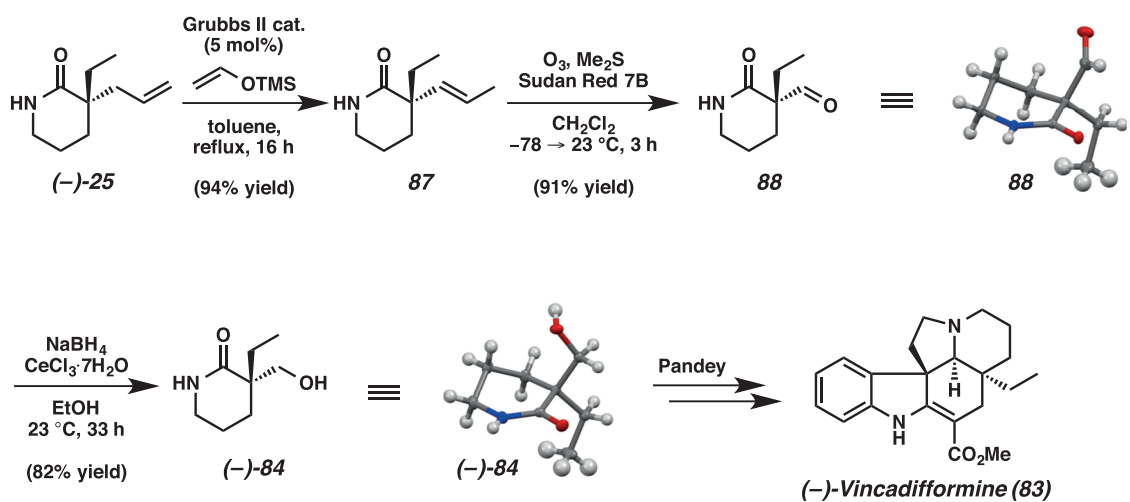
Recently, Pandey reported a highly efficient synthesis of (+)-vincadifformine (Scheme 3.14).¹⁰⁷ The key step in the synthesis was an iminium ion cascade reaction that formed the fused ring systems by coupling 3,3-disubstituted tetrahydropyridine **81** with indole derivative **82**. The former coupling partner was derived from chiral α -quaternary lactam (+)-**84**, which was constructed using a chiral auxiliary strategy. We envisioned that chiral lactam **84** could again be readily accessed by our palladium-catalyzed enantioselective alkylation chemistry.

Scheme 3.14 Pandey's approach to (+)-vincadifformine



The formal synthesis of (–)-vincadifformine commenced with ruthenium-catalyzed isomerization of the terminal olefin moiety in unprotected piperidinone (–)-**25** to produce internal olefin **87** (Scheme 3.15).¹¹⁰ Ozonolysis of the double bond furnished aldehyde **88**, which was reduced under Luche conditions to alcohol (–)-**84**, a compound identical in structure and enantiomeric to the intermediate employed by Pandey in the synthesis of (+)-vincadifformine.

Scheme 3.15 Formal total synthesis of (–)-vincadifformine

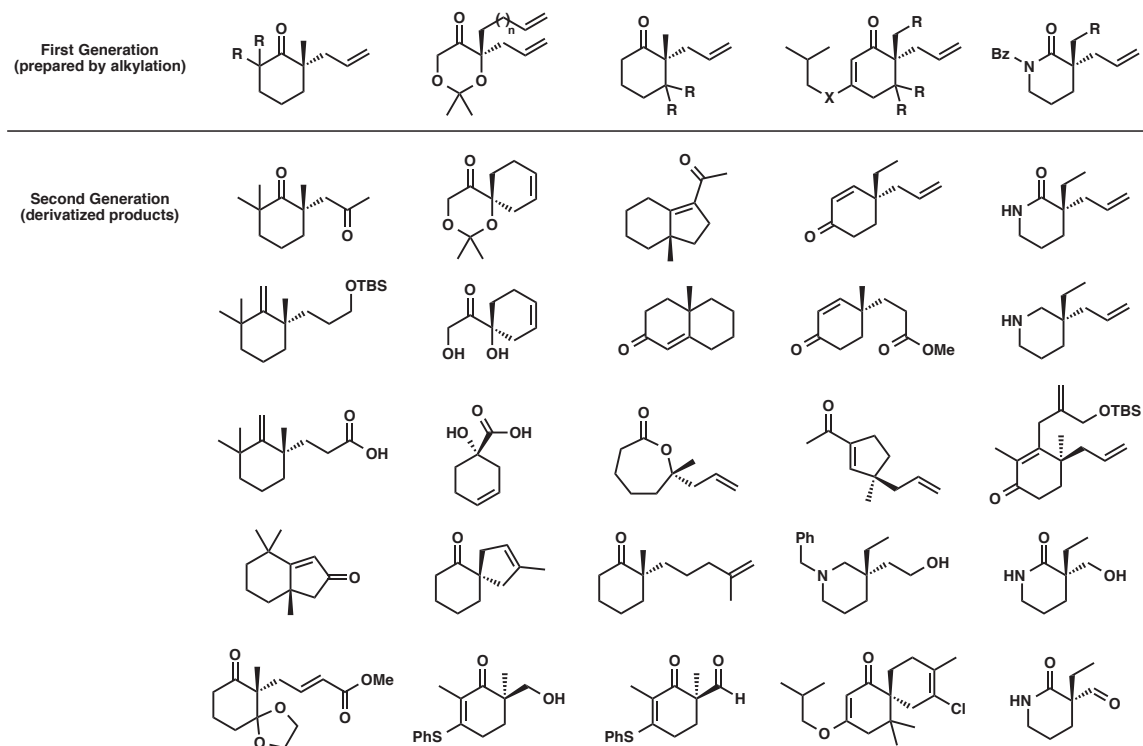


3.9 Conclusions

The development of a series of Pd-catalyzed methods for constructing stereogenic quaternary carbons has provided two generations of building blocks (Figure 3.2). The described derivatization enabled the formal total syntheses of an array of classic natural products including sugar derivatives, terpenes, and alkaloids, adding significantly to the growing list of uses for this powerful C–C bond construction. An efficient route to the sesquiterpenoid (–)-thujopsene (**37**) has been delineated, allowing access to the

compound's natural antipode. Our lab's novel approach to quinic acid (**51**) allowed access to either enantiomer of this important substance. We have also intercepted a key intermediate in Danishefsky's synthesis of dysidiolide (**56**), rendering the former racemic route enantioselective. Additionally, a rapid approach to a compound in Meyers' formal synthesis of aspidospermine (**63**) granted access to the natural product without the use of a chiral auxiliary. Finally, we have demonstrated the application of lactam alkylation products in the catalytic asymmetric syntheses of rhazinilam (**71**), quebrachamine (**75**), and vincadifformine (**83**). The powerful catalytic enantioselective allylic alkylation will undoubtedly enable new synthetic endeavors in the context of both academic and industrial research.

Figure 3.2 Two generations of building blocks



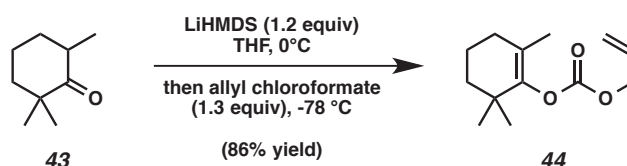
3.10 Experimental Section

3.10.1 Materials and Methods

Unless stated otherwise, reactions were conducted in flame-dried glassware under an atmosphere of nitrogen using anhydrous solvents (either freshly distilled or passed through activated alumina columns). Chloroform, stabilized with ethanol, was stored in the dark over oven-dried 4Å molecular sieves. Absolute ethanol, methanol, and *N,N*-dimethyl acetamide were used as purchased. 2,2,6-Trimethylcyclohexanone (**43**) was used as received. TMEDA and *i*-Pr₂NH were distilled from CaH₂. All other commercially obtained reagents were used as received unless specified otherwise. (*S*)-*t*-Bu-PHOX ligand **L1** was prepared according to known methods.¹¹¹ Reaction temperatures were controlled using an IKAmag temperature modulator. Thin-layer chromatography (TLC) was conducted with E. Merck silica gel 60 F254 pre-coated plates (0.25 mm) and visualized using UV at 254 nm, *p*-anisaldehyde, potassium permanganate, and iodine vapor over sand. TLC data include R_f, eluent, and method of visualization. ICN silica gel (particle size 0.032-0.063 mm), SilliaFlash P60 Academic silica gel (0.040-0.063 mm), or Florisil (Aldrich) was used for flash column chromatography. Analytical chiral HPLC analyses were performed with an Agilent 1100 Series HPLC using a chiralcel OD or AD normal-phase column (250 x 4.6 mm) employing 2.0–3.0% ethanol in hexane isocratic elution and a flow rate of 0.1 mL/min with visualization at 254nm. Analytical chiral GC analysis was performed with an Agilent 6850 GC using a GT-A column (0.25m x 30.00m) employing an 80 °C isotherm and a flow rate of 1.0 mL/min. ¹H NMR spectra were recorded on a Varian Mercury 300 (at 300 MHz) or a Varian Inova 500 (at 500 MHz) and are reported relative to the residual solvent peak (δ 7.26 for CDCl₃ and δ 7.16

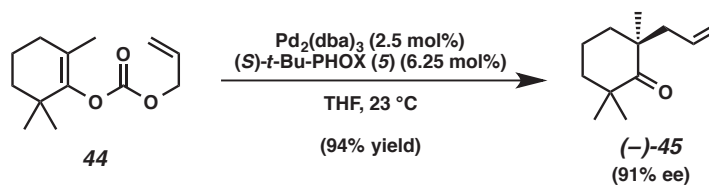
for C₆D₆). Data for ¹H NMR spectra are reported as follows: chemical shift (δ ppm), multiplicity, coupling constant (Hz),¹¹² and integration. ¹³C NMR spectra were recorded on a Varian Mercury 300 (at 75 MHz) or a Varian Inova 500 (at 125 MHz) and are reported relative to the residual solvent peak (δ 77.2 for CDCl₃ and δ 128.4 for C₆D₆). Data for ¹³C NMR spectra are reported in terms of chemical shift, and integration (where appropriate). IR spectra were recorded on a Perkin Elmer Spectrum BXII spectrometer and are reported in frequency of absorption (cm⁻¹). IR samples were thin films deposited on sodium chloride plates by evaporation from a solvent (usually CDCl₃), which is recorded. Optical rotations were measured with a Jasco P-1010 polarimeter, using a 100 mm path-length cell. High-resolution mass spectra were obtained from the California Institute of Technology Mass Spectral Facility. Melting points were determined on a Thomas-Hoover melting point apparatus and are uncorrected.

3.10.2 Syntheses of Compounds Related to Thujopsene



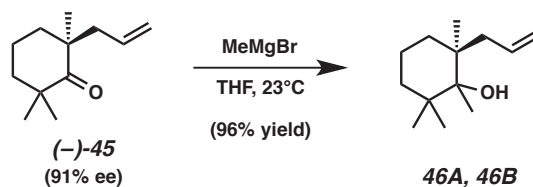
Enol Carbonate 44.¹¹³ A solution of LiHMDS (1.0 M in THF, 57.5 mL, 57.5 mmol) was added to THF (300 mL), then cooled to 0 °C. A solution of 2,2,6-trimethylcyclohexanone (**43**) (6.67 g, 47.6 mmol) in THF (10 mL) was added. The reaction was stirred at 0 °C for 1 h, then cooled to -78 °C and fitted with an addition funnel, which was charged with a solution of allyl chloroformate (6.56 mL, 61.8 mmol) in THF (200 mL). The solution was added dropwise over 30 min. Then the reaction was warmed to 23 °C. After 13 h, the reaction was poured into a mixture of sat. aq NH₄Cl (100 mL), water (100 mL), and

hexane (100 mL). After 10 min, the organic phase was collected and the aqueous phase extracted with Et₂O (3 x 75 mL). All organic layers were combined, washed with brine (100 mL), dried (Na₂SO₄), filtered, and concentrated. The residue was purified by flash chromatography on silica gel (2:98 Et₂O/hexane eluent), affording enol carbonate **44** (9.19 g, 86% yield) as a clear oil. $R_f = 0.43$ (10% EtOAc in hexanes); ¹H NMR (300 MHz, CDCl₃) δ 5.96 (app. ddt, $J_{d1} = 17.1$ Hz, $J_{d2} = 10.7$ Hz, $J_t = 5.8$ Hz, 1H), 5.38 (app. ddq, $J_{d1} = 17.3$ Hz, $J_{d2} = 8.3$ Hz, $J_q = 1.4$ Hz, 1H), 5.28 (app. ddq, $J_{d1} = 10.5$ Hz, $J_{d2} = 4.4$ Hz, $J_q = 1.1$ Hz, 1H), 4.65 (app. ddt, $J_{d1} = 10.2$ Hz, $J_{d2} = 5.7$ Hz, $J_t = 1.4$ Hz, 2H), 2.05 (t, $J = 5.5$ Hz, 2H), 1.77–1.52 (m, 4H), 1.50 (s, 3H), 1.04 (s, 6H); ¹³C NMR (75 MHz, CDCl₃) δ 153.5, 148.1, 131.8, 120.9, 119.1, 68.7, 39.4, 35.1, 31.4, 26.9, 19.3, 16.7; IR (Neat Film NaCl) 2965, 2934, 2868, 2838, 1759, 1459, 1363, 1271, 1238, 1138, 1025, 993, 937 cm⁻¹; HRMS (EI+) m/z calc'd for C₁₃H₂₀O [M]⁺: 224.1413, found 224.1408.



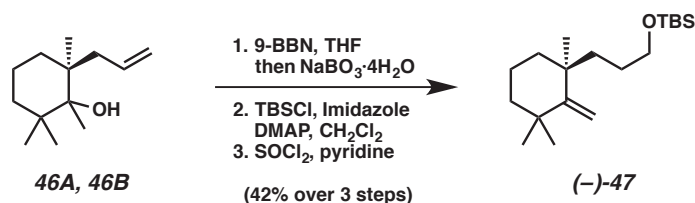
Allyl Ketone (-)-45. A round bottom flask was flame-dried under argon and cycled into the glovebox. It was charged with Pd₂(dba)₃ (242 mg, 0.264 mmol, 6.25 mol%) and (*S*)-*t*-Bu-PHOX (**L1**, 256 mg, 0.661 mmol, 2.5 mol%). Then, THF (317 mL) was introduced. The red mixture was stirred for 20 min at 25 °C. Then, enol carbonate **44** (2.37 g, 10.57 mmol, 1.00 equiv) in THF (10 mL) was added. After the reaction was gauged complete using TLC analysis, it was removed from the glovebox, then concentrated. PhH (~20 mL) was added. After concentrating a second time, more PhH (~20 mL) was added. The

solution was purified by flash chromatography on silica gel (2:98 Et₂O/hexane eluent), affording allyl ketone (–)-**45** (1.72 g, 94% yield) as a clear oil in 91% ee as determined by chiral HPLC analysis. $R_f = 0.48$ (10% EtOAc in hexanes); ¹H NMR (300 MHz, CDCl₃) δ 5.64 (dddd, $J = 17.1$ Hz, 10.5 Hz, 7.7 Hz, 6.9 Hz, 1H), 5.05 (app. ddt, $J_{d1} = 6.3$ Hz, $J_{d2} = 2.2$ Hz, $J_t = 1.1$ Hz, 1H), 4.98 (app. ddt, $J_{d1} = 13.8$ Hz, $J_{d2} = 2.5$ Hz, $J_t = 1.4$ Hz, 1H), 2.32 (app. ddt, $J_{d1} = 13.8$ Hz, $J_{d2} = 6.9$ Hz, $J_t = 1.4$ Hz, 1H), 2.16 (app. ddt, $J_{d1} = 13.8$ Hz, $J_{d2} = 6.9$ Hz, $J_t = 1.4$ Hz, 1H) 1.87–1.47 (m, 6H), 1.15 (s, 3H), 1.09 (s, 3H), 1.08 (s, 3H); ¹³C NMR (75 MHz, CDCl₃) δ 219.8, 134.7, 118.0, 47.7, 44.6, 44.0, 39.9, 37.0, 28.0, 27.3, 25.7, 17.9; IR (Neat Film NaCl) 3077, 2979, 2964, 2933, 2869, 1697, 1463, 1382, 999, 914 cm⁻¹; HRMS (EI+) m/z calc'd for C₁₂H₂₀O [M]⁺: 180.1514, found 180.1506; $[\alpha]_D^{24} -36.3^\circ$ (c 0.140, CHCl₃, 91% ee).



Alcohols 46A and 46B. A round-bottom flask was charged with a solution of allyl ketone (–)-**45** (1.02 g, 5.65 mmol, 1.00 equiv, 91% ee) and THF (55.5 mL). Then, methyl magnesium bromide (3.0 M in Et₂O, 9.25 mL, 27.8 mmol, 5.00 equiv) was gradually introduced at 23 °C. After 24 h, the reaction was carefully quenched at 0 °C with sat. aq NH₄Cl (30 mL). Then H₂O (50 mL) was added, along with hexanes (50 mL). The biphasic mixture was extracted with Et₂O (2 x 30 mL). All organic layers were combined, dried (Na₂SO₄), filtered, and concentrated. The wet residue was taken up in CHCl₃ and dried again with Na₂SO₄, then filtered. The filtrate was concentrated, giving a 1:1 mixture

of diastereomeric alcohols **46A** and **46B** (1.04 g, 94% yield) as a colorless oil. $R_f = 0.59$ (10% EtOAc in hexanes); $^1\text{H NMR}$ (300 MHz, CDCl_3) (both diastereomers) δ 5.84 (app. dddd, $J = 19.4$ Hz, 14.6 Hz, 7.4 Hz, 7.2 Hz, 2H), 5.01 (app. d, $J = 11.1$ Hz, 2H), 5.00 (app. d, $J = 14.6$ Hz, 2H), 2.44 (app. ddd, $J = 12.6$ Hz, 11.1 Hz, 7.5 Hz, 2H), 2.07 (app. ddd, $J = 19.4$ Hz, 13.6 Hz, 7.7 Hz, 2H), 1.62–1.46 (m, 4H), 1.44–1.36 (m, 4H), 1.28–1.10 (m, 2H), 1.14 (app. s, 6H), 1.07 (s, 3H), 1.06 (s, 3H), 1.10 (s, 3H), 0.99 (s, 3H), 0.98–0.86 (m, 2H), 0.97 (s, 3H), 0.95 (s, 3H); $^{13}\text{C NMR}$ (75 MHz, CDCl_3) (both diastereomers) δ 136.8, 136.4, 117.0, 116.8, 78.2, 77.9, 43.8, 42.0, 41.6, 41.2, 39.2, 39.0, 37.2, 36.9, 33.6, 33.0, 28.3, 28.2, 26.6, 25.8, 22.9, 22.2, 18.6, 18.5, 18.3, 18.1; IR (Neat Film NaCl) 3504 (broad), 3074, 2930, 2867, 1638, 1454, 1378, 1305, 1071, 998, 910 cm^{-1} ; HRMS (EI+) m/z calc'd for $\text{C}_{13}\text{H}_{24}\text{O}$ $[\text{M}]^+$: 196.1827, found 196.1803.



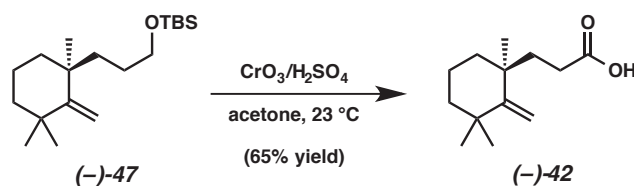
Methylene Cyclohexane (-)-47. A 20 mL scintillation vial containing a mixture of diastereomeric alcohols **46A** and **46B** (72 mg, 0.367 mmol, 1.00 equiv, 91% ee) was treated with a solution of 9-borabicyclo[3.3.1]nonane in THF (0.5 M, 0.90 mL, 0.45 mmol, 1.23 equiv) at 23 °C. The reaction was stirred for 2.5 h. Then the reaction was cooled to 0 °C, and H_2O (1 mL) was carefully added, followed by $\text{NaBO}_3 \cdot 4\text{H}_2\text{O}$ (219 g, 1.42 mmol, 3.88 equiv). The biphasic reaction mixture was stirred vigorously at 23 °C for 2 h, diluted with water, and extracted with CH_2Cl_2 (4 x 1 mL). All organic layers were combined, dried (Na_2SO_4), filtered, and concentrated. The residue was purified by flash

chromatography on silica gel (25% → 33% → 50% EtOAc in hexanes), giving an oil containing two diastereomeric products, which was immediately used in the next reaction.

This mixture was transferred to a 20 mL scintillation vial. Imidazole (39 mg, 0.57 mmol), 4-dimethylaminopyridine (1 mg, 0.00885 mmol), and anhydrous CH₂Cl₂ (1.0 mL) were introduced, followed by a solution of TBSCl (48 mg, 0.314 mmol) in anhydrous CH₂Cl₂ (1.0 mL) at 23 °C. A white precipitate quickly formed. After 10 min, the reaction was diluted with hexanes (4 mL), filtered, and concentrated. The residue was purified by flash chromatography on silica gel (5:95 EtOAc:hexane eluent), affording a diastereomeric mixture of silyl ethers. This composite was carried on to the next reaction without further characterization.

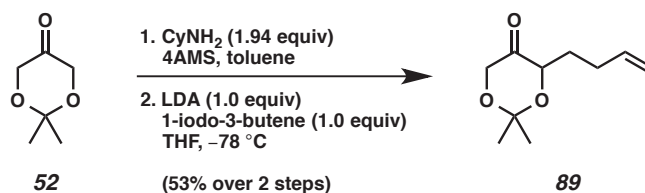
The mixture of silyl ethers was transferred to a 20 mL scintillation vial, which was charged with pyridine (freshly distilled from CaH₂, 1.5 mL). After cooling to 0 °C, SOCl₂ (36 μL, 0.50 mmol) was slowly introduced. After stirring 1 h at 0 °C and another 1 h at 23 °C, H₂O (5 mL) was carefully added, followed by Et₂O (8 mL). The organic phase was collected, and the aqueous layer was extracted with Et₂O (2 x 10 mL). All organic layers were combined and washed with 1.0 M aq CuSO₄ (4 x 5 mL). The aqueous washings were back-extracted with Et₂O (1 x 10 mL). All organic layers were combined, dried (Na₂SO₄), filtered, and concentrated. The residue was purified by flash chromatography on silica gel (1% → 2% Et₂O in hexanes), giving pure methylene cyclohexane (–)-**47** (48 mg, 42% yield from **46A** and **46B**) as a colorless oil. R_f = 0.71 (10% EtOAc in hexanes); ¹H NMR (300 MHz, CDCl₃) δ 5.00 (app. s, 1H), 4.79 (app. s, 1H), 3.57 (app. t, J = 6.6 Hz, 2H), 1.80–1.64 (m, 2H), 1.62–1.16 (m, 8H), 1.11 (s, 3H),

1.10 (s, 3H), 1.04 (s, 3H), 0.89 (s, 9H), 0.04 (s, 6H); ^{13}C NMR (75 MHz, CDCl_3) δ 160.5, 108.7, 64.1, 41.8, 40.8, 39.4, 36.6, 36.5, 32.8, 29.9, 29.8, 28.4, 26.2 (3C), 18.7, 18.6, 5.0 (2C); IR (Neat Film NaCl) 3100, 2955, 2929, 2858, 1623, 1472, 1382, 1361, 1255, 1100, 940, 900, 836, 774 cm^{-1} ; HRMS (EI+) m/z calc'd for $\text{C}_{19}\text{H}_{38}\text{SiO}$ $[\text{M}]^+$: 310.2692, found 310.2689; $[\alpha]_{\text{D}}^{24}$ -18.8° (c 1.90, CHCl_3 , 91% ee).



Carboxylic Acid (-)-42. A vessel containing methylene cyclohexane (-)-47 (48 mg, 0.154 mmol) was charged with acetone (ACS grade, 2.5 mL), then treated with Jones reagent (1.0 M CrO_3 , 4.0 H_2SO_4 in H_2O) (1.0 mL, dropwise from a glass pipet) at 23°C . After 15 min, the reaction was carefully quenched with sat. aq Na_2SO_3 (2 mL). CHCl_3 (5 mL) was added, followed by H_2O (5 mL) and 6 M aq HCl (4 mL). After 5 min, the reaction was extracted with CHCl_3 (3 x 10 mL). All organic layers were combined, dried (Na_2SO_4), filtered, and concentrated. The residue was purified by flash chromatography on silica gel (6% \rightarrow 14% Et_2O in CH_2Cl_2), giving carboxylic acid (-)-42 (21 mg, 65% yield) as a colorless oil. $R_f = 0.17$ (10% EtOAc in hexanes); ^1H NMR (300 MHz, CDCl_3) δ 5.06 (app. s, 1H), 4.80 (app. s, 1H), 2.36–2.04 (m, 3H), 1.82–1.66 (m, 2H), 1.60–1.30 (m, 5H), 1.11 (s, 3H), 1.10 (s, 3H), 1.05 (s, 3H); ^{13}C NMR (75 MHz, CDCl_3) δ 159.3, 109.6, 41.5, 40.6, 39.2, 36.5, 34.7, 32.7, 29.61, 29.56, 18.6; IR (Neat Film NaCl) 3000 (broad), 2927, 1708, 1462, 1414, 1380, 1296, 1095, 902 cm^{-1} ; HRMS (EI+) m/z calc'd for $\text{C}_{13}\text{H}_{22}\text{O}$ $[\text{M}]^+$: 210.1620, found 210.1618; $[\alpha]_{\text{D}}^{24}$ -27.8° (c 1.205, CHCl_3 , 91% ee).

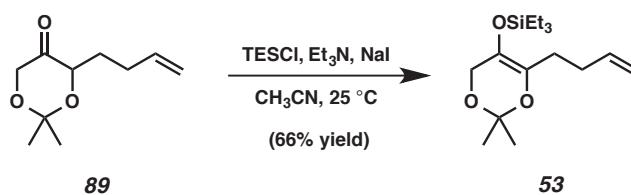
3.10.3 Syntheses of Compounds Related to Quinic Acid



Dioxanone 89.¹¹⁴ To a solution of 2,2-dimethyl-1,3-dioxan-5-one **52** (5.0 g, 38.4 mmol, 1.0 equiv) in toluene (125 mL, 0.3 M) were added 4Å molecular sieves (5.0 g) and cyclohexylamine (8.50 mL, 74.3 mmol, 1.94 equiv) at room temperature (ca. 25 °C). The mixture was stirred for 14 h, before the molecular sieves were removed by filtration. The filtrate was concentrated under reduced pressure to give crude imine (7.95 g).

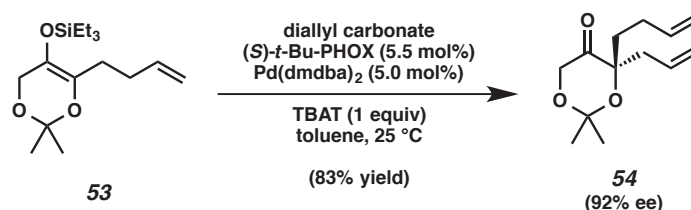
Lithium diisopropylamine was prepared in a separate flask by dropwise addition of *n*-BuLi (2.50 M in hexanes, 15.4 mL, 38.5 mmol, 1.0 equiv) via syringe to a solution of diisopropylamine (5.40 mL, 38.5 mmol, 1.0 equiv) in THF (60 mL, 0.64 M) at 0 °C. The solution was stirred at 0 °C for 10 min, and then cooled to -78 °C. A solution of the imine (7.95 g) in THF (40.0 mL) was added dropwise via syringe to the resulting LDA solution at -78 °C. The reaction mixture was warmed to -35 °C, and stirred for 2 h, after which it was re-cooled to -78 °C, and 1-iodo-3-butene (7.00 g, 38.4 mmol, 1.0 equiv) was added. The reaction was warmed to room temperature (ca. 25 °C) over 3 h. Saturated aq NH₄Cl (60 mL) was added to the reaction mixture, and the mixture was stirred at room temperature overnight. The mixture was extracted with Et₂O (3 x 50 mL). The combined organic layers were washed with brine (30 mL), dried over MgSO₄, and filtered. Solvent was removed under reduced pressure, and the residue was purified by flash chromatography (20% Et₂O in pentane on silica gel) to give dioxanone **89** (3.75 g, 53% yield over 2 steps) as a colorless oil. *R_f* = 0.38 (20% Et₂O in hexanes); ¹H NMR

(300 MHz, CDCl₃) δ 5.85–5.72 (m, 1H), 5.09–4.98 (m, 2H), 4.29–4.21 (m, 2H), 3.98 (d, *J* = 16.8 Hz, 1H), 2.30–2.08 (m, 2H), 2.03–1.92 (m, 1H), 1.70–1.58 (m, 1H), 1.45 (s, 3H), 1.44 (s, 3H); ¹³C NMR (75 MHz, CDCl₃) δ 210.0, 137.7, 115.8, 101.0, 73.8, 66.8, 29.3, 27.6, 24.1, 23.9; IR (Neat Film NaCl) 2988, 2938, 2884, 1748, 1642, 1434, 1376, 1251, 1225, 1175, 1103, 1071, 916, 864 cm⁻¹; HRMS (EI+) *m/z* calc'd for C₁₀H₁₆O₃ [M]⁺: 184.1100, found 184.1131.



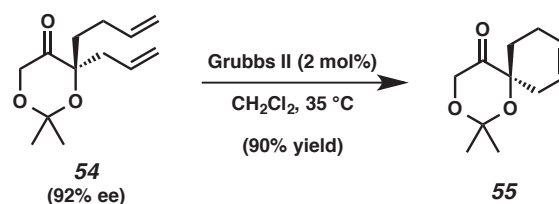
Triethylsilyl Enol Ether 53.¹¹⁴ To a solution of dioxanone **89** (0.58 g, 3.16 mmol, 1.0 equiv), Et₃N (0.71 mL, 5.09 mmol, 1.6 equiv) and sodium iodide (0.62 g, 4.14 mmol, 1.3 equiv) in acetonitrile (5.0 mL, 0.63 M) was added triethylsilyl chloride (0.69 mL, 4.11 mmol, 1.3 equiv) at room temperature (ca. 25 °C). After the mixture was stirred for 20 h, pentane (10 mL) was added. The mixture was stirred at room temperature for 2 min, before the pentane was decanted. After additional pentane extractions (5 x 10 mL), the combined pentane extracts were washed with water (20 mL) and then with brine (20 mL), dried over Na₂SO₄, and concentrated under reduced pressure. The residue was purified by flash chromatography (1% Et₂O in petroleum ether on silica gel) to give triethylsilyl enol ether **53** (0.623 g, 66% yield) as a colorless oil. *R_f* = 0.58 (10% Et₂O in hexanes); ¹H NMR (300 MHz, CDCl₃) δ 5.90–5.77 (m, 1H), 5.07–5.0 (m, 1H), 5.0–4.93 (m, 1H), 4.05 (s, 2H), 2.30–2.13 (m, 4H), 1.43 (s, 6H), 0.98 (t, *J* = 7.8 Hz, 9H), 0.65 (q, *J* = 7.8 Hz, 6H); ¹³C NMR (75 MHz, CDCl₃) δ 138.5, 137.2, 125.7, 114.8, 98.2, 61.1, 30.9, 27.0,

24.3, 6.9, 5.6; IR (Neat Film NaCl) 2995, 2957, 2914, 2878, 2838, 1383, 1369, 1277, 1223, 1198, 1147, 1085, 1006, 857, 745, 730 cm^{-1} ; HRMS (EI+) m/z calc'd for $\text{C}_{16}\text{H}_{30}\text{O}_3\text{Si}$ $[\text{M}]^+$: 298.1964, found 298.1967.

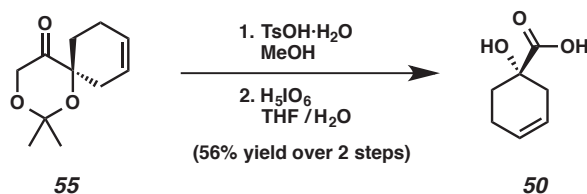


Diene 54.¹¹⁴ A 100 mL round-bottom flask was flame dried under vacuum and back-filled with argon. Pd(dmdba)₂ (20.3 mg, 0.025 mmol, 0.05 equiv), (*S*)-*t*-Bu-PHOX (10.6 mg, 0.027 mmol, 0.055 equiv), and TBAT (270 mg, 0.50 mmol, 1.0 equiv) were added to the flask. The system was evacuated under vacuum and backfilled with argon (3 x). Toluene (15 mL, 0.033 M) was added by syringe and the mixture was stirred at room temperature (ca. 25 °C) for 30 min. Diallyl carbonate (75.2 μL , 0.52 mmol, 1.05 equiv) and triethylsilyl enol ether **53** (149 mg, 0.50 mmol, 1.0 equiv) were added sequentially. When the reaction was complete by TLC (after ca. 9 h), the reaction mixture was loaded onto a silica gel column and eluted with 2% Et₂O in petroleum ether to give diene **54** (93.0 mg, 83% yield, 92% ee) as a colorless oil. R_f = 0.33 (10% Et₂O in hexanes); ¹H NMR (300 MHz, CDCl₃) δ 5.86–5.70 (m, 2H), 5.11–4.92 (m, 4H), 4.19 (d, J = 18.0 Hz, 2H), 4.15 (d, J = 18.0 Hz, 2H), 2.60–2.45 (m, 2H), 2.27–1.95 (m, 2H), 1.93–1.69 (m, 2H), 1.51 (s, 3H), 1.48 (s, 3H); ¹³C NMR (75 MHz, CDCl₃) δ 210.5, 138.2, 132.4, 119.1, 115.0, 100.1, 84.5, 67.4, 41.9, 36.1, 27.7, 27.3, 26.5; IR (Neat Film NaCl) 3079, 2987, 2941, 1738 1642, 1427, 1382 1372, 1232, 1209, 1168, 1148, 1098, 998, 915 cm^{-1} ; HRMS

(EI+) m/z calc'd for $C_{13}H_{20}O_3$ $[M]^+$: 224.1412, found 224.1416; $[\alpha]_D^{20.2} +7.04^\circ$ (c 1.030, CH_2Cl_2 , 92% ee).

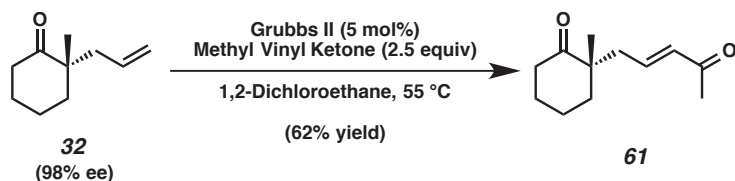


Cyclohexene 55.¹¹⁴ To a solution of diene **54** (60 mg, 0.268 mmol, 1.0 equiv) in CH_2Cl_2 (10 mL) was added Grubbs second generation catalyst (4.6 mg, 0.0054 mmol, 0.02 equiv) at room temperature. After the mixture was stirred at 35 °C for 40 h, it was concentrated under reduced pressure. The residue was purified by flash chromatography (2% Et_2O in petroleum ether on silica gel) to give the cyclohexene **55** (47.3 mg, 90% yield) as a colorless oil. $R_f = 0.24$ (10% Et_2O in hexanes); 1H NMR (300 MHz, $CDCl_3$) δ 5.80–5.70 (m, 1H), 5.67–5.58 (m, 1H), 4.27 (s, 2H), 2.60–2.47 (m, 1H), 2.38–2.18 (m, 2H), 2.17–1.81 (m, 3H), 1.51 (s, 3H), 1.47 (s, 3H); ^{13}C NMR (75 MHz, $CDCl_3$) δ 211.1, 126.4, 122.8, 100.5, 79.9, 66.6, 33.5, 29.9, 27.7, 26.3, 21.8; IR (Neat Film NaCl) 3030, 2991, 2938, 2911, 1739, 1429, 1382, 1372, 1259, 1230, 1200, 1155, 1099, 1062, 999, 886, 836, 778, 651 cm^{-1} ; HRMS (EI+) m/z calc'd for $C_{11}H_{16}O_3$ $[M]^+$: 196.1100, found 196.1139; $[\alpha]_D^{20.2} -20.9^\circ$ (c 1.045, CH_2Cl_2 , 92% ee).

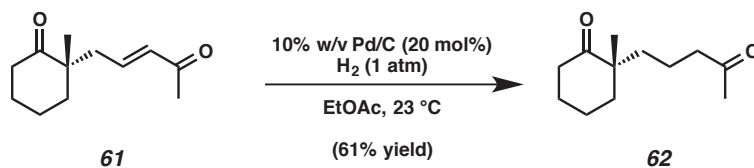


Carboxylic Acid 50.¹¹⁴ To a solution of cyclohexene **55** (40 mg, 0.20 mmol, 1.0 equiv) in MeOH (4 mL, 0.05 M) was added *p*-toluenesulfonic acid monohydrate (3.9 mg, 0.02 mmol, 0.1 equiv) at room temperature (24 °C). After the mixture was stirred for 3 h, Et₃N (0.1 mL) was added. The mixture was concentrated under reduced pressure to give a yellow oil. The oil was diluted with EtOAc (10 mL), filtered through SiO₂ (1 mL), and concentrated under reduced pressure to furnish a white solid (35 mg). The solid was dissolved in THF (0.4 mL) and water (0.2 mL), and the colorless solution was cooled to 0 °C (ice water bath). H₅IO₆ (46 mg, 0.20 mmol, 1 equiv) was added to the solution. The mixture was allowed to warm to room temperature (26 °C) over 10 minutes, and then stirred for 2 h. The reaction was diluted with water (0.5 mL), and extracted with EtOAc (4 x 15 mL). Extracts were dried over Na₂SO₄ and concentrated under reduced pressure. The white solid was purified by column chromatography over silica gel (ca. 9 mL) with 2:1 Hexanes:EtOAc to give carboxylic acid **50** (16.3 mg, 56% yield, 92% ee) as a white solid: mp 79–81 °C; ¹H NMR (300 MHz, CDCl₃) δ 5.88–5.79 (m, 1H), 5.72–5.61 (m, 1H), 2.79–2.62 (m, 1H), 2.37–2.11 (m, 4H), 1.95–1.80 (m, 1H); ¹³C NMR (75 MHz, CDCl₃) δ 181.5, 126.6, 122.6, 72.6, 34.9, 30.6, 21.4; IR (Neat Film NaCl) 3432, 3032, 2929, 2624, 1736, 1443, 1370, 1356, 1318, 1253, 1216, 1092, 1064, 982, 939, 886, 773, 746, 650, 736 cm⁻¹; HRMS (EI+) *m/z* calc'd for C₈H₁₂O₃ [M]⁺: 143.0708, found 143.0708; [α]_D^{20.7} +31.7° (*c* 0.310, CH₂Cl₂, 92% ee).

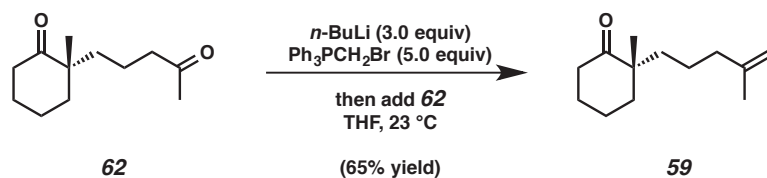
3.10.4 Syntheses of Compounds Related to Dysidiolide



Keto-Enone 61.¹¹³ A vial was charged with allyl ketone **32** (45.2 mg, 0.297 mmol, 1.0 equiv, 98% ee), followed by a solution of methyl vinyl ketone (61.8 μL , 0.743 mmol, 2.5 equiv) in 1,2-dichloroethane (1.5 mL). Then, Grubbs 2nd generation catalyst (12.6 mg, 14.9 μmol , 5 mol%) was added. The vessel was sealed and warmed to 55 $^\circ\text{C}$ for 24 h. The reaction transitioned from maroon to deep green. The reaction was cooled to 23 $^\circ\text{C}$ and concentrated. The residue was purified by flash chromatography on silica gel (hexanes \rightarrow 20% EtOAc in hexanes), giving keto-enone **61** (35.7 mg, 62% yield) as a pale brown oil. $R_f = 0.23$ (20% EtOAc in hexanes); $^1\text{H NMR}$ (300 MHz, CDCl_3) δ 6.70 (app. dt, $J_d = 15.9$ Hz, $J_t = 7.4$ Hz, 1H), 6.03 (app. d, $J = 15.9$ Hz, 1H), 2.50–2.26 (m, 2H), 2.40 (app. d, $J = 6.9$ Hz, 1H), 2.39 (app. d, $J = 6.9$ Hz, 1H), 2.22 (s, 3H), 1.91–1.81 (m, 2H), 1.80–1.60 (m, 4H), 1.12 (s, 3H); $^{13}\text{C NMR}$ (75 MHz, CDCl_3) δ 214.6, 198.4, 144.1, 134.2, 48.7, 41.0, 38.9, 38.7, 27.4, 26.9, 23.1, 21.1; IR (Neat Film NaCl) 2935, 2866, 1704, 1672, 1626, 1426, 1361, 1254, 1124, 986 cm^{-1} ; HRMS (EI+) m/z calc'd for $\text{C}_{12}\text{H}_{18}\text{O}_2$ $[\text{M}]^+$: 194.1307, found 194.1336; $[\alpha]_D^{22} -1.14^\circ$ (c 1.415, CHCl_3 , 98% ee).



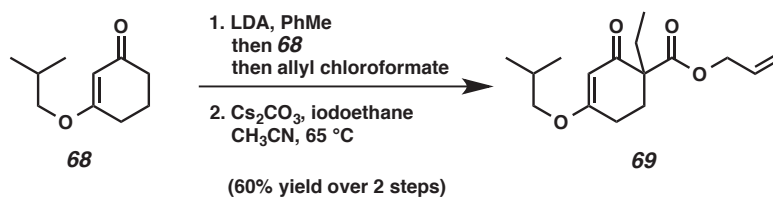
Diketone 62.¹¹³ A round-bottom flask containing keto-enone **61** (28.0 mg, 0.144 mmol, 1.0 equiv) in EtOAc (3.0 mL) was sparged with argon for 2 min. Pd/C (10% w/w) (30.6 mg, 28.8 μmol , 20 mol) was introduced, and the reaction was cooled to $-78\text{ }^{\circ}\text{C}$. It was purged/backfilled with vacuum/ H_2 (1 atm) (3 x) and warmed to $23\text{ }^{\circ}\text{C}$ and stirred under H_2 (1 atm) for 12 h. More EtOAc (5 mL) was added, and the reaction was sparged with argon to remove residual H_2 . The material was filtered through a plug of silica gel with the aide of EtOAc. The filtrate was concentrated, affording diketone **62** (17.3 mg, 61% yield) as a pale yellow oil. $R_f = 0.26$ (20% EtOAc in hexanes); $^1\text{H NMR}$ (300 MHz, CDCl_3) δ 2.40 (app. t, $J = 6.6\text{ Hz}$, 2H), 2.36 (app. t, $J = 5.5\text{ Hz}$, 2H), 2.11 (s, 3H), 1.90–1.44 (m, 9H), 1.36 (app. d, $J = 7.7\text{ Hz}$, 1H), 1.15 (s, 3H); $^{13}\text{C NMR}$ (75 MHz, CDCl_3) δ 216.0, 208.8, 48.6, 44.0, 39.2, 38.9, 37.0, 30.1, 27.6, 22.7, 21.2, 18.2; IR (Neat Film NaCl) 2936, 2865, 1705, 1452, 1360, 1167, 1123, 1099 cm^{-1} ; HRMS (EI+) m/z calc'd for $\text{C}_{12}\text{H}_{20}\text{O}_2$ $[\text{M}]^+$: 196.1463, found 196.1469; $[\alpha]_{\text{D}}^{22} -42.3^{\circ}$ (c 0.865, CHCl_3 , 98% ee).



Keto-Olefin 59. A round-bottom flask was charged with methyl triphenyl phosphonium bromide (weighed in glovebox, 260 mg, 0.688 mmol, 5.0 equiv). THF (5.5 mL) was introduced, followed by $n\text{-BuLi}$ (2.5 M in hexane, 165 μL , 0.413 mmol, 3.0 equiv) at $23\text{ }^{\circ}\text{C}$. After stirring for 1 h, a solution of diketone **62** (27.0 mg, 0.138 mmol, 1.0 equiv) in THF (2.0 mL) was added. 30 min later, the reaction was quenched with sat. aq NH_4Cl (4.0 mL). Then, the reaction was diluted with H_2O (20 mL) and hexane (15 mL). The

biphasic mixture was extracted with EtOAc (4 x 20 mL). All organic layers were combined, dried (Na₂SO₄), filtered, and concentrated. The residue was purified by flash chromatography on silica gel (hexanes → 2% EtOAc in hexanes), giving keto-olefin **59** (17.3 mg, 65% yield) as a colorless oil. R_f = 0.75 (20% EtOAc in hexanes); ¹H NMR (300 MHz, CDCl₃) δ 4.70 (app. s, 1H), 4.65 (app. s, 1H), 2.46–2.26 (m, 2H), 1.98 (app. t, J = 7.1 Hz, 2H), 1.94–1.84 (m, 1H), 1.82–1.50 (m, 5H), 1.68 (s, 3H), 1.47–1.39 (m, 1H), 1.38 (app. ddd, J = 26.4 Hz, 12.6 Hz, 4.1 Hz, 1H), 1.22–1.10 (m, 2H), 1.14 (s, 3H); ¹³C NMR (75 MHz, CDCl₃) δ 216.3, 145.7, 110.3, 48.7, 39.6, 39.0, 38.4, 37.2, 27.7, 22.8, 22.5, 21.7, 21.2; IR (Neat Film NaCl) 3074, 2936, 2865, 1707, 1650, 1452, 1376, 1260, 1096, 1020, 886, 804 cm⁻¹; HRMS (EI+) m/z calc'd for C₁₃H₂₂O [M]⁺: 194.1671, found 194.1680; $[\alpha]_D^{21}$ -49.8° (c 0.865, CHCl₃, 98% ee).

3.10.5 Syntheses of Compounds Related to Aspidospermine

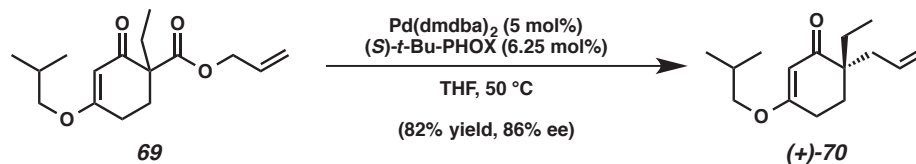


α-Ethyl-α-Allyloxycarbonyl Vinylous Ester 69. A round-bottom flask was flamedried under argon and charged with dry PhMe (320 mL). Then, *i*-Pr₂NH (12.81 mL, 91.3 mmol, 2.05 equiv) was introduced. The reaction was cooled to -78 °C, and *n*-BuLi (2.5 M in hexane, 35.68 mL, 89.2 mmol, 2.00 equiv) was added slowly. The reaction was warmed to 0 °C for 15 min, then promptly cooled back to -78 °C. Then, a solution of vinylous ester **68** (7.50 g, 44.6 mmol, 1.00 equiv) in PhMe (20 mL) was added at -78

°C over a 5 min period. After 40 min had passed, the reaction was treated with allyl chloroformate (4.97 mL, 46.8 mmol, 1.05 equiv) over a 5 min timeframe at -78 °C. After 15 min, the reaction was warmed to 23 °C and stirred for 1 h, during which the reaction went from yellow to orange. Then, 1.0 M aq KHSO₄ (127 mL) was added with vigorous stirring, causing the reaction to turn yellow. The organic phase was collected. The aqueous layer was extracted with Et₂O (2 x 50 mL). All organic layers were combined, dried (Na₂SO₄), filtered, and concentrated, giving a crude α -allyloxycarbonyl vinylogous ester as an orange oil, which was immediately used in the next reaction.

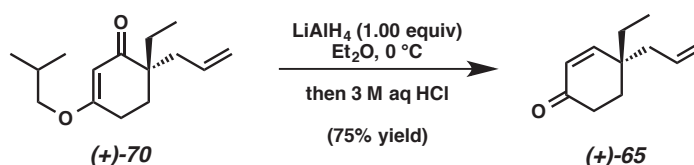
A round-bottom flask containing the crude vinylogous ester was charged with CH₃CN (45 mL), followed by iodoethane (14.26 mL, 178.4 mmol, 4.0 equiv relative to **68**). Anhydrous Cs₂CO₃ (29.06 g, 89.2 mmol, 2.0 equiv relative to **68**) was introduced, and the reaction was stirred vigorously at 65 °C for 12 h. The reaction was cooled to 23 °C and filtered over glass frits. The filtrate was concentrated in vacuo, and the residue was purified by flash column chromatography on silica gel (hexane \rightarrow 15% EtOAc in hexanes), giving semipure **69**. The product-containing fractions were combined and concentrated, and the resulting residue was purified on a second silica gel flash column (5% EtOAc in CH₂Cl₂), giving pure α -ethyl- α -allyloxycarbonyl vinylogous ester **69** (7.47 g, 60% yield over 2 steps) as a yellow oil. $R_f = 0.44$ (20% EtOAc in hexanes); ¹H NMR (300 MHz, CDCl₃) δ 5.83 (ddt, $J_{d1} = 16.2$ Hz, $J_{d2} = 10.7$ Hz, $J_t = 5.7$ Hz, 1H), 5.31 (s, 1H), 5.24 (app. ddd, $J = 16.2$ Hz, 2.9 Hz, 1.5 Hz, 1H), 5.15 (app. ddd, $J = 10.7$ Hz, 2.9 Hz, 1.5 Hz, 1H), 4.56 (app. dt, $J_d = 5.4$ Hz, $J_t = 1.5$ Hz, 2H), 3.54 (d, $J = 6.7$ Hz, 2H), 2.68–2.28 (m, 2H), 2.42–2.26 (m, 1H), 1.99 (dq, $J_d = 22.2$ Hz, $J_q = 7.4$ Hz, 1H), 1.97–1.85 (m, 2H), 1.78 (dq, $J_d = 22.2$ Hz, $J_q = 7.4$ Hz, 1H), 0.92 (d, $J = 6.9$ Hz, 6H), 0.86 (t, $J = 7.4$

Hz, 3H); ^{13}C NMR (75 MHz, CDCl_3) δ 195.8, 176.8, 171.6, 131.9, 118.2, 102.2, 74.9, 65.5, 56.3, 27.77, 27.76, 27.0, 26.4, 19.1, 9.1; IR (Neat Film NaCl) 3083, 2963, 2939, 2879, 1731, 1664, 1610, 1470, 1384, 1236, 1195, 1178, 1119, 998, 919 cm^{-1} ; HRMS (EI+) m/z calc'd for $\text{C}_{16}\text{H}_{24}\text{O}_4$ $[\text{M}]^+$: 280.1687, found 280.1687.



Allyl Vinylogous Ester (+)-70. In the glovebox, a flamedried round-bottom flask was charged with Pd(dmdba)_2 (40.8 mg, 50.0 μmol , 5.00 mol%) and $(S)\text{-}t\text{-butyl}$ phosphinooxazoline (24.2 mg, 62.5 μmol , 6.25 mol%) and removed from the glovebox. THF (30 mL) was added, and the reaction stirred at 23 °C for 30 min. Then, a solution of $\alpha\text{-ethyl-}\alpha\text{-allyloxycarbonyl}$ vinylogous ester **69** (280 mg, 1.00 mmol, 1.00 equiv) in THF (3.0 mL) was added. The reactor was quickly fitted with a reflux condenser, and the reaction was heated to 50 °C under N_2 for 24 h. During this time the reaction went from orange to green. The reaction was cooled to 23 °C and concentrated. The residue was purified by flash chromatography on silica gel (hexanes \rightarrow 5% EtOAc in hexanes), giving allyl vinylogous ester (+)-**70** (193.4 mg, 82% yield) in 86% ee (as determined by chiral HPLC assay) as a yellow oil. R_f = 0.58 (20% EtOAc in hexanes); ^1H NMR (300 MHz, CDCl_3) δ 5.73 (app. dddd, J = 17.0 Hz, 10.5 Hz, 7.7 Hz, 6.9 Hz, 1H), 5.24 (s, 1H), 5.08–5.04 (m, 1H), 5.04–5.00 (m, 1H), 3.57 (d, J = 6.6 Hz, 2H), 2.42 (app. td, J_t = 6.6 Hz, J_d = 2.5 Hz, 2H), 2.38 (app. dd, J = 14.0 Hz, 7.1 Hz, 1H), 2.19 (app. dd, J = 14.0 Hz, 7.1 Hz, 1H), 1.85 (app. t, J = 6.6 Hz, 2H), 2.01 (app. septuplet, J = 6.6 Hz, 1H), 1.61 (dq,

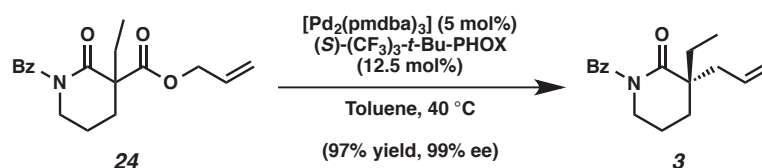
$J_d = 22.2$ Hz, $J_q = 7.4$ Hz, 1H), 1.55 (dq, $J_d = 22.2$ Hz, $J_q = 7.4$ Hz, 1H), 0.97 (d, $J = 6.6$ Hz, 6H), 0.84 (t, $J = 7.4$ Hz, 3H); ^{13}C NMR (75 MHz, CDCl_3) δ 203.0, 176.0, 134.8, 117.8, 102.0, 74.8, 46.6, 39.4, 29.0, 27.9, 27.6, 25.8, 19.2, 8.5; IR (Neat Film NaCl) 3074, 2963, 2936, 2878, 1652, 1612, 1384, 1193, 1178, 1003 cm^{-1} ; HRMS (EI+) m/z calc'd for $\text{C}_{15}\text{H}_{24}\text{O}_2$ $[\text{M}]^+$: 236.1776, found 236.1788; $[\alpha]_D^{24} +10.4^\circ$ (c 0.675, CHCl_3 , 86% ee).



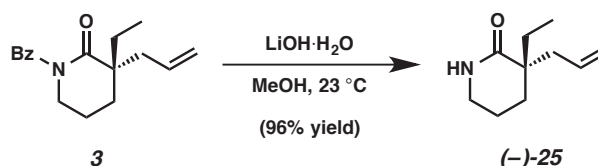
γ -Ethyl- γ -Allyl Enone (+)-65. A round-bottom flask was charged with allyl vinylogous ester (+)-70 (50.0 mg, 0.212 mmol, 95% ee, 1.00 equiv), and the reactor was purged with vacuum/argon (1 x). Et_2O (10.0 mL) was introduced, and the reaction was cooled to 0 $^\circ\text{C}$. LiAlH_4 (8.0 mg, 0.212 mmol, 1.00 equiv) was then added, and the reaction was stirred for 1 h. The 3 M aq HCl (10.0 mL) was very cautiously added at 0 $^\circ\text{C}$. Once the addition was complete, the reaction was warmed to 23 $^\circ\text{C}$ and stirred vigorously for 5 h. The reaction was transferred to a separatory funnel and extracted with Et_2O (3 x 10 mL). All organic layers were combined, dried (Na_2SO_4), filtered, and concentrated. The residue, which contained some H_2O , was dissolved in CHCl_3 and dried with Na_2SO_4 . The mixture was filtered, and the filtrate was concentrated, affording γ -ethyl- γ -allyl enone (+)-65 (26.2 mg, 75% yield) as a colorless, volatile oil. $R_f = 0.57$ (20% EtOAc in hexanes); ^1H NMR (300 MHz, CDCl_3) δ 6.69 (d, $J = 10.4$ Hz, 1H), 5.91 (d, $J = 10.4$ Hz, 1H), 5.74 (app. ddt, $J_{d1} = 16.7$ Hz, $J_{d2} = 9.9$ Hz, $J_t = 7.4$ Hz, 1H), 5.10 (app. d, $J = 9.9$ Hz, 1H), 5.08

(app. d, $J = 16.7$ Hz, 1H), 2.42 (app. t, $J = 6.9$ Hz, 2H), 2.21 (app. d, $J = 7.4$ Hz, 2H), 1.86 (app. t, $J = 6.9$ Hz, 2H), 1.53 (dq, $J_d = 22.2$ Hz, $J_q = 7.4$ Hz, 1H), 1.47 (dq, $J_d = 22.2$ Hz, $J_q = 7.4$ Hz, 1H), 0.90 (t, $J = 7.4$ Hz, 3H); ^{13}C NMR (75 MHz, CDCl_3) δ 199.9, 158.3, 133.7, 128.4, 118.7, 41.9, 38.7, 34.0, 30.6, 30.4, 8.5; IR (Neat Film NaCl) 3077, 2966, 2929, 2880, 1682, 1452, 1387, 916, 800 cm^{-1} ; HRMS (EI+) m/z calc'd for $\text{C}_{11}\text{H}_{16}\text{O}$ $[\text{M}]^+$: 164.1201, found 164.1207; $[\alpha]_{\text{D}}^{25} +27.5^\circ$ (c 0.524, CHCl_3 , 95% ee).

3.10.6 Syntheses of Compounds Related to Rhazinilam



Benzoyl Lactam 3.¹¹⁵ See Chapter 2 for synthetic procedure and characterization data of benzoyl lactam 3.



Piperidin-2-one (-)-25.¹¹⁵ See Chapter 2 for synthetic procedure and characterization data of piperidin-2-one (-)-25.

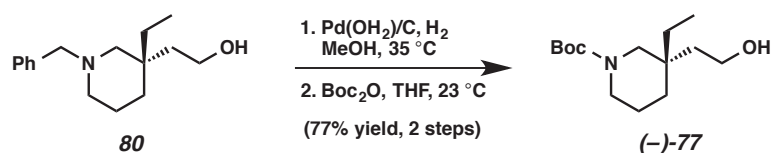
3.10.7 Syntheses of Compounds Related to Quebrachamine



Alcohol 56.¹¹⁵ To a vigorously stirred mixture of benzoyl lactam **3** (291 mg, 1.07 mmol, 1.00 equiv) and NaIO₄ (915 mg, 4.28 mmol, 4.00 equiv) in CCl₄ (4.3 mL), MeCN (4.3 mL), and H₂O (6.5 mL) was added RuCl₃·H₂O (11.0 mg, 0.053 mmol, 0.05 equiv). After 28 h, the reaction mixture was diluted with half-saturated brine (30 mL) and extracted with CH₂Cl₂ (5 x 25 mL). The combined organics were washed with half-saturated brine, dried (Na₂SO₄), and concentrated under reduced pressure. The resulting residue was suspended in Et₂O (30 mL) and filtered through a pad of celite. The celite pad was washed with Et₂O (2 x 15 mL), and the combined filtrate was concentrated under reduced pressure. This crude residue was used in the next step without further purification.

With cooling from a room temperature bath, the above residue was dissolved in THF (19 mL) and then treated with lithium aluminum hydride (487 mg, 12.9 mmol, 12.0 equiv) (*Caution: Gas evolution and exotherm*). The reaction mixture was stirred at ambient temperature for 12 h and then warmed to 40 °C for an additional 12 h. The reaction mixture was then cooled (0 °C) and dropwise treated with brine (20 mL, *Caution: Gas evolution and exotherm*). Once gas evolution had ceased the reaction mixture was diluted with half-saturated brine (20 mL) and EtOAc (20 mL). The phases were separated and the aqueous phase was extracted with EtOAc (5 x 50 mL). The combined organic phases were dried (Na₂SO₄), filtered, and concentrated under reduced pressure. The resulting oil was purified by flash chromatography (3 x 12 cm SiO₂, 35 to 70% EtOAc in hexanes) to afford alcohol **80** as a colorless oil (162 mg, 61% yield for

two steps). $R_f = 0.36$ (75% EtOAc in hexanes); $^1\text{H NMR}$ (500 MHz, CDCl_3) δ 7.35–7.24 (m, 5H), 3.80–3.72 (m, 1H), 3.71–3.60 (m, 2H), 3.31 (br s, 1H), 2.85–2.70 (br s, 2H), 2.00–1.70 (br s, 4H), 1.66–1.45 (m, 3H), 1.35–1.10 (m, 3H), 0.81 (t, $J = 7.5$ Hz, 3H); $^{13}\text{C NMR}$ (126 MHz, CDCl_3) δ 129.5, 128.4, 127.4, 63.9, 63.4, 59.4, 52.9, 39.9, 35.9, 35.1, 33.4, 22.4, 7.5; IR (Neat Film NaCl) 3345 (br), 2933, 2793, 1453, 1350, 1115, 1040, 1028, 739 cm^{-1} ; HRMS (MM: ESI-APCI+) m/z calc'd for $\text{C}_{16}\text{H}_{26}\text{NO}$ $[\text{M}+\text{H}]^+$: 248.2009, found 248.2016.

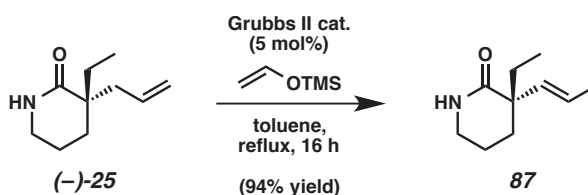


Alcohol (-)-77.¹¹⁵ A mixture of alcohol **80** (162.3 mg, 0.656 mmol, 1.00 equiv) and 20% $\text{Pd(OH)}_2/\text{C}$ (50 mg) in MeOH (15 mL) was stirred under an H_2 atmosphere for 3.5 h. The reaction mixture was filtered through a pad of celite. The celite pad was washed with MeOH (2 x 15 mL), and the combined filtrate was concentrated under reduced pressure. This crude residue was used in the next step without further purification.

To a solution of the above residue in THF (10 mL) was added Boc_2O (150 mg, 0.689 mmol, 1.05 equiv). After stirring for 24 h, the reaction mixture was concentrated under reduced pressure and partitioned between CH_2Cl_2 (20 mL) and saturated aqueous NaHCO_3 (20 mL). The organic layer was dried (Na_2SO_4), filtered, and concentrated under reduced pressure. The resulting oil was purified by flash chromatography (2 x 20 cm SiO_2 , 15 to 35% EtOAc in hexanes) to afford alcohol (-)-77 as a colorless oil (130 mg, 77% yield for two steps). $R_f = 0.34$ (35% EtOAc in hexanes); $^1\text{H NMR}$ (500 MHz, CDCl_3) δ 3.74–3.60 (m, 2H), 3.48 (br s, 1H), 3.31 (br s, 1H), 3.20 (br s, 1H), 2.96 (br s,

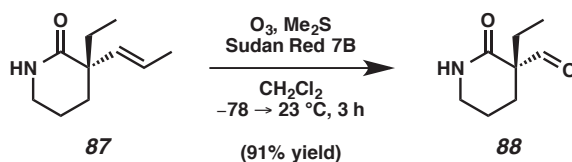
1H), 2.16 (br s, 1H), 1.66–1.55 (m, 1H), 1.55–1.42 (m, 3H), 1.44 (s, 9H), 1.40–1.27 (m, 2H), 1.25–1.15 (m, 1H), 0.83 (t, $J = 7.5$ Hz, 3H); ^{13}C NMR (126 MHz, CDCl_3) δ 155.2, 79.4, 58.7, 52.5, 44.5, 36.1, 35.3, 34.6, 28.4, 27.6, 21.2, 7.4; IR (Neat Film NaCl) 3439 (br), 2967, 2934, 2861, 1693, 1670, 1429, 1365, 1275, 1248, 1162, 1045, 865, 767 cm^{-1} ; HRMS (MM: ESI-APCI+) m/z calc'd for $\text{C}_{14}\text{H}_{28}\text{NO}_3$ $[\text{M}+\text{H}]^+$: 258.2064, found 258.2069; $[\alpha]_{\text{D}}^{25} -7.0^\circ$ (c 1.13, CHCl_3 , 96% ee).

3.10.8 Syntheses of Compounds Related to Vincadifformine



Disubstituted Alkene 87.¹¹⁶ To a solution of (-)-**25** (108 mg, 0.65 mmol, 1.0 equiv) and vinyloxytrimethylsilane (0.96 mL, 6.46 mmol, 10 equiv) in toluene (34 mL) was added at rt Grubbs 2nd generation catalyst (27.4 mg, 5 mol%). The purple reaction mixture was immersed in an oil bath (125 °C) (color changed to yellow) and refluxed for 16 h. The reaction mixture was then concentrated under reduced pressure and the residue was purified by column chromatography (50% EtOAc in hexanes \rightarrow EtOAc) to afford **87** (102 mg, 93% conv., 94%) as a brown oil. $R_f = 0.20$ (50% EtOAc in hexanes); ^1H NMR (500 MHz, CDCl_3) δ 5.94 (brs, 1H), 5.55–5.42 (m, 2H), 3.31–3.22 (m, 2H), 1.91–1.66 (m, 5H), 1.69 (d, $J = 5.4$ Hz, 3H), 1.64–1.54 (m, 1H), 0.84 (t, $J = 7.4$ Hz, 3H); ^{13}C NMR (126 MHz, CDCl_3) δ 175.7, 134.8, 124.7, 48.1, 42.7, 31.5, 29.3, 19.1, 18.1, 8.4; IR (Neat Film NaCl) 3203, 3074, 2936, 2876, 1654, 1489, 1447, 1354, 1298, 1209, 979, 852 cm^{-1} ;

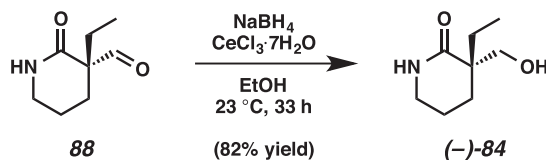
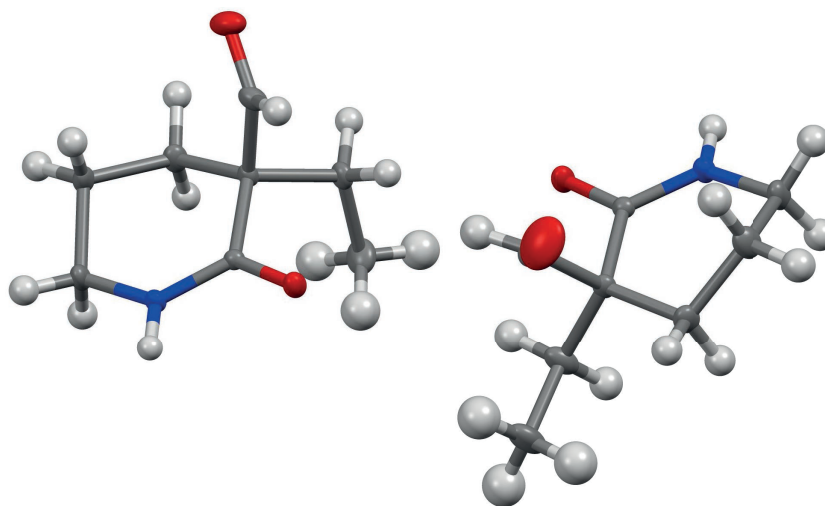
HRMS (MM: ESI-APCI+) m/z calc'd for $C_{10}H_{17}NO$ $[M+H]^+$: 168.1383, found 168.1385; $[\alpha]_D^{24} +10.2^\circ$ (c 1.270, $CHCl_3$).



Aldehyde 88. Ozone was bubbled through a cooled (-78°C) solution of **87** (100 mg, 0.60 mmol, 1.0 equiv) in CH_2Cl_2 (6.0 mL with one drop of sat. Sudan Red 7B CH_2Cl_2 solution) until the reaction mixture turned from bright purple to colorless. Then, the ozone generator was turned off and oxygen was bubbled through for a few minutes. Then, the argon flow was turned on and dimethylsulfide (0.88 mL, 12.0 mmol, 20 equiv) was added dropwise at -78°C . After stirring for 30 min at that temperature, the reaction mixture was allowed to warm to rt over 2.5 h. The reaction mixture was then concentrated under reduced pressure and the residue was purified by column chromatography (67% EtOAc in hexanes \rightarrow EtOAc) to afford **88** (84.7 mg, 91%) as beige crystalline solid. X-ray quality crystals sublimed under high vacuum at rt. $R_f = 0.36$ (EtOAc); ^1H NMR (500 MHz, $CDCl_3$) δ 9.63 (s, 1H), 6.54 (brs, 1H), 3.34–3.20 (m, 2H), 2.33–2.20 (m, 1H), 2.05–1.93 (m, 1H), 1.89–1.75 (m, 2H), 1.73–1.62 (m, 1H), 1.62–1.52 (m, 1H), 0.87 (t, $J = 7.5$ Hz, 3H); ^{13}C NMR (126 MHz, $CDCl_3$) δ 201.2, 171.1, 58.9, 42.5, 27.3, 24.1, 20.2, 8.2; IR (Neat Film NaCl) 3290, 2941, 2877, 1727, 1660, 1488, 1462, 1450, 1353, 1323 cm^{-1} ; HRMS (MM: ESI-APCI+) m/z calc'd for $C_8H_{13}NO_2$ $[M+H]^+$: 156.1019, found 156.1021; $[\alpha]_D^{24} -54.6^\circ$ (c 1.305, $CHCl_3$); mp: 63–65 $^\circ\text{C}$. X-

ray structure has been deposited in the Cambridge Database (CCDC) under the deposition number 1000826.

Figure 3.3 Crystal structure of **88** (ellipsoids, 50% probability level)

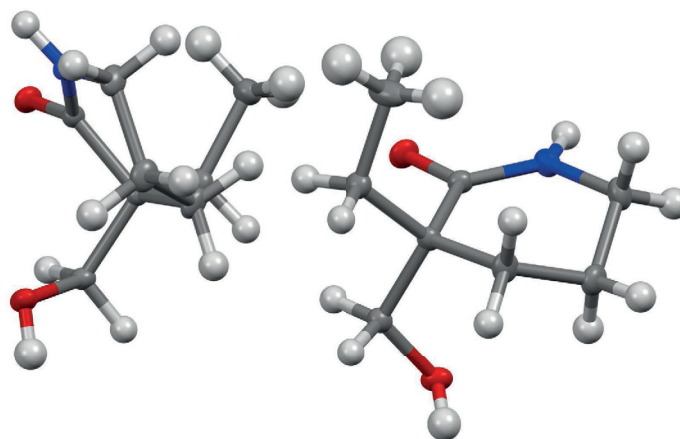


Alcohol (-)-84. To a suspension of NaBH₄ (49.4 mg, 1.3 mmol, 5.0 equiv) and CeCl₃•7H₂O (146 mg, 0.39 mmol, 1.5 equiv) in EtOH (4.0 mL) was added at 0 °C solid **88** (40.5 mg, 0.26 mmol, 1.0 equiv) in one portion, after evolution of hydrogen gas had subsided. After stirring for 33 h at 23 °C, the heterogeneous reaction mixture was quenched with sat. NH₄Cl (15 mL) and diluted with CH₂Cl₂ (20 mL). The layers were separated and the aqueous layer was extracted with CH₂Cl₂ (20 mL). Since phase separation was tedious due to the presence of boronic acid salts (emulsion), the aqueous layer was then basified with 6 M NaOH (2 mL) and was extracted with CH₂Cl₂ (2 x 20 mL). The combined organic extracts were dried over MgSO₄ and the solvent was

removed under reduced pressure. The residue was purified by column chromatography (50% → 67% acetone in hexanes) to afford (–)-**84** (33.8 mg, 82%) as a colorless, viscous oil. $R_f = 0.33$ (67% acetone in hexanes); $^1\text{H NMR}$ (500 MHz, CDCl_3) δ 6.66 (brs, 1H), 3.85 (brs, 1H), 3.59–3.45 (m, 2H), 3.32–3.20 (m, 2H), 1.89–1.64 (m, 5H), 1.47 (ddd, $J = 13.7$ Hz, 10.0 Hz, 3.6 Hz, 1H), 0.88 (t, $J = 7.5$ Hz, 3H); $^{13}\text{C NMR}$ (126 MHz, CDCl_3) δ 178.3, 67.4, 45.3, 42.2, 26.9, 26.5, 19.4, 7.9. IR (Neat Film NaCl) 3289, 2939, 2875, 1643, 1492, 1355, 1324, 1208, 1055 cm^{-1} ; HRMS (MM: ESI-APCI+) m/z calc'd for $\text{C}_8\text{H}_{15}\text{NO}_2$ $[\text{M}+\text{H}]^+$: 158.1176, found 158.1179. $[\alpha]_{\text{D}}^{24} -12.9^\circ$ (c 1.69, CHCl_3) (Lit.¹¹⁷ for (R)-**65**: $[\alpha]_{\text{D}}^{27} +13.5^\circ$ (c 1.05, CHCl_3)).

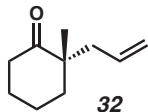
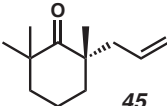
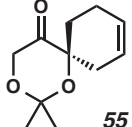
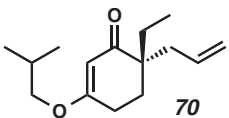
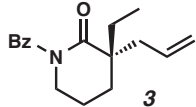
During the synthesis of the racemic compound, alcohol (±)-**84** solidified upon storage in the freezer to give a white crystalline solid: mp: 91–93 °C. X-ray quality crystals were obtained by slow diffusion of heptane (with a few drops of benzene) into a solution of the alcohol in EtOAc at 23 °C. X-ray structure has been deposited in the Cambridge Database (CCDC) under the deposition number 1002339.

Figure 3.4 Crystal structure of (±)-**84** (ellipsoids, 50% probability level)



3.10.9 Methods for the Determination of Enantiomeric Excess

Table 3.1 Analytical GC and HPLC assays and retention times

entry	product	assay conditions	retention time of major isomer (min)	retention time of minor isomer (min)	% ee
1	 32	Chiral GC Agilent GT-A 100 °C isotherm	11.1	12.7	88
2	 45	Chiral GC Agilent GT-A 80 °C isotherm	29.1	30.5	91
3	 55	HPLC Chiralpak AD Hexanes isocratic, 1.0 mL/min 220 nm	11.462	10.307	92
4	 70	HPLC Chiralcel OD 2% EtOH in hexanes isocratic, 1.0 mL/min 254 nm	7.4	8.2	86
5	 3	SFC Chiralcel OJ-H 3% MeOH in CO ₂ isocratic, 5.0 mL/min 254 nm	3.85	2.49	99

3.11 Notes and References

- (1) Trost, B. M.; Jiang, C. *Synthesis* **2006**, 369–396.
- (2) Mohr, J. T.; Stoltz, B. M. *Chem. Asian J.* **2007**, 2, 1476–1491.
- (3) Behenna, D. C.; Mohr, J. T.; Sherden, N. H.; Marinescu, S. C.; Harned, A. M.; Tani, K.; Seto, M.; Ma, S.; Novák, Z.; Krout, M. R.; McFadden, R. M.; Roizen, J. L.; Enquist, J. A., Jr.; White, D. E.; Levine, S. R.; Petrova, K. V.; Iwashita, A.; Virgil, S. C.; Stoltz, B. M. *Chem. — Eur. J.* **2011**, 17, 14199–14223.

-
- (4) McFadden, R. M.; Stoltz, B. M. *J. Am. Chem. Soc.* **2006**, *128*, 7738–7739.
 - (5) White, D. E.; Stewart, I. C.; Grubbs, R. H.; Stoltz, B. M. *J. Am. Chem. Soc.* **2008**, *130*, 810–811.
 - (6) Enquist, J. A., Jr.; Stoltz, B. M. *Nature* **2008**, *453*, 1228–1231.
 - (7) Enquist, J. A., Jr.; Virgil, S. C.; Stoltz, B. M. *Chem. — Eur. J.* **2011**, *17*, 9957–9969.
 - (8) Enquist, J. A., Jr.; Stoltz, B. M. *Nat. Prod. Rep.* **2009**, *26*, 661–680.
 - (9) Levine, S. R.; Krout, M. R.; Stoltz, B. M. *Org. Lett.* **2009**, *11*, 289–292.
 - (10) Petrova, K. V.; Mohr, J. T.; Stoltz, B. M. *Org. Lett.* **2009**, *11*, 293–295.
 - (11) White, D. E.; Stewart, I. C.; Seashore-Ludlow, B. A.; Grubbs, R. H.; Stoltz, B. M. *Tetrahedron* **2010**, *66*, 4668–4686.
 - (12) Day, J. J.; McFadden, R. M.; Virgil, S. C.; Kolding, H.; Alleva, J. L.; Stoltz, B. M. *Angew. Chem., Int. Ed.* **2011**, *50*, 6814–6818.
 - (13) Wei, Y.; Zhao, D.; Ma, D. *Angew. Chem., Int. Ed.* **2013**, *52*, 12988–12991.
 - (14) Xu, Z.; Wang, Q.; Zhu, J. *J. Am. Chem. Soc.* **2013**, *135*, 19127–19130.
 - (15) Hu, Q.-Y.; Zhou, G.; Corey, E. J. *J. Am. Chem. Soc.* **2004**, *126*, 13708–13713.
 - (16) Ko, S. Y.; Lee, A. W. M.; Masamune, S.; Reed, L. A., III.; Sharpless, K. B.; Walker, F. J. *Science* **1983**, *220*, 949–951.
 - (17) Inamori, Y.; Morita, Y.; Sakagami, Y.; Okabe, T.; Ishida, N. *Biocontrol Science* **2006**, *11*, 49–54.
 - (18) Chetty, G. L.; Dev, S. *Tetrahedron Lett.* **1965**, *6*, 3773–3776.
 - (19) Ito, S.; Endo, K.; Honma, H.; Ota, K. *Tetrahedron Lett.* **1965**, *6*, 3777–3781.

-
- (20) Oh, I.; Yang, W.-Y.; Park, J.; Lee, S.; Mar, W.; Oh, K.-B.; Shin, J. *Arch. Pharm. Res.* **2011**, *34*, 2141–2147.
- (21) Yano, M. *J. Soc. Chem. Ind. Jpn.* **1913**, *16*, 443–463.
- (22) Uchida, S. *J. Soc. Chem. Ind. Jpn.* **1928**, *31*, 501–503.
- (23) Miyazaki, Y. *Mokuzai Gakkaishi* **1996**, *42*, 624–626.
- (24) Hiramatsu, Y.; Miyazaki, Y. *J. Wood. Sci.* **2001**, *47*, 13–17.
- (25) Dauben, W. G.; Ashcraft, A. C. *J. Am. Chem. Soc.* **1963**, *85*, 3673–3676.
- (26) Büchi, G.; White, J. D. *J. Am. Chem. Soc.* **1964**, *86*, 2884–2887.
- (27) Mori, K.; Ohki, M.; Kobayashi, A.; Matsui, M. *Tetrahedron* **1970**, *26*, 2815–2819.
- (28) McMurry, J. E.; Blaszczyk, L. C. *J. Org. Chem.* **1974**, *39*, 2217–2222.
- (29) Branca, S. J.; Lock, R. L.; Smith, A. B., III. *J. Org. Chem.* **1977**, *42*, 3165–3168.
- (30) Johnson, C. R.; Barbachyn, M. R. *J. Am. Chem. Soc.* **1982**, *104*, 4290–4291.
- (31) Lee, E.; Shin, I.-J.; Kim, T.-S. *J. Am. Chem. Soc.* **1990**, *112*, 260–264.
- (32) Zhang, C. X.; Fang, L. J.; Bi, F. Q.; Li, Y. L. *Chinese Chem. Lett.* **2008**, *19*, 256–258.
- (33) Srikrishna, A.; Anebouselvy, K. *J. Org. Chem.* **2001**, *66*, 7102–7106.
- (34) Behenna, D. C.; Stoltz, B. M. *J. Am. Chem. Soc.* **2004**, *126*, 15044–15045.
- (35) Rapado, L. P.; Bulugahapitiya, V.; Renaud, P. *Helv. Chim. Acta* **2000**, *83*, 1625–1632.
- (36) Wolinsky, J.; Novak, R.; Vasilev, R. *J. Org. Chem.* **1964**, *29*, 3596–3598.
- (37) Barco, A.; Benetti, S.; De Risi, C.; Marchetti, P.; Pollini, G. P.; Zanirato, V. *Tetrahedron: Asymmetry* **1997**, *8*, 3515–3545.
- (38) Garg, N. K.; Caspi, D. D.; Stoltz, B. M. *J. Am. Chem. Soc.* **2004**, *126*, 9552–9553.

-
- (39) Garg, N. K.; Caspi, D. D.; Stoltz, B. M. *J. Am. Chem. Soc.* **2005**, *127*, 5970–5978.
- (40) Garg, N. K.; Stoltz, B. M. *Chem. Commun.* **2006**, 3769–3779.
- (41) Garg, N. K.; Caspi, D. D.; Stoltz, B. M. *Synlett* **2006**, 3081–3087.
- (42) Rohloff, J. C.; Kent, K. M.; Postich, M. J.; Becker, M. W.; Chapman, H. H.; Kelly, D. E.; Lew, W.; Louie, M. S.; McGee, L. R.; Prisbe, E. J.; Schultze, L. M.; Yu, R. H.; Zhang, L. *J. Org. Chem.* **1998**, *63*, 4545–4550.
- (43) Seto, M.; Roizen, J. L.; Stoltz, B. M. *Angew. Chem., Int. Ed.* **2008**, *47*, 6873–6876.
- (44) Scholl, M.; Ding, S.; Lee, C. W.; Grubbs, R. H. *Org. Lett.* **1999**, *1*, 953–956.
- (45) Gunasekera, S. P.; McCarthy, P. J.; Kelly-Borges, M. *J. Am. Chem. Soc.* **1996**, *118*, 8759–8760.
- (46) Millar, J. B. A.; Russel, P. *Cell* **1992**, *68*, 407–410.
- (47) Boukouvalas, J.; Cheng, Y.-X.; Robichaud, J. *J. Org. Chem.* **1998**, *63*, 228–229.
- (48) Magnuson, S. R.; Sepp-Lorenzino, L.; Rosen, N.; Danishefsky, S. J. *J. Am. Chem. Soc.* **1998**, *120*, 1615–1616.
- (49) Miyaoka, H.; Kajiwara, Y.; Yamada, Y. *Tetrahedron Lett.* **2000**, *41*, 911–914.
- (50) Takahashi, M.; Dodo, K.; Hashimoto, Y.; Shirai, R. *Tetrahedron Lett.* **2000**, *41*, 2111–2114.
- (51) Demeke, D.; Forsyth, C. *Org. Lett.* **2000**, *2*, 3967–3969.
- (52) Miyaoka, H.; Yamada, Y. *Bull. Chem. Soc. Jpn.* **2002**, *75*, 203–222.
- (53) Demeke, D.; Forsyth, C. J. *Tetrahedron* **2002**, *58*, 6531–6544.
- (54) Corey, E. J.; Roberts, B. E. *J. Am. Chem. Soc.* **1997**, *119*, 12425–12431.
- (55) Miyaoka, H.; Kajiwara, Y.; Hara, Y.; Yamada, Y. *J. Org. Chem.* **2001**, *66*, 1429–1435.

-
- (56) Jung, M. E.; Nishimura, N. *Org. Lett.* **2001**, *3*, 2113–2115.
- (57) Mohr, J. T.; Behenna, D. C.; Harned, A. M.; Stoltz, B. M. *Angew. Chem., Int. Ed.*, **2005**, *44*, 6924–6927.
- (58) Mohr, J. T.; Krout, M. R.; Stoltz, B. M. *Org. Synth.* **2009**, *86*, 194–211.
- (59) Saxton, J. E. In *The Alkaloids*; Cordell, G. A., Ed.; Academic Press: New York, 1998; Vol. 51, Chapter 1.
- (60) Stork, G.; Dolfini, J. E. *J. Am. Chem. Soc.* **1963**, *85*, 2872–2873.
- (61) Ban, Y.; Sato, Y.; Inoue, I.; Nagai, M.; Oishi, T.; Terashima, M.; Yonematsu, O.; Kanaoka, Y. *Tetrahedron Lett.* **1965**, *6*, 2261–2268.
- (62) Lawton, G.; Saxton, J. E.; Smith, A. J. *Tetrahedron* **1997**, *33*, 1641–1653.
- (63) Meyers, A. I.; Berney, D. *J. Org. Chem.* **1989**, *54*, 4673–4676.
- (64) Stork, G.; Dolfini, J. E. *J. Am. Chem. Soc.* **1963**, *85*, 2872–2873.
- (65) Spessard, S. J.; Stoltz, B. M. *Org. Lett.* **2002**, *4*, 1943–1946.
- (66) Stork, G.; Danheiser, R. L. *J. Org. Chem.* **1973**, *38*, 1775–1776.
- (67) Bennett, N. B.; Hong, A. Y.; Harned, A. M.; Stoltz, B. M. *Org. Biomol. Chem.* **2012**, *10*, 56–59.
- (68) Banerji, A.; Majumder, P. L.; Chatterjee, A. G. *Phytochemistry* **1970**, *9*, 1491–1493.
- (69) Linde, H. H. A. *Helv. Chim. Acta* **1965**, *48*, 1822–1842.
- (70) Thoison, O.; Guénard, D.; Sévenet, T.; Kan-Fan, C.; Quirion, J.-C.; Husson, H. P.; Deverre, J.-R.; Chan, K. C.; Potier, P. *C. R. Acad. Sci. Paris II* **1987**, *304*, 157–160.
- (71) Abraham, D. J.; Rosenstein, R. D.; Lyon, R. L.; Fong, H. H. S. *Tetrahedron Lett.* **1972**, *13*, 909–912.

-
- (72) Alazard, J.-P.; Millet-Paillusson, C.; Boyé, O.; Guénard, D.; Chiaroni, A.; Riche, C.; Thal, C. *Bioorg. Med. Chem. Lett.* **1991**, *1*, 725–728.
- (73) Edler, M. C.; Yang, G.; Jung, M. K.; Bai, R.; Bornmann, W. G.; Hamel, E. *Arch. Biochem. Biophys.* **2009**, *487*, 98–104.
- (74) For a review, see: Kholod, I.; Vallat, O.; Buciumas, A.-M.; Neier, R. *Heterocycles* **2011**, *82*, 917–948.
- (75) Ratcliffe, A. H.; Smith, G. F.; Smith, G. N. *Tetrahedron Lett.* **1973**, *14*, 5179–5184.
doi:
- (76) Johnson, J. A.; Sames, D. *J. Am. Chem. Soc.* **2000**, *122*, 6321–6322.
- (77) Bowie, A. L.; Hughes, C. C.; Trauner, D. *Org. Lett.* **2005**, *7*, 5207–5209.
- (78) Johnson, J. A.; Ning, L.; Sames, D. *J. Am. Chem. Soc.* **2002**, *124*, 6900–6903.
- (79) Banwell, M. G.; Beck, D. A. S.; Willis, A. C. *ARKIVOC* **2006**, *3*, 163–174.
- (80) Liu, Z.; Wasmuth, A. S.; Nelson, S. G. *J. Am. Chem. Soc.* **2006**, *128*, 10352–10353.
- (81) Gu, Z.; Zakarian, A. *Org. Lett.* **2010**, *12*, 4224–4227.
- (82) Sugimoto, K.; Toyoshima, K.; Nonaka, S.; Kotaki, K.; Ueda, H.; Tokuyama, H. *Angew. Chem., Int. Ed.* **2013**, *52*, 7168–7171.
- (83) Magnus, P.; Rainey, T. *Tetrahedron* **2001**, *57*, 8647–8651.
- (84) Behenna, D. C.; Liu, Y.; Yurino, T.; Kim, J.; White, D. E.; Virgil, S. C.; Stoltz, B. M. *Nature Chem.* **2012**, *4*, 130–133.
- (85) Saxton, J. E. In *The Alkaloids. Alkaloids of the Aspidospermine Group*; Cordell, G. A., Ed.; Academic Press: New York, 1998; Vol. 51, Chapter 1.
- (86) Deutsch, H. F.; Evenson, M. A.; Drescher, P.; Sparwasser, C.; Madsen, P. O. *J. Pharm. Biomed. Anal.* **1994**, *12*, 1283–1287.

-
- (87) Coldham, I.; Burrell, A. J. M.; White, L. E.; Adams, H.; Oram, N. *Angew. Chem., Int. Ed.* **2007**, *46*, 6159–6162.
- (88) Bajtos, B.; Pagenkopf, B. L. *Eur. J. Org. Chem.* **2009**, 1072–1077.
- (89) Hsu, S.-W.; Cheng, H.-Y.; Huang, A.-C.; Ho, T.-L.; Hou, D.-R. *Eur. J. Org. Chem.* **2014**, 3109–3115.
- (90) Temme, O.; Taj, S.-A.; Andersson, P. G. *J. Org. Chem.* **1998**, *63*, 6007–6015.
- (91) Kozmin, S. A.; Iwama, T.; Huang, Y.; Rawal, V. H. *J. Am. Chem. Soc.* **2002**, *124*, 4628–4641.
- (92) Sattely, E. S.; Meek, S. J.; Malcolmson, S. J.; Schrock, R. R.; Hoveyda, A. H. *J. Am. Chem. Soc.* **2009**, *131*, 943–953.
- (93) Amat, M.; Lozano, O.; Escolano, C.; Molins, E.; Bosch, J. *J. Org. Chem.* **2007**, *72*, 4431–4439.
- (94) Smith, G. F.; Wahid, M. A. *J. Chem. Soc.* **1963**, 4002–4004.
- (95) Szántay, C. *Pure Appl. Chem.* **1990**, *62*, 1299–1302.
- (96) Danieli, B.; Lesma, G.; Palmisano, G. *J. Chem. Soc., Chem. Commun.* **1981**, 908–909.
- (97) Sági, J.; Szabó, L.; Baitz-Gács, E.; Kalaus, G.; Szántay, C. *Tetrahedron* **1988**, *44*, 4619–4629.
- (98) Calabi, L.; Danieli, B.; Lesma, G.; Palmisano, G. *J. Chem. Soc., Perkin Trans. 1* **1982**, 1371–1379.
- (99) Kutney, J. P.; Chan, K. K.; Failli, A.; Fromson, J. M.; Gletsos, C.; Nelson, V. R. *J. Am. Chem. Soc.* **1968**, *90*, 3891–3893.

-
- (100) Laronze, P. J.-Y.; Laronze-Fontaine, J.; Lévy, J.; Le Men, J. *Tetrahedron Lett.* **1974**, *15*, 491–494.
- (101) Kuehne, M. E.; Roland, D. M.; Hafter, R. *J. Org. Chem.* **1978**, *43*, 3705–3710.
- (102) Barsi, M.-C.; Das, B. C.; Fourrey, J.-L.; Sundaramoorthi, R. *J. Chem. Soc., Chem. Commun.* **1985**, 88–89.
- (103) Yoshida, K.; Nomura, S.; Ban, Y. *Tetrahedron* **1985**, *41*, 5495–5501.
- (104) Kalaus, G.; Greiner, I.; Kajtár-Peredy, M.; Brlik, J.; Szabó, L.; Szántay, C. *J. Org. Chem.* **1993**, *58*, 1434–1442.
- (105) Kobayashi, S.; Peng, G.; Fukuyama, T. *Tetrahedron Lett.* **1999**, *40*, 1519–1522.
- (106) Kuehne, M. E.; Podhorez, D. E. *J. Org. Chem.* **1985**, *50*, 924–929.
- (107) Pandey, G.; Kumara, P. C. *Org. Lett.* **2011**, *13*, 4672–4675.
- (108) Jones, S. B.; Simmons, B.; Mastracchio, A.; MacMillan, D. W. C. *Nature* **2011**, *475*, 183–188.
- (109) Zhao, S.; Andrade, R. B. *J. Am. Chem. Soc.* **2013**, *135*, 13334–13337.
- (110) Arisawa, M.; Terada, Y.; Nakagawa, M.; Nishida, A. *Angew. Chem., Int. Ed.* **2002**, *41*, 4732–4734.
- (111) (a) Peer, M.; de Jong, J. C.; Kiefer, M.; Langer, T.; Riech, H.; Schell, H.; Sennhenn, P.; Sprinz, J.; Steinhagen, H.; Wiese, B.; Helmchen, G. *Tetrahedron* **1996**, *52*, 7547–7583. (b) Tani, K.; Behenna, D. C.; McFadden, R. M.; Stoltz, B. M. *Org. Lett.* **2007**, *9*, 2529–2931.
- (112) When a subscript is shown with the coupling constant, it indicates what type of splitting the constant is associated with. For example (td, $J_t = 5.0$ Hz, $J_d = 3.3$ Hz,

1H) indicates that the triplet splitting has a 5.0 Hz coupling constant and the doublet has a 3.3 Hz coupling constant.

(113) Behenna, D. C.; Stoltz, B. M. *J. Am. Chem. Soc.* **2004**, *126*, 15044–15045.

(114) Seto, M.; Roizen, J. L.; Stoltz, B. M. *Angew. Chem., Int. Ed.* **2008**, *47*, 6873–6876.

(115) Behenna, D. C.; Liu, Y.; Yurino, T.; Kim, J.; White, D. E.; Virgil, S. C.; Stoltz, B.

M. *Nature Chem.* **2012**, *4*, 130–133.

(116) Arisawa, M.; Terada, Y.; Nakagawa, M.; Nishida, A. *Angew. Chem., Int. Ed.* **2002**,

41, 4732–4734.

(117) Pandey, G.; Kumara, P. C. *Org. Lett.* **2011**, *13*, 4672–4675.

APPENDIX 2

Spectra Relevant to Chapter 3

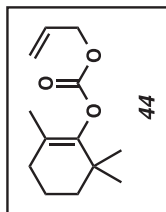
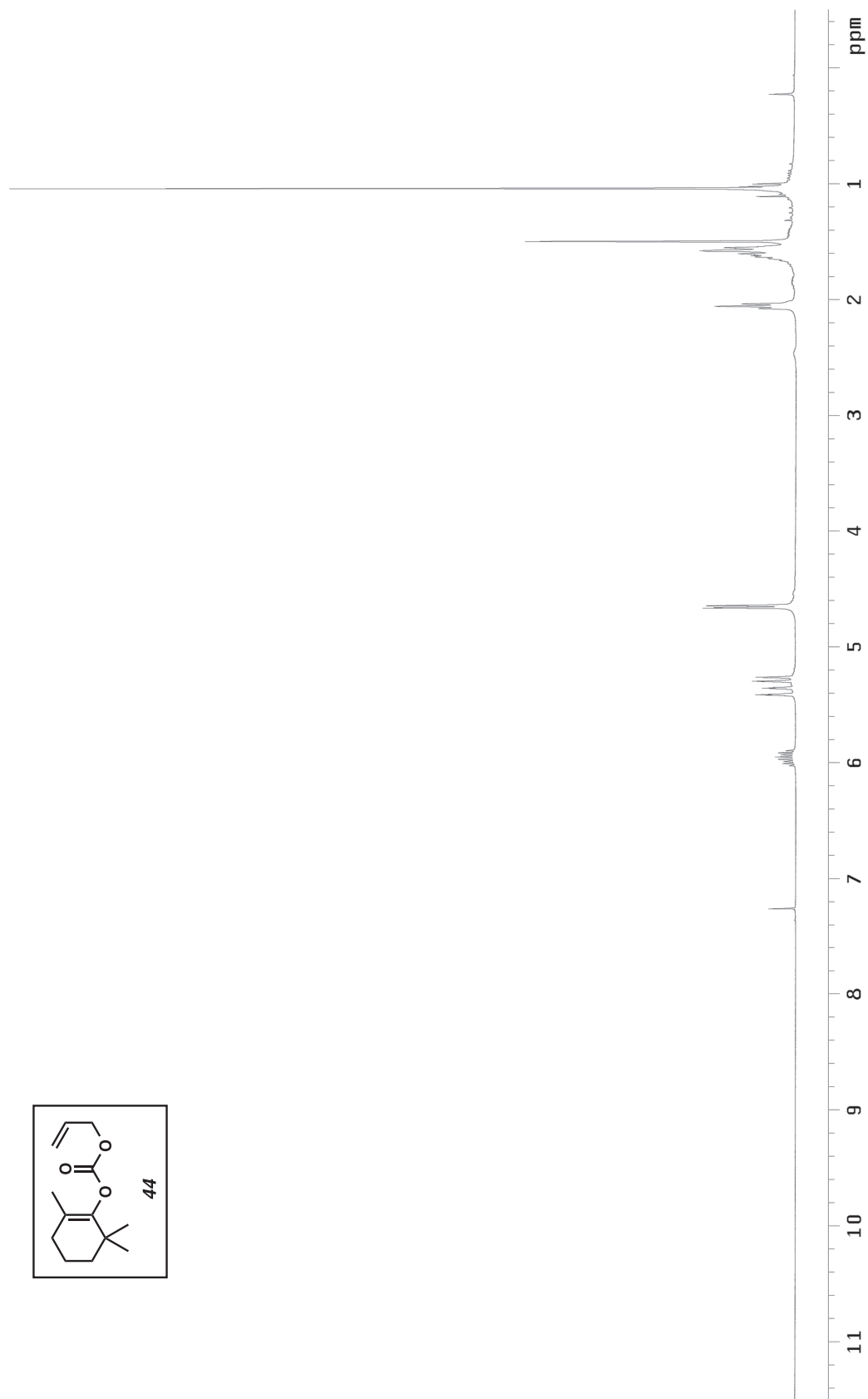


Figure A2.1 ^1H NMR (300 MHz, CDCl_3) of compound 44.

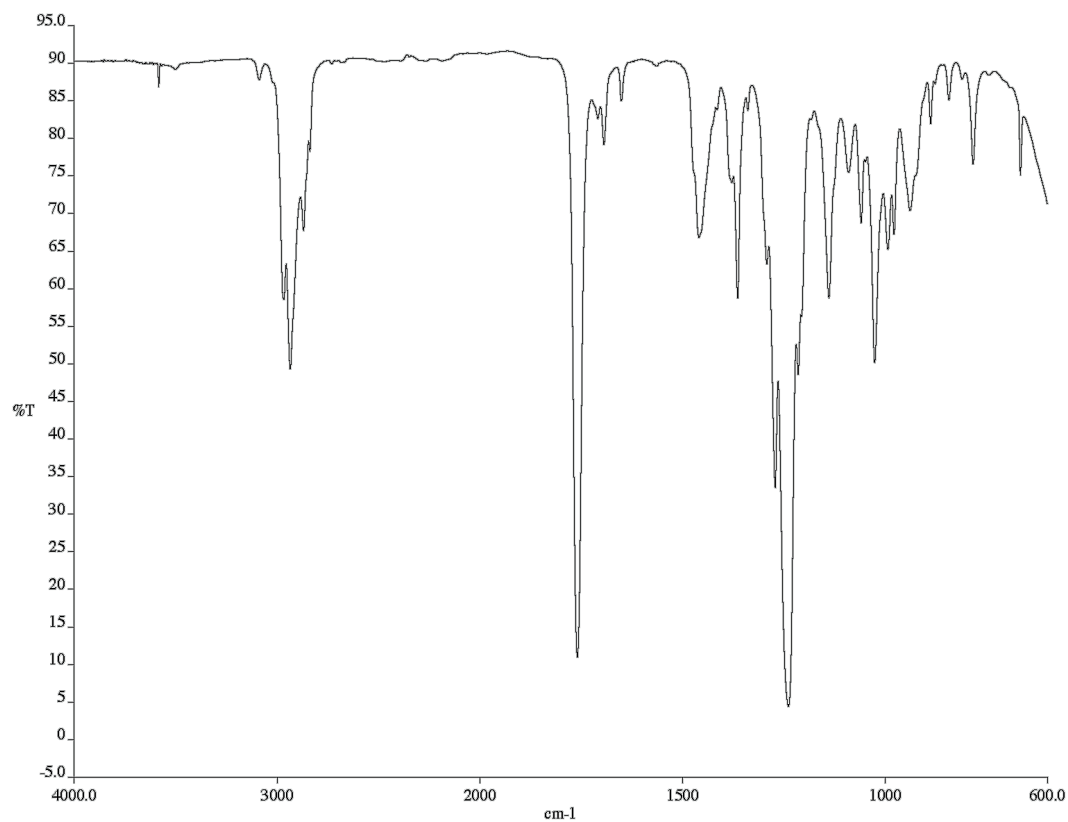


Figure A2.2 Infrared spectrum (Thin Film, NaCl) of compound **44**.

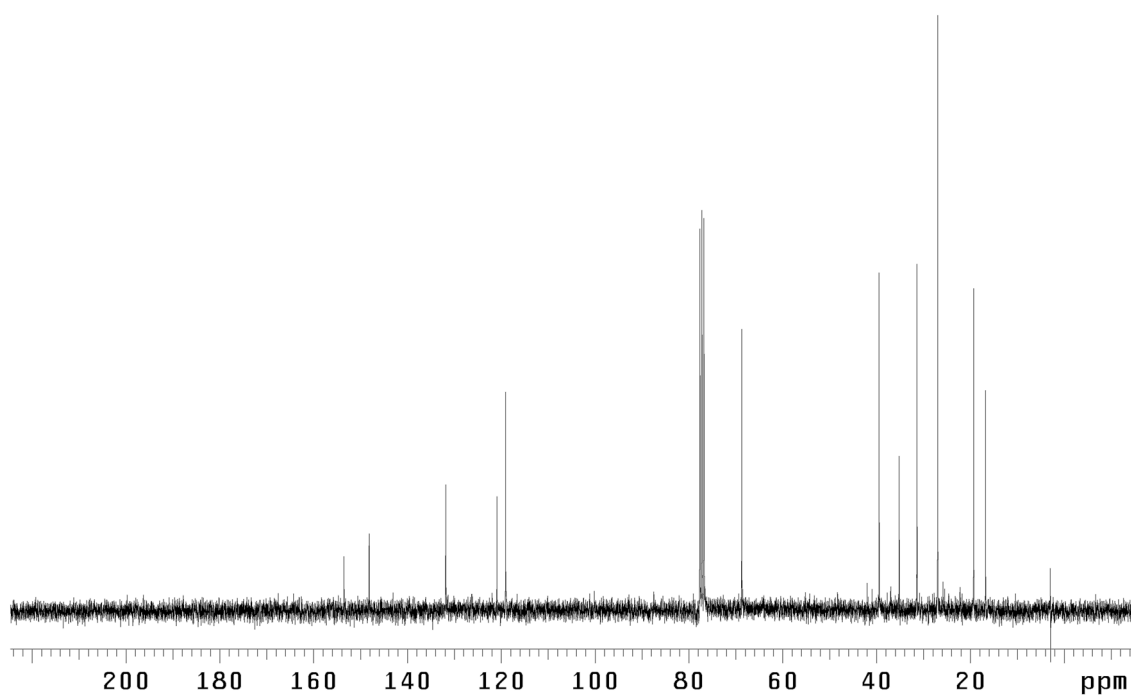


Figure A2.3 ¹³C NMR (75 MHz, CDCl₃) of compound **44**.

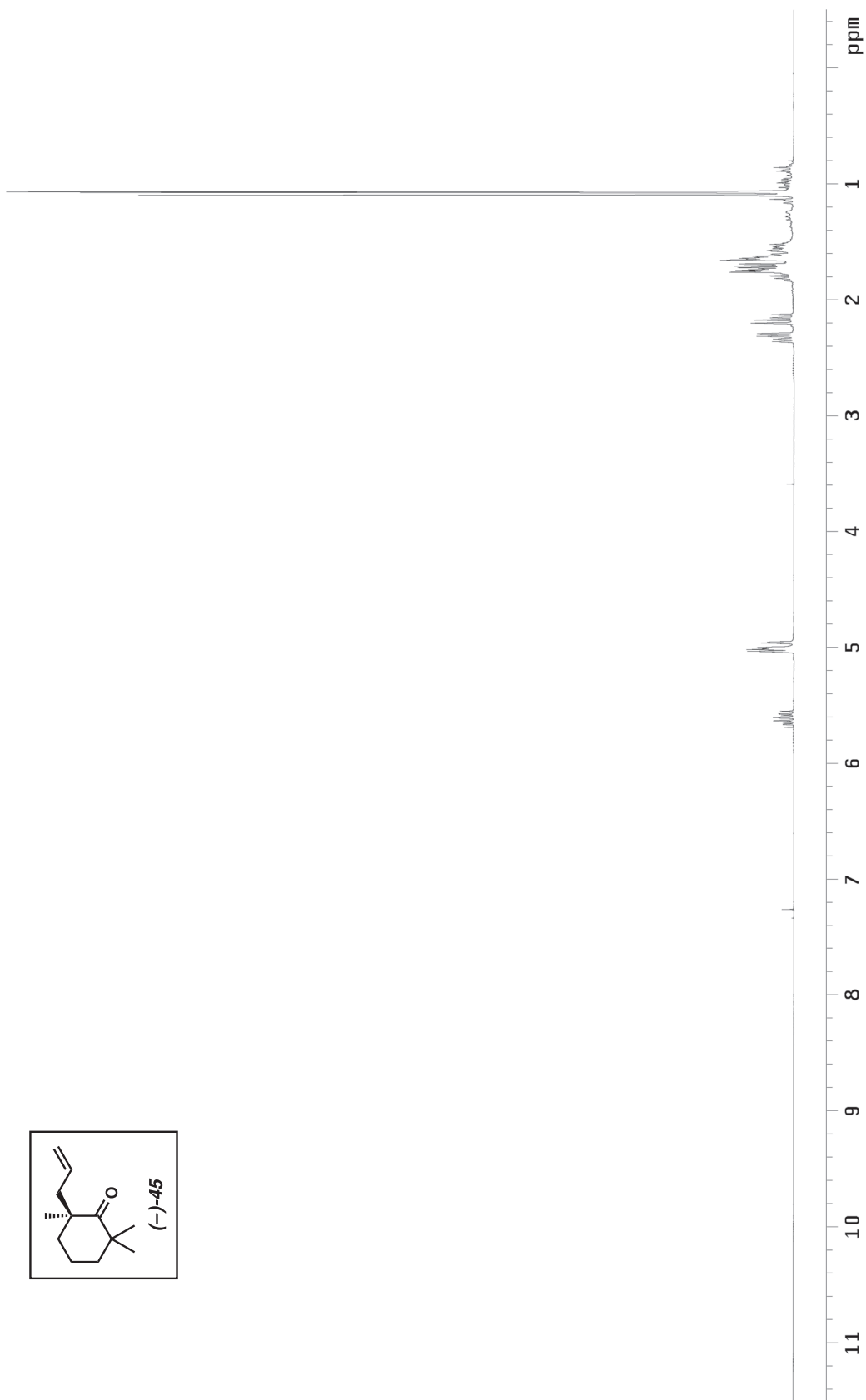


Figure A2.4 ^1H NMR (300 MHz, CDCl_3) of compound **45**.

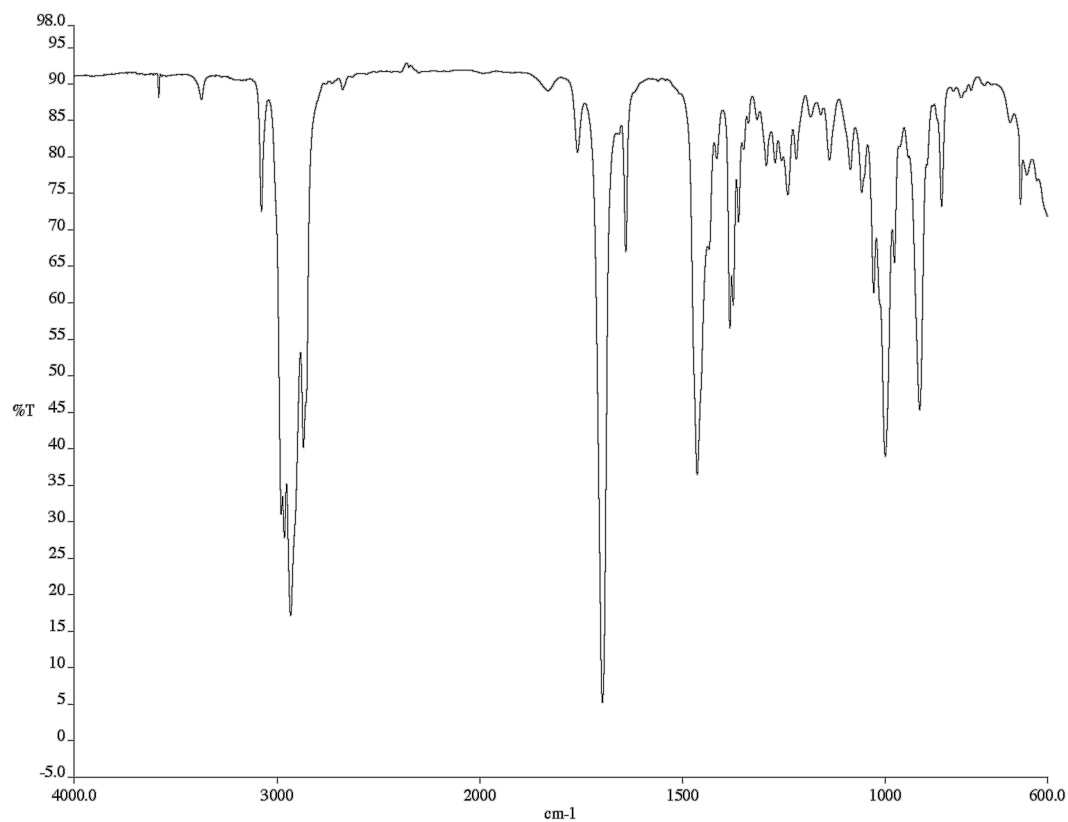


Figure A2.5 Infrared spectrum (Thin Film, NaCl) of compound **45**.

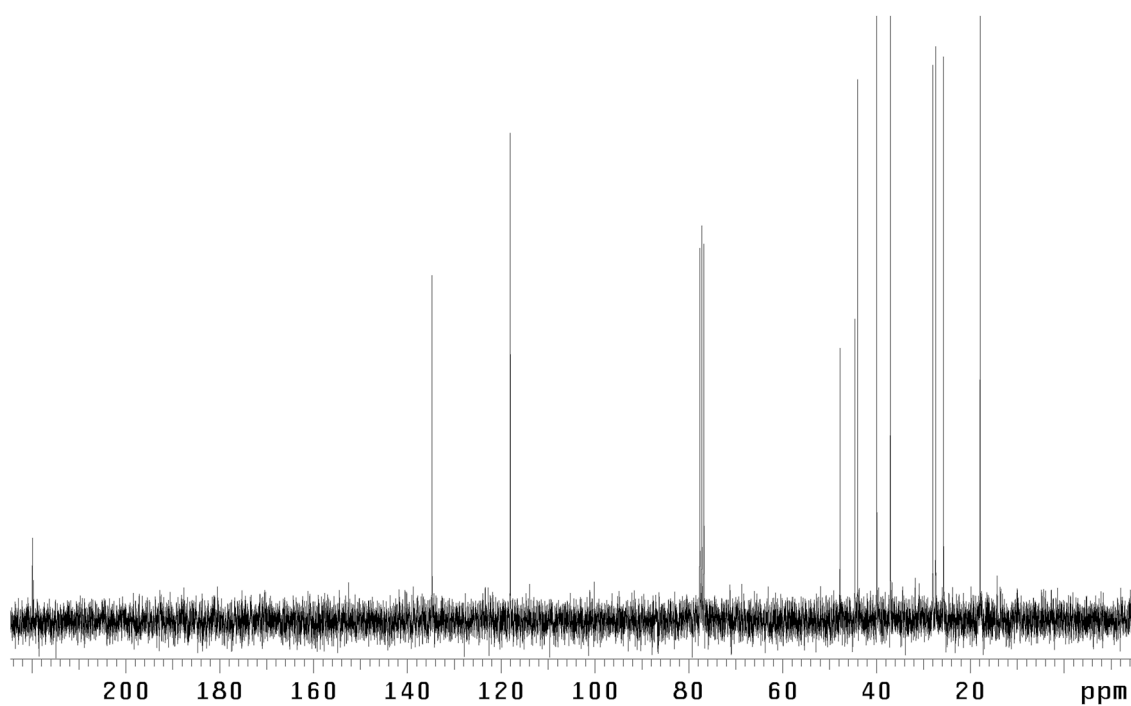


Figure A2.6 ¹³C NMR (75 MHz, CDCl₃) of compound **45**.

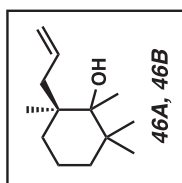
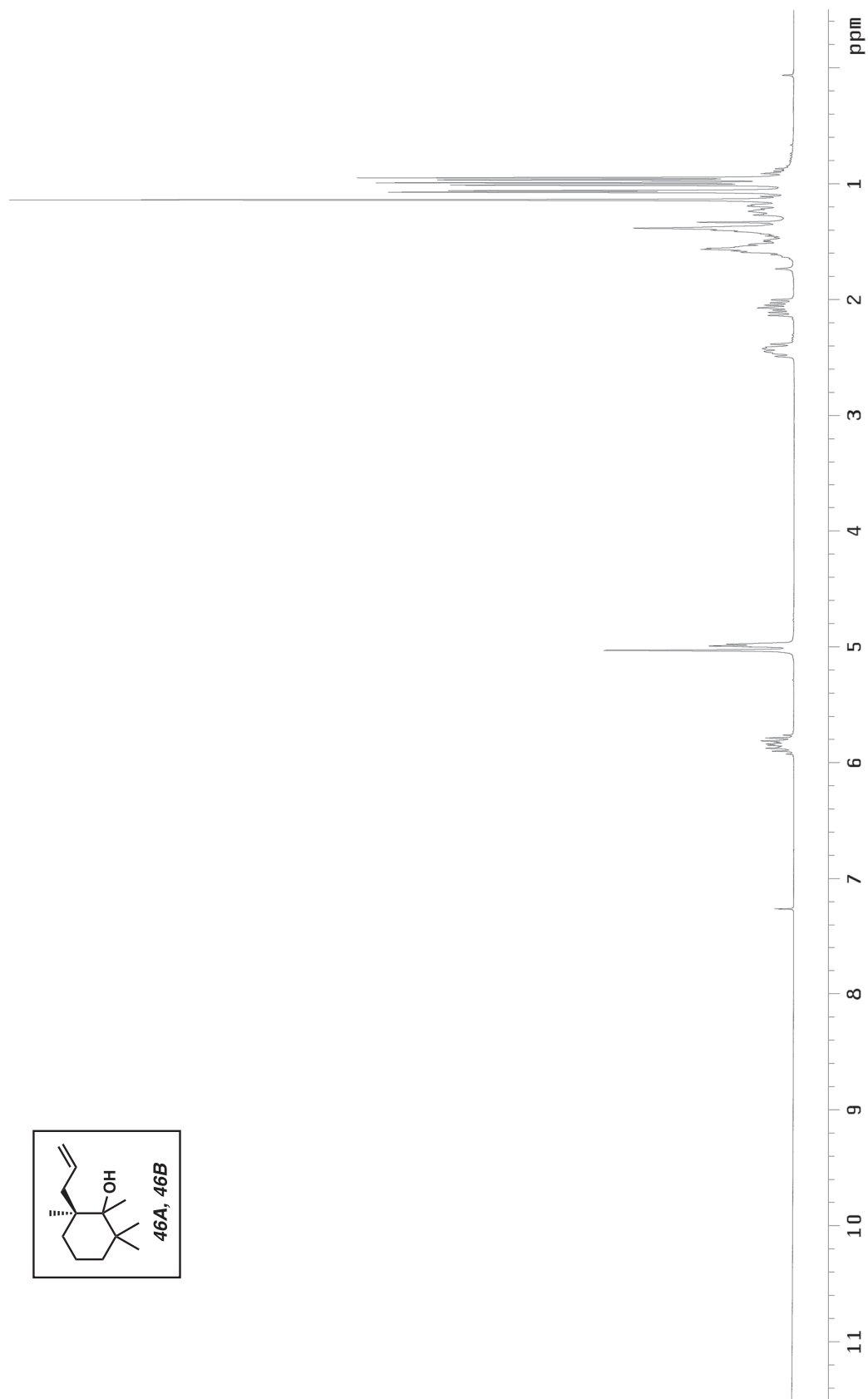


Figure A2.7 ^1H NMR (300 MHz, CDCl_3) of compounds 46A and 46B.

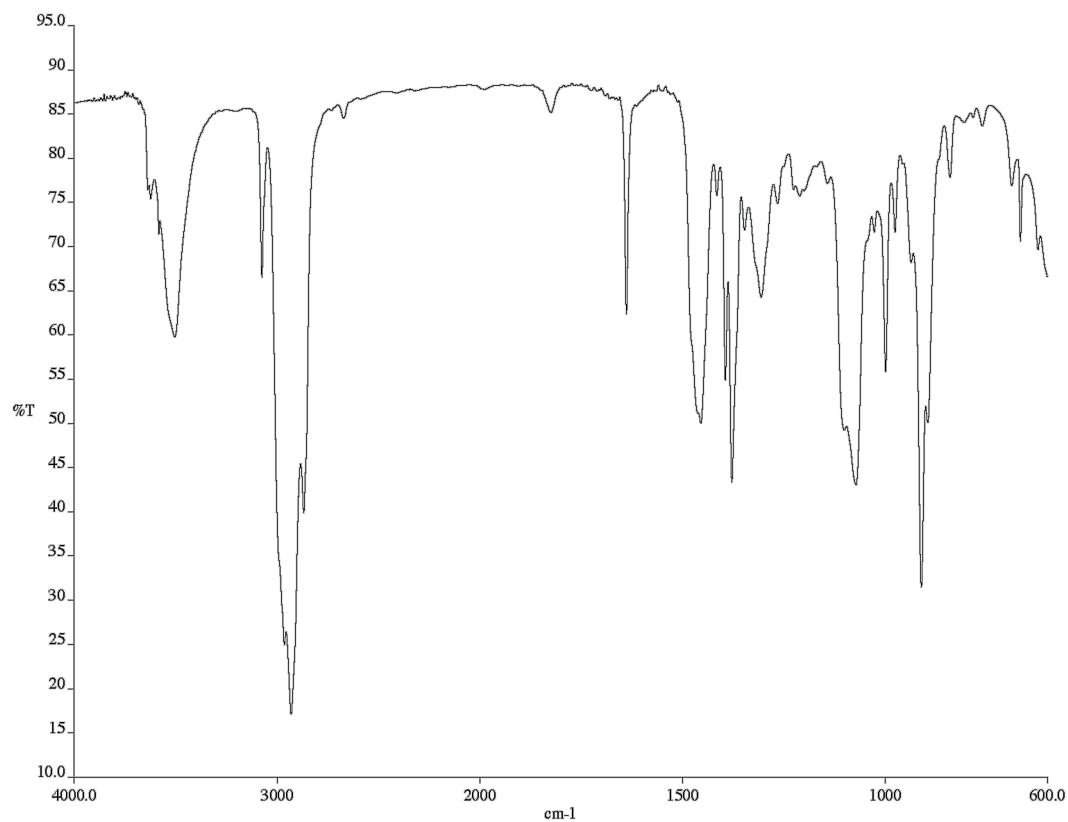


Figure A2.8 Infrared spectrum (Thin Film, NaCl) of compound **46A** and **46B**.

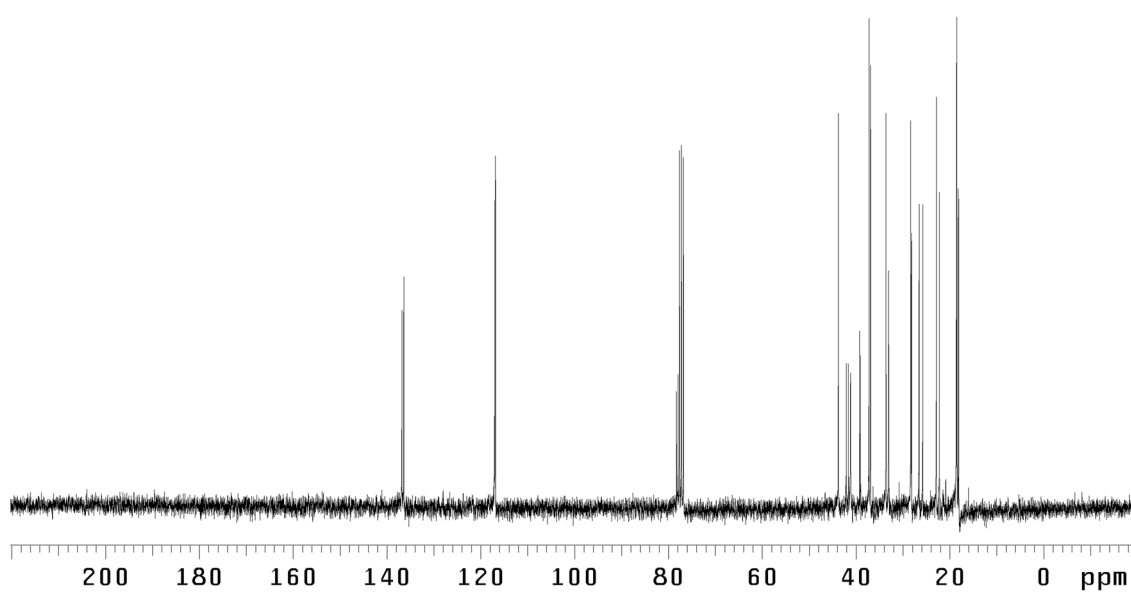


Figure A2.9 ¹³C NMR (75 MHz, CDCl₃) of compounds **46A** and **46B**.

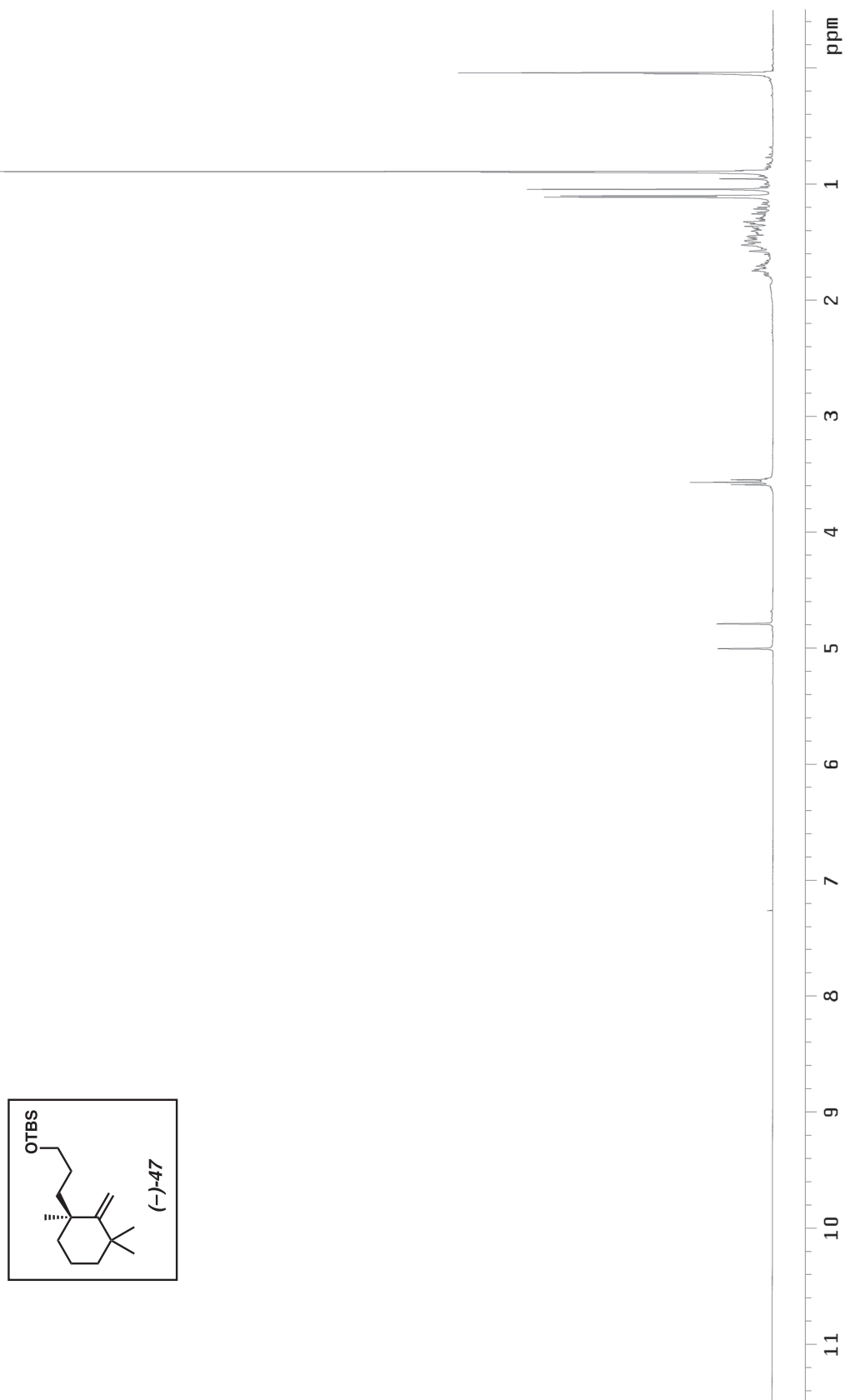


Figure A2.10 ¹H NMR (300 MHz, CDCl₃) of compound 47.

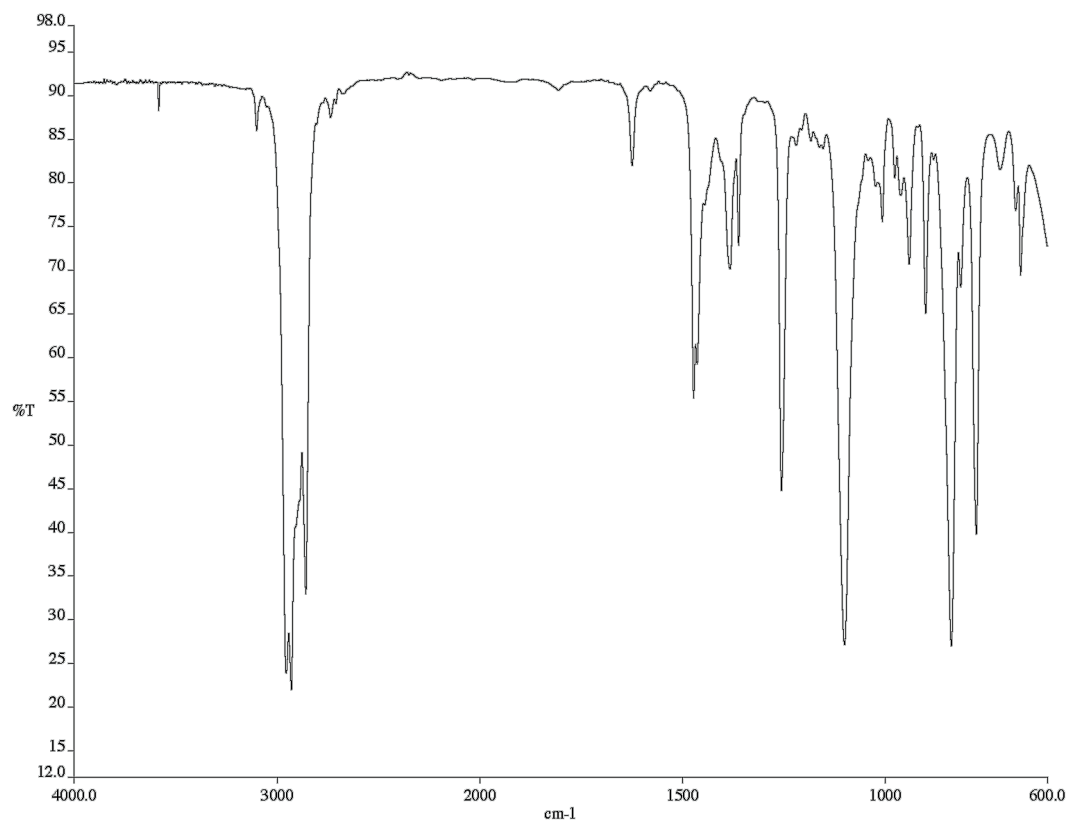


Figure A2.11 Infrared spectrum (Thin Film, NaCl) of compound 47.

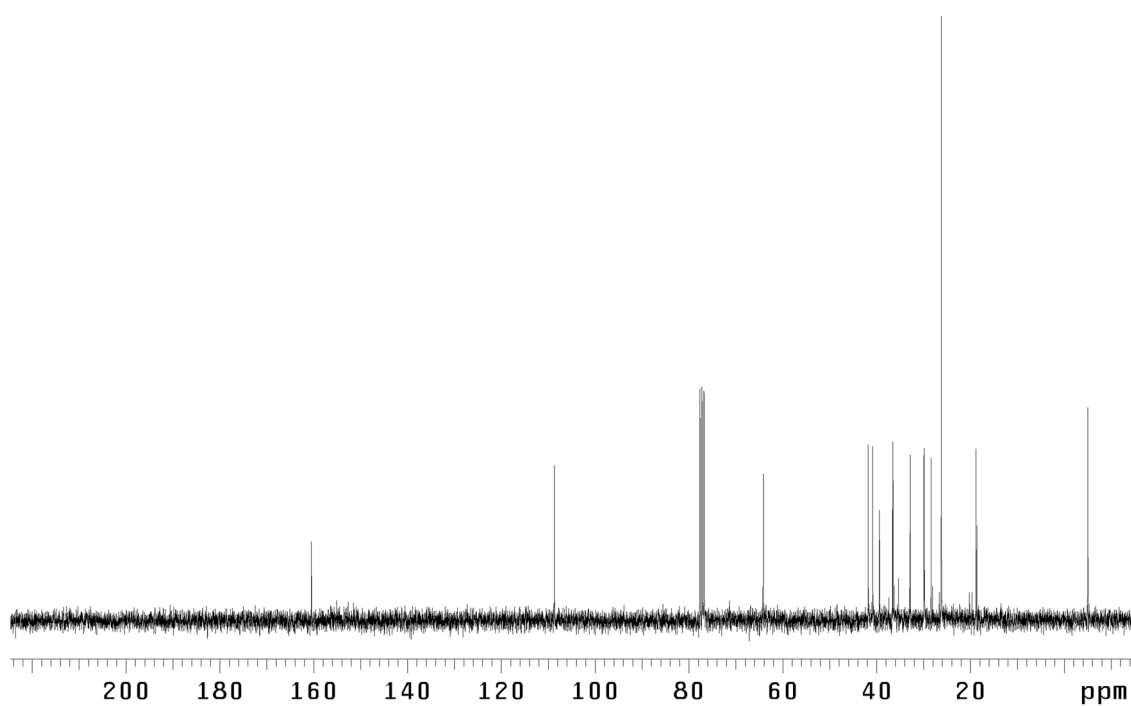
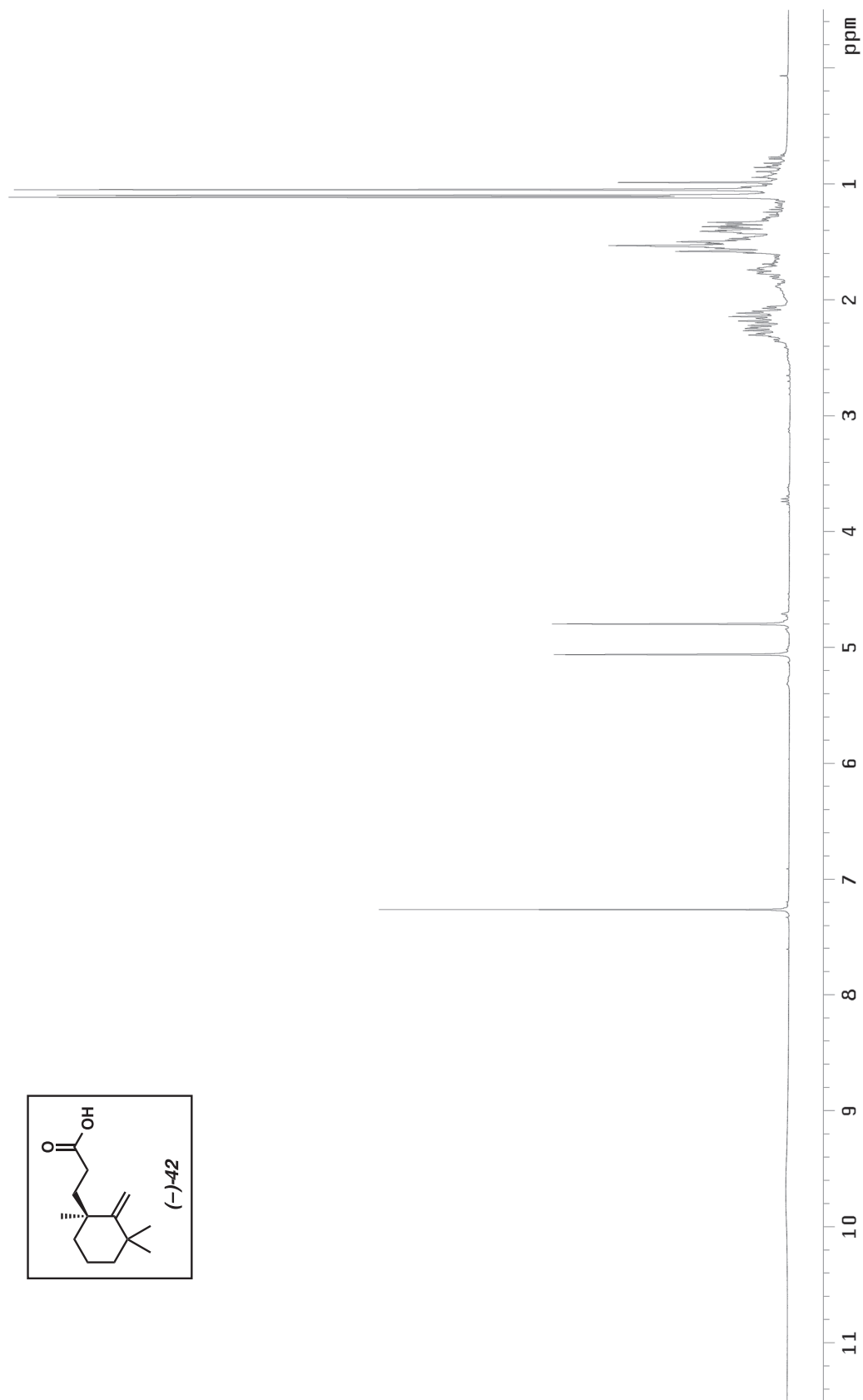


Figure A2.12 ¹³C NMR (75 MHz, CDCl₃) of compound 47.

Figure A2.13 ^1H NMR (300 MHz, CDCl_3) of compound 42.

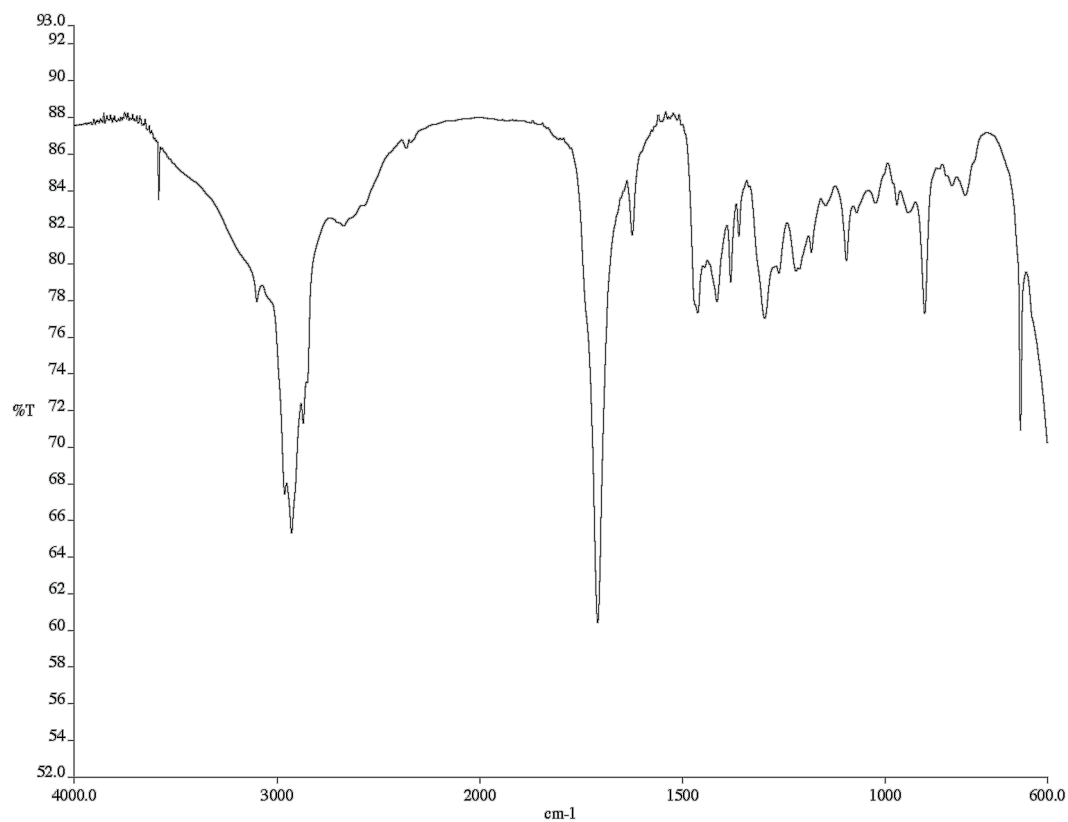


Figure A2.14 Infrared spectrum (Thin Film, NaCl) of compound **42**.

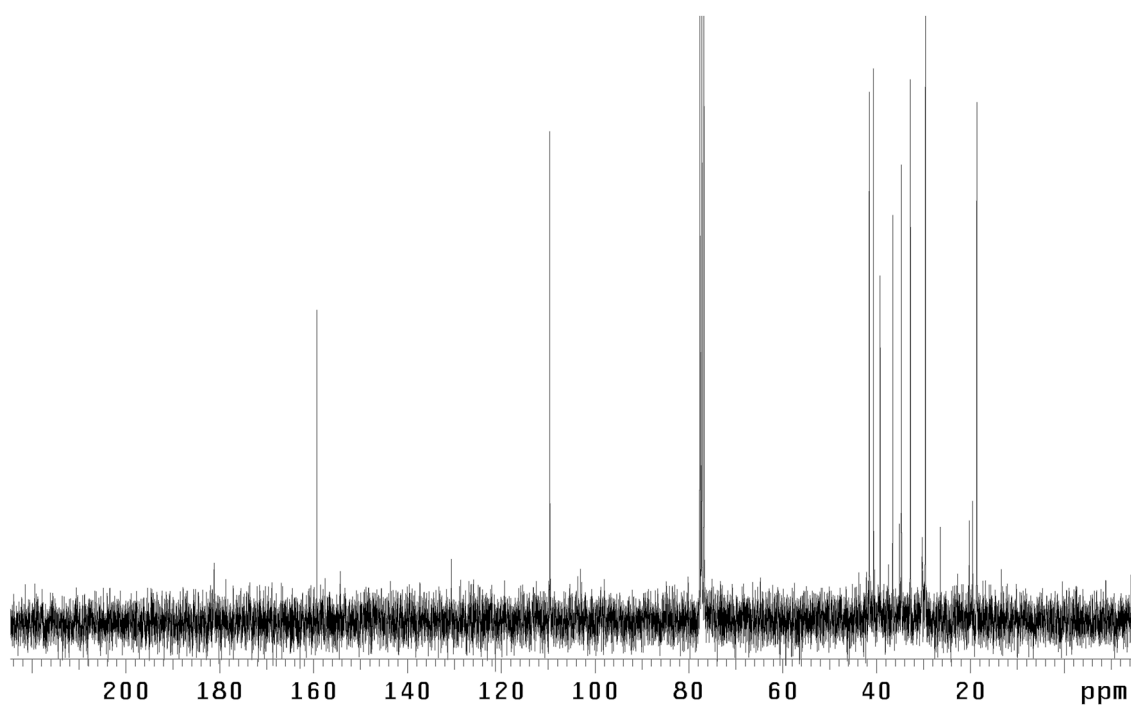


Figure A2.15 ¹³C NMR (75 MHz, CDCl₃) of compound **42**.

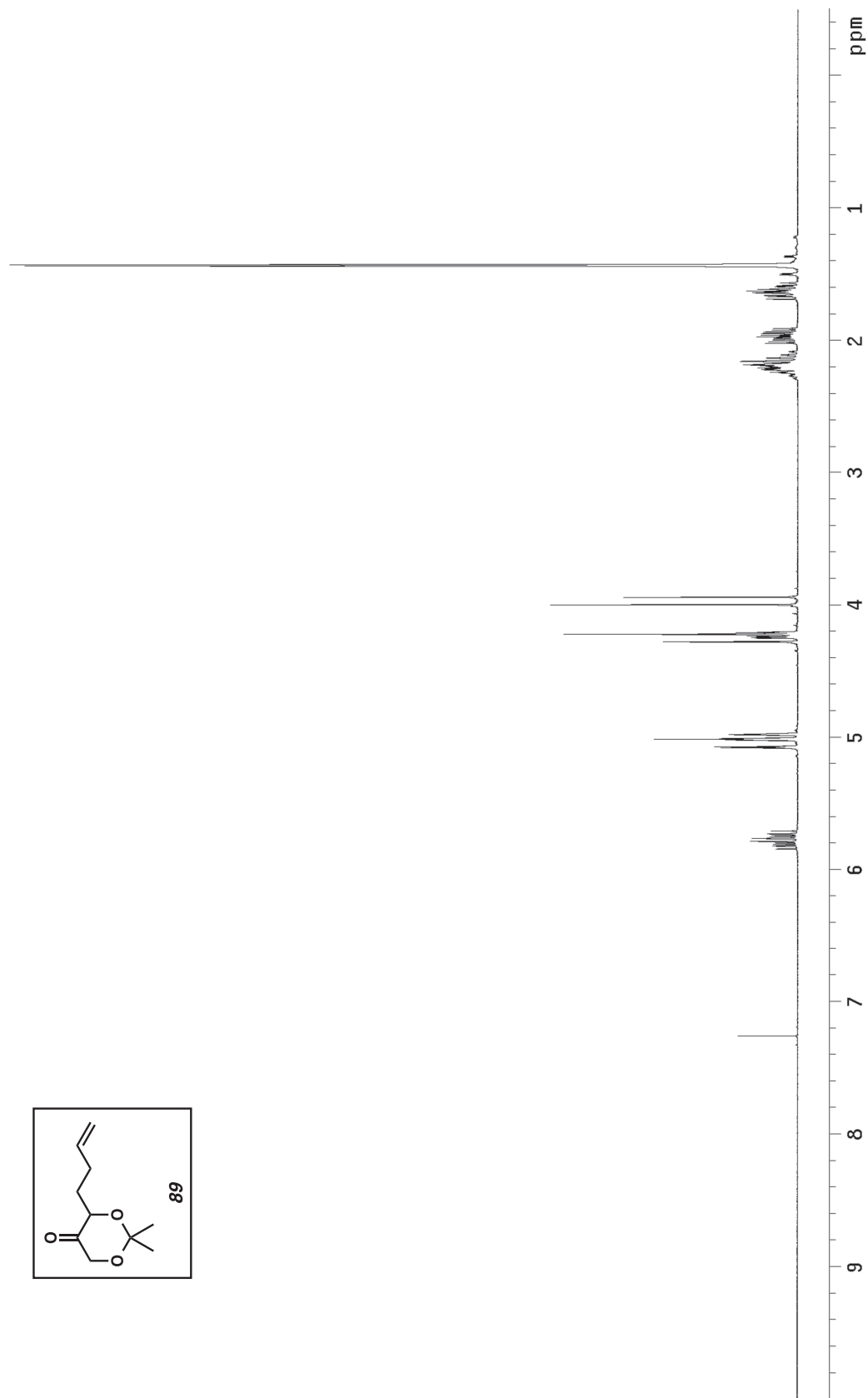


Figure A2.16 ^1H NMR (300 MHz, CDCl_3) of compound **89**.

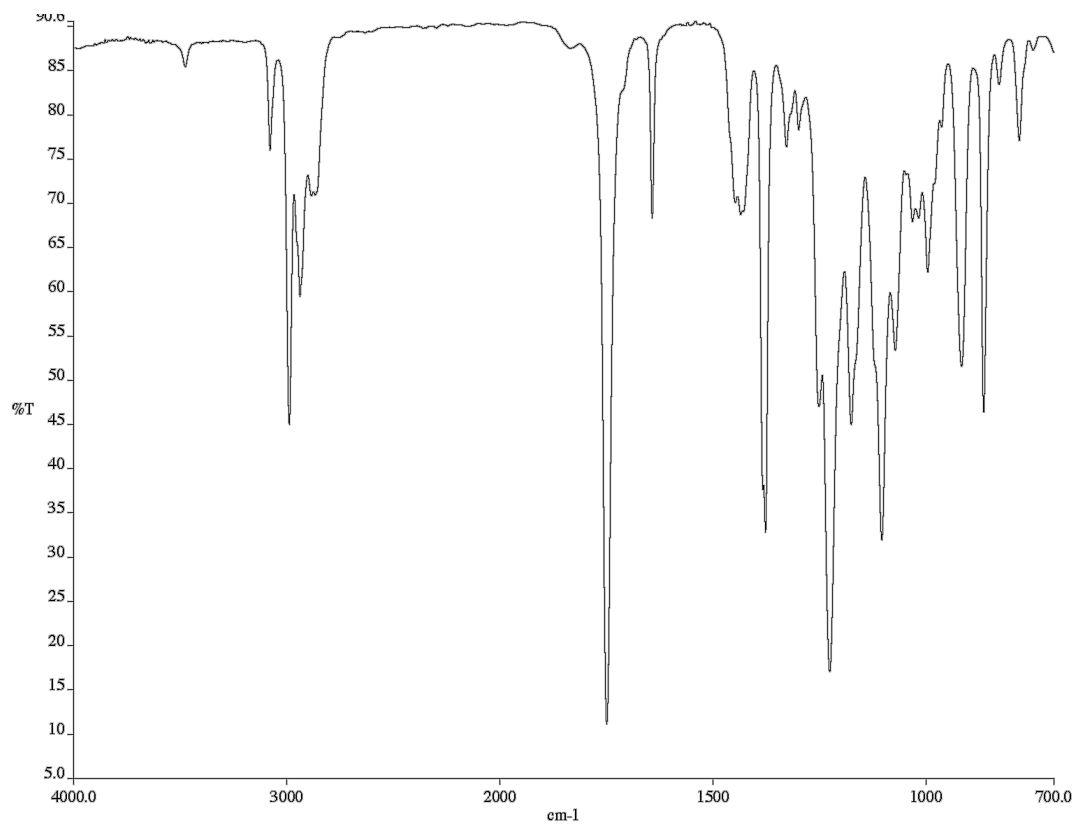


Figure A2.17 Infrared spectrum (Thin Film, NaCl) of compound **89**.

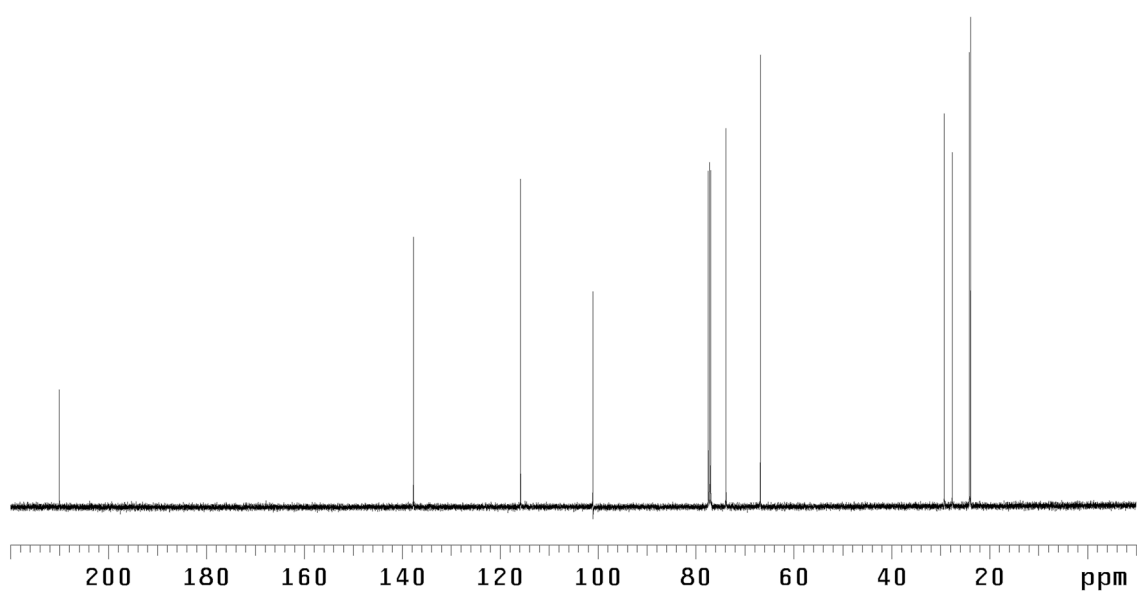


Figure A2.18 ¹³C NMR (75 MHz, CDCl₃) of compound **89**.

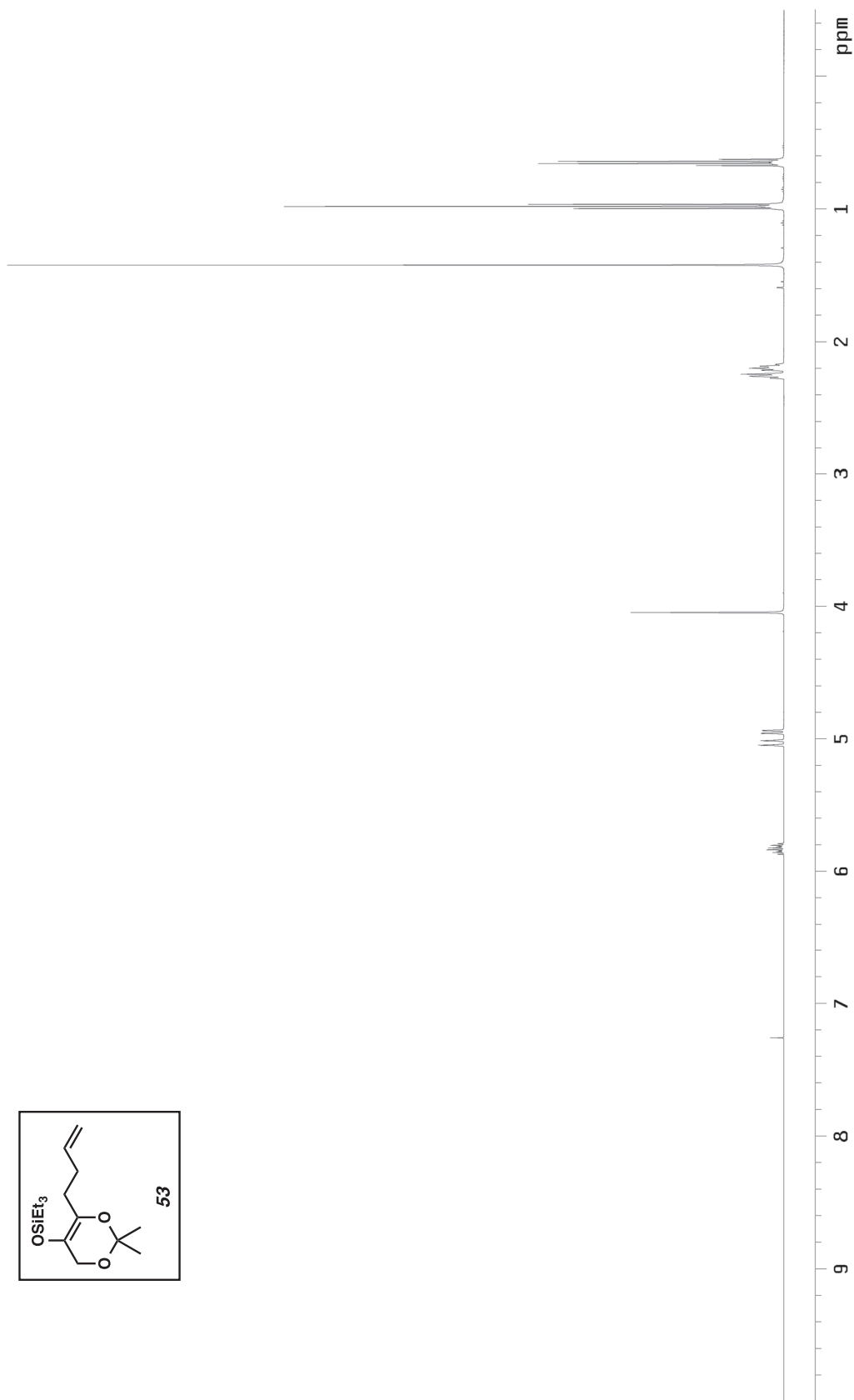


Figure A2.19 ^1H NMR (500 MHz, CDCl_3) of compound **53**.

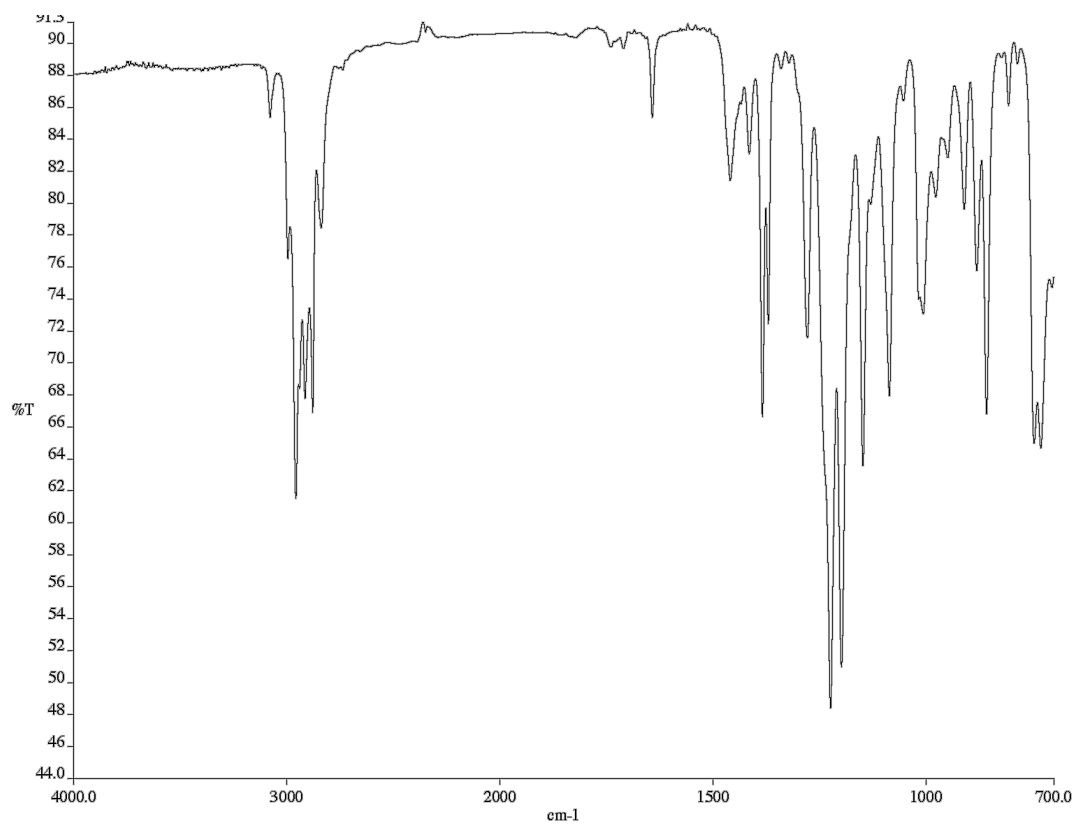


Figure A2.20 Infrared spectrum (Thin Film, NaCl) of compound **53**.

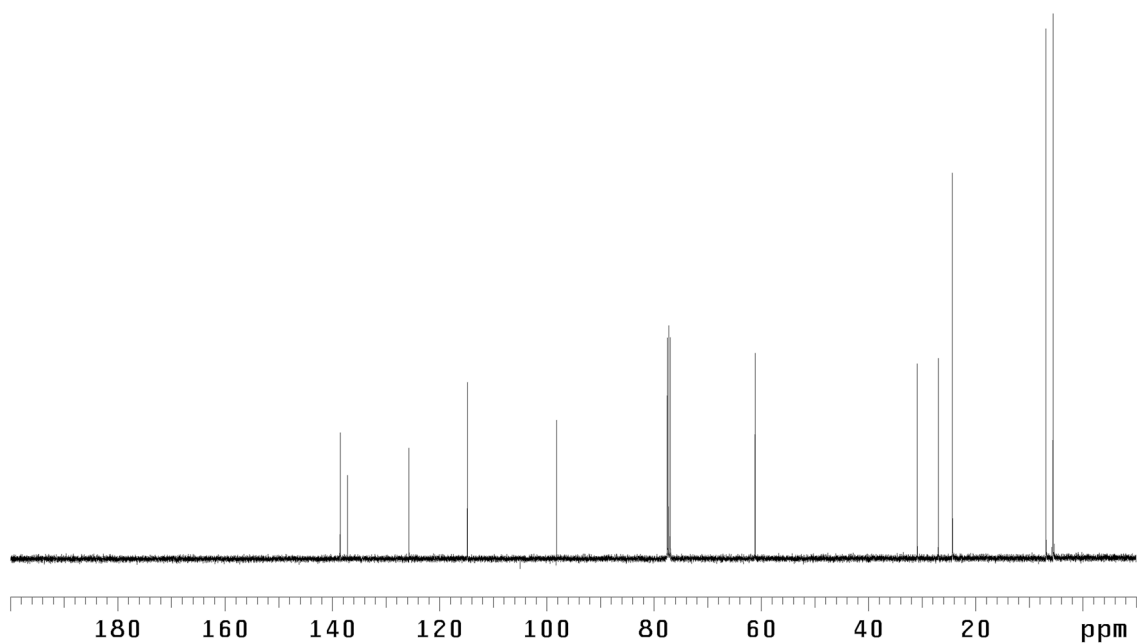


Figure A2.21 ¹³C NMR (125 MHz, CDCl₃) of compound **53**.

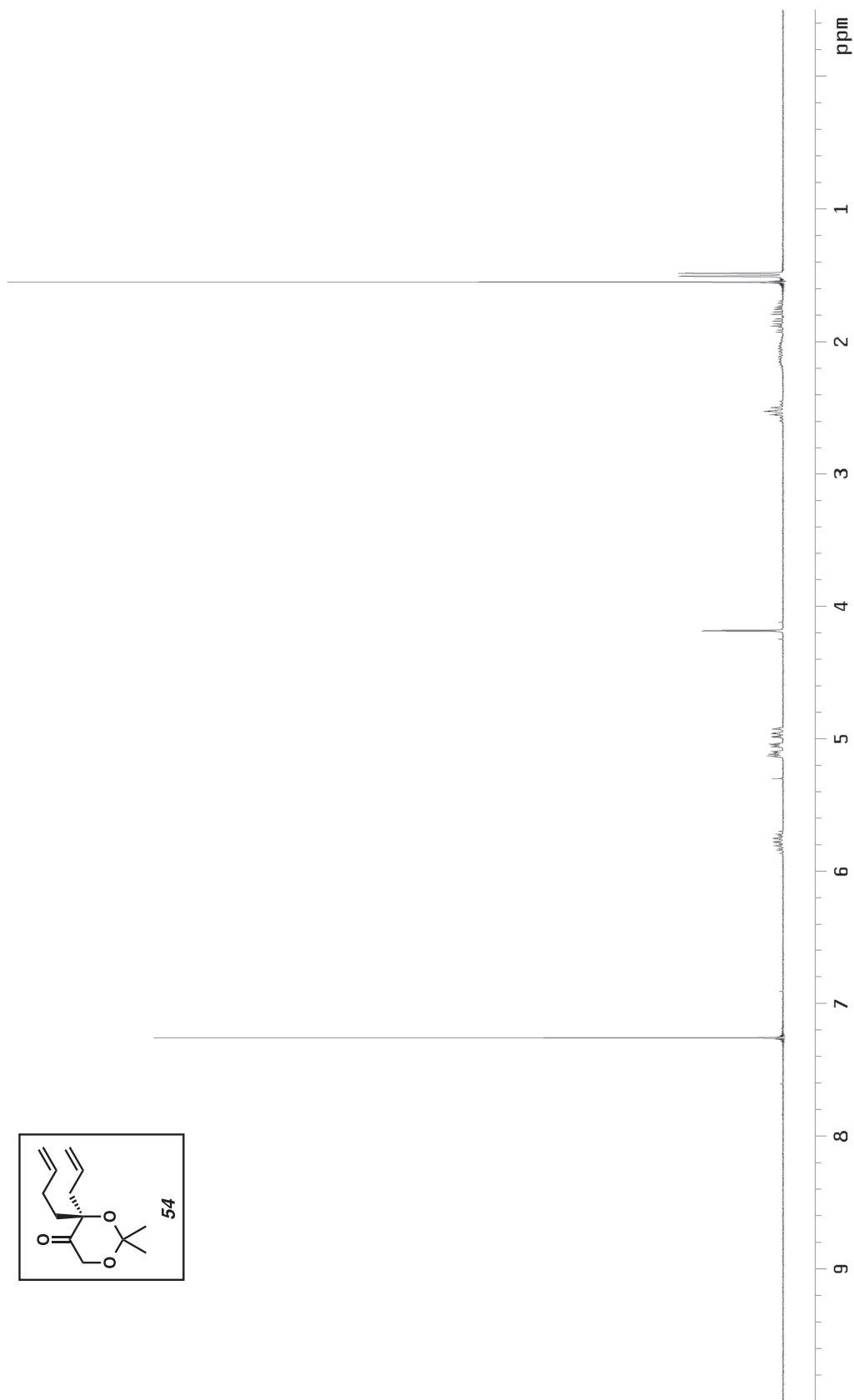


Figure A2.22 ^1H NMR (300 MHz, CDCl_3) of compound **54**.

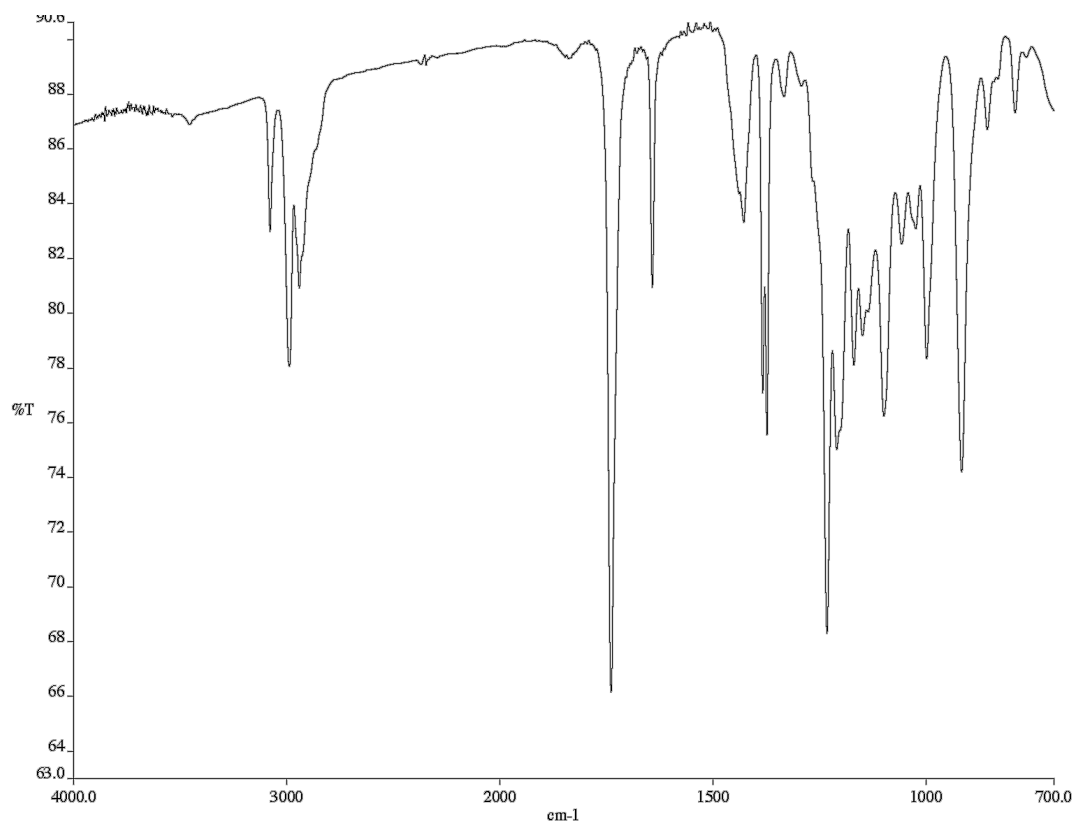


Figure A2.23 Infrared spectrum (Thin Film, NaCl) of compound **54**.

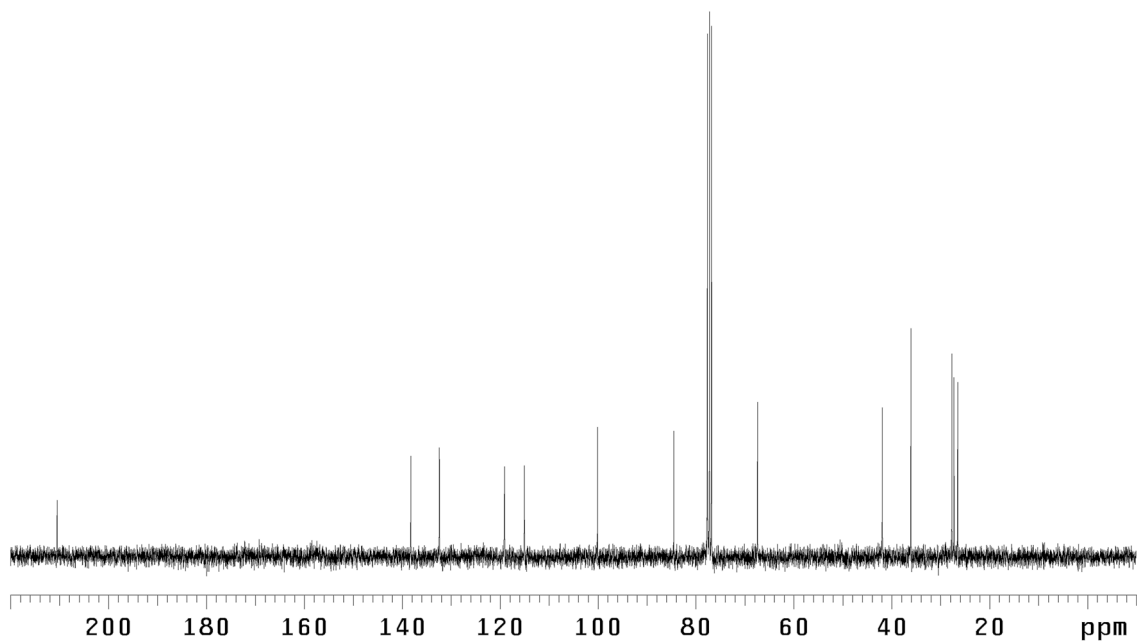


Figure A2.24 ¹³C NMR (75 MHz, CDCl₃) of compound **54**.

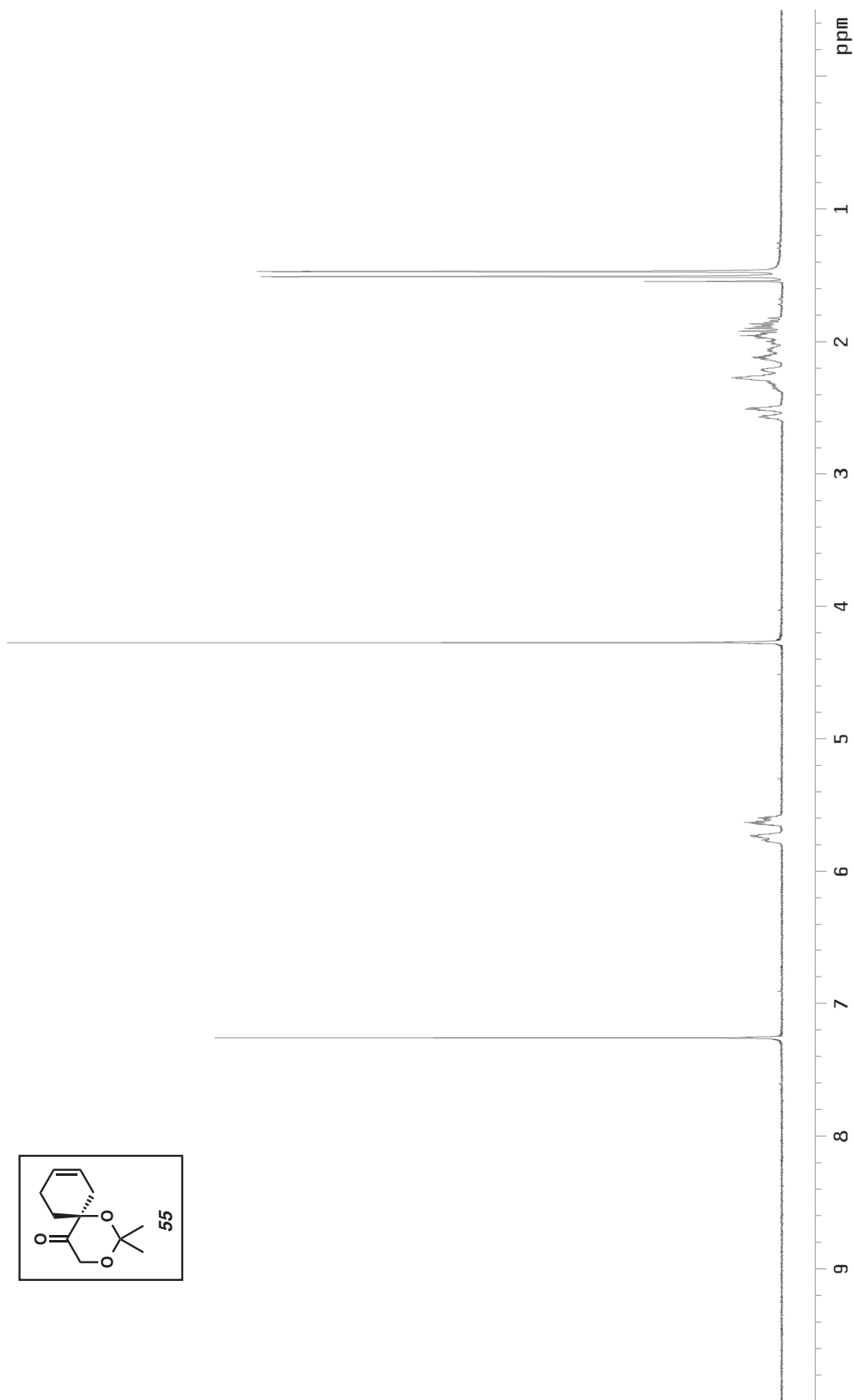


Figure A2.25 ^1H NMR (300 MHz, CDCl_3) of compound **55**.

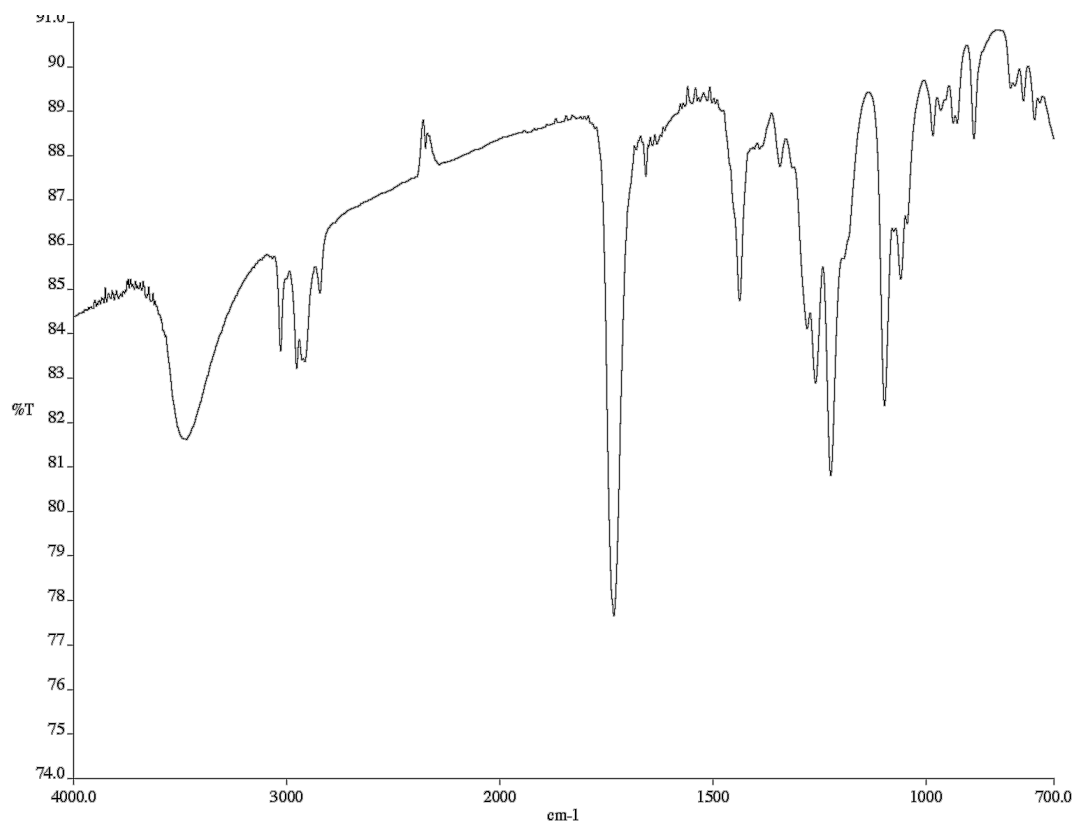


Figure A2.26 Infrared spectrum (Thin Film, NaCl) of compound **55**.

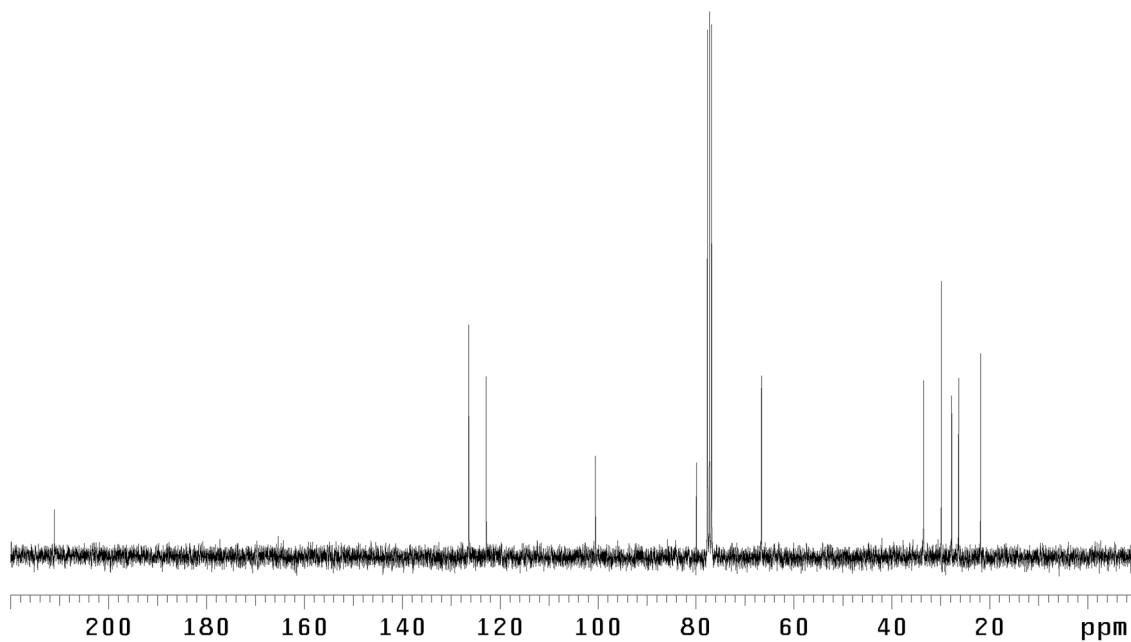
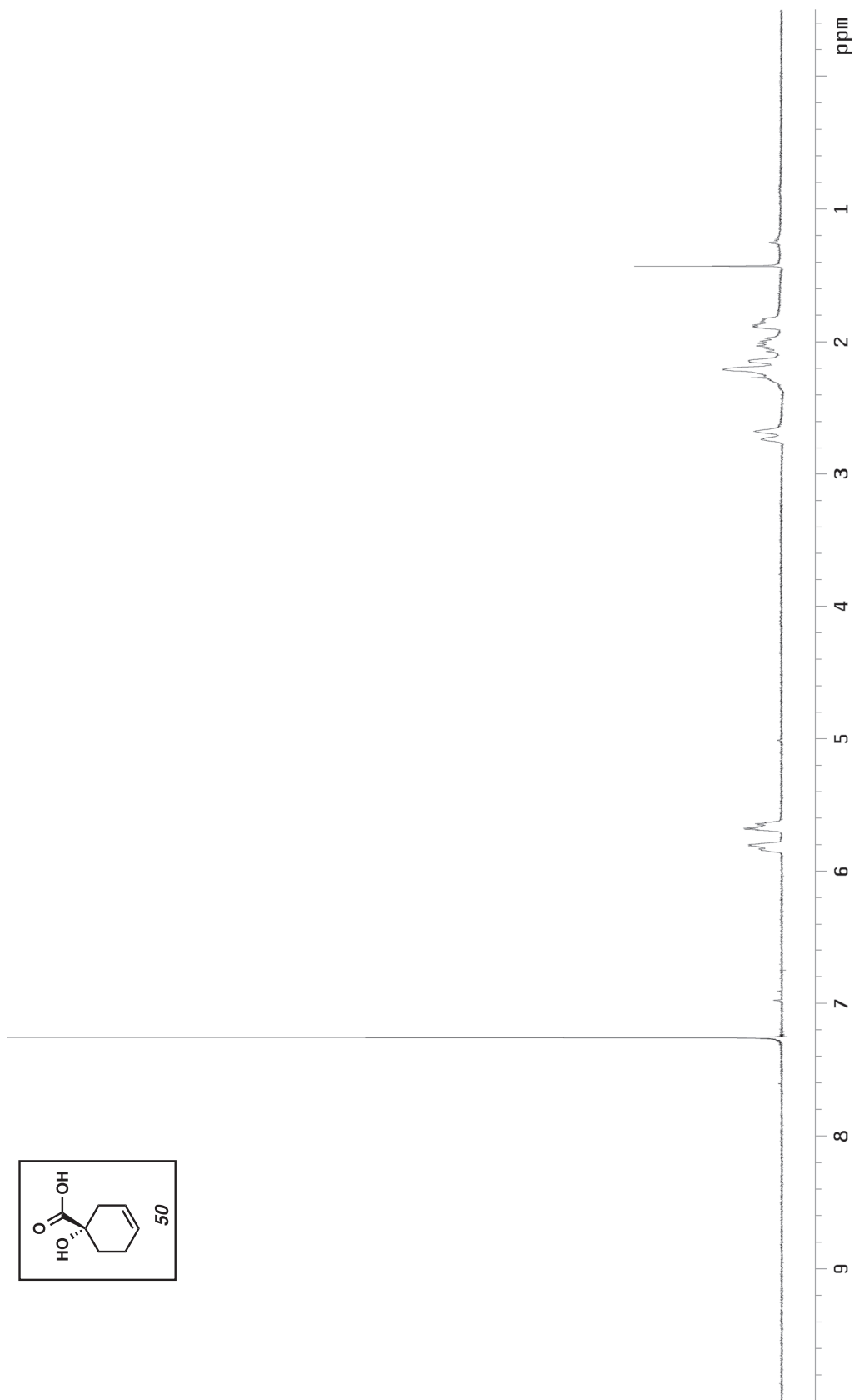


Figure A2.27 ¹³C NMR (75 MHz, CDCl₃) of compound **55**.



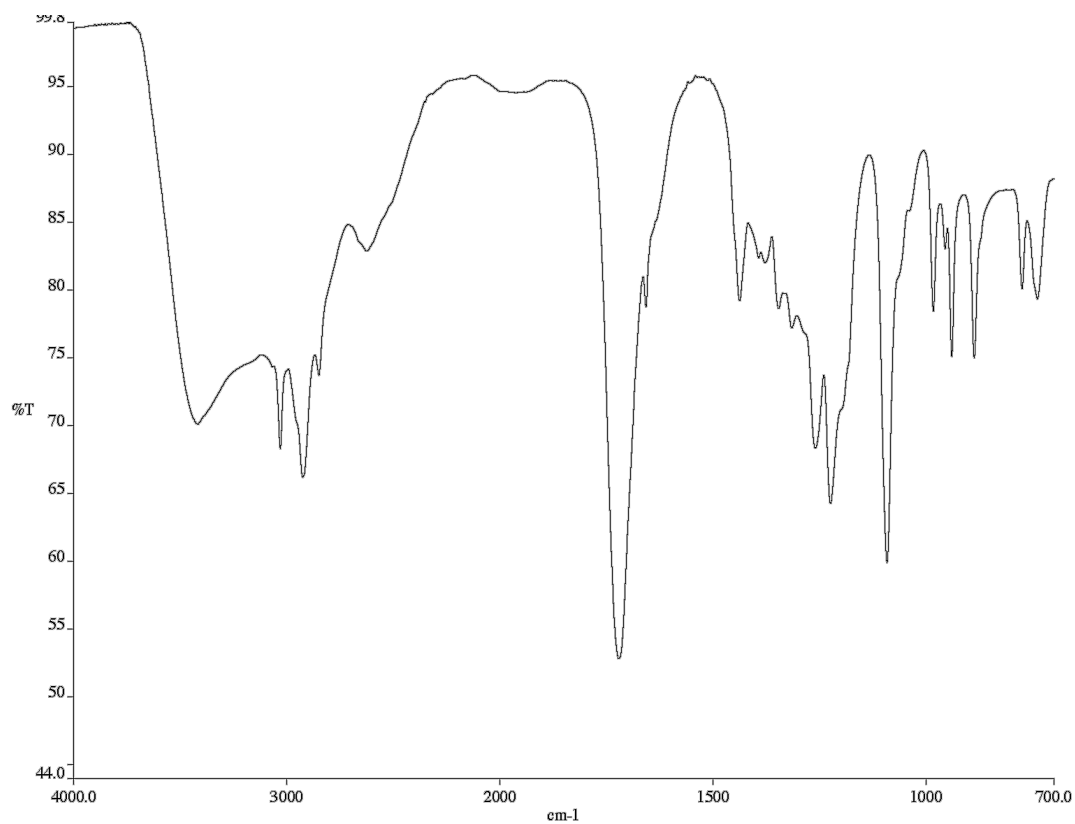


Figure A2.29 Infrared spectrum (Thin Film, NaCl) of compound **50**.

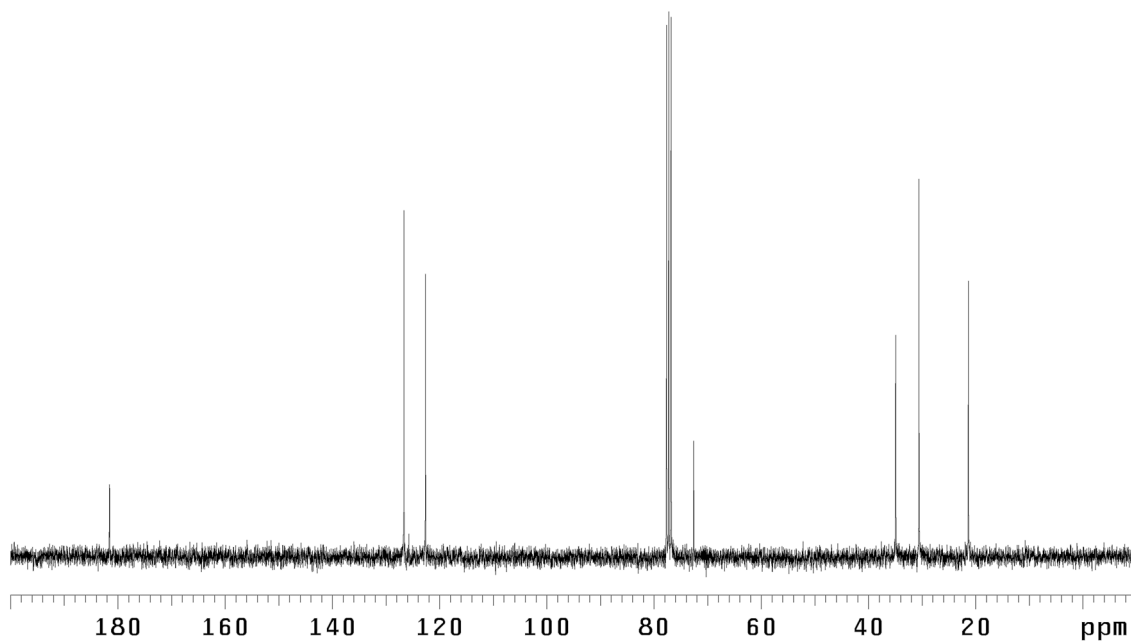


Figure A2.30 ¹³C NMR (75 MHz, CDCl₃) of compound **50**.

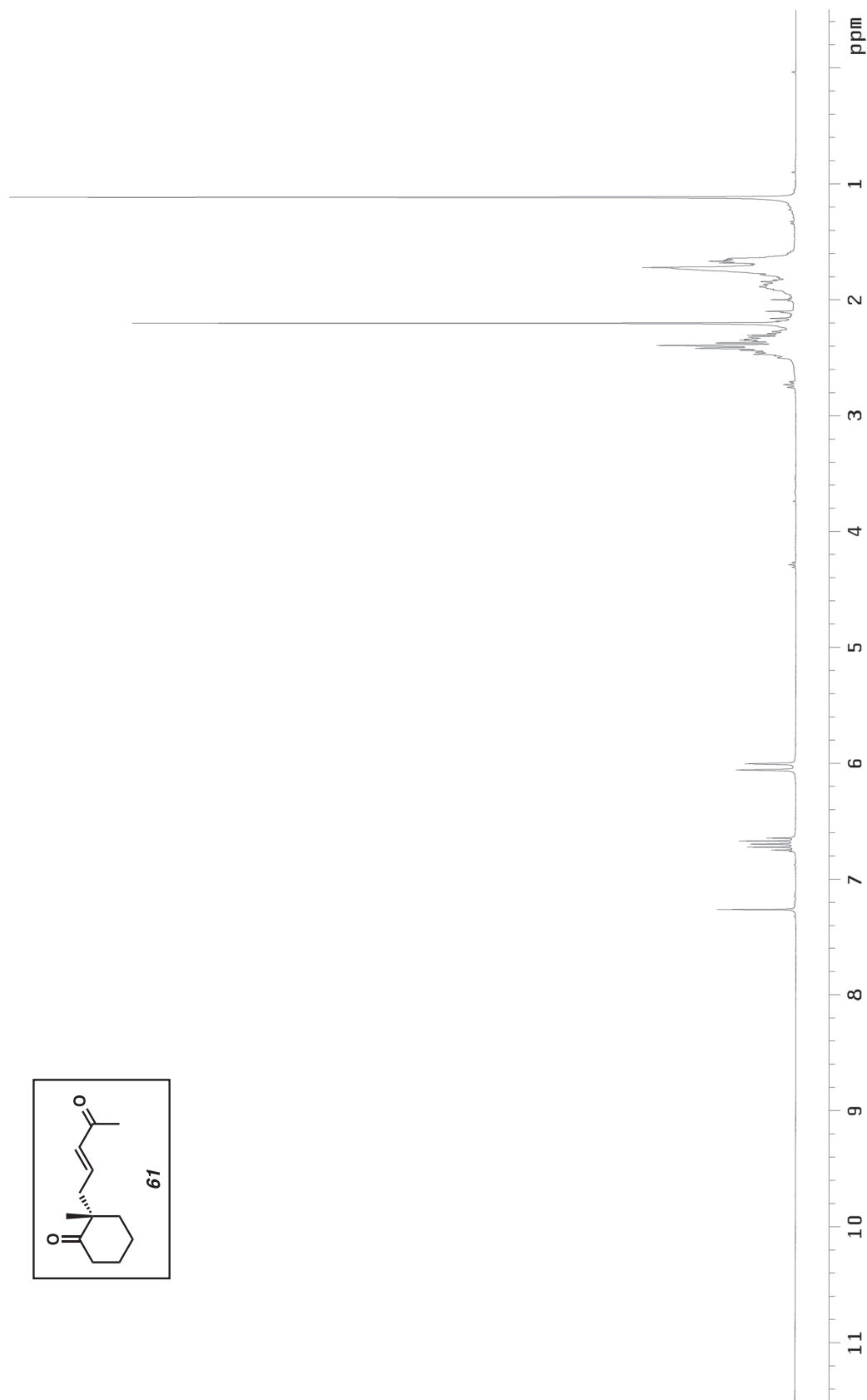


Figure A2.31 ^1H NMR (300 MHz, CDCl_3) of compound **61**.

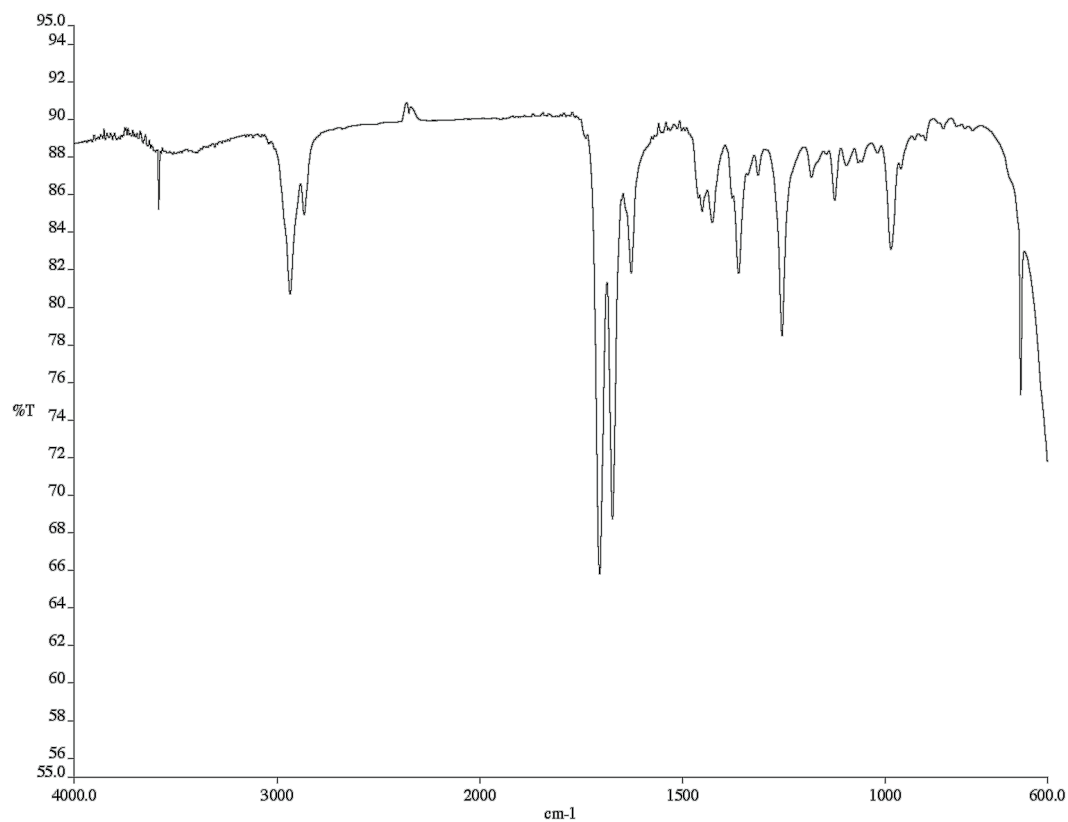


Figure A2.32 Infrared spectrum (Thin Film, NaCl) of compound **61**.

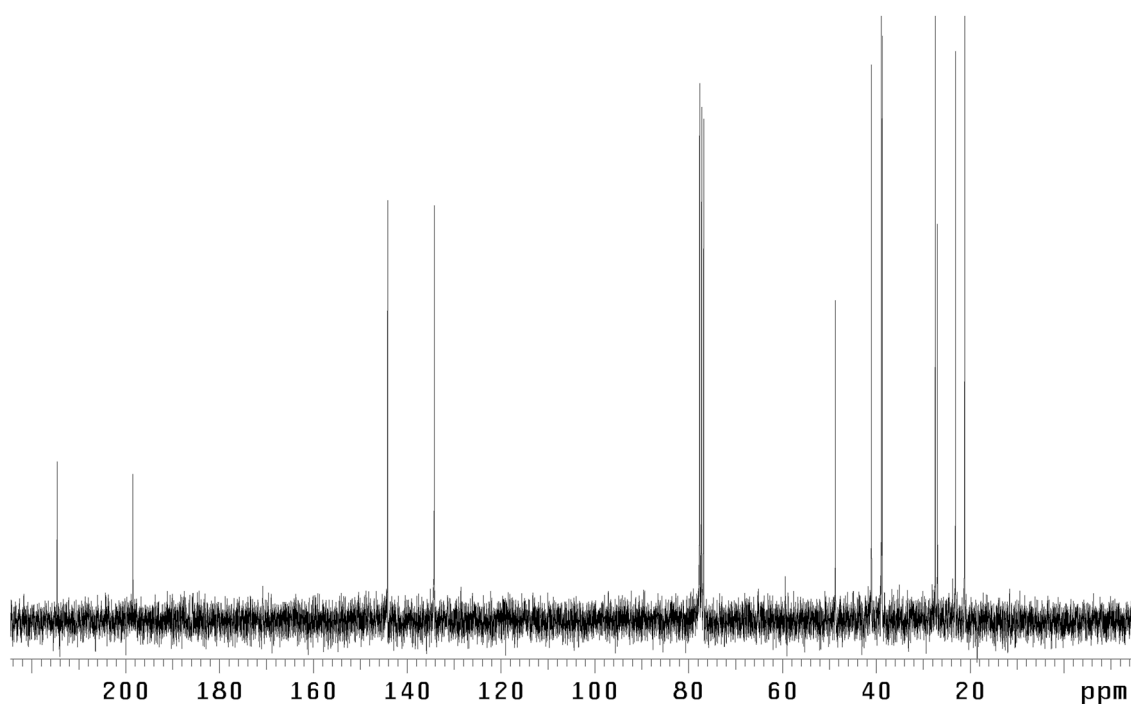


Figure A2.33 ¹³C NMR (75 MHz, CDCl₃) of compound **61**.

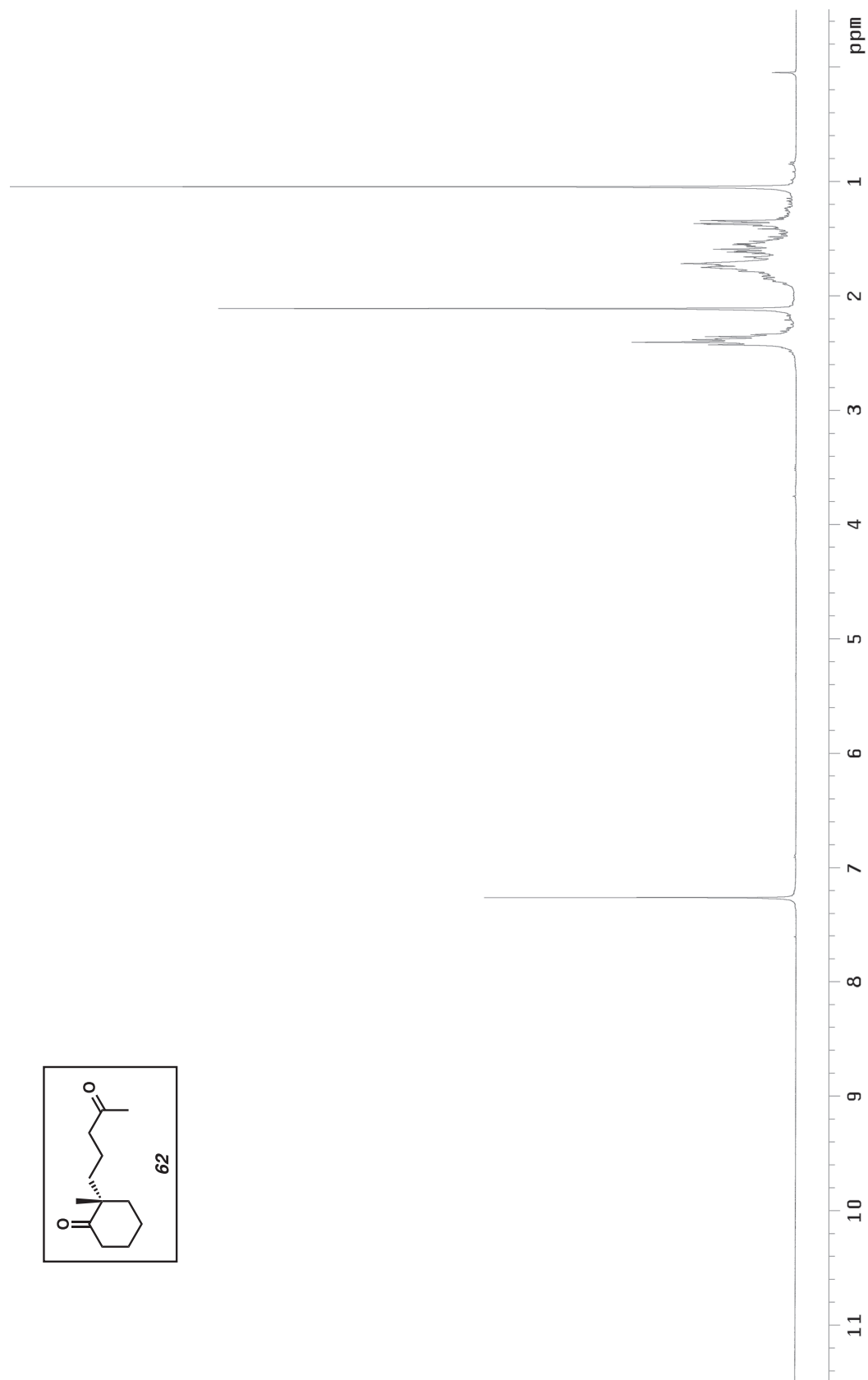


Figure A2.34 ^1H NMR (300 MHz, CDCl_3) of compound **62**.

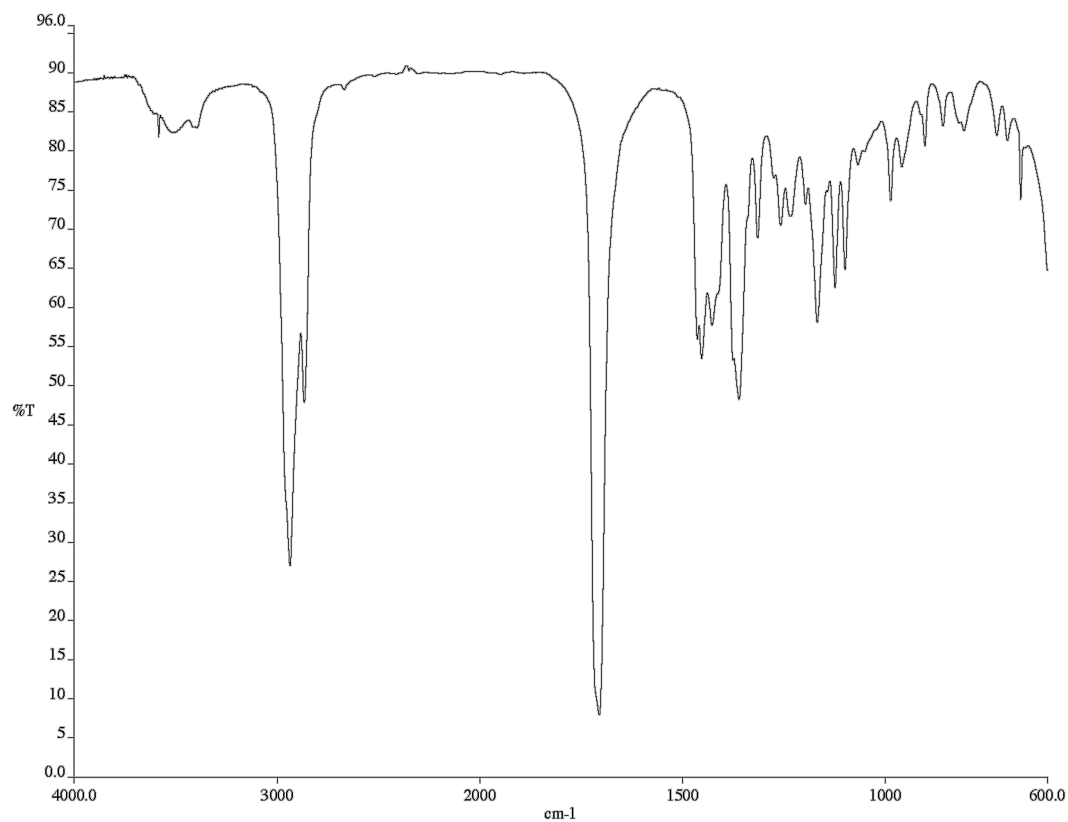


Figure A2.35 Infrared spectrum (Thin Film, NaCl) of compound **62**.

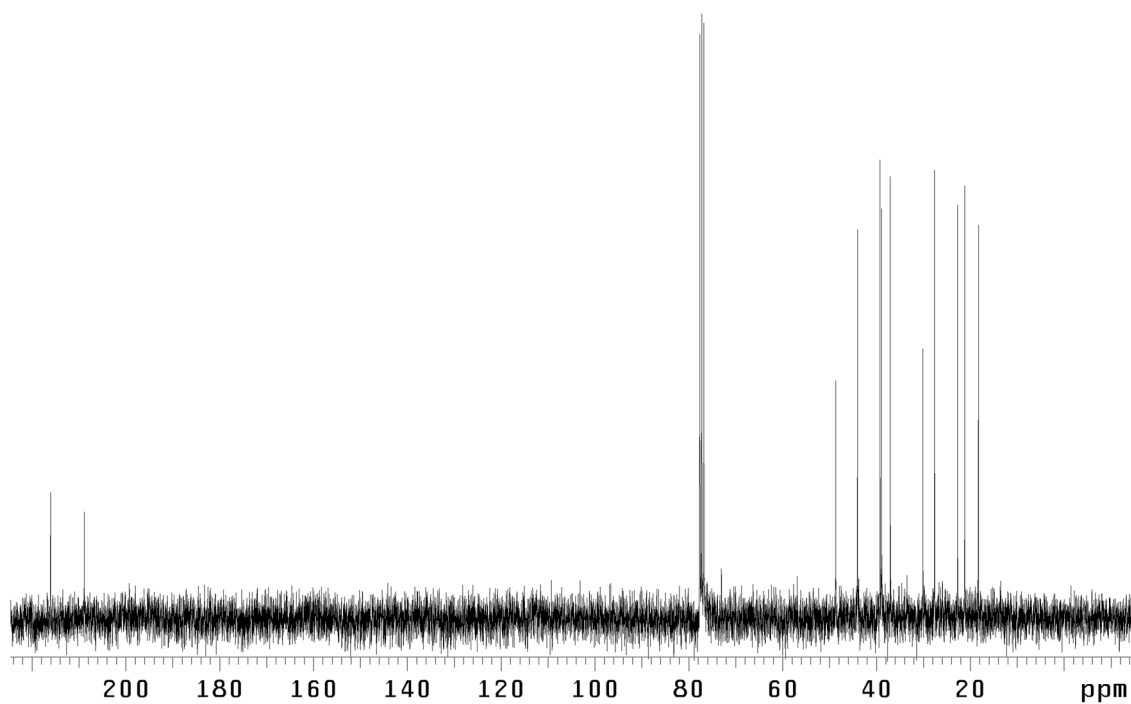


Figure A2.36 ¹³C NMR (75 MHz, CDCl₃) of compound **62**.

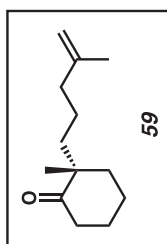
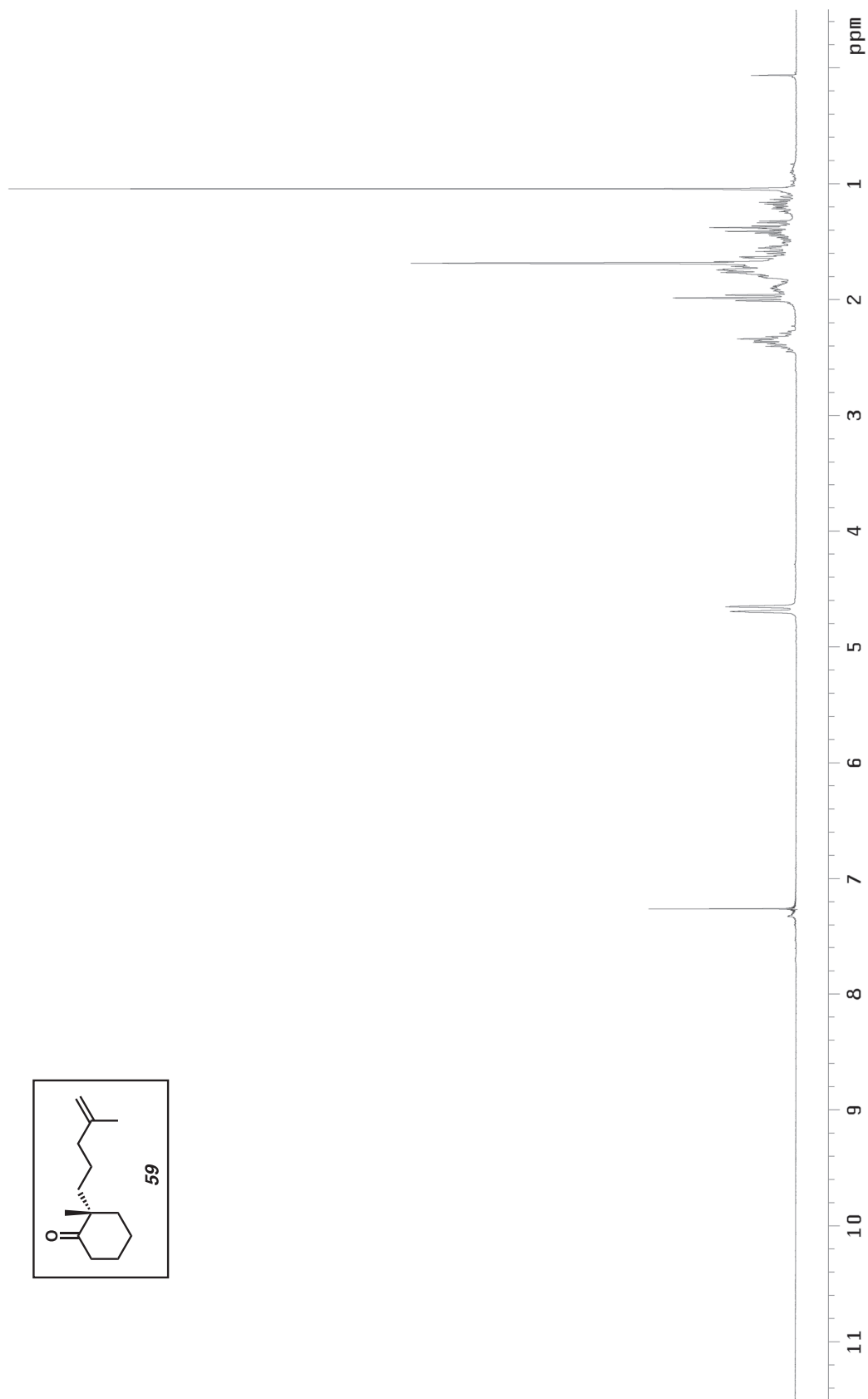


Figure A2.37 ^1H NMR (300 MHz, CDCl_3) of compound **59**.

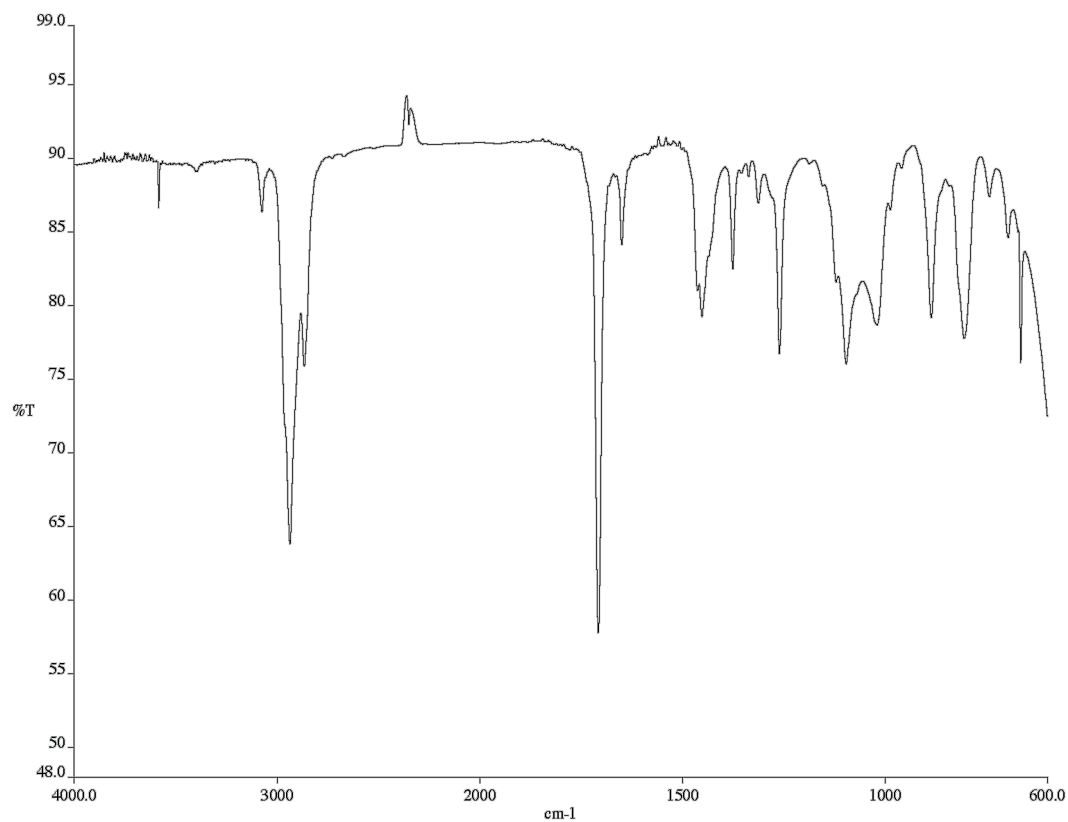


Figure A2.38 Infrared spectrum (Thin Film, NaCl) of compound **59**.

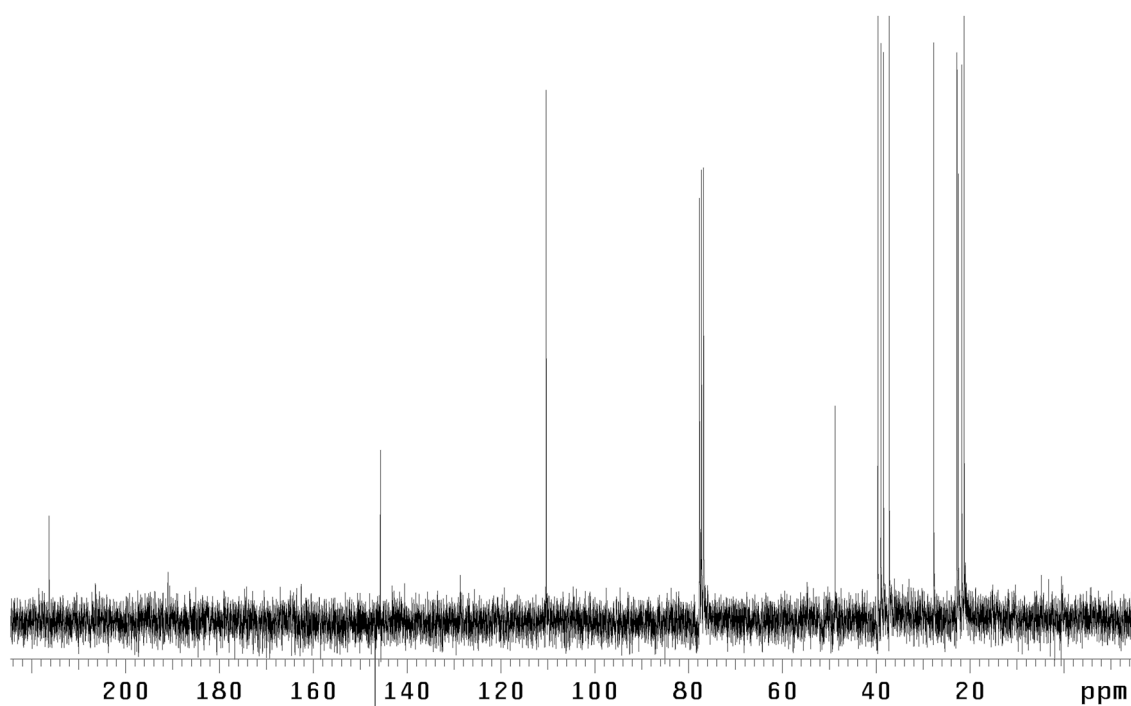


Figure A2.39 ¹³C NMR (75 MHz, CDCl₃) of compound **59**.

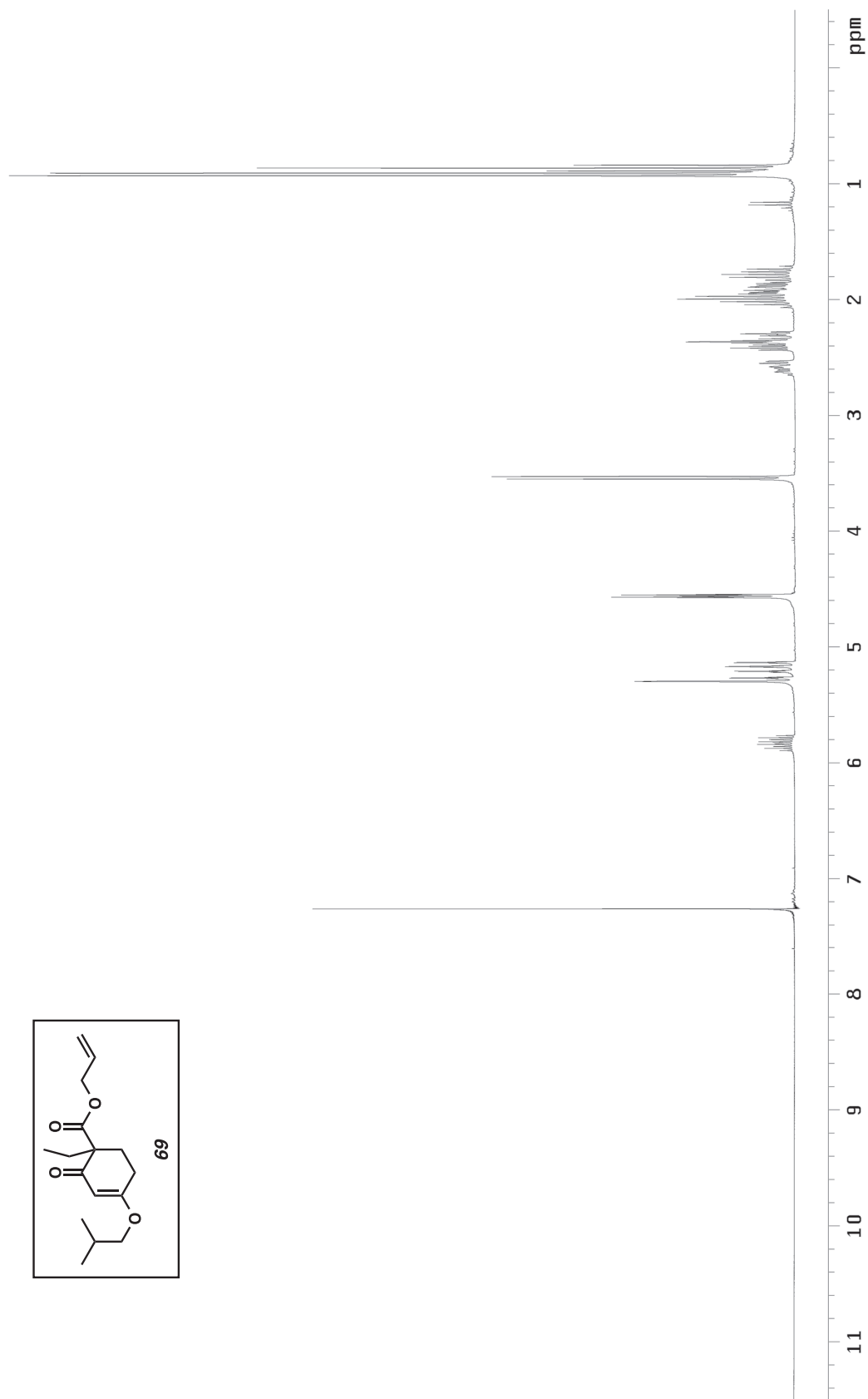


Figure A2.40 ^1H NMR (300 MHz, CDCl_3) of compound **69**.

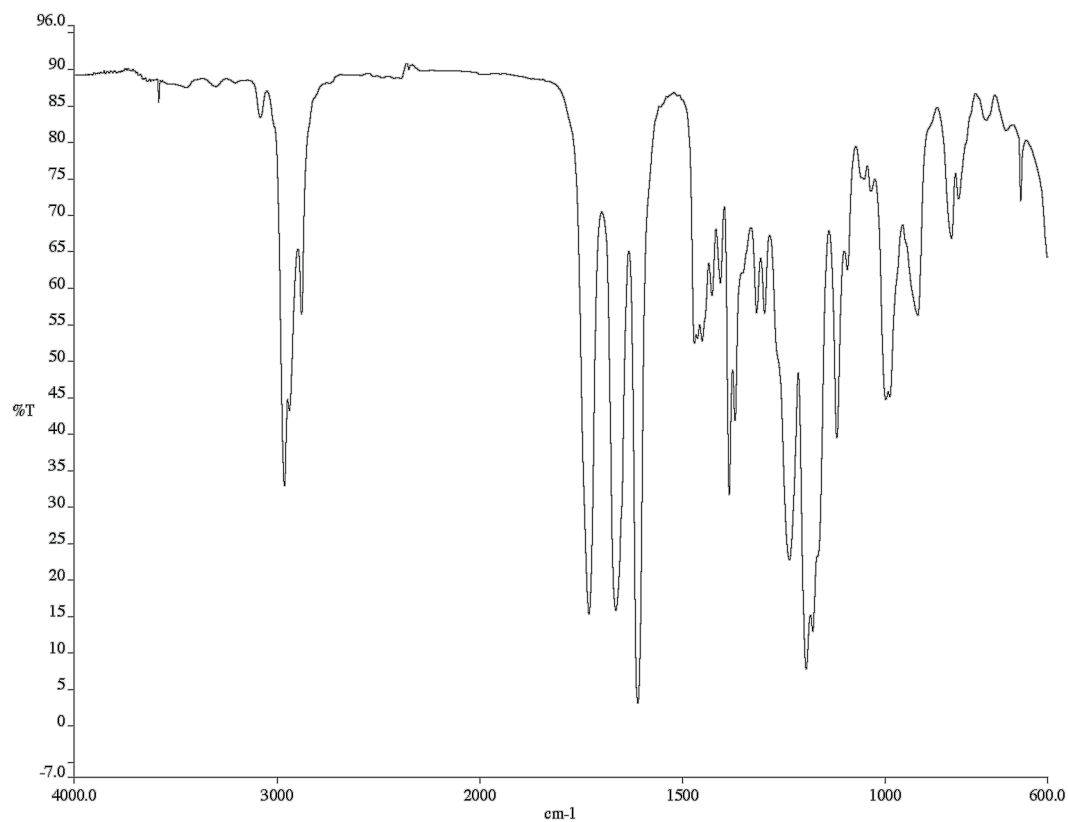


Figure A2.41 Infrared spectrum (Thin Film, NaCl) of compound **69**.

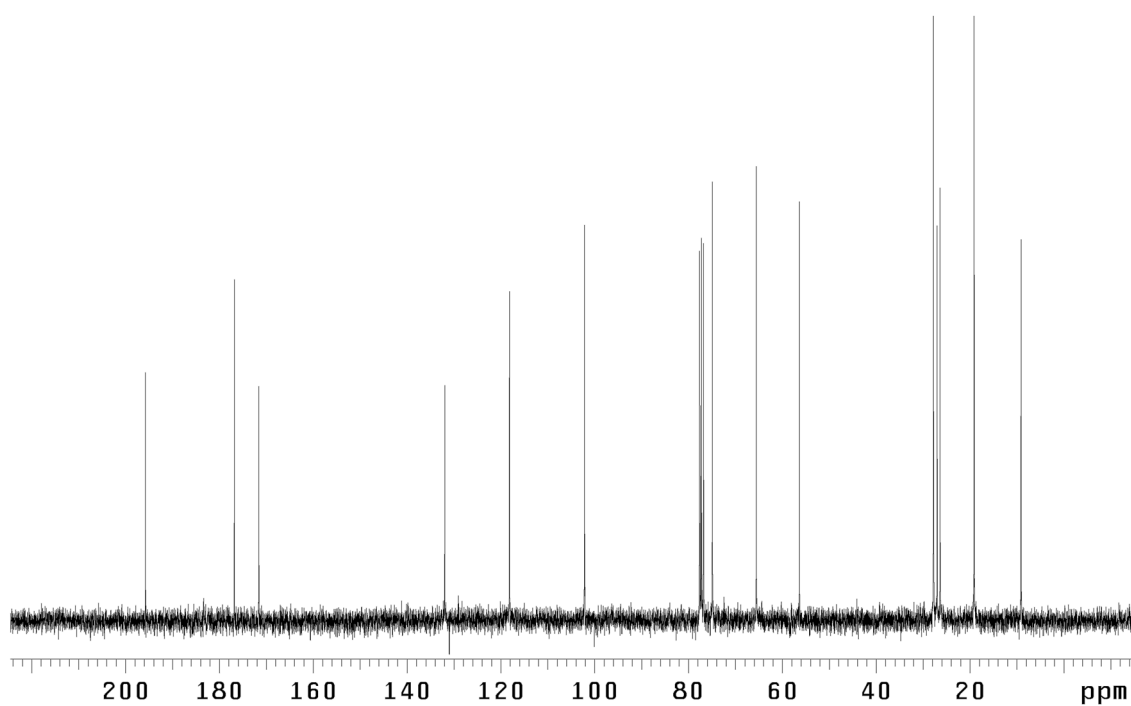


Figure A2.42 ¹³C NMR (75 MHz, CDCl₃) of compound **69**.

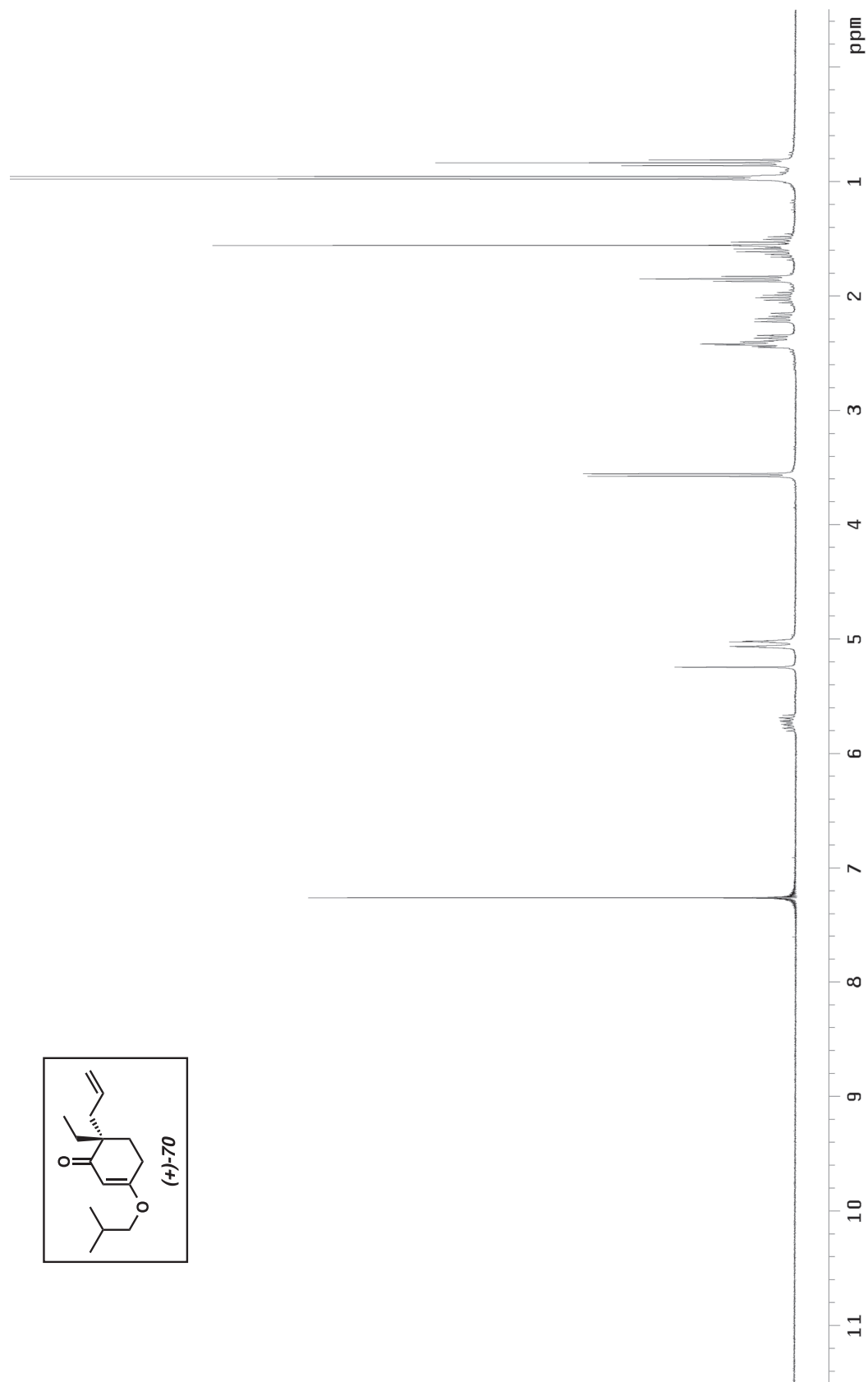


Figure A2.43 ^1H NMR (300 MHz, CDCl_3) of compound **70**.

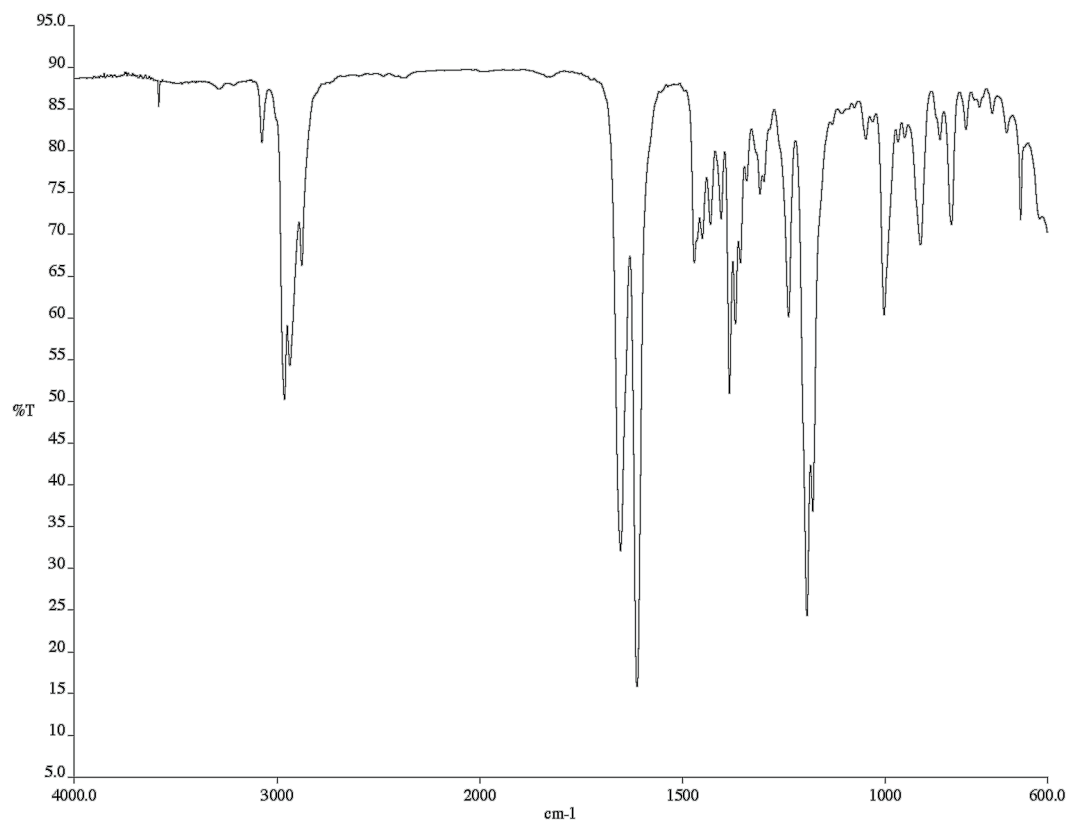


Figure A2.44 Infrared spectrum (Thin Film, NaCl) of compound **70**.

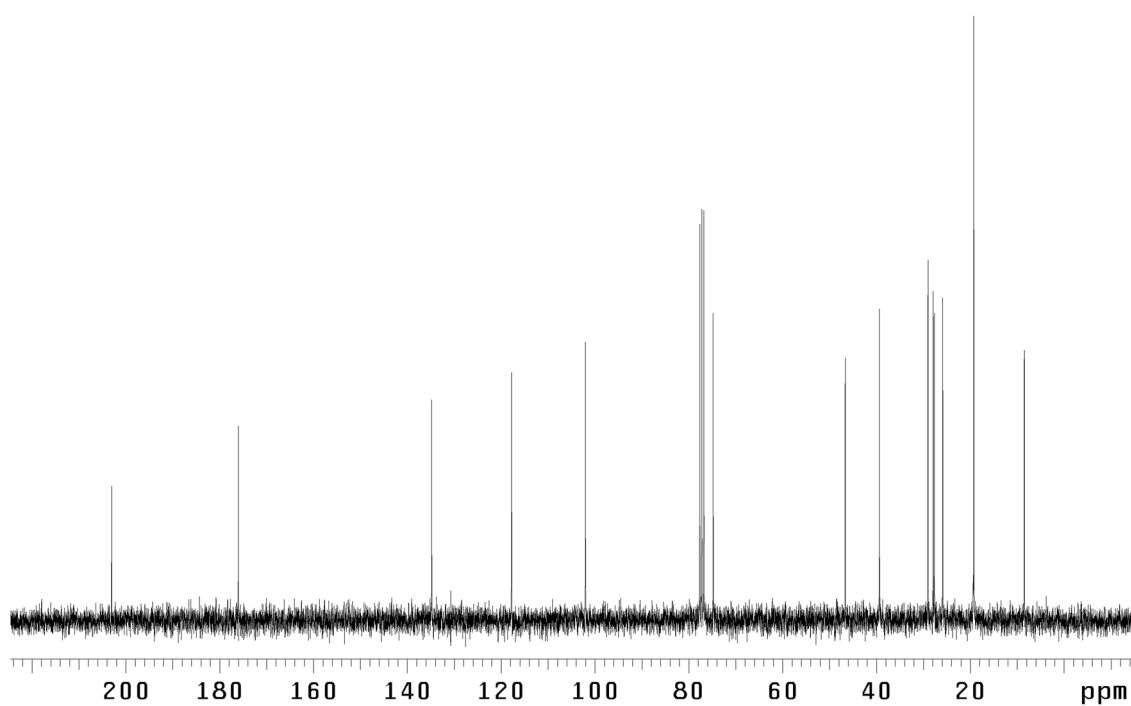


Figure A2.45 ¹³C NMR (75 MHz, CDCl₃) of compound **70**.

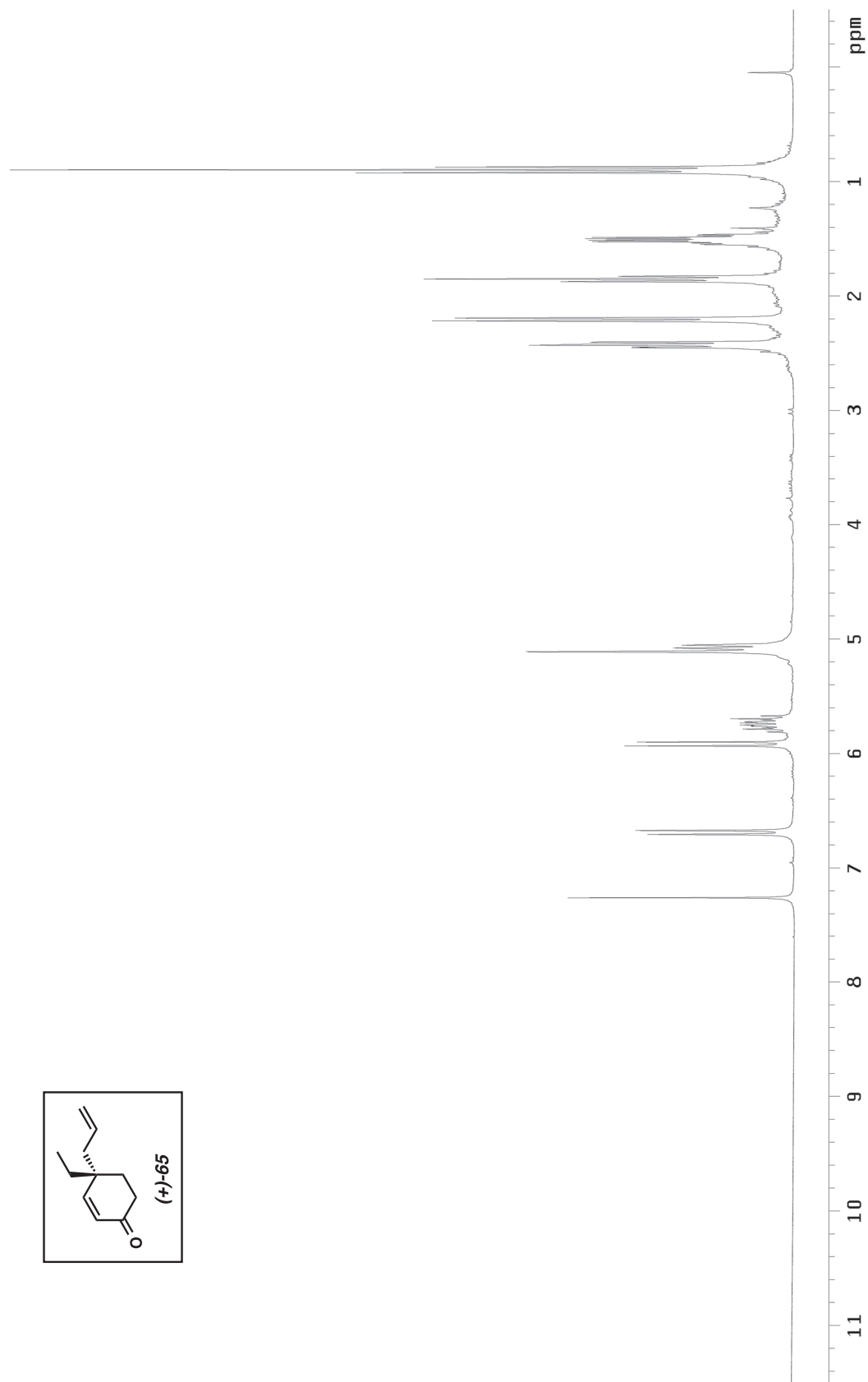


Figure A2.46 ¹H NMR (300 MHz, CDCl₃) of compound 65.

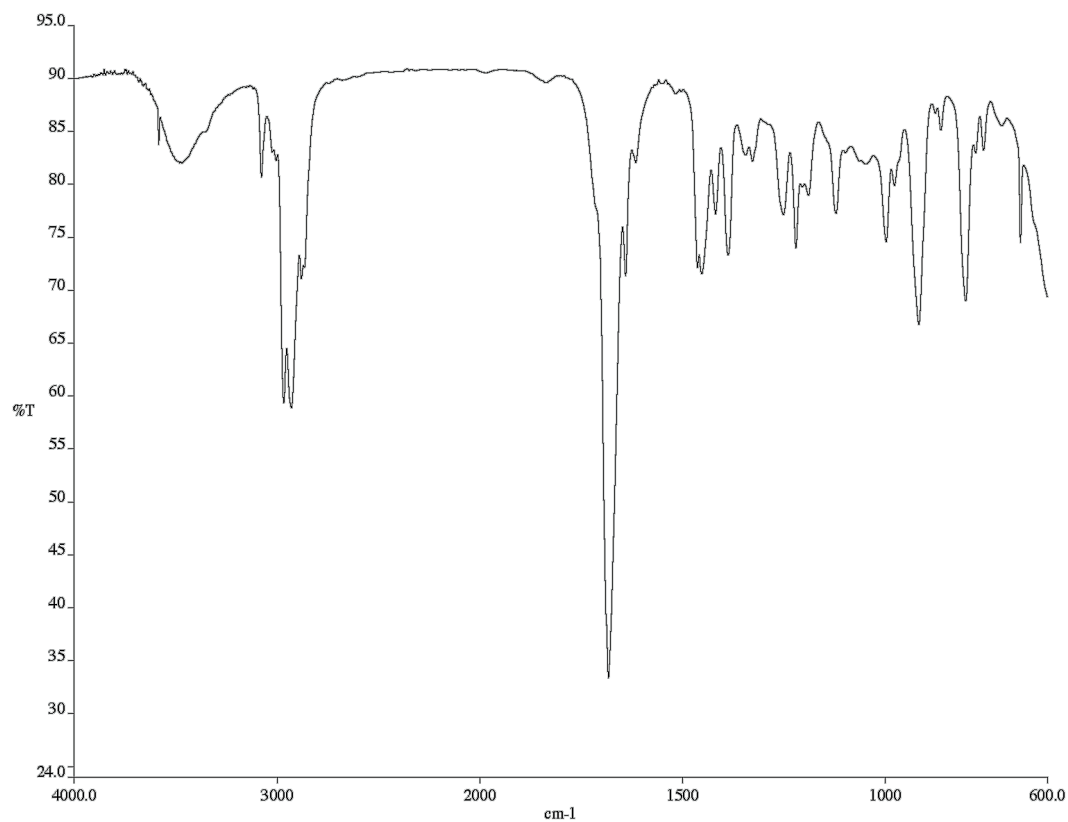


Figure A2.47 Infrared spectrum (Thin Film, NaCl) of compound **65**.

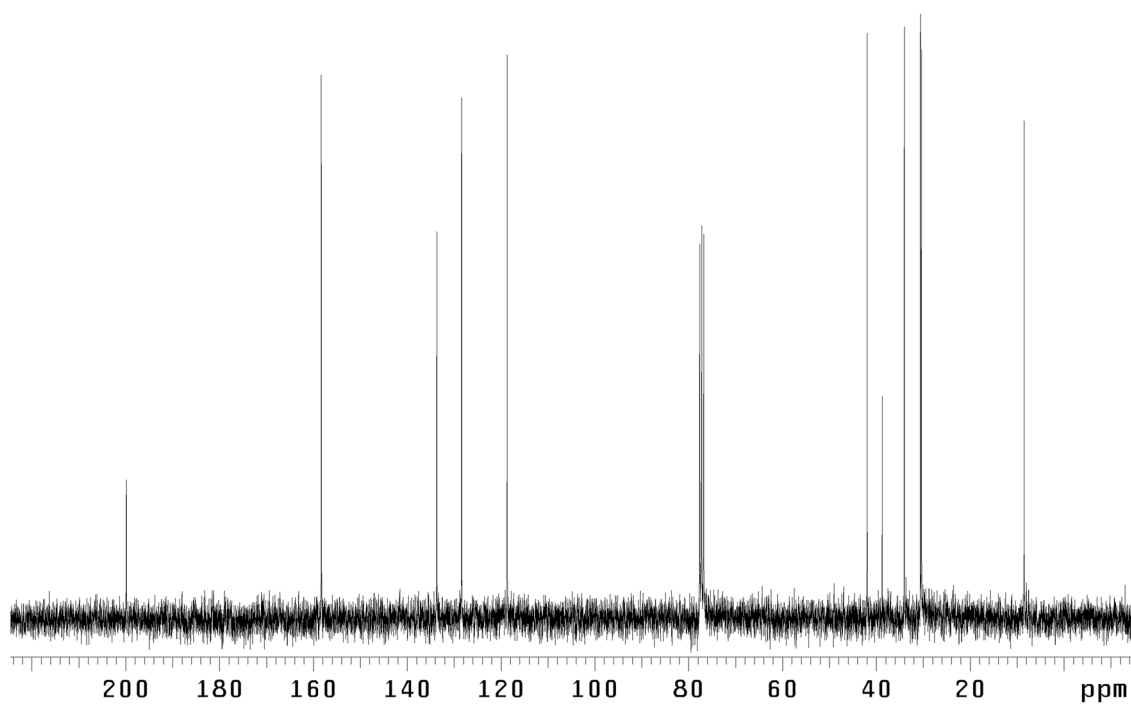


Figure A2.48 ¹³C NMR (75 MHz, CDCl₃) of compound **65**.

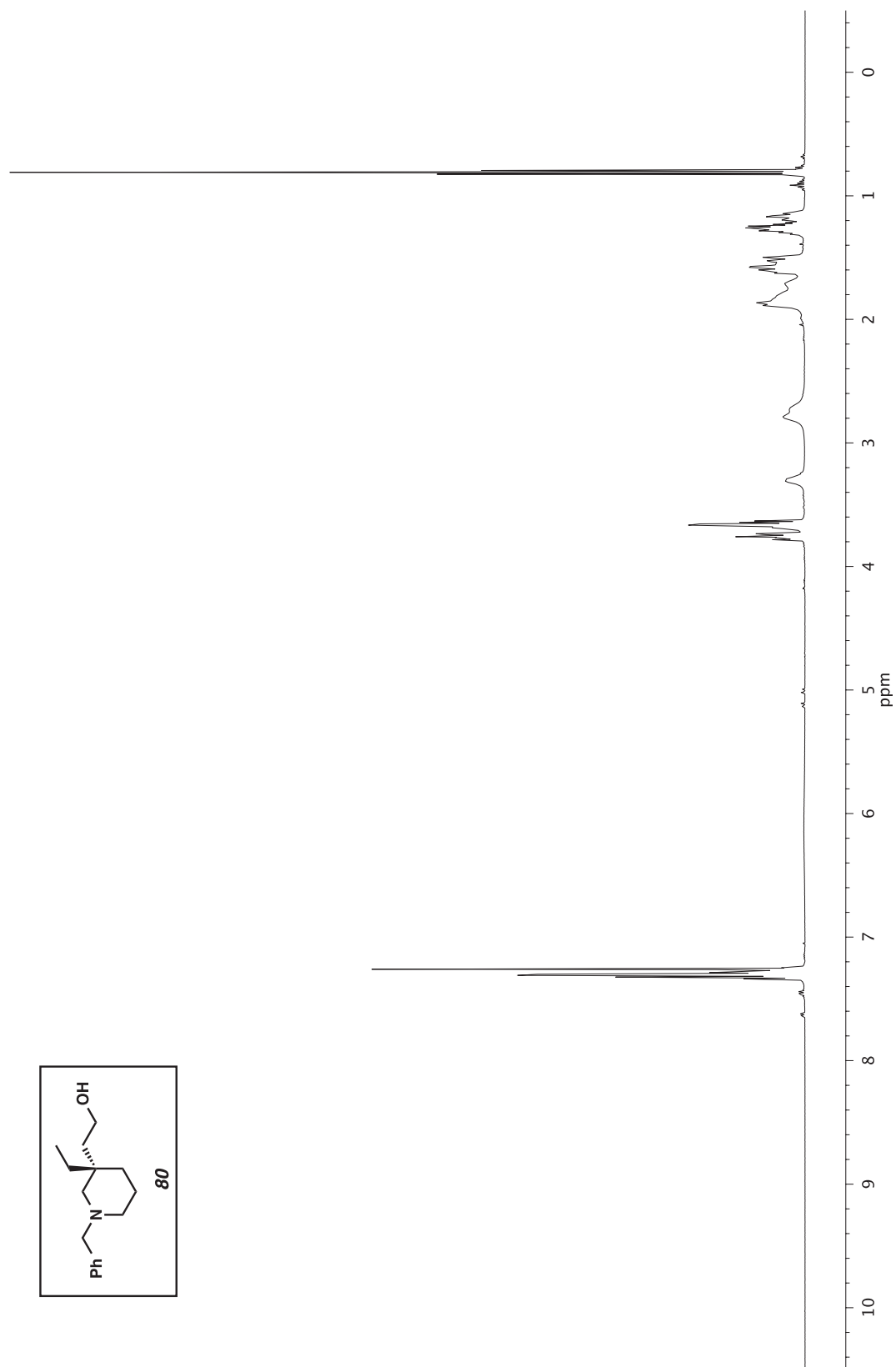


Figure A2.49 ^1H NMR (500 MHz, CDCl_3) of compound **80**.

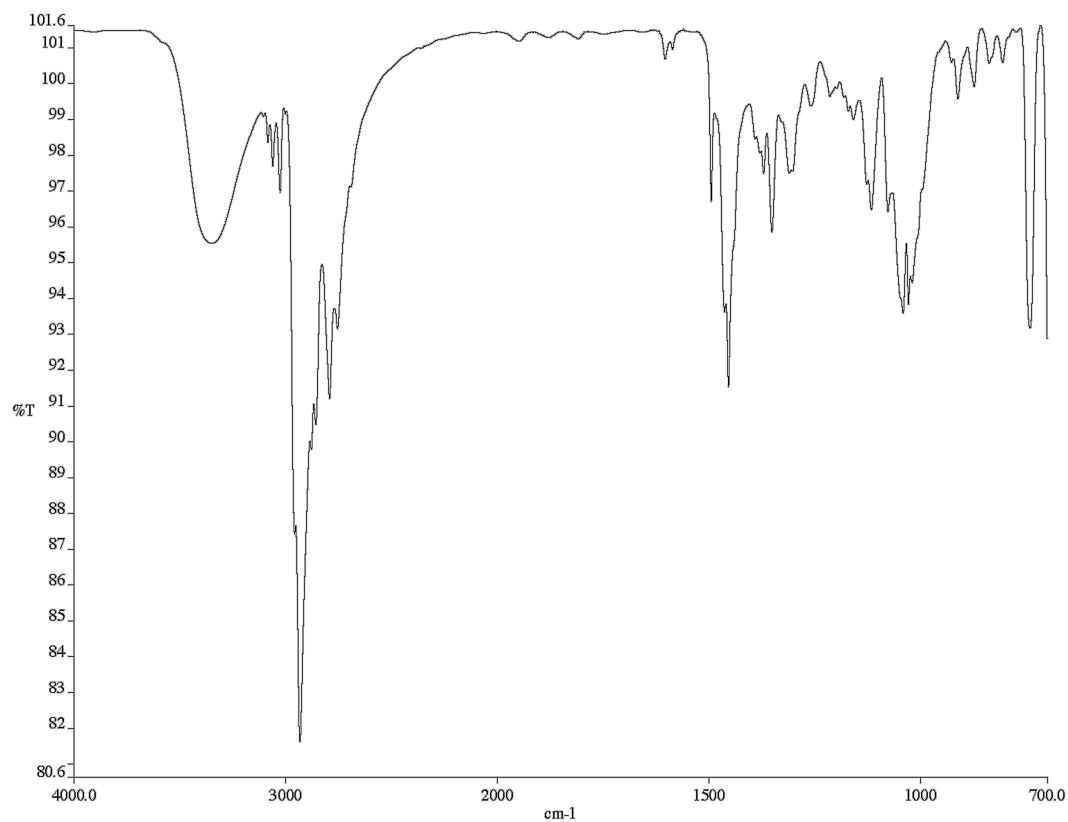


Figure A2.50 Infrared spectrum (Thin Film, NaCl) of compound **80**.

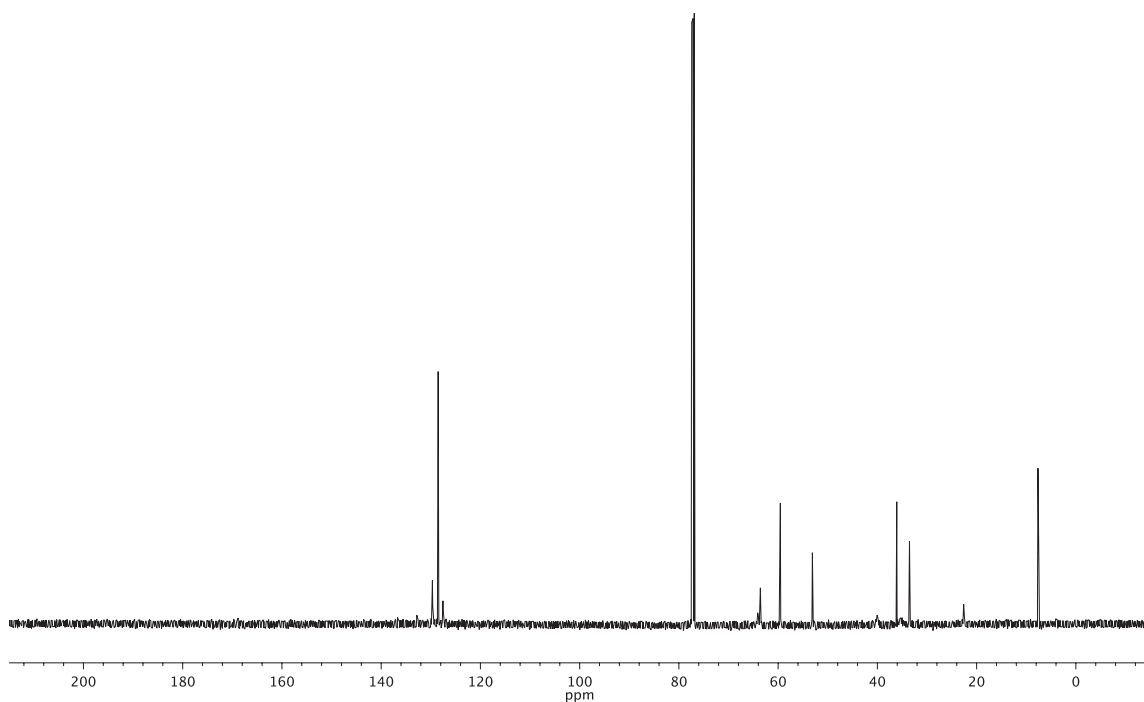


Figure A2.51 ¹³C NMR (126 MHz, CDCl₃) of compound **80**.

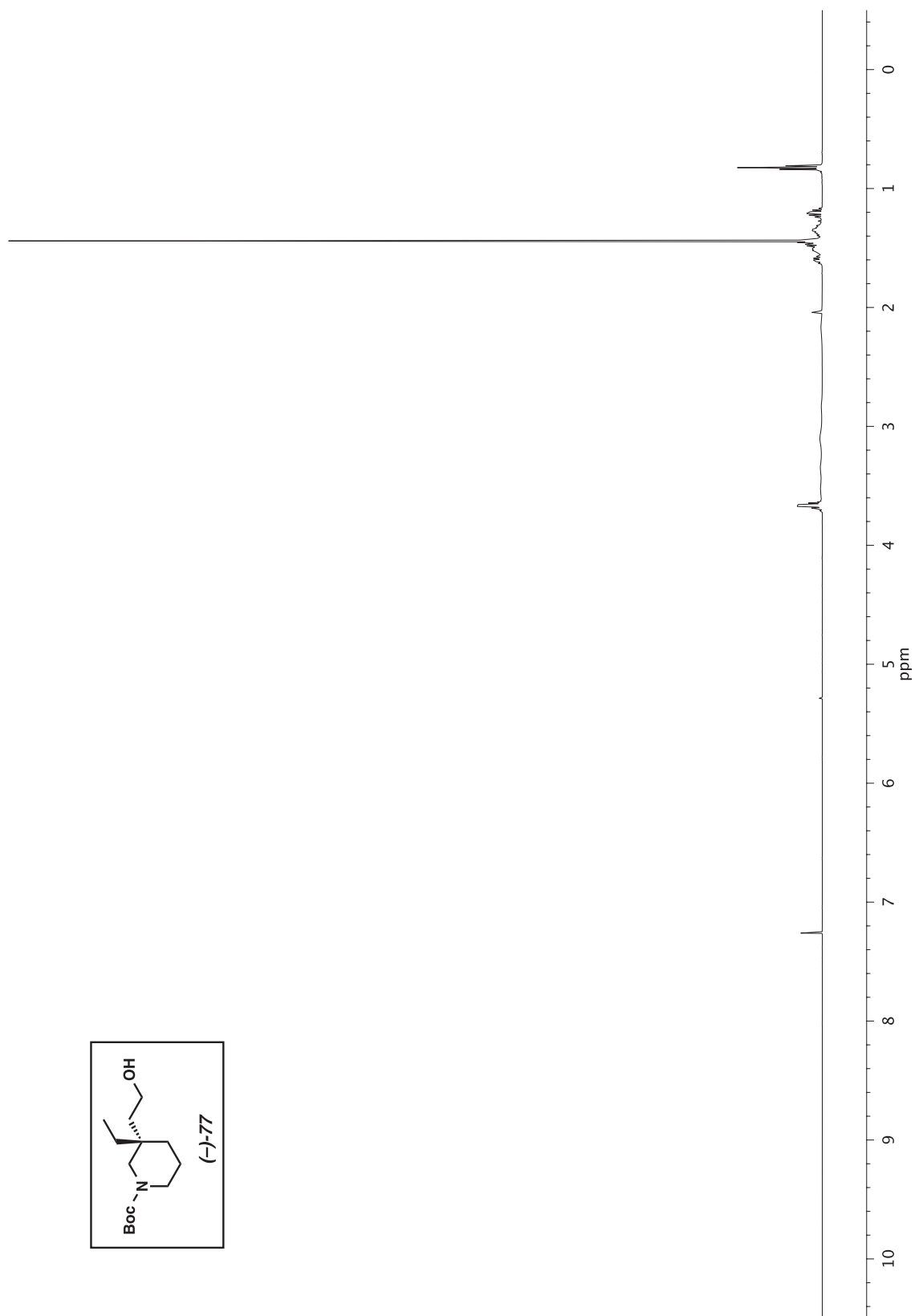


Figure A2.52 ¹H NMR (500 MHz, CDCl₃) of compound 77.

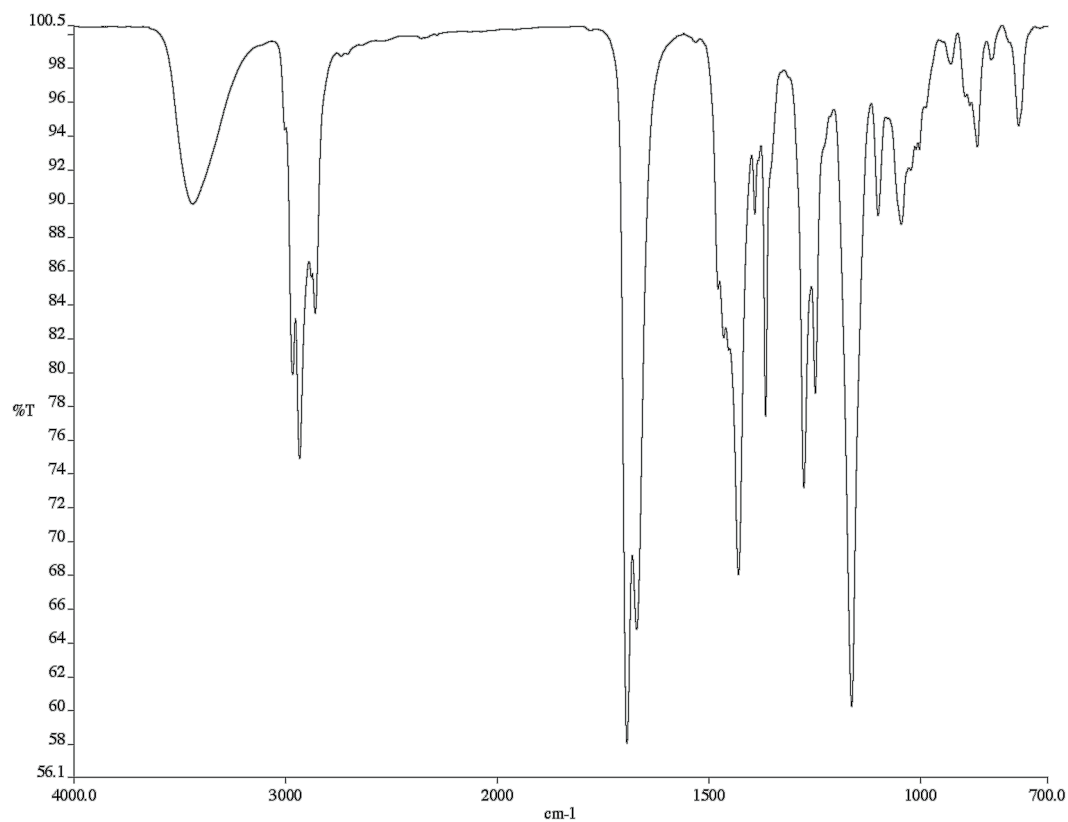


Figure A2.53 Infrared spectrum (Thin Film, NaCl) of compound 77.

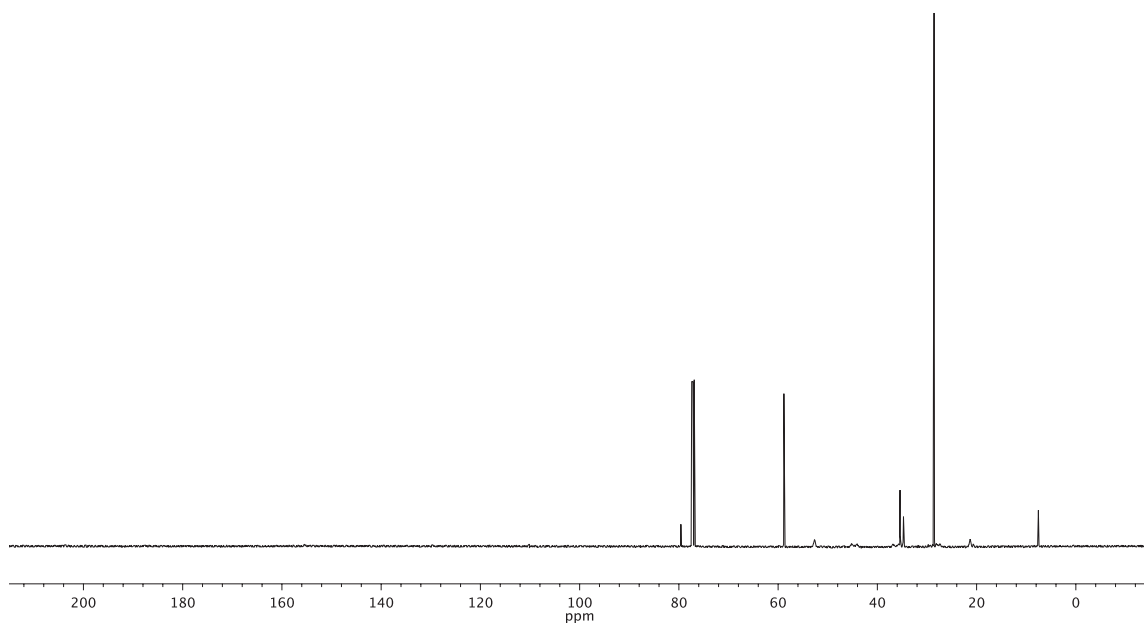


Figure A2.54 ¹³C NMR (126 MHz, CDCl₃) of compound 77.

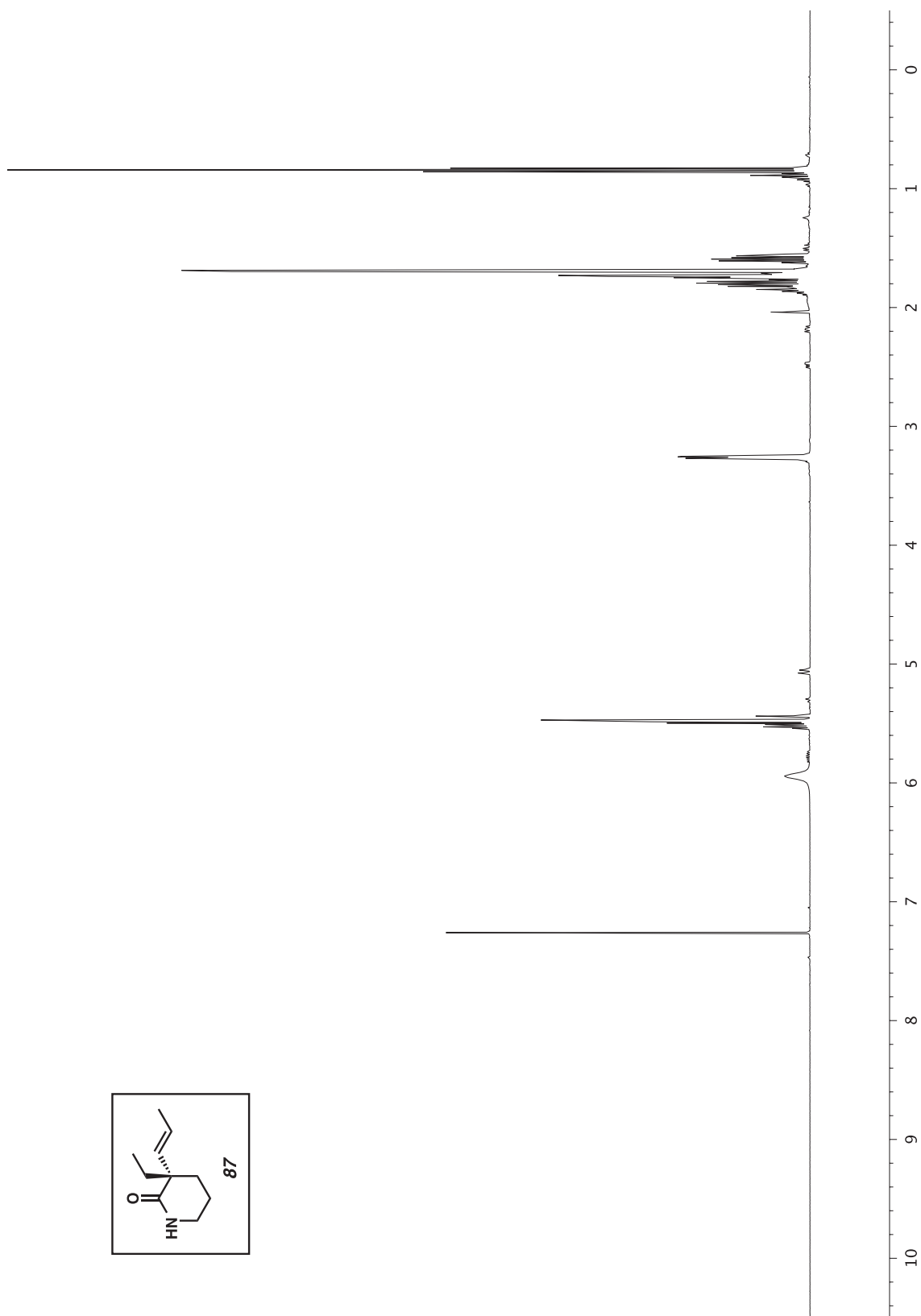


Figure A2.55 ^1H NMR (500 MHz, CDCl_3) of compound **87**.

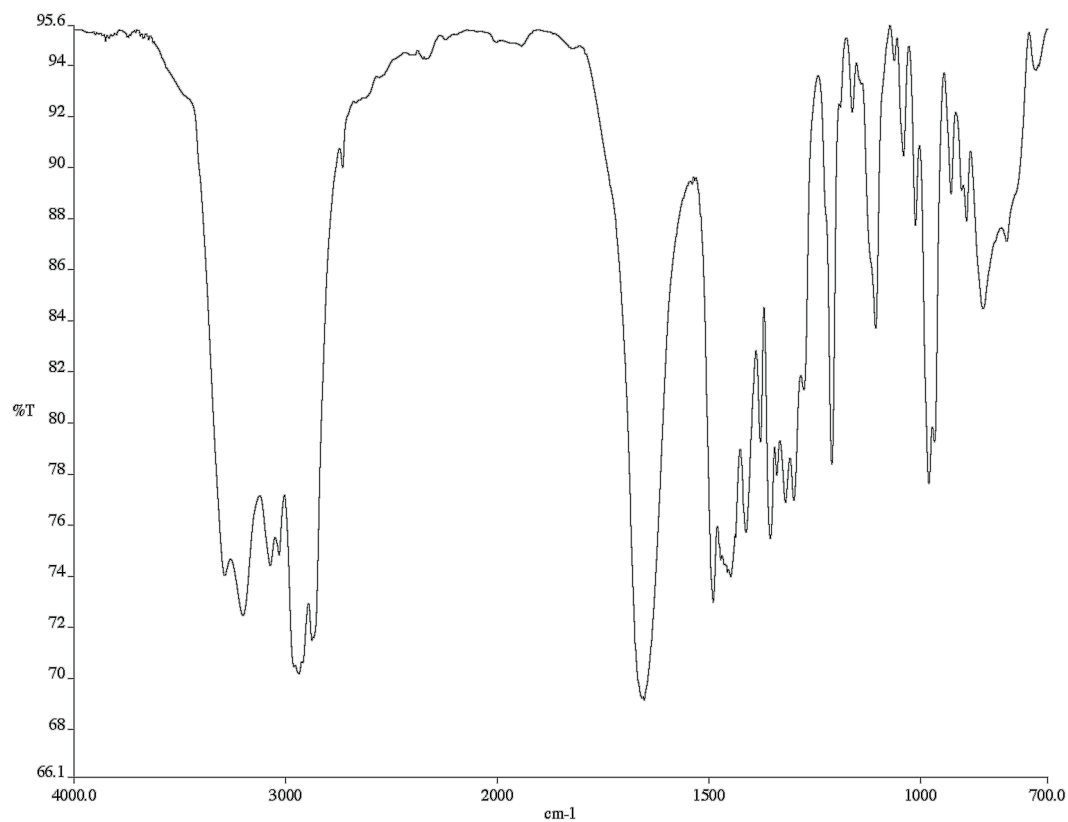


Figure A2.56 Infrared spectrum (Thin Film, NaCl) of compound **87**.

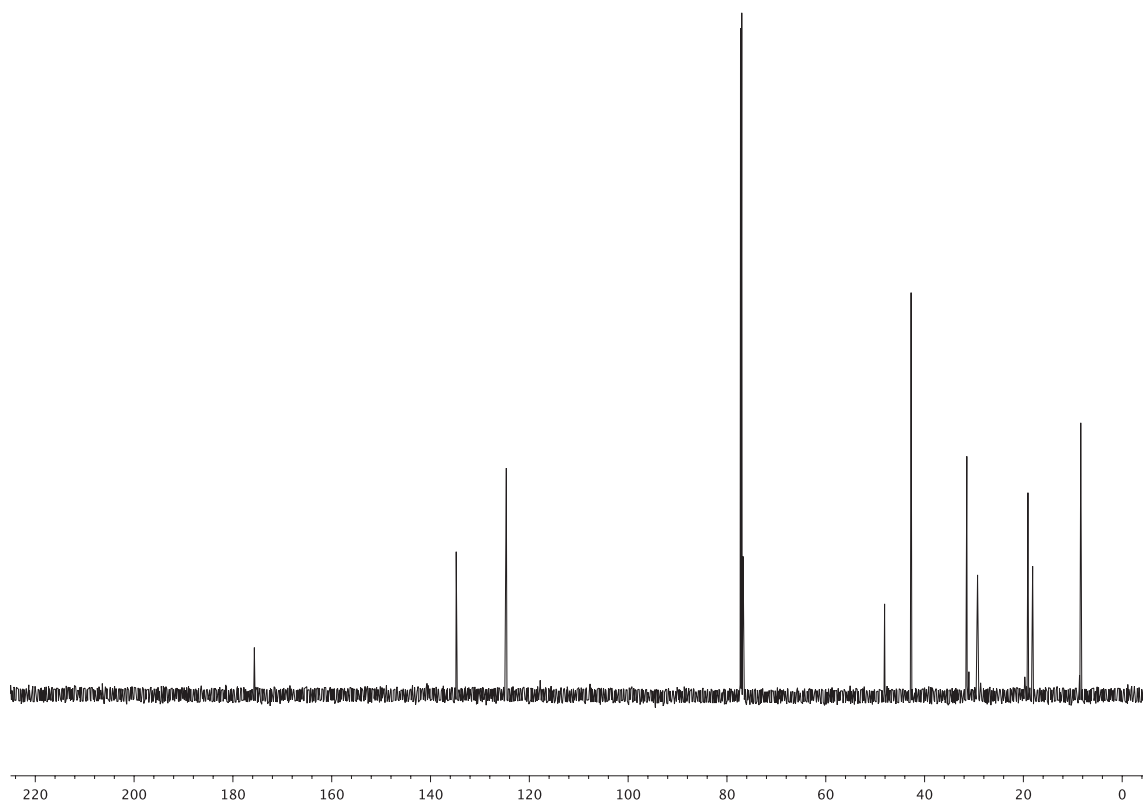


Figure A2.57 ¹³C NMR (126 MHz, CDCl₃) of compound **87**.

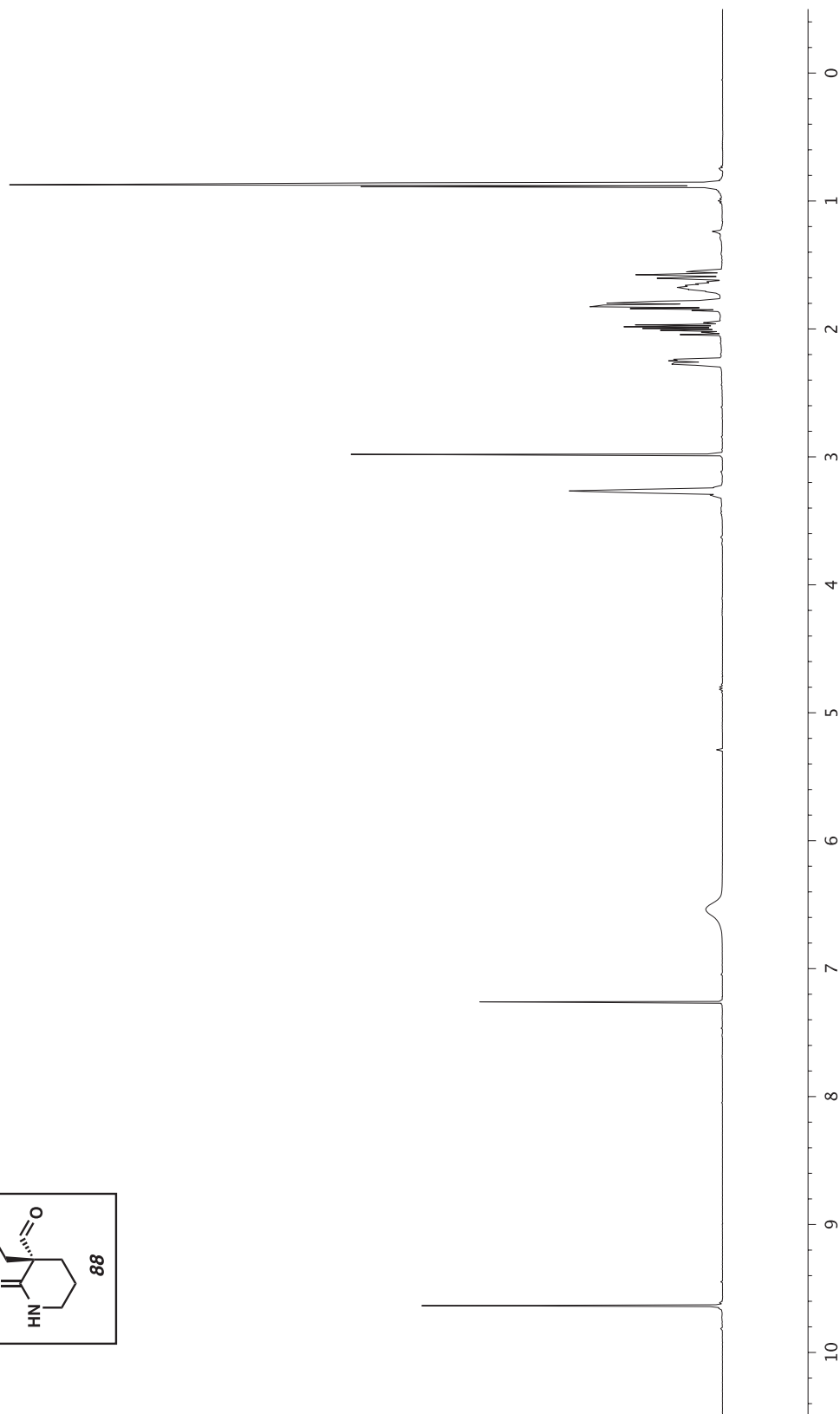
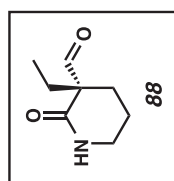


Figure A2.58 ¹H NMR (500 MHz, CDCl₃) of compound **88**.

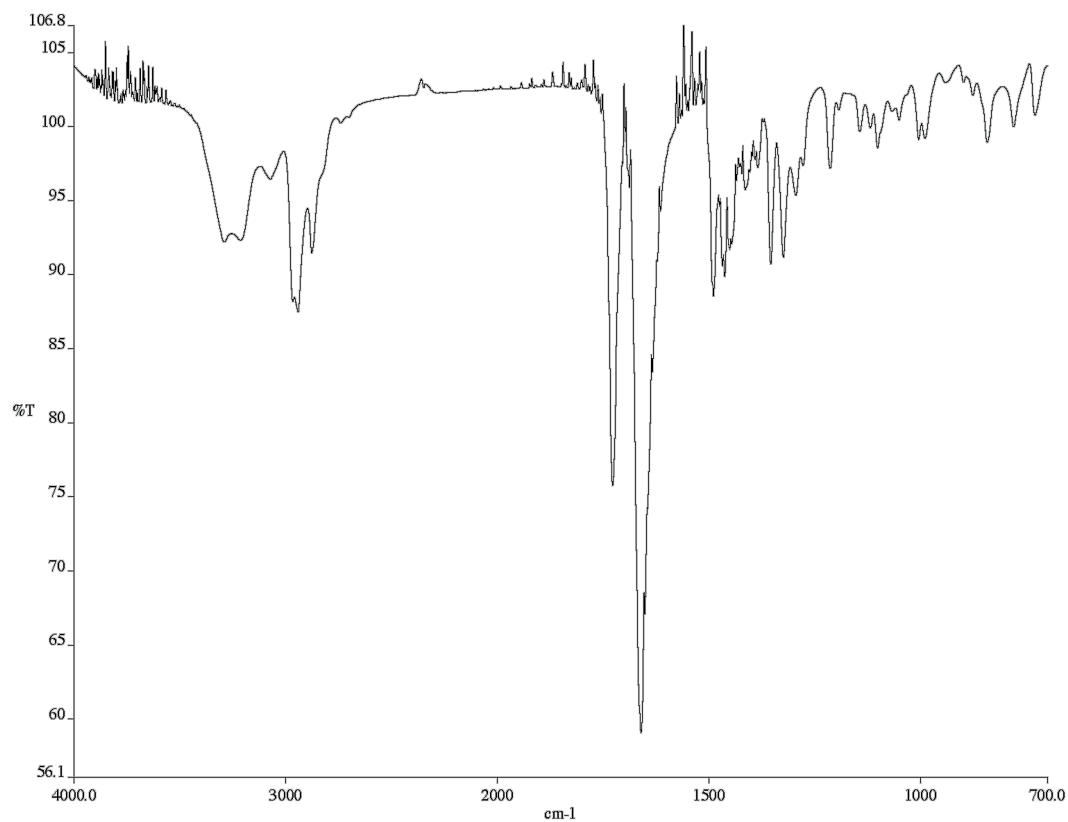


Figure A2.59 Infrared spectrum (Thin Film, NaCl) of compound **88**.

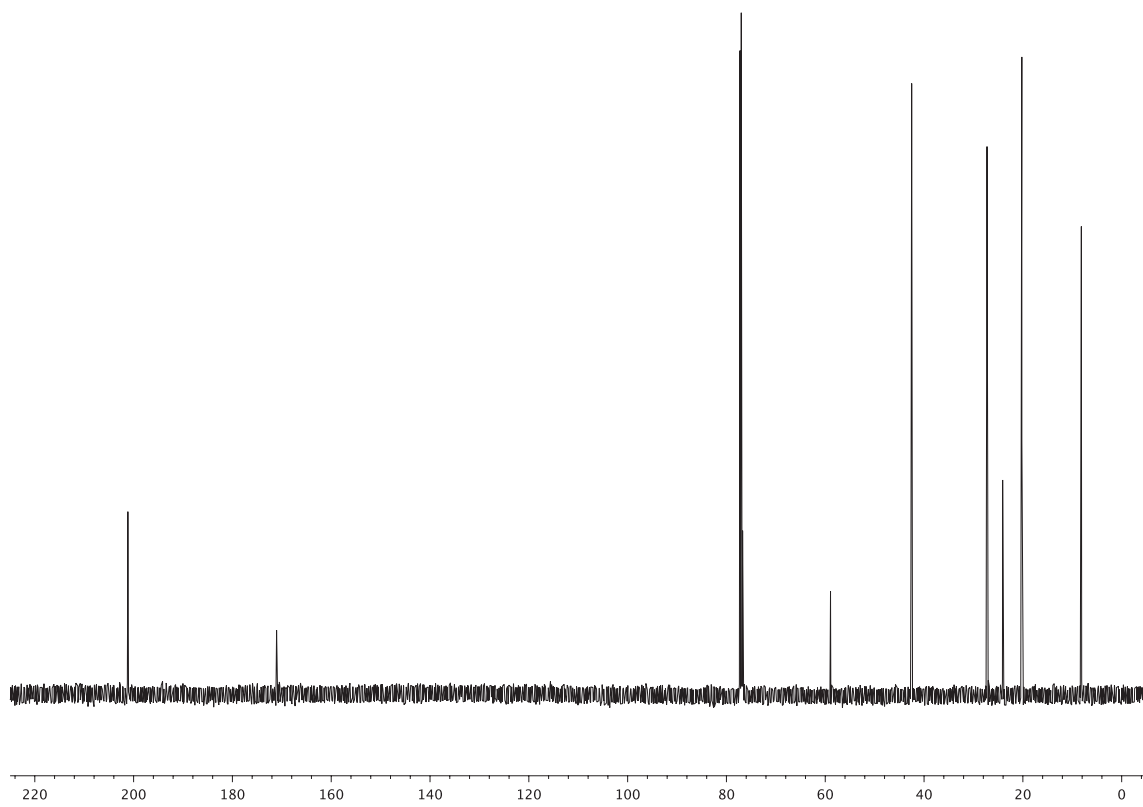


Figure A2.60 ¹³C NMR (126 MHz, CDCl₃) of compound **88**.

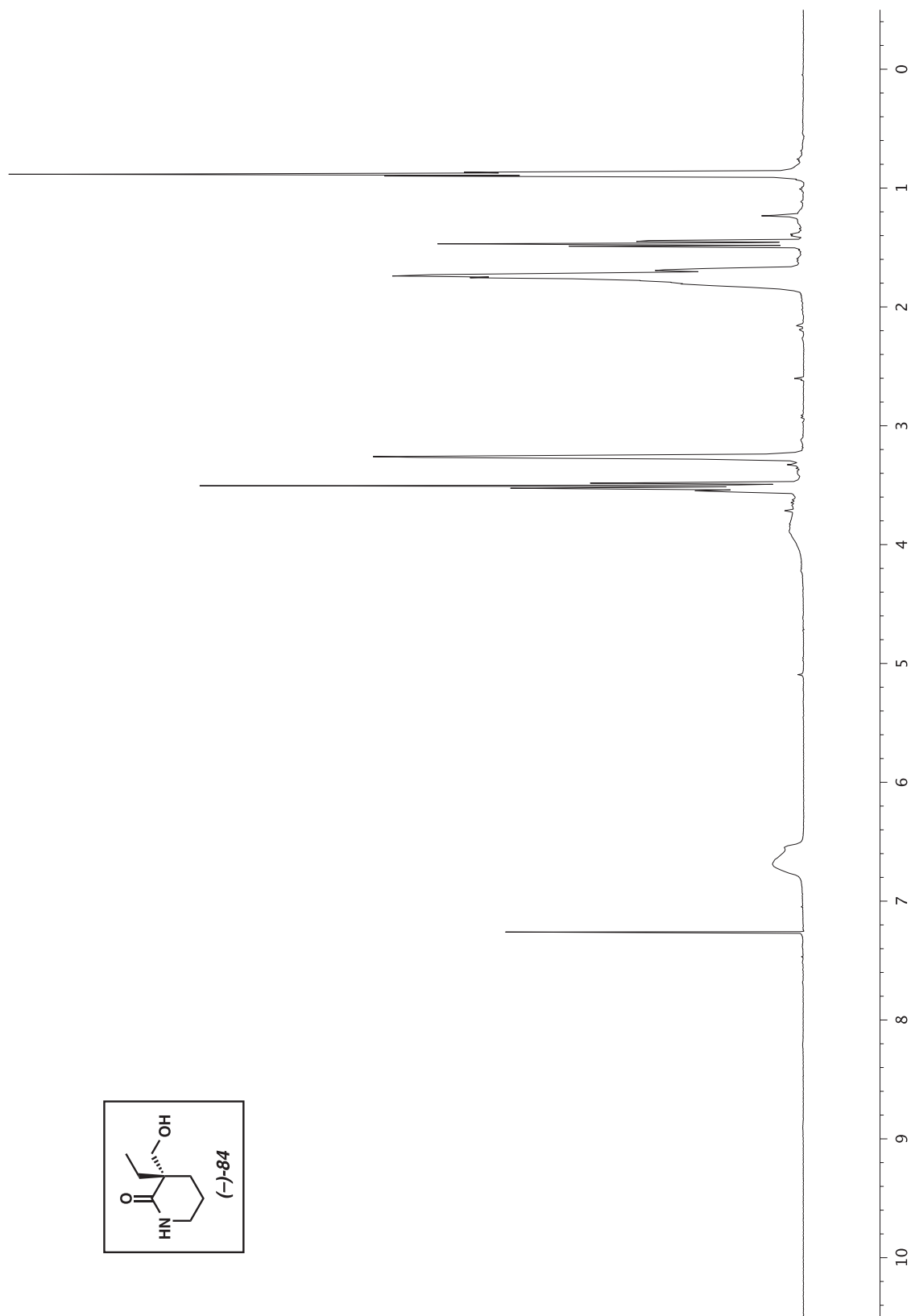


Figure A2.61 ^1H NMR (500 MHz, CDCl_3) of compound **84**.

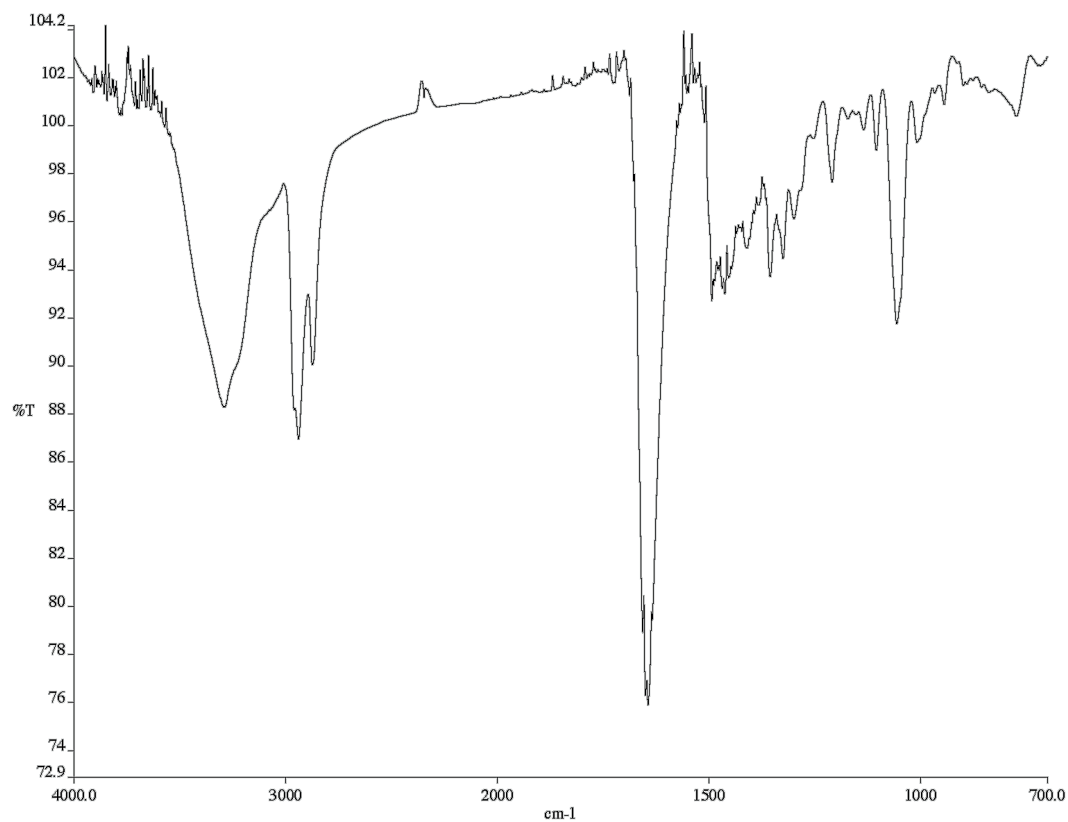


Figure A2.62 Infrared spectrum (Thin Film, NaCl) of compound **84**.

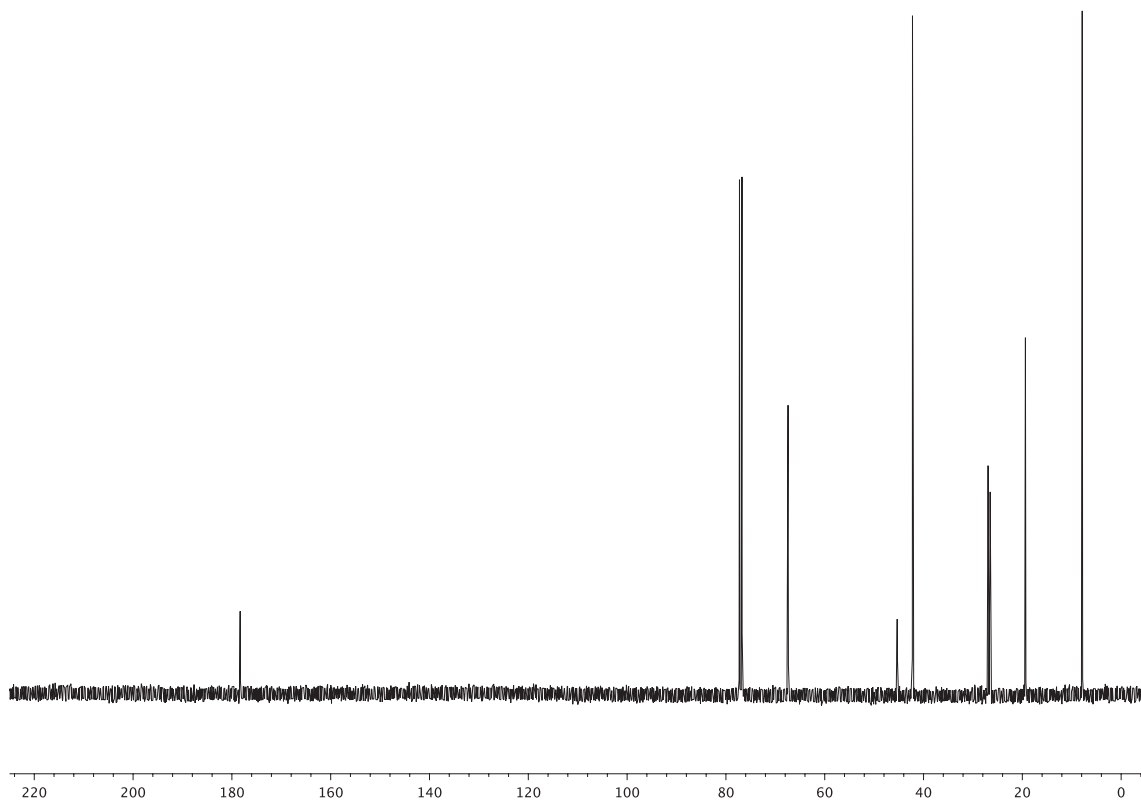


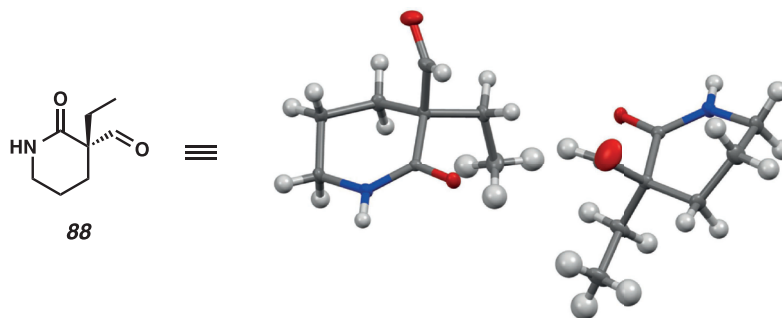
Figure A2.63 ¹³C NMR (126 MHz, CDCl₃) of compound **84**.

APPENDIX 3

X-Ray Crystallographic Data Relevant to Chapter 3

X-Ray Structure Determination

Low-temperature diffraction data (ϕ - and ω -scans) were collected on a Bruker Kappa diffractometer coupled to a Apex II CCD detector with graphite monochromated Mo K_α radiation ($\lambda = 0.71073 \text{ \AA}$) for the structure of compound **88** and (\pm)-**84**. The structure was solved by direct methods using SHELXS¹ and refined against F^2 on all data by full-matrix least squares with SHELXL-2013² using established refinement techniques.³ All non-hydrogen atoms were refined anisotropically. Unless otherwise noted, all hydrogen atoms were included into the model at geometrically calculated positions and refined using a riding model. The isotropic displacement parameters of all hydrogen atoms were fixed to 1.2 times the U value of the atoms they are linked to (1.5 times for methyl groups).



Compound **88** crystallizes in the monoclinic space group $P2_1$ with two molecules in the asymmetric unit. The coordinates for the hydrogen atoms bound to N1 and N2 were located in the difference Fourier synthesis and refined semi-freely with the help of a distance restraint. The N-H distances were restrained to be $0.88(4) \text{ \AA}$. The absolute configuration was determined during the synthetic procedure and is consistent with the

¹ Sheldrick, G. M. *Acta Cryst.* **1990**, A46, 467–473.

² Sheldrick, G. M. *Acta Cryst.* **2008**, A64, 112–122.

³ Müller, P. *Crystallography Reviews* **2009**, 15, 57–83.

diffraction data. Bayesian statistics P2(true) 0.977, P3(true)... 0.680, P3(rac-twin) 0.304, P3(false) .. 0.016.⁴

Table A3.1 Crystal data and structure refinement for **88**.

Identification code	A14103	
CCDC Deposition Number	1000826	
Empirical formula	C ₈ H ₁₃ N O ₂	
Formula weight	155.19	
Temperature	100(2) K	
Wavelength	0.71073 Å	
Crystal system	Monoclinic	
Space group	P 21	
Unit cell dimensions	a = 8.1906(13) Å	α = 90°.
	b = 10.4809(17) Å	β = 110.678(7)°.
	c = 10.3279(16) Å	γ = 90°.
Volume	829.5(2) Å ³	
Z	4	
Density (calculated)	1.243 Mg/m ³	
Absorption coefficient	0.089 mm ⁻¹	
F(000)	336	
Crystal size	0.700 x 0.070 x 0.050 mm ³	
Theta range for data collection	2.108 to 36.313°.	
Index ranges	-13 ≤ h ≤ 13, -17 ≤ k ≤ 17, -17 ≤ l ≤ 17	
Reflections collected	39923	
Independent reflections	8043 [R(int) = 0.0504]	
Completeness to theta = 25.242°	100.0 %	
Absorption correction	Semi-empirical from equivalents	
Max. and min. transmission	0.7474 and 0.6748	
Refinement method	Full-matrix least-squares on F ²	

⁴ Hoft, R.; Straver, L.; Spek, A. *J. Appl. Cryst.* **2008**, *41*, 96–103.

Data / restraints / parameters	8043 / 3 / 207
Goodness-of-fit on F^2	1.034
Final R indices [$I > 2\sigma(I)$]	R1 = 0.0436, wR2 = 0.1030
R indices (all data)	R1 = 0.0578, wR2 = 0.1104
Absolute structure parameter	0.0(4)
Extinction coefficient	n/a
Largest diff. peak and hole	0.439 and -0.239 $e \cdot \text{\AA}^{-3}$

Table A3.2 Atomic coordinates ($\times 10^4$) and equivalent isotropic displacement parameters ($\text{\AA}^2 \times 10^3$) for **88**. $U(\text{eq})$ is defined as one third of the trace of the orthogonalized U^{ij} tensor.

	x	y	z	U(eq)
C(1)	5129(2)	2251(1)	3426(1)	11(1)
O(1)	4972(1)	2819(1)	2328(1)	15(1)
C(2)	6748(2)	1423(1)	4116(1)	12(1)
C(6)	6594(2)	318(1)	3110(2)	17(1)
O(2)	7134(2)	-744(1)	3455(1)	25(1)
C(7)	8414(2)	2137(1)	4138(1)	16(1)
C(8)	8695(2)	3426(2)	4864(2)	25(1)
C(3)	6914(2)	931(1)	5548(1)	17(1)
C(4)	5150(2)	517(1)	5581(2)	19(1)
C(5)	3940(2)	1663(1)	5263(2)	18(1)
N(1)	3887(1)	2283(1)	3982(1)	13(1)
C(11)	10512(2)	4123(1)	1308(1)	12(1)
O(3)	10666(1)	3510(1)	2374(1)	16(1)
C(12)	8793(2)	4826(1)	554(1)	14(1)
C(16)	7434(2)	3755(2)	91(2)	24(1)
O(4)	6589(2)	3526(2)	-1097(2)	47(1)
C(17)	8355(2)	5646(2)	1638(2)	23(1)
C(18)	6550(2)	6260(2)	1077(2)	30(1)
C(13)	8826(2)	5624(2)	-676(2)	20(1)
C(14)	9870(2)	4978(2)	-1451(2)	24(1)
C(15)	11737(2)	4807(2)	-482(2)	21(1)
N(2)	11786(1)	4161(1)	787(1)	16(1)

Table A3.3 Bond lengths [\AA] and angles [$^\circ$] for **88**

C(1)-O(1)	1.2460(15)
C(1)-N(1)	1.3336(16)
C(1)-C(2)	1.5334(17)
C(2)-C(3)	1.5262(19)
C(2)-C(6)	1.5311(19)
C(2)-C(7)	1.5497(18)
C(6)-O(2)	1.2037(18)
C(6)-H(6)	0.9500
C(7)-C(8)	1.523(2)
C(7)-H(7A)	0.9900
C(7)-H(7B)	0.9900
C(8)-H(8A)	0.9800
C(8)-H(8B)	0.9800
C(8)-H(8C)	0.9800
C(3)-C(4)	1.5208(19)
C(3)-H(3A)	0.9900
C(3)-H(3B)	0.9900
C(4)-C(5)	1.5176(19)
C(4)-H(4A)	0.9900
C(4)-H(4B)	0.9900
C(5)-N(1)	1.4617(17)
C(5)-H(5A)	0.9900
C(5)-H(5B)	0.9900
N(1)-H(1N)	0.901(17)
C(11)-O(3)	1.2420(16)
C(11)-N(2)	1.3334(17)
C(11)-C(12)	1.5352(17)
C(12)-C(13)	1.5286(19)
C(12)-C(16)	1.533(2)
C(12)-C(17)	1.552(2)
C(16)-O(4)	1.202(2)
C(16)-H(16)	0.9500
C(17)-C(18)	1.526(2)
C(17)-H(17A)	0.9900
C(17)-H(17B)	0.9900
C(18)-H(18A)	0.9800
C(18)-H(18B)	0.9800

C(18)-H(18C)	0.9800
C(13)-C(14)	1.521(2)
C(13)-H(13A)	0.9900
C(13)-H(13B)	0.9900
C(14)-C(15)	1.514(2)
C(14)-H(14A)	0.9900
C(14)-H(14B)	0.9900
C(15)-N(2)	1.4625(18)
C(15)-H(15A)	0.9900
C(15)-H(15B)	0.9900
N(2)-H(2N)	0.851(17)
O(1)-C(1)-N(1)	122.04(11)
O(1)-C(1)-C(2)	119.17(11)
N(1)-C(1)-C(2)	118.69(11)
C(3)-C(2)-C(6)	111.08(11)
C(3)-C(2)-C(1)	114.09(10)
C(6)-C(2)-C(1)	105.21(10)
C(3)-C(2)-C(7)	111.85(10)
C(6)-C(2)-C(7)	103.66(11)
C(1)-C(2)-C(7)	110.25(10)
O(2)-C(6)-C(2)	124.42(13)
O(2)-C(6)-H(6)	117.8
C(2)-C(6)-H(6)	117.8
C(8)-C(7)-C(2)	114.49(12)
C(8)-C(7)-H(7A)	108.6
C(2)-C(7)-H(7A)	108.6
C(8)-C(7)-H(7B)	108.6
C(2)-C(7)-H(7B)	108.6
H(7A)-C(7)-H(7B)	107.6
C(7)-C(8)-H(8A)	109.5
C(7)-C(8)-H(8B)	109.5
H(8A)-C(8)-H(8B)	109.5
C(7)-C(8)-H(8C)	109.5
H(8A)-C(8)-H(8C)	109.5
H(8B)-C(8)-H(8C)	109.5
C(4)-C(3)-C(2)	110.99(10)
C(4)-C(3)-H(3A)	109.4
C(2)-C(3)-H(3A)	109.4
C(4)-C(3)-H(3B)	109.4

C(2)-C(3)-H(3B)	109.4
H(3A)-C(3)-H(3B)	108.0
C(5)-C(4)-C(3)	108.79(11)
C(5)-C(4)-H(4A)	109.9
C(3)-C(4)-H(4A)	109.9
C(5)-C(4)-H(4B)	109.9
C(3)-C(4)-H(4B)	109.9
H(4A)-C(4)-H(4B)	108.3
N(1)-C(5)-C(4)	110.86(11)
N(1)-C(5)-H(5A)	109.5
C(4)-C(5)-H(5A)	109.5
N(1)-C(5)-H(5B)	109.5
C(4)-C(5)-H(5B)	109.5
H(5A)-C(5)-H(5B)	108.1
C(1)-N(1)-C(5)	126.55(11)
C(1)-N(1)-H(1N)	115.4(13)
C(5)-N(1)-H(1N)	118.0(13)
O(3)-C(11)-N(2)	121.64(11)
O(3)-C(11)-C(12)	119.05(11)
N(2)-C(11)-C(12)	119.30(11)
C(13)-C(12)-C(16)	111.43(11)
C(13)-C(12)-C(11)	113.70(11)
C(16)-C(12)-C(11)	103.98(11)
C(13)-C(12)-C(17)	111.89(12)
C(16)-C(12)-C(17)	107.65(12)
C(11)-C(12)-C(17)	107.73(10)
O(4)-C(16)-C(12)	123.93(15)
O(4)-C(16)-H(16)	118.0
C(12)-C(16)-H(16)	118.0
C(18)-C(17)-C(12)	113.55(12)
C(18)-C(17)-H(17A)	108.9
C(12)-C(17)-H(17A)	108.9
C(18)-C(17)-H(17B)	108.9
C(12)-C(17)-H(17B)	108.9
H(17A)-C(17)-H(17B)	107.7
C(17)-C(18)-H(18A)	109.5
C(17)-C(18)-H(18B)	109.5
H(18A)-C(18)-H(18B)	109.5
C(17)-C(18)-H(18C)	109.5
H(18A)-C(18)-H(18C)	109.5

H(18B)-C(18)-H(18C)	109.5
C(14)-C(13)-C(12)	111.85(12)
C(14)-C(13)-H(13A)	109.2
C(12)-C(13)-H(13A)	109.2
C(14)-C(13)-H(13B)	109.2
C(12)-C(13)-H(13B)	109.2
H(13A)-C(13)-H(13B)	107.9
C(15)-C(14)-C(13)	109.24(13)
C(15)-C(14)-H(14A)	109.8
C(13)-C(14)-H(14A)	109.8
C(15)-C(14)-H(14B)	109.8
C(13)-C(14)-H(14B)	109.8
H(14A)-C(14)-H(14B)	108.3
N(2)-C(15)-C(14)	110.44(12)
N(2)-C(15)-H(15A)	109.6
C(14)-C(15)-H(15A)	109.6
N(2)-C(15)-H(15B)	109.6
C(14)-C(15)-H(15B)	109.6
H(15A)-C(15)-H(15B)	108.1
C(11)-N(2)-C(15)	126.69(11)
C(11)-N(2)-H(2N)	115.7(14)
C(15)-N(2)-H(2N)	117.6(14)

Table A3.4 Anisotropic displacement parameters ($\text{\AA}^2 \times 10^3$) for **88**. The anisotropic displacement factor exponent takes the form: $-2p^2[h^2 a^* U^{11} + \dots + 2hk a^* b^* U^{12}]$

	U^{11}	U^{22}	U^{33}	U^{23}	U^{13}	U^{12}
C(1)	9(1)	11(1)	11(1)	0(1)	2(1)	0(1)
O(1)	14(1)	18(1)	13(1)	4(1)	5(1)	2(1)
C(2)	9(1)	14(1)	12(1)	1(1)	4(1)	1(1)
C(6)	13(1)	19(1)	19(1)	-4(1)	5(1)	2(1)
O(2)	21(1)	17(1)	36(1)	-3(1)	7(1)	3(1)
C(7)	9(1)	20(1)	18(1)	2(1)	5(1)	-1(1)
C(8)	23(1)	26(1)	26(1)	-7(1)	8(1)	-11(1)
C(3)	13(1)	22(1)	14(1)	7(1)	3(1)	4(1)
C(4)	18(1)	18(1)	23(1)	9(1)	11(1)	4(1)
C(5)	18(1)	20(1)	21(1)	8(1)	12(1)	5(1)

N(1)	11(1)	15(1)	15(1)	4(1)	6(1)	4(1)
C(11)	11(1)	12(1)	12(1)	0(1)	3(1)	0(1)
O(3)	14(1)	20(1)	14(1)	6(1)	5(1)	4(1)
C(12)	11(1)	16(1)	13(1)	4(1)	3(1)	3(1)
C(16)	14(1)	24(1)	30(1)	7(1)	1(1)	-2(1)
O(4)	34(1)	52(1)	37(1)	-1(1)	-7(1)	-20(1)
C(17)	20(1)	30(1)	17(1)	2(1)	5(1)	11(1)
C(18)	25(1)	39(1)	28(1)	7(1)	11(1)	18(1)
C(13)	18(1)	22(1)	18(1)	9(1)	7(1)	6(1)
C(14)	25(1)	31(1)	16(1)	8(1)	8(1)	7(1)
C(15)	21(1)	26(1)	21(1)	11(1)	12(1)	6(1)
N(2)	12(1)	19(1)	16(1)	6(1)	6(1)	4(1)

Table A3.5 Hydrogen coordinates ($\times 10^4$) and isotropic displacement parameters ($\text{\AA}^2 \times 10^3$) for **88**.

	x	y	z	U(eq)
H(6)	6035	481	2149	21
H(7A)	9440	1590	4603	19
H(7B)	8351	2267	3172	19
H(8A)	7744	4005	4359	38
H(8B)	9810	3787	4891	38
H(8C)	8712	3315	5811	38
H(3A)	7729	199	5795	20
H(3B)	7401	1612	6241	20
H(4A)	4651	-162	4887	22
H(4B)	5288	172	6506	22
H(5A)	2750	1385	5174	22
H(5B)	4350	2280	6037	22
H(1N)	2940(20)	2750(20)	3510(20)	16
H(16)	7250	3243	786	29
H(17A)	8425	5102	2439	27
H(17B)	9243	6327	1974	27
H(18A)	6455	6781	265	45
H(18B)	6381	6801	1793	45
H(18C)	5656	5591	812	45

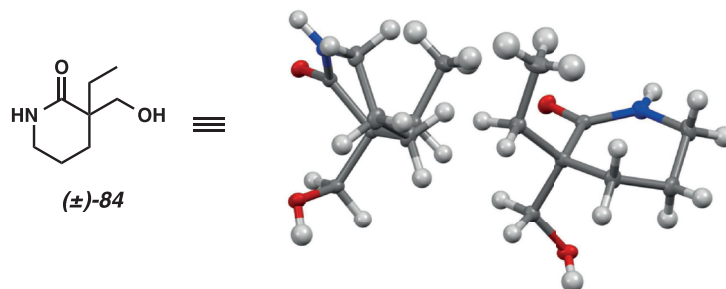
H(13A)	7615	5763	-1318	23
H(13B)	9345	6468	-340	23
H(14A)	9351	4138	-1802	28
H(14B)	9842	5508	-2252	28
H(15A)	12388	4297	-946	25
H(15B)	12309	5651	-249	25
H(2N)	12730(20)	3790(20)	1260(20)	19

Table A3.6 Hydrogen bonds for **88** [Å and °].

D-H...A	d(D-H)	d(H...A)	d(D...A)	<(DHA)
C(5)-H(5B)...O(2)#1	0.99	2.55	3.277(2)	130.3
N(1)-H(1N)...O(3)#2	0.901(17)	1.984(17)	2.8771(15)	171(2)
N(2)-H(2N)...O(1)#3	0.851(17)	2.047(17)	2.8963(15)	177(2)

Symmetry transformations used to generate equivalent atoms:

#1 -x+1,y+1/2,-z+1 #2 x-1,y,z #3 x+1,y,z



Compound (±)-**84** crystallizes in the triclinic space group $P\bar{1}$ with two molecules in the asymmetric unit. The structure was refined with two twin domains related by a 2-fold axis, twin law $(-100/0-10/001)$. The twin ratio refined to 0.1275(16):0.8725(16). The highest electron density maxima are located on the bonds between atoms.

Table A3.7 Crystal data and structure refinement for (±)-**84**.

Identification code	A14199	
CCDC Deposition Number	1002339	
Empirical formula	C ₈ H ₁₅ N O ₂	
Formula weight	157.21	
Temperature	100(2) K	
Wavelength	0.71073 Å	
Crystal system	Triclinic	
Space group	P -1	
Unit cell dimensions	$a = 6.0486(5) \text{ \AA}$	$\alpha = 89.349(5)^\circ$.
	$b = 11.6947(9) \text{ \AA}$	$\beta = 88.952(5)^\circ$.
	$c = 11.8938(9) \text{ \AA}$	$\gamma = 84.996(5)^\circ$.
Volume	$837.94(11) \text{ \AA}^3$	

Z	4
Density (calculated)	1.246 Mg/m ³
Absorption coefficient	0.089 mm ⁻¹
F(000)	344
Crystal size	0.250 x 0.200 x 0.150 mm ³
Theta range for data collection	1.713 to 35.630°.
Index ranges	-9<=h<=9, -19<=k<=19, -19<=l<=19
Reflections collected	48695
Independent reflections	7714 [R(int) = 0.0550]
Completeness to theta = 25.242°	100.0 %
Absorption correction	Semi-empirical from equivalents
Max. and min. transmission	0.7471 and 0.6469
Refinement method	Full-matrix least-squares on F ²
Data / restraints / parameters	7714 / 4 / 214
Goodness-of-fit on F ²	1.078
Final R indices [I>2sigma(I)]	R1 = 0.0793, wR2 = 0.2239
R indices (all data)	R1 = 0.1022, wR2 = 0.2511
Extinction coefficient	n/a
Largest diff. peak and hole	0.709 and -0.413 e.Å ⁻³

Table A3.8 Atomic coordinates ($\times 10^4$) and equivalent isotropic displacement parameters ($\text{\AA}^2 \times 10^3$) for (\pm)-**84**. $U(\text{eq})$ is defined as one third of the trace of the orthogonalized U^{ij} tensor.

	x	y	z	U(eq)
N(1)	5794(3)	6168(2)	5728(2)	17(1)
C(1)	5529(3)	5411(2)	6563(2)	14(1)
O(1)	6927(2)	4579(1)	6721(1)	19(1)
C(2)	3485(3)	5561(2)	7352(2)	13(1)
C(3)	1921(3)	6634(2)	7084(2)	18(1)
C(6)	2270(3)	4459(2)	7288(2)	16(1)
O(2)	1294(2)	4312(1)	6233(1)	18(1)
C(7)	4304(3)	5600(2)	8571(2)	17(1)
C(8)	5917(4)	6501(2)	8764(2)	27(1)
C(4)	1908(3)	6950(2)	5834(2)	19(1)
C(5)	4248(4)	7153(2)	5440(2)	20(1)
N(101)	11065(3)	1082(1)	9237(1)	16(1)
C(101)	10787(3)	325(2)	8443(2)	13(1)
O(101)	12055(2)	-576(1)	8353(1)	17(1)
C(102)	8897(3)	540(2)	7617(2)	13(1)
C(103)	7567(3)	1713(2)	7772(2)	18(1)
C(106)	7405(3)	-457(2)	7767(2)	15(1)
O(102)	6312(2)	-464(1)	8840(1)	17(1)
C(107)	9890(3)	448(2)	6410(2)	16(1)
C(108)	11805(3)	1187(2)	6147(2)	21(1)
C(104)	7387(4)	2097(2)	8991(2)	20(1)
C(105)	9683(4)	2151(2)	9448(2)	19(1)

Table A3.9 Bond lengths [\AA] and angles [$^\circ$] for (\pm)-**84**.

N(1)-C(1)	1.340(3)
N(1)-C(5)	1.461(3)
N(1)-H(1N)	0.869(17)
C(1)-O(1)	1.247(2)
C(1)-C(2)	1.537(2)
C(2)-C(3)	1.538(2)
C(2)-C(6)	1.542(3)

C(2)-C(7)	1.542(3)
C(3)-C(4)	1.528(3)
C(3)-H(3A)	0.9900
C(3)-H(3B)	0.9900
C(6)-O(2)	1.415(2)
C(6)-H(6A)	0.9900
C(6)-H(6B)	0.9900
O(2)-H(2O)	0.820(18)
C(7)-C(8)	1.520(3)
C(7)-H(7A)	0.9900
C(7)-H(7B)	0.9900
C(8)-H(8A)	0.9800
C(8)-H(8B)	0.9800
C(8)-H(8C)	0.9800
C(4)-C(5)	1.520(3)
C(4)-H(4A)	0.9900
C(4)-H(4B)	0.9900
C(5)-H(5A)	0.9900
C(5)-H(5B)	0.9900
N(101)-C(101)	1.324(2)
N(101)-C(105)	1.464(2)
N(101)-H(01N)	0.880(17)
C(101)-O(101)	1.252(2)
C(101)-C(102)	1.524(2)
C(102)-C(103)	1.539(2)
C(102)-C(106)	1.543(3)
C(102)-C(107)	1.547(3)
C(103)-C(104)	1.522(3)
C(103)-H(10A)	0.9900
C(103)-H(10B)	0.9900
C(106)-O(102)	1.426(2)
C(106)-H(10C)	0.9900
C(106)-H(10D)	0.9900
O(102)-H(02O)	0.822(18)
C(107)-C(108)	1.531(3)
C(107)-H(10E)	0.9900
C(107)-H(10F)	0.9900
C(108)-H(10G)	0.9800
C(108)-H(10H)	0.9800
C(108)-H(10I)	0.9800

C(104)-C(105)	1.507(3)
C(104)-H(10J)	0.9900
C(104)-H(10K)	0.9900
C(105)-H(10L)	0.9900
C(105)-H(10M)	0.9900
C(1)-N(1)-C(5)	126.10(16)
C(1)-N(1)-H(1N)	121(2)
C(5)-N(1)-H(1N)	113(2)
O(1)-C(1)-N(1)	121.07(17)
O(1)-C(1)-C(2)	118.75(16)
N(1)-C(1)-C(2)	120.18(15)
C(1)-C(2)-C(3)	113.54(15)
C(1)-C(2)-C(6)	107.54(14)
C(3)-C(2)-C(6)	111.31(15)
C(1)-C(2)-C(7)	108.13(14)
C(3)-C(2)-C(7)	110.52(15)
C(6)-C(2)-C(7)	105.42(15)
C(4)-C(3)-C(2)	112.97(15)
C(4)-C(3)-H(3A)	109.0
C(2)-C(3)-H(3A)	109.0
C(4)-C(3)-H(3B)	109.0
C(2)-C(3)-H(3B)	109.0
H(3A)-C(3)-H(3B)	107.8
O(2)-C(6)-C(2)	113.33(15)
O(2)-C(6)-H(6A)	108.9
C(2)-C(6)-H(6A)	108.9
O(2)-C(6)-H(6B)	108.9
C(2)-C(6)-H(6B)	108.9
H(6A)-C(6)-H(6B)	107.7
C(6)-O(2)-H(2O)	109(3)
C(8)-C(7)-C(2)	114.14(17)
C(8)-C(7)-H(7A)	108.7
C(2)-C(7)-H(7A)	108.7
C(8)-C(7)-H(7B)	108.7
C(2)-C(7)-H(7B)	108.7
H(7A)-C(7)-H(7B)	107.6
C(7)-C(8)-H(8A)	109.5
C(7)-C(8)-H(8B)	109.5
H(8A)-C(8)-H(8B)	109.5

C(7)-C(8)-H(8C)	109.5
H(8A)-C(8)-H(8C)	109.5
H(8B)-C(8)-H(8C)	109.5
C(5)-C(4)-C(3)	109.48(17)
C(5)-C(4)-H(4A)	109.8
C(3)-C(4)-H(4A)	109.8
C(5)-C(4)-H(4B)	109.8
C(3)-C(4)-H(4B)	109.8
H(4A)-C(4)-H(4B)	108.2
N(1)-C(5)-C(4)	110.39(16)
N(1)-C(5)-H(5A)	109.6
C(4)-C(5)-H(5A)	109.6
N(1)-C(5)-H(5B)	109.6
C(4)-C(5)-H(5B)	109.6
H(5A)-C(5)-H(5B)	108.1
C(101)-N(101)-C(105)	126.71(16)
C(101)-N(101)-H(01N)	117(2)
C(105)-N(101)-H(01N)	116(2)
O(101)-C(101)-N(101)	121.24(16)
O(101)-C(101)-C(102)	118.64(16)
N(101)-C(101)-C(102)	120.12(15)
C(101)-C(102)-C(103)	113.21(15)
C(101)-C(102)-C(106)	106.96(14)
C(103)-C(102)-C(106)	111.53(15)
C(101)-C(102)-C(107)	108.21(14)
C(103)-C(102)-C(107)	110.07(15)
C(106)-C(102)-C(107)	106.57(14)
C(104)-C(103)-C(102)	113.37(15)
C(104)-C(103)-H(10A)	108.9
C(102)-C(103)-H(10A)	108.9
C(104)-C(103)-H(10B)	108.9
C(102)-C(103)-H(10B)	108.9
H(10A)-C(103)-H(10B)	107.7
O(102)-C(106)-C(102)	113.08(15)
O(102)-C(106)-H(10C)	109.0
C(102)-C(106)-H(10C)	109.0
O(102)-C(106)-H(10D)	109.0
C(102)-C(106)-H(10D)	109.0
H(10C)-C(106)-H(10D)	107.8
C(106)-O(102)-H(02O)	104(3)

C(108)-C(107)-C(102)	115.97(16)
C(108)-C(107)-H(10E)	108.3
C(102)-C(107)-H(10E)	108.3
C(108)-C(107)-H(10F)	108.3
C(102)-C(107)-H(10F)	108.3
H(10E)-C(107)-H(10F)	107.4
C(107)-C(108)-H(10G)	109.5
C(107)-C(108)-H(10H)	109.5
H(10G)-C(108)-H(10H)	109.5
C(107)-C(108)-H(10I)	109.5
H(10G)-C(108)-H(10I)	109.5
H(10H)-C(108)-H(10I)	109.5
C(105)-C(104)-C(103)	109.30(17)
C(105)-C(104)-H(10J)	109.8
C(103)-C(104)-H(10J)	109.8
C(105)-C(104)-H(10K)	109.8
C(103)-C(104)-H(10K)	109.8
H(10J)-C(104)-H(10K)	108.3
N(101)-C(105)-C(104)	111.07(16)
N(101)-C(105)-H(10L)	109.4
C(104)-C(105)-H(10L)	109.4
N(101)-C(105)-H(10M)	109.4
C(104)-C(105)-H(10M)	109.4
H(10L)-C(105)-H(10M)	108.0

Symmetry transformations used to generate equivalent atoms:

Table A3.10 Anisotropic displacement parameters ($\text{\AA}^2 \times 10^3$) for (\pm)-**84**. The anisotropic displacement factor exponent takes the form: $-2p^2[h^2 a^* U^{11} + \dots + 2 h k a^* b^* U^{12}]$

	U^{11}	U^{22}	U^{33}	U^{23}	U^{13}	U^{12}
N(1)	16(1)	17(1)	17(1)	0(1)	4(1)	0(1)
C(1)	12(1)	13(1)	16(1)	-3(1)	1(1)	1(1)
O(1)	13(1)	19(1)	23(1)	-1(1)	1(1)	6(1)
C(2)	11(1)	12(1)	15(1)	-1(1)	2(1)	2(1)
C(3)	17(1)	15(1)	21(1)	0(1)	3(1)	6(1)
C(6)	15(1)	14(1)	18(1)	0(1)	1(1)	-1(1)

O(2)	12(1)	22(1)	19(1)	-5(1)	1(1)	-1(1)
C(7)	18(1)	19(1)	15(1)	-1(1)	0(1)	-1(1)
C(8)	26(1)	36(1)	21(1)	-10(1)	3(1)	-14(1)
C(4)	20(1)	15(1)	22(1)	2(1)	-3(1)	5(1)
C(5)	25(1)	15(1)	20(1)	3(1)	2(1)	0(1)
N(101)	16(1)	14(1)	16(1)	-1(1)	-4(1)	0(1)
C(101)	12(1)	11(1)	15(1)	0(1)	0(1)	1(1)
O(101)	12(1)	15(1)	22(1)	0(1)	-1(1)	4(1)
C(102)	13(1)	12(1)	14(1)	0(1)	-2(1)	2(1)
C(103)	20(1)	15(1)	19(1)	-2(1)	-5(1)	7(1)
C(106)	12(1)	15(1)	17(1)	-1(1)	-1(1)	-2(1)
O(102)	12(1)	24(1)	17(1)	2(1)	0(1)	-1(1)
C(107)	18(1)	17(1)	14(1)	-1(1)	1(1)	-2(1)
C(108)	20(1)	23(1)	20(1)	2(1)	-1(1)	-6(1)
C(104)	22(1)	15(1)	21(1)	-2(1)	0(1)	7(1)
C(105)	26(1)	12(1)	18(1)	-2(1)	-3(1)	1(1)

Table A3.11 Hydrogen coordinates ($\times 10^4$) and isotropic displacement parameters ($\text{\AA}^2 \times 10^3$) for (\pm)-**84**.

	x	y	z	U(eq)
H(1N)	6870(40)	6050(30)	5240(20)	20
H(3A)	395	6497	7333	21
H(3B)	2382	7289	7516	21
H(6A)	3338	3788	7444	19
H(6B)	1096	4481	7881	19
H(2O)	-50(30)	4450(30)	6300(30)	27
H(7A)	3002	5752	9081	20
H(7B)	5034	4837	8773	20
H(8A)	7266	6324	8307	41
H(8B)	6301	6502	9561	41
H(8C)	5225	7259	8549	41
H(4A)	1357	6320	5398	23
H(4B)	903	7652	5709	23
H(5A)	4271	7279	4615	24
H(5B)	4714	7851	5800	24

H(01N)	12130(40)	910(30)	9720(20)	19
H(10A)	8287	2297	7320	22
H(10B)	6055	1670	7480	22
H(10C)	6274	-400	7173	18
H(10D)	8323	-1193	7668	18
H(02O)	5030(30)	-580(30)	8690(30)	26
H(10E)	10420	-365	6274	19
H(10F)	8687	659	5873	19
H(10G)	11282	2000	6225	31
H(10H)	12348	1044	5376	31
H(10I)	13012	991	6673	31
H(10J)	6554	2863	9038	24
H(10K)	6574	1549	9444	24
H(10L)	10384	2800	9088	23
H(10M)	9577	2290	10268	23

Table A3.12 Hydrogen bonds for (\pm)-**84** [\AA and $^\circ$].

D-H...A	d(D-H)	d(H...A)	d(D...A)	\angle (DHA)
N(1)-H(1N)...O(2)#1	0.869(17)	2.08(2)	2.926(2)	163(3)
O(2)-H(2O)...O(1)#2	0.820(18)	1.880(19)	2.686(2)	168(4)
C(4)-H(4A)...O(2)	0.99	2.54	3.168(3)	121.0
N(101)-H(01N)...O(102)#3	0.880(17)	2.01(2)	2.858(2)	161(3)
O(102)-H(02O)...O(101)#2	0.822(18)	1.849(19)	2.664(2)	171(4)
C(104)-H(10K)...O(102)	0.99	2.49	3.128(3)	122.0

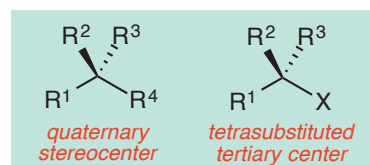
Symmetry transformations used to generate equivalent atoms:

#1 -x+1,-y+1,-z+1 #2 x-1,y,z #3 -x+2,-y,-z+2

APPENDIX 4

*Catalytic Enantioselective Construction of Quaternary Stereocenters:
Assembly of Key Building Blocks for the Synthesis of Biologically Active
Molecules[‡]*

CONSPECTUS: The ever-present demand for drugs with better efficacy and fewer side effects continually motivates scientists to explore the vast chemical space.



Traditionally, medicinal chemists have focused much attention on achiral or so-called “flat” molecules. More recently, attention has shifted toward molecules with stereogenic centers since their three-dimensional structures represent a much larger fraction of the chemical space and have a number of superior properties compared with flat aromatic

[‡] This account was written in collaboration with Seo-Jung Han and Dr. Wen-Bo Liu, and was partially adapted from the publication: Liu, Y.; Han, S.-J.; Liu, W.-B.; Stoltz, B. M. *Acc. Chem. Res.* **2015**, *48*, 740–751. Copyright 2015 American Chemical Society.

compounds. Quaternary stereocenters, in particular, add greatly to the three-dimensionality and novelty of the molecule. Nevertheless, synthetic challenges in building quaternary stereocenters have largely prevented their implementation in drug discovery. The lack of effective and broadly general methods for enantioselective formation of quaternary stereocenters in simple molecular scaffolds has prompted us to investigate new chemistry and develop innovative tools and solutions. In this Account, we describe three approaches to constructing quaternary stereocenters: nucleophilic substitution of 3-haloindoles, conjugate addition of boronic acids to cyclic enones, and allylic alkylation of enolates. In the first approach, malonic ester nucleophiles attack electrophilic 3-halooxindoles, mediated by a copper(II)-bisoxazoline catalyst. A variety of oxindoles containing a benzylic quaternary stereocenter can be accessed through this method. However, it is only applicable to the specialized 3,3-disubstituted oxindole system. To access benzylic quaternary stereocenters in a more general context, we turned our attention to the enantioselective conjugate addition of carbon nucleophiles to α,β -unsaturated carbonyl acceptors. We discovered that in the presence of catalytic palladium-pyridinooxazoline complex, arylboronic acids add smoothly to β -substituted cyclic enones to furnish ketones with a β -benzylic quaternary stereocenter in high yields and enantioselectivities. The reaction is compatible with a wide range of arylboronic acids, β -substituents, and ring sizes. Aside from benzylic quaternary stereocenters, a more challenging motif is a quaternary stereocenter not adjacent to an aromatic group. Such centers represent more general structures in chemical space, but are more difficult to form by asymmetric catalysis. To address this greater challenge, and motivated by the greater reward, we entered the field of palladium-catalyzed asymmetric allylic alkylation

of prochiral enolate nucleophiles about a decade ago. On the basis of Tsuji's work, which solved the issue of positional selectivity for unsymmetrical ketones, we discovered that the phosphinooxazoline ligand effectively rendered this reaction enantioselective. Extensive investigations since then have revealed that the reaction exhibits broad scope and accepts a range of substrate classes, each with its unique advantage in synthetic applications. A diverse array of carbonyl compounds bearing α -quaternary stereocenters are obtained in excellent yields and enantioselectivities, and more possibilities have yet to be explored. As an alternative to palladium catalysis, we also studied iridium-catalyzed asymmetric allylic alkylations that generate vicinal quaternary and tertiary stereocenters in a single transformation. Overall, these methods provide access to small molecule building blocks with a single quaternary stereocenter, can be applied to various molecular scaffolds, and tolerate a wide range of functional groups. We envision that the chemistry reported in this Account will be increasingly useful in drug discovery and design.

A4.1 Introduction

As humanity settles into the second decade of the 21st Century, science continues to press forward with new advances that alter our experiences on a daily basis. The fields of medicinal and pharmaceutical chemistry are no different, with new medicines becoming available to treat the most threatening and problematic maladies of the day. Although the landscape of drug discovery and the pharmaceutical industry continue to change, particularly with the vibrant increase in new types of large molecule medicinal agents, small molecule chemistry is likely to continue to play a critical role in the discovery of new active pharmaceutical ingredients (API) well into the future. Therefore,

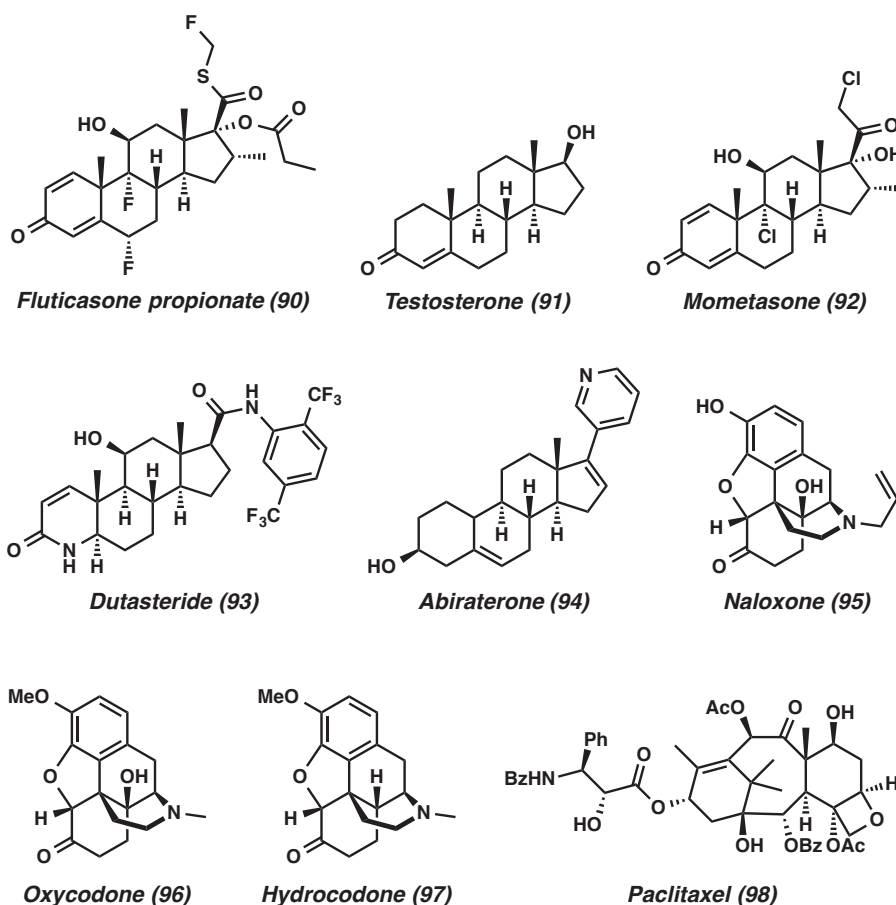
it is critical that academic chemists continue to develop thoughtful strategies, implement sound tactical maneuvers, and invent robust new technologies for the synthesis of biologically rich, complex small molecules that will allow medicinal chemists to explore new molecular space with functional compounds having better properties.

For many years, medicinal chemists have focused attention on achiral aromatic and heteroaromatic molecules as potential drug candidates.¹ This is in part due to the relative ease of their preparation, especially since the emergence of cross-coupling chemistries and parallel synthesis, and their biased population in screening suites at most companies. While many of such compounds have been developed into successful drugs, their lack of stereochemistry presents a number of drawbacks at a fundamental level. First, achiral or “flat” molecules occupy only a small fraction of chemical space. From a structural diversity perspective, a vast number of possibilities have not been explored. Second, the two-dimensional nature of aromatic molecules implies that their interaction with target proteins, which have a three-dimensional structure, will be limited. Therefore, high selectivity for binding to the desired protein (for instance) over undesired ones is difficult to achieve, and side effects such as cytotoxicity often pose a challenge. Finally, polyaromatic molecules tend to interact strongly with one another due to π -stacking, thereby resulting in low solubility and poor bioavailability.

A promising solution to the issues raised above is to incorporate sp^3 -hybridized carbon stereocenters into the molecule. This topic has been the subject of recent review articles and essays.² In particular, quaternary stereocenters, which bear four different carbon substituents at the four vertices of a tetrahedron, add greatly to the three-dimensionality of a molecule. However, construction of quaternary stereocenters via

chemical synthesis is extremely challenging.³ While 21 compounds out of the top 200 drugs by US retail sales in 2012⁴ have quaternary stereocenters (>10%, examples shown in Figure A4.1), all of those structures are derived from natural products. These include terpenoid (**90–94** and **98**) and morphine (**95–97**) derivatives, where the quaternary stereocenters are made by nature and the API is typically produced by peripheral derivatization. *Within those 200 top pharmaceuticals, none have a quaternary stereocenter built by chemical synthesis.* This dichotomy reflects the paucity of synthetic methods available for the construction of quaternary stereocenters and consequently the lack of their applications in drug discovery.

Figure A4.1 Drug molecules containing quaternary stereocenters



Traditional chemical approaches to quaternary stereocenters include the Claisen rearrangement⁵ and the Diels–Alder reaction.⁶ While these reactions are well established, the formation of the quaternary stereocenter is often accompanied by formation of other stereocenters nearby. From a drug discovery perspective, this potentially introduces unnecessary complexity, collaterally obscuring structure-activity relationship (SAR) studies. Construction of a single quaternary stereocenter in a simple molecular scaffold is much more desirable. Most critical would be to develop robust methods that allow one to perform rigorous SAR studies while maintaining the quaternary center as a constant.

During the past decade, our research group has strategically tackled this problem by implementing an array of orthogonal approaches. The most well studied tactics that have emerged from our laboratories involve the alkylation of 3-halooxindole electrophiles, the conjugate addition of boronic acids to cyclic enones, and the allylic alkylation of enolates. In all three approaches, we have achieved catalytic asymmetric construction of quaternary stereocenters in high yield and enantioselectivity with broad substrate scope. We believe that these methods will greatly expand the medicinal chemist's synthetic toolbox and facilitate access to potential drug candidates containing quaternary stereocenters.

A4.2 Enantioselective Syntheses of C(3) All-Carbon Quaternary Centers on oxindoles by Alkylation of 3-Bromooxindoles

3,3-Disubstituted oxindoles and their derivatives are widely encountered in numerous biologically active natural products⁷ and pharmaceutical compounds.⁸ A considerable amount of effort has thus been devoted toward the construction of 3,3-

disubstituted oxindoles over the past decade.^{9,10} However, a non-traditional use of the oxindole core as an electrophile rather than as a nucleophile toward the catalytic enantioselective generation of C(3) quaternary substituted oxindoles was unprecedented and discovered by our laboratory.

In 2007, we reported a method for the construction of 3,3-disubstituted oxindoles in good yields by alkylation of malonate nucleophiles with 3-halooxindoles as electrophiles, presumably via indolones **100** (Scheme A4.1A).¹¹ Additionally, by employing these mild conditions, we could access the core structures of the complex polycyclic alkaloid natural products communesin F (**108**) and perophoramidine (**109**, Scheme A4.1B).¹² In view of these promising results, we turned our attention to the asymmetric synthesis of C(3) all-carbon quaternary substituted oxindoles.¹³ We envisioned that employing a chiral Lewis acid catalyst would facilitate an asymmetric variant of our alkylation reactions under mild basic conditions. Gratifyingly, we found that smooth enantioselective alkylation of 3-bromooxindole by malonates was achieved in good yields and high enantioselectivities by implementing a chiral Cu-BOX catalyst with a weakly coordinating counter ion such as SbF₆ (Table A4.1). A variety of substituted alkyl chain lengths were tolerated in the chemistry, as were numerous functional groups. Additionally, 3-aryl-3-chlorooxindoles were also alkylated to produce the corresponding 3,3-disubstituted oxindoles in good yields and high enantioselectivities. Our method stands as one of the only that allows the preparation of both C3-alkyl and C3-aryl quaternary oxindoles with a single catalyst system.

Scheme A4.1 Alkylations of 3-halooxindoles

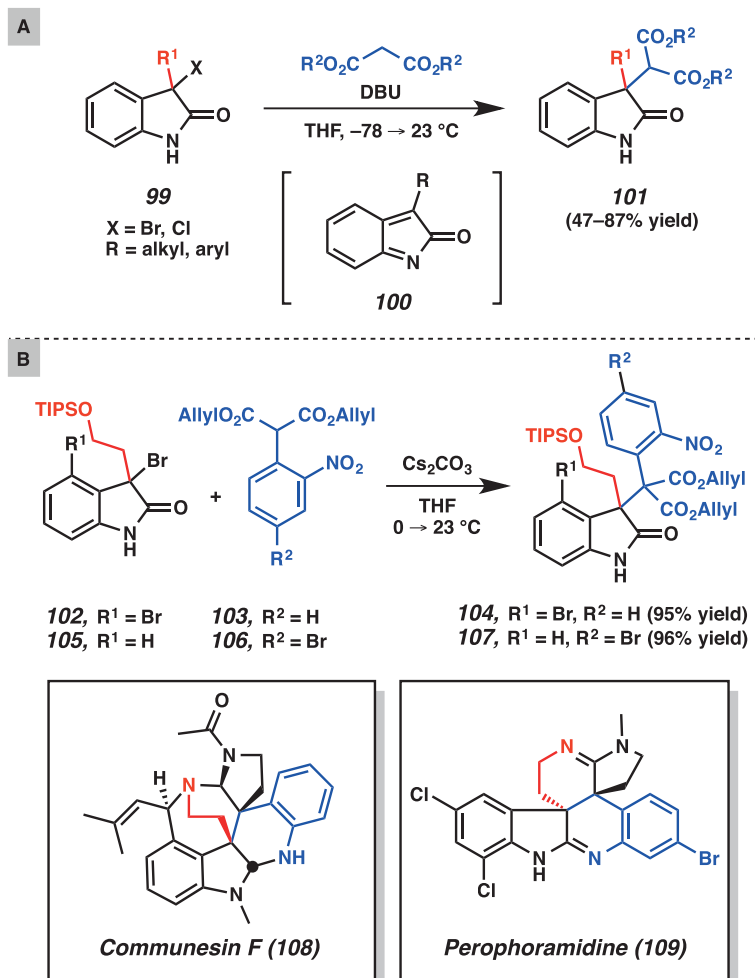
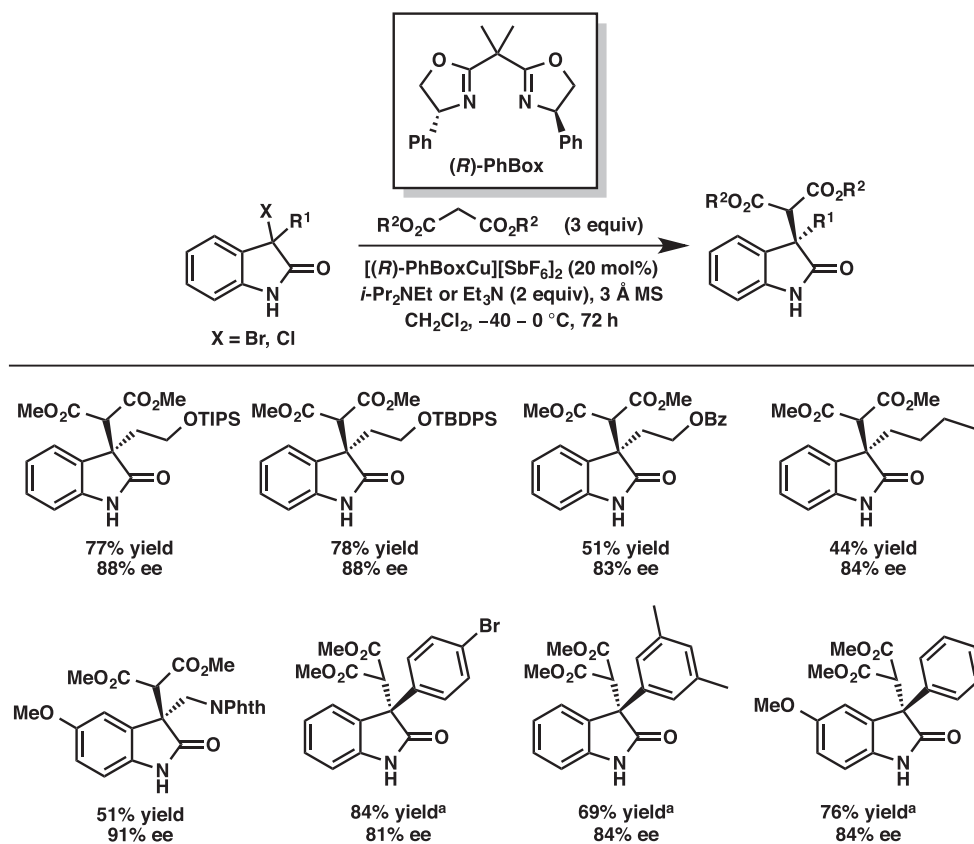
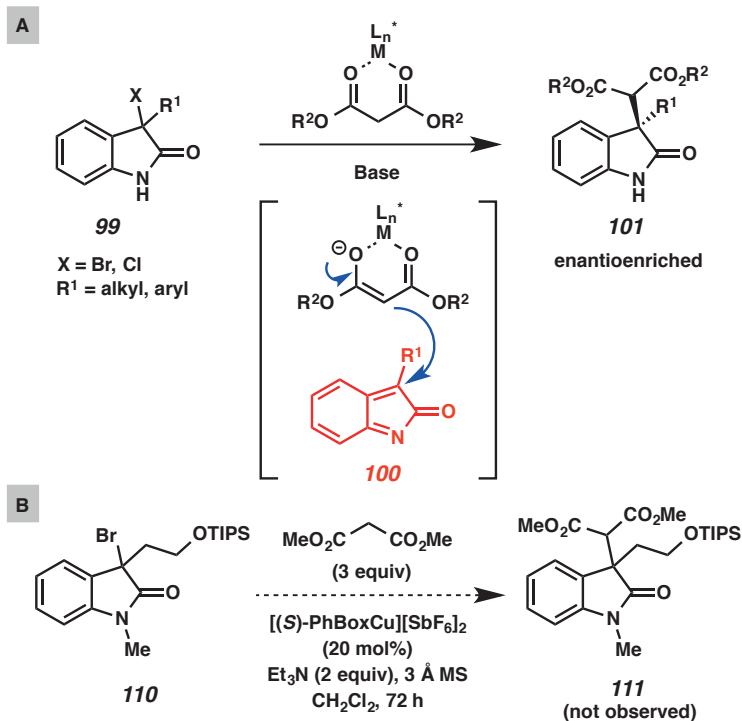


Table A4.1 Enantioselective alkylation of 3-haloindoles



^a Used 3-aryl-3-chloroindoles as substrates and (*S*)-PhBox as ligand.

Mechanistically, we envision that prochiral indolone **100** is likely to be an intermediate, since racemic starting materials remain throughout the course of the reaction and are converted to products of high ee (Scheme A4.2A), and alkylation reactions employing *N*-Me oxindole **110** as electrophiles are unsuccessful under our standard conditions (Scheme A4.2B).

Scheme A4.2 Alkylations of 3-halooxindoles via reactive prochiral indolone **100**

A4.3 Palladium-Catalyzed Asymmetric Conjugate Addition of Arylboronic Acids to Cyclic Enones to Furnish Benzylic Quaternary Centers

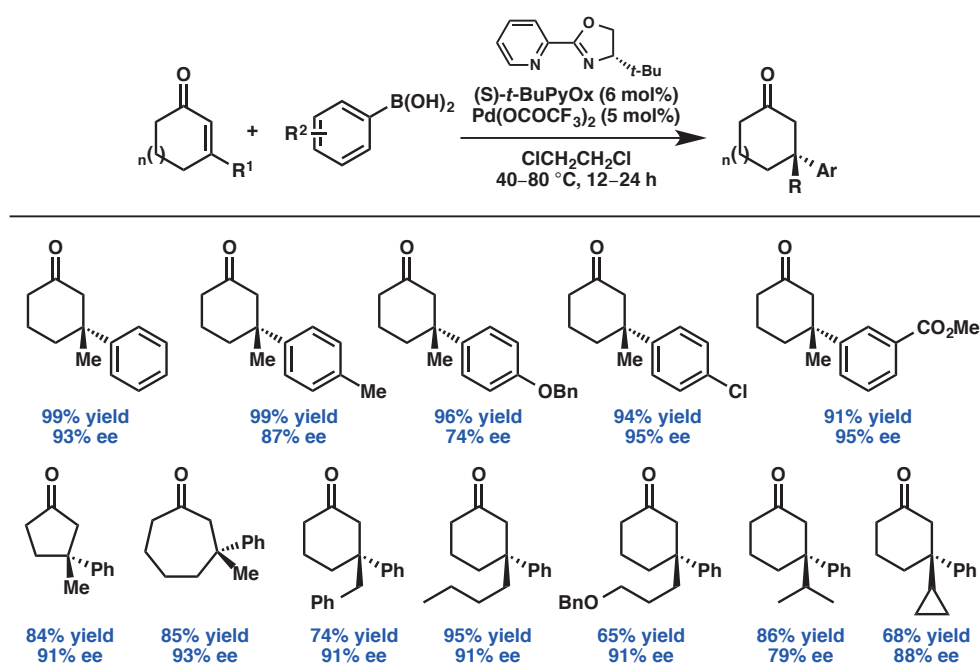
Although the alkylation of malonate nucleophiles to halooxindoles produces a quaternary benzylic carbon stereocenter, it does so in a very specialized system, the 3,3-disubstituted oxindole series. In order to produce benzylic quaternary centers in a more general way, we turned to the catalytic asymmetric conjugate addition of a carbon-based nucleophiles to β -substituted α,β -unsaturated carbonyl acceptors.¹⁴ For transition metal approaches, there have been two successful major catalytic systems, copper and rhodium. To date, most nucleophiles employed in copper-catalyzed conjugate additions are highly reactive organometallic species such as diorganozinc,¹⁵ triorganoaluminum,¹⁶ and organomagnesium reagents.¹⁷ The air- and moisture-sensitive nature of these

nucleophiles requires strictly anhydrous reaction conditions. On the other hand, air-stable organoboron reagents have been used in rhodium-catalyzed conjugate additions,¹⁸ although there are relatively few examples of quaternary stereocenter formation.¹⁹ In one report, it was shown that sodium tetraarylborates and arylboroxines could add to β,β -disubstituted enones to deliver β -quaternary ketones.²⁰ From a practical standpoint, using commercially available arylboronic acids as nucleophiles will make conjugate addition a much more valuable method for quaternary stereocenter generation. Additionally, the ultra-high cost of rhodium can often be prohibitive. As a remedy for these substantial hurdles, we embarked on a program to develop Pd catalysts that could be employed with aryl boronic acids for this purpose.

Palladium-catalyzed conjugate addition of arylboronic acids to enones has been widely studied and has led to development of addition reactions that form enantioenriched tertiary stereocenters.²¹ More recently, Lu reported a bipyridine-palladium complex-catalyzed conjugate addition to form quaternary stereocenters in racemic form.²² We envisioned that by using chiral ligands, enantioselective formation of quaternary stereocenters might be achieved.²³ With 3-methyl-2-cyclohexenone and phenylboronic acid as model reactants, we examined a range of reaction parameters, and discovered that a combination of easily accessible chiral pyridinooxazoline (PyOx) ligand, a commercial palladium(II) trifluoroacetate precatalyst, and 1,2-dichloroethane as solvent provided the desired β -quaternary ketone in high yield and excellent ee. Notably, the reaction was not sensitive to oxygen or moisture, and thus could be performed under ambient atmosphere without the need for anhydrous solvents.

With the optimal conditions in hand, we explored the substrate scope of palladium-catalyzed conjugate addition of arylboronic acids to cyclic enones (Table A4.2). In addition to a variety of substituents on the aromatic ring of the boronic acid, 5-, 6-, and 7-membered cyclic enones are all competent substrates for the reaction. Enones bearing more complex substituents at the β -position also undergo conjugate addition smoothly to afford the corresponding β -quaternary ketones in good yields and good to high ee.

Table A4.2 Asymmetric addition of arylboronic acids to 3-substituted cyclic enones



During scale-up studies, we found that addition of water was necessary for the complete conversion of starting material (Scheme A4.3). With 5 equiv of water, a 22 mmol scale reaction proceeded smoothly to furnish 3-methyl-3-phenylcyclohexanone (**114**) in 97% yield and 91% ee. Further investigation revealed that addition of water and

ammonium hexafluorophosphate had a synergistic effect in increasing reaction rate. Thus, more challenging substrates such as *ortho*-substituted arylboronic acid could also be employed in conjugate addition to give the desired products in much better yields compared with the previous conditions (Table A4.3).²⁴

Scheme A4.3 Large scale conjugate additions

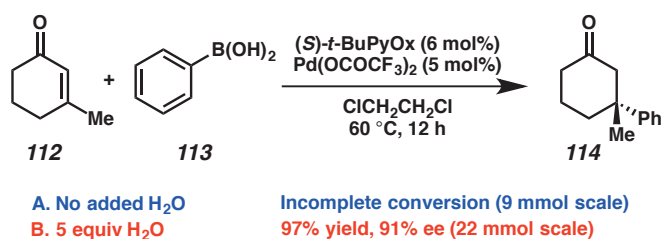
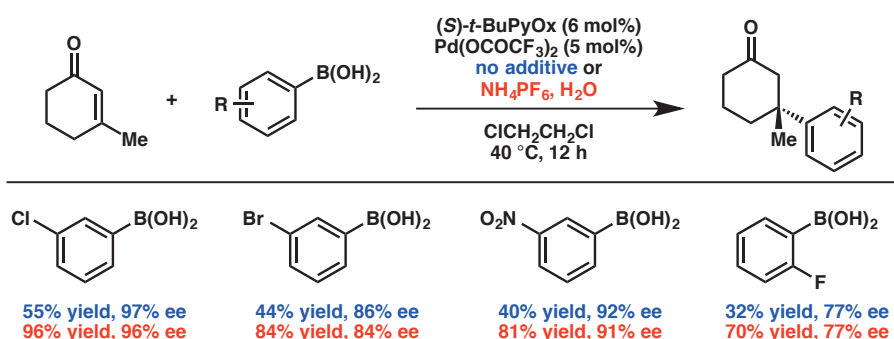


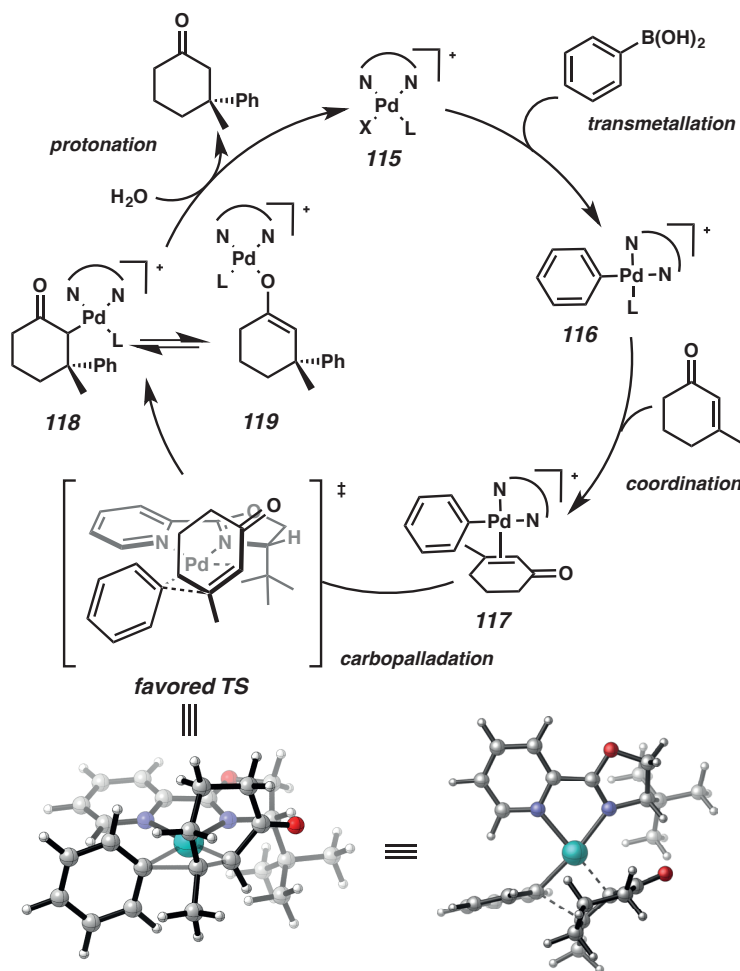
Table A4.3 Increased yields under new reaction conditions



Finally, a series of experimental and computational mechanistic studies revealed that a likely mechanistic path for the reaction is shown in Scheme A4.4.²⁴ The catalytic cycle consists of transmetalation from boron to palladium, insertion of the enone substrate into the aryl-metal bond, and protonolysis of the resulting palladium-enolate **119**. These investigations suggest that the bond-forming palladium species is an arylpalladium(II) cation (**117**), and enantioselectivity is governed by steric repulsions

between the *t*-Bu group of the chiral ligand and the α -methylene hydrogens of the cyclohexenone substrate.

Scheme A4.4 Mechanistic rationale for the asymmetric conjugate addition



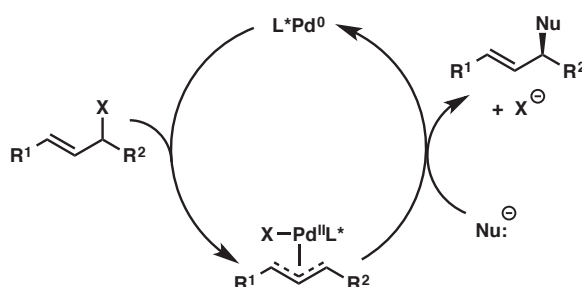
A4.4 Palladium-Catalyzed Enantioselective Allylic Alkylation of Prochiral Enolates

The first two sections of this manuscript discuss benzylic quaternary centers, yet a potentially greater challenge to asymmetric catalysis lies in bond forming chemistries that have no proximal aromatic groups. It is often the case that asymmetric reactions may function at benzylic positions and then fail upon extension to the alkyl variant. For the

construction of quaternary centers, the case is no different. It was precisely this limitation, and our concomitant efforts in the context of a multi-step synthesis, that guided our entry into this entire field, more than a decade ago.²⁵

Palladium-catalyzed asymmetric allylic alkylation is a powerful C–C bond forming process that allows for the construction of stereogenic centers.²⁶ A typical catalytic cycle involves the oxidative generation of a π -allylpalladium intermediate from an allyl electrophile, followed by nucleophilic attack on the allyl terminus, resulting in reduction of the metal center (Scheme A4.5). The pioneering earlier works of Trost,²⁷ Helmchen,²⁸ and others focused mainly on prochiral allyl electrophiles. Although this reaction mode enjoys success with a broad range of substrates and has found numerous applications in natural products synthesis, it typically produces only tertiary stereocenters. Formation of quaternary stereocenters by C-nucleophilic addition to prochiral allyl electrophiles has been carried out with other metals, such as copper.²⁹

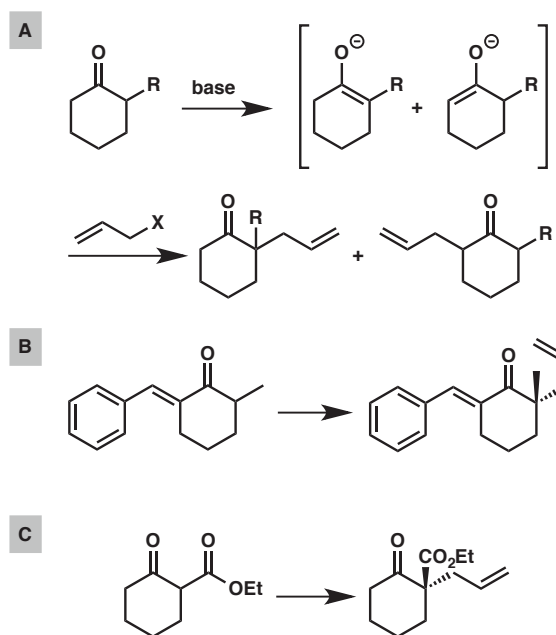
Scheme A4.5 General mechanism of Pd-catalyzed Asymmetric Allylic Alkylation



Another mode of reactivity makes use of a prochiral nucleophile. A quaternary stereocenter may be formed if the nucleophile possesses three distinct substituents. One typical example of such nucleophiles is a tetrasubstituted enolate, generated by

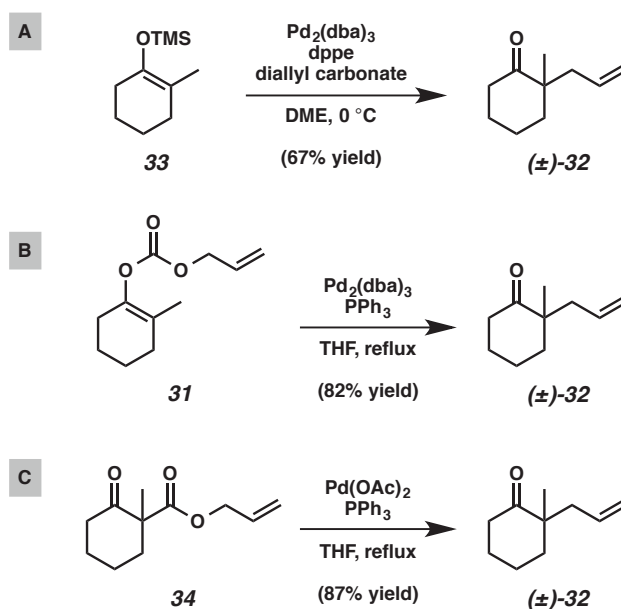
deprotonation of a carbonyl compound. However, position-selective enolate generation can be particularly challenging if the carbonyl compound bears multiple, similarly acidic α -protons. For example, deprotonation and alkylation of nonsymmetrical ketones generally lead to an intractable mixture of positional isomers (Scheme A4.6A). To address this selectivity issue, two strategies have been classically pursued. One of them installs a blocking group at the undesired α -position (Scheme A4.6B).³⁰ The other strategy introduces an electron-withdrawing group at one of the α -positions to dramatically lower its pK_a and stabilize the enolate thus formed (Scheme A4.6C).³¹ Although these tactics circumvent the positional selectivity problem, they require additional functional groups that potentially need removal or manipulation, thus reducing overall efficiency and synthetic utility.

Scheme A4.6 Challenges in alkylation of nonsymmetrical ketones



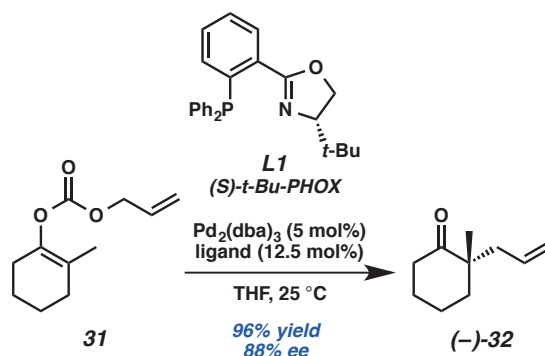
We were drawn to the pioneering work of Tsuji to provide an alternative solution to this position selectivity problem in the context of enantioselective catalysis. In the early 1980s, the Tsuji group reported the non-enantioselective allylic alkylation of silyl enol ethers, enol carbonates, and β -ketoesters derived from nonsymmetrical, nonstabilized ketones, in the presence of catalytic palladium and phosphine ligand (Scheme A4.7).³² The first substrate class involves separate nucleophiles and electrophiles (Scheme A4.7A), while the other two classes build the latent enolate nucleophile and the allyl electrophile into one molecule (Scheme A4.7B and C). The Tsuji allylic alkylation furnishes simple α -quaternary ketones with high positional fidelity, and the reaction proceeds under mild and nearly neutral conditions, with no exogenous base required. Despite these important advantages, the Tsuji allylic alkylation saw little application in organic synthesis for two decades and no asymmetric version was known until our first report in 2004.³³

Scheme A4.7 The Tsuji allylic alkylation



We became interested in developing an enantioselective variant of the Tsuji allylic alkylation because of its regiochemical fidelity and the synthetic utility of its products. We envisioned that a chiral phosphine ligand might impart asymmetric induction in the reaction, leading to preferential formation of one of the enantiomers. With allyl enol carbonate **31** as substrate, we examined a number of chiral bidentate phosphine ligands of various scaffolds and different chelating atoms and were pleased to discover that the phosphinooxazoline ligand (*S*)-*t*-Bu-PHOX (**L1**) provided excellent reactivity and high enantioselectivity (96% yield, 88% ee; see Scheme A4.8).

Scheme A4.8 Discovery of an enantioselective catalyst system for the asymmetric Tsuji allylic alkylation

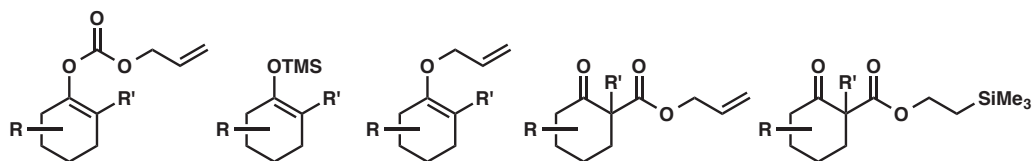


Since this initial discovery, we have intensely investigated the scope of this catalysis and found it to be extensive. From a practical standpoint, an important finding was our ability to initiate the chemistry starting from a range of substrate classes. Specifically, in addition to the prototypical enol allyl carbonate, silyl enol ethers, allyl β -ketoesters, allyl enol ethers, and trimethyl silyl ethyl keto esters can serve as nearly equivalent masked enolate substrates (Figure A4.2). The electrophilic allyl unit can bear

carbonates, acetates, sulphonates, and in some instances even halides as the leaving group. The great flexibility in substrate choice allows for strategic implementation in the context of multi-step synthesis, with each substrate class engendering different and unique tactical advantages.

Figure A4.2 Substrate possibilities for the enantioselective alkylation reaction

Masked enolate synthons:

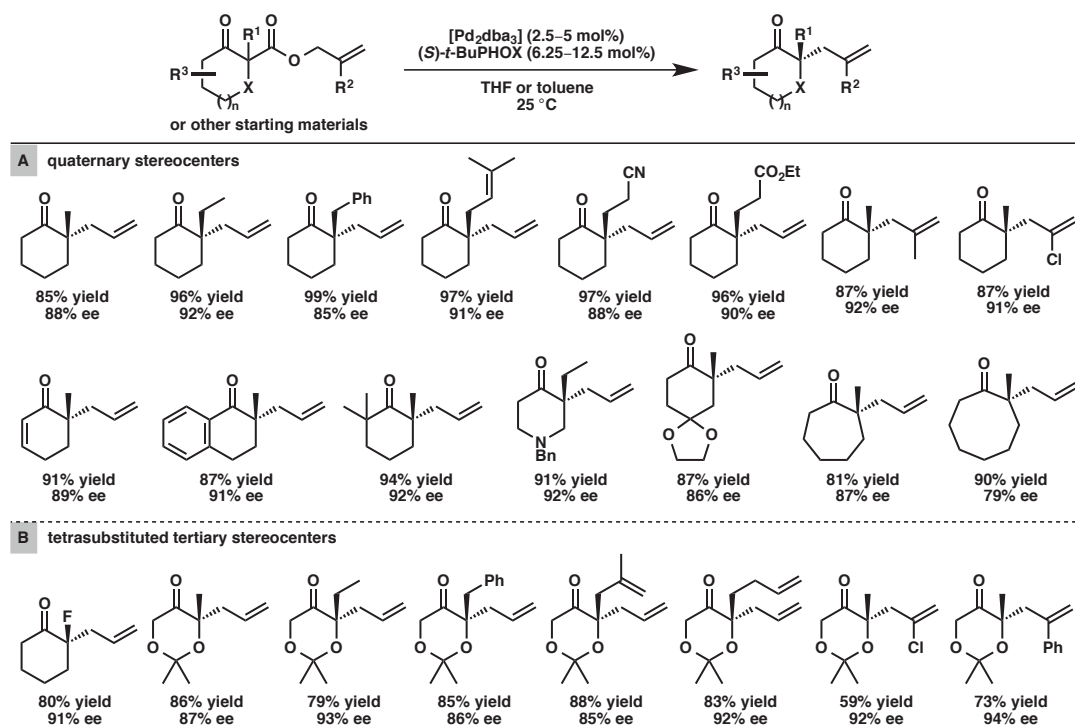


Allylic Electrophiles:



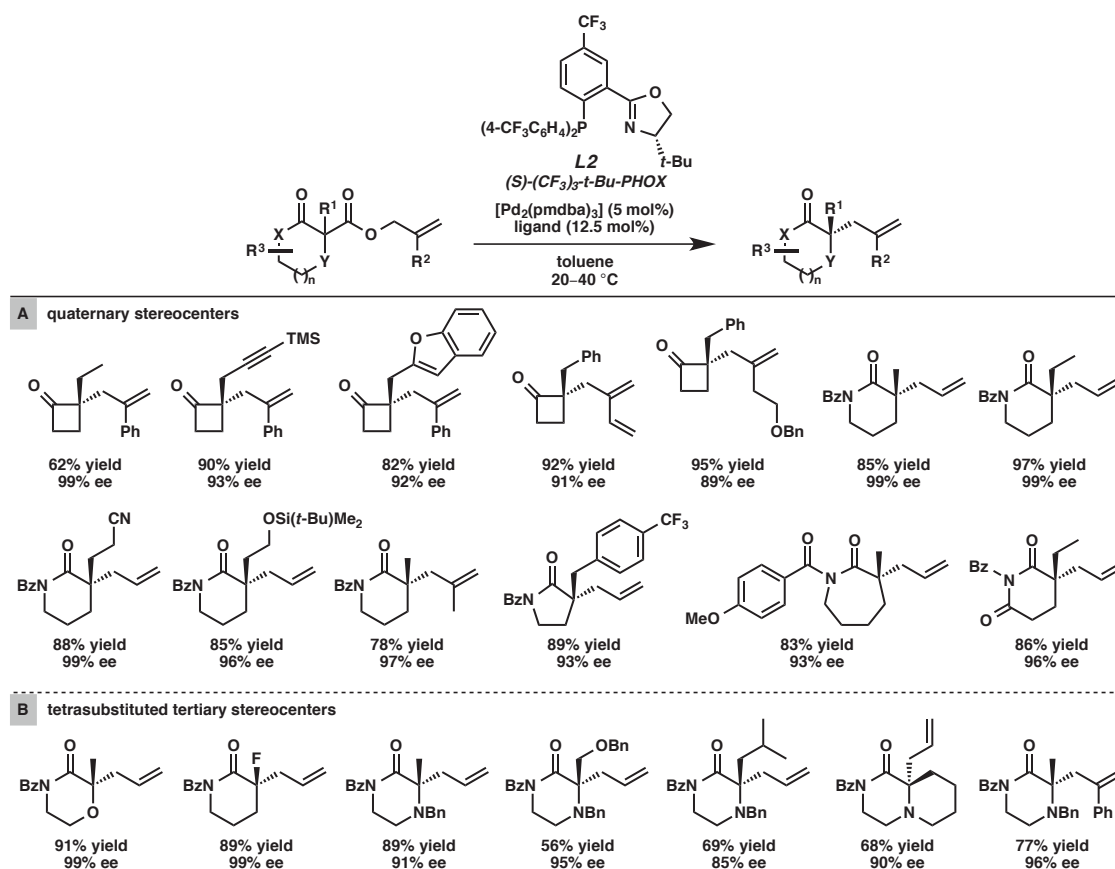
A wide array of quaternary ketones with various scaffolds and substituents can be accessed through our allylic alkylation chemistry with high yield and enantioselectivity (Table A4.4).^{33,34} Substitutions at the α -position, the 2-allyl position, and on the ring are all well tolerated. Substrates with seven- and eight-membered rings undergo the alkylation reaction smoothly. In addition to quaternary stereocenters, fully substituted tertiary centers can also be built by the reaction.³⁵

Table A4.4 Enantioselective allylic alkylation of cyclic ketone enolates



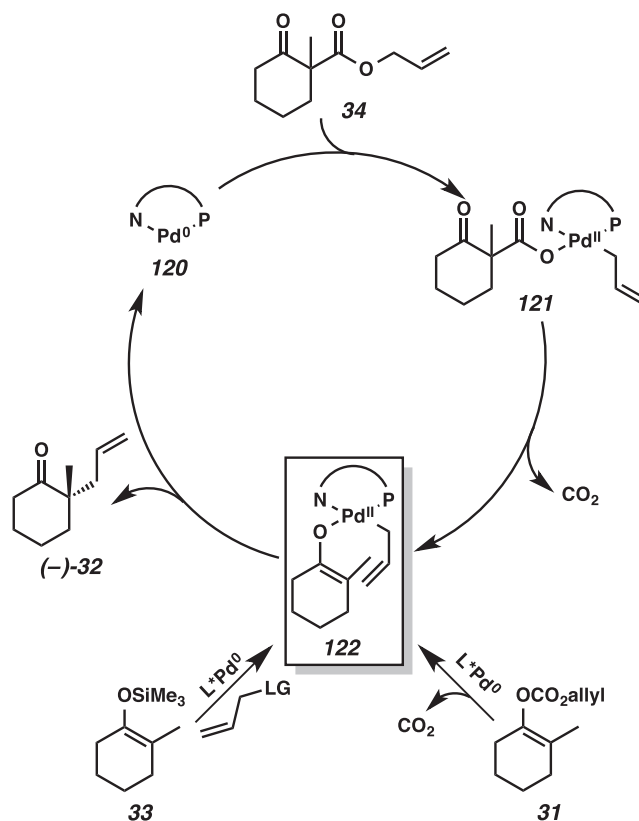
During our investigations, we became aware of the ligand electronic effects on reaction rate and selectivity. In many cases, the electron-deficient phosphinoxazoline ligand (*S*)-(CF₃)₃-*t*-Bu-PHOX (**L2**, Table A4.5) lead to faster reaction rates and higher enantioselectivities, as compared with the standard (*S*)-*t*-Bu-PHOX ligand. This modification of ligand electronics allowed us to improve the reaction's performance with more challenging classes of substrates such as cyclobutanones³⁶ and lactams.³⁷ Fully substituted tertiary carbonyl compounds, such as morpholinones,³⁷ α -fluorolactams,³⁷ and piperazines³⁸ can all be obtained through this chemistry.

Table A4.5 Enantioselective allylic alkylation of cyclobutanone and lactam enolates



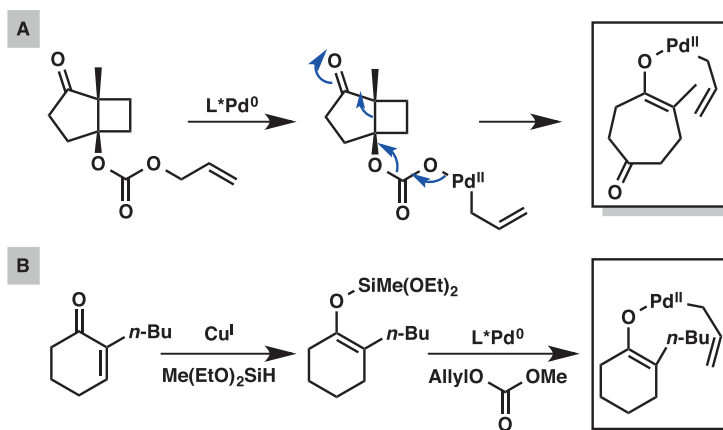
A mechanistic rationale has been proposed for the catalytic cycle (Scheme A4.9). Oxidative addition of Pd(0) to the allyl–O bond of **34** generates complex **121**, which undergoes decarboxylation to form allyl palladium enolate **122**, a key intermediate that can be formed from other starting materials such as silyl enol ether **33** and allyl enol carbonate **31**. Reductive elimination furnishes quaternary ketone product (–)-**32** and regenerates the active Pd(0) catalyst **120**.

Scheme A4.9 Proposed mechanism for palladium-catalyzed allylic alkylation



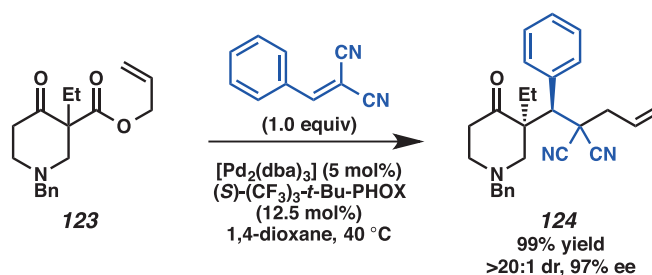
For the past decade, other labs have also contributed significantly to the field with related methods. Trost reported related palladium-catalyzed asymmetric allylic alkylation using a C₂-symmetric diamine-based ligand.³⁹ Nakamura and Paquin each expanded the scope of our method for the enantioselective synthesis of α -fluoroketones using the Pd/(*S*)-*t*-Bu-PHOX catalyst system.⁴⁰ Tunge employed the same catalyst/ligand combination for the deacylative allylic alkylation of ketones.⁴¹ The requisite allyl palladium enolate species can also be generated by fragmentation of fused 5-4 ring systems⁴² (Scheme A4.10A) or copper-catalyzed conjugate addition of silanes to enones (Scheme A4.10B).⁴³

Scheme A4.10 Generation of palladium enolate intermediates from other starting materials



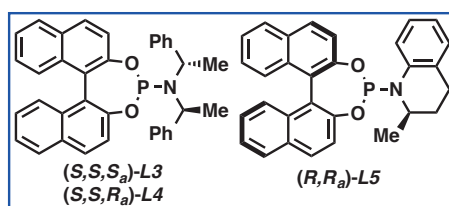
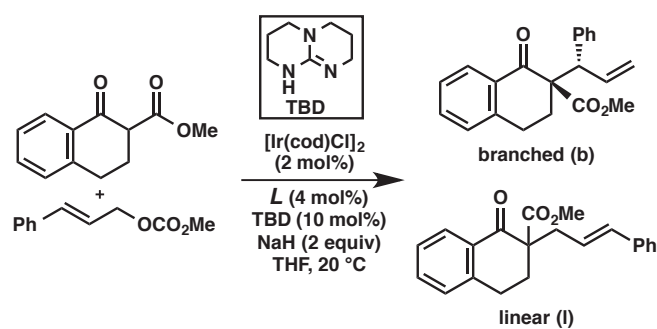
Since the reaction involves an enolate nucleophile, we envisioned trapping it with electrophiles other than the allyl fragment. Such electrophiles need to meet two requirements: 1) they do not interfere with oxidative addition or enolate generation; and 2) their reaction with the enolate is faster than direct enolate allylic alkylation. After examination of various carbon electrophiles, we found that arylidenemalononitrile-type Michael acceptors exhibited desired reactivity and produced cyclic ketones bearing adjacent quaternary and tertiary stereocenters (Scheme A4.11).⁴⁴

Scheme A4.11 Asymmetric enolate alkylation cascade with different electrophiles



A4.5 Iridium-Catalyzed Allylic Alkylation for the Construction of Vicinal Quaternary and Tertiary Stereocenters

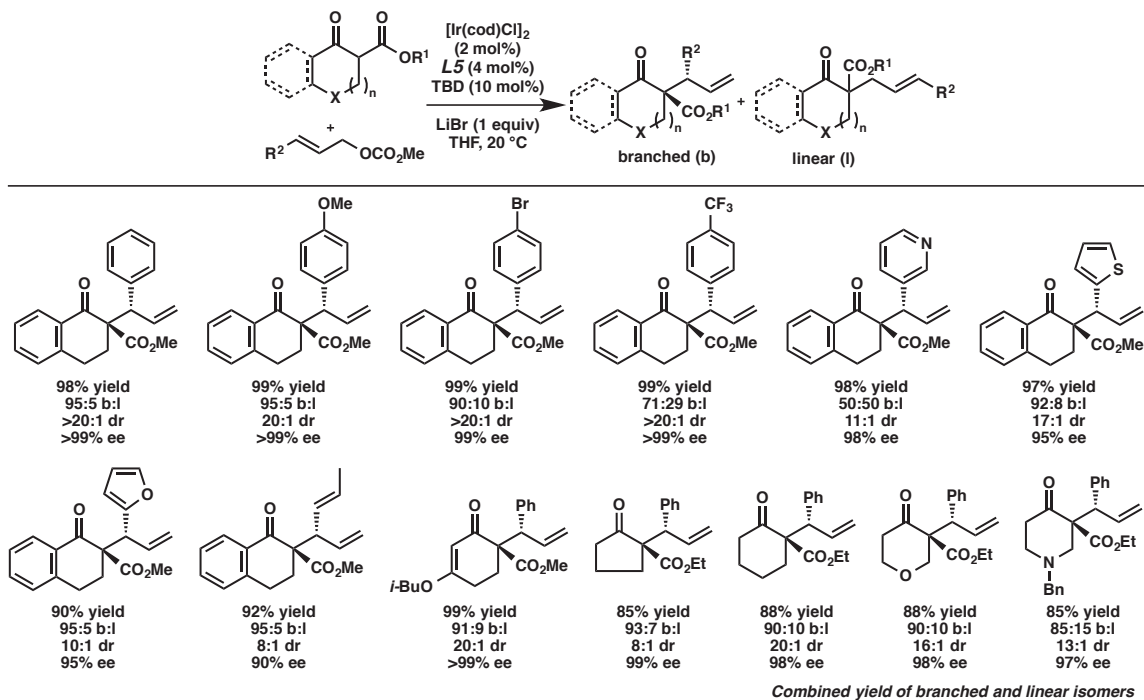
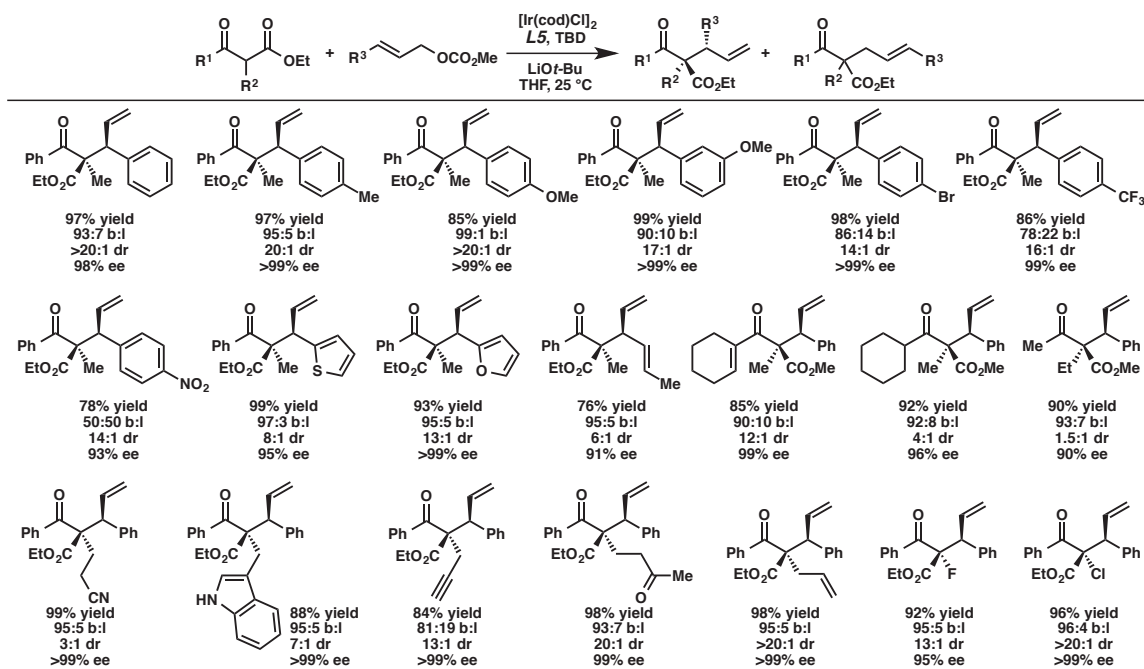
Based on the intriguing diastereochemical issues encountered in the Pd-enolate trapping chemistry, we became interested in other methods for direct generation of vicinal quaternary-tertiary relationships. Recently, by employing prochiral α -substituted cyclic β -ketoester enolates as nucleophiles, we developed an Ir-catalyzed direct enantioselective allylic alkylation reaction for the construction of vicinal quaternary-tertiary arrays.^{45,46} We explored the reaction with commonly used iridium catalyst systems, derived from $[\text{Ir}(\text{cod})\text{Cl}]_2$ and phosphoramidite ligands. The catalyst derived from Feringa ligand (**L3**)⁴⁷ affords the desired branched product in an equal amount of two diastereoisomers (1:1 dr), although the ee of the isomers are nearly perfect (96% and 99% ee, respectively; see Scheme A4.12).⁴⁸ In contrast, the $[\text{Ir}(\text{cod})\text{Cl}]_2 \cdot N$ -arylphosphoramidite (**L5**) complex⁴⁹ was found to furnish the desired product in 98% ee, >20:1 dr and excellent branched to linear ratio.

Scheme A4.12 Ir-catalyzed allylic alkylation of cyclic α -substituted β -ketoesters

ligand	b:l	for branched	
		dr	ee (%)
L3	>95:5	1:1	96
L4	>95:5	1:2	32 (3) ^a
L5	95:5	>20:1	98

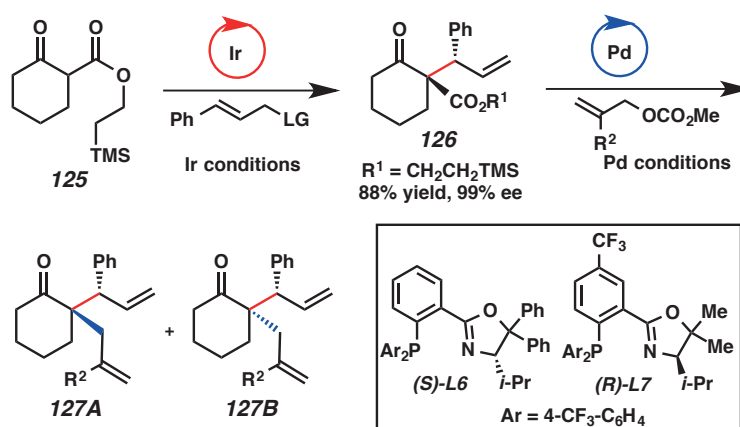
^a (ee) for alternate diastereomer.

The reaction proceeds with high yield and selectivity using a wide range of substrates variable on the enolate portion as well as the electrophile (Table A4.6). With further exploration, we found that a modified protocol is amenable to acyclic β -ketoesters as well, again with tolerance to a wide array of substituent groups and functionality (Table A4.7).⁵⁰

Table A4.6 Selected substrates of Ir-catalyzed allylic alkylation of cyclic α -substituted β -ketoestersTable A4.7 Selected examples of Ir-catalyzed allylic alkylation of acyclic α -substituted β -ketoesters

Combining our fluoride-triggered decarboxylative allylic alkylation⁵¹ and the iridium chemistry together, we have developed a sequential double allylic alkylation procedure to selectively program the diastereomer that is furnished within the stereochemical dyad. We found that 2-(trimethylsilyl)ethyl β -ketoester substrates successfully engage in iridium-catalyzed allylic alkylation to generate the desired product with excellent regio- and enantioselectivity. Subsequently, treatment of the product (**126**) with allyl methyl carbonate and catalyst derived from Pd₂(dba)₃ and PHOX ligand (**L6**), in the presence of tetrabutylammonium difluorotriphenylsilicate (TBAT), generated the desired dialkylated α -quaternary ketone **127B** in good yield and diastereoselectivity (Table A4.8, entry 1). Through choice of ligand, we can alter the selectivity to favor the ketone **127A** in high dr (12:1–18:1) and yield (80–87%) with several 2-substituted allyl carbonates (entries 2–4).

Table A4.8 Sequential allylic alkylation catalyzed by iridium and palladium complexes



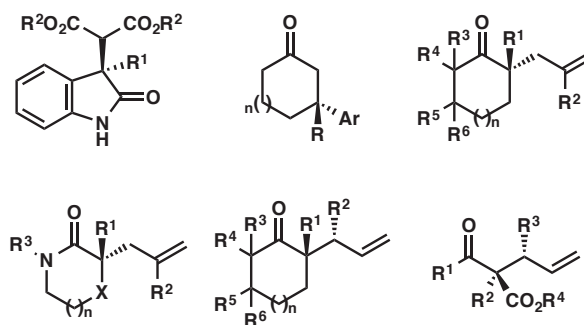
entry	ligand	R ²	dr (127A : 127B)	yield (%)
1	L6	H	1:8	91
2	L7	H	18:1	85
3	L7	Ph	13:1	87
4	L7	Me	12:1	80

Ir conditions: [Ir(cod)Cl]₂ (2 mol%), **L5** (4 mol%), TBD (10 mol%), LiBr (1 equiv), in THF at 25 °C. Pd conditions: Pd₂(dba)₃ (5 mol%), ligand (12.5 mol%), TBAT (1.2 equiv), allyl carbonate (1.2 equiv), in THF at 25 °C.

A4.6 Conclusions

The development of a suite of catalytic asymmetric transformations by our group for the preparation of quaternary stereocenters provides access to a broad range of enantioenriched, high-value, small molecule building blocks (Figure A4.3). We have developed methods that readily produce 3,3-disubstituted oxindoles, β -quaternary ketones, α -quaternary ketones, and α -quaternary lactams. These building blocks can be further derivatized to a much larger collection of compounds bearing quaternary stereogenicity. We anticipate that the synthetic methods developed by our group and the advancements that synthetic chemists are making as a whole toward the synthesis of challenging stereochemically rich molecules will find increasing future application in drug discovery and design. These methods move us into previously unexplored chemical space that may be brought to bear on problems of a medicinal nature, with potential enhancements in biochemical, pharmacological, and physiological properties.

Figure A4.3 Enantioenriched building blocks accessible by our synthetic methods



A4.7 Notes and References

- (1) Ritchie, T. J.; Macdonald, S. J. F. *Drug Discov. Today* **2009**, *14*, 1011–1020.

-
- (2) Lovering, F.; Bikker, J.; Humblet, C. *J. Med. Chem.* **2009**, *52*, 6752–6756.
- (3) (a) Trost, B. M.; Jiang, C. *Synthesis* **2006**, 369–396. (b) Corey, E. J.; Guzman-Perez, A. *Angew. Chem., Int. Ed.* **1998**, *37*, 388–401.
- (4)
- http://cbc.arizona.edu/njardarson/group/sites/default/files/Top200%20Pharmaceutical%20Products%20by%20US%20Retail%20Sales%20in%202012_0.pdf
- (5) Castro, A. M. M. *Chem. Rev.* **2004**, *104*, 2939–3002.
- (6) Corey, E. J. *Angew. Chem., Int. Ed.* **2002**, *41*, 1650–1667.
- (7) (a) Galliford, C. V.; Scheidt, K. A. *Angew. Chem., Int. Ed.* **2007**, *46*, 8748–8758. (b) Marti, C.; Carreira, E. M. *J. Am. Chem. Soc.* **2005**, *127*, 11505–11515. (c) Edmondson, S.; Danishefsky, S. J.; Sepp-Lorenzino, L.; Rosen, N. *J. Am. Chem. Soc.* **1999**, *121*, 2147–2155.
- (8) Ding, K.; Lu, Y.; Nikolovska-Coleska, Z.; Wang, G.; Qiu, S.; Shangary, S.; Gao, W.; Qin, D.; Stuckey, J.; Krajewski, K.; Roller, P. P.; Wang, S. *J. Med. Chem.* **2006**, *49*, 3432–3435.
- (9) Reviews: (a) Zhou, F.; Liu, Y.-L.; Zhou, J. *Adv. Synth. Catal.* **2010**, *352*, 1381–1407. (b) Klein, J. E. M. N.; Taylor, R. J. K. *Eur. J. Org. Chem.* **2011**, 6821–6841. (c) Dalpozzo, R.; Bartoli, G.; Bencivenni, G. *Chem. Soc. Rev.* **2012**, *41*, 7247–7290. (d) Singh, G. S.; Desta, Z. Y. *Chem. Rev.* **2012**, *112*, 6104–6155.
- (10) Recent examples: (a) Hu, F.-L.; Wei, Y.; Shi, M. *Chem. Commun.* **2014**, *50*, 8912–8914. (b) Cao, Z.-Y.; Wang, Y.-H.; Zeng, X.-P.; Zhou, J. *Tetrahedron Lett.* **2014**, *55*, 2571–2584. (c) Trost, B. M.; Osipov, M. *Angew. Chem., Int. Ed.* **2013**, *52*, 9176–9181.

-
- (11) Krishnan, S.; Stoltz, B. M. *Tetrahedron Lett.* **2007**, *48*, 7571–7573.
- (12) Han, S.-J. Vogt, F.; Krishnan, S.; May, J. A.; Gatti, M.; Virgil, S. C. Stoltz, B. M. *Org. Lett.* **2014**, *16*, 3316–3319.
- (13) Ma, S.; Han, X.; Krishnan, S.; Virgil, S. C.; Stoltz, B. M. *Angew. Chem., Int. Ed.* **2009**, *48*, 8037–8041.
- (14) Hawner, C.; Alexakis, A. *Chem. Commun.* **2010**, *46*, 7295–7306.
- (15) Hird, A. W.; Hoveyda, A. H. *J. Am. Chem. Soc.* **2005**, *127*, 14988–14989.
- (16) d'Augustin, M.; Palais, L.; Alexakis, A. *Angew. Chem., Int. Ed.* **2005**, *44*, 1376–1378.
- (17) Martin, D.; Kehrl, S.; d'Augustin, M.; Clavier, H.; Mauduit, M.; Alexakis, A. *J. Am. Chem. Soc.* **2006**, *128*, 8416–8417.
- (18) Takaya, Y.; Ogasawara, M.; Hayashi, T. *J. Am. Chem. Soc.* **1998**, *120*, 5579–5580.
- (19) Shintani, R.; Duan, W.-L.; Hayashi, T. *J. Am. Chem. Soc.* **2006**, *128*, 5628–5629.
- (20) Shintani, R.; Tsutsumi, Y.; Nagaosa, M.; Nishimura, T.; Hayashi, T. *J. Am. Chem. Soc.* **2009**, *131*, 13588–13589.
- (21) Gutnov, A. *Eur. J. Org. Chem.* **2008**, 4547–4554.
- (22) Lin, S.; Lu, X. *Org. Lett.* **2010**, *12*, 2536–2539.
- (23) Kikushima, K.; Holder, J. C.; Gatti, M.; Stoltz, B. M. *J. Am. Chem. Soc.* **2011**, *133*, 6902–6905.
- (24) Holder, J. C.; Zou, L.; Marziale, A. N.; Liu, P.; Lan, Y.; Gatti, M.; Kikushima, K.; Houk, K. N.; Stoltz, B. M. *J. Am. Chem. Soc.* **2013**, *135*, 14996–15007.
- (25) Behenna, D. C.; Stoltz, B. M. *Top. Organomet. Chem.* **2013**, *44*, 281–314.
- (26) Trost, B. M.; Van Vranken, D. L. *Chem. Rev.* **1996**, *96*, 395–422.

-
- (27) Trost, B. M. *J. Org. Chem.* **2004**, *69*, 5813–5837.
- (28) Helmchen, G. *J. Organomet. Chem.* **1999**, *576*, 203–214.
- (29) Luchaco-Cullis, C. A.; Mizutani, H.; Murphy, K. E.; Hoveyda, A. H. *Angew. Chem., Int. Ed.* **2001**, *40*, 1456–1460.
- (30) Trost, B. M.; Schroeder, G. M. *J. Am. Chem. Soc.* **1999**, *121*, 6759–6760.
- (31) (a) Hayashi, T.; Kanehira, K.; Hagihara, T.; Kumada, M. *J. Org. Chem.* **1988**, *53*, 113–120. (b) Sawamura, M.; Nagata, H.; Sakamoto, H.; Ito, Y. *J. Am. Chem. Soc.* **1992**, *114*, 2586–2592. (c) Trost, B. M.; Radinov, R.; Grenzer, E. M. *J. Am. Chem. Soc.* **1997**, *119*, 7879–7880.
- (32) (a) Shimizu, I.; Yamada, T.; Tsuji, J. *Tetrahedron Lett.* **1980**, *21*, 3199–3202. (b) Tsuji, J.; Minami, I.; Shimizu, I. *Tetrahedron Lett.* **1983**, *24*, 1793–1796.
- (33) Behenna, D. C.; Stoltz, B. M. *J. Am. Chem. Soc.* **2004**, *126*, 15044–15045.
- (34) Mohr, J. T.; Behenna, D. C.; Harned, A. M.; Stoltz, B. M. *Angew. Chem., Int. Ed.* **2005**, *44*, 6924–6927.
- (35) Seto, M.; Roizen, J. L.; Stoltz, B. M. *Angew. Chem., Int. Ed.* **2008**, *47*, 6873–6876.
- (36) Reeves, C. M.; Eidamshaus, C.; Kim, J.; Stoltz, B. M. *Angew. Chem., Int. Ed.* **2013**, *52*, 6718–6721.
- (37) Behenna, D. C.; Liu, Y.; Yurino, T.; Kim, J.; White, D. E.; Virgil, S. C.; Stoltz, B. M. *Nature Chem.* **2012**, *4*, 130–133.
- (38) Korch, K. M.; Eidamshaus, C.; Behenna, D. C.; Nam, S.; Home, D.; Stoltz, B. M. *Angew. Chem., Int. Ed.* **2015**, *54*, 179–183.
- (39) Trost, B. M.; Xu, J. *J. Am. Chem. Soc.* **2005**, *127*, 2846–2847.

-
- (40) (a) Nakamura, M.; Hajra, A.; Endo, K.; Nakamura, E. *Angew. Chem., Int. Ed.* **2005**, *44*, 7248–7251. (b) Bélanger, É.; Cantin, K.; Messe, O.; Tremblay, M.; Paquin, J.-F. *J. Am. Chem. Soc.* **2007**, *129*, 1034–1035.
- (41) Grenning, A. J.; Van Allen, C. K.; Maji, T.; Lang, S. B.; Tunge, J. A. *J. Org. Chem.* **2013**, *78*, 7281–7287.
- (42) Schulz, S. R.; Blechert, S. *Angew. Chem., Int. Ed.* **2007**, *46*, 3966–3970.
- (43) Nahra, F.; Macé, Y.; Lambin, D.; Riant, O. *Angew. Chem., Int. Ed.* **2013**, *52*, 3208–3212.
- (44) Streuff, J.; White, D. E.; Virgil, S. C.; Stoltz, B. M. *Nature Chem.* **2010**, *2*, 192–196.
- (45) Liu, W.-B.; Reeves, C. M.; Virgil, S. C.; Stoltz, B. M. *J. Am. Chem. Soc.* **2013**, *135*, 10626–10629.
- (46) For the first examples: (a) Takeuchi, R.; Kashio, M. *Angew. Chem., Int. Ed. Engl.* **1997**, *36*, 263–265. (b) Janssen, J. P.; Helmchen, G. *Tetrahedron Lett.* **1997**, *38*, 8025–8026. For reviews: (c) Helmchen, G.; Dahnz, A.; Dübon, P.; Schelwies, M.; Weihofen, R. *Chem. Commun.* **2007**, 675–691. (d) Hartwig, J. F.; Pouy, M. J. *Top. Organomet. Chem.* **2011**, *34*, 169–208. (e) Tosatti, P.; Nelson, A.; Marsden, S. P. *Org. Biomol. Chem.* **2012**, *10*, 3147–3163.
- (47) Teichert, J. F.; Feringa, B. L. *Angew. Chem., Int. Ed.* **2010**, *49*, 2486–2528.
- (48) (a) Wu, Q.-F.; He, H.; Liu, W.-B.; You, S.-L. *J. Am. Chem. Soc.* **2010**, *132*, 11418–11419. (b) Kanayama, T.; Yoshida, K.; Miyabe, H.; Takemoto, Y. *Angew. Chem., Int. Ed.* **2003**, *42*, 2054–2056. (c) Chen, W.; Hartwig, J. F. *J. Am. Chem. Soc.* **2013**,

-
- 135, 2068–2071. (d) Krautwald, S.; Sarlah, D.; Schafroth, M. A.; Carreira, E. M. *Science* **2013**, *340*, 1065–1068.
- (49) Liu, W.-B.; Zheng, C.; Zhuo, C.-X.; Dai, L.-X.; You, S.-L. *J. Am. Chem. Soc.* **2012**, *134*, 4812–4821.
- (50) Liu, W.-B.; Reeves, C. M.; Stoltz, B. M. *J. Am. Chem. Soc.* **2013**, *135*, 17298–17301.
- (51) Reeves, C. M.; Behenna, D. C.; Stoltz, B. M. *Org. Lett.* **2014**, *16*, 2314–2317.

CHAPTER 4

Palladium-Catalyzed Decarbonylative Dehydration of Fatty Acids for the Synthesis of Linear Alpha Olefins[†]

4.1 Introduction

Linear alpha olefins represent an important class of industrial chemicals with a wide range of applications. They are used as co-monomers for ethylene polymerization¹ as well as precursors to plasticizers, lubricants, and surfactants.² Currently, these olefins are mainly produced by oligomerization of ethylene,³ which, in turn, is derived from petroleum. As the world's oil reserves continue to diminish, development of renewable feedstocks for the production of alpha olefins becomes increasingly important. One obvious choice is ethylene from biomass-derived ethanol.⁴ A potentially more direct

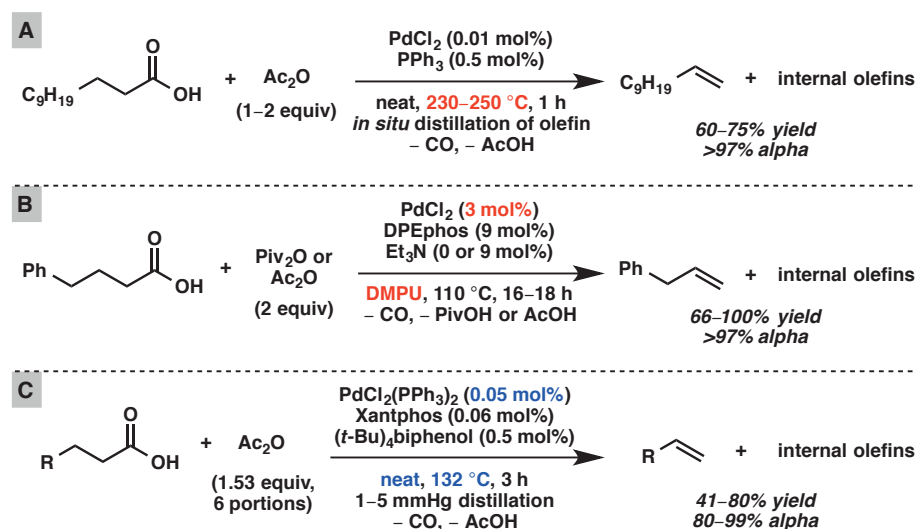
[†] This work was performed in collaboration with Kelly E. Kim, Dr. Myles B. Herbert, and Dr. Alexey Fedorov, and was partially adapted from the publication: Liu, Y.; Kim, K. E.; Herbert, M. B.; Fedorov, A.; Grubbs, R. H.; Stoltz, B. M. *Adv. Synth. Catal.* **2014**, *356*, 130–136. Copyright 2014 John Wiley & Sons, Inc.

method is the decarbonylative dehydration of long chain fatty acids. The latter route is particularly attractive because fatty acids are inexpensive and readily available starting materials derived from many natural sources. Since natural fatty acids contain an even number of carbon atoms, their corresponding alpha olefins will be odd-numbered after decarbonylative dehydration. Moreover, conventional ethylene oligomerization processes deliver only even-numbered alpha olefins,³ and odd-numbered olefins are largely inaccessible and prohibitively expensive.⁵ These odd-numbered olefins are valuable building blocks in the synthesis of various fine chemicals such as lepidopteran insect pheromones, but are currently far too costly to be practical.⁶ Therefore, the development of an efficient and economic process for fatty acid decarbonylative dehydration is highly desirable.

Many strategies to convert fatty acids to alpha olefins have been pursued. Lead tetraacetate-mediated oxidative decarboxylation is a classical method.⁷ Alternative protocols that avoid stoichiometric toxic reagents have also been developed, such as Kolbe electrolysis⁸ and silver-catalyzed oxidative decarboxylation.⁹ However, these reactions proceed through highly reactive radical intermediates, and thus suffer from low yields due to many side reactions. A more recent approach entails the transition metal-catalyzed decarbonylative dehydration of fatty acids. A variety of transition metals including rhodium,¹⁰ iridium,¹¹ palladium,¹² and iron¹³ have been shown to catalyze decarbonylative dehydration reactions. To date, palladium has demonstrated the highest activity, and catalyst loadings as low as 0.01 mol% have been reported independently by Miller^{12a} and Kraus^{12b} (Scheme 4.1A). Unfortunately, their methods require very high temperatures (230–250 °C). In addition, it is necessary to distill the olefin product from

the reaction mixture as soon as it is formed in order to prevent double bond isomerization, and therefore only volatile olefins can be produced this way. Decarbonylation processes under milder conditions have been developed independently by Gooßen^{12c} and Scott^{12d} (Scheme 4.1B). Although their reactions proceed at 110 °C, much higher palladium catalyst loading (3 mol%) and an expensive, high-boiling-point solvent (DMPU) are required. We envisioned that by judicious choice of ligand set for palladium and other parameters, the most advantageous aspects of these two systems could be combined. Herein we report a palladium-catalyzed decarbonylative dehydration using low catalyst loading under relatively mild and solvent-free conditions to produce alpha olefins in good yield and high selectivity (Scheme 4.1C).

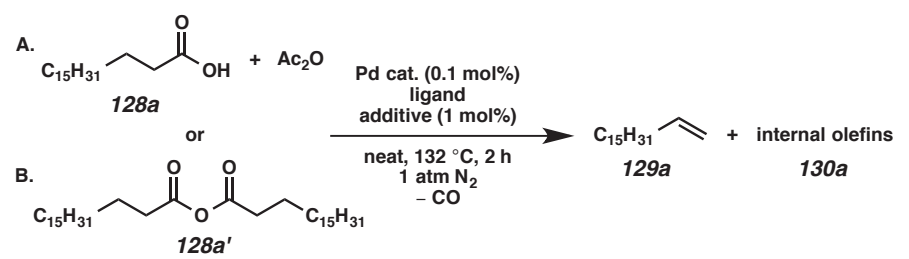
Scheme 4.1 Palladium-catalyzed decarbonylative dehydration. (A) High temperature processes (Miller, Kraus). (B) Low temperature processes (Gooßen, Scott). (C) This research.

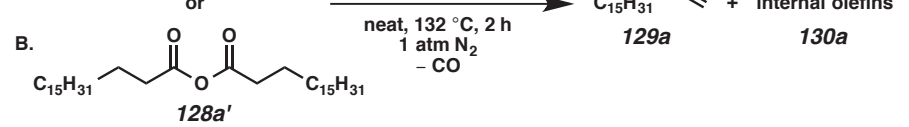


4.2 Optimization of Reaction Conditions

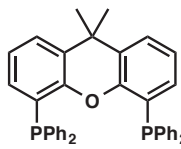
At the outset of our study, we examined the palladium-catalyzed decarbonylative dehydration of stearic acid (**128a**) in neat acetic anhydride as the dehydrating agent (Table 4.1). A preliminary survey of phosphine ligands revealed Xantphos to be an optimal and unique ligand for the transformation (entries 1–4). It is believed that acetic anhydride converts the stearic acid into stearic anhydride in situ, which then undergoes oxidative addition by Pd(0) to initiate the catalytic cycle.¹² Considering that acetic anhydride itself could compete with stearic anhydride for oxidative addition at the metal center, we sought to simplify the system by using pre-formed stearic anhydride (**128a'**) alone. To our surprise, the decarbonylation of neat stearic anhydride with the same catalyst was exceedingly slow (only 12% yield, 120 TON, in 2 h; entry 5). Comparing the two systems, we found that the former had one equivalent of acid in it, while the latter was acid-free. Thus, we posited that acid might play a role in promoting reactivity. Consequently we added 1 mol% isophthalic acid to the system, and the yield rose to 22% (entry 6). When the ligand-to-metal ratio was reduced from 4:1 to 1.2:1, the yield dramatically increased to 92%, but the selectivity dropped to 31% (entry 7). Since it has been shown previously that triphenylphosphine can inhibit olefin isomerization,^{12a} we used PdCl₂(PPh₃)₂ instead of PdCl₂(nbd) (nbd = norbornadiene), and we were delighted to observe an increase in selectivity to 54% with negligible erosion in yield (90%; entry 8). Finally, we examined a number of protic additives (entries 9–12), and found that (*t*-Bu)₄biphenol gave the optimal overall performance to furnish the highest yield of alpha olefin (entry 12).

Table 4.1 Effects of catalyst, ligand, and additive ^a

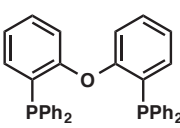
A. 

B. 

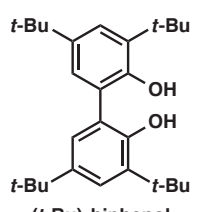
Entry	Rxn	Pd cat.	Ligand (mol%)	Additive	Yield (%) ^b	Alpha (%) ^b	Y x A (%) ^c
1	A	PdCl ₂ (nbd)	PPh ₃ (0.8)	--	0	--	0
2	A	PdCl ₂ (nbd)	dppp (0.4)	--	0	--	0
3	A	PdCl ₂ (nbd)	DPEphos (0.4)	--	43	59	25
4	A	PdCl ₂ (nbd)	Xantphos (0.4)	--	60	55	33
5	B	PdCl ₂ (nbd)	Xantphos (0.4)	--	12	100	12
6	B	PdCl ₂ (nbd)	Xantphos (0.4)	isophthalic acid	22	96	21
7	B	PdCl ₂ (nbd)	Xantphos (0.12)	isophthalic acid	92	31	29
8	B	PdCl ₂ (PPh ₃) ₂	Xantphos (0.12)	isophthalic acid	90	54	49
9	B	PdCl ₂ (PPh ₃) ₂	Xantphos (0.12)	<i>p</i> -TsOH·H ₂ O	86	5	4
10	B	PdCl ₂ (PPh ₃) ₂	Xantphos (0.12)	salicylamide	60	90	54
11	B	PdCl ₂ (PPh ₃) ₂	Xantphos (0.12)	2,2'-biphenol	59	91	54
12	B	PdCl ₂ (PPh ₃) ₂	Xantphos (0.12)	(<i>t</i> -Bu) ₄ biphenol	84	70	59



Xantphos



DPEphos



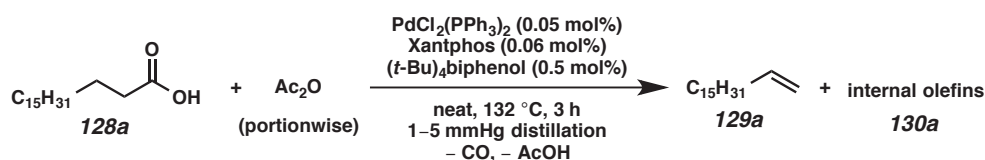
(*t*-Bu)₄biphenol

^a Conditions: A) 1 equiv **128a** (5 mmol), 2 equiv Ac₂O; B) 1 equiv **128a'** (5 mmol). ^b Determined by ¹H NMR with methyl benzoate as internal standard. Alpha = **129a**/(**129a**+**130a**). ^c Y x A = Yield x Alpha.

One major limitation of using pre-formed stearic anhydride as the substrate is that only half of the molecule can be converted to the olefin while the other half is wasted as stearic acid, so the maximum theoretical yield based on the acid is 50%. Control experiments also revealed that the buildup of acid in the reaction mixture was responsible for olefin isomerization and erosion of alpha selectivity. We envisioned that portionwise addition of acetic anhydride to the reaction mixture and distillation of acetic acid in situ could transform stearic acid back into its anhydride, thereby reducing acid concentration

and increasing the yield and selectivity (Table 4.2). When two portions of acetic anhydride were added to the reaction mixture with immediate distillation of acetic acid, once every 1.5 hours, the olefin product was obtained in 69% yield based on stearic acid and 62% selectivity (entry 1). Furthermore, when three portions of acetic anhydride were added, once every hour, the olefin product was obtained in 67% yield and 86% alpha selectivity (entry 2). Finally, when six portions of acetic anhydride were added, once every half hour, the olefin product was obtained in 67% isolated yield and 89% alpha selectivity (entry 3). The selectivity trend clearly shows that the more frequently acetic anhydride is added to dehydrate stearic acid, the higher the alpha selectivity. This is a remarkable result in that it is possible to maintain high selectivity without having to distill the olefin product out of the reaction mixture as it forms.

Table 4.2 Portionwise addition of acetic anhydride ^a



Entry	Equiv of Ac ₂ O	Yield (%) ^b	Alpha (%) ^b
1	1+0.5 (once every 1.5 hours)	69	62
2	1+0.5+0.25 (once every hour)	67	86
3	1+0.14+0.12+0.1+0.09+0.08 (once every half hour)	68 (67)	89

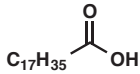
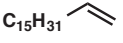
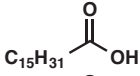
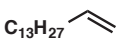
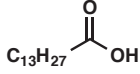
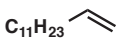
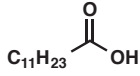
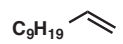
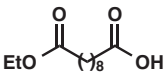
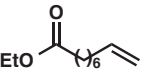
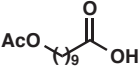
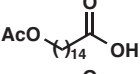
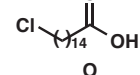
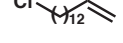
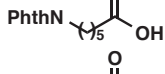
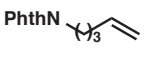
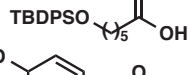
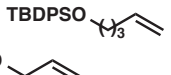
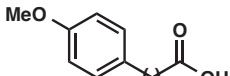
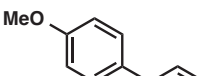
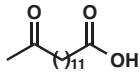
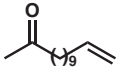
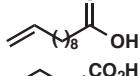
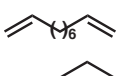
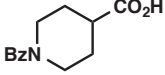
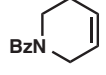
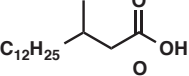
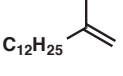
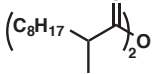
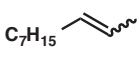
^a 20 mmol **128a**. ^b Determined by ¹H NMR (isolated yield in parentheses).

4.3 Study of Reaction Scope

With the optimized conditions in hand, we explored the decarbonylative dehydration of a variety of fatty acid substrates, as shown in Table 4.3. Common

saturated fatty acids with carbon numbers from 12 to 18 all provided the corresponding olefin in good yield and high alpha selectivity (entries 1–4). In particular, volatile olefins were formed with exceptionally high selectivities (entries 3 and 4). Terminally functionalized fatty acids were also competent substrates, and functional groups such as esters, chlorides, imides, silyl ethers, ketones, terminal olefins, and substituted aromatics were all well tolerated (entries 5–13). Notably, allylbenzene derivative **129k** was formed with 91% alpha selectivity (entry 11), which is impressive considering the significant thermodynamic driving force for isomerization into conjugation with the aromatic ring. Carboxylic acids with α - or β -substituents were considerably less reactive (entries 14–16). Nevertheless, catalyst turnovers up to 400 could be achieved for these challenging substrates. Compared to previous reports by Miller^{12a} and Kraus,^{12b} our reaction exhibits a much broader scope, does not require distillation of the olefin products to maintain high selectivity, and is compatible with various heteroatom-containing functional groups.

Table 4.3 Substrate scope study^a

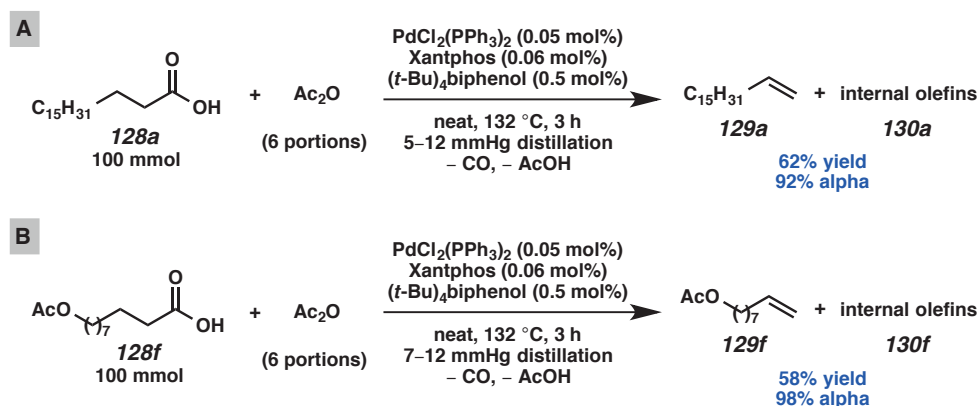
$\text{R}-\text{CH}_2-\text{CH}_2-\text{COOH} \quad \mathbf{128} + \text{Ac}_2\text{O} \xrightarrow[\text{1-5 mmHg distillation, -CO, -AcOH}]{\text{PdCl}_2(\text{PPh}_3)_2 (0.05 \text{ mol}\%), \text{Xantphos} (0.06 \text{ mol}\%), (t\text{-Bu})_4\text{biphenol} (0.5 \text{ mol}\%), \text{neat, 132 }^\circ\text{C, 3 h}}$		$\text{R}-\text{CH}=\text{CH}_2 \quad \mathbf{129} + \text{internal olefins} \quad \mathbf{130}$			
Entry	Substrate	Product	Yield (%) ^b	TON	Alpha (%) ^c
1	 128a	 129a	67	1340	89
2	 128b	 129b	41	820	97
3	 128c	 129c	65	1300	99
4	 128d	 129d	73	1460	99
5 ^{de}	 128e	 129e	63	1260	98
6 ^d	 128f	 129f	67	1340	96
7 ^d	 128g	 129g	60	1200	89
8	 128h	 129h	75	1500	86
9	 128i	 129i	76	1520	83
10	 128j	 129j	64	1280	80
11	 128k	 129k	80	1600	91
12	 128l	 129l	49	980	88
13	 128m	 129m	59	1180	87
14 ^f	 128n	 129n	20 80 ^h	400 320 ^h	-- ^g -- ^h
15	 128o	 129o	19	380	-- ^g
16 ⁱ	 128p'	 130p	71	71	-- ^j

^a Conditions: 20 mmol **1**, 6 portions of Ac₂O, 1+0.14+0.12+0.10+0.09+0.08 equiv, added every 30 min. ^b Isolated yield (column chromatography). ^c Determined by ¹H NMR. ^d Purified by distillation. ^e 18.5 mmol **128e**. ^f PdCl₂(nbd) (0.05 mol%), PPh₃ (0.05 mol%), Xantphos (0.06 mol%), 1.5 h, 3 portions of Ac₂O (1+0.15+0.10 equiv). ^g Single isomer observed. ^h PdCl₂(PPh₃)₂ (0.25 mol%), Xantphos (0.30 mol%), (t-Bu)₄biphenol (1 mol%), **129n**:**130n** = 49:51. ⁱ 2-methyldecanoic anhydride (10 mmol), no Ac₂O, PdCl₂(nbd) (1 mol%), Xantphos (1.1 mol%), salicylamide (2 mol%), 160 °C, 10 mmHg distillation, 10 h, **130p**:**129p** = 73:27.

4.4 Large Scale Reactions

Since this process requires no solvent and low catalyst loading, it can be readily scaled up (Scheme 4.2). In a laboratory setting, a 100 mmol scale (28.4 g stearic acid or 23.0 g 10-acetoxydecanoic acid) decarbonylative dehydration was easily carried out in a 100 mL round-bottom flask. Compared with small-scale reactions, the large-scale ones afforded products in similar yields and slightly higher alpha selectivity. When the olefin is sufficiently volatile, it is distilled out together with the acetic acid (Table 4.3, entries 3–6, 11, and 13). Although distillation of olefin is not necessary in order to maintain high selectivity (e.g. Scheme 4.2A), it is convenient to do so for volatile olefins (Scheme 4.2B).

Scheme 4.2 Large-scale decarbonylative dehydration of stearic acid and 10-acetoxydecanoic acid

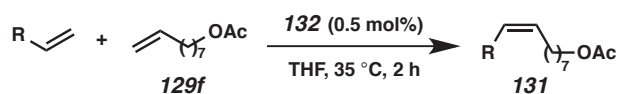


4.5 Synthetic Utility of Alpha Olefin Products

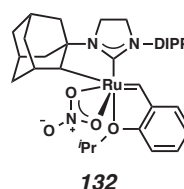
The olefin products thus obtained are important building blocks in chemical synthesis. For example, 8-nonyl acetate (**129f**) is a precursor to insect pheromones **131a** (Oriental fruit moth pheromone)¹⁴ and **131b** (Figure-of-Eight moth pheromone).¹⁵

Aided by *Z*-selective cross metathesis catalyst **132**, olefin **129f** reacts with 1-pentene or 1-hexene to afford pheromones **131a** or **131b** in 58% and 48% yield, respectively, and >98% *Z*-selectivity (Table 4.4).^{6b}

Table 4.4 Synthesis of pheromones **131a** and **131b** from olefin **129f**



Product	R	Yield (%) ^a	<i>Z</i> (%) ^b
131a	C ₃ H ₇	58	>98
131b	C ₄ H ₉	48	>98



^a 4.8 mmol **129f**. ^b Determined by ¹H NMR.

4.6 Concluding Remarks

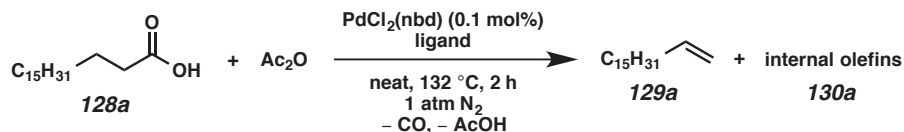
In summary, we have developed a highly efficient palladium-catalyzed decarbonylative dehydration process that converts carboxylic acids (e.g. fatty acids) to linear alpha olefins in good yield and with high selectivity. The reaction requires low palladium catalyst loading and proceeds under solvent-free and relatively mild conditions. In situ distillation of the olefin product is not necessary, and a wide range of functionalized and unfunctionalized carboxylic acids can be transformed into their corresponding olefins. Process development for large-scale production is underway and will be reported in due course. A small-scale application in natural product synthesis is presented in Chapter 5.

4.7 Experimental Section

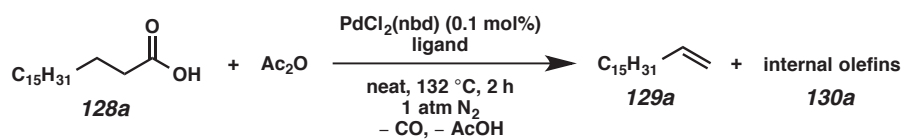
4.7.1 Materials and Methods

Unless otherwise stated, reactions were performed in flame-dried glassware under a nitrogen atmosphere or under vacuum without the use of solvents. Reaction progress was monitored by ^1H NMR analysis of the crude reaction mixture. Silicycle SiliaFlash® P60 Academic Silica gel (particle size 40–63 nm) was used for flash chromatography. ^1H NMR spectra were recorded on a Varian Inova 500 MHz spectrometer and are reported relative to residual CHCl_3 (δ 7.26 ppm) or DMSO (δ 2.50 ppm). ^{13}C NMR spectra were recorded on a Varian Inova 500 MHz spectrometer (125 MHz) and are reported relative to CHCl_3 (δ 77.16 ppm) or DMSO (δ 39.52 ppm). Data for ^1H NMR are reported as follows: chemical shift (δ ppm) (multiplicity, coupling constant (Hz), integration). Multiplicities are reported as follows: s = singlet, d = doublet, t = triplet, q = quartet, p = pentet, sept = septuplet, m = multiplet, br s = broad singlet, br d = broad doublet, app = apparent. Data for ^{13}C NMR are reported in terms of chemical shifts (δ ppm). IR spectra were obtained by use of a Perkin Elmer Spectrum BXII spectrometer using thin films deposited on NaCl plates and reported in frequency of absorption (cm^{-1}). High-resolution mass spectra (HRMS) were provided by the California Institute of Technology Mass Spectrometry Facility using a JEOL JMS-600H High Resolution Mass Spectrometer by positive-ion FAB, or obtained with an Agilent 6200 Series TOF using Agilent G1978A Multimode source in negative electrospray ionization (ESI⁻), negative atmospheric pressure chemical ionization (APCI⁻), or negative mixed ionization mode (NMM: ESI⁻-APCI⁻). Reagents were purchased from Sigma-Aldrich, Acros Organics, Strem, or Alfa Aesar and used as received unless otherwise stated.

4.7.2 General Procedure for Optimization Reactions (Route A)



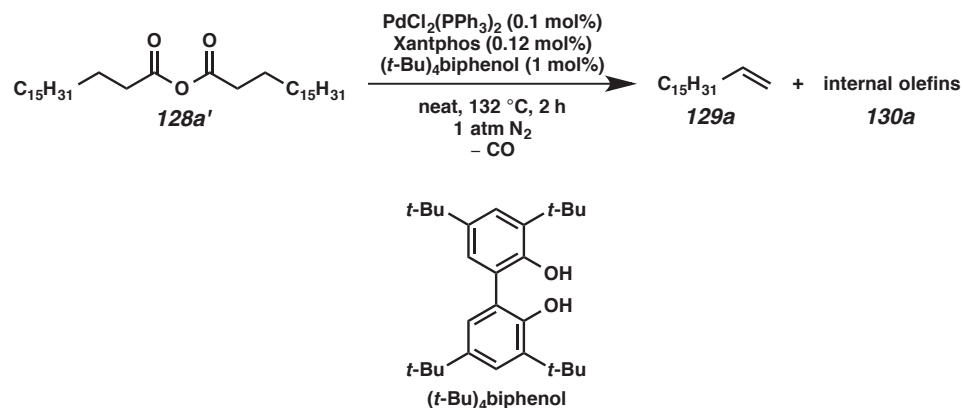
To a 20 x 150 mm Kimble glass tube equipped with a magnetic stir bar was added PdCl₂(nbd) (0.005 mmol, 0.1 mol%), ligand (monophosphine: 0.04 mmol, 0.8 mol%; diphosphine: 0.02 mmol, 0.4 mol%), and stearic acid **128a** (5 mmol, 1 equiv). The tube was sealed with a rubber septum, evacuated and refilled with N₂ (x 3), and acetic anhydride (10 mmol, 2 equiv) was added via syringe. The reaction tube placed in a preheated 132 °C oil bath (glass thermometer reading = 132 °C, IKA reading = 140 °C) and stirred for 2 h. The oil bath was removed, and methyl benzoate (internal standard, 5 mmol, 1 equiv) was added and the resulting mixture stirred for 1 min. An aliquot of the crude mixture was taken by pipette and analyzed by ¹H NMR. The results of additional ligand screen are shown in Table 4.5.

Table 4.5 Additional ligand screen ^a

Entry	Ligand (mol%)	Yield (%) ^b	Alpha (%) ^b	Y x A (%) ^c
1	PPh ₃ (0.8)	0	--	0
2	P(4-MeOC ₆ H ₄) ₃ (0.8)	0	--	0
3	P(4-CF ₃ C ₆ H ₄) ₃ (0.8)	0	--	0
4	P(2-furyl) ₃ (0.8)	0	--	0
5	P(<i>o</i> -tolyl) ₃ (0.8)	0	--	0
6	PCy ₃ (0.8)	0	--	0
7	RuPhos (0.8)	0	--	0
8	dppe (0.4)	0	--	0
9	dppp (0.4)	0	--	0
10	dppb (0.4)	0	--	0
11	dppf (0.4)	0	--	0
12	<i>rac</i> -BINAP (0.4)	0	--	0
13	DPEphos (0.4)	43	59	25
14	Xantphos (0.4)	60	55	33

^a 128a (5 mmol, 1 equiv), Ac₂O (2 equiv). ^b Determined by ¹H NMR with methyl benzoate as internal standard. ^c Y x A = Yield x Alpha.

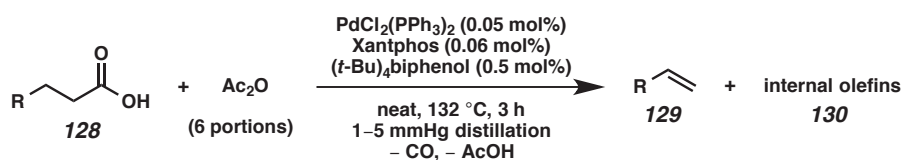
4.7.3 General Procedure for Optimization Reactions (Route B)



The procedure for the representative reaction (Table 4.1, entry 12) is shown as follows. To a 20 x 150 mm Kimble glass tube equipped with a magnetic stir bar was added PdCl₂(PPh₃)₂ (0.005 mmol, 0.1 mol%), Xantphos (0.006 mmol, 0.12 mol%), (*t*-

Bu₄biphenol (0.05 mmol, 1 mol%), and stearic anhydride **128a'** (5 mmol, 1 equiv). The tube was sealed with a rubber septum, evacuated and refilled with N₂ (x 3), and placed in a preheated 132 °C oil bath and stirred for 2 h. The oil bath was removed, and methyl benzoate (internal standard, 5 mmol, 1 equiv) was added and the resulting mixture stirred for 1 min. An aliquot of the crude mixture was taken by pipette and analyzed by ¹H NMR.

4.7.4 General Procedure for Preparative Pd-Catalyzed Decarbonylative Dehydration



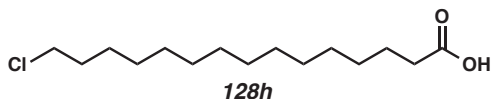
A 15 mL round-bottom flask was charged with PdCl₂(PPh₃)₂ (0.01 mmol, 0.05 mol%), Xantphos (0.012 mmol, 0.06 mol%), (t-Bu)₄biphenol (0.1 mmol, 0.5 mol%), and fatty acid substrate (20 mmol, 1 equiv). The flask was equipped with a distillation head and a 25 mL round-bottom receiving flask. The closed system was connected to a vacuum manifold, equipped with a needle valve and a digital vacuum gauge. The system was evacuated and refilled with N₂ (x 3), and the first portion of acetic anhydride (20 mmol, 1 equiv) was added via syringe through the septum that seals the top of the distillation head. The flask was lowered into a 20 °C oil bath and gradually heated to 132 °C in 23 min.[†] When oil bath temperature rose to 122 °C, the needle valve was closed, switched to vacuum, and the needle valve carefully and slowly opened to allow

[†] When the reaction was performed at 100 mmol scale with high-melting substrates such as stearic acid, the reaction flask was first heated to 85 °C until all solid melted, and then to 132 °C. Overall heating time from 20 to 132 °C was approximately 40 min.

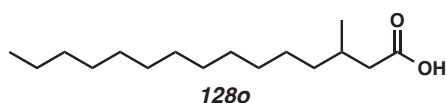
distillation of acetic acid into a receiving flask, which was cooled to $-78\text{ }^{\circ}\text{C}$. When the oil bath temperature reached $130\text{ }^{\circ}\text{C}$, time was recorded as $t = 0$. After distillation ceased (about $t = 3\text{ min}$), the needle valve was opened fully and a vacuum of 1–5 mmHg was drawn. At $t = 30\text{ min}$, the system was refilled with N_2 , and the second portion of acetic anhydride (2.8 mmol, 0.14 equiv) was added via syringe. The system was then gradually ($t = 35\text{ min}$) resubjected to a vacuum of 1–5 mmHg. Acetic anhydride was added as follows (0.12, 0.10, 0.09, 0.08 equiv) in the same manner every 30 min. The reaction was stopped at $t = 3\text{ h}$ and allowed to cool to ambient temperature. The residual reaction mixture was purified by flash chromatography. If it contained solids, it was suction-filtered first and the solids washed with hexanes, and the filtrate was concentrated and purified by chromatography. In cases where the product was distilled together with acetic acid, the distillate was added dropwise to a saturated NaHCO_3 solution, stirred for 30 min, and the resulting mixture was extracted with dichloromethane (30 mL x 3). The combined extracts were dried over Na_2SO_4 , filtered and concentrated. The crude product was then subjected to flash chromatography or distillation to afford the olefin in pure form.

4.7.5 Spectroscopic Data for Acid Substrates

Saturated fatty acids **128a–128d** and **128m** are commercially available. Carboxylic acids **128e**,¹⁶ **128f**,¹⁷ **128g**,¹⁸ **128i**,¹⁹ **128j**,²⁰ **128k**,²¹ **128l**,²² and **128n**²³ are known compounds and prepared according to literature methods.

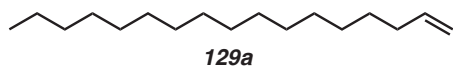


15-Chloropentadecanoic acid (128h). ^1H NMR (500 MHz, CDCl_3) δ 3.52 (t, $J = 6.8$ Hz, 2H), 2.34 (t, $J = 7.5$ Hz, 2H), 1.79–1.73 (m, 2H), 1.62 (p, $J = 7.5$ Hz, 2H), 1.46–1.20 (m, 20H); ^{13}C NMR (126 MHz, CDCl_3) δ 180.6, 45.3, 34.2, 32.8, 29.7, 29.7, 29.7, 29.7, 29.6, 29.6, 29.4, 29.2, 29.0, 27.0, 24.8; IR (Neat Film) 2916, 2848, 1701, 1462, 1410, 1302, 943, 721 cm^{-1} ; HRMS (NMM: ESI-APCI $^-$) m/z calc'd for $\text{C}_{15}\text{H}_{28}\text{O}_2\text{Cl}$ $[\text{M}-\text{H}]^-$: 275.1783, found 275.1794.

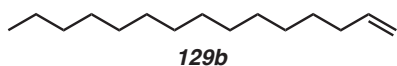


3-Methylpentadecanoic acid (128o). ^1H NMR (500 MHz, CDCl_3) δ 2.35 (dd, $J = 15.0$, 5.9 Hz, 1H), 2.14 (dd, $J = 15.0$, 8.2 Hz, 1H), 2.01–1.90 (m, 1H), 1.38–1.15 (m, 22H), 0.96 (d, $J = 6.7$ Hz, 3H), 0.88 (t, $J = 6.9$ Hz, 3H); ^{13}C NMR (126 MHz, CDCl_3) δ 180.1, 41.8, 36.8, 32.1, 30.3, 29.9, 29.8, 29.8, 29.8, 29.8, 29.8, 29.5, 27.0, 22.9, 19.8, 14.3; IR (Neat Film) 2914, 2852, 1701, 1473, 1410, 1300, 1151, 1123, 954, 715; HRMS (NMM: ESI-APCI $^-$) m/z calc'd for $\text{C}_{16}\text{H}_{31}\text{O}_2$ $[\text{M}-\text{H}]^-$: 255.2330, found 255.2328.

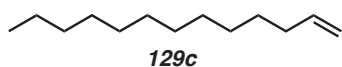
4.7.6 Spectroscopic Data for Olefin Products



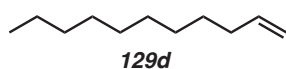
1-Heptadecene (129a).²⁴ ^1H NMR (500 MHz, CDCl_3) δ 5.82 (ddt, $J = 16.9$, 10.2, 6.7 Hz, 1H), 5.07–4.86 (m, 2H), 2.11–1.98 (m, 2H), 1.49–1.08 (m, 26H), 0.88 (t, $J = 6.9$ Hz, 3H).



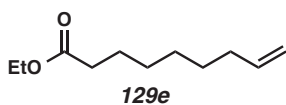
1-Pentadecene (129b).²⁵ ^1H NMR (500 MHz, CDCl_3) δ 5.82 (ddt, $J = 16.9, 10.2, 6.7$ Hz, 1H), 5.07–4.85 (m, 2H), 2.11–1.97 (m, 2H), 1.46–1.08 (m, 22H), 0.88 (t, $J = 6.9$ Hz, 3H).



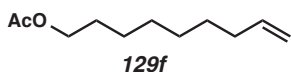
1-Tridecene (129c).²⁶ ^1H NMR (500 MHz, CDCl_3) δ 5.82 (ddt, $J = 17.0, 10.1, 6.7$ Hz, 1H), 5.09–4.83 (m, 2H), 2.11–1.97 (m, 2H), 1.48–1.11 (m, 18H), 0.88 (t, $J = 6.9$ Hz, 3H).



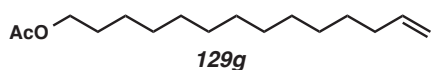
1-Undecene (129d).²⁷ ^1H NMR (500 MHz, CDCl_3) δ 5.82 (ddt, $J = 16.9, 10.2, 6.7$ Hz, 1H), 5.08–4.84 (m, 2H), 2.11–1.98 (m, 2H), 1.47–1.09 (m, 14H), 0.88 (t, $J = 6.9$ Hz, 3H).



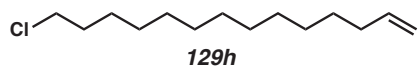
Ethyl non-8-enoate (129e).²⁸ ^1H NMR (500 MHz, CDCl_3) δ 5.80 (ddt, $J = 16.6, 9.9, 6.8$ Hz, 1H), 5.07–4.87 (m, 2H), 4.12 (q, $J = 7.2$ Hz, 2H), 2.28 (t, $J = 7.5$ Hz, 2H), 2.10–1.98 (m, 2H), 1.69–1.54 (m, 2H), 1.46–1.28 (m, 6H), 1.25 (t, $J = 7.1$ Hz, 3H).



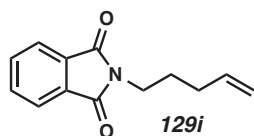
Non-8-en-1-yl acetate (129f).²⁹ ¹H NMR (500 MHz, CDCl₃) δ 5.80 (ddt, *J* = 16.9, 10.2, 6.7 Hz, 1H), 5.07–4.87 (m, 2H), 4.05 (t, *J* = 6.8 Hz, 2H), 2.14–1.94 (m, 5H), 1.70–1.52 (m, 2H), 1.47–1.18 (m, 8H).



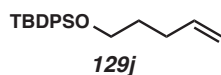
Tetradec-13-en-1-yl acetate (129g).³⁰ ¹H NMR (500 MHz, CDCl₃) δ 5.81 (ddt, *J* = 16.8, 10.1, 6.8 Hz, 1H), 5.08–4.86 (m, 2H), 4.05 (t, *J* = 6.8 Hz, 2H), 2.11–1.98 (m, 5H), 1.69–1.53 (m, 2H), 1.45–1.09 (m, 18H).



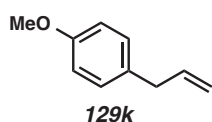
14-Chlorotetradec-1-ene (129h). ¹H NMR (500 MHz, CDCl₃) δ 5.81 (ddt, *J* = 17.0, 10.2, 6.7 Hz, 1H), 5.07–4.86 (m, 2H), 3.53 (t, *J* = 6.8 Hz, 2H), 2.11–1.98 (m, 2H), 1.77 (dt, *J* = 14.5, 6.9 Hz, 2H), 1.50–1.10 (m, 18H); ¹³C NMR (126 MHz, CDCl₃) δ 139.4, 114.2, 45.3, 34.0, 32.8, 29.8, 29.7, 29.7, 29.6, 29.6, 29.3, 29.1, 29.0, 27.0; IR (Neat Film, NaCl) 3076, 2925, 2854, 1641, 1465, 1309, 993, 966, 909, 723 cm⁻¹; HRMS (FAB+) *m/z* calc'd for C₁₄H₂₇³⁵Cl [M]⁺: 230.1801, found 230.1808.



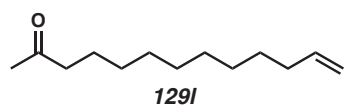
2-(Pent-4-en-1-yl)isoindoline-1,3-dione (129i).³¹ ¹H NMR (500 MHz, CDCl₃) δ 7.89–7.73 (m, 2H), 7.73–7.58 (m, 2H), 5.77 (ddt, *J* = 16.9, 10.2, 6.6 Hz, 1H), 5.10–4.87 (m, 2H), 3.74–3.57 (m, 2H), 2.17–2.00 (m, 2H), 1.74 (p, *J* = 7.5 Hz, 2H).



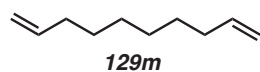
tert-Butyl(pent-4-en-1-yloxy)diphenylsilane (129j).³² ^1H NMR (500 MHz, CDCl_3) δ 7.67 (dt, $J = 6.5, 1.5$ Hz, 4H), 7.39 (dddd, $J = 14.4, 8.3, 6.0, 2.1$ Hz, 6H), 5.80 (ddt, $J = 16.9, 10.2, 6.6$ Hz, 1H), 5.09–4.87 (m, 2H), 3.68 (t, $J = 6.5$ Hz, 2H), 2.15 (tdd, $J = 8.1, 6.8, 1.4$ Hz, 2H), 1.73–1.60 (m, 2H), 1.05 (s, 9H).



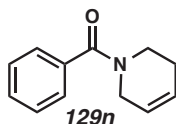
1-Allyl-4-methoxybenzene (129k).³³ ^1H NMR (500 MHz, CDCl_3) δ 7.17–7.06 (m, 2H), 6.91–6.78 (m, 2H), 5.96 (ddt, $J = 16.8, 10.1, 6.7$ Hz, 1H), 5.13–4.99 (m, 2H), 3.79 (s, 3H), 3.34 (d, $J = 6.7$ Hz, 2H).



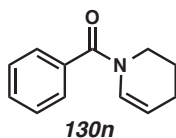
Tridec-12-en-2-one (129l).³⁴ ^1H NMR (500 MHz, CDCl_3) δ 5.81 (ddt, $J = 16.9, 10.1, 6.7$ Hz, 1H), 5.06–4.87 (m, 2H), 2.41 (t, $J = 7.5$ Hz, 2H), 2.13 (s, 3H), 2.09–1.97 (m, 2H), 1.62–1.49 (m, 2H), 1.46–1.11 (m, 12H).



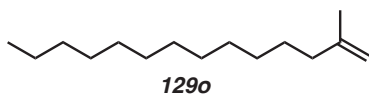
Deca-1,9-diene (129m).³⁵ ^1H NMR (500 MHz, CDCl_3) δ 5.81 (ddt, $J = 17.0, 10.2, 6.7$ Hz, 2H), 5.08–4.86 (m, 4H), 2.11–1.98 (m, 4H), 1.48–1.21 (m, 8H).



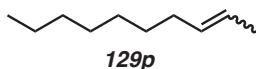
(3,6-Dihydropyridin-1(2H)-yl)(phenyl)methanone (129n).³⁶ ¹H NMR (500 MHz, DMSO-*d*₆, 130 °C) δ 7.41 (ddd, *J* = 24.3, 6.8, 3.4 Hz, 5H), 5.90–5.82 (m, 1H), 5.78–5.64 (m, 1H), 4.00 (p, *J* = 2.8 Hz, 2H), 3.56 (t, *J* = 5.8 Hz, 2H), 2.16 (dp, *J* = 8.7, 3.2 Hz, 2H).



(3,4-Dihydropyridin-1(2H)-yl)(phenyl)methanone (129n).³⁷ ¹H NMR (500 MHz, DMSO-*d*₆, 130 °C) δ 7.45 (tdd, *J* = 6.0, 3.9, 2.4 Hz, 5H), 6.78–6.61 (m, 1H), 4.97 (dt, *J* = 8.2, 3.9 Hz, 1H), 3.72–3.60 (m, 2H), 2.09 (tdd, *J* = 6.2, 3.8, 2.0 Hz, 2H), 1.85 (p, *J* = 6.1 Hz, 2H).

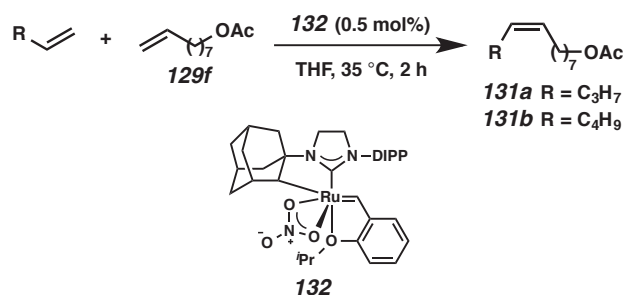


2-Methyltetradec-1-ene (129o).³⁸ ¹H NMR (500 MHz, CDCl₃) δ 4.72–4.63 (m, 2H), 2.00 (t, *J* = 7.7 Hz, 2H), 1.71 (s, 3H), 1.47–1.11 (m, 20H), 0.88 (t, *J* = 6.9 Hz, 3H).

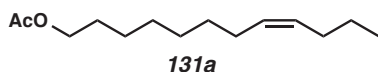


(E)- and (Z)-2-decene (129p).³⁹ ¹H NMR (500 MHz, CDCl₃) δ 5.48–5.35 (m, 2H), 2.07–1.93 (m, 2H), 1.64 (d, *J* = 4.2 Hz, 3H, *E*-olefin), 1.60 (d, *J* = 6.1 Hz, 3H, *Z*-olefin), 1.43–1.20 (m, 10H), 0.88 (t, *J* = 6.6 Hz, 3H).

4.7.7 General Procedure for Pheromone Synthesis by Ru-Catalyzed Cross Metathesis^{6b}

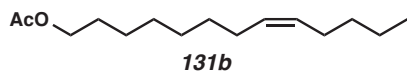


In a glovebox, a 20 mL vial was charged with 8-nonenyl acetate (**129f**,^{††} 1.0 mL, 4.8 mmol), 1-pentene or 1-hexene (48 mmol), and THF (2.6 mL). Ruthenium metathesis catalyst **132** (16 mg, 0.024 mmol, 0.5 mol%) was added and the reaction was stirred at 35 °C in an open vial for 2 hours. The vial was removed from the glovebox, quenched with ethyl vinyl ether (2.5 mL) and stirred for 30 minutes. The solvent was then removed *in vacuo*. The crude mixture was passed through a SiO₂ plug (hexane to 4% ethyl acetate in hexanes) to provide a mixture of unreacted 8-nonenyl acetate and pheromone **131**. Pheromone **131** was isolated by distillation using a Kugelrohr apparatus.



(*Z*)-dodec-8-en-1-yl acetate (**131a**).^{6a} ¹H NMR (500 MHz, CDCl₃) δ 5.35 (2H, m), 4.04 (2H, t, *J* = 6.8 Hz), 2.04 (3H, s), 2.01 (4H, m), 1.61 (2H, m), 1.27–1.39 (10H, m), 0.89 (3H, t, *J* = 7.4 Hz).

^{††} An inseparable mixture of olefin isomers **129f** and **130f** was used for this reaction. For **131a**, the mixture was 98% alpha (**129f**:**130f** = 98:2); for **131b**, the mixture was 96% alpha (**129f**:**130f** = 96:4).



(Z)-tridec-8-en-1-yl acetate (131b).^{6b} ¹H NMR (500 MHz, CDCl₃) δ 5.34 (m, 2H), 4.05 (t, *J* = 6.8 Hz, 2H), 2.00–2.04 (m, 7H), 1.60–1.63 (m, 2H), 1.29–1.36 (m, 12H), 0.88–0.91 (m, 3H).

4.8 Notes and References

- (1) Ittel, S. D.; Johnson, L. K.; Brookhart, M. *Chem. Rev.* **2000**, *100*, 1169–1203.
- (2) (a) Marquis, D. M., Sharman, S. H.; House, R.; Sweeney, W. A. *J. Am. Oil Chem. Soc.* **1966**, *43*, 607–614. (b) Franke, R.; Selent, D.; Börner, A. *Chem. Rev.* **2012**, *112*, 5675–5732.
- (3) (a) Al-Jarallah, A. M.; Anabtawi, J. A.; Siddiqui, M. A. B.; Aitani, A. M.; Al-Sa'doun, A. W. *Catal. Today* **1992**, *14*, 1–121. (b) Small, B. L.; Brookhart, M. *J. Am. Chem. Soc.* **1998**, *120*, 7143–7144.
- (4) Ouyang, J.; Kong, F.; Su, G.; Hu, Y.; Song, Q. *Catal. Lett.* **2009**, *132*, 64–74.
- (5) Prices of acids and olefins (Sigma-Aldrich, 10/5/2013):

Acid	\$/kg	Olefin	\$/kg
Decanoic (C ₁₀)	16.28	1-Nonene (C ₉)	12,080.00
		1-Decene (C ₁₀)	55.87
Lauric (C ₁₂)	14.20	1-Undecene (C ₁₁)	7,240.00
		1-Dodecene (C ₁₂)	187.60
Myristic (C ₁₄)	11.76	1-Tridecene (C ₁₃)	23,800.00
		1-Tetradecene (C ₁₄)	47.74
Palmitic (C ₁₆)	7.68	1-Pentadecene (C ₁₅)	24,722.58
		1-Hexadecene (C ₁₆)	2,758.62
Stearic (C ₁₈)	13.20	1-Heptadecene (C ₁₇)	69,500.00

-
- (6) (a) Herbert, M. B.; Marx, V. M.; Pederson, R. L.; Grubbs, R. H. *Angew. Chem., Int. Ed.* **2013**, *52*, 310–314. (b) Rosebrugh, L. E.; Herbert, M. B.; Marx, V. M.; Keitz, B. K.; Grubbs, R. H. *J. Am. Chem. Soc.* **2013**, *135*, 1276–1279.
- (7) Bacha, J. D.; Kochi, J. K. *Tetrahedron* **1968**, *24*, 2215–2226.
- (8) Kolbe, H. *Justus Liebigs Ann. Chem.* **1849**, *69*, 257–294.
- (9) (a) Anderson, J. M.; Kochi, J. K. *J. Org. Chem.* **1969**, *35*, 986–989. (b) van der Klis, F.; van den Hoorn, M. H.; Blaauw, R.; van Haveren, J.; van Es, D. S. *Eur. J. Lipid Sci. Technol.* **2011**, *113*, 562–571.
- (10) Foglia, T. A.; Barr, P. A. *J. Am. Oil Chem. Soc.* **1976**, *53*, 737–741.
- (11) Maetani, S.; Fukuyama, T.; Suzuki, N.; Ishihara, D.; Ryu, I. *Organometallics* **2011**, *30*, 1389–1394.
- (12) (a) Miller, J. A.; Nelson, J. A.; Byrne, M. P. *J. Org. Chem.* **1993**, *58*, 18–20. (b) Kraus, G. A.; Riley, S. *Synthesis* **2012**, *44*, 3003–3005. (c) Gooßen, L. J.; Rodríguez, N. *Chem. Commun.* **2004**, 724–725. (d) Le Nôtre, J.; Scott, E. L.; Franssen, M. C. R.; Sanders, J. P. M. *Tetrahedron Lett.* **2010**, *51*, 3712–3715. (e) Miranda, M. O.; Pietrangelo, A.; Hillmyer, M. A.; Tolman, W. B. *Green Chem.* **2012**, *14*, 490–494.
- (13) Maetani, S.; Fukuyama, T.; Suzuki, N.; Ishihara, D.; Ryu, I. *Chem. Commun.* **2012**, *48*, 2552–2554.
- (14) Baker, T. C.; Cardé, R. T.; Miller, J. R. *J. Chem. Ecol.* **1980**, *6*, 749–758.
- (15) Subchev, M.; Toth, M.; Wu, D.; Stanimirova, L.; Toshova, T.; Karpati, Z. *J. Appl. Ent.* **2000**, *124*, 197–199.
- (16) Regourd, J.; Ali, A. A.; Thompson, A. *J. Med. Chem.* **2007**, *50*, 1528–1536.

-
- (17) Kazlauskas, R.; Murphy, P. T.; Wells, R. J.; Blackman, A. J. *Aust. J. Chem.* **1982**, *35*, 113–120.
- (18) Melliou, E.; Chinou, I. *J. Agric. Food Chem.* **2005**, *53*, 8987–8992.
- (19) Guenin, E.; Monteil, M.; Bouchemal, N.; Prange, T.; Lecouvey, M. *Eur. J. Org. Chem.* **2007**, 3380–3391.
- (20) Oppolzer, W.; Radinov, R. N.; El-Sayed, E. *J. Org. Chem.* **2001**, *66*, 4766–4770.
- (21) Ohishi, T.; Zhang, L.; Nishiura, M.; Hou, Z. *Angew. Chem., Int. Ed.* **2011**, *50*, 8114–8117.
- (22) Kaiser, R.; Lamparsky, D. *Helv. Chim. Acta* **1978**, *61*, 2671–2680.
- (23) Wang, Z.; Zhu, L.; Yin, F.; Su, Z.; Li, Z.; Li, C. *J. Am. Chem. Soc.* **2012**, *134*, 4258–4263.
- (24) Barton, D. H. R.; Boivin, J.; Crépon, E.; Sarma, J.; Togo, H.; Zard, S. Z. *Tetrahedron* **1991**, *47*, 7091–7108.
- (25) Burns, D. H.; Miller, J. D.; Chan, H.-K.; Delaney, M. O. *J. Am. Chem. Soc.* **1997**, *119*, 2125–2133.
- (26) Rojas, G.; Wagener, K. B. *J. Org. Chem.* **2008**, *73*, 4962–4970.
- (27) Vijai Kumar Reddy, T.; Prabhavathi Devi, B. L. A.; Prasad, R. B. N.; Poornima, M.; Ganesh Kumar, C. *Bioorg. Med. Chem. Lett.* **2012**, *22*, 4678–4680.
- (28) Ravu, V. R.; Leung, G. Y. C.; Lim, C. S.; Ng, S. Y.; Sum, R. J.; Chen, D. Y.-K. *Eur. J. Org. Chem.* **2011**, 463–468.
- (29) Mori, K. *Tetrahedron* **2009**, *65*, 3900–3909.
- (30) Lin, J.; Liu, F.; Wang, Y.; Liu, M. *Synth. Commun.* **1995**, *25*, 3457–3461.
- (31) Whittaker, A. M.; Lalic, G. *Org. Lett.* **2013**, *15*, 1112–1115.

-
- (32) Dias, D. A.; Kerr, M. A. *Org. Lett.* **2009**, *11*, 3694–3697.
- (33) Ackermann, L.; Kapdi, A. R.; Schulzke, C. *Org. Lett.* **2010**, *12*, 2298–2301.
- (34) Arbain, D.; Dasman, N.; Ibrahim, S.; Sargent, M. V. *Aust. J. Chem.* **1990**, *43*, 1949–1952.
- (35) Garwood, R. F.; Naser-ud-Din; Scott, C. J.; Weedon, B. C. L. *J. Chem. Soc., Perkin Trans. 1* **1973**, 2714–2721.
- (36) Olofson, R. A.; Abbott, D. E. *J. Org. Chem.* **1984**, *49*, 2795–2799.
- (37) Gigant, N.; Chausset-Boissarie, L.; Belhomme, B.-C.; Poisson, T.; Pannecoucke, X.; Isabelle, G. *Org. Lett.* **2013**, *15*, 278–281.
- (38) Pearlman, B. A.; Putt, S. R.; Fleming, J. A. *J. Org. Chem.* **1985**, *50*, 3625–3626.
- (39) Yanagisawa, A.; Habaue, S.; Yasue, K.; Yamamoto, H. *J. Am. Chem. Soc.* **1994**, *116*, 6130–6141.

APPENDIX 5

Spectra Relevant to Chapter 4

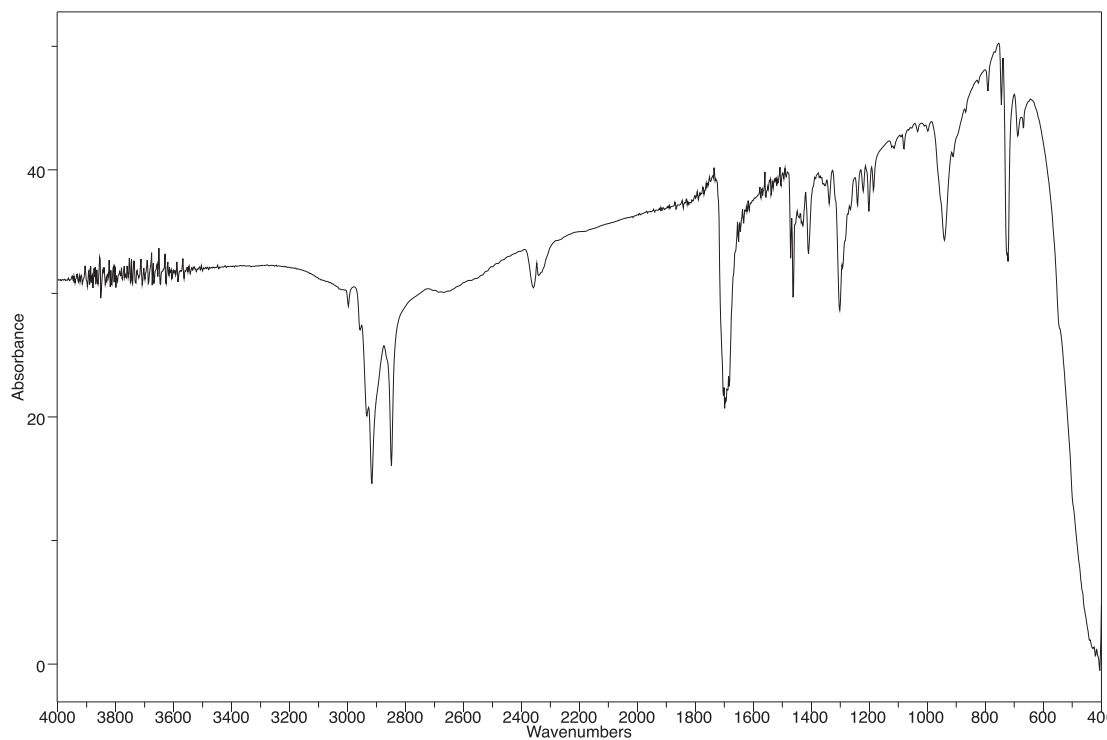


Figure A5.2 Infrared spectrum (Thin Film, NaCl) of compound **128h**.

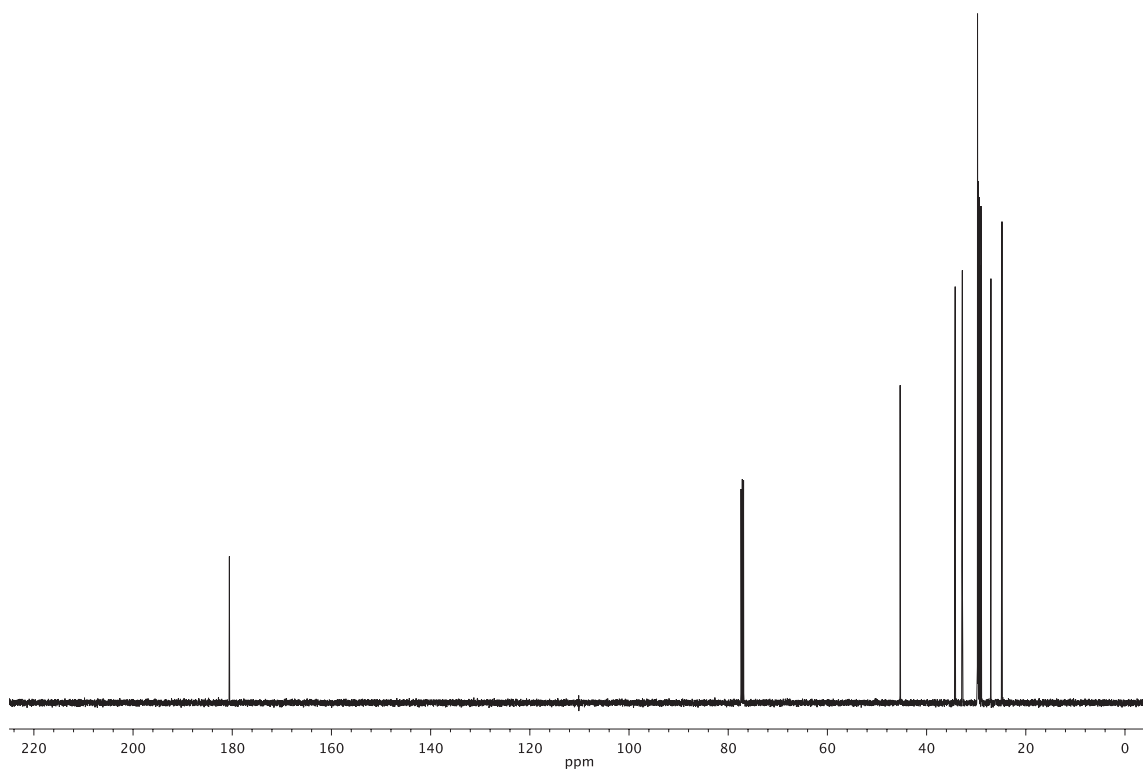


Figure A5.3 ¹³C NMR (126 MHz, CDCl₃) of compound **128h**.

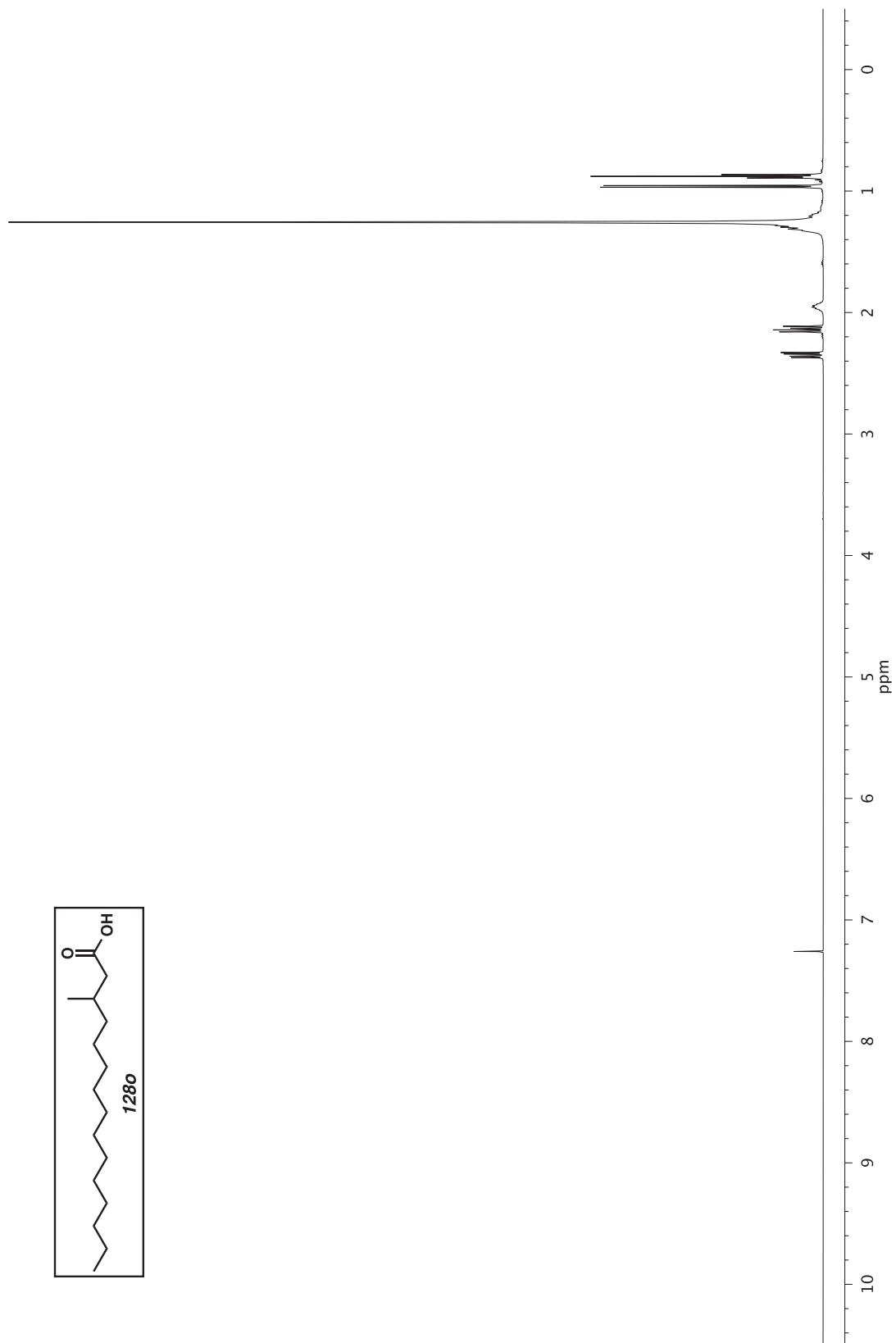


Figure A5.4 ^1H NMR (500 MHz, CDCl_3) of compound 1280.

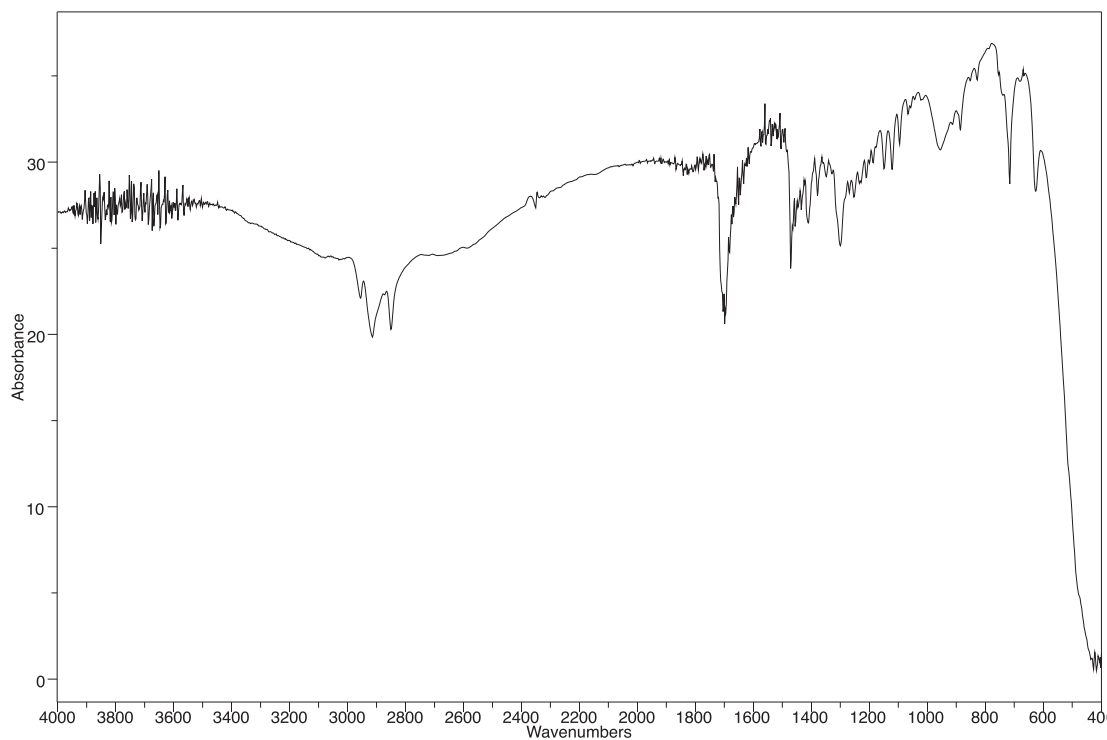


Figure A5.5 Infrared spectrum (Thin Film, NaCl) of compound **128o**.

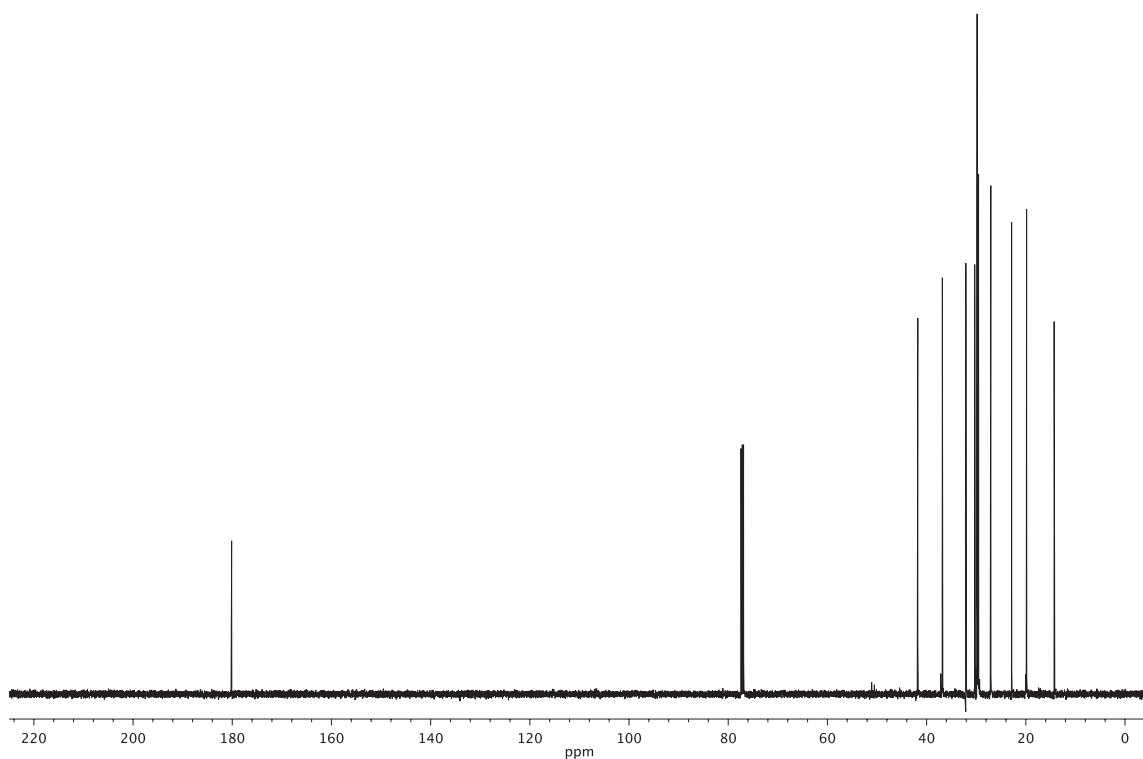


Figure A5.6 ¹³C NMR (126 MHz, CDCl₃) of compound **128o**.

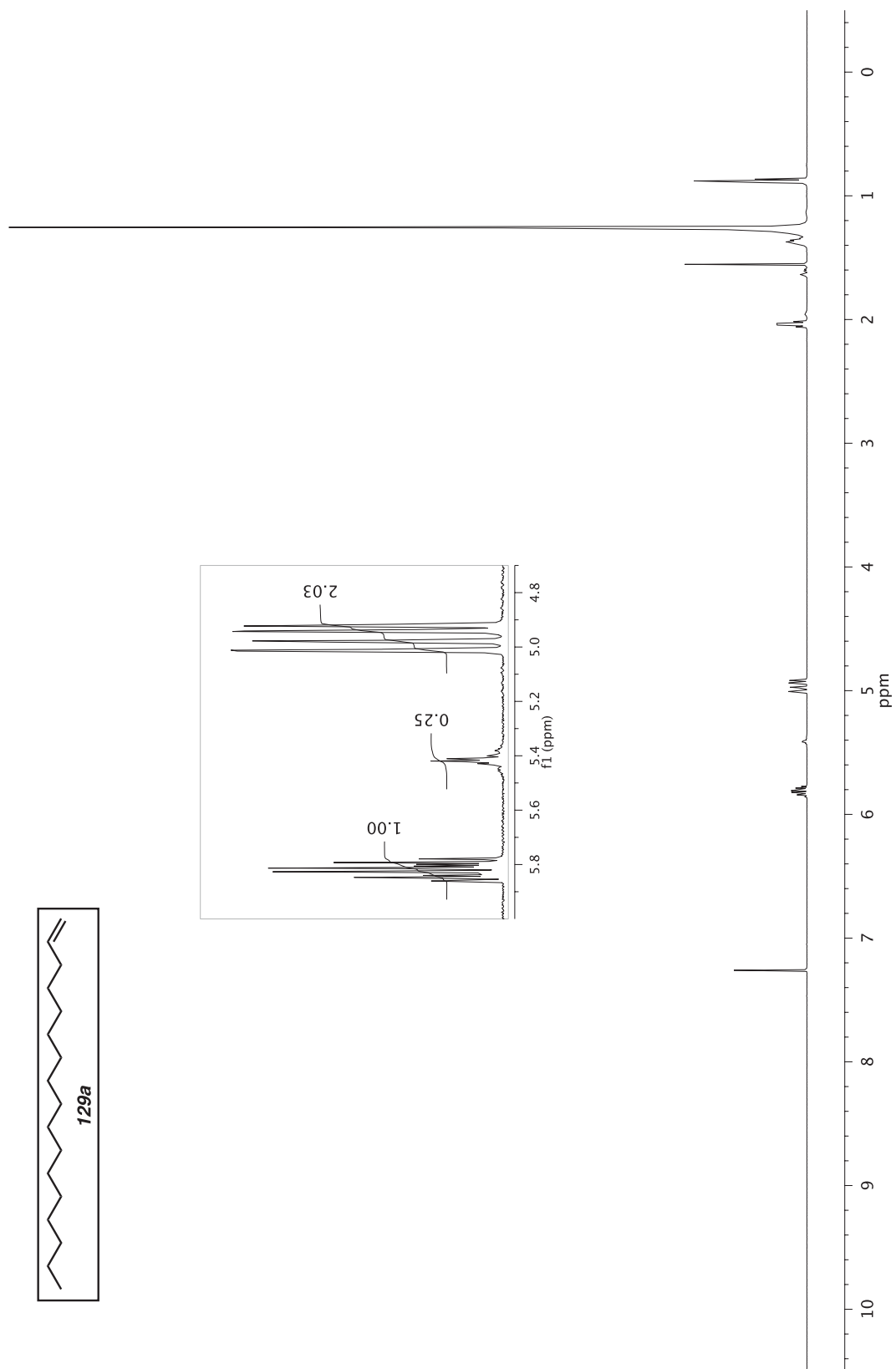


Figure A5.7 ^1H NMR (500 MHz, CDCl_3) of compound **129a**.

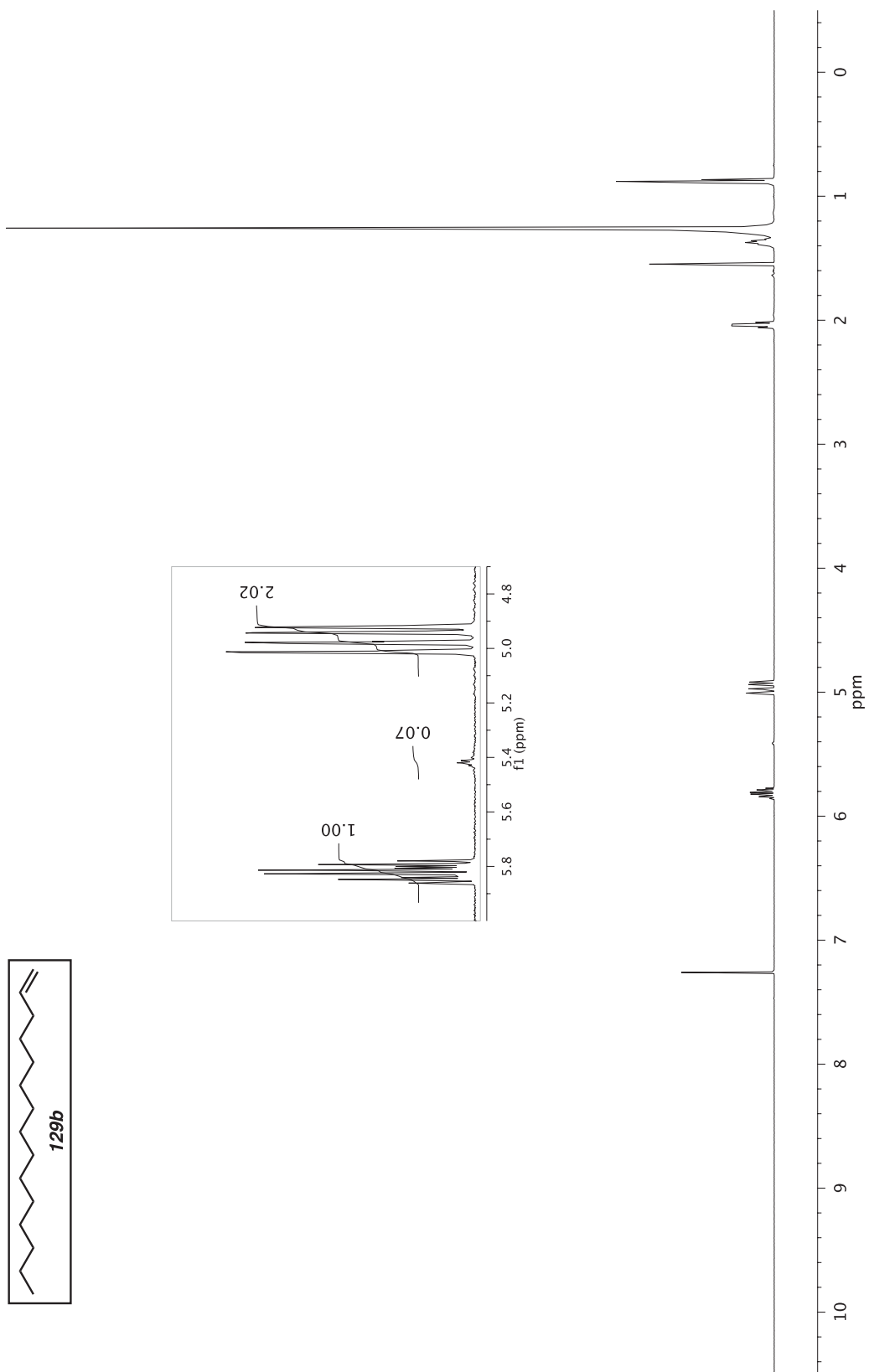


Figure A5.8 ^1H NMR (500 MHz, CDCl_3) of compound **129b**.

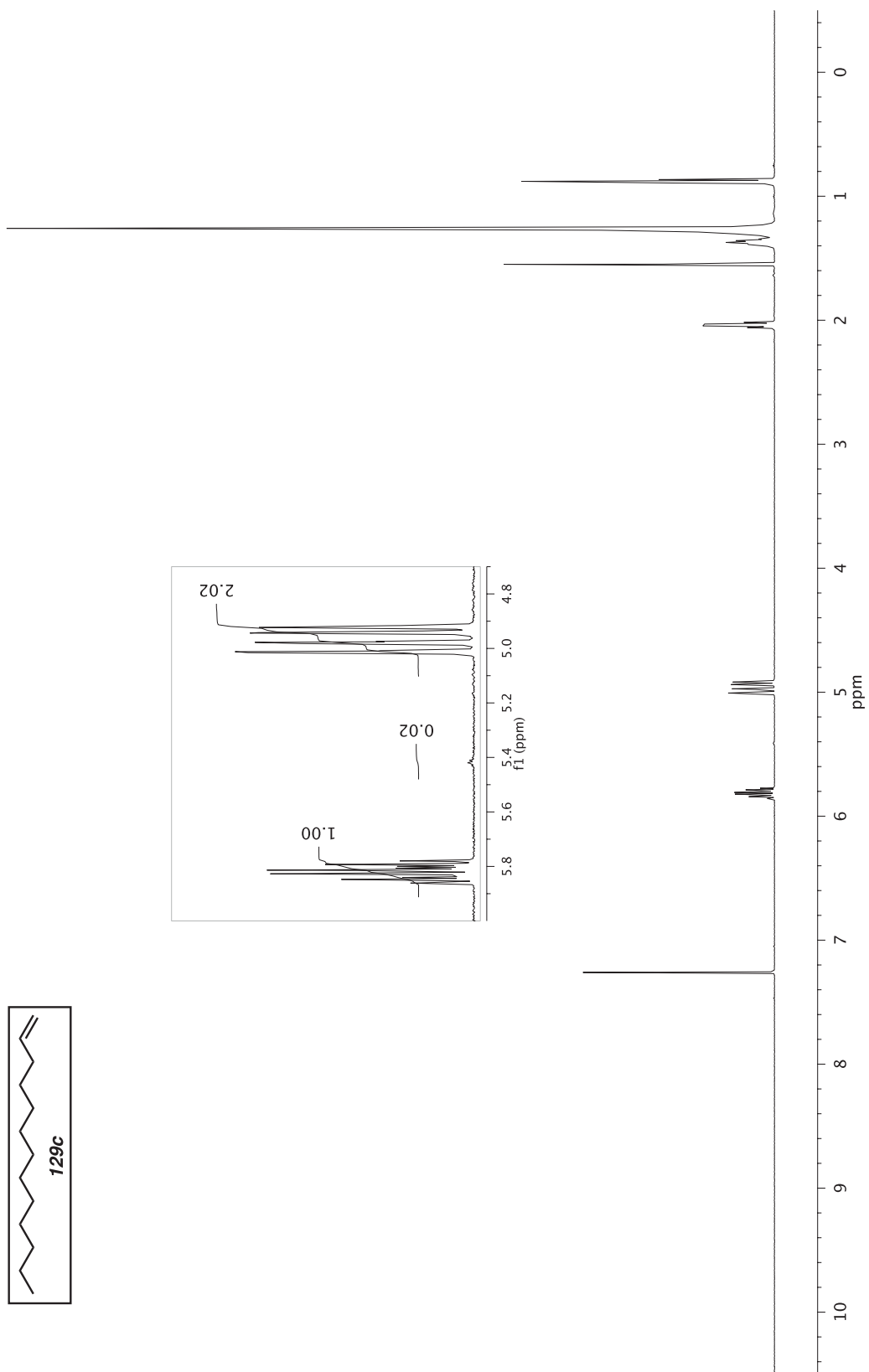


Figure A5.9 ^1H NMR (500 MHz, CDCl_3) of compound **129c**.

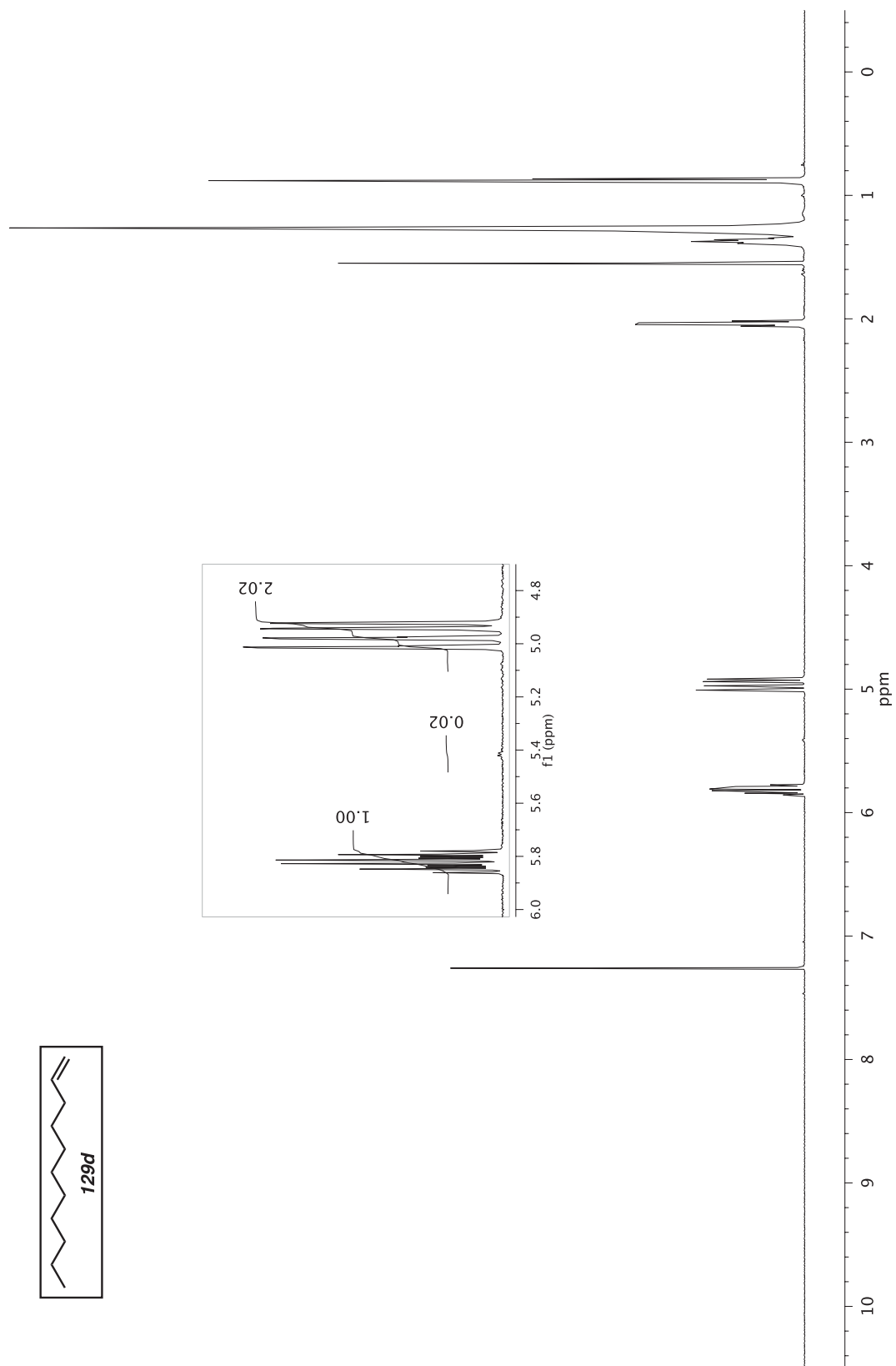


Figure A5.10 ^1H NMR (500 MHz, CDCl_3) of compound **129d**.

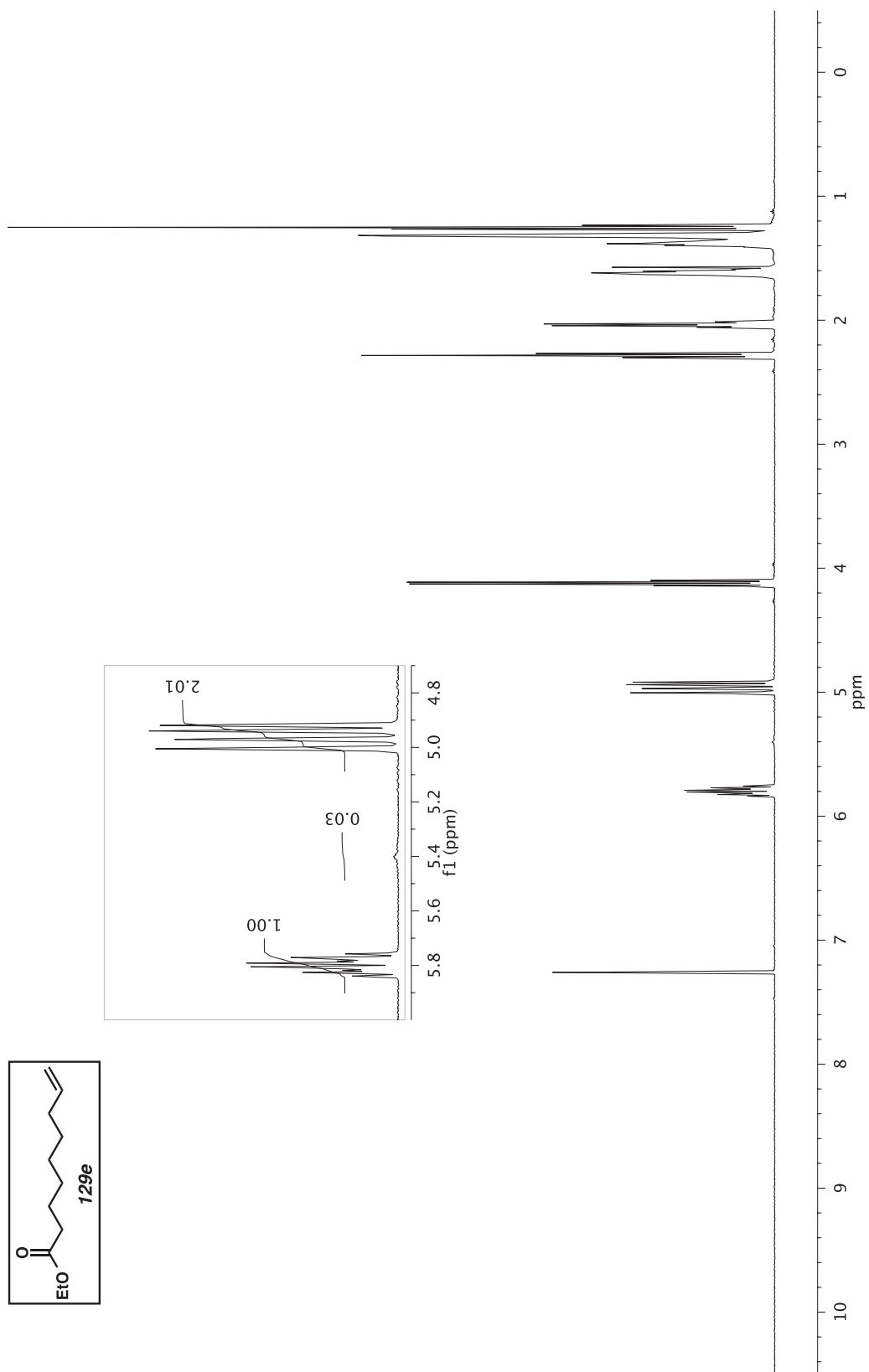


Figure A5.11 ^1H NMR (500 MHz, CDCl_3) of compound **129e**.

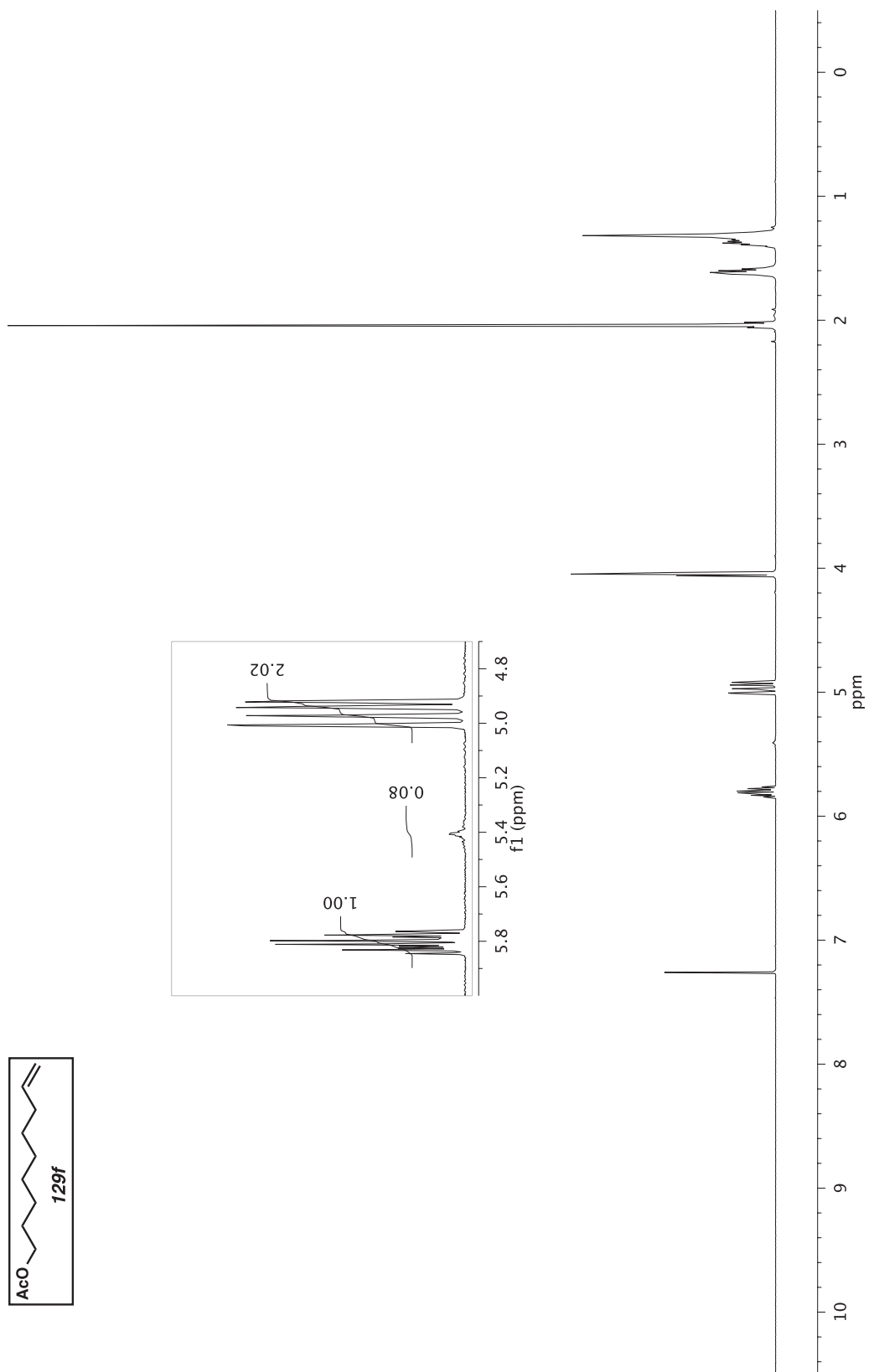


Figure A5.12 ^1H NMR (500 MHz, CDCl_3) of compound **129f**.

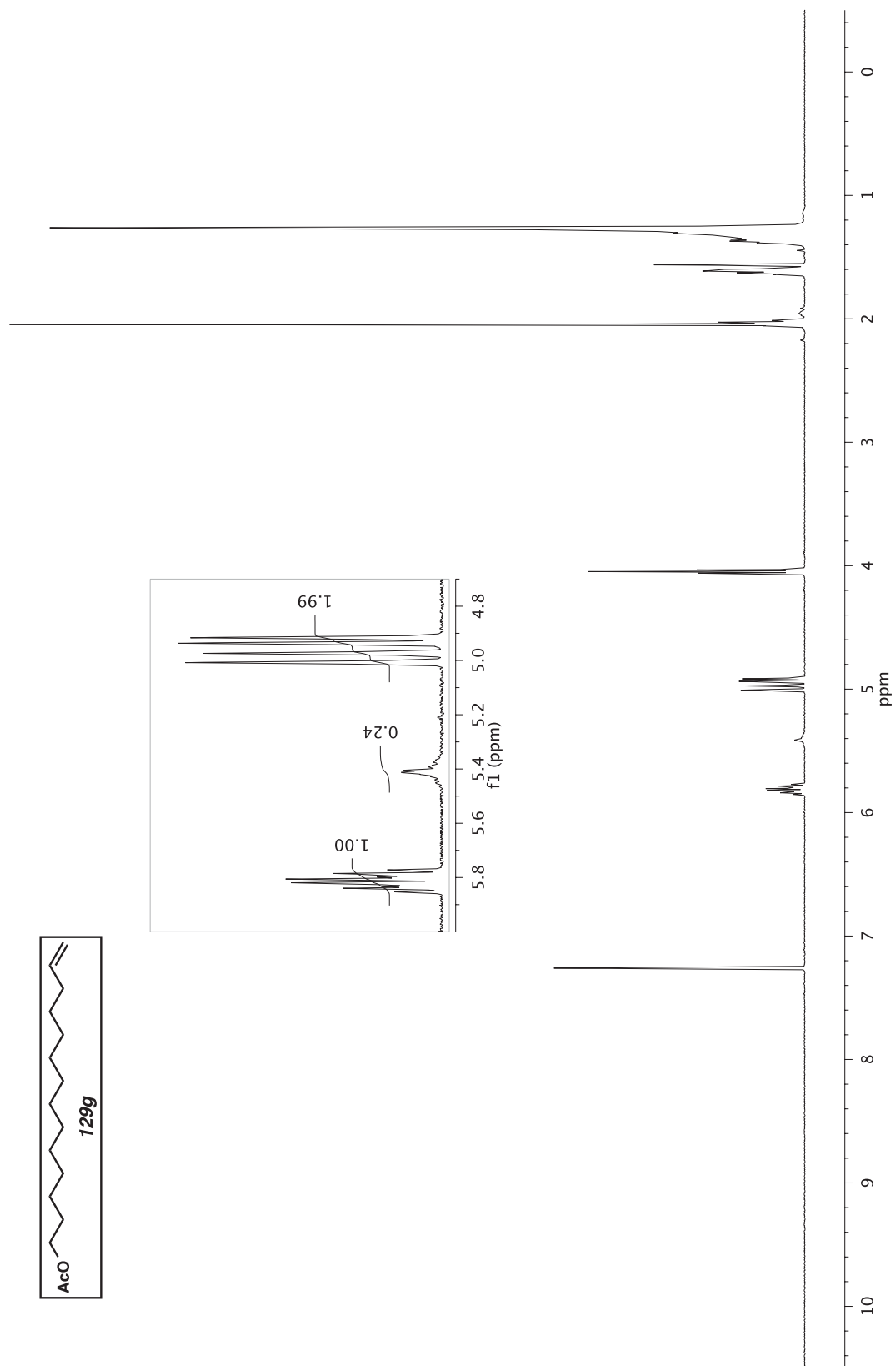


Figure A5.13 ^1H NMR (500 MHz, CDCl_3) of compound **129g**.

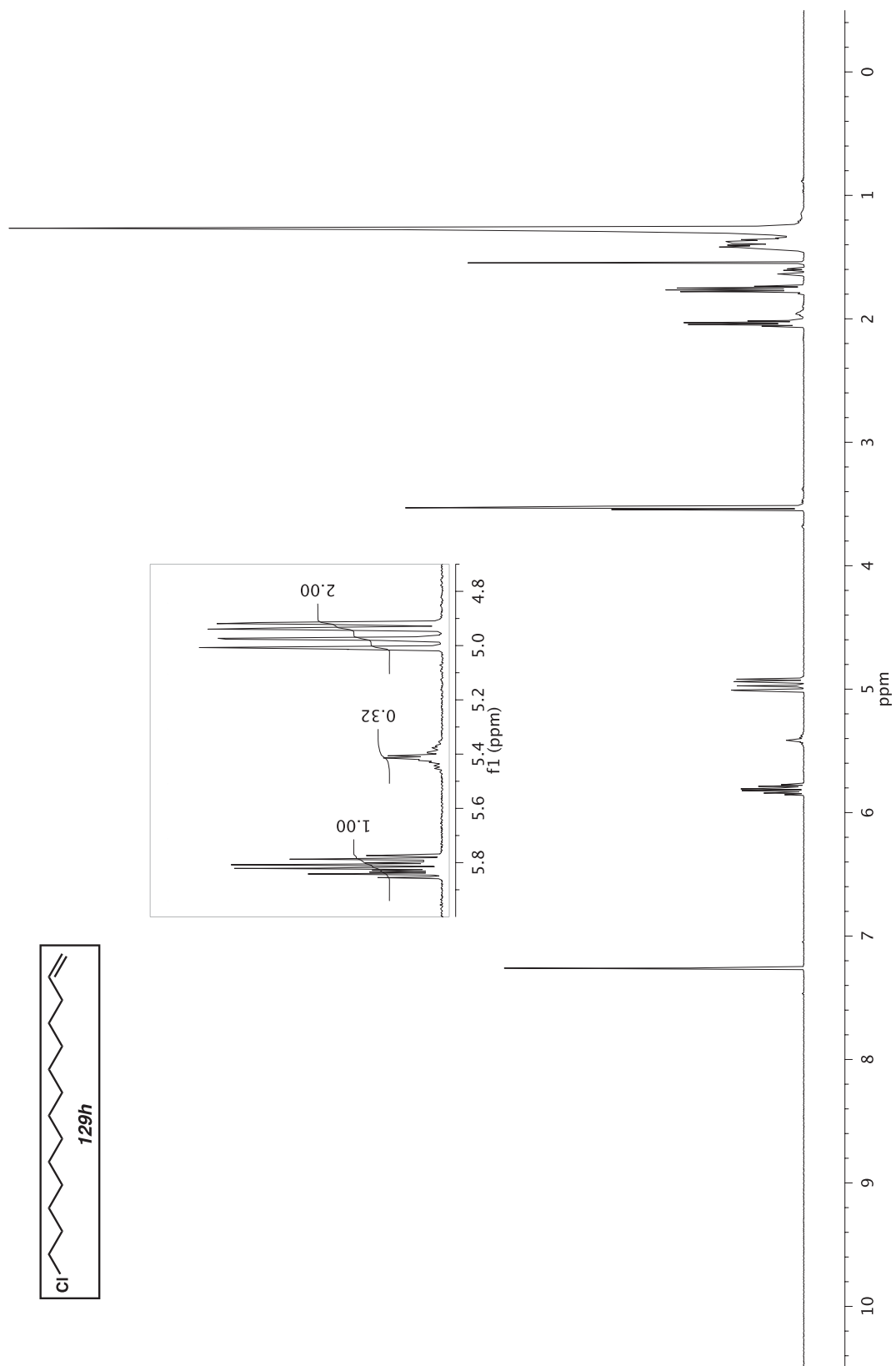


Figure A5.14 ^1H NMR (500 MHz, CDCl_3) of compound **129h**.

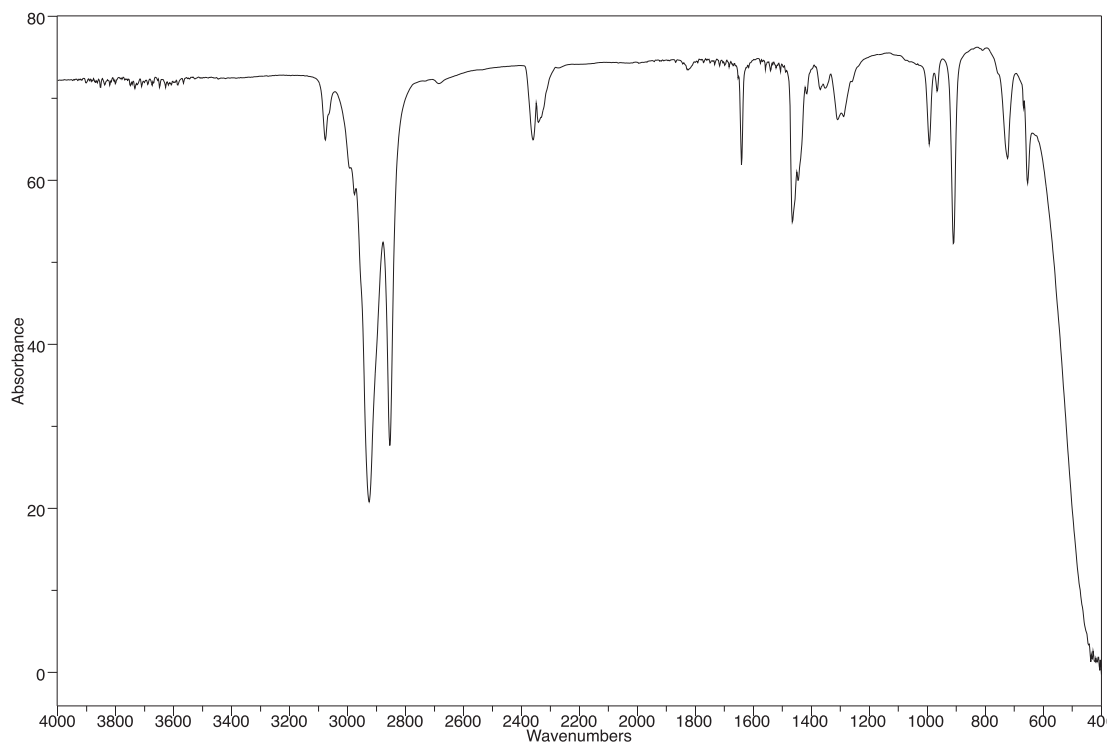


Figure A5.15 Infrared spectrum (Thin Film, NaCl) of compound **129h**.

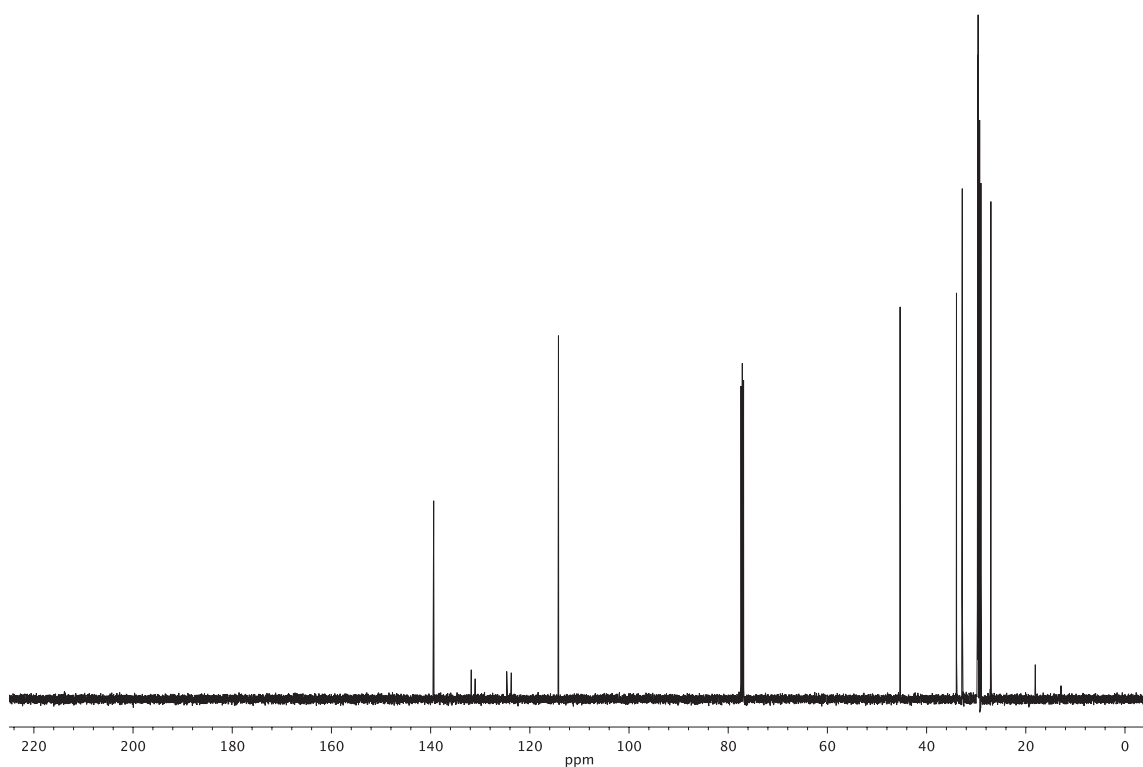
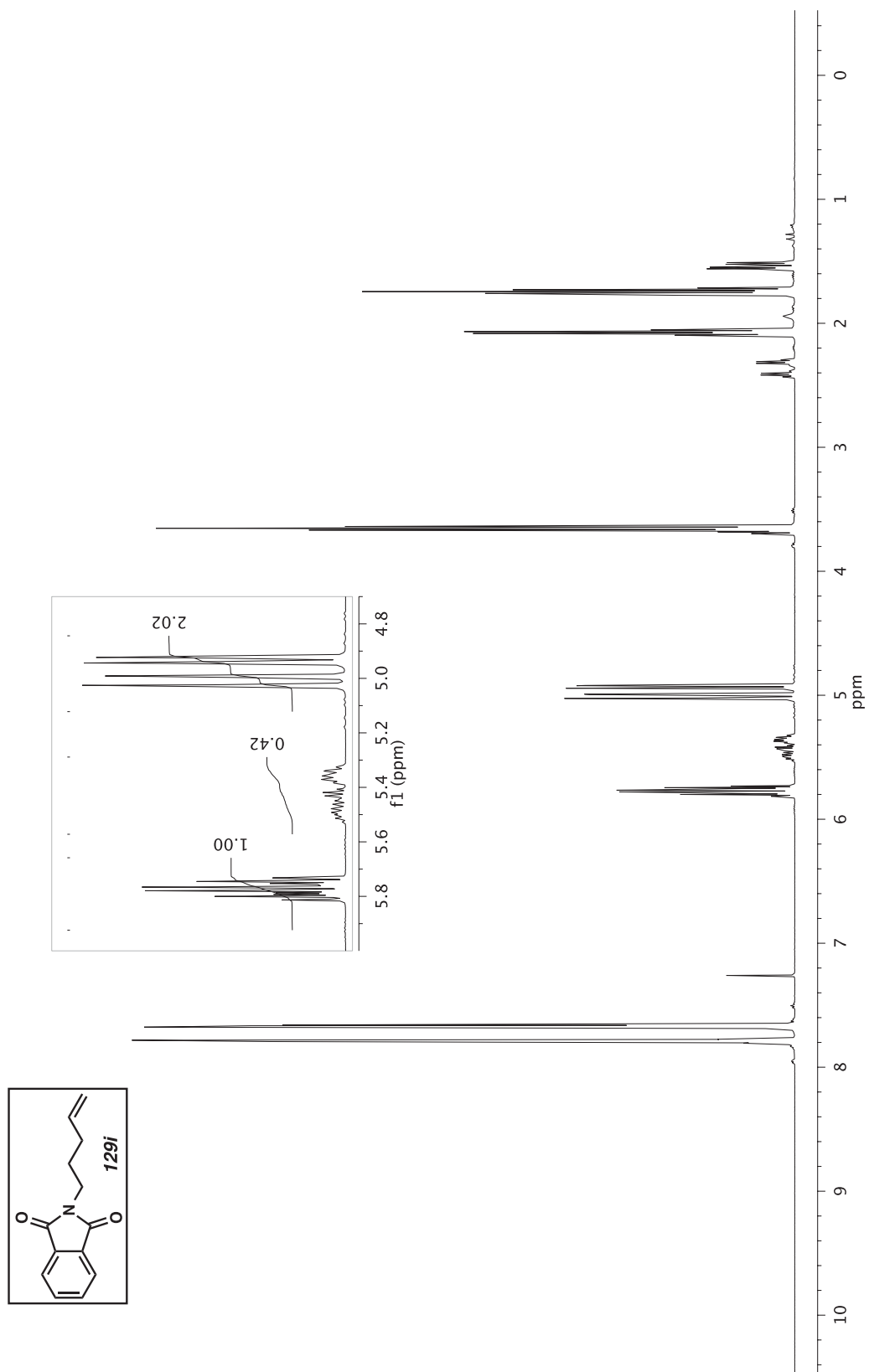
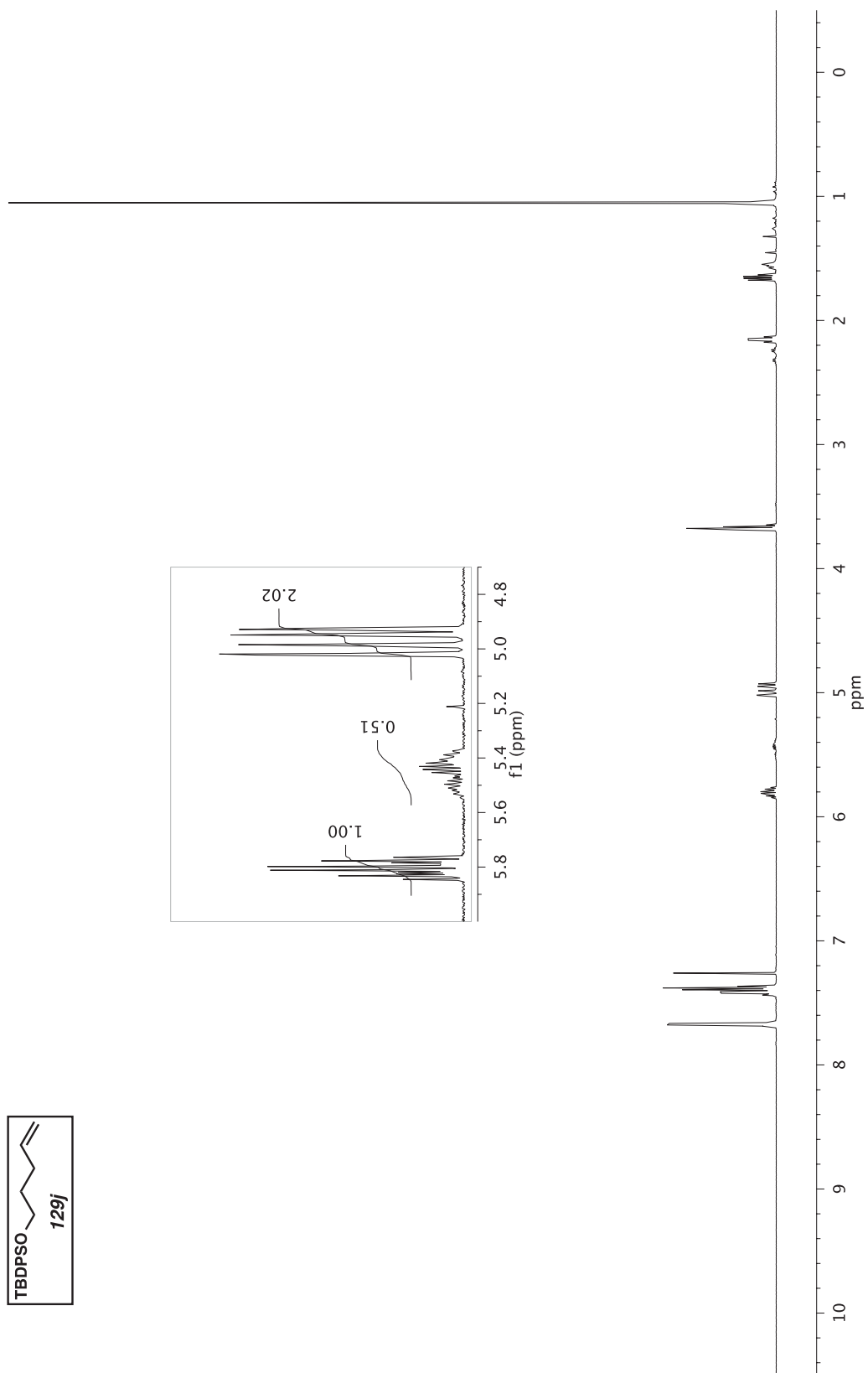


Figure A5.16 ¹³C NMR (126 MHz, CDCl₃) of compound **129h**.

Figure A5.17 ^1H NMR (500 MHz, CDCl_3) of compound **129i**.



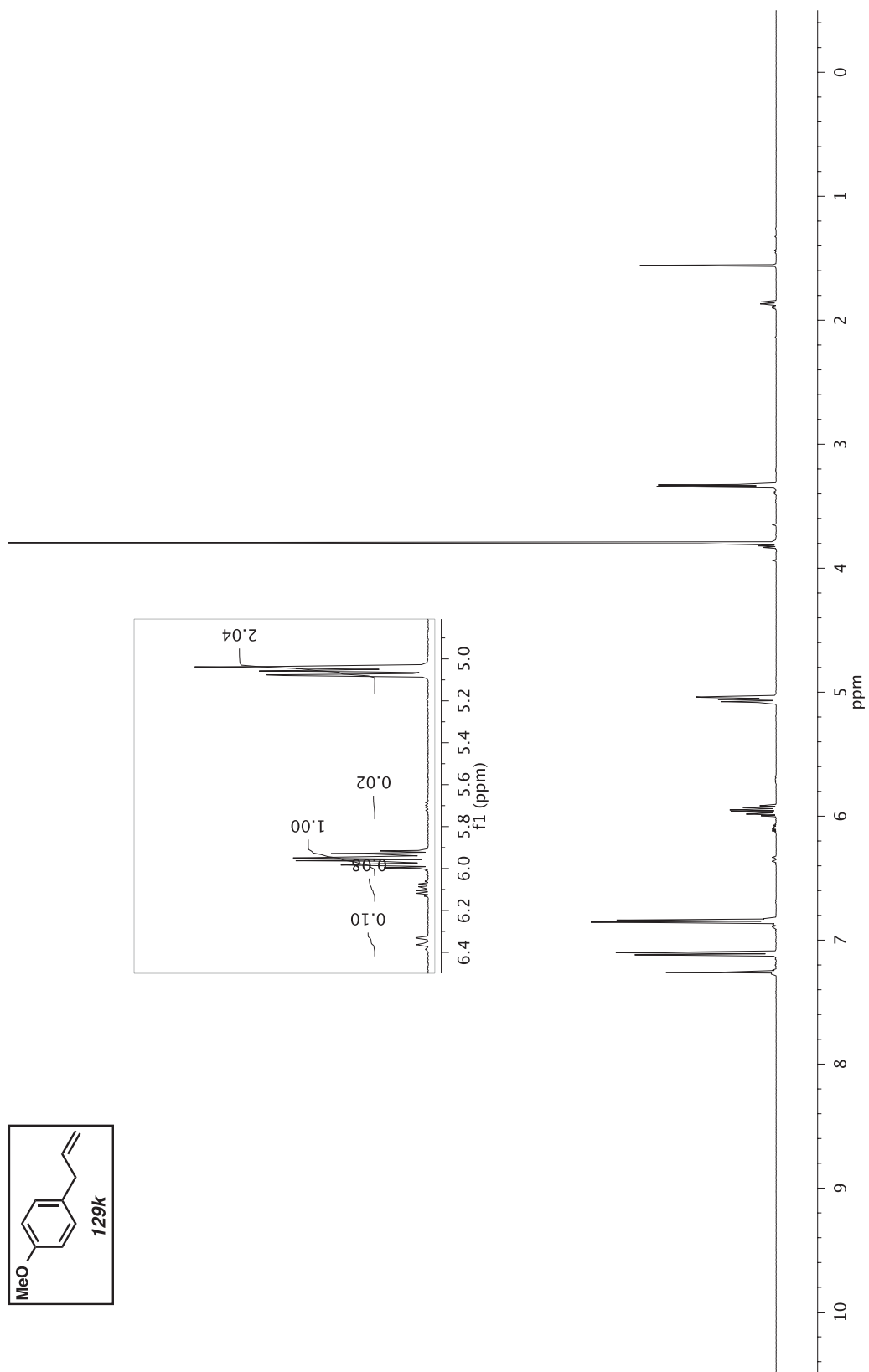


Figure A5.19 ^1H NMR (500 MHz, CDCl_3) of compound **129k**.

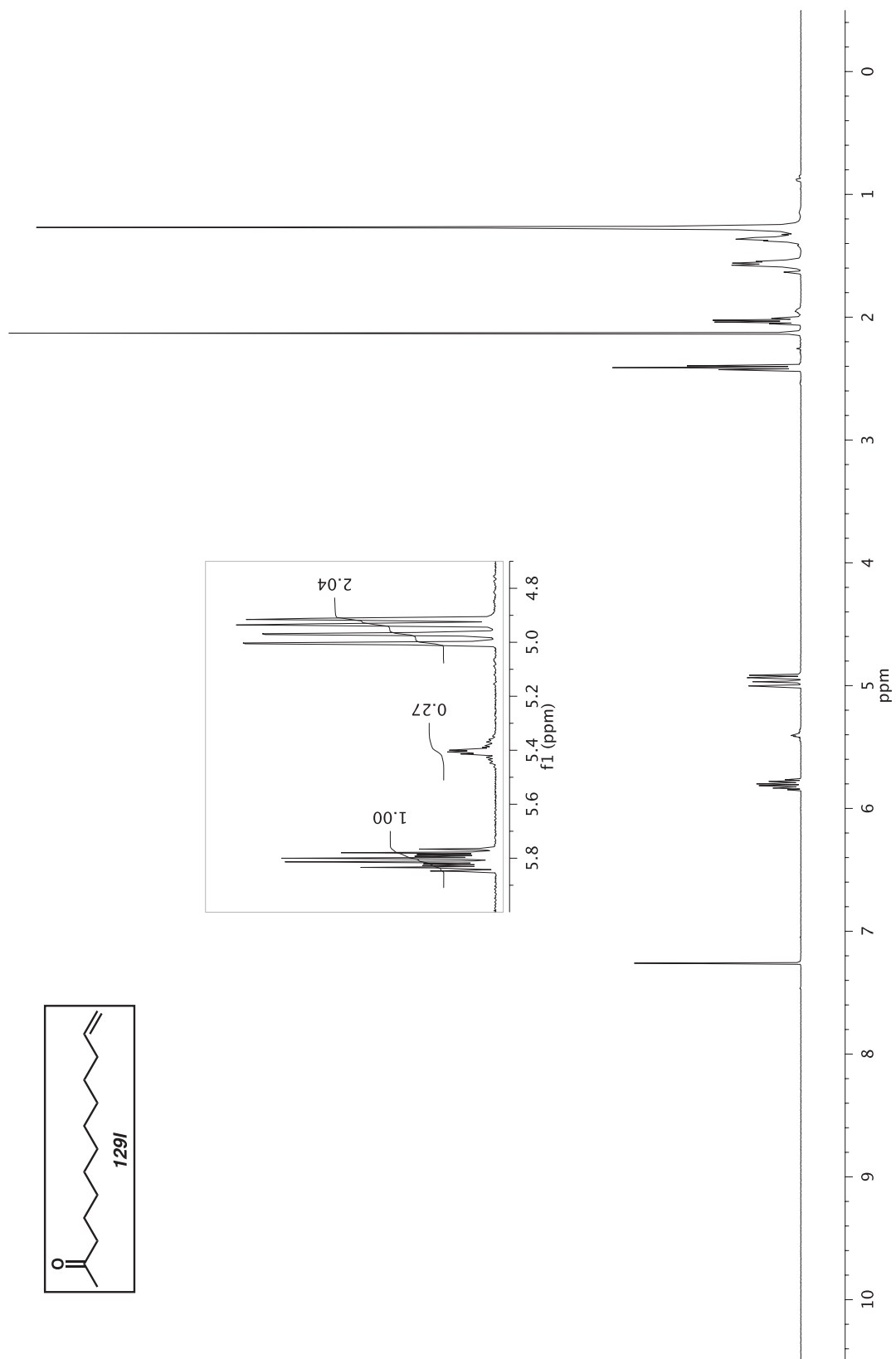


Figure A5.20 ^1H NMR (500 MHz, CDCl_3) of compound **129I**.

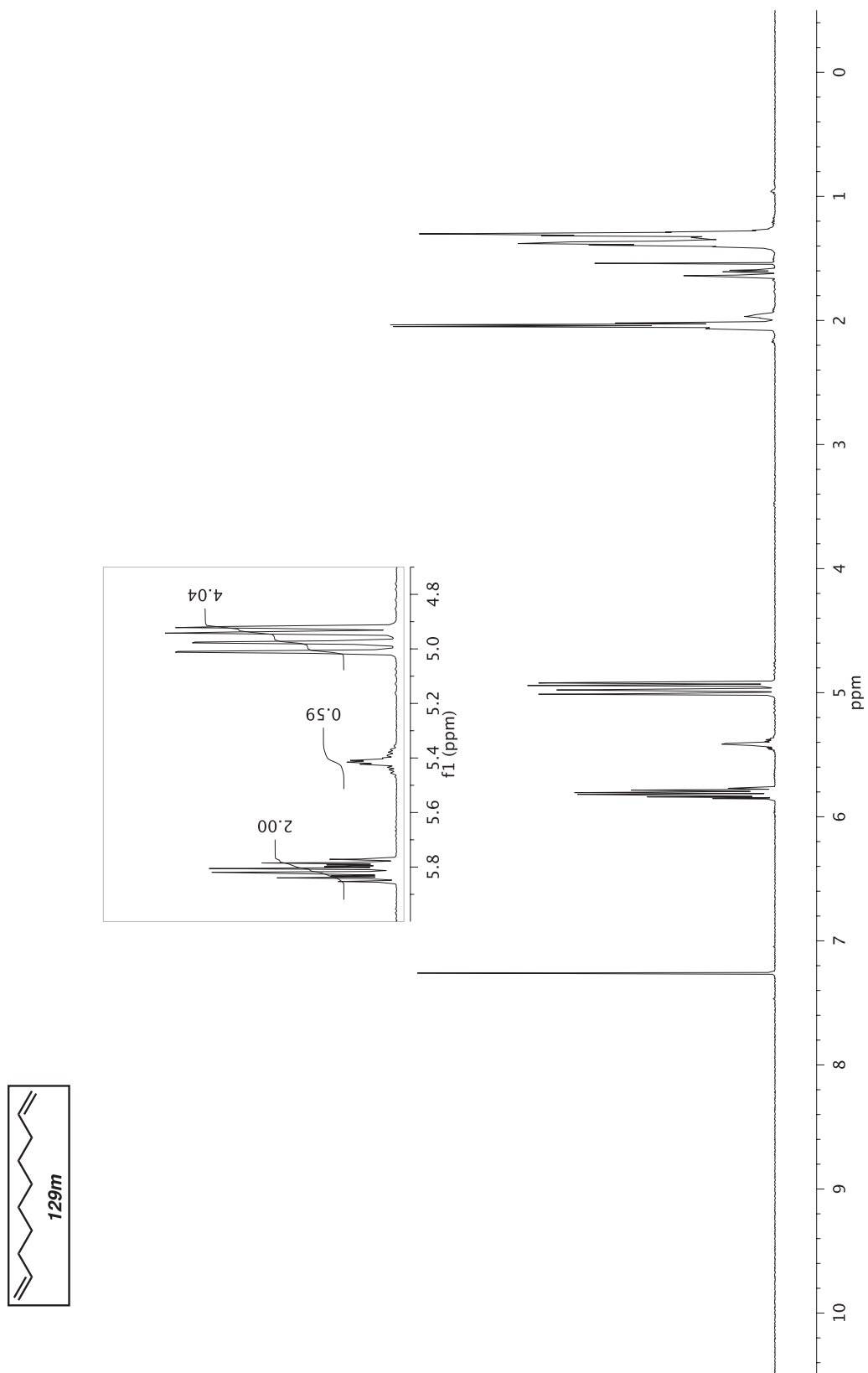


Figure A5.21 ^1H NMR (500 MHz, CDCl_3) of compound **129m**.

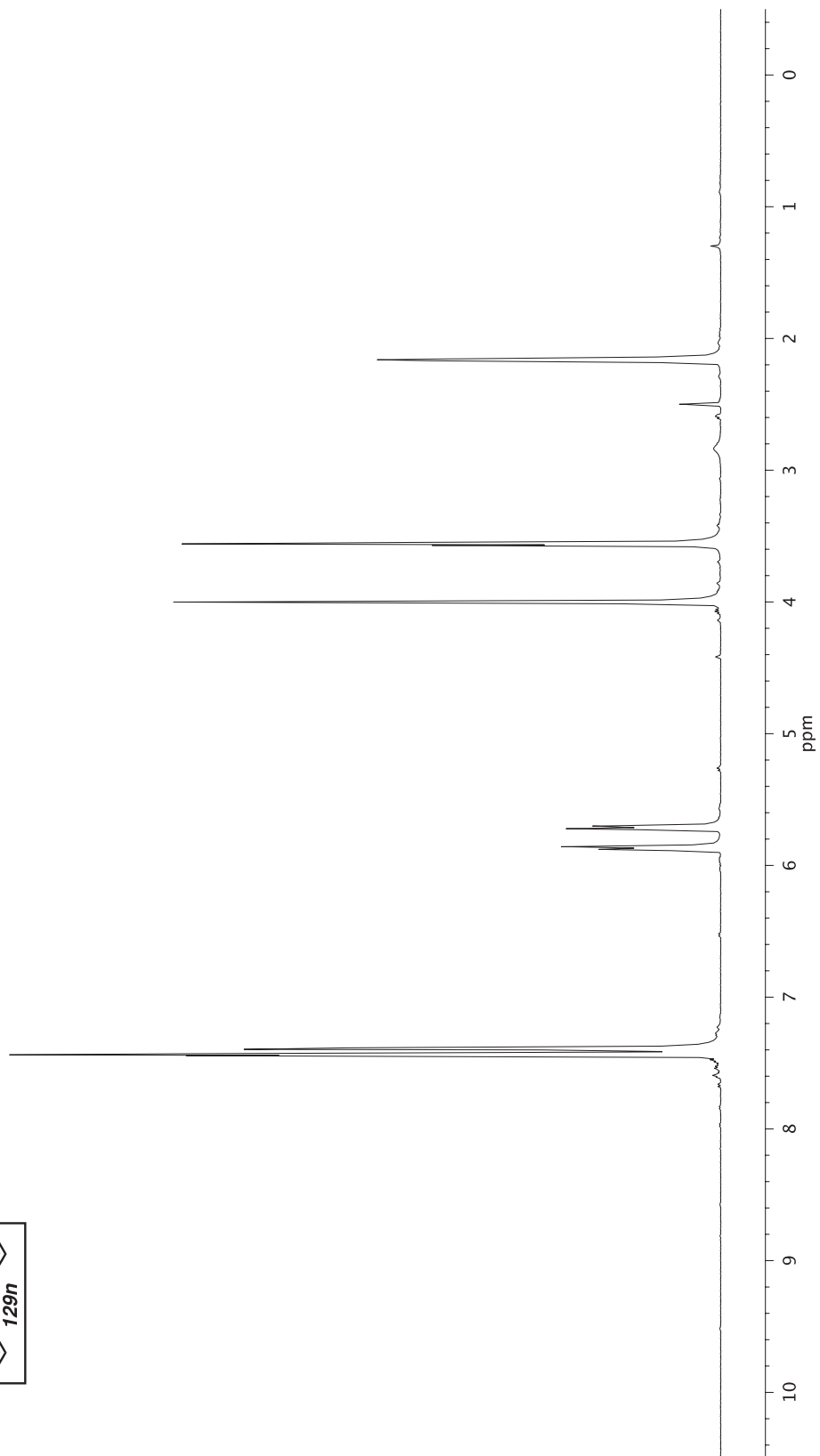
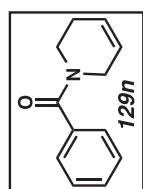


Figure A5.22 ¹H NMR (500 MHz, DMSO-d₆, 130 °C) of compound 129n.

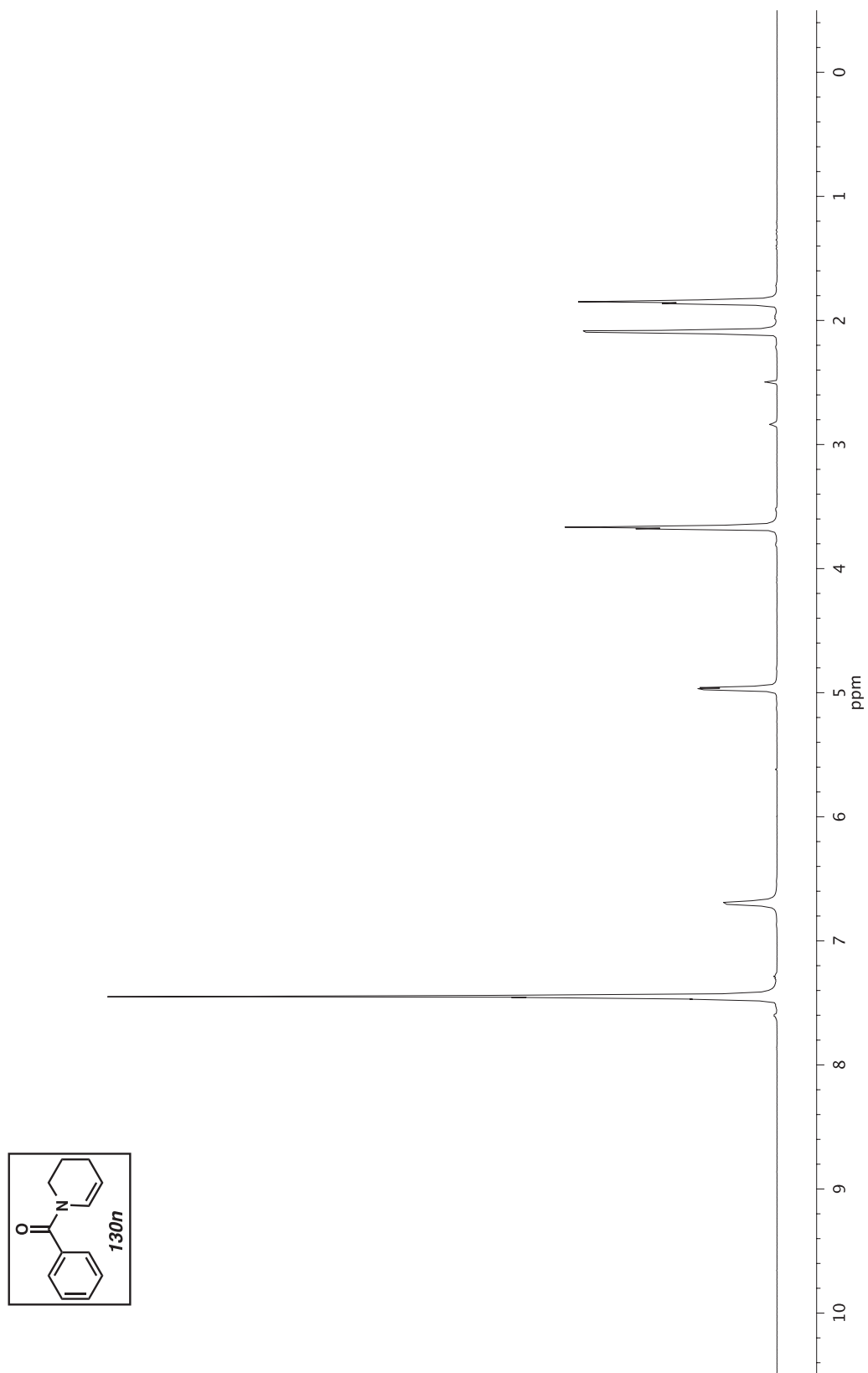


Figure A5.23 ^1H NMR (500 MHz, DMSO-d_6 , $130\text{ }^\circ\text{C}$) of compound **130n**.

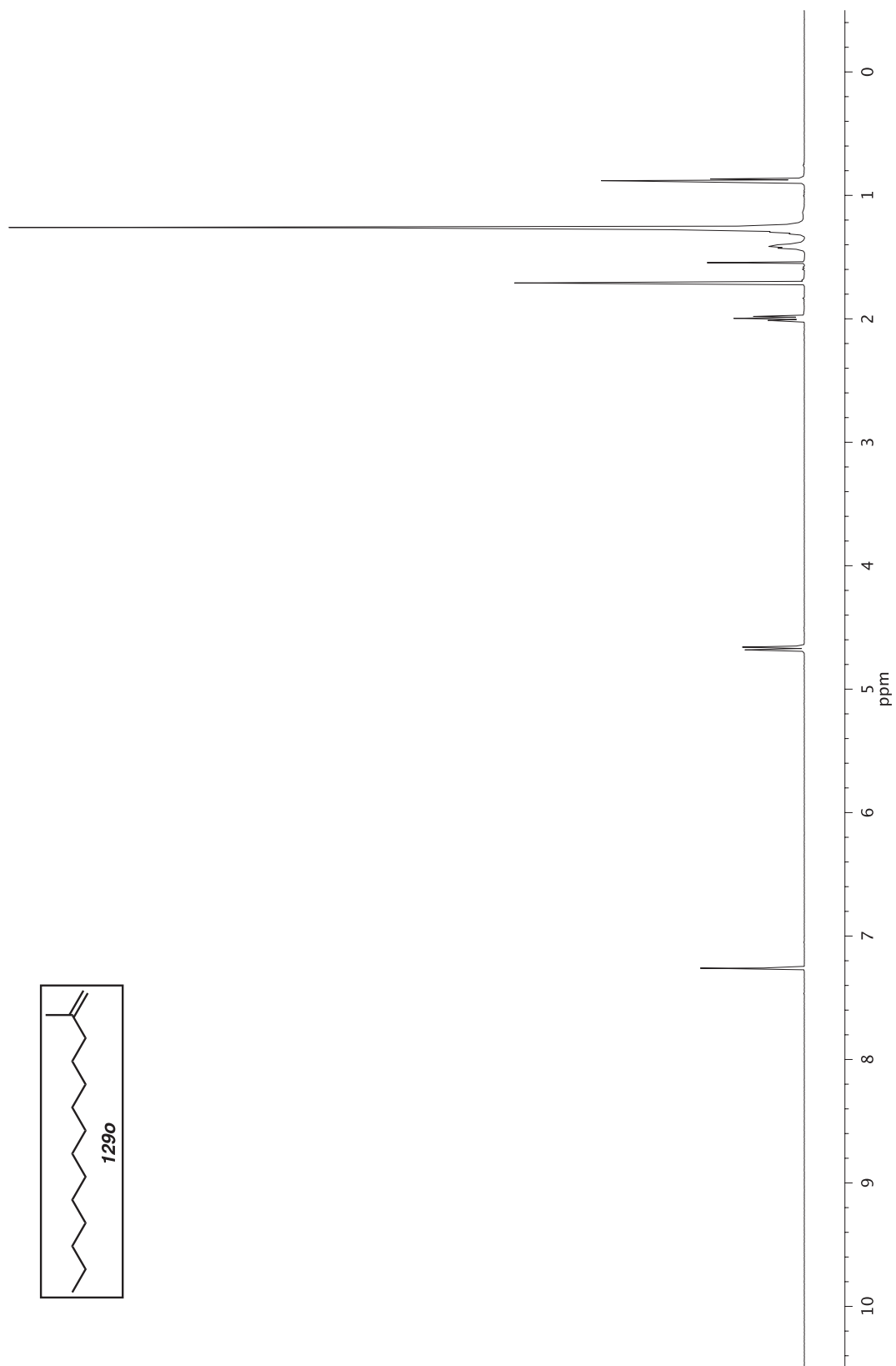


Figure A5.24 ¹H NMR (500 MHz, CDCl₃) of compound **1290**.

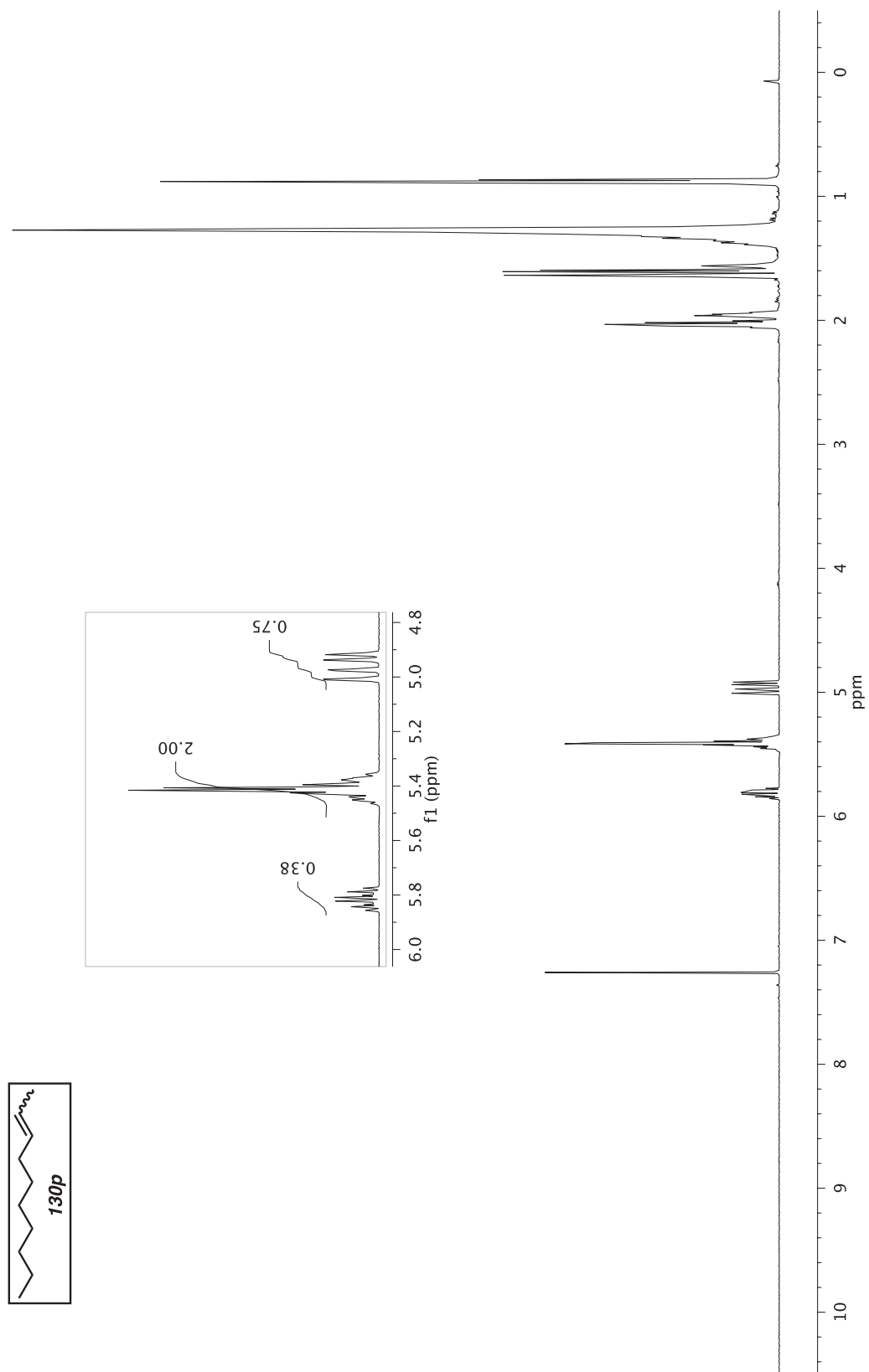


Figure A5.25 ^1H NMR (500 MHz, CDCl_3) of compound **130p**.

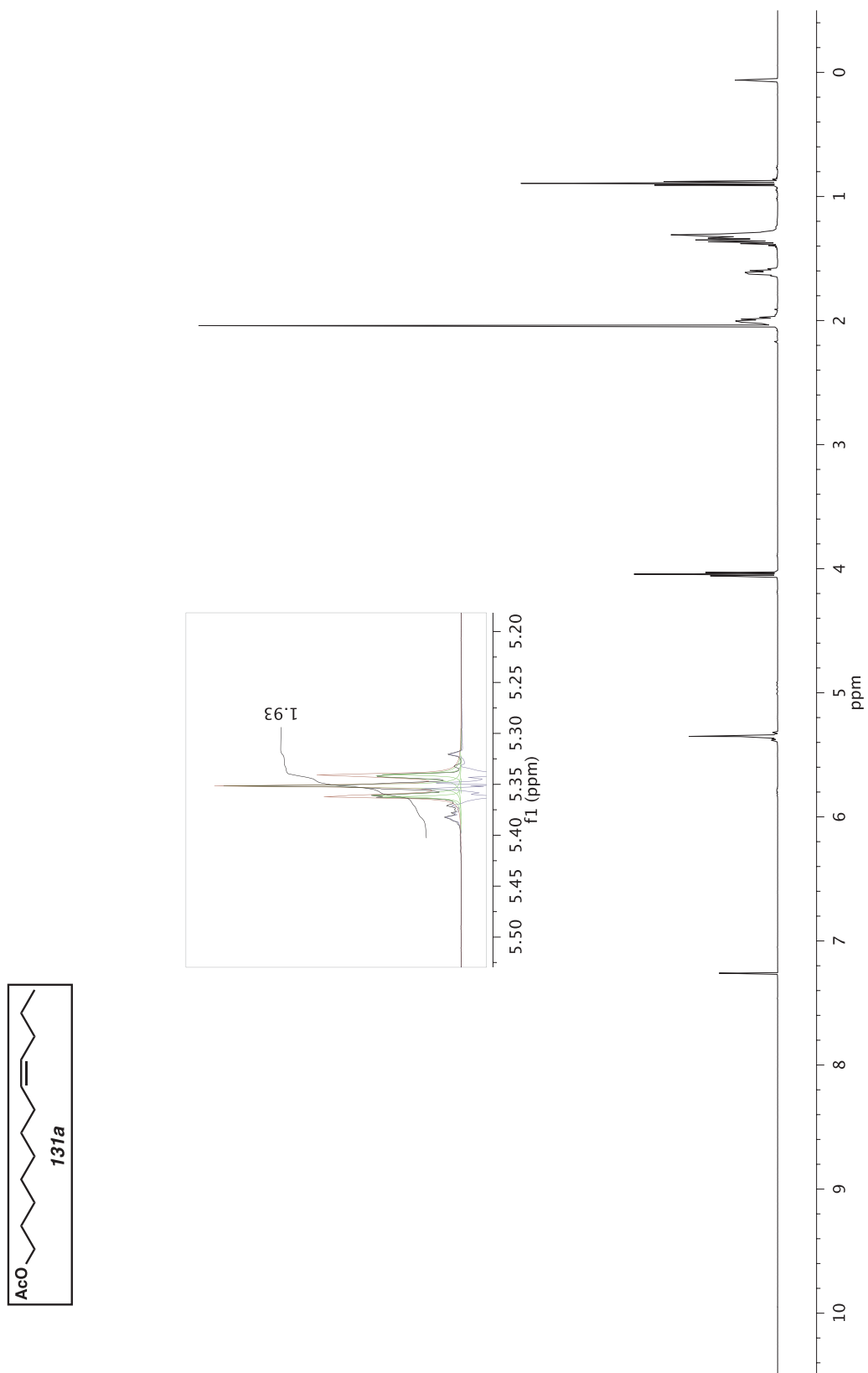


Figure A5.26 ^1H NMR (500 MHz, CDCl_3) of compound **131a**.

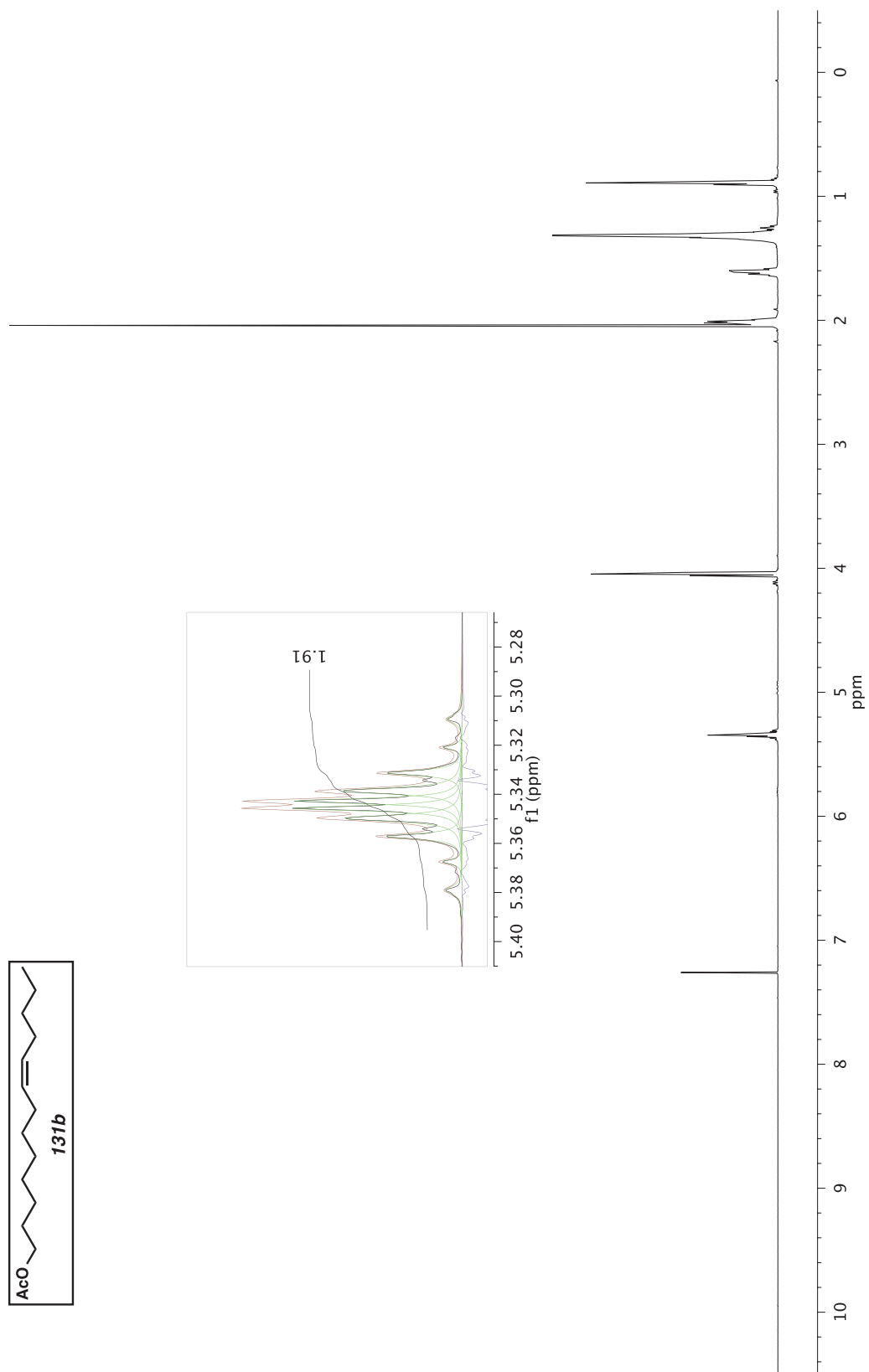


Figure A5.27 ^1H NMR (500 MHz, CDCl_3) of compound **131b**.

CHAPTER 5

Palladium-Catalyzed Decarbonylative Dehydration for the Synthesis of α -Vinyl Carbonyl Compounds and Total Synthesis of (-)-Aspewentin B[†]

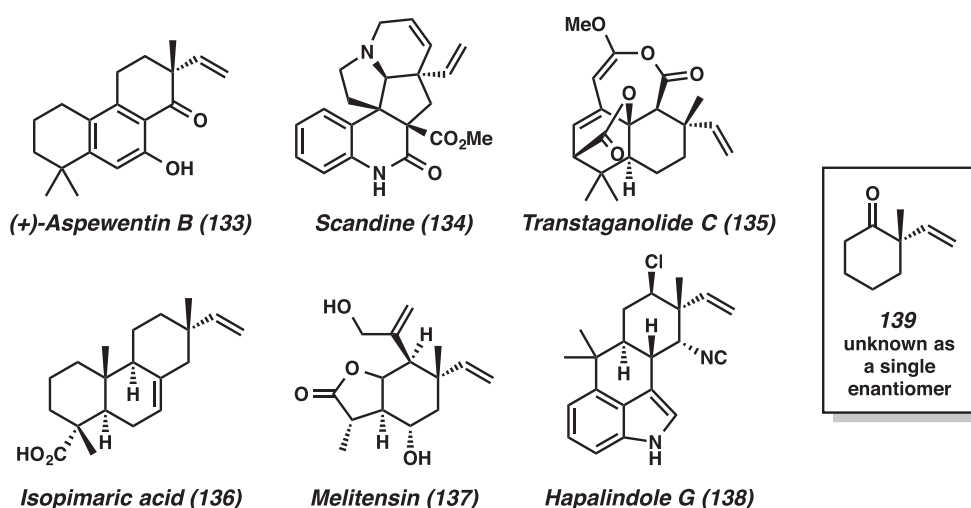
5.1 Introduction

An all-carbon quaternary center bearing an ethylene substituent is a common structural motif in many natural products (Figure 5.1).¹ An important approach to the construction of this unit is the α -vinylation of carbonyl compounds. Two general methods have been developed. One is the direct coupling of an enolate nucleophile with a vinyl electrophile such as an alkenyl ether,² vinyl bromide,³ or acetylene itself.^{4,5} Although this approach can be extended to alkenylations as well, and asymmetric versions are known,^{3a,3c,4c} the scope of the enolate nucleophile is generally limited to 1,3-dicarbonyl compounds⁴ or those with only one enolizable position.^{2,3,5b} A second tactic

[†] This work was partially adapted from a manuscript in preparation for submission to *Angew. Chem., Int. Ed.*

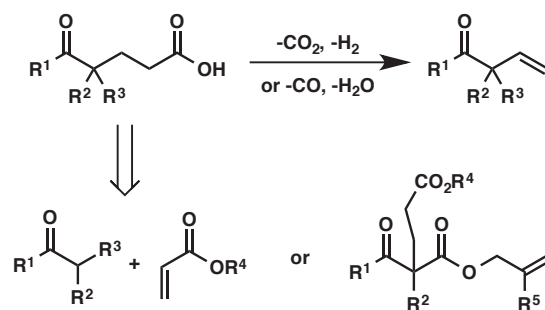
involves addition of the enolate nucleophile to a vinyl surrogate such as vinyl sulfoxide,⁶ (phenylseleno)acetaldehyde,⁷ or ethylene oxide,⁸ followed by elimination. However, there are few reports of stereoselective additions that form the quaternary stereocenter,⁹ and none are catalytic or enantioselective. Due to these constraints, even the simplest 2-methyl-2-vinylcyclohexanone (**139**) is not known as a single enantiomer in the literature.

Figure 5.1 Natural products with ethylene substituents



We envisioned an alternative approach to access α -vinyl carbonyl compounds, by employing a decarboxylative elimination of δ -oxocarboxylic acids (Scheme 5.1). These acids may be prepared by addition of an enolate nucleophile to an acrylate acceptor¹⁰ or by palladium-catalyzed allylic alkylation.¹¹ Both methods allow for the enantioselective construction of the requisite quaternary stereocenter.

Scheme 5.1 Decarboxylative approach to vinylation

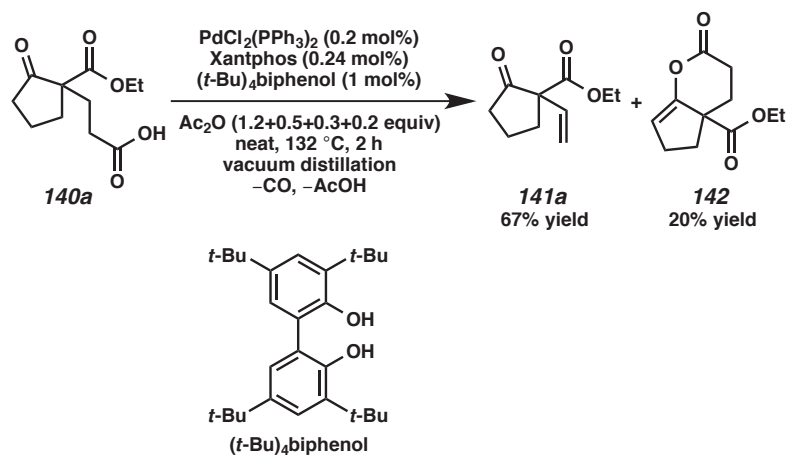


Recently, we reported on the palladium-catalyzed decarbonylative dehydration of fatty acids to form terminal olefins of one less carbon.¹² Due to the importance of α -vinyl carbonyl compounds and the challenges in their preparation, we became interested in applying our decarbonylative dehydration chemistry as an alternative strategy to α -vinylation. Since the carboxylic acid, which bears a quaternary center two atoms away from the reactive carboxyl group, is more hindered than a simple fatty acid, we expected that the reaction conditions would need to be tuned for this particular class of substrates. Additionally, from a practical standpoint, our previous studies were typically conducted on ~5 g fatty acid substrate without solvent, under vacuum distillation conditions. Thus, a smaller scale alternative for implementation on laboratory scale and in the context of multistep organic synthesis would need to be developed.

At the outset of our investigation, we prepared carboxylic acid **140a** and subjected it to palladium-catalyzed decarbonylative dehydration condition, with slightly higher loading of catalyst, ligand, and additive (Scheme 5.2). We were pleased to isolate vinyl cyclopentanone **141a** in 67% yield, along with cyclic lactone **142** in 20% yield as a byproduct. This result demonstrated that steric bulk at the quaternary center does not

significantly retard the reaction, but proximal functionality (e.g. the ketone) could alter the reaction pathway.

Scheme 5.2 Decarbonylative dehydration of δ -oxocarboxylic acid **140a**



5.2 Study of Reaction Scope

With this exciting initial result in hand, we proceeded to investigate the scope of the reaction (Table 5.1). First, we synthesized (*R*)-3-(1-methyl-2-oxocyclohexyl)propanoic acid (**140b**) by enantioselective d'Angelo Michael addition,¹⁰ and subjected it to decarbonylative dehydration (entry 2). We were delighted to obtain the desired product, (*R*)-2-methyl-2-vinylcyclohexanone (*ent*-**139**), in 60% yield and 92% ee. Likewise, 2-ethyl-2-vinylcyclohexanone (**141c**) was prepared in a similar fashion. Carboxylic acids bearing allyl or 2-methylallyl substituents, which can be prepared via palladium-catalyzed allylic alkylation,¹¹ also underwent decarbonylative dehydration smoothly to provide the corresponding 2-allyl-2-vinyl-substituted cyclohexanones **141d** and **141e** (entries 4 and 5), the latter in 91% ee from enantioenriched acid **140e**. It is worth noting that double bond isomerization in the allyl moiety is negligible for **141d** and

does not occur at all for **141e**. Aside from cyclic substrates, we examined acyclic ones (entries 6–9), and found that α -vinyl ketone **141f**, ester **141g**, and aldehyde **141h** can all be prepared in good yields. More complex scaffolds such as acid **140i**, obtained by oxidative cleavage of testosterone,¹³ also undergo the reaction to provide tricyclic vinyl compound **141i** (entry 10). While the reaction can be carried out in the absence of a solvent at a fairly large scale (5 mmol, entries 1–7), we found that for smaller scale synthesis it is more convenient to use NMP as solvent along with slightly modified conditions (entries 8–10).¹⁴

Table 5.1 Decarbonylative dehydration of δ -oxocarboxylic acids

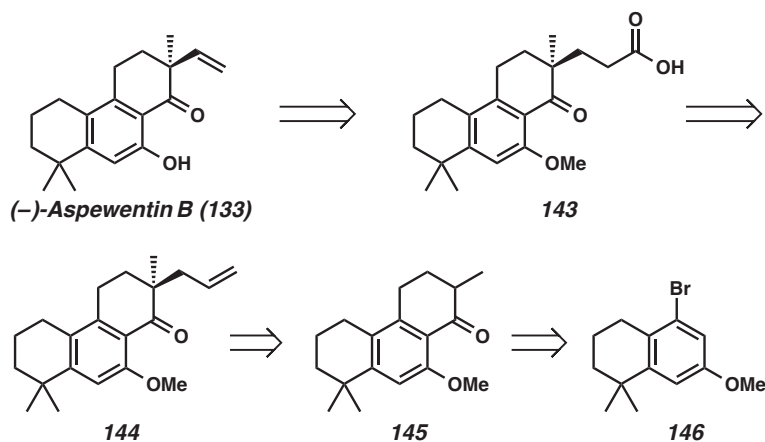
entry ^a	δ -oxocarboxylic acid	product	yield
1			67%
2			60% 92% ee
3			66%
4			54% ^b
5			69% 92% ee
6			75%
7 8 ^c			50% 51%
9 ^c			77%
10 ^c			41%

^a 5 mmol scale. ^b Isolated as a 95:5 mixture of desired product and internal olefin isomer. ^c Condition: 0.5 mmol substrate (1 equiv), benzoic anhydride (1.2 equiv), PdCl₂(nbd) (1 mol%), Xantphos (1.2 mol%), NMP (0.25 mL), 1 atm N₂, 132 °C, 3 h.

5.3 Total Synthesis of (-)-Aspewentin B

To further demonstrate the utility of our decarbonylative dehydration approach to vinylation, we embarked on a total synthesis of aspewentin B (**133**, Figure 5.1), a norditerpene natural product isolated from *Aspergillus wentii*.^{15,16} This terpenoid contains an α -vinyl quaternary cyclohexanone scaffold, and is therefore ideally suited for our chemistry. Retrosynthetically (Scheme 5.3), we envisioned that the vinyl group could be formed by decarbonylative dehydration of δ -oxocarboxylic acid **143**, which might be obtained by elaboration of allyl ketone **144**.¹⁷ The quaternary stereocenter would be set by palladium-catalyzed enantioselective allylic alkylation of tricyclic ketone **145**, which could be built from known aryl bromide **146**.¹⁸

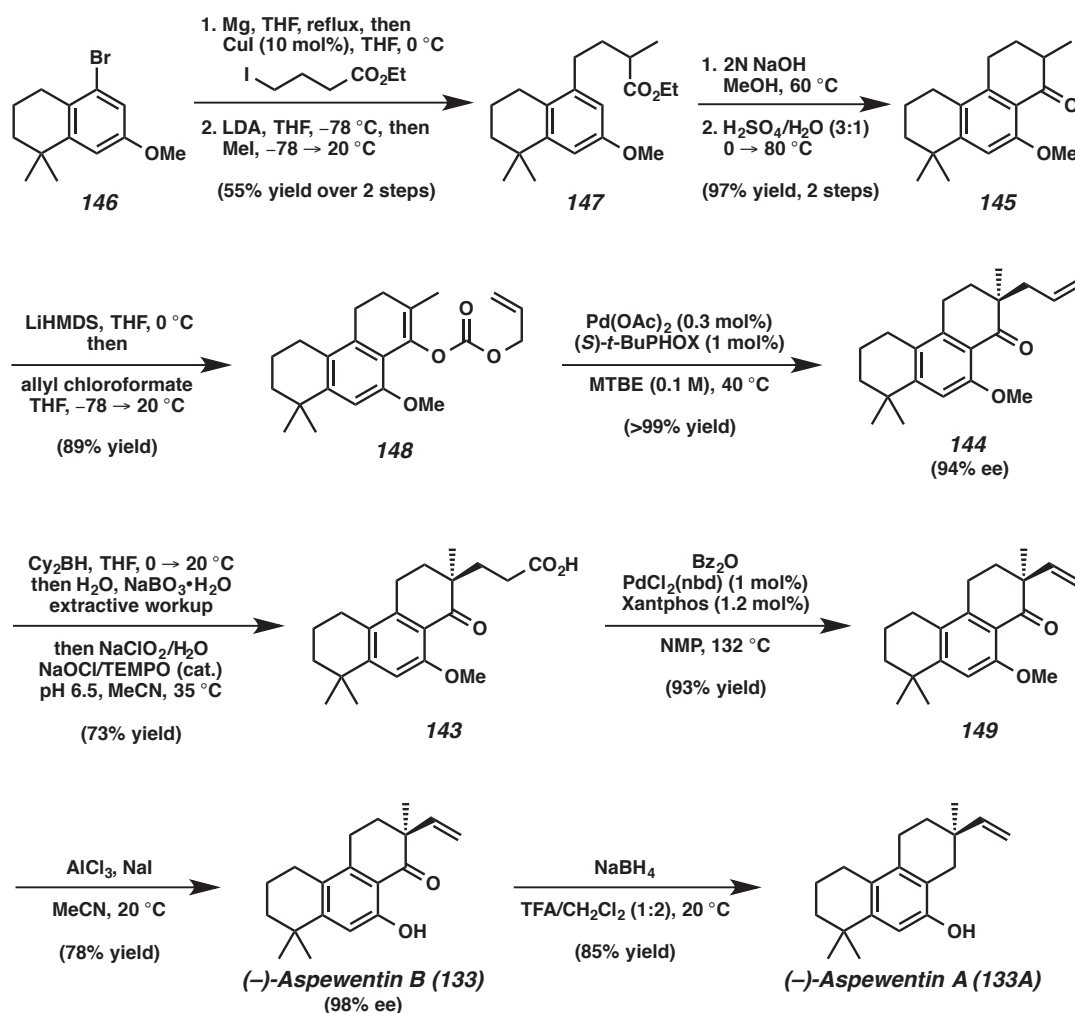
Scheme 5.3 Retrosynthetic analysis of (-)-aspewentin B



We commenced our total synthesis by copper-catalyzed coupling of a Grignard reagent derived from aryl bromide **146** with ethyl 4-iodobutyrate (Scheme 5.4). α -Methylation of the coupled product led to ester **147**, which was hydrolyzed to the corresponding carboxylic acid and then cyclized under acidic conditions to form tricyclic

ketone **145**. The ketone was converted to the corresponding allyl enol carbonate (**148**), and subjected to palladium-catalyzed enantioselective decarboxylative allylic alkylation to afford allyl ketone **144** in nearly quantitative yield and 94% ee. Interestingly, the allylic alkylation reaction proceeds efficiently with low palladium catalyst loading.¹⁹ Hydroboration of the terminal olefin of **144** with dicyclohexylborane and oxidation with sodium perborate, followed by further oxidation with sodium chlorite catalyzed by TEMPO and bleach, delivered carboxylic acid **143** in 73% yield. Gratifyingly, palladium-catalyzed decarbonylative dehydration furnished α -vinyl ketone **149** in 93% yield.²⁰ Removal of the *O*-methyl group provided (–)-aspewentin B (**133**) in 78% yield.²¹ Reduction of the ketone moiety of **133** using sodium borohydride and trifluoroacetic acid furnishes (–)-aspewentin A (**133A**) in 85% yield.²²

Scheme 5.4 Total synthesis of (-)-aspewentin B



5.4 Concluding Remarks

In summary, we have developed a new approach to access α -vinyl quaternary carbonyl compounds via palladium-catalyzed decarbonylative dehydration of δ -oxocarboxylic acids. A variety of acids with different scaffolds and functional groups were transformed into the corresponding α -vinyl carbonyl compounds in moderate to good yields. We have also applied the method to the first enantioselective total synthesis

of (-)-aspewentin B. Further applications of this transformation in natural product synthesis are currently ongoing in our lab and will be reported in due course.

5.5 Experimental Section

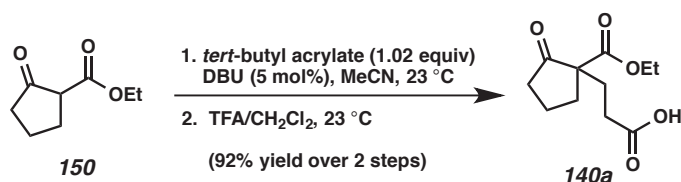
5.5.1 Materials and Methods

Unless otherwise stated, reactions were performed in flame-dried glassware under a nitrogen atmosphere using dry, deoxygenated solvents, or under vacuum without the use of solvents. Solvents were dried by passage through an activated alumina column under argon.²³ Reaction progress was monitored by thin-layer chromatography (TLC) or ¹H NMR analysis of the crude reaction mixture. TLC was performed using E. Merck silica gel 60 F254 pre-coated glass plates (0.25 mm) and visualized by UV fluorescence quenching, *p*-anisaldehyde, phosphomolybdic acid, or KMnO₄ staining. Silicycle SiliaFlash® P60 Academic Silica gel (particle size 40–63 nm) was used for flash chromatography. ¹H NMR and ¹³C NMR spectra were recorded on a Varian Inova 500 (500 MHz and 126 MHz, respectively) or a Bruker CryoProbe Prodigy 400 spectrometer (400 MHz and 101 MHz, respectively) and are reported relative to residual CHCl₃ (δ 7.26 ppm and δ 77.16 ppm, respectively). Data for ¹H NMR are reported as follows: chemical shift (δ ppm) (multiplicity, coupling constant (Hz), integration). Multiplicities are reported as follows: s = singlet, d = doublet, t = triplet, q = quartet, p = pentet, sept = septuplet, m = multiplet, br s = broad singlet, br d = broad doublet, app = apparent. Data for ¹³C NMR are reported in terms of chemical shifts (δ ppm). IR spectra were obtained by use of a Perkin Elmer Spectrum BXII spectrometer using thin films deposited on NaCl plates and reported in frequency of absorption (cm⁻¹). Optical rotations were measured

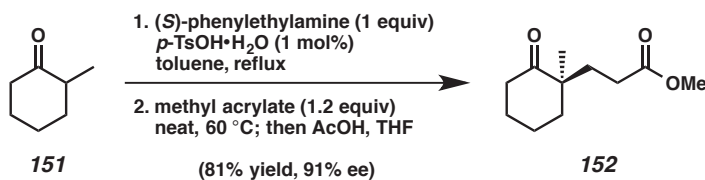
with a Jasco P-2000 polarimeter operating on the sodium D line (589 nm), using a 100 mm path-length cell and are reported as: $[\alpha]_D^T$ (concentration in g/100 mL, solvent). Analytical chiral GC was performed with an Agilent 6850 GC utilizing a G-TA (30 m x 0.25 mm) column (1.0 mL/min carrier gas flow). Analytical chiral HPLC was performed with an Agilent 1100 Series HPLC utilizing a Chiralpak (AD-H or AS) or Chiralcel (OD-H, OJ-H, or OB-H) columns (4.6 mm x 25 cm) obtained from Daicel Chemical Industries, Ltd. Analytical chiral SFC was performed with a Mettler SFC supercritical CO₂ analytical chromatography system utilizing Chiralpak (AD-H, AS-H or IC) or Chiralcel (OD-H, OJ-H, or OB-H) columns (4.6 mm x 25 cm) obtained from Daicel Chemical Industries, Ltd. High-resolution mass spectra (HRMS) were provided by the California Institute of Technology Mass Spectrometry Facility using a JEOL JMS-600H High Resolution Mass Spectrometer (EI+ or FAB+), or obtained with an Agilent 6200 Series TOF using Agilent G1978A Multimode source in electrospray ionization (ESI), atmospheric pressure chemical ionization (APCI), or mixed ionization mode (MM: ESI-APCI).

Reagents were purchased from Sigma-Aldrich, Acros Organics, Strem, or Alfa Aesar and used as received unless otherwise stated. *i*-Pr₂NH was distilled from calcium hydride prior to use. (*S*)-*t*-BuPHOX was prepared by a known method.²⁴

5.5.2 Preparation of Carboxylic Acid Substrates

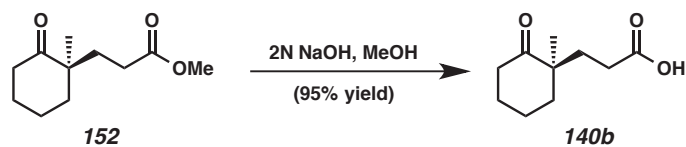


3-(1-(Ethoxycarbonyl)-2-oxocyclopentyl)propanoic acid (140a). A flame-dried 100 mL round-bottom flask was charged with a magnetic stir bar, anhydrous MeCN (30 mL), β -keto ester **150** (2.9 mL, 20 mmol, 1 equiv), *tert*-butyl acrylate (3.0 mL, 20.6 mmol, 1.02 equiv), and DBU (0.15 mL, 1 mmol, 0.05 equiv). The light yellow reaction mixture was stirred at 23 °C. After 12 h, TLC analysis indicated complete consumption of starting material. Solvents were evaporated, and the crude residue was purified by flash column chromatography on silica gel (10→16→25% EtOAc in hexanes) to afford a colorless oil (5.22 g). To a solution of this oil (1.42 g) in CH₂Cl₂ (4 mL) was added trifluoroacetic acid (4 mL). The reaction mixture was stirred at 23 °C for 30 min and concentrated under reduced pressure. Removal of remaining trifluoroacetic acid by azeotropic evaporation from toluene (5 mL x 5) afforded carboxylic acid **140a** (1.14 g, 92% yield over 2 steps) as a viscous colorless oil. $R_f = 0.1$ (25% EtOAc in hexanes); ¹H NMR (500 MHz, CDCl₃) δ 7.86 (br s, 1H), 4.17 (q, $J = 7.1$ Hz, 2H), 2.59 (ddd, $J = 16.3, 10.2, 5.7$ Hz, 1H), 2.53–2.36 (m, 3H), 2.30 (dt, $J = 19.0, 8.0$ Hz, 1H), 2.19 (ddd, $J = 14.2, 10.2, 5.7$ Hz, 1H), 2.09–1.92 (m, 3H), 1.89 (dt, $J = 13.1, 7.4$ Hz, 1H), 1.25 (t, $J = 7.1$ Hz, 3H); ¹³C NMR (126 MHz, CDCl₃) δ 214.7, 178.6, 171.1, 61.8, 59.2, 38.0, 34.0, 29.6, 28.2, 19.7, 14.2; IR (Neat Film, NaCl) 2979, 1713, 1408, 1158, 1028 cm⁻¹; HRMS (MM: ESI-APCI-) m/z calc'd for C₁₁H₁₅O₅ [M-H]⁻: 227.0925, found 227.0925.

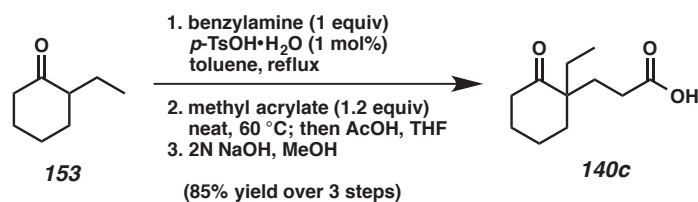


Methyl (R)-3-(1-methyl-2-oxocyclohexyl)propanoate (152). Synthesis of **152** was based on a literature procedure.¹⁰ A 100 mL round-bottom flask was charged with a magnetic stir bar, 2-methylcyclohexanone (**151**, 3.7 mL, 30.6 mmol, 1 equiv), (*S*)-phenylethylamine (3.71 g, 30.6 mmol, 1 equiv), *p*-toluenesulfonic acid hydrate (58 mg, 0.306 mmol, 0.01 equiv), and toluene (30 mL). The flask was equipped with a Dean-Stark trap filled with toluene and a reflux condenser. The reaction mixture was heated at reflux for 3.5 h. The Dean-Stark trap was replaced with a distillation head, and the toluene was distilled off under reduced pressure. The residue was cooled to 60 °C under nitrogen and methyl acrylate (3.4 mL, 36.7 mmol, 1.2 equiv) was added. The reaction mixture was stirred at 60 °C for 12 h. After cooling to ambient temperature, the reaction mixture was quantitatively transferred to a 250 mL round-bottom flask by rinsing with THF (50 mL total). Aqueous 20% acetic acid (30 mL) was added and the solution was stirred at 23 °C for 5 h. THF was evaporated under reduced pressure and 1N HCl (11 mL) was added. The biphasic mixture was extracted with Et₂O (25 mL x 3). The combined organic layers were washed with H₂O and brine, dried over Na₂SO₄, filtered, and concentrated under reduced pressure. The residue was purified by flash column chromatography on silica gel (5→6→10→12% EtOAc in hexanes) to afford δ-keto ester **152** (4.96 g, 81% yield over 2 steps) as a light brown oil. *R*_f = 0.4 (16% EtOAc in hexanes); ¹H NMR (500 MHz, CDCl₃) δ 3.66 (s, 3H), 2.46–2.26 (m, 3H), 2.22–2.10 (m, 1H), 2.11–1.98 (m, 1H), 1.93–1.67 (m, 6H), 1.67–1.54 (m, 1H), 1.07 (d, *J* = 2.7 Hz, 3H); ¹³C NMR (126 MHz, CDCl₃) δ 215.4, 174.2, 51.8, 48.0, 39.4, 38.8, 32.6, 29.1, 27.6, 22.5, 21.1; IR (Neat Film, NaCl) 2936, 2865, 1740, 1705, 1437, 1378, 1304, 1197, 1172, 1123,

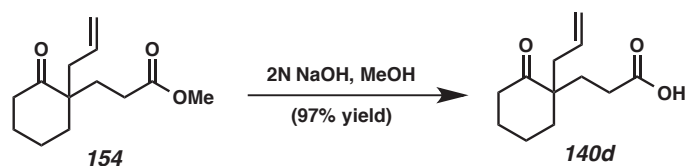
988 cm^{-1} ; HRMS (ESI-APCI+) m/z calc'd for $\text{C}_{11}\text{H}_{19}\text{O}_3$ $[\text{M}+\text{H}]^+$: 199.1329, found 199.1325; $[\alpha]_{\text{D}}^{25} +31.5$ (c 3.00, EtOH, 91% ee).



(R)-3-(1-Methyl-2-oxocyclohexyl)propanoic acid (140b). To a solution of **152** (2.37 g, 11.9 mmol, 1.0 equiv) in MeOH (11 mL) was added aqueous 2N NaOH (7.8 mL, 15.5 mmol, 1.3 equiv). The reaction mixture was stirred at 23 °C for 2 h, then MeOH was evaporated under reduced pressure. The aqueous layer was washed with Et_2O (10 mL x 1), acidified with 1N HCl (25 mL), and extracted with Et_2O (25 mL x 3). The combined organic layers were dried over Na_2SO_4 , filtered, and concentrated under reduced pressure to a wet residue. The residue was redissolved in CH_2Cl_2 , dried over Na_2SO_4 , filtered, and concentrated under reduced pressure to afford carboxylic acid **140b** (2.14 g, 95% yield) as a light yellow viscous oil. $R_f = 0.1$ (25% EtOAc in hexanes); ^1H NMR (500 MHz, CDCl_3) δ 2.43–2.31 (m, 3H), 2.22 (ddd, $J = 16.8, 13.2, 5.2$ Hz, 1H), 2.06–1.96 (m, 1H), 1.89–1.68 (m, 6H), 1.66–1.56 (m, 1H), 1.08 (s, 3H); ^{13}C NMR (126 MHz, CDCl_3) δ 215.5, 179.7, 48.0, 39.3, 38.8, 32.4, 29.1, 27.5, 22.6, 21.1; IR (Neat Film, NaCl) 2936, 1706, 1455, 1312, 1224, 1124, 1097, 902, 856 cm^{-1} ; HRMS (ESI-APCI-) m/z calc'd for $\text{C}_{10}\text{H}_{15}\text{O}_3$ $[\text{M}-\text{H}]^-$: 183.1027, found 183.1034; $[\alpha]_{\text{D}}^{25} +36.0$ (c 4.77, EtOH, 91% ee).

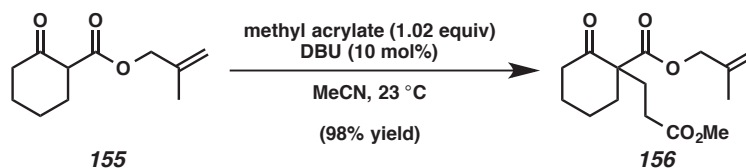


3-(1-Ethyl-2-oxocyclohexyl)propanoic acid (140c). Using 2-ethylcyclohexanone (**153**) as starting material, the procedure for the synthesis of **140b** was followed to provide carboxylic acid **140c** (3.85 g, 85% yield over 3 steps) as a white solid. $R_f = 0.1$ (25% EtOAc in hexanes); ¹H NMR (500 MHz, CDCl₃) δ 2.45–2.26 (m, 3H), 2.23–2.12 (m, 1H), 1.93–1.58 (m, 9H), 1.54–1.43 (m, 1H), 0.77 (t, $J = 7.8$ Hz, 3H); ¹³C NMR (126 MHz, CDCl₃) δ 215.1, 179.9, 51.1, 39.2, 35.8, 28.9, 28.8, 27.3, 27.2, 20.8, 7.8; IR (Neat Film, NaCl) 2939, 2868, 1704, 1455, 1423, 1312, 1229, 1127, 1091 cm⁻¹; HRMS (ESI-APCI-) m/z calc'd for C₁₁H₁₇O₃ [M-H]⁻: 197.1183, found 197.1187.



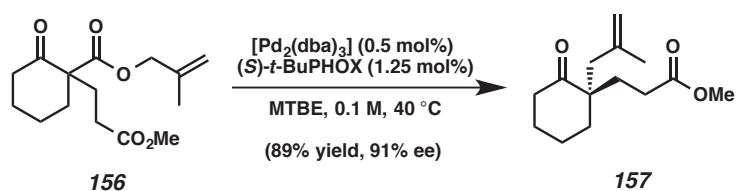
3-(1-Allyl-2-oxocyclohexyl)propanoic acid (140d). Basic hydrolysis of known δ -keto ester **154**¹¹ (2.24 g, 10.0 mmol, 1.0 equiv) afforded carboxylic acid **140d** (2.04 g, 97% yield) as a viscous colorless oil. $R_f = 0.1$ (25% EtOAc in hexanes); ¹H NMR (500 MHz, CDCl₃) δ 10.52 (br s, 1H), 5.64 (dq, $J = 17.0, 7.7$ Hz, 1H), 5.11–5.02 (m, 2H), 2.44–2.28 (m, 4H), 2.28–2.20 (m, 1H), 2.16 (ddd, $J = 16.4, 11.2, 5.1$ Hz, 1H), 1.96 (ddd, $J = 15.8, 11.2, 5.0$ Hz, 1H), 1.88–1.65 (m, 7H); ¹³C NMR (126 MHz, CDCl₃) δ 214.4, 179.7, 133.1, 118.7, 50.9, 39.2, 39.1, 36.2, 29.5, 28.7, 27.1, 20.8; IR (Neat Film, NaCl) 2937,

2866, 1704, 1419, 1312, 1221, 1126, 995, 917 cm^{-1} ; HRMS (ESI-APCI-) m/z calc'd for $\text{C}_{12}\text{H}_{17}\text{O}_3$ $[\text{M}-\text{H}]^-$: 209.1183, found 209.1190.

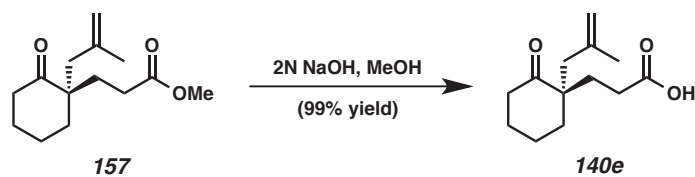


2-Methylallyl 1-(3-methoxy-3-oxopropyl)-2-oxocyclohexane-1-carboxylate (156). A

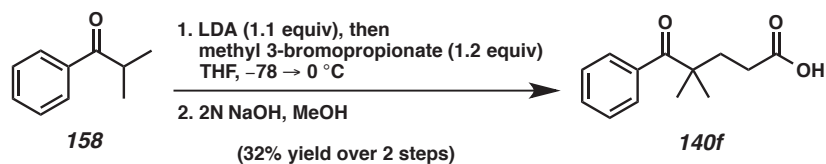
flame-dried 100 mL round-bottom flask was charged with a magnetic stir bar, MeCN (30 mL), β -keto ester **155** (3.32 g, 16.9 mmol, 1.0 equiv), methyl acrylate (1.6 mL, 17.3 mmol, 1.02 equiv), and DBU (0.25 mL, 1.69 mmol, 0.1 equiv). The light yellow reaction mixture was stirred at 23 $^\circ\text{C}$. After 14 h, TLC analysis indicated complete consumption of starting material. Solvents were evaporated, and the crude residue was purified by flash column chromatography on silica gel (8 \rightarrow 16% EtOAc in hexanes) to afford ester **156** (4.69 g, 98% yield) as a colorless oil. R_f = 0.4 (16% EtOAc in hexanes); ^1H NMR (500 MHz, CDCl_3) δ 4.96 (d, J = 16.1 Hz, 2H), 4.54 (s, 2H), 3.65 (s, 3H), 2.54–2.34 (m, 4H), 2.30–2.15 (m, 2H), 2.06–1.89 (m, 2H), 1.82–1.74 (m, 1H), 1.73 (s, 3H), 1.71–1.57 (m, 2H), 1.54–1.43 (m, 1H); ^{13}C NMR (126 MHz, CDCl_3) δ 207.4, 173.6, 171.5, 139.2, 114.2, 68.8, 60.2, 51.8, 41.1, 36.4, 29.8, 29.5, 27.6, 22.6, 19.7; IR (Neat Film, NaCl) 2948, 2867, 1738, 1715, 1436, 1307, 1176, 1135, 990, 907 cm^{-1} ; HRMS (ESI-APCI+) m/z calc'd for $\text{C}_{15}\text{H}_{23}\text{O}_5$ $[\text{M}+\text{H}]^+$: 283.1540, found 283.1533.



Methyl (*R*)-3-(1-(2-methylallyl)-2-oxocyclohexyl)propanoate (157**).** In a nitrogen-filled glove box, a 250 mL Schlenk flask was charged with a magnetic stir bar, Pd₂(dba)₃ (32 mg, 0.035 mmol, 0.005 equiv), (*S*)-*t*-BuPHOX (34 mg, 0.0875 mmol, 0.0125 equiv), and MTBE (40 mL). The solution was stirred at ambient temperature for 30 min. Then additional MTBE (21 mL) and **156** (1.98 g, 7.0 mmol, 1.0 equiv) were added via syringe. The syringe was rinsed with MTBE (3 mL x 3) to ensure complete transfer of **156**. The Schlenk flask was sealed and taken out of the glove box. The reaction mixture was stirred at 40 °C for 28 h, then concentrated under reduced pressure. The crude residue was purified by flash column chromatography on silica gel (6→10% EtOAc in hexanes) to afford δ-keto ester **157** (1.49 g, 89% yield) as a colorless oil. *R_f* = 0.5 (16% EtOAc in hexanes); ¹H NMR (500 MHz, CDCl₃) δ 4.83 (s, 1H), 4.65 (s, 1H), 3.64 (s, 3H), 2.47 (dt, *J* = 14.0, 6.5 Hz, 1H), 2.42–2.27 (m, 4H), 2.15–2.06 (m, 1H), 2.02–1.92 (m, 1H), 1.91–1.65 (m, 7H), 1.64 (s, 3H); ¹³C NMR (126 MHz, CDCl₃) δ 214.4, 174.2, 141.9, 115.4, 51.8, 51.0, 42.9, 39.4, 36.7, 30.5, 28.9, 27.2, 24.5, 20.9; IR (Neat Film, NaCl) 2943, 2865, 1738, 1699, 1436, 1374, 1173, 1128, 1080, 895 cm⁻¹; HRMS (ESI-APCI+) *m/z* calc'd for C₁₄H₂₃O₃ [M+H]⁺: 239.1642, found 239.1633; [α]_D²⁵ +9.0 (*c* 1.00, CHCl₃, 91% ee).

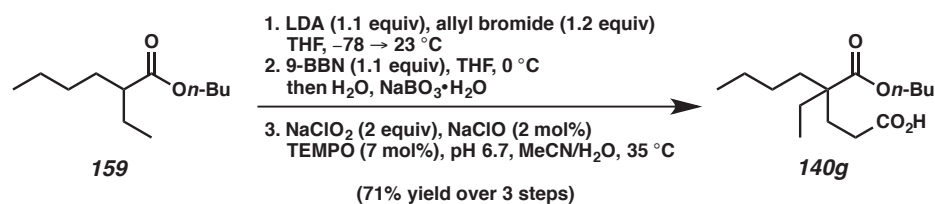


(R)-3-(1-(2-Methylallyl)-2-oxocyclohexyl)propanoic acid (140e). Basic hydrolysis of δ -keto ester **157** (1.49 g, 6.25 mmol, 1 equiv) afforded carboxylic acid **140e** (1.39 g, 99% yield) as a white solid. $R_f = 0.1$ (25% EtOAc in hexanes); $^1\text{H NMR}$ (500 MHz, CDCl_3) δ 4.82 (s, 1H), 4.64 (s, 1H), 2.54–2.43 (m, 1H), 2.43–2.27 (m, 4H), 2.15 (ddd, $J = 16.4, 10.8, 5.5$ Hz, 1H), 1.96–1.69 (m, 7H), 1.69–1.63 (m, 1H), 1.62 (s, 3H); $^{13}\text{C NMR}$ (126 MHz, CDCl_3) δ 214.7, 179.9, 141.7, 115.5, 51.0, 43.0, 39.3, 36.7, 30.1, 28.9, 27.1, 24.4, 20.9; IR (Neat Film, NaCl) 3074, 2940, 2866, 1704, 1455, 1312, 1219, 1128, 896 cm^{-1} ; HRMS (ESI-APCI $^-$) m/z calc'd for $\text{C}_{13}\text{H}_{19}\text{O}_3$ $[\text{M}-\text{H}]^-$: 223.1340, found 223.1345; $[\alpha]_{\text{D}}^{25} +5.4$ (c 1.00, CHCl_3 , 91% ee).



4,4-Dimethyl-5-oxo-5-phenylpentanoic acid (140f). A flame-dried 100 mL round-bottom flask was charged with a magnetic stir bar, THF (26 mL), and cooled to 0 °C. A solution of *n*-butyllithium in hexanes (2.5 M, 5.7 mL, 14.3 mmol, 1.1 equiv) was added, followed by dropwise addition of diisopropylamine (2.0 mL, 14.3 mmol, 1.1 equiv). The light yellow solution was stirred at 0 °C for 10 min, then cooled to -78 °C in a dry ice-acetone bath. Isobutyrophenone (**158**, 2.0 mL, 13 mmol, 1.0 equiv) was added dropwise. The orange-red solution was stirred at the same temperature for 30 min, and methyl 3-bromopropionate (1.7 mL, 15.6 mmol, 1.2 equiv) was added dropwise. The dry ice-

acetone bath was removed, and the yellow reaction mixture was warmed to 0 °C and stirred for an additional 2 h. The reaction was quenched with half saturated aqueous NH₄Cl solution (30 mL) and extracted with Et₂O (30 mL x 2). The combined organic layers were washed with H₂O and brine, dried over Na₂SO₄, filtered, and concentrated under reduced pressure. The crude residue was purified by flash column chromatography on silica gel (5% EtOAc in hexanes) to afford a colorless oil (1.20 g), which was subjected to basic hydrolysis to provide carboxylic acid **140f** (0.93 g, 32% yield over 2 steps) as a viscous colorless oil. $R_f = 0.1$ (25% EtOAc in hexanes); ¹H NMR (400 MHz, CDCl₃) δ 7.69–7.65 (m, 2H), 7.50–7.45 (m, 1H), 7.43–7.37 (m, 2H), 2.36–2.29 (m, 2H), 2.13–2.07 (m, 2H), 1.34 (s, 6H); ¹³C NMR (101 MHz, CDCl₃) δ 208.2, 179.7, 138.6, 131.3, 128.4, 127.8, 47.2, 35.3, 29.9, 26.0; IR (Neat Film, NaCl) 2972, 1709, 1597, 1444, 1303, 1200, 962, 719, 700 cm⁻¹; HRMS (ESI-APCI-) m/z calc'd for C₁₃H₁₅O₃ [M-H]⁻: 219.1027, found 219.1035.



4-(Butoxycarbonyl)-4-ethyloctanoic acid (140g). A flame-dried 50 mL round-bottom flask was charged with a magnetic stir bar, THF (10 mL), and cooled to 0 °C. A solution of *n*-butyllithium in hexanes (2.5 M, 2.4 mL, 6.09 mmol, 1.1 equiv) was added, followed by dropwise addition of diisopropylamine (0.93 mL, 6.65 mmol, 1.2 equiv). The light yellow solution was stirred at 0 °C for 10 min, then cooled to -78 °C in a dry ice-acetone bath. Butyl ester **159** (1.11 g, 5.54 mmol, 1.0 equiv) was added dropwise. The solution

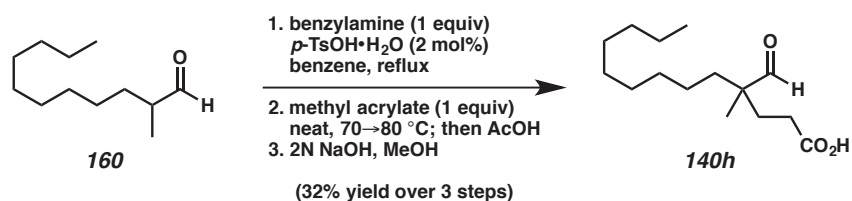
was stirred at the same temperature for 40 min, and allyl bromide (0.58 mL, 6.65 mmol, 1.2 equiv) was added dropwise. After stirring at $-78\text{ }^{\circ}\text{C}$ for 1 h, the dry ice-acetone bath was removed, and the yellow reaction mixture was warmed to $23\text{ }^{\circ}\text{C}$ and stirred for an additional 1 h. The reaction was quenched with half saturated aqueous NH_4Cl solution (10 mL) and extracted with hexanes (30 mL x 2). The combined organic layers were washed with H_2O , dried over Na_2SO_4 , filtered, and concentrated under reduced pressure. The crude residue was purified by flash column chromatography on silica gel (3% Et_2O in hexanes) to afford the allylated ester as a colorless oil (1.24 g, $R_f = 0.8$ (10% Et_2O in hexanes)), which was used directly in the next reaction.

A solution of 9-BBN in THF (0.5 M, 10 mL, 5.0 mmol, 1.1 equiv) was added to a 50 mL round-bottom flask containing the allylated ester (1.24 g, 4.5 mmol, 1.0 equiv) at $0\text{ }^{\circ}\text{C}$. After 10 min, the ice bath was removed, and the reaction mixture was stirred for another 3 h. Water (10 mL) was added to the reaction mixture, followed by careful portionwise addition of sodium perborate hydrate (1.78 g, 17.8 mmol, 4.0 equiv) to oxidize the organoborane intermediate to the corresponding alcohol. The biphasic mixture was stirred for 40 min, and extracted with EtOAc (25 mL x 3). The combined organic layers were dried over Na_2SO_4 , filtered, and concentrated under reduced pressure. The crude residue was purified by flash column chromatography on silica gel (16 \rightarrow 25% EtOAc in hexanes) to afford the desired primary alcohol as a colorless oil (1.14 g, $R_f = 0.4$ (25% EtOAc in hexanes)), which was used directly in the next reaction.

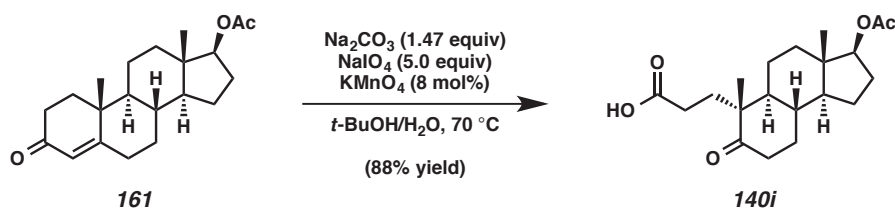
Oxidation of the primary alcohol to the corresponding carboxylic acid was carried out following a literature procedure.²⁵ A 100 mL round-bottom flask was charged with a magnetic stir bar, the primary alcohol (517 mg, 2.0 mmol, 1.0 equiv), TEMPO (22 mg,

0.14 mmol, 0.07 equiv), MeCN (10 mL), H₂O (2 mL), and aqueous phosphate buffer (0.33 M in NaH₂PO₄ and 0.33 M in Na₂HPO₄, 7.5 mL), and stirred at 20 °C for 5 min. Solid NaClO₂ (452 mg, 4.0 mmol, 2.0 equiv) was added to the flask and the reaction mixture was stirred for 2 min when the solid dissolved. A solution of NaClO (0.26 wt%, 1.1 mL, 0.04 mmol, 0.02 equiv) was added, and the reaction mixture immediately turned dark red. The flask was placed in a pre-heated 35 °C oil bath and stirred for 14 h. TLC analysis showed complete consumption of the alcohol. To the reaction mixture was added H₂O (15 mL) and 2N NaOH (4 mL) to bring the solution's pH to 10. The biphasic mixture was poured into an ice-cold solution of Na₂SO₃ (610 mg) in H₂O (10 mL), stirred for 30 min, and extracted with Et₂O (30 mL x 1). The ethereal layer was back-extracted with 0.7N NaOH (8 mL x 2). The alkaline aqueous layers were combined and acidified with 6N HCl (12 mL), and extracted with EtOAc (25 mL x 3). The combined EtOAc extracts were washed with H₂O, dried over Na₂SO₄, filtered, and concentrated under reduced pressure to a liquid/solid mixture. The mixture was dissolved in Et₂O and solid impurities were filtered off. The filtrate was concentrated and purified by flash column chromatography on silica gel (5% MeOH in CH₂Cl₂) to afford carboxylic acid **140g** (485 mg, 71% yield over 3 steps) as a viscous colorless oil. $R_f = 0.3$ (25% EtOAc in hexanes); ¹H NMR (500 MHz, CDCl₃) δ 10.27 (br s, 1H), 4.07 (t, $J = 6.6$ Hz, 2H), 2.29–2.19 (m, 2H), 1.95–1.85 (m, 2H), 1.64–1.55 (m, 4H), 1.55–1.49 (m, 2H), 1.43–1.33 (m, 2H), 1.33–1.23 (m, 2H), 1.20–1.05 (m, 2H), 0.93 (t, $J = 7.4$ Hz, 3H), 0.89 (t, $J = 7.4$ Hz, 3H), 0.79 (t, $J = 7.5$ Hz, 3H); ¹³C NMR (126 MHz, CDCl₃) δ 179.9, 176.7, 64.4, 48.8, 34.0, 30.8, 29.3, 28.6, 27.2, 26.2, 23.3, 19.3, 14.1, 13.8, 8.4; IR (Neat Film, NaCl) 2961, 2875, 1716,

1458, 1207, 1133, 947 cm^{-1} ; HRMS (ESI-APCI $^-$) m/z calc'd for $\text{C}_{15}\text{H}_{27}\text{O}_4$ $[\text{M}-\text{H}]^-$: 271.1915, found 271.1923.



4-Formyl-4-methyltridecanoic acid (140h). Using 2-methylundecanal (**160**) as starting material, the procedure for the synthesis of **140b** was followed (Note: the conjugate addition reaction was allowed to proceed for 20 h at 70 $^\circ\text{C}$ and then 28 h at 80 $^\circ\text{C}$) to provide carboxylic acid **140h** (481 mg, 32% yield over 3 steps) as a colorless oil. $R_f = 0.2$ (25% EtOAc in hexanes); ^1H NMR (500 MHz, CDCl_3) δ 11.35 (br s, 1H), 9.41 (s, 1H), 2.34–2.19 (m, 2H), 1.93–1.83 (m, 1H), 1.82–1.72 (m, 1H), 1.53–1.37 (m, 2H), 1.33–1.09 (m, 14H), 1.02 (s, 3H), 0.86 (t, $J = 6.5$ Hz, 3H); ^{13}C NMR (126 MHz, CDCl_3) δ 205.9, 179.7, 48.5, 35.6, 32.0, 30.3, 29.6, 29.5, 29.4, 29.4, 29.1, 23.9, 22.8, 18.2, 14.2; IR (Neat Film, NaCl) 2924, 2853, 1711, 1458, 1300, 1225, 913 cm^{-1} ; HRMS (ESI-APCI $^-$) m/z calc'd for $\text{C}_{15}\text{H}_{27}\text{O}_3$ $[\text{M}-\text{H}]^-$: 255.1966, found 255.1976.

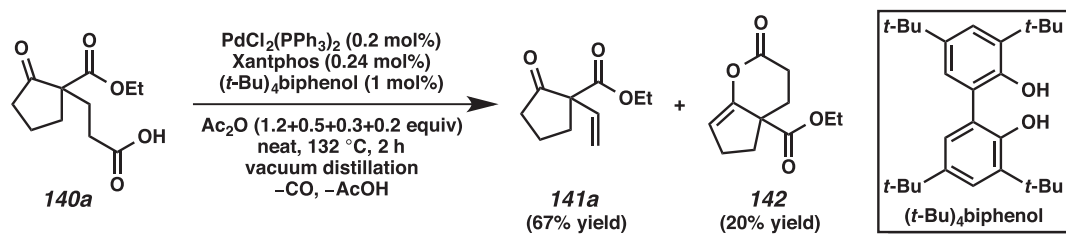


3-((3S,3aS,5aS,6R,9aS,9bS)-3-Acetoxy-3a,6-dimethyl-7-oxododecahydro-1H-cyclopenta[*a*]naphthalen-6-yl)propanoic acid (140i). Carboxylic acid **140i** was prepared based on a literature procedure.²⁶ A 250 mL round-bottom flask was charged

with a magnetic stir bar, testosterone acetate **161** (661 mg, 2.0 mmol, 1.0 equiv), Na₂CO₃ (312 mg, 2.94 mmol, 1.47 equiv), *t*-BuOH (21 mL) and H₂O (1 mL). The flask was placed in a pre-heated 70 °C oil bath, and a hot solution of NaIO₄ (2.14 g, 10.0 mmol, 5.0 equiv) and KMnO₄ (25 mg, 0.16 mmol, 0.08 equiv) in H₂O (21 mL) was added. The reaction mixture was stirred at 70 °C for 20 min when TLC analysis indicated complete consumption of starting material. The flask was cooled to ambient temperature, and 1N HCl (100 mL) was added. After stirring 2 min, the reaction mixture was extracted with EtOAc (30 mL x 3). The combined organic layers were dried over Na₂SO₄, filtered, and concentrated under reduced pressure. The residue was purified by flash column chromatography on silica gel (50% EtOAc in hexanes) to afford carboxylic acid **140i** (664 mg, 88% yield) as a solid/liquid mixture, which was recrystallized from hexanes:EtOAc 2:1 to give a white solid. $R_f = 0.4$ (50% EtOAc in hexanes); ¹H NMR (500 MHz, CDCl₃) δ 4.58 (t, $J = 8.5$ Hz, 1H), 2.63–2.44 (m, 1H), 2.40–2.14 (m, 4H), 2.14–2.06 (m, 1H), 2.04 (s, 3H), 1.99–1.89 (m, 1H), 1.85–1.30 (m, 8H), 1.29–1.14 (m, 3H), 1.12 (s, 3H), 1.10–1.02 (m, 1H), 0.84 (s, 3H); ¹³C NMR (126 MHz, CDCl₃) δ 214.6, 179.6, 171.3, 82.5, 50.5, 50.2, 48.0, 42.7, 38.0, 36.4, 34.8, 30.9, 29.3, 29.2, 27.5, 23.7, 21.3, 21.1, 20.5, 12.2; IR (Neat Film, NaCl) 2941, 1732, 1705, 1448, 1375, 1248, 1043, 952, 735 cm⁻¹; HRMS (ESI-APCI-) m/z calc'd for C₂₀H₂₉O₅ [M-H]⁻: 349.2020, found 349.2037.

5.5.3 Palladium-Catalyzed Decarbonylative Dehydration of Carboxylic Acids

General Procedure A: Large Scale Distillation Process



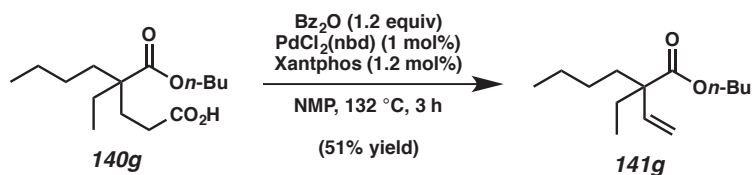
Ethyl 2-oxo-1-vinylcyclopentane-1-carboxylate (141a). A flame-dried 15 mL round-bottom flask was charged with a magnetic stir bar, $\text{PdCl}_2(\text{PPh}_3)_2$ (7.0 mg, 0.01 mmol, 0.002 equiv), Xantphos (6.9 mg, 0.012 mmol, 0.0024 equiv), $(t\text{-Bu})_4\text{biphenol}$ ²⁷ (20.5 mg, 0.05 mmol, 0.01 equiv), and carboxylic acid **140a** (1.14 g, 5.0 mmol, 1.0 equiv). The flask was equipped with a distillation head and a 25 mL round-bottom receiving flask. The closed system was connected to a vacuum manifold and equipped with a needle valve. The system was evacuated and backfilled with N_2 (x 3), and the first portion of acetic anhydride (6.0 mmol, 1.2 equiv) was added via syringe through the septum that seals the top of the distillation head. The flask was lowered into a pre-heated 60 °C oil bath and gradually heated to 132 °C in 18 min. When the oil bath temperature reached 122 °C, the needle valve was closed, switched to vacuum, and the needle valve carefully and slowly opened to allow distillation of acetic acid into a receiving flask, which was cooled to -78 °C. When the oil bath temperature reached 130 °C, time was recorded as $t = 0$. After distillation ceased (about $t = 3$ min), the needle valve was opened fully and a vacuum of 1–5 mmHg was drawn. At $t = 30$ min, the system was backfilled with N_2 , and the second portion of acetic anhydride (2.5 mmol, 0.5 equiv) was added via syringe. The system was then gradually ($t = 35$ min) resubjected to a vacuum of 1–5 mmHg. Acetic anhydride was added as follows (0.3, 0.2 equiv) in the same manner every 30 min. The

reaction was stopped at $t = 2$ h and allowed to cool under N_2 to ambient temperature. The distillate was added to a saturated aqueous solution of $NaHCO_3$, stirred for 20 min, and the biphasic mixture was extracted with CH_2Cl_2 (20 mL x 3). The combined extracts were dried over Na_2SO_4 and filtered into a 250 round-bottom flask. To this filtrate were added the residual dark red reaction mixture and the washings of the distillation head's inside (with ~5 mL CH_2Cl_2). The solvents were evaporated and the residue was purified by flash column chromatography on silica gel (5→8% EtOAc in hexanes for **141a** and then 16% EtOAc in hexanes for **142**) to afford vinyl ketone **141a** (613 mg, 67% yield) as a colorless, fragrant oil. $R_f = 0.5$ (16% EtOAc in hexanes); 1H NMR (500 MHz, $CDCl_3$) δ 6.04 (dd, $J = 17.6, 10.7$ Hz, 1H), 5.28 (d, $J = 10.7$ Hz, 1H), 5.19 (d, $J = 17.6$ Hz, 1H), 4.18 (q, $J = 7.2$ Hz, 2H), 2.63–2.55 (m, 1H), 2.45–2.27 (m, 2H), 2.23–2.15 (m, 1H), 2.07–1.87 (m, 2H), 1.25 (t, $J = 7.1$ Hz, 3H); ^{13}C NMR (126 MHz, $CDCl_3$) δ 212.5, 170.4, 134.5, 117.0, 63.5, 61.9, 37.7, 32.9, 19.6, 14.2; IR (Neat Film, NaCl) 2980, 1753, 1729, 1635, 1456, 1406, 1255, 1142, 1034, 927 cm^{-1} ; HRMS (EI+) m/z calc'd for $C_{10}H_{14}O_3$ $[M]^+$: 182.0943, found 182.0939.

Ethyl 2-oxo-3,4,5,6-tetrahydrocyclopenta[*b*]pyran-4a(2*H*)-carboxylate (142). The above reaction also furnished enol lactone **142** (206 mg, 20% yield) as a colorless oil. $R_f = 0.2$ (16% EtOAc in hexanes); 1H NMR (500 MHz, $CDCl_3$) δ 5.30 (app. s, 1H), 4.20 (q, $J = 7.1$ Hz, 2H), 2.76–2.62 (m, 2H), 2.55–2.42 (m, 3H), 2.35–2.26 (m, 1H), 1.96–1.84 (m, 1H), 1.84–1.73 (m, 1H), 1.26 (t, $J = 7.1$ Hz, 3H); ^{13}C NMR (126 MHz, $CDCl_3$) δ 173.3, 167.4, 151.6, 108.0, 61.8, 50.8, 35.9, 29.5, 28.1, 26.7, 14.2; IR (Neat Film, NaCl)

2940, 2862, 1768, 1726, 1668, 1456, 1248, 1159, 1124, 1020, 891, 805 cm^{-1} ; HRMS (EI+) m/z calc'd for $\text{C}_{11}\text{H}_{14}\text{O}_4$ $[\text{M}]^+$: 210.0892, found 210.0910.

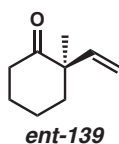
General Procedure B: Small Scale Nondistillation Process



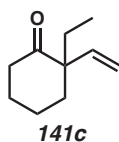
Butyl 2-ethyl-2-vinylhexanoate (141g). A flame-dried 20 x 150 mm Kimax culture tube was charged with a magnetic stir bar, $\text{PdCl}_2(\text{nbd})$ (1.3 mg, 0.005 mmol, 0.01 equiv), Xantphos (3.5 mg, 0.006 mmol, 0.012 equiv), carboxylic acid **140g** (136 mg, 0.5 mmol, 1.0 equiv), and benzoic anhydride (136 mg, 0.6 mmol, 1.2 equiv). The tube was sealed with a rubber septum, and the system was evacuated and backfilled with N_2 (x 3). NMP (0.25 mL) was added via syringe. The reaction mixture was stirred at 20 °C for 2 min, then placed in a pre-heated 132 °C oil bath and stirred for 3 h. After cooling to ambient temperature, Et_3N (0.3 mL) was added, and the mixture was purified by flash column chromatography on silica gel (2% Et_2O in hexanes) to afford vinyl ester **141g** (58 mg, 51% yield) as a colorless oil. $R_f = 0.5$ (10% Et_2O in hexanes); ^1H NMR (500 MHz, CDCl_3) δ 5.98 (dd, $J = 17.8, 10.9$ Hz, 1H), 5.17 (d, $J = 11.0$ Hz, 1H), 5.07 (d, $J = 17.8$ Hz, 1H), 4.08 (t, $J = 6.6$ Hz, 2H), 1.77–1.69 (m, 2H), 1.69–1.63 (m, 2H), 1.63–1.55 (m, 2H), 1.45–1.23 (m, 4H), 1.23–1.08 (m, 2H), 0.93 (t, $J = 7.4$ Hz, 3H), 0.88 (t, $J = 7.4$ Hz, 3H), 0.80 (t, $J = 7.4$ Hz, 3H); ^{13}C NMR (126 MHz, CDCl_3) δ 175.7, 140.3, 114.3, 64.5, 52.9, 35.7, 30.9, 29.0, 26.7, 23.4, 19.4, 14.1, 13.8, 8.9; IR (Neat Film, NaCl) 2960, 2874,

1731, 1459, 1380, 1240, 1206, 1136, 1001, 915 cm^{-1} ; HRMS (EI+) m/z calc'd for $\text{C}_{14}\text{H}_{26}\text{O}_2$ $[\text{M}]^+$: 226.1933, found 226.1933.

5.5.4 Spectroscopic Data for Pd-Catalyzed Decarbonylative Dehydration Products

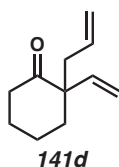


(R)-2-Methyl-2-vinylcyclohexan-1-one (ent-139). Ketone **ent-139** was prepared according to General Procedure A and isolated by silica gel chromatography (3% Et_2O in hexanes) as a colorless, fragrant oil. 60% yield. $R_f = 0.6$ (20% Et_2O in hexanes); ^1H NMR (500 MHz, CDCl_3) δ 5.97 (dd, $J = 17.8, 10.8$ Hz, 1H), 5.13 (d, $J = 10.8$ Hz, 1H), 4.98 (d, $J = 17.7$ Hz, 1H), 2.56–2.45 (m, 1H), 2.37–2.28 (m, 1H), 2.01–1.90 (m, 2H), 1.84–1.65 (m, 3H), 1.65–1.56 (m, 1H), 1.15 (s, 3H); ^{13}C NMR (126 MHz, CDCl_3) δ 213.6, 142.7, 114.9, 52.2, 39.9, 39.3, 27.8, 24.0, 21.8; IR (Neat Film, NaCl) 2932, 2864, 1709, 1635, 1450, 1371, 1313, 1123, 1093, 986, 918 cm^{-1} ; HRMS (EI+) m/z calc'd for $\text{C}_9\text{H}_{14}\text{O}$ $[\text{M}]^+$: 138.1045, found 138.1026; $[\alpha]_D^{25} +113.2$ (c 1.03, CHCl_3 , 92% ee).

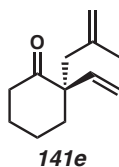


2-Ethyl-2-vinylcyclohexan-1-one (141c). Ketone **141c** was prepared according to General Procedure A and isolated by silica gel chromatography (2% Et_2O in hexanes) as a colorless, fragrant oil. 66% yield. $R_f = 0.4$ (10% Et_2O in hexanes); ^1H NMR (500 MHz, CDCl_3) δ 5.90 (dd, $J = 17.8, 10.9$ Hz, 1H), 5.19 (d, $J = 10.9$ Hz, 1H), 4.96 (d, $J =$

17.7 Hz, 1H), 2.52–2.41 (m, 1H), 2.36–2.27 (m, 1H), 1.98–1.83 (m, 2H), 1.80–1.53 (m, 6H), 0.79 (t, $J = 7.5$ Hz, 3H); ^{13}C NMR (126 MHz, CDCl_3) δ 213.3, 141.5, 115.5, 55.5, 39.6, 35.6, 29.8, 27.4, 21.6, 8.2; IR (Neat Film, NaCl) 2938, 2863, 1707, 1448, 1313, 1230, 1124, 993, 918 cm^{-1} ; HRMS (EI+) m/z calc'd for $\text{C}_{10}\text{H}_{16}\text{O}$ $[\text{M}]^+$: 152.1201, found 152.1176.

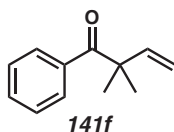


2-Allyl-2-vinylcyclohexan-1-one (141d). Ketone **141d** was prepared according to General Procedure A and isolated by silica gel chromatography (3% Et_2O in hexanes) as a colorless, fragrant oil. 54% yield. $R_f = 0.4$ (10% Et_2O in hexanes); ^1H NMR (500 MHz, CDCl_3) δ 5.86 (dd, $J = 17.7, 10.8$ Hz, 1H), 5.68 (ddt, $J = 18.0, 11.1, 7.3$ Hz, 1H), 5.22 (d, $J = 10.8$ Hz, 1H), 5.05–4.95 (m, 3H), 2.54–2.45 (m, 1H), 2.42–2.27 (m, 3H), 1.99–1.88 (m, 2H), 1.81–1.60 (m, 4H); ^{13}C NMR (126 MHz, CDCl_3) δ 212.7, 141.4, 134.3, 117.9, 116.2, 54.9, 42.0, 39.6, 36.0, 27.3, 21.6; IR (Neat Film, NaCl) 3077, 2936, 2864, 1708, 1636, 1448, 1314, 1222, 1124, 998, 916 cm^{-1} ; HRMS (EI+) m/z calc'd for $\text{C}_{11}\text{H}_{16}\text{O}$ $[\text{M}]^+$: 164.1201, found 164.1173.

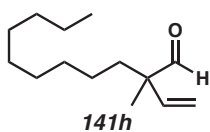


(S)-2-(2-Methylallyl)-2-vinylcyclohexan-1-one (141e). Ketone **141e** was prepared according to General Procedure A and isolated by silica gel chromatography (2→3%

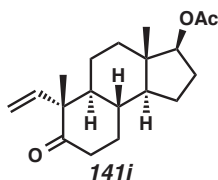
Et₂O in hexanes) as a colorless, fragrant oil. 69% yield. $R_f = 0.4$ (10% Et₂O in hexanes); ¹H NMR (500 MHz, CDCl₃) δ 5.94 (dd, $J = 18.1, 11.1$ Hz, 1H), 5.19 (d, $J = 10.8$ Hz, 1H), 4.98 (d, $J = 17.8$ Hz, 1H), 4.80 (s, 1H), 4.65 (s, 1H), 2.55–2.43 (m, 2H), 2.43–2.32 (m, 2H), 2.01–1.87 (m, 2H), 1.79–1.66 (m, 4H), 1.65 (s, 3H); ¹³C NMR (126 MHz, CDCl₃) δ 212.3, 142.5, 142.4, 115.8, 115.0, 54.8, 45.5, 39.5, 36.0, 27.1, 25.0, 21.7; IR (Neat Film, NaCl) 3075, 2938, 2863, 1707, 1641, 1448, 1125, 919, 892 cm⁻¹; HRMS (EI+) m/z calc'd for C₁₂H₁₈O [M]⁺: 178.1358, found 178.1350; $[\alpha]_D^{25} +129.5$ (c 1.00, CHCl₃, 92% ee).



2,2-Dimethyl-1-phenylbut-3-en-1-one (141f). Ketone **141f** was prepared according to General Procedure A and isolated by silica gel chromatography (2.5% Et₂O in hexanes) as a colorless oil. 75% yield. $R_f = 0.4$ (10% Et₂O in hexanes); ¹H NMR (500 MHz, CDCl₃) δ 7.89–7.85 (m, 2H), 7.49–7.43 (m, 1H), 7.40–7.35 (m, 2H), 6.19 (dd, $J = 17.6, 10.6$ Hz, 1H), 5.26–5.18 (m, 2H), 1.40 (s, 6H); ¹³C NMR (126 MHz, CDCl₃) δ 204.8, 144.0, 137.2, 131.8, 129.4, 128.1, 114.2, 50.3, 26.2; IR (Neat Film, NaCl) 3084, 2975, 2933, 1679, 1634, 1446, 1258, 971, 918, 719, 694 cm⁻¹; HRMS (EI+) m/z calc'd for C₁₂H₁₄O [M]⁺: 174.1045, found 174.1069.



2-Methyl-2-vinylundecanal (141h). Aldehyde **141h** was prepared according to General Procedure B and isolated by silica gel chromatography (2% Et₂O in hexanes) as a colorless, fragrant oil. 77% yield. $R_f = 0.5$ (10% Et₂O in hexanes); ¹H NMR (500 MHz, CDCl₃) δ 9.38 (s, 1H), 5.79 (dd, $J = 17.6, 10.8$ Hz, 1H), 5.25 (d, $J = 10.8$ Hz, 1H), 5.11 (d, $J = 17.5$ Hz, 1H), 1.57 (td, $J = 9.6, 5.9$ Hz, 2H), 1.25 (br s, 14H), 1.15 (s, 3H), 0.87 (t, $J = 6.7$ Hz, 3H); ¹³C NMR (126 MHz, CDCl₃) δ 203.2, 139.1, 116.6, 52.9, 35.7, 32.0, 30.3, 29.7, 29.6, 29.4, 24.0, 22.8, 17.8, 14.3; IR (Neat Film, NaCl) 2927, 2854, 1732, 1463, 998, 920 cm⁻¹; HRMS (EI+) m/z calc'd for C₁₄H₂₆O [M]⁺: 210.1984, found 210.2009.

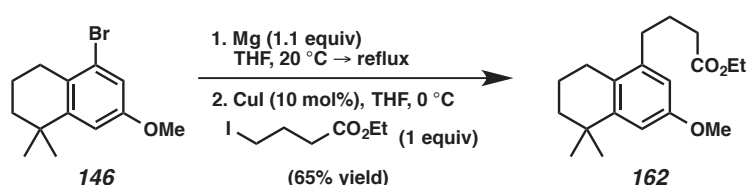


(3S,3aS,5aS,6R,9aS,9bS)-3a,6-dimethyl-7-oxo-6-vinyldodecahydro-1H-

cyclopenta[a]naphthalen-3-yl acetate (141i). Ketone **141i** was prepared according to General Procedure B and isolated by silica gel chromatography (10→14% EtOAc in hexanes) as a white solid. 41% yield. $R_f = 0.3$ (16% EtOAc in hexanes); ¹H NMR (500 MHz, CDCl₃) δ 5.78 (dd, $J = 17.6, 10.9$ Hz, 1H), 5.24 (d, $J = 10.9$ Hz, 1H), 5.02 (d, $J = 17.6$ Hz, 1H), 4.59 (t, $J = 8.5$ Hz, 1H), 2.61 (td, $J = 14.3, 6.3$ Hz, 1H), 2.37–2.30 (m, 1H), 2.24–2.14 (m, 1H), 2.03 (s, 3H), 2.02–1.95 (m, 1H), 1.83–1.62 (m, 3H), 1.58–1.47 (m, 1H), 1.45–1.33 (m, 3H), 1.32–1.25 (m, 2H), 1.24 (s, 3H), 1.18–1.05 (m, 2H), 0.85 (s, 3H); ¹³C NMR (126 MHz, CDCl₃) δ 214.3, 171.2, 141.7, 114.7, 82.4, 54.6, 51.0, 50.4, 43.0, 38.0, 36.4, 34.8, 31.2, 27.6, 23.6, 21.9, 21.3, 15.2, 12.3; IR (Neat Film, NaCl) 2946,

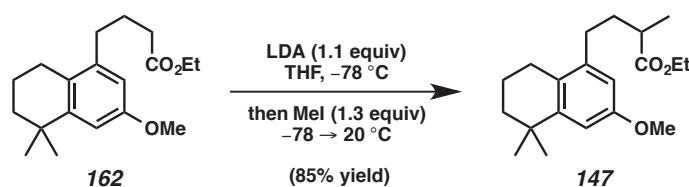
2845, 1735, 1696, 1373, 1250, 1041, 922 cm^{-1} ; HRMS (EI+) m/z calc'd for $\text{C}_{19}\text{H}_{28}\text{O}_3$ [M]⁺: 304.2039, found 304.2044.

5.5.5 Total Synthesis of (-)-Aspewentin B and Related Compounds



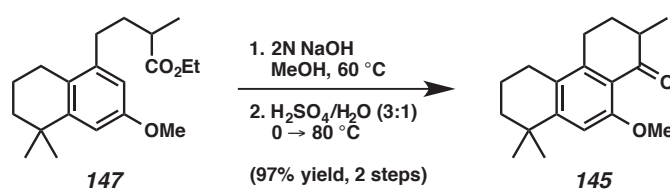
Ester 162. A 100 mL 2-necked round-bottom flask was charged with a magnetic stir bar and magnesium turnings (560 mg, 23.0 mmol, 1.1 equiv). The flask was equipped with a reflux condenser, flame-dried under vacuum, and allowed to cool to ambient temperature under N_2 . THF (3 mL) was added, followed by a small portion (2 mL) of a solution of bromoarene **146**¹⁸ (5.63 g, 20.9 mmol, 1.0 equiv) in THF (8.5 mL). DIBAL-H (0.4 mL, 1.0 M in hexanes, 0.4 mmol, 0.02 equiv) was added, and the reaction mixture was gently heated to reflux using a heat gun. Grignard reagent formation initiated as the reaction mixture turned dark with a strong exotherm. The remainder of the bromoarene solution in THF (ca. 6.5 mL) was added dropwise to maintain a gentle reflux. After addition was finished, the reaction mixture was further refluxed for 1 h, and allowed to cool to ambient temperature under N_2 . The dark gray solution of Grignard reagent was taken up in a syringe and added dropwise to a separate 100 mL round-bottom flask containing a stirred suspension of CuI (400 mg, 2.09 mmol, 0.1 equiv) and ethyl 4-iodobutyrate (5.06 g, 20.9 mmol, 1.0 equiv) in THF (20 mL) at 0 °C. After 15 min, the reaction mixture was warmed to 20 °C and quenched with aqueous NH_4Cl and NaHSO_4 solution. The layers were separated, and the aqueous layer was extracted with EtOAc (30 mL x 3). The

combined organic layers were dried over Na_2SO_4 , filtered, and concentrated under reduced pressure. Flash column chromatography on silica gel (3→4→10% EtOAc in hexanes) furnished ester **162** (4.16 g, 65% yield) as a colorless oil. $R_f = 0.5$ (10% EtOAc in hexanes); ^1H NMR (500 MHz, CDCl_3) δ 6.78 (s, 1H), 6.56 (s, 1H), 4.15 (q, $J = 7.2$ Hz, 2H), 3.79 (s, 3H), 2.62 (t, $J = 6.4$ Hz, 2H), 2.60–2.55 (m, 2H), 2.39 (t, $J = 7.4$ Hz, 2H), 1.95–1.85 (m, 2H), 1.84–1.76 (m, 2H), 1.66–1.60 (m, 2H), 1.30–1.25 (m, 9H); ^{13}C NMR (126 MHz, CDCl_3) δ 173.7, 157.3, 147.6, 140.7, 126.6, 112.1, 110.2, 60.4, 55.3, 39.0, 34.5, 34.3, 32.9, 32.2, 26.6, 25.3, 19.8, 14.4; IR (Neat Film, NaCl) 2930, 1734, 1603, 1465, 1304, 1254, 1188, 1116, 1065, 847 cm^{-1} ; HRMS (MM: ESI-APCI+) m/z calc'd for $\text{C}_{19}\text{H}_{29}\text{O}_3$ $[\text{M}+\text{H}]^+$: 305.2111, found 305.2105.



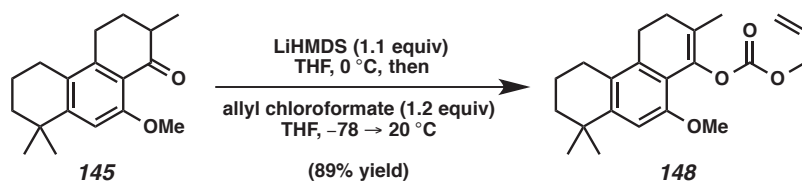
Ester 147. To a stirred solution of *n*-BuLi (3.2 mL, 2.5 M in hexanes, 8.10 mmol, 1.1 equiv) in THF (12 mL) was added *i*-Pr₂NH (1.2 mL, 8.83 mmol, 1.2 equiv) dropwise at 0 °C. The light yellow solution was stirred for 5 min, then cooled to -78 °C in a dry ice-acetone bath. A solution of ester **162** (2.24 g, 7.36 mmol, 1.0 equiv) in THF (6 mL) was added dropwise, followed by washings of the syringe (THF, 1 mL x 2). The reaction mixture was stirred at -78 °C for 15 min, and iodomethane (0.60 mL, 9.57 mmol, 1.3 equiv) was added dropwise. After stirring at -78 °C for another 45 min, the reaction mixture was allowed to warm to 20 °C, and quenched with aqueous 1N HCl (ca. 30 mL). The layers were separated, and the aqueous layer was extracted with EtOAc (30 mL x 3).

The combined organic layers were dried over Na_2SO_4 , filtered, and concentrated under reduced pressure. Flash column chromatography on silica gel (2.5→3% EtOAc in hexanes) furnished ester **147** (1.99 g, 85% yield) as a colorless oil. $R_f = 0.6$ (10% EtOAc in hexanes); ^1H NMR (500 MHz, CDCl_3) δ 6.77 (s, 1H), 6.56 (s, 1H), 4.16 (q, $J = 7.1$ Hz, 2H), 3.79 (s, 3H), 2.61 (t, $J = 6.5$ Hz, 2H), 2.58–2.48 (m, 3H), 1.98–1.88 (m, 1H), 1.84–1.75 (m, 2H), 1.71–1.58 (m, 3H), 1.30–1.26 (m, 9H), 1.22 (d, $J = 7.0$ Hz, 3H); ^{13}C NMR (126 MHz, CDCl_3) δ 176.7, 157.4, 147.6, 141.0, 126.5, 112.0, 110.2, 60.4, 55.3, 39.8, 39.0, 34.6, 34.3, 32.2, 32.2, 31.3, 26.6, 19.8, 17.4, 14.5; IR (Neat Film, NaCl) 2935, 1732, 1605, 1467, 1304, 1255, 1156, 1126, 1053, 864 cm^{-1} ; HRMS (FAB+) m/z calc'd for $\text{C}_{20}\text{H}_{30}\text{O}_3$ $[\text{M}]^+$: 318.2195, found 318.2202.



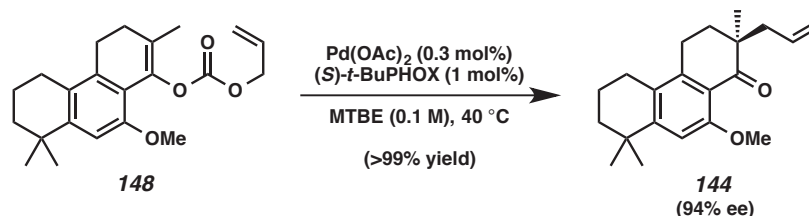
Ketone 145. To a 50 mL round-bottom flask containing ester **147** (1.96 g, 6.16 mmol, 1.0 equiv) was added a magnetic stir bar, MeOH (9 mL), and aqueous 2N NaOH (4.6 mL, 9.24 mmol, 1.5 equiv). The reaction mixture was stirred at 60 °C for 4 h and cooled to ambient temperature. Most of the MeOH was evaporated under reduced pressure, and the alkaline solution was acidified with 1N HCl (15 mL) and extracted with CH_2Cl_2 (20 mL x 3). The combined organic layers were dried over Na_2SO_4 , filtered, and concentrated under reduced pressure to the crude carboxylic acid as a colorless oil, which was used immediately for the next reaction.

The crude carboxylic acid was added dropwise to a mixture of conc. H₂SO₄ and H₂O (28 mL total, 3:1 v/v) at 0 °C via pipette. Washings of the pipette (Et₂O, 2 mL x 3) were also added. The cooling bath was removed, and the reaction mixture was stirred for 15 min, and then placed in a pre-heated 80 °C oil bath. After 20 min, the reaction mixture was allowed to cool to ambient temperature, diluted with ice water (ca. 90 mL), and extracted with EtOAc (30 mL x 3). The combined organic layers were dried over Na₂SO₄, filtered, and concentrated under reduced pressure. Flash column chromatography on silica gel (2.5→3% Et₂O in CH₂Cl₂) furnished ketone **145** (1.64 g, 97% yield over 2 steps) as a white solid. *R_f* = 0.7 (10% Et₂O in CH₂Cl₂); ¹H NMR (500 MHz, CDCl₃) δ 6.83 (s, 1H), 3.87 (s, 3H), 2.85 (dt, *J* = 17.6, 4.0 Hz, 1H), 2.72 (ddd, *J* = 17.0, 11.0, 5.2 Hz, 1H), 2.60–2.47 (m, 3H), 2.20–2.10 (m, 1H), 1.91–1.71 (m, 3H), 1.69–1.57 (m, 2H), 1.30 (s, 6H), 1.19 (d, *J* = 6.7 Hz, 3H); ¹³C NMR (126 MHz, CDCl₃) δ 200.7, 158.0, 152.2, 144.3, 126.3, 120.9, 108.4, 56.1, 56.1, 43.1, 38.4, 31.7, 31.7, 30.7, 27.1, 26.8, 19.4, 15.5; IR (Neat Film, NaCl) 2928, 1685, 1591, 1559, 1457, 1317, 1246, 1102, 1012 cm⁻¹; HRMS (MM: ESI-APCI+) *m/z* calc'd for C₁₈H₂₅O₂ [M+H]⁺: 273.1849, found 273.1855.



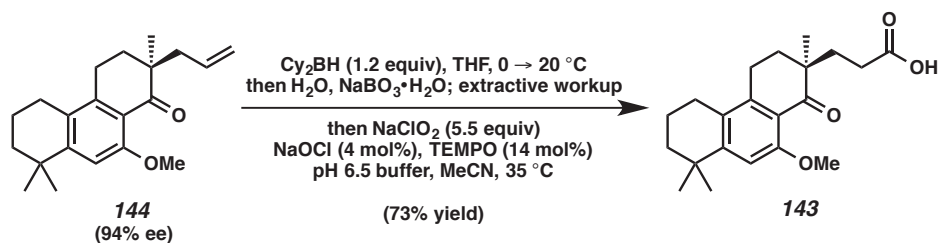
Allyl enol carbonate 148. To a stirred solution of LiHMDS (1.11 g, 6.61 mmol, 1.1 equiv) in THF (10 mL) at 0 °C was added a solution of ketone **145** (1.64 g, 6.01 mmol, 1.0 equiv) in THF (5 mL) via syringe. Washings of the syringe (THF, 1.5 mL x 2) were also added. The deep red solution was stirred at 0 °C for 1 h. In a separate, flame-dried

200 mL round-bottom flask, THF (34 mL) and allyl chloroformate (0.77 mL, 7.21 mmol, 1.2 equiv) were added, and the solution was cooled to $-78\text{ }^{\circ}\text{C}$ in a dry ice-acetone bath. To this cooled solution was added the deep red enolate solution dropwise via cannula (ca. 15 min addition time). The reaction mixture was stirred at $-78\text{ }^{\circ}\text{C}$ for another 15 min, and the cold bath was removed. After warming to room temperature, the reaction was quenched with half saturated NH_4Cl solution (ca. 50 mL). The layers were separated, and the aqueous layer was extracted with EtOAc (30 mL x 3). The combined organic layers were dried over Na_2SO_4 , filtered, and concentrated under reduced pressure. Flash column chromatography on silica gel (3 \rightarrow 5% EtOAc in hexanes) furnished allyl enol carbonate **148** (1.91 g, 89% yield) as a white solid. $R_f = 0.6$ (16% EtOAc in hexanes); ^1H NMR (500 MHz, CDCl_3) δ 6.74 (s, 1H), 6.06–5.96 (m, 1H), 5.41 (d, $J = 17.1$ Hz, 1H), 5.29 (d, $J = 10.4$ Hz, 1H), 4.70 (d, $J = 5.8$ Hz, 2H), 3.75 (s, 3H), 2.67 (t, $J = 8.0$ Hz, 2H), 2.56 (t, $J = 6.5$ Hz, 2H), 2.27 (t, $J = 8.0$ Hz, 2H), 1.85 (s, 3H), 1.83–1.76 (m, 2H), 1.64–1.58 (m, 2H), 1.27 (s, 6H); ^{13}C NMR (126 MHz, CDCl_3) δ 153.4, 152.8, 146.3, 140.3, 136.1, 132.0, 126.0, 123.5, 118.8, 117.2, 109.1, 68.7, 56.4, 38.7, 34.4, 31.9, 28.7, 27.5, 24.2, 19.7, 16.4; IR (Neat Film, NaCl) 2929, 1762, 1670, 1592, 1465, 1363, 1247, 1107, 1046 cm^{-1} ; HRMS (FAB+) m/z calc'd for $\text{C}_{22}\text{H}_{28}\text{O}_4$ $[\text{M}]^+$: 356.1988, found 356.1979.



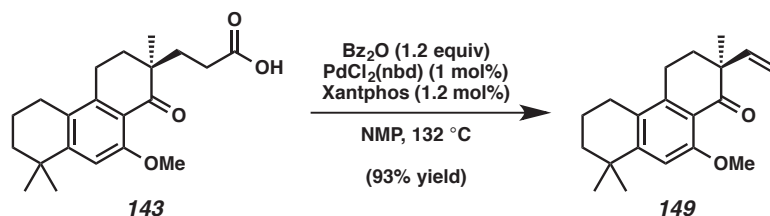
α -Allyl ketone 144. In a nitrogen-filled glove box, a 100 mL Schlenk flask was charged with $\text{Pd}(\text{OAc})_2$ (2.7 mg, 0.012 mmol, 0.003 equiv), (S) -*t*-BuPHOX (15.5 mg, 0.0399

mmol, 0.01 equiv), and MTBE (15 mL). The solution was stirred at ambient temperature for 30 min. Another portion of MTBE (15 mL) was added, and then allyl enol carbonate **148** (1.42 g, 3.99 mmol, 1.0 equiv) was added as a solid to the reaction mixture. Washings of the vial containing **148** (MTBE, 2.5 mL x 4) were also added. The Schlenk flask was sealed with a Kontes valve, brought out of the glove box, and placed in a pre-heated 40 °C oil bath. The reaction mixture was stirred at this temperature for 17 h, at which time TLC analysis indicated complete conversion of starting material. Evaporation of solvent and flash column chromatography on silica gel (10% EtOAc in hexanes) afforded α -allyl ketone **144** (1.24 g, >99% yield) as a viscous colorless oil. R_f = 0.4 (16% EtOAc in hexanes); $^1\text{H NMR}$ (500 MHz, CDCl_3) δ 6.83 (s, 1H), 5.86–5.75 (m, 1H), 5.08–5.00 (m, 2H), 3.87 (s, 3H), 2.80–2.66 (m, 2H), 2.52 (t, J = 6.5 Hz, 2H), 2.37 (dd, J = 13.8, 7.5 Hz, 1H), 2.28 (dd, J = 13.9, 7.3 Hz, 1H), 1.98 (dt, J = 13.2, 6.4 Hz, 1H), 1.88–1.78 (m, 3H), 1.69–1.60 (m, 2H), 1.30 (s, 3H), 1.29 (s, 3H), 1.14 (s, 3H); $^{13}\text{C NMR}$ (126 MHz, CDCl_3) δ 202.1, 158.7, 152.2, 143.7, 134.7, 126.1, 119.8, 117.9, 108.6, 56.1, 45.1, 41.4, 38.4, 34.9, 32.9, 31.7, 31.7, 27.0, 23.6, 21.9, 19.5; IR (Neat Film, NaCl) 2928, 1684, 1591, 1559, 1457, 1318, 1245, 1104, 1016, 913 cm^{-1} ; HRMS (MM: ESI-APCI+) m/z calc'd for $\text{C}_{21}\text{H}_{29}\text{O}_2$ $[\text{M}+\text{H}]^+$: 313.2162, found 313.2158; $[\alpha]_{\text{D}}^{25}$ -13.1 (c 1.00, CHCl_3 , 94% ee).



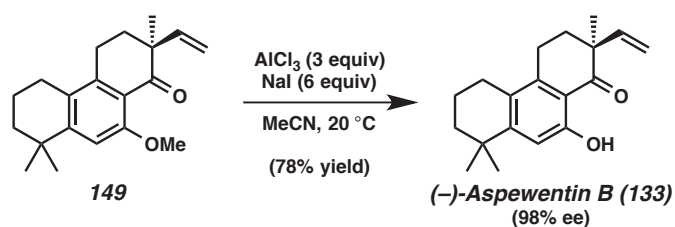
Carboxylic acid 143. A flame-dried 25 mL round-bottom flask was charged with a magnetic stir bar, $\text{BH}_3\cdot\text{SMe}_2$ (0.6 mL, 2.0 M in THF, 1.2 mmol, 1.2 equiv), and THF (0.5 mL). The solution was cooled to 0 °C in an ice bath, and cyclohexene (0.23 mL, 2.3 mmol, 2.3 equiv) was added. After stirring at 0 °C for 1 h, a solution of α -allyl ketone **144** (312 mg, 1.0 mmol, 1.0 equiv) in THF (0.6 mL) was added. The vial containing **144** was washed with THF (0.6 mL x 2) and the washings were also added. The white slurry soon turned into a light yellow and clear solution (ca. 5 min). The ice bath was removed, and the solution was stirred at 20 °C for 12 h. TLC analysis then indicated almost complete consumption of starting material. To the solution was added H_2O (1 mL) and $\text{NaBO}_3\cdot\text{H}_2\text{O}$ (350 mg). Additional H_2O (10 mL) was added to break up the white solid formed in the mixture. The aqueous phase was extracted with EtOAc (15 mL x 3). The combined organic layers were dried over Na_2SO_4 , filtered, concentrated under reduced pressure, and quantitatively transferred to a 50 mL round-bottom flask. To this flask was added a magnetic stir bar, TEMPO (22 mg, 0.14 mmol, 0.14 equiv), MeCN (5 mL), H_2O (2.6 mL), and aqueous phosphate buffer (0.33 M in NaH_2PO_4 and 0.33 M in Na_2HPO_4 , 4 mL), and stirred at 20 °C for 5 min. Solid NaClO_2 (622 mg, 5.5 equiv) was added to the flask and the reaction mixture was stirred for 2 min when the solid dissolved. A solution of NaClO (0.26 wt%, 1.2 mL, 0.04 mmol, 0.04 equiv) was added, and the reaction mixture immediately turned dark red. The flask was placed in a pre-heated 35 °C oil bath and stirred for 53 h. TLC analysis showed complete consumption of the alcohol. After cooling to 23 °C, 2N NaOH (5 mL) was added, followed by a solution of Na_2SO_3 (0.88 g) in H_2O (6 mL). The mixture was stirred vigorously for 30 min, and extracted with Et₂O (30 mL x 1). The ethereal layer was discarded. The alkaline aqueous layer was acidified

with 8N HCl (ca. 3 mL), and extracted with EtOAc (30 mL x 1). The EtOAc layer was washed with 1N HCl (10 mL) and H₂O (10 mL), dried over Na₂SO₄, filtered, and concentrated under reduced pressure to afford carboxylic acid **143** (252 mg, 73% yield) as a viscous light brown oil. Recrystallization from hexanes/EtOAc gave pure **143** as white crystals. $R_f = 0.4$ (67% EtOAc in hexanes); ¹H NMR (500 MHz, CDCl₃) δ 6.82 (s, 1H), 3.85 (s, 3H), 2.82–2.68 (m, 2H), 2.51 (t, $J = 6.5$ Hz, 2H), 2.44 (dt, $J = 16.5, 8.1$ Hz, 1H), 2.34 (dt, $J = 16.5, 8.2$ Hz, 1H), 1.98 (dt, $J = 13.1, 6.3$ Hz, 1H), 1.94–1.79 (m, 5H), 1.66–1.60 (m, 2H), 1.30 (s, 3H), 1.29 (s, 3H), 1.15 (s, 3H); ¹³C NMR (126 MHz, CDCl₃) δ 201.8, 179.5, 158.6, 152.5, 143.4, 126.2, 119.5, 108.6, 56.0, 44.5, 38.4, 34.9, 33.5, 31.7, 31.7, 31.6, 29.4, 27.0, 23.6, 21.9, 19.4; IR (Neat Film, NaCl) 2931, 1708, 1674, 1591, 1558, 1460, 1318, 1245, 1227, 1103, 913, 731 cm⁻¹; HRMS (MM: ESI-APCI+) m/z calc'd for C₂₁H₂₉O₄ [M+H]⁺: 345.2060, found 345.2047; $[\alpha]_D^{25} -1.5$ (c 1.00, CHCl₃).



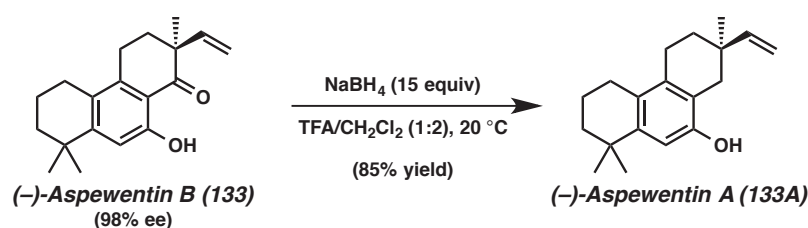
α -Vinyl ketone 149. Following General Procedure B, palladium-catalyzed decarbonylative dehydration of carboxylic acid **143** (172 mg, 0.5 mmol, 1.0 equiv) and flash column chromatography on silica gel (7→10% EtOAc in hexanes) furnished α -vinyl ketone **149** (140 mg, 93% yield) as a colorless oil. $R_f = 0.3$ (16% EtOAc in hexanes); ¹H NMR (500 MHz, CDCl₃) δ 6.82 (s, 1H), 6.01 (dd, $J = 17.7, 10.9$ Hz, 1H), 5.08–4.98 (m, 2H), 3.86 (s, 3H), 2.81–2.68 (m, 2H), 2.58–2.43 (m, 2H), 2.08 (dt, $J =$

13.8, 5.1 Hz, 1H), 2.00–1.90 (m, 1H), 1.89–1.73 (m, 2H), 1.68–1.55 (m, 2H), 1.28 (s, 6H), 1.27 (s, 3H); ^{13}C NMR (126 MHz, CDCl_3) δ 199.9, 158.5, 152.3, 143.7, 141.1, 126.0, 120.2, 114.4, 108.5, 56.1, 49.0, 38.4, 34.9, 34.5, 31.7, 31.6, 27.0, 24.0, 23.4, 19.4; IR (Neat Film, NaCl) 2928, 1684, 1591, 1559, 1458, 1318, 1245, 1105, 1020, 915 cm^{-1} ; HRMS (MM: ESI-APCI+) m/z calc'd for $\text{C}_{20}\text{H}_{27}\text{O}_2$ $[\text{M}+\text{H}]^+$: 299.2006, found 299.1992; $[\alpha]_{\text{D}}^{25}$ -43.2 (c 1.00, CHCl_3).



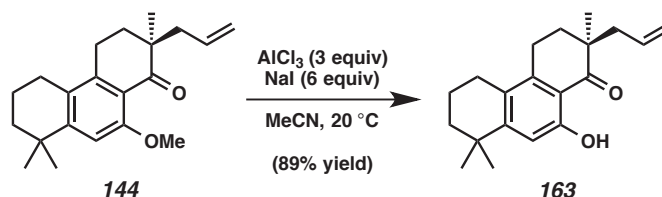
(-)-Aspewentin B (133). A 50 mL round-bottom flask was charged with a magnetic stir bar, NaI (329 mg, 2.20 mmol, 6.0 equiv), AlCl_3 (146 mg, 1.10 mmol, 3.0 equiv), and MeCN (4 mL) in air. To this slurry was added a solution of α -vinyl ketone **149** (109 mg, 0.37 mmol, 1.0 equiv) in MeCN (6 mL). The reaction mixture immediately turned yellow-orange. After stirring for 5 min, the reaction was quenched with 1N HCl (30 mL) and extracted with CH_2Cl_2 (10 mL x 4). The combined organic layers were dried over Na_2SO_4 , filtered, and concentrated under reduced pressure. Flash column chromatography on silica gel (2.5% Et_2O in hexanes) furnished (-)-aspewentin B (**133**, 82 mg, 78% yield) as a light yellow oil. $R_f = 0.7$ (16% EtOAc in hexanes); ^1H NMR (500 MHz, CDCl_3) δ 12.40 (s, 1H), 6.84 (s, 1H), 5.98 (dd, $J = 17.7, 10.8$ Hz, 1H), 5.13 (d, $J = 10.7$ Hz, 1H), 5.03 (d, $J = 17.6$ Hz, 1H), 2.81–2.69 (m, 2H), 2.59–2.44 (m, 2H), 2.14–2.06 (m, 1H), 2.04–1.94 (m, 1H), 1.88–1.73 (m, 2H), 1.68–1.55 (m, 2H), 1.33 (s, 3H), 1.27 (s, 6H); ^{13}C NMR (126 MHz, CDCl_3) δ 207.2, 160.9, 156.1, 142.3, 140.5, 124.7, 115.1, 114.6, 113.3,

47.9, 38.3, 35.0, 34.4, 31.7, 31.6, 26.9, 23.4, 23.3, 19.4; IR (Neat Film, NaCl) 2929, 1635, 1464, 1358, 1222, 1083, 920, 809 cm^{-1} ; HRMS (FAB+) m/z calc'd for $\text{C}_{19}\text{H}_{25}\text{O}_2$ $[\text{M}+\text{H}]^+$: 285.1855, found 285.1842; $[\alpha]_{\text{D}}^{25}$ -90.5 (c 0.20, MeOH, 98% ee).

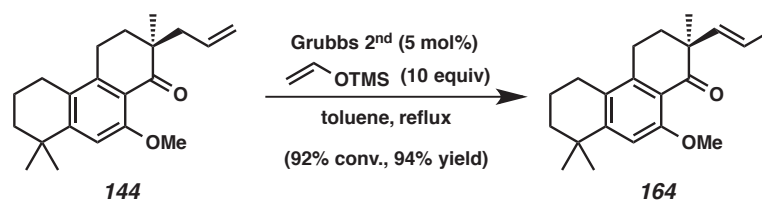


(-)-Aspewentin A (133A). A 20 mL scintillation vial was charged with a magnetic stir bar and NaBH_4 (38 mg, 1.0 mmol, 10 equiv). Trifluoroacetic acid (1 mL) was added carefully with stirring. Solids soon dissolved, with a slight exotherm. A solution of (-)-aspewentin B (**1**, 29 mg, 0.10 mmol, 1.0 equiv) in CH_2Cl_2 (2 mL) was added, and the reaction mixture immediately turned yellow. After stirring 1 h, additional NaBH_4 (7.5 mg, 0.20 mmol, 2.0 equiv) was added. After 45 min, a third portion of NaBH_4 (11 mg, 0.30 mmol, 3.0 equiv, 15 equiv total) was added. After stirring another 2 h, the reaction was quenched with saturated aq. NaHCO_3 solution (ca. 15 mL). Care should be taken during addition of NaHCO_3 due to rapid gas evolution. The biphasic mixture was extracted with EtOAc (15 mL x 2). The combined organic layers were dried over Na_2SO_4 , filtered, and concentrated under reduced pressure. Flash column chromatography on silica gel (9% Et_2O in hexanes) furnished (-)-aspewentin A (**133A**, 23 mg, 85% yield) as a light orange oil. $R_f = 0.4$ (20% Et_2O in hexanes); ^1H NMR (500 MHz, CDCl_3) δ 6.67 (s, 1H), 5.90 (dd, $J = 17.5, 10.7$ Hz, 1H), 5.08–4.88 (m, 2H), 4.69 (br s, 1H), 2.66 (d, $J = 16.3$ Hz, 1H), 2.57 (t, $J = 6.7$ Hz, 2H), 2.50 (t, $J = 6.5$ Hz, 2H), 2.46 (d, $J = 16.3$ Hz, 1H), 1.86–1.79 (m, 2H), 1.76–1.70 (m, 1H), 1.69–1.60 (m, 3H),

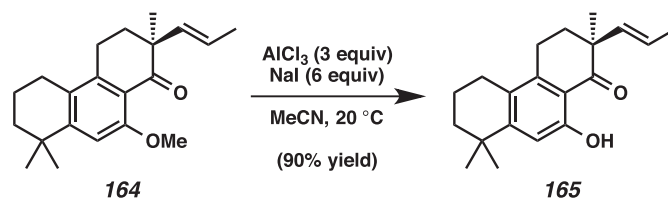
1.27 (d, $J = 1.6$ Hz, 6H), 1.11 (s, 3H); ^{13}C NMR (126 MHz, CDCl_3) δ 151.3, 147.2, 143.9, 135.2, 126.5, 119.7, 111.2, 110.0, 38.8, 34.5, 34.5, 34.1, 33.9, 32.1, 32.0, 26.8, 26.0, 24.4, 19.7; IR (Neat Film, NaCl) 3307, 2923, 1606, 1456, 1418, 1324, 1252, 1019, 910, 858 cm^{-1} ; HRMS (FAB+) m/z calc'd for $\text{C}_{19}\text{H}_{26}\text{O}$ $[\text{M}]^+$: 270.1984, found 270.1972; $[\alpha]_{\text{D}}^{25} - 38.6$ (c 0.20, MeOH).



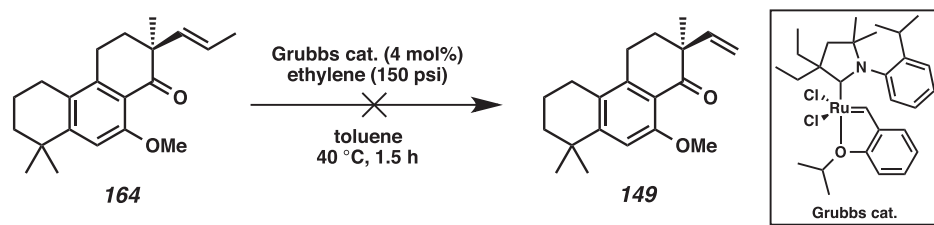
Ketone 163. Using α -allyl ketone **144** as starting material (20 mg, 0.064 mmol, 1.0 equiv), and following the same procedure as that for (–)-aspewentin B (**1**), ketone **163** was obtained (17 mg, 89% yield) as a colorless oil. $R_f = 0.7$ (16% EtOAc in hexanes); ^1H NMR (500 MHz, CDCl_3) δ 12.47 (s, 1H), 6.84 (s, 1H), 5.83–5.72 (m, 1H), 5.13–5.05 (m, 2H), 2.82–2.66 (m, 2H), 2.52 (t, $J = 6.5$ Hz, 2H), 2.46 (dd, $J = 13.9, 7.3$ Hz, 1H), 2.26 (dd, $J = 13.8, 7.5$ Hz, 1H), 2.08–1.98 (m, 1H), 1.90–1.77 (m, 3H), 1.65–1.59 (m, 2H), 1.28 (s, 6H), 1.19 (s, 3H); ^{13}C NMR (126 MHz, CDCl_3) δ 209.1, 161.0, 156.0, 142.2, 133.8, 124.7, 118.6, 114.2, 113.4, 44.1, 41.2, 38.3, 35.0, 32.6, 31.6, 31.6, 26.9, 23.0, 22.2, 19.4; IR (Neat Film, NaCl) 2930, 1634, 1464, 1360, 1220, 1190, 919, 811 cm^{-1} ; HRMS (MM: ESI-APCI+) m/z calc'd for $\text{C}_{20}\text{H}_{27}\text{O}_2$ $[\text{M}+\text{H}]^+$: 299.2006, found 299.1999; $[\alpha]_{\text{D}}^{25} - 23.5$ (c 0.20, MeOH).



Ketone 164. To a solution of α -allyl ketone **144** (109 mg, 0.349 mmol, 1.0 equiv) and vinyloxytrimethylsilane (0.52 mL, 3.49 mmol, 10.0 equiv) in toluene (19 mL) was added Grubbs 2nd generation catalyst (14.8 mg, 0.01745 mmol, 0.05 equiv) at 20 °C. The purple reaction mixture was immersed in a pre-heated 128°C oil bath (color changed to yellow) and refluxed for 16 h. The reaction mixture was concentrated under reduced pressure. The residue was purified by flash column chromatography on silica gel (10% EtOAc in hexanes) to afford ketone **164** (103 mg, 92% conv., 94% yield) as a colorless oil. R_f = 0.4 (16% EtOAc in hexanes); ¹H NMR (500 MHz, CDCl₃) δ 6.82 (s, 1H), 5.60 (d, J = 15.9 Hz, 1H), 5.48–5.38 (m, 1H), 3.86 (s, 3H), 2.79–2.66 (m, 2H), 2.58–2.45 (m, 2H), 2.08–1.99 (m, 1H), 1.96–1.88 (m, 1H), 1.87–1.74 (m, 2H), 1.68–1.56 (m, 5H), 1.30 (s, 3H), 1.28 (s, 3H), 1.24 (s, 3H); ¹³C NMR (126 MHz, CDCl₃) δ 200.4, 158.6, 152.1, 143.9, 133.6, 126.0, 125.0, 120.2, 108.5, 56.1, 48.2, 38.4, 35.1, 34.9, 31.8, 31.6, 27.0, 24.1, 24.0, 19.5, 18.5; IR (Neat Film, NaCl) 2928, 1683, 1591, 1558, 1456, 1318, 1245, 1106, 1020, 966 cm⁻¹; HRMS (MM: ESI-APCI+) m/z calc'd for C₂₁H₂₉O₂ [M+H]⁺: 313.2162, found 313.2154; $[\alpha]_D^{25}$ -49.0 (c 1.00, CHCl₃).



Ketone 165. Using ketone **164** as starting material (35 mg, 0.112 mmol, 1.0 equiv), and following the same procedure as that for (–)-aspewentin B (**133**), ketone **165** was obtained (30 mg, 90% yield) as a colorless oil. $R_f = 0.7$ (16% EtOAc in hexanes); ^1H NMR (500 MHz, CDCl_3) δ 12.46 (s, 1H), 6.84 (s, 1H), 5.57 (d, $J = 15.9$ Hz, 1H), 5.49–5.39 (m, 1H), 2.79–2.67 (m, 2H), 2.59–2.44 (m, 2H), 2.09–2.00 (m, 1H), 2.00–1.91 (m, 1H), 1.89–1.74 (m, 2H), 1.66 (d, $J = 5.9$ Hz, 3H), 1.64–1.55 (m, 2H), 1.30 (s, 3H), 1.28 (s, 6H); ^{13}C NMR (126 MHz, CDCl_3) δ 207.7, 160.9, 155.9, 142.5, 133.1, 125.9, 124.6, 114.6, 113.3, 47.1, 38.3, 35.1, 35.0, 31.7, 31.6, 26.9, 23.9, 23.5, 19.4, 18.4; IR (Neat Film, NaCl) 2929, 1634, 1464, 1359, 1267, 1221, 1191, 964 cm^{-1} ; HRMS (MM: ESI-APCI+) m/z calc'd for $\text{C}_{20}\text{H}_{27}\text{O}_2$ $[\text{M}+\text{H}]^+$: 299.2006, found 299.2002; $[\alpha]_{\text{D}}^{25} -65.1$ (c 0.20, MeOH).



Ethenolysis of 164. In a nitrogen-filled glove box, a Fisher-Porter bottle was charged with a magnetic stir bar, toluene (10 mL), and Grubbs catalyst (1.7 mg, 0.0028 mmol, 0.04 equiv). A solution of **164** (22 mg, 0.07 mmol, 1.0 equiv) in toluene (0.2 mL) was added. The head of the Fisher-Porter bottle was equipped with a pressure gauge, and a

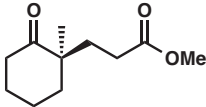
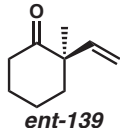
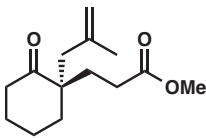
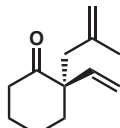
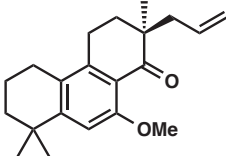
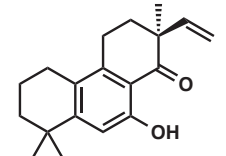
dip-tube was adapted on the bottle. The system was sealed and taken out of the glove box and connected to the ethylene line. The vessel was then purged with ethylene (polymer purity 99.9% from Matheson Tri Gas) for 5 min, pressurized to 150 psi, and placed in an oil bath at 40 °C. After stirring for 1.5 h, the solvent was evaporated, and the residue was diluted in EtOAc and passed through a short plug of silica gel to remove the ruthenium catalyst. The filtrate was concentrated under reduced pressure, and ¹H NMR analysis of the residue showed starting material **164** remaining, and no peaks corresponding to the desired product **149**.

Table 5.2 Comparison of Synthetic and Natural Aspewentin B

Synthetic (-)-Aspewentin B	Natural (+)-Aspewentin B¹⁵
<i>¹H NMR (500 MHz, CDCl₃)</i>	<i>¹H NMR (500 MHz, CDCl₃)</i>
12.40 (s, 1H)	12.40 (s, 1H)
6.84 (s, 1H)	6.84 (s, 1H)
5.98 (dd, <i>J</i> = 17.7, 10.8 Hz, 1H)	5.98 (dd, <i>J</i> = 17.6, 10.8 Hz, 1H)
5.13 (d, <i>J</i> = 10.7 Hz, 1H)	5.14 (d, <i>J</i> = 10.8 Hz, 1H)
5.03 (d, <i>J</i> = 17.6 Hz, 1H)	5.03 (d, <i>J</i> = 17.6 Hz, 1H)
2.81–2.69 (m, 2H)	2.75 (m, 2H)
2.59–2.44 (m, 2H)	2.51 (m, 2H)
2.14–2.06 (m, 1H)	2.10 (m, 1H)
2.04–1.94 (m, 1H)	2.00 (m, 1H)
1.88–1.73 (m, 2H)	1.81 (m, 2H)
1.68–1.55 (m, 2H)	1.61 (m, 2H)
1.33 (s, 3H)	1.33 (s, 3H)
1.27 (s, 6H)	1.28 (s, 3H), 1.27 (s, 3H)
<i>¹³C NMR (126 MHz, CDCl₃)</i>	<i>¹³C NMR (125 MHz, CDCl₃)</i>
207.2	207.1
160.9	160.8
156.1	156.2
142.3	142.2
140.5	140.4
124.7	124.6
115.1	115.0
114.6	114.4
113.3	113.3
47.9	47.8
38.3	38.2
35.0	34.9
34.4	34.3
31.7	31.6
31.6	31.5
26.9	26.8
23.4	23.3
23.3	23.2
19.4	19.3
<i>Optical Rotation</i>	<i>Optical Rotation</i>
$[\alpha]_D^{25} -90.5$ (c 0.20, MeOH, 98% ee)	$[\alpha]_D^{20} +23.3$ (c 0.20, MeOH)

5.5.6 Methods for the Determination of Enantiomeric Excess

Table 5.3 Analytical HPLC and SFC assays and retention times

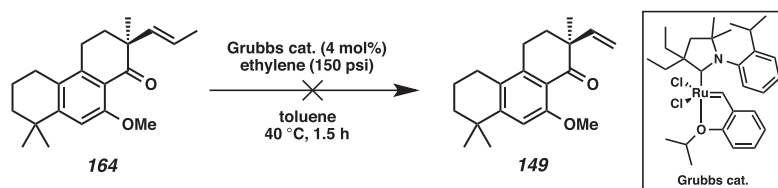
entry	compound	assay conditions	retention time of major isomer (min)	retention time of minor isomer (min)	% ee
1	 152	HPLC Chiralcel OD-H 10% IPA in hexanes isocratic, 1.0 mL/min 220 nm	6.43	5.93	91
2	 ent-139	GC G-TA 60 °C isotherm 5 min then ramp 2 °C/min	24.20	23.92	92
3	 157	HPLC Chiralcel OD-H 5% IPA in hexanes isocratic, 1.0 mL/min 210 nm	8.08	9.99	91
4	 141e	HPLC Chiralpak AS 0.2% IPA in hexanes isocratic, 1.0 mL/min 210 nm	9.50	7.89	92
5	 144	SFC Chiralcel OB-H 3% MeOH in CO ₂ isocratic, 3.0 mL/min 254 nm	8.82	6.41	94
6	 (-)-Aspewentin B (133)	HPLC Chiralpak AD 0.5% IPA in hexanes isocratic, 1.0 mL/min 210 nm	7.22	6.56	98

5.6 Notes and References

- (1) (a) Bernauer, K.; Englert, G.; Vetter, W.; Weiss, E. *Helv. Chim. Acta* **1969**, *52*, 1886–1905. (b) Moore, R. E.; Cheuk, C.; Patterson, G. M. L. *J. Am. Chem. Soc.* **1984**, *106*, 6456–6457. (c) Masuda, T.; Masuda, K.; Shiragami, S.; Jitoe, A.; Nakatani, N. *Tetrahedron* **1992**, *48*, 6787–6792. (d) Rubal, J. J.; Moreno-Dorado, F. J.; Guerra, F. M.; Jorge, Z. D.; Saouf, A.; Akssira, M.; Mellouki, F.; Romero-Garrido, R.; Massanet, G. M. *Phytochemistry* **2007**, *68*, 2480–2486.
- (2) Nishimoto, Y.; Ueda, H.; Yasuda, M.; Baba, A. *Angew. Chem., Int. Ed.* **2012**, *51*, 8073–8076.
- (3) (a) Chieffi, A.; Kamikawa, K.; Åhman, J.; Fox, J. M.; Buchwald, S. L. *Org. Lett.* **2001**, *3*, 1897–1900. (b) Huang, J.; Bunel, E.; Faul, M. M. *Org. Lett.* **2007**, *9*, 4343–4346. (c) Taylor, A. M.; Altman, R. A.; Buchwald, S. L. *J. Am. Chem. Soc.* **2009**, *131*, 9900–9901.
- (4) (a) Nakamura, M.; Endo, K.; Nakamura, E. *Org. Lett.* **2005**, *7*, 3279–3281. (b) Endo, K.; Hatakeyama, T.; Nakamura, M.; Nakamura, E. *J. Am. Chem. Soc.* **2007**, *129*, 5264–5271. (c) Fujimoto, T.; Endo, K.; Tsuji, H.; Nakamura, M.; Nakamura, E. *J. Am. Chem. Soc.* **2008**, *130*, 4492–4496.
- (5) (a) Yamaguchi, M.; Tsukagoshi, T.; Arisawa, M. *J. Am. Chem. Soc.* **1999**, *121*, 4074–4075. (b) Arisawa, M.; Miyagawa, C.; Yoshimura, S.; Kido, Y.; Yamaguchi, M. *Chem. Lett.* **2001**, 1080–1081.
- (6) Tanikaga, R.; Sugihara, H.; Tanaka, K.; Kaji, A. *Synthesis* **1977**, 299–301.
- (7) (a) Kowalski, C. J.; Dung, J.-S. *J. Am. Chem. Soc.* **1980**, *102*, 7950–7951. (b) Clive, D. L. J.; Russell, C. G.; Suri, S. C. *J. Org. Chem.* **1982**, *41*, 1632–1641.

-
- (8) Nozoye, T.; Shibnuma, Y.; Nakai, T.; Hatori, Y. *Chem. Pharm. Bull.* **1988**, *36*, 4980–4985.
- (9) (a) Meyers, A. I.; Hanreich, R.; Wanner, K. T. *J. Am. Chem. Soc.* **1985**, *107*, 7776–7778. (b) Kawashima, H.; Kaneko, Y.; Sakai, M.; Kobayashi, Y. *Chem. – Eur. J.* **2014**, *20*, 272–278.
- (10) Pfau, M.; Revial, G.; Guingant, A.; d’Angelo, J. *J. Am. Chem. Soc.* **1985**, *107*, 273–274.
- (11) Mohr, J. T.; Behenna, D. C.; Harned, A. M.; Stoltz, B. M. *Angew. Chem., Int. Ed.* **2005**, *44*, 6924–6927.
- (12) Liu, Y.; Kim, K. E.; Herbert, M. B.; Fedorov, A.; Grubbs, R. H.; Stoltz, B. M. *Adv. Synth. Catal.* **2014**, *356*, 130–136.
- (13) de Avellar, I. G. J.; Vierhapper, F. W. *Tetrahedron* **2000**, *56*, 9957–9965.
- (14) The small-scale reactions were performed under 1 atm N₂ (no distillation). Acetic anhydride was found to be unsuitable under such conditions, while benzoic anhydride proved to be optimal.
- (15) Miao, F.-P.; Liang, X.-R.; Liu, X.-H.; Ji, N.-Y. *J. Nat. Prod.* **2014**, *77*, 429–432.
- (16) The natural product has (+)-stereochemistry we synthesized the (–)-enantiomer due to the ready availability of the (*S*)-*t*-BuPHOX ligand.
- (17) The enantioselective Michael addition does not work for 1-tetralone substrates. For details, see: d’Angelo, J.; Desmaële, D.; Dumas, F.; Guingant, A. *Tetrahedron Asymmetry* **1992**, *3*, 459–505.
- (18) Allergan, Inc. Patent WO2005/58301 A1, 2005.
- (19) Stoltz, B. M. et al. Manuscript submitted to *Adv. Synth. Catal.*

(20) An alternative route from allyl ketone **144** to vinyl ketone **149** involves isomerization of the double bond to the internal position followed by ethenolysis. While the isomerization proceeded smoothly using the protocol developed by Nishida (Arisawa, M.; Terada, Y.; Nakagawa, M.; Nishida, A. *Angew. Chem., Int. Ed.* **2002**, *41*, 4732–4734) to afford internal olefin **164**, attempts at ethenolysis of the resulting internal olefin were unsuccessful, likely due to steric bulk at the adjacent quaternary center. See Experimental Section (5.5) for details.



(21) Spectroscopic data (^1H and ^{13}C NMR) and exact mass of the synthetic compound matches those of natural (+)-aspewentin B. Optical rotation, however, is significantly different (synthetic compound: $[\alpha]_{\text{D}}^{25} -90.5$ (c 0.20, MeOH, 94% ee); natural product: $[\alpha]_{\text{D}}^{20} +23.3$ (c 0.20, MeOH)). HPLC analysis showed the synthetic compound to be of 98% ee. Based on the stereoselectivity of the Pd-PHOX catalyst in previous examples, we reasoned that the absolute configuration of our synthetic compound is opposite to that of the natural product, and thus the sign of optical rotation is correct. The difference in magnitude may arise from the possibility that the natural product is a scalemic mixture (i.e. not enantiopure). For a review on non-enantiopure natural products, see: Finefield, J. M.; Sherman, D. H.; Kreitman, M.; Williams, R. M. *Angew. Chem., Int. Ed.* **2012**, *51*, 4802–4836. Another possibility is that the isolated natural product contained a small amount of impurity that had a large effect on optical rotation.

-
- (22) G. Quandt, G. Höfner, K. T. Wanner, *Bioorg. Med. Chem.* **2013**, *21*, 3363–3378.
- (23) Pangborn, A. M.; Giardello, M. A.; Grubbs, R. H.; Rosen, R. K.; Timmers, F. J. *Organometallics* **1996**, *15*, 1518–1520.
- (24) Peer, M.; de Jong, J. C.; Kiefer, M.; Langer, T.; Rieck, H.; Schell, H.; Sennhenn, P.; Sprinz, J.; Steinhagen, H.; Wiese, B.; Helmchen, G. *Tetrahedron* **1996**, *52*, 7547–7583.
- (25) Zhao, M. M.; Li, J.; Mano, E.; Song, Z. J.; Tschaen, D. M. *Org. Syn.* **2005**, *81*, 195–203.
- (26) Borthakur, M.; Boruah, R. C. *Steroids* **2008**, *73*, 637–641.
- (27) Straub, B. F.; Wrede, M.; Schmid, K.; Rominger, F. *Eur. J. Inorg. Chem.* **2010**, 1907–1911.

APPENDIX 6

Spectra Relevant to Chapter 5

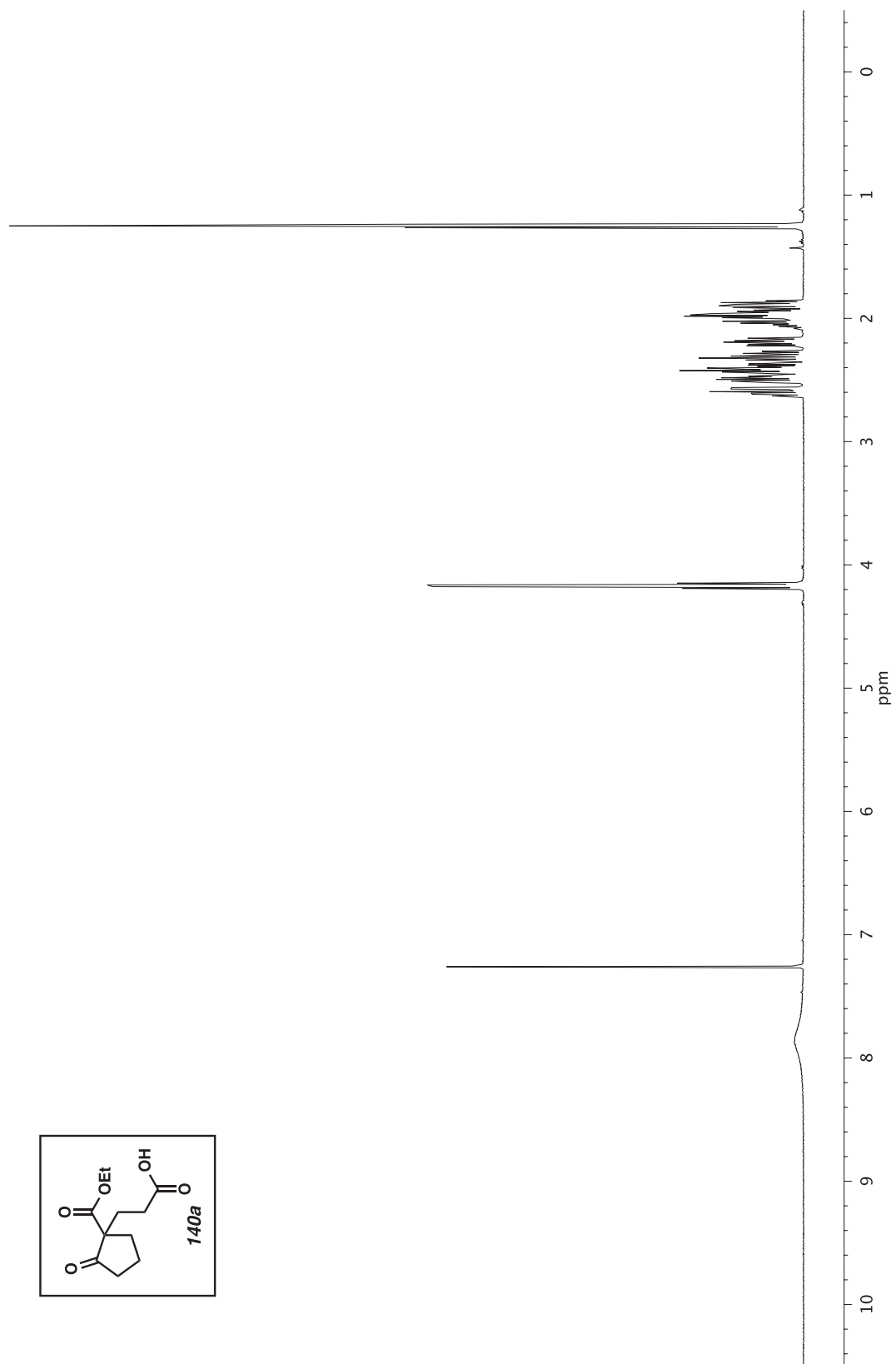


Figure A6.1 ^1H NMR (500 MHz, CDCl_3) of compound **140a**.

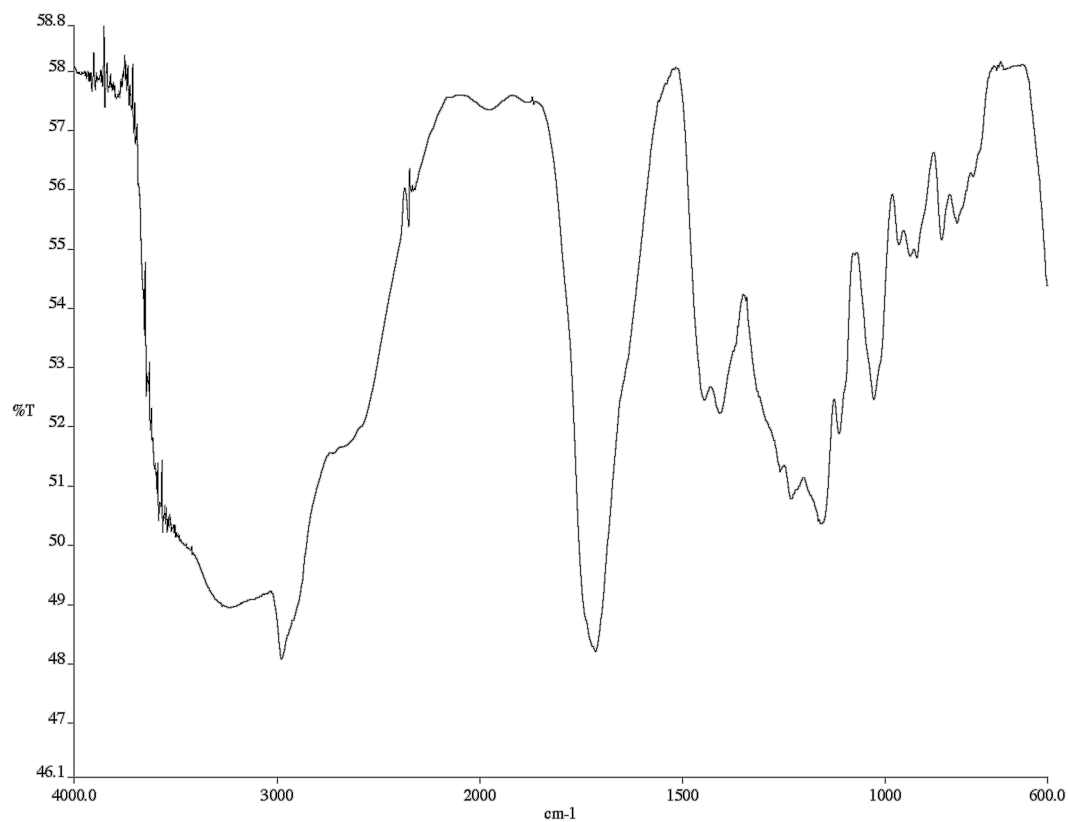


Figure A6.2 Infrared spectrum (Thin Film, NaCl) of compound **140a**.

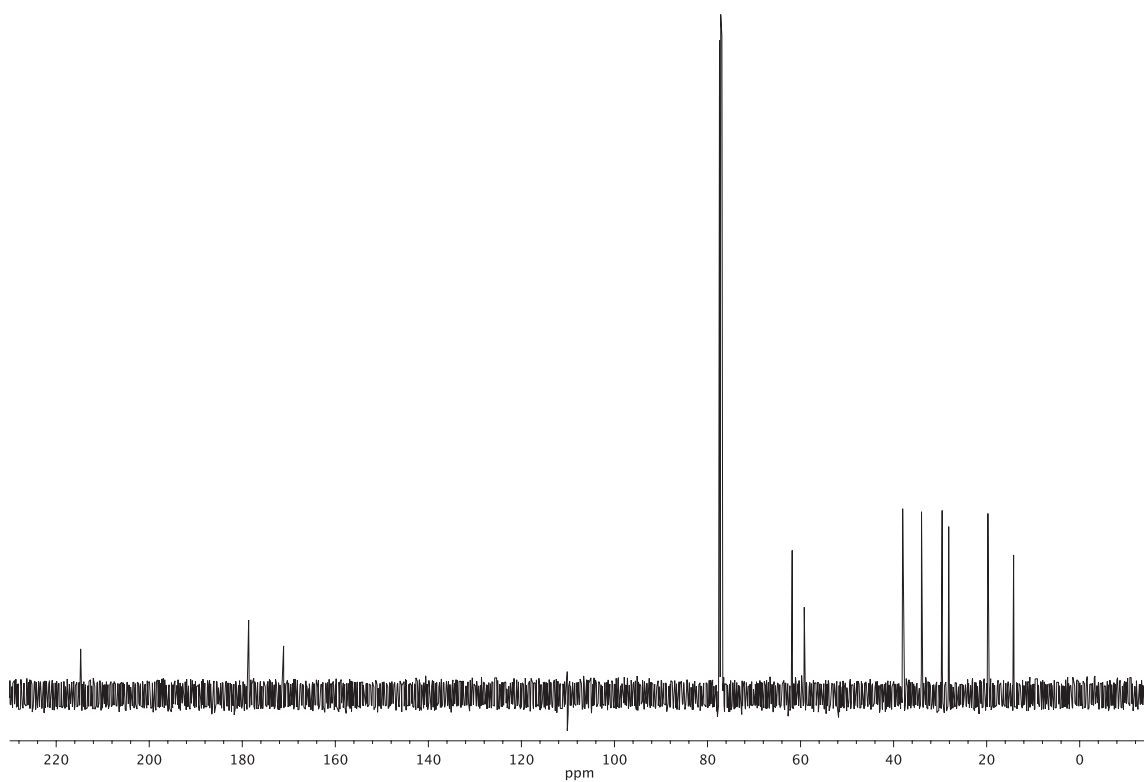


Figure A6.3 ¹³C NMR (126 MHz, CDCl₃) of compound **140a**.

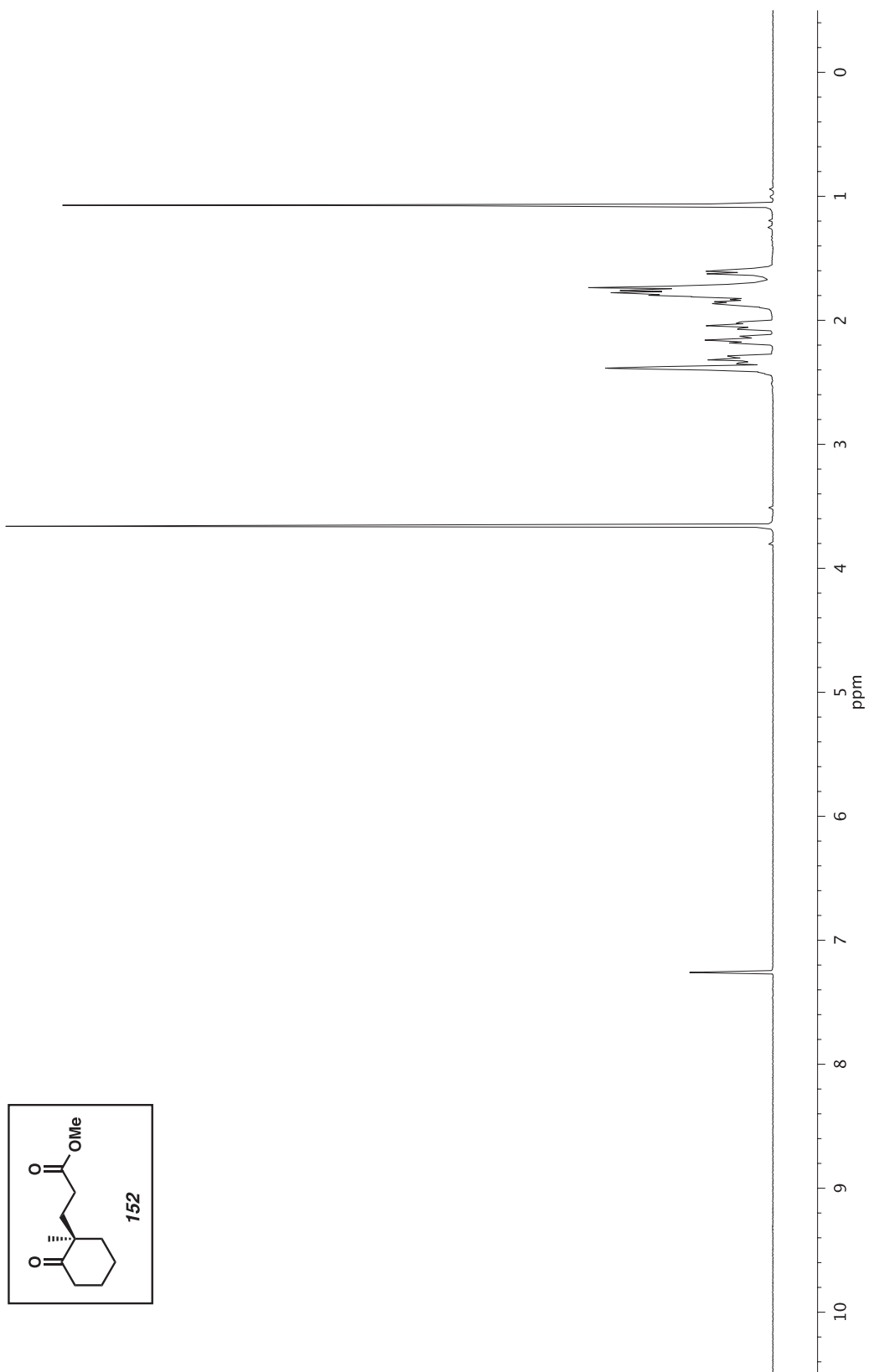


Figure A6.4 ^1H NMR (500 MHz, CDCl_3) of compound **152**.

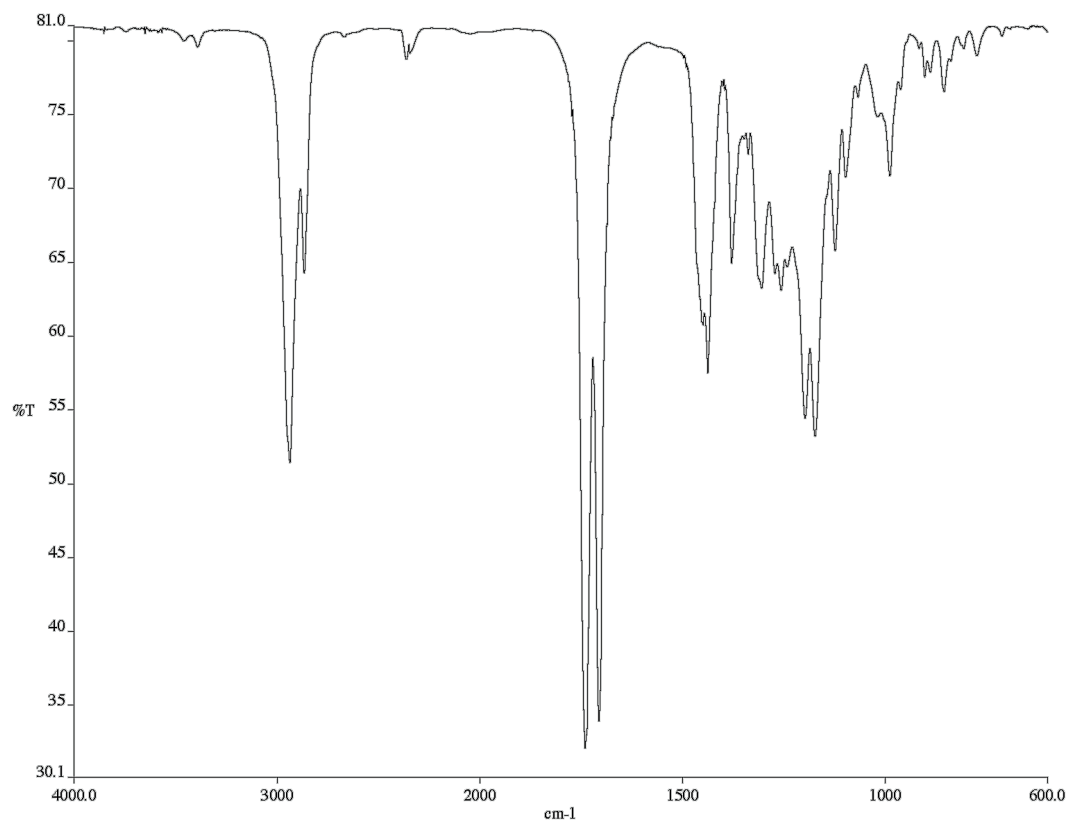


Figure A6.5 Infrared spectrum (Thin Film, NaCl) of compound **152**.

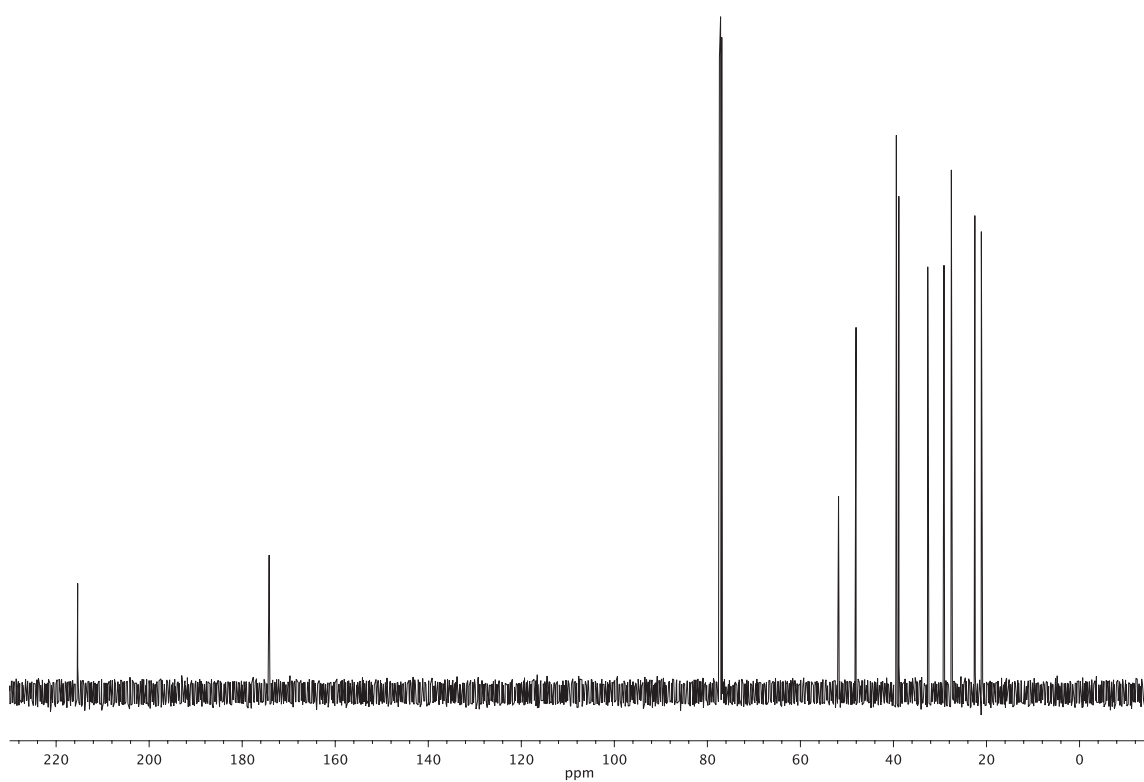


Figure A6.6 ¹³C NMR (126 MHz, CDCl₃) of compound **152**.

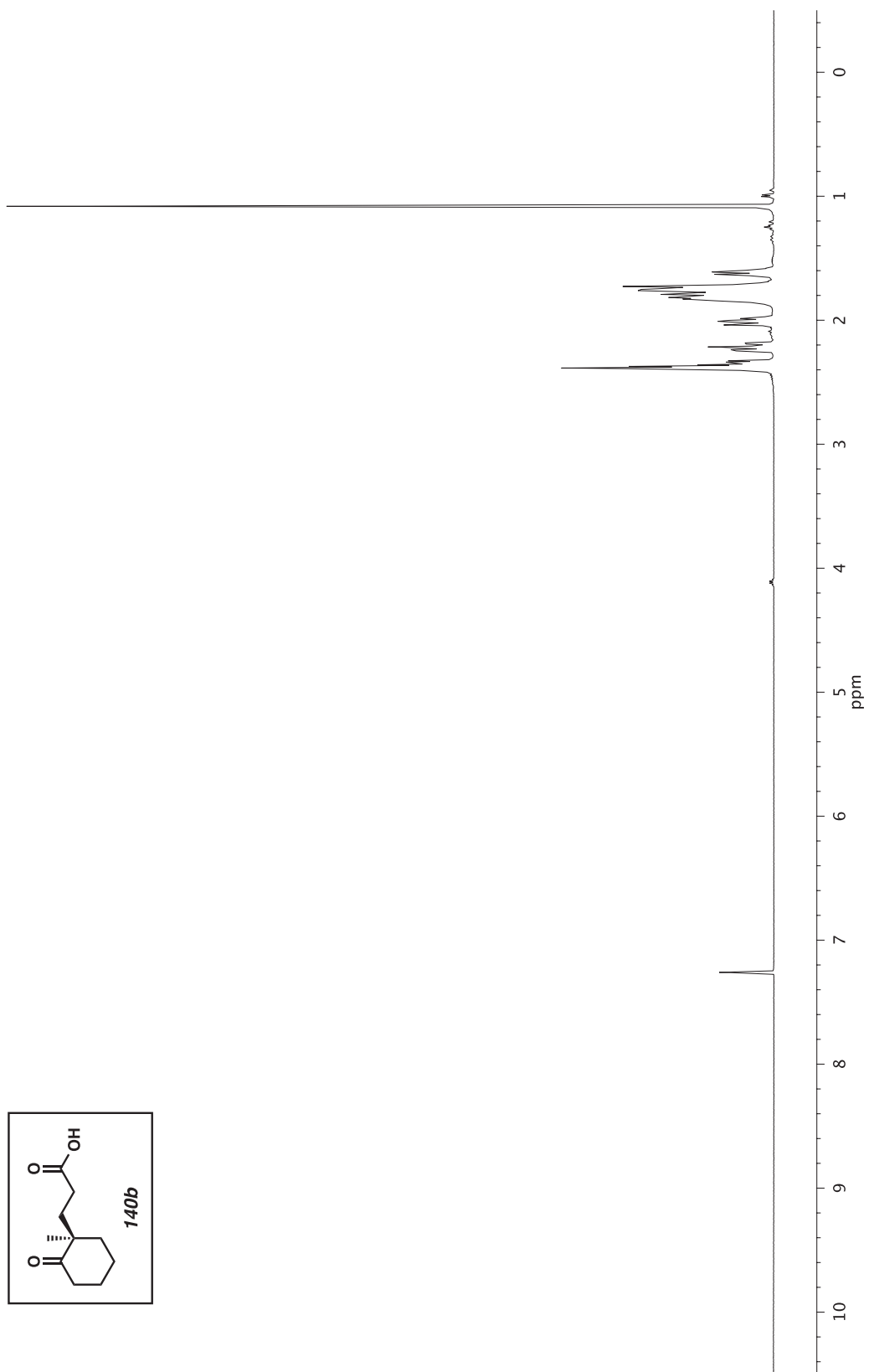


Figure A6.7 ^1H NMR (500 MHz, CDCl_3) of compound **140b**.

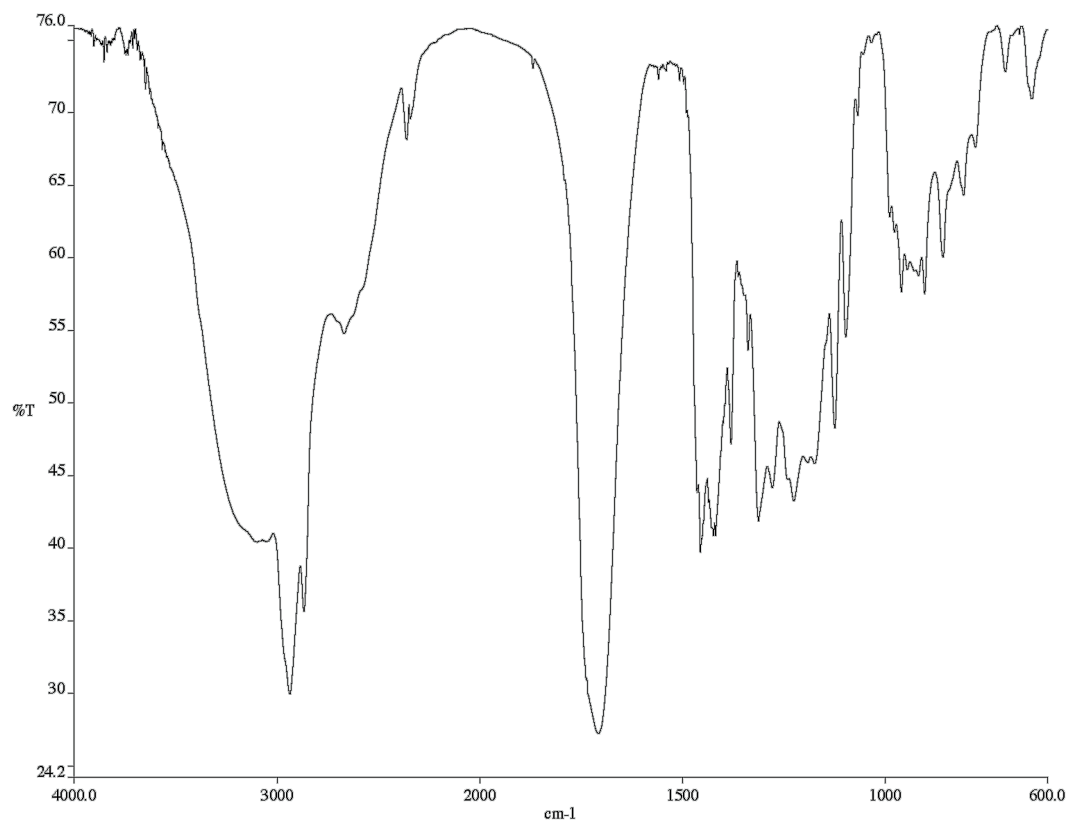


Figure A6.8 Infrared spectrum (Thin Film, NaCl) of compound **140b**.

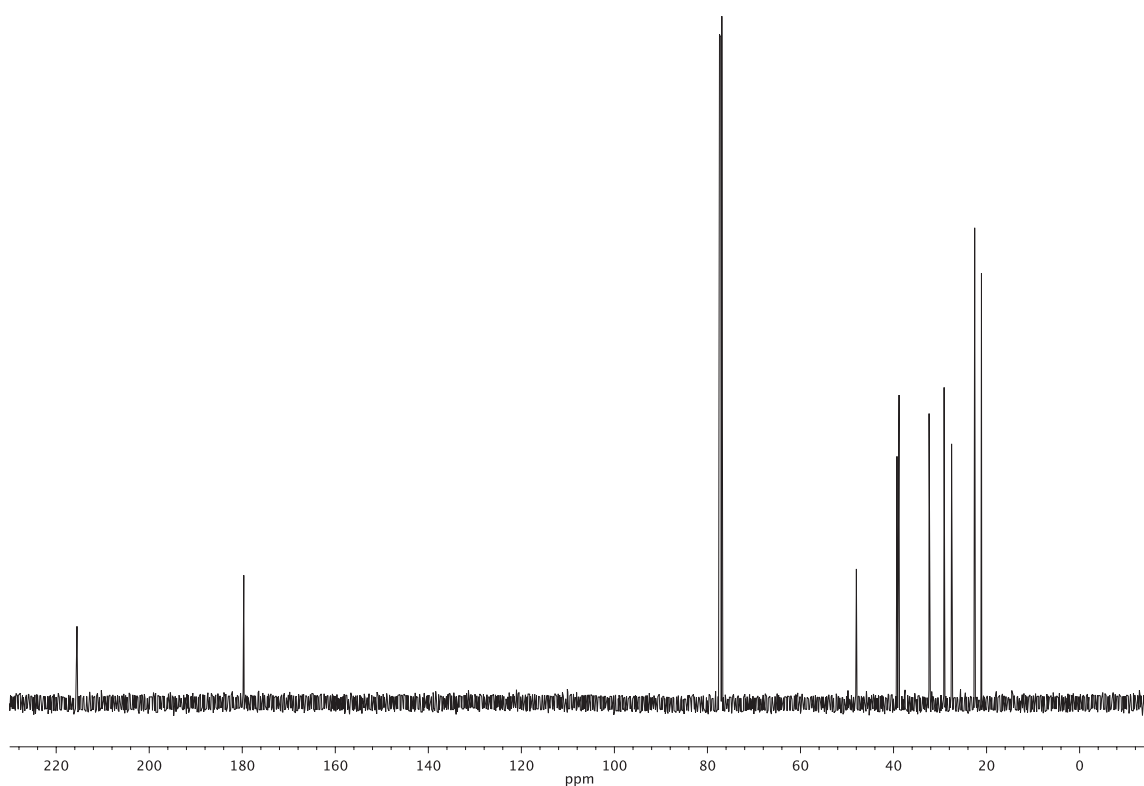


Figure A6.9 ¹³C NMR (126 MHz, CDCl₃) of compound **140b**.

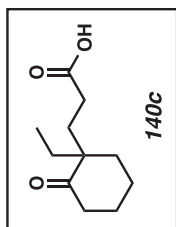
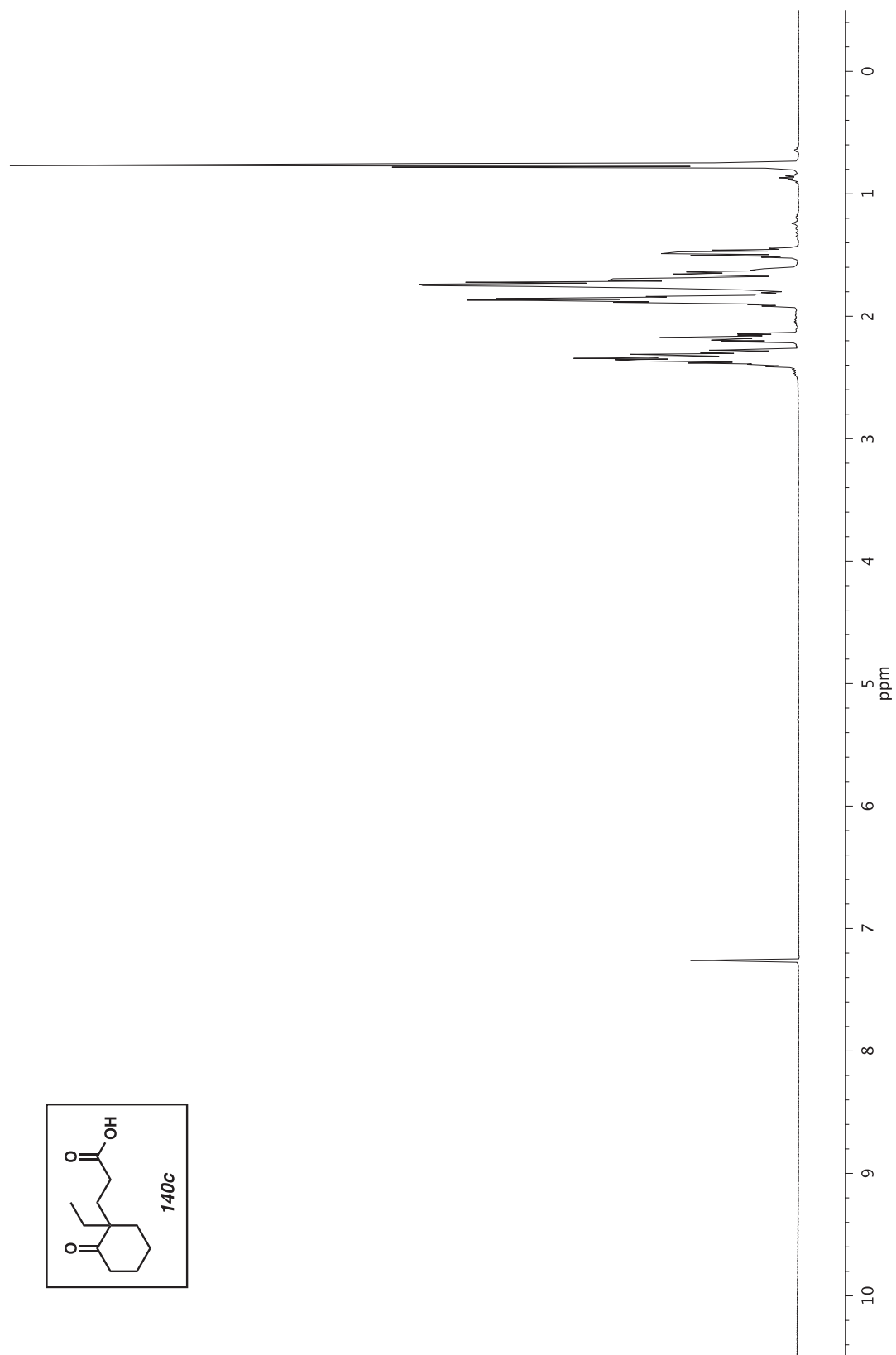


Figure A6.10 ^1H NMR (500 MHz, CDCl_3) of compound **140c**.

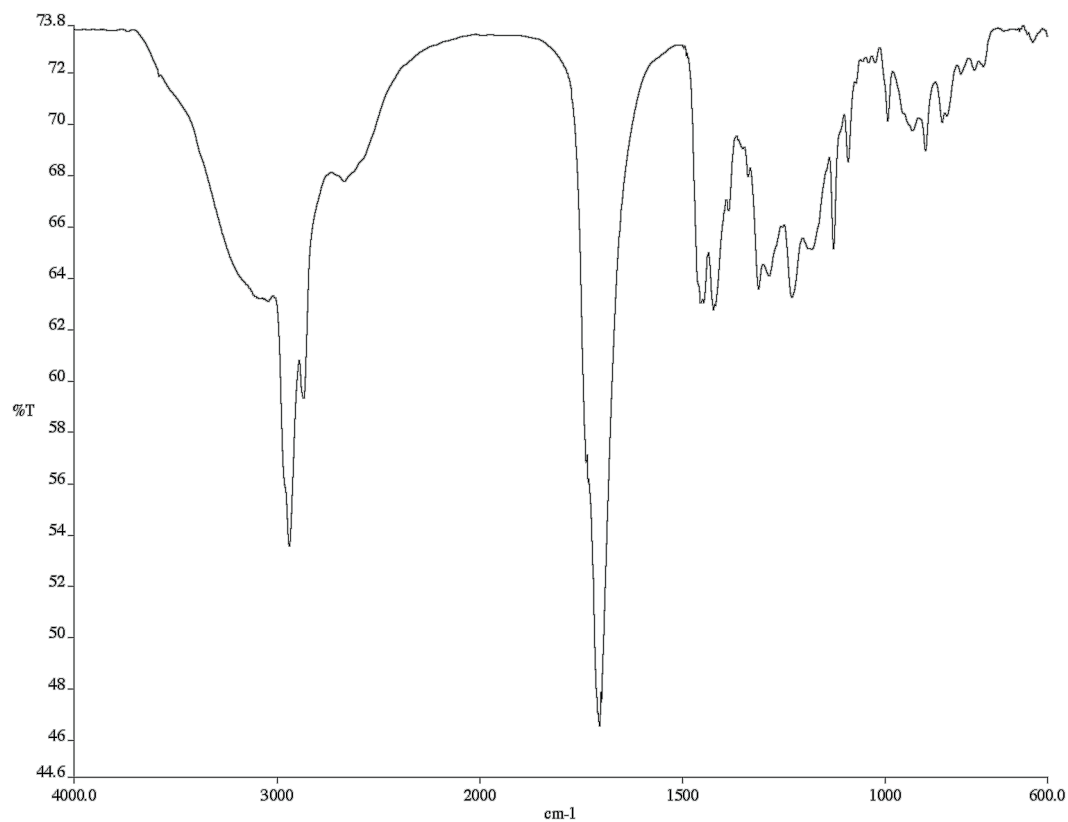


Figure A6.11 Infrared spectrum (Thin Film, NaCl) of compound **140c**.

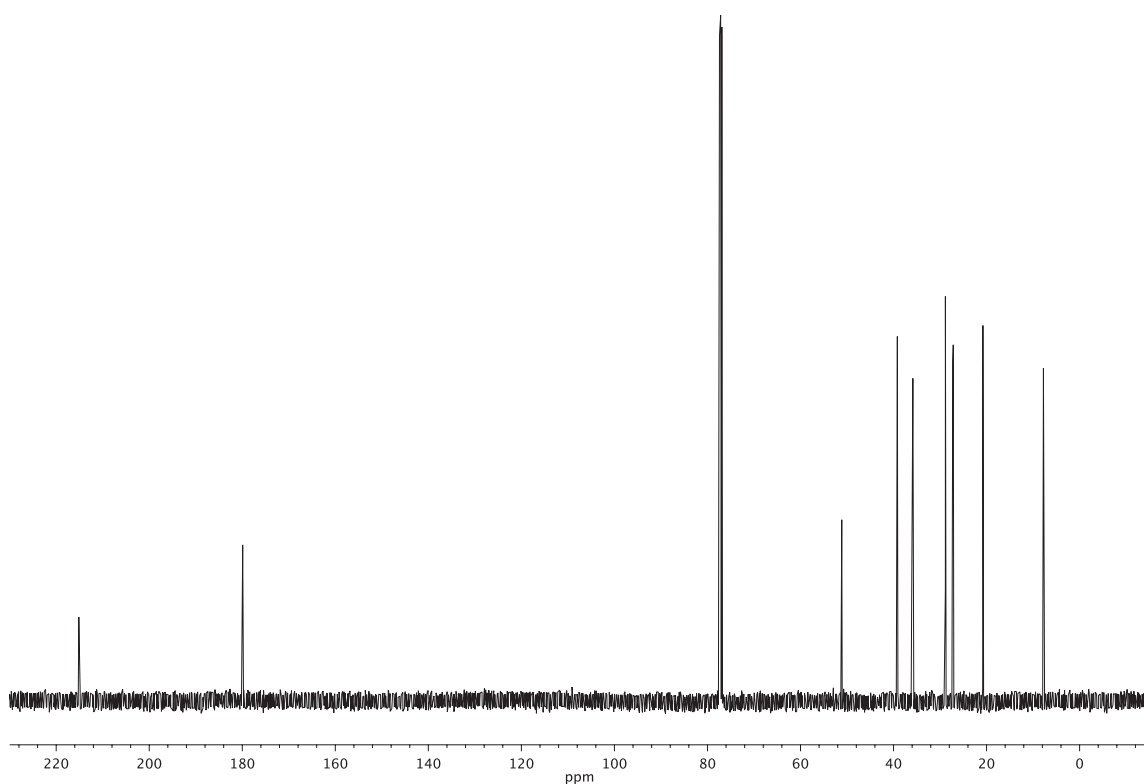


Figure A6.12 ¹³C NMR (126 MHz, CDCl₃) of compound **140c**.

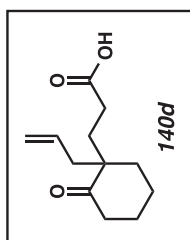
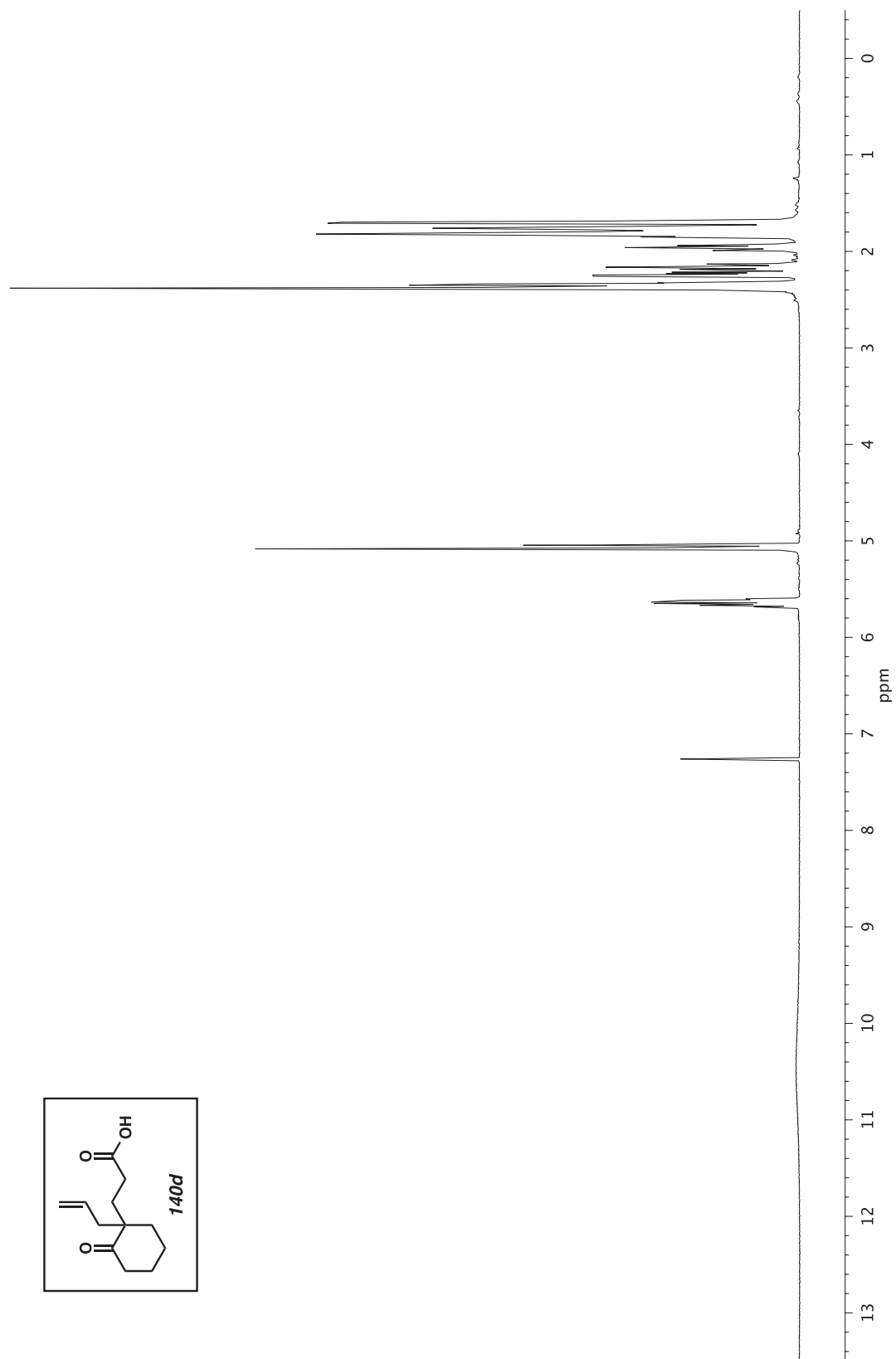


Figure A6.13 ^1H NMR (500 MHz, CDCl_3) of compound **140d**.

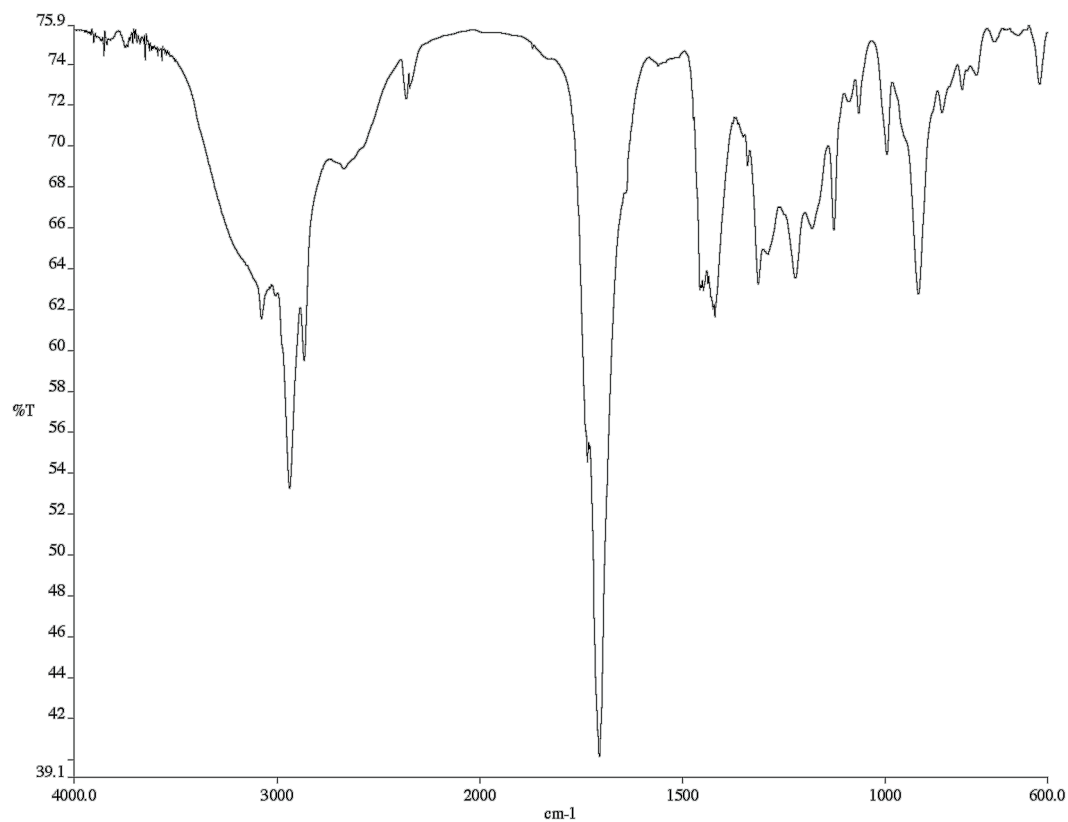


Figure A6.14 Infrared spectrum (Thin Film, NaCl) of compound **140d**.

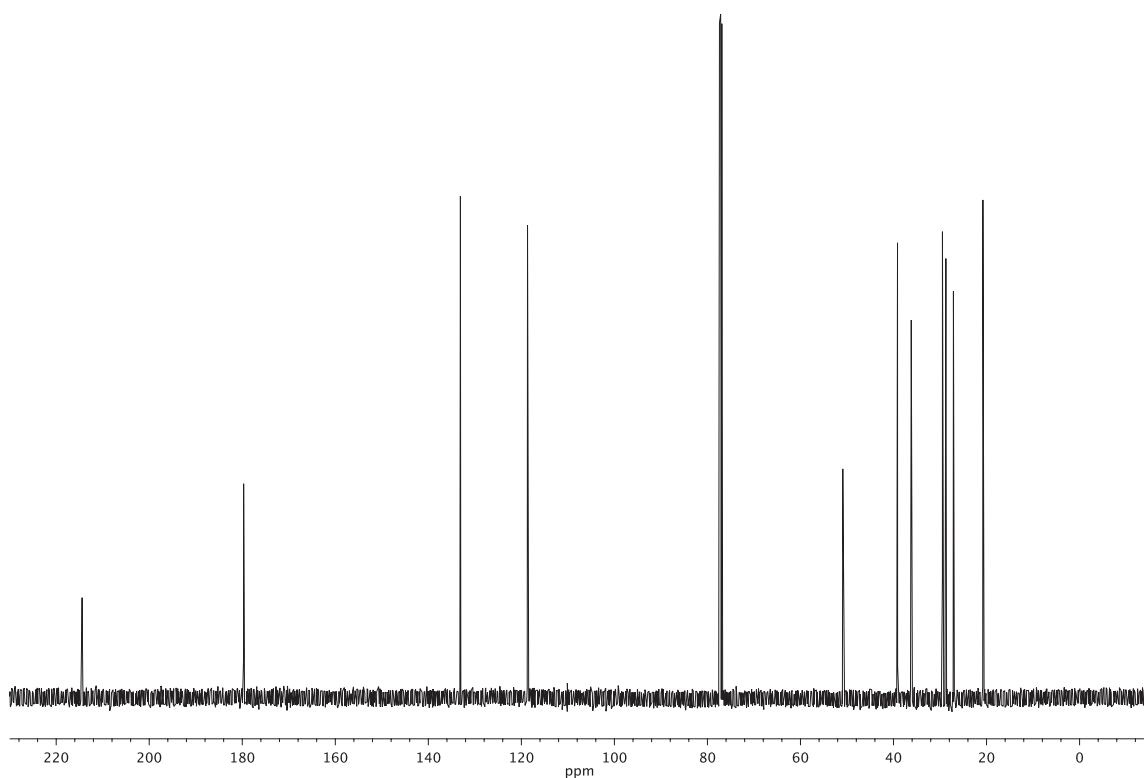


Figure A6.15 ¹³C NMR (126 MHz, CDCl₃) of compound **140d**.

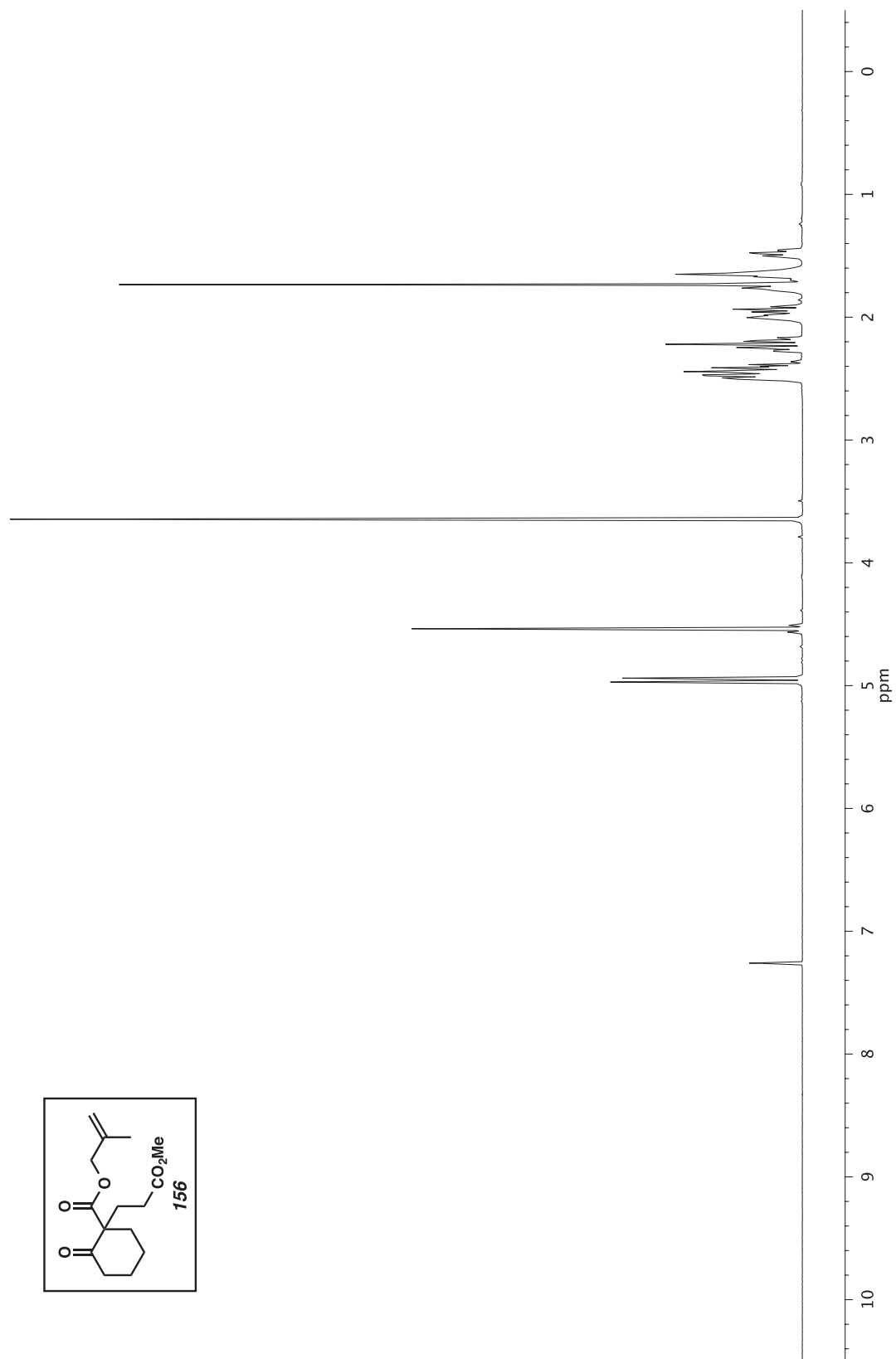


Figure A6.16 ^1H NMR (500 MHz, CDCl_3) of compound **156**.

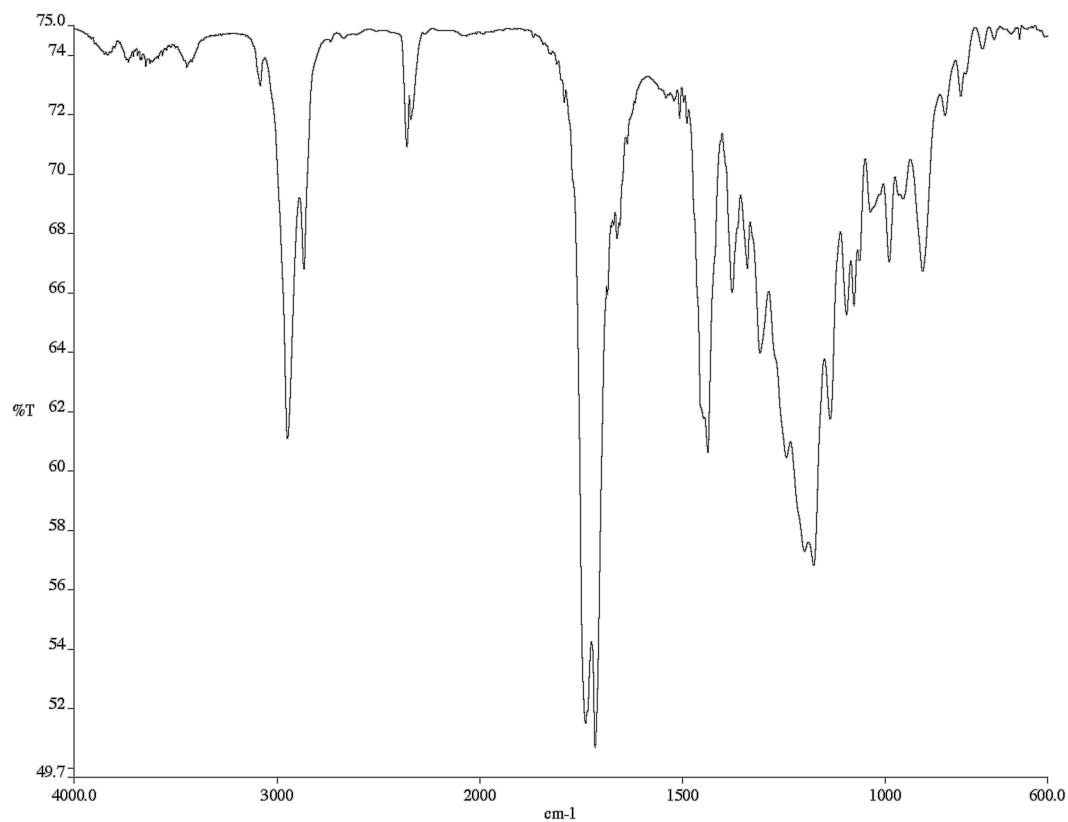


Figure A6.17 Infrared spectrum (Thin Film, NaCl) of compound **156**.

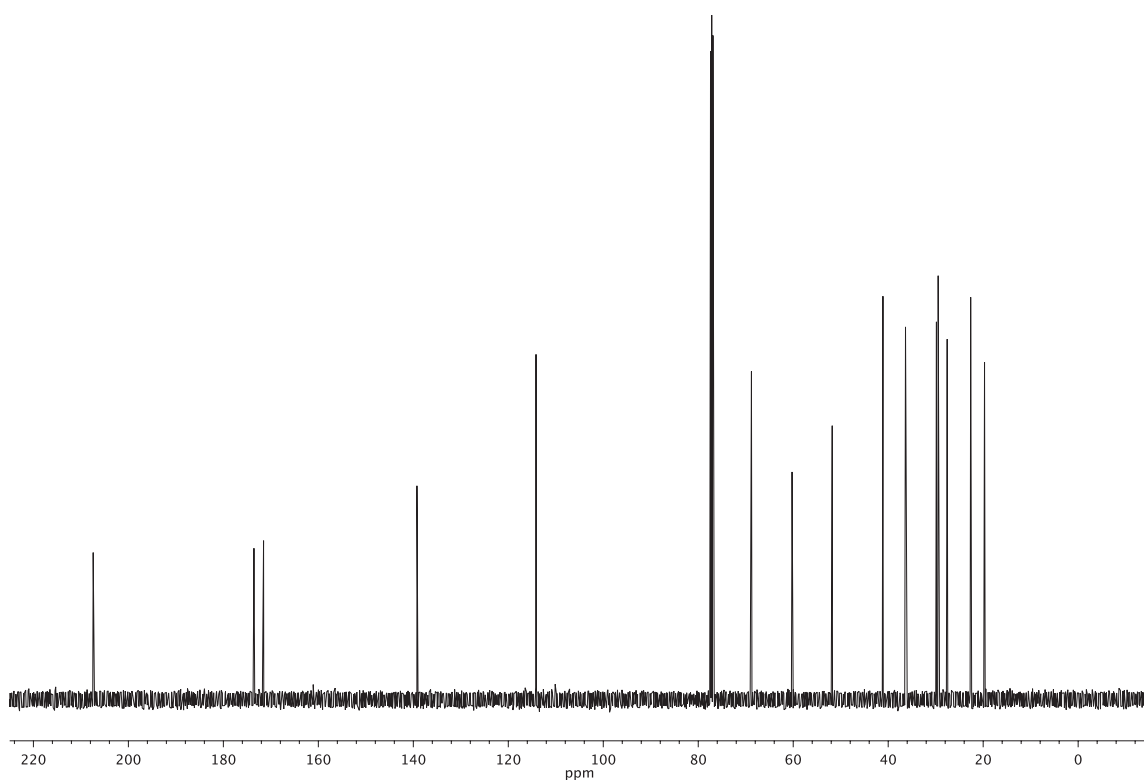


Figure A6.18 ¹³C NMR (126 MHz, CDCl₃) of compound **156**.

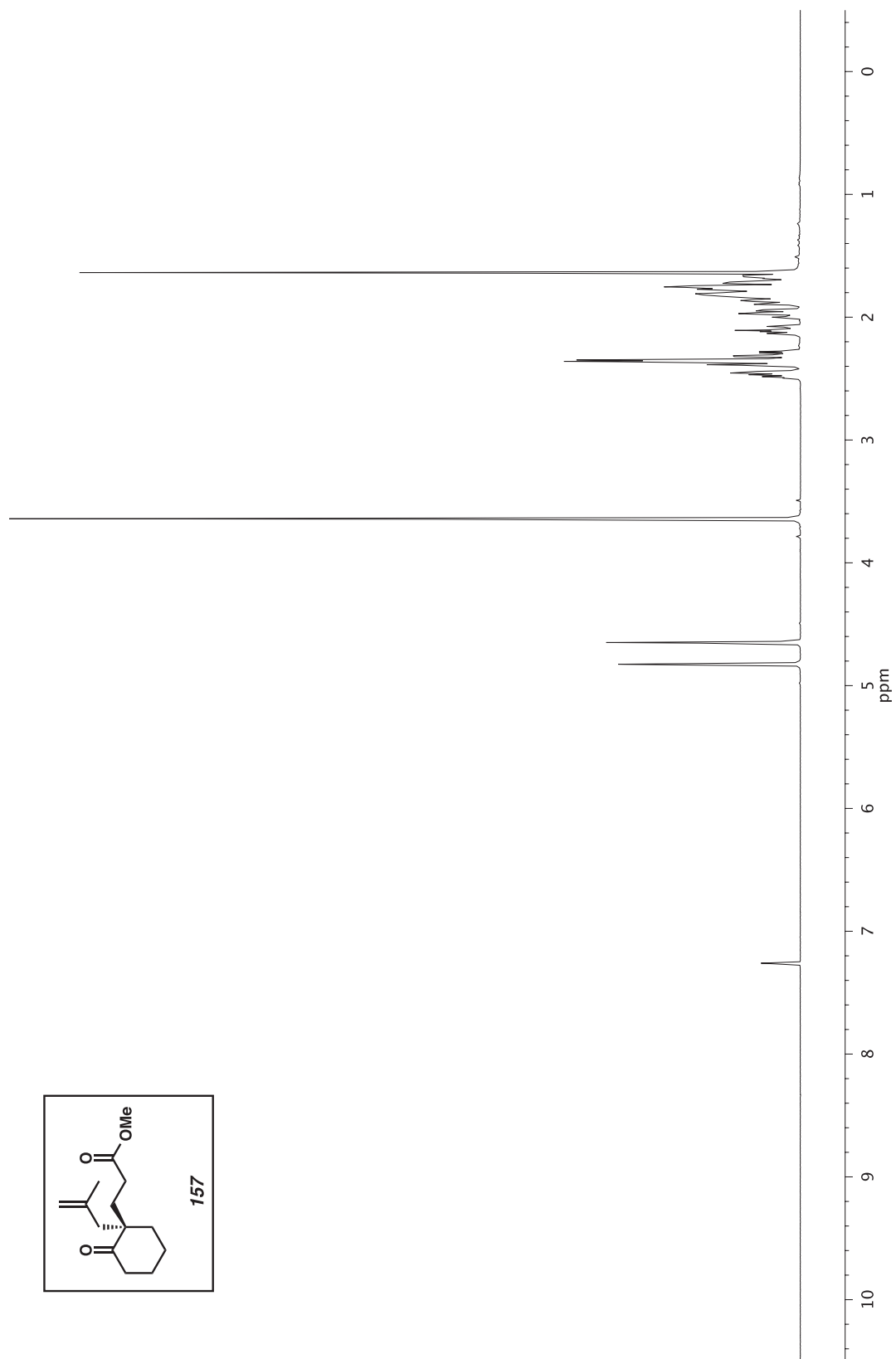


Figure A6.19 ^1H NMR (500 MHz, CDCl_3) of compound **157**.

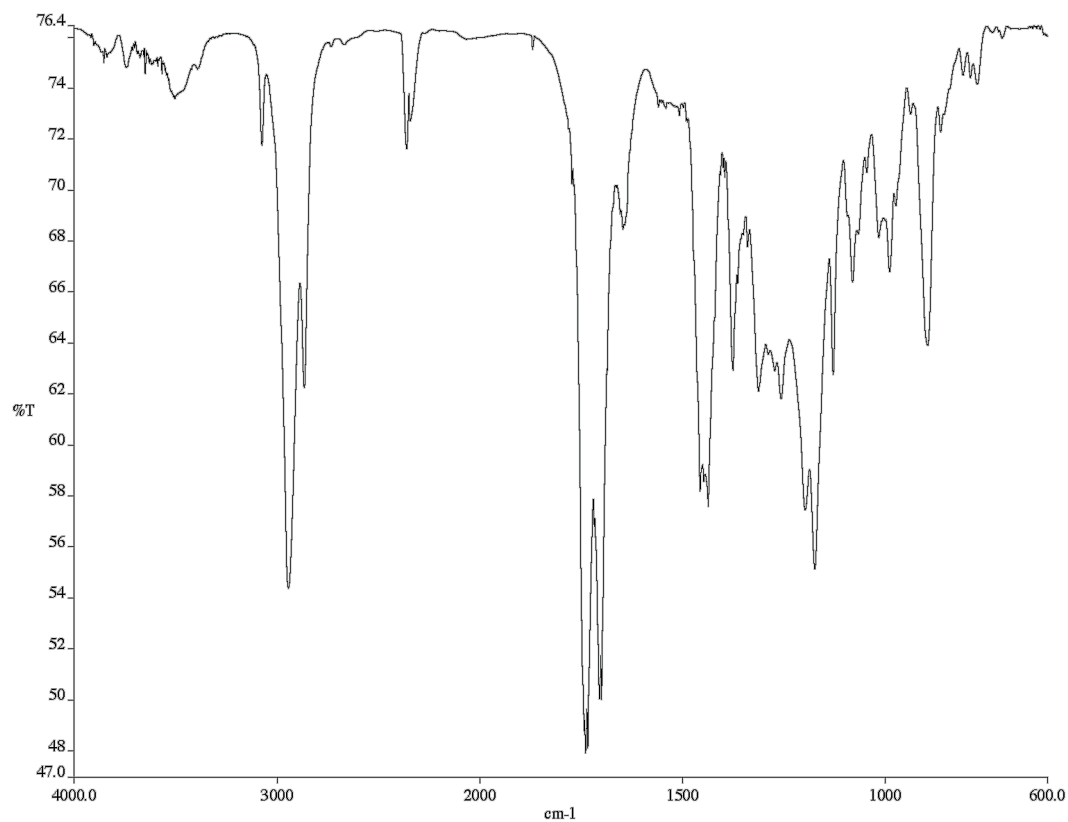


Figure A6.20 Infrared spectrum (Thin Film, NaCl) of compound **157**.

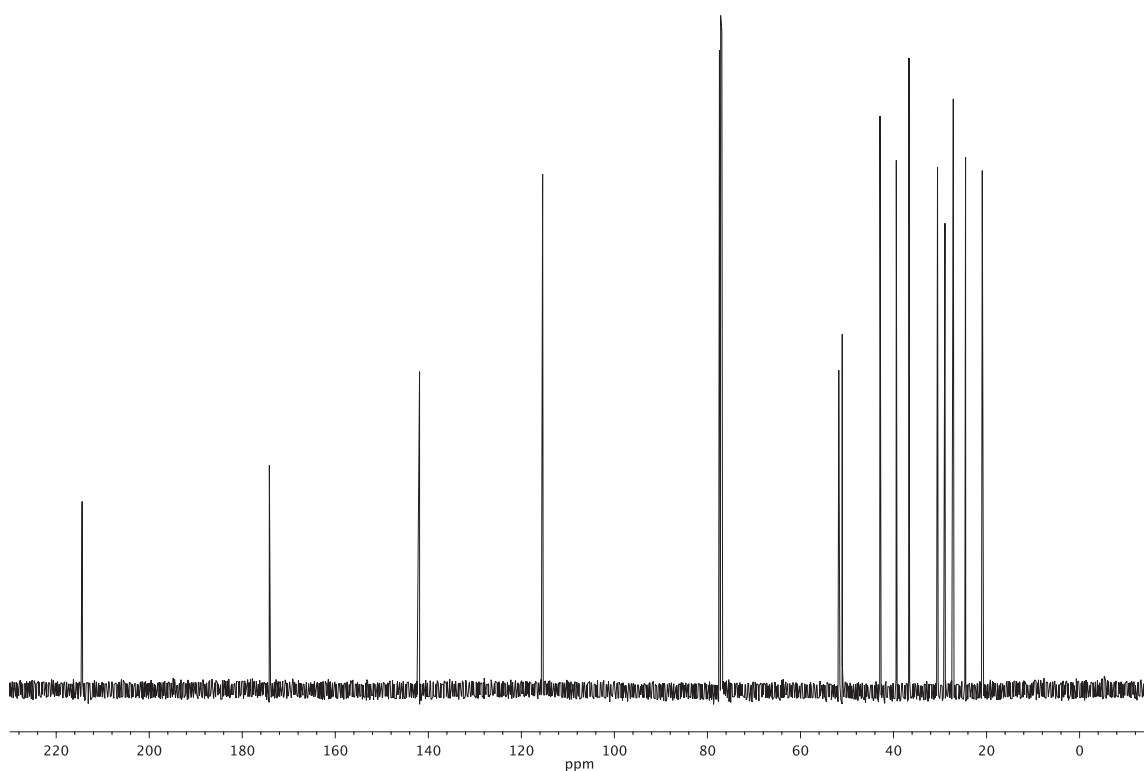


Figure A6.21 ¹³C NMR (126 MHz, CDCl₃) of compound **157**.

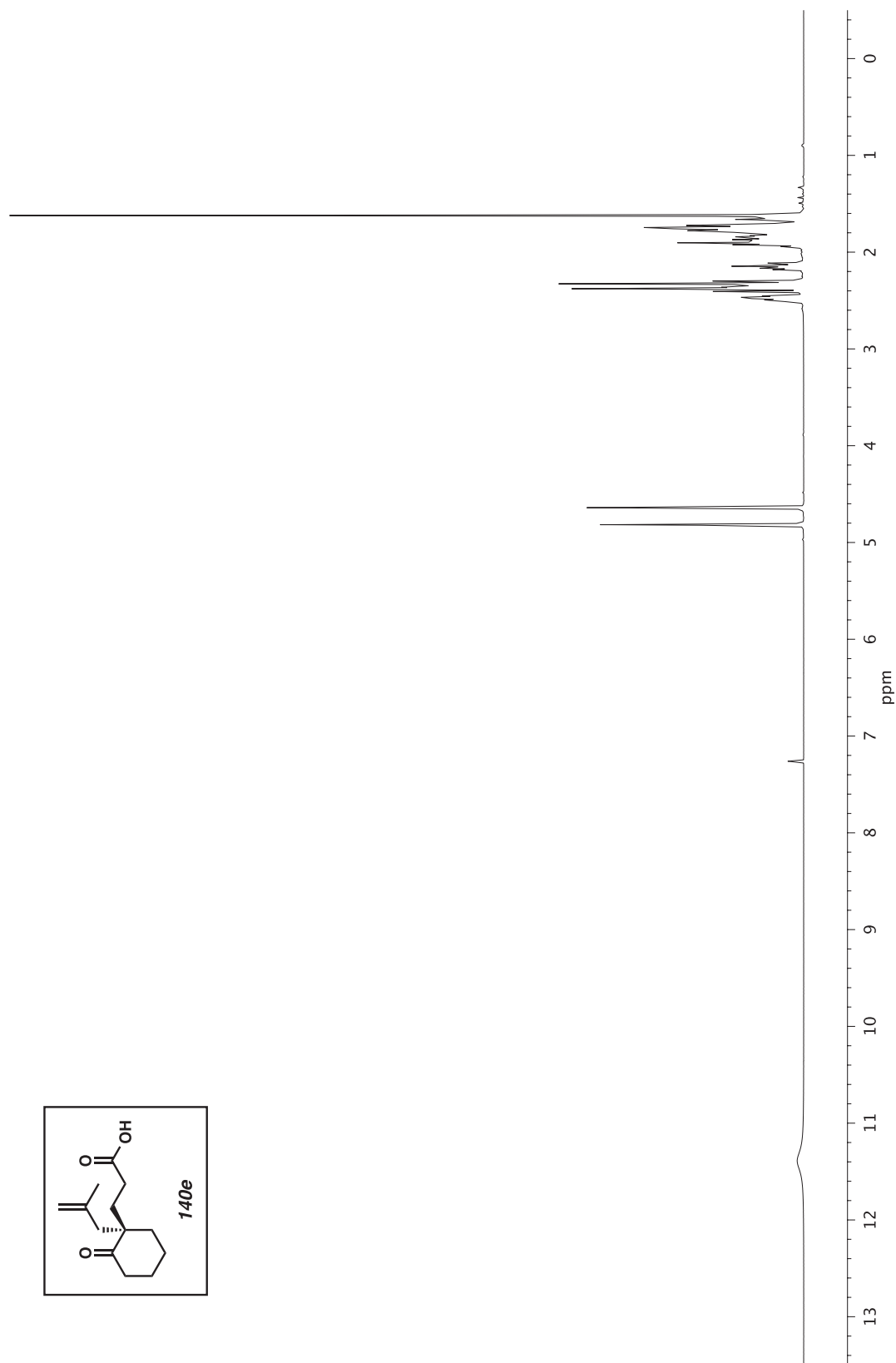


Figure A6.22 ^1H NMR (500 MHz, CDCl_3) of compound **140e**.

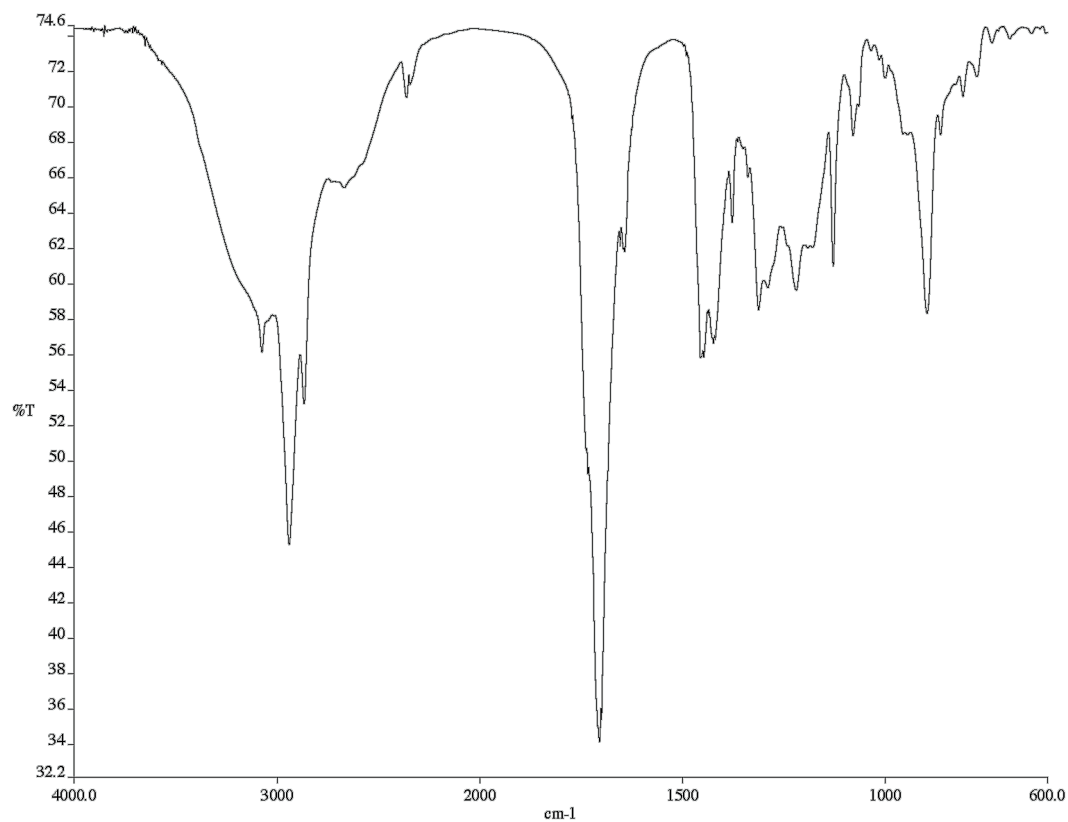


Figure A6.23 Infrared spectrum (Thin Film, NaCl) of compound **140e**.

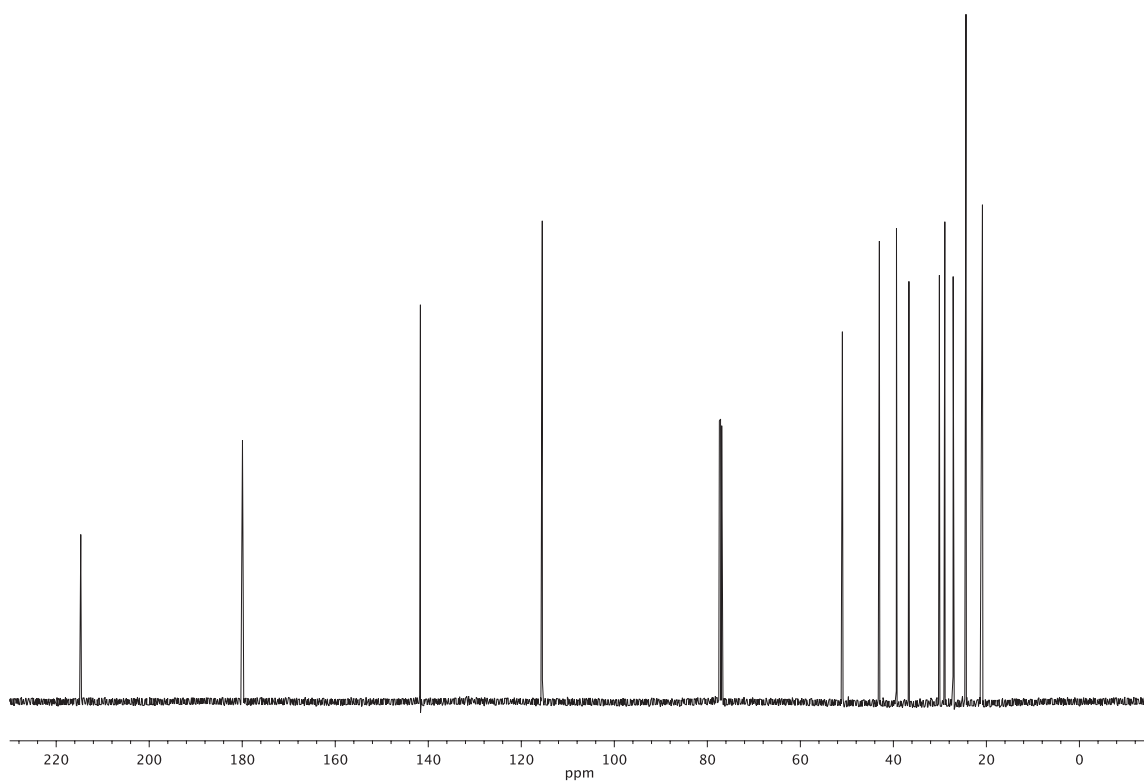


Figure A6.24 ¹³C NMR (126 MHz, CDCl₃) of compound **140e**.

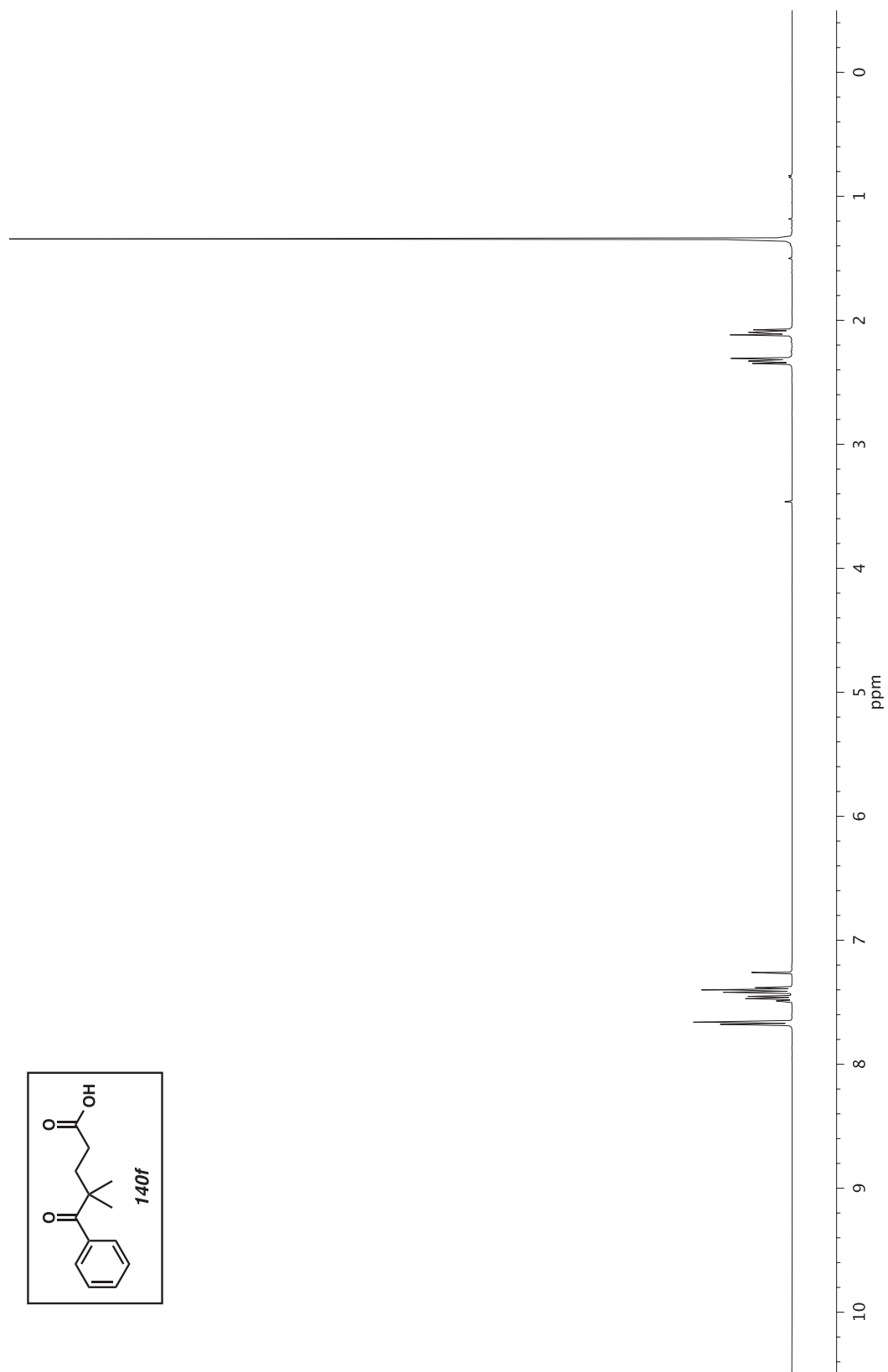


Figure A6.25 ^1H NMR (400 MHz, CDCl_3) of compound **140f**.

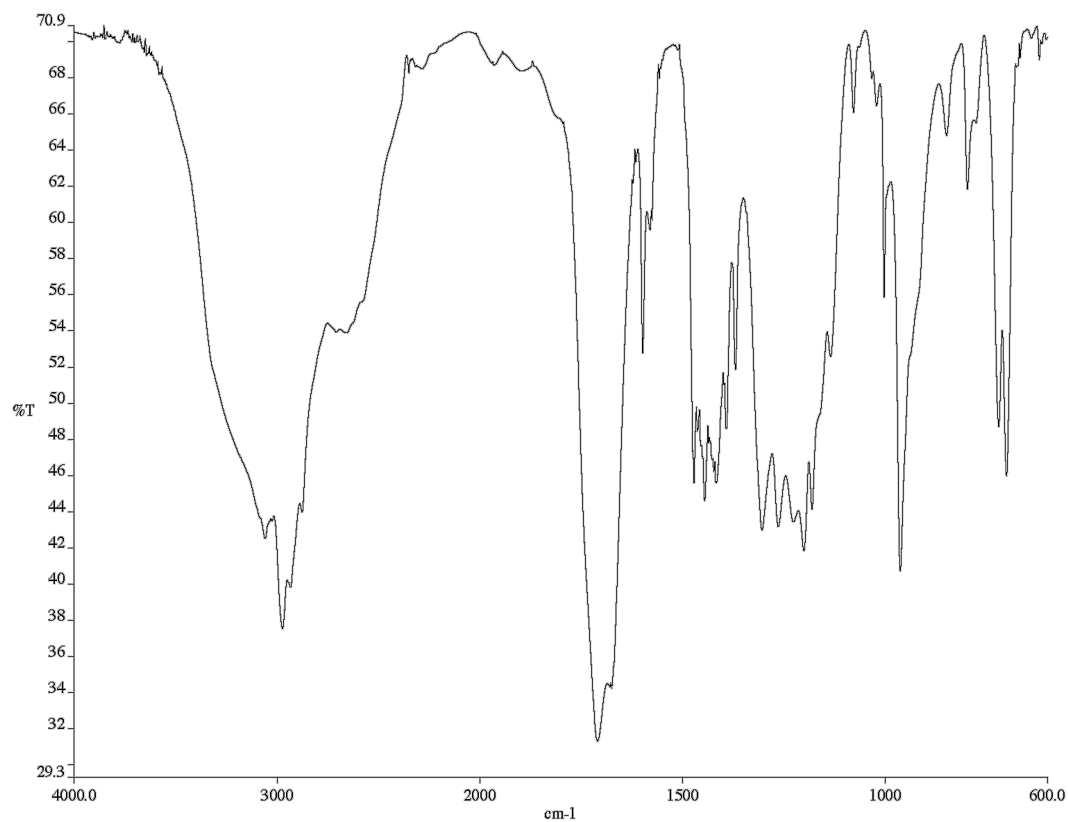


Figure A6.26 Infrared spectrum (Thin Film, NaCl) of compound **140f**.

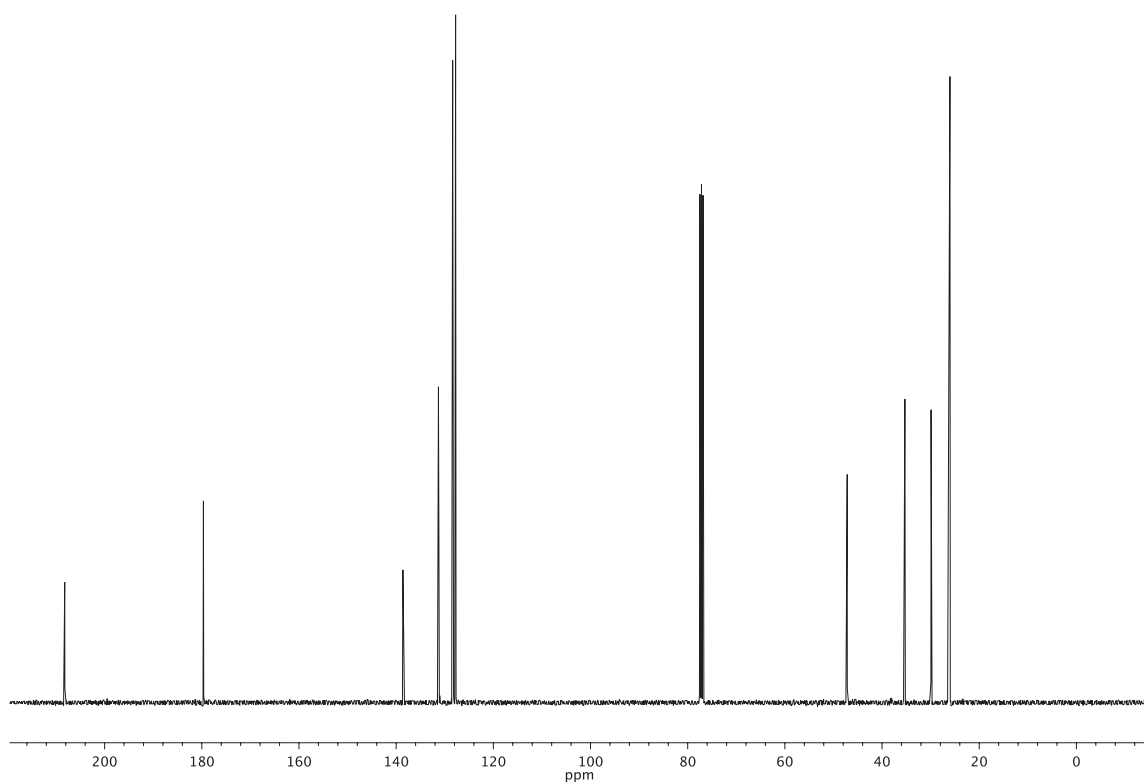


Figure A6.27 ¹³C NMR (101 MHz, CDCl₃) of compound **140f**.

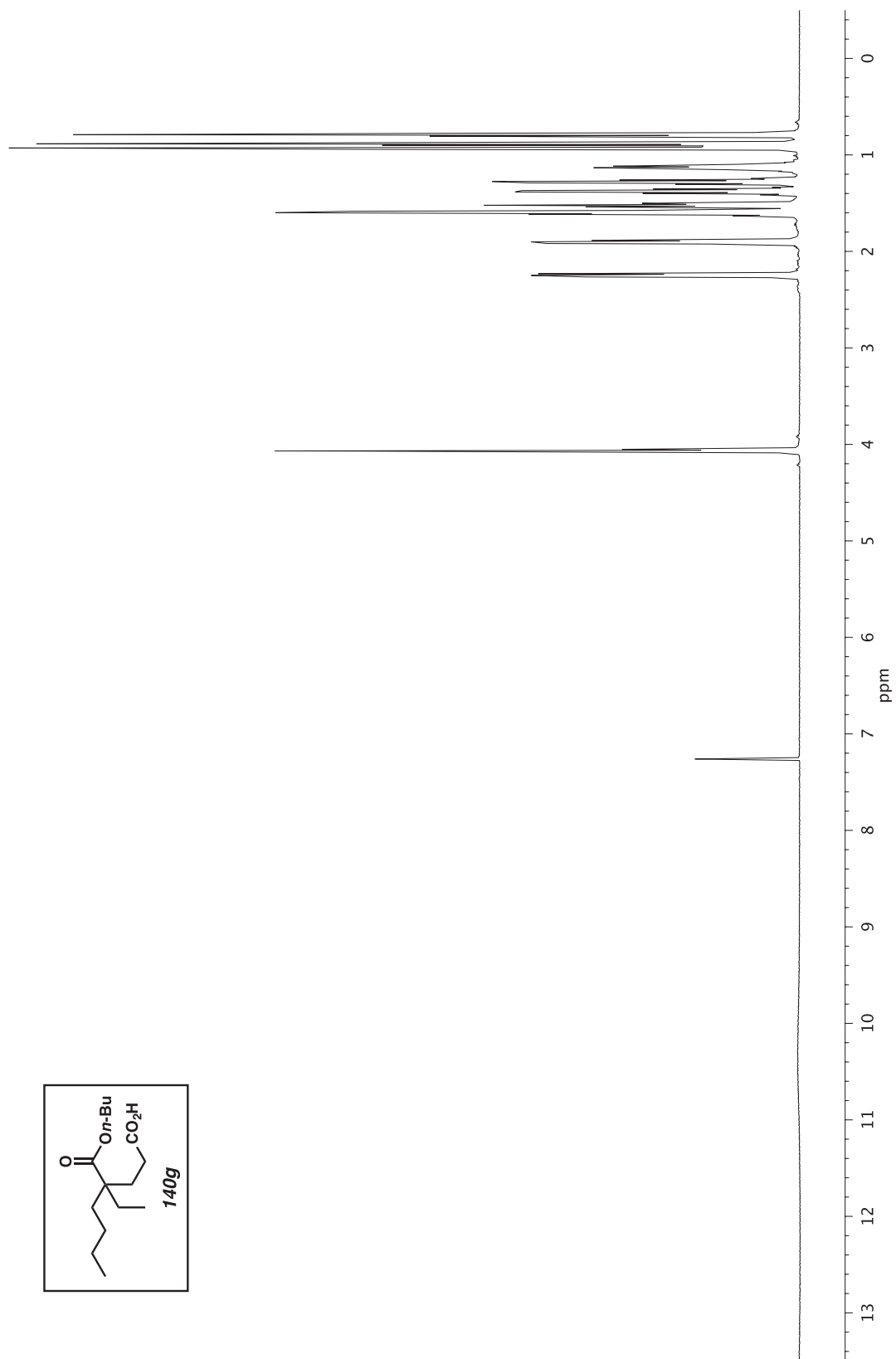


Figure A6.28 ¹H NMR (500 MHz, CDCl₃) of compound 140g.

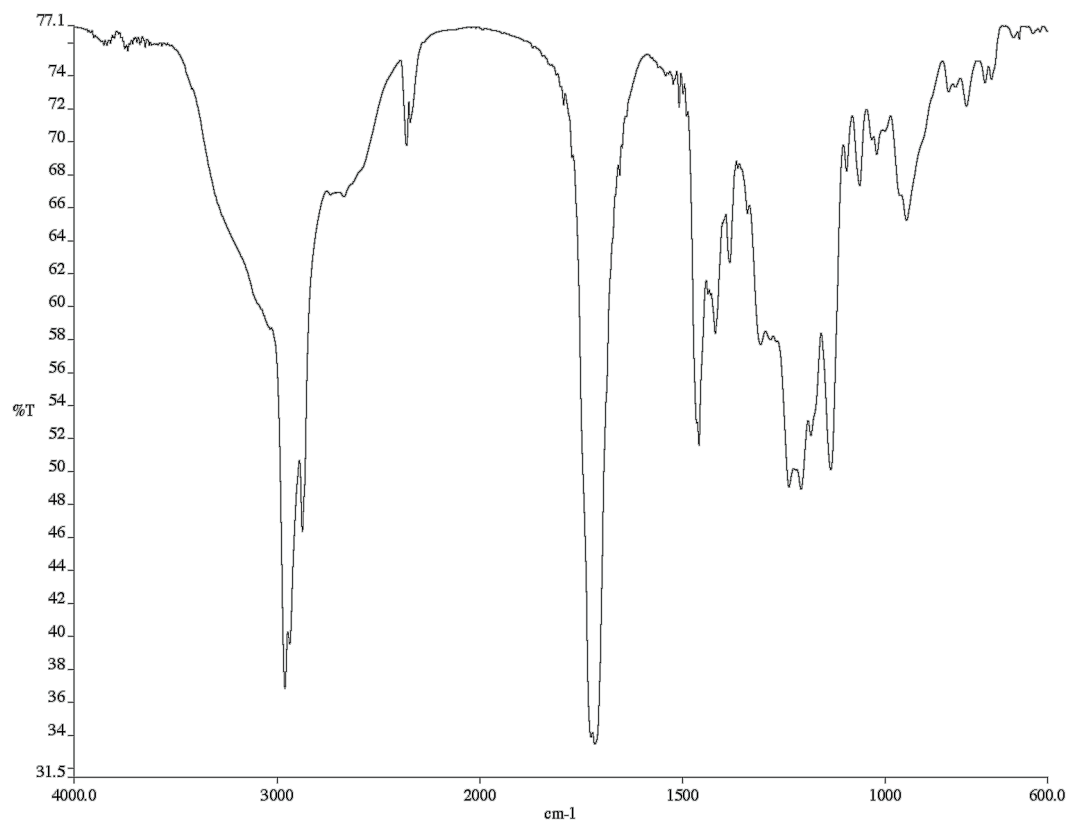


Figure A6.29 Infrared spectrum (Thin Film, NaCl) of compound **140g**.

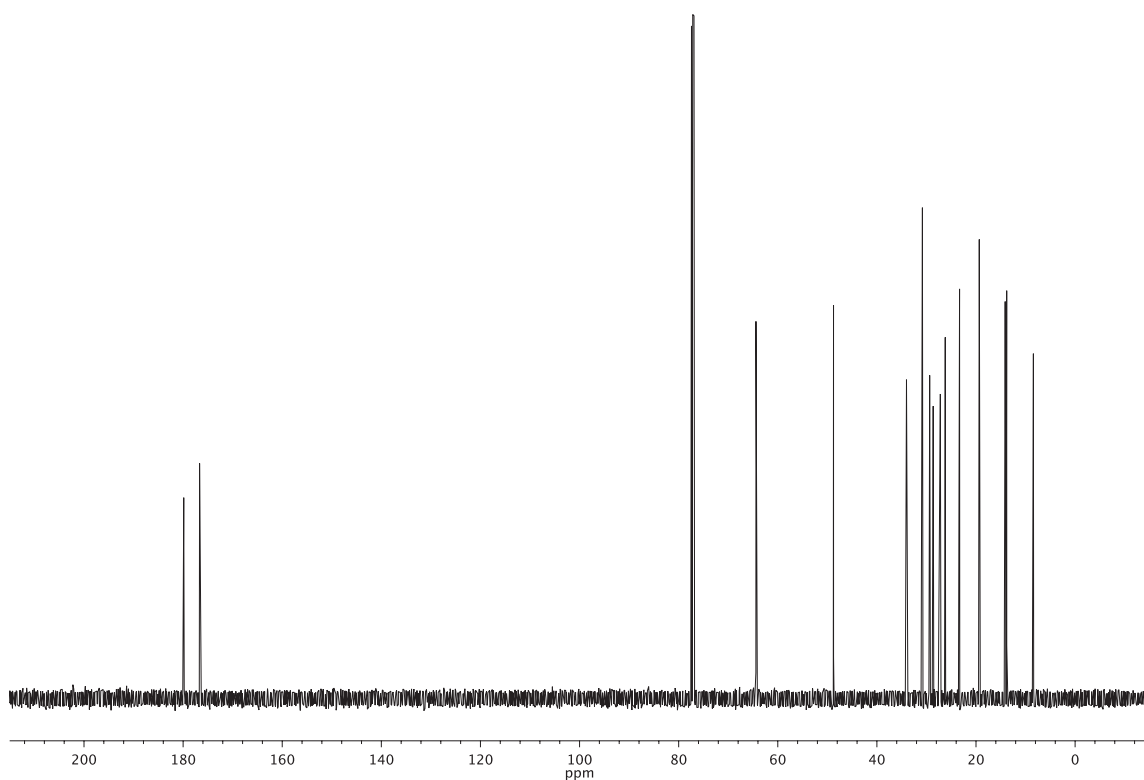


Figure A6.30 ¹³C NMR (126 MHz, CDCl₃) of compound **140g**.

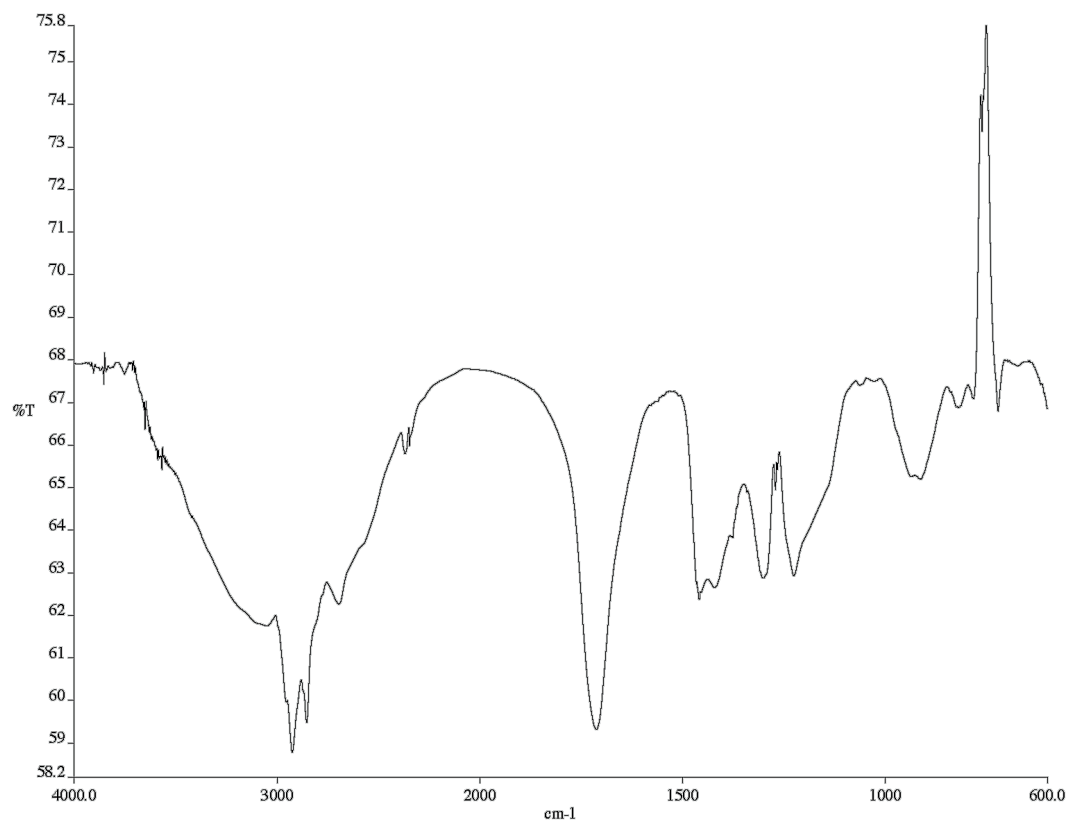


Figure A6.32 Infrared spectrum (Thin Film, NaCl) of compound **140h**.

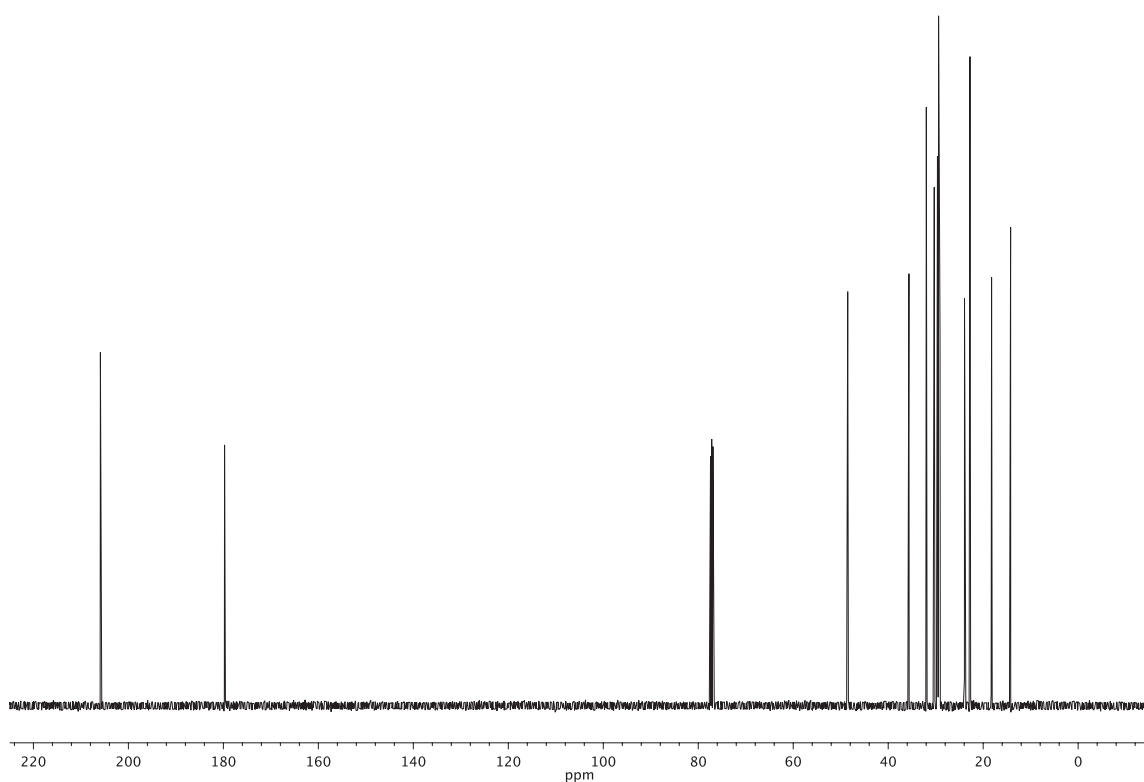


Figure A6.33 ¹³C NMR (126 MHz, CDCl₃) of compound **140h**.

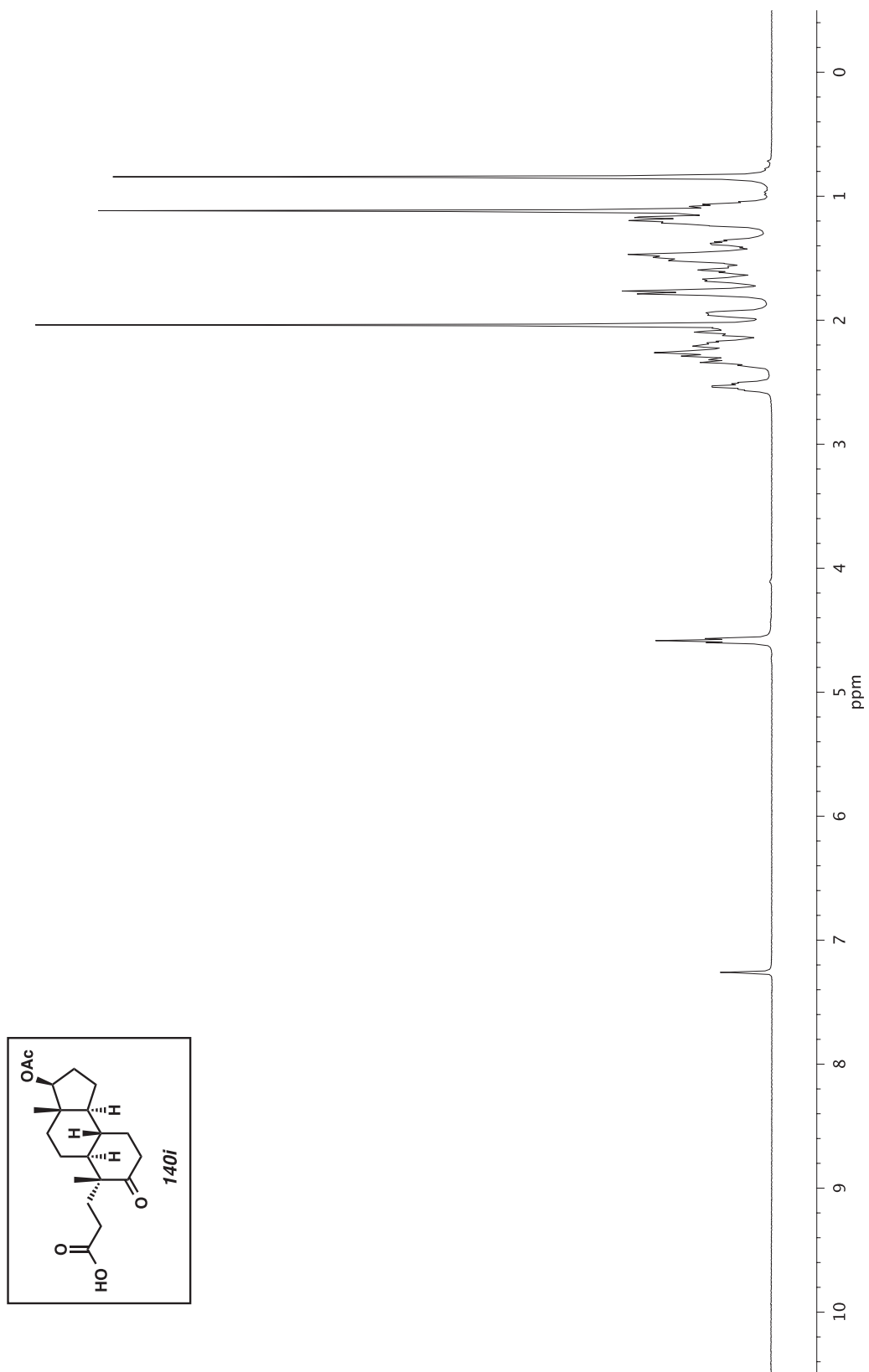


Figure A6.34 ^1H NMR (500 MHz, CDCl_3) of compound **140i**.

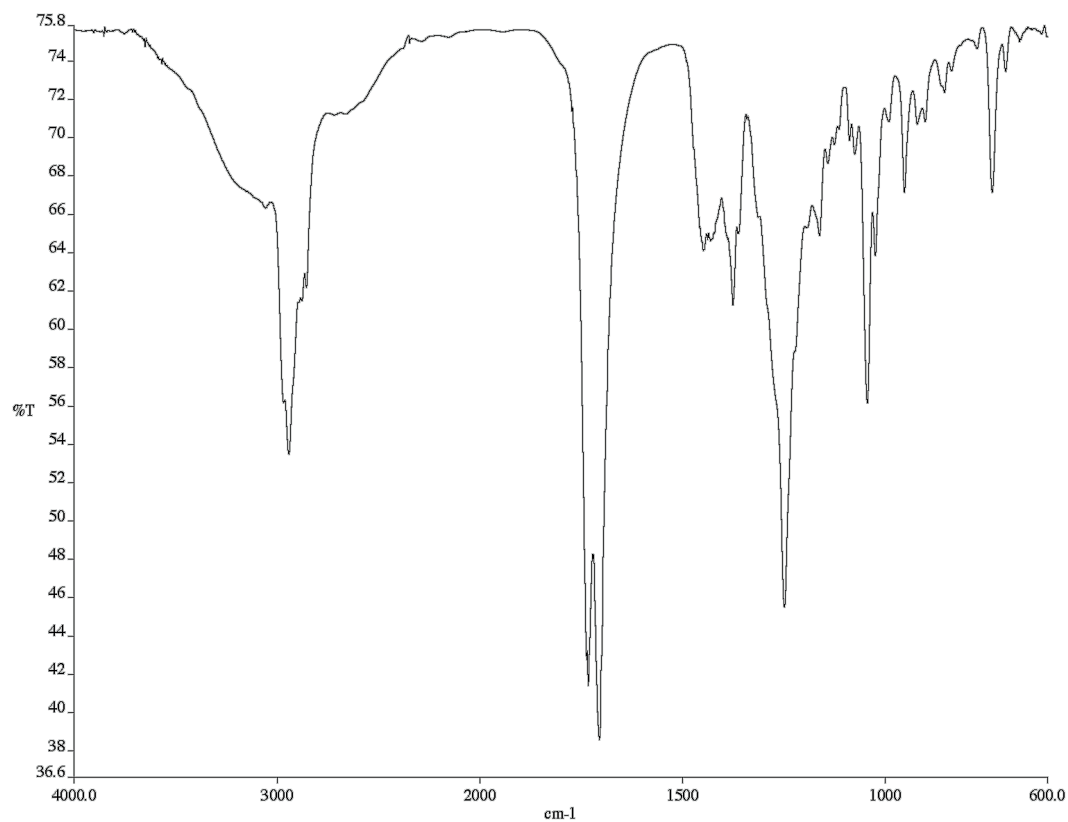


Figure A6.35 Infrared spectrum (Thin Film, NaCl) of compound **140i**.

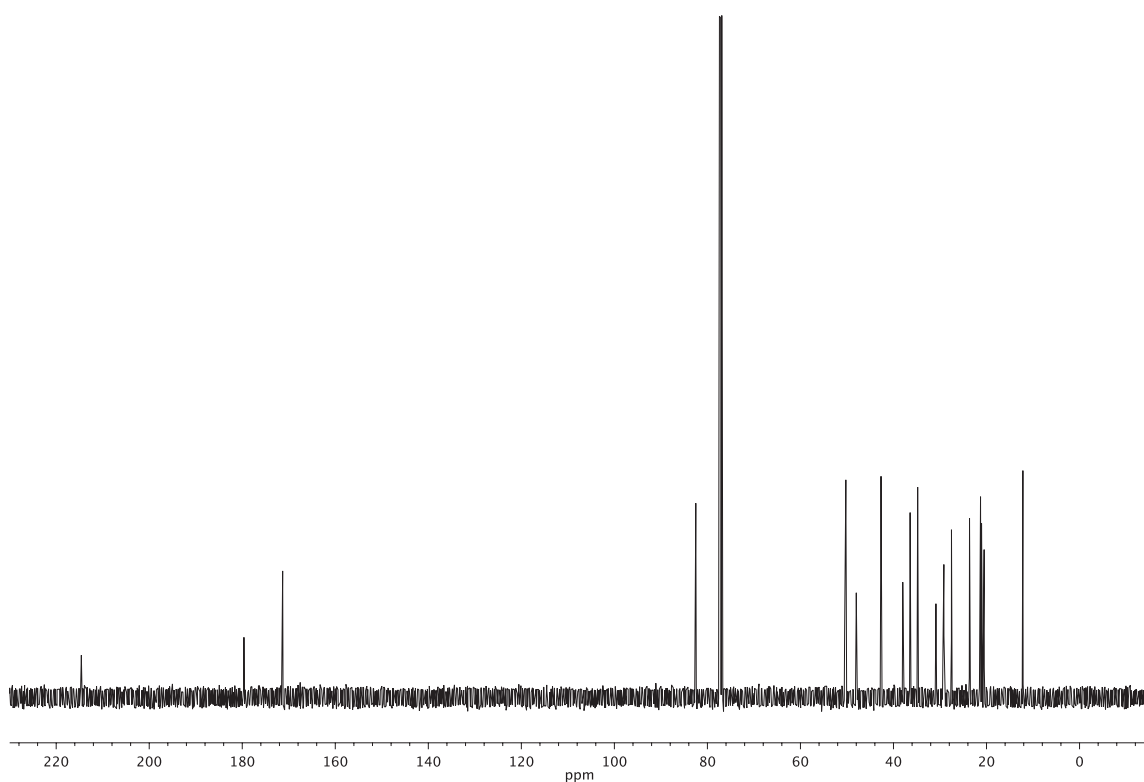


Figure A6.36 ¹³C NMR (126 MHz, CDCl₃) of compound **140i**.

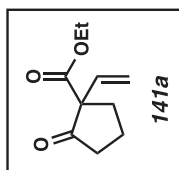
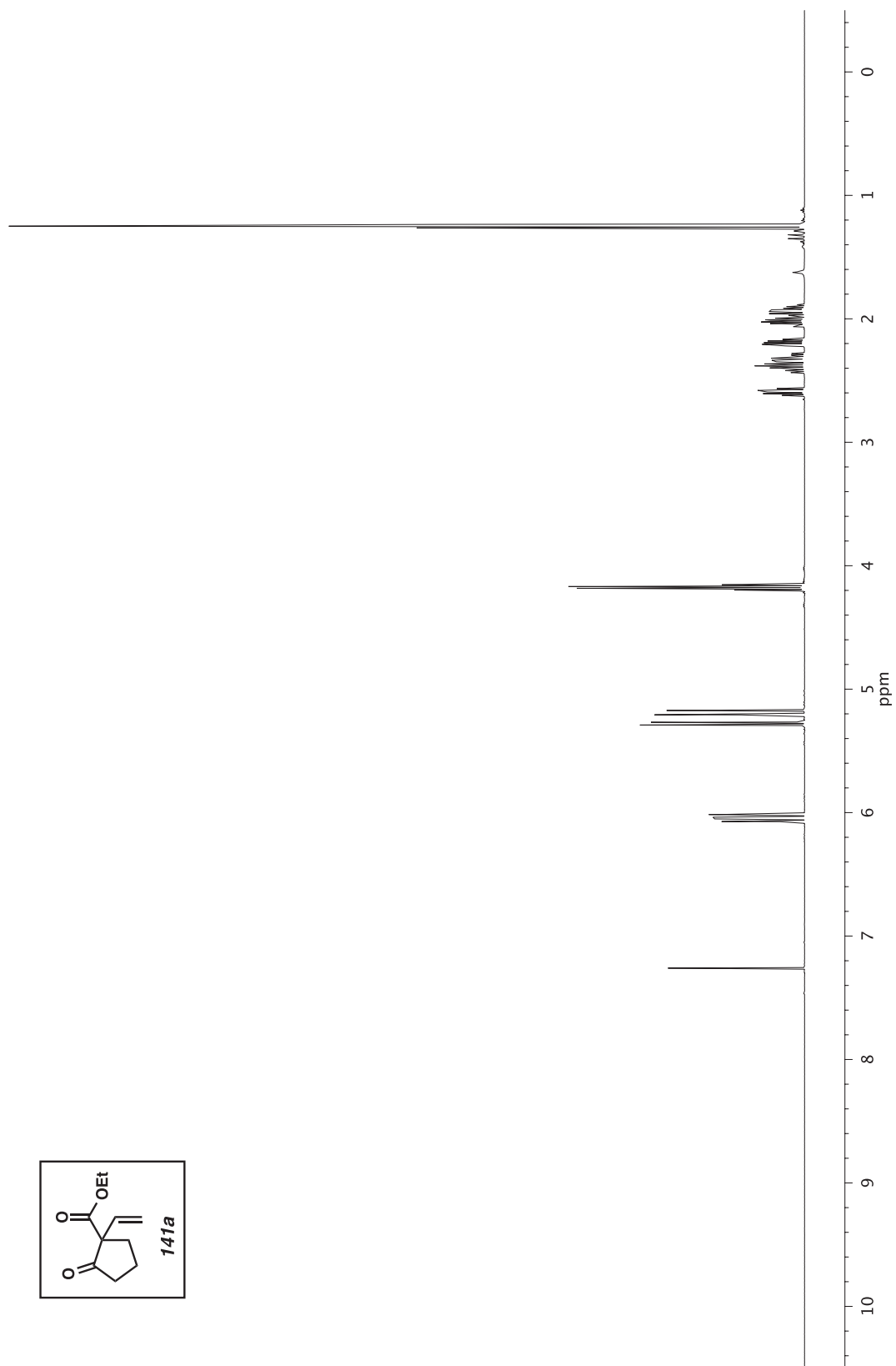


Figure A6.37 ^1H NMR (500 MHz, CDCl_3) of compound **141a**.

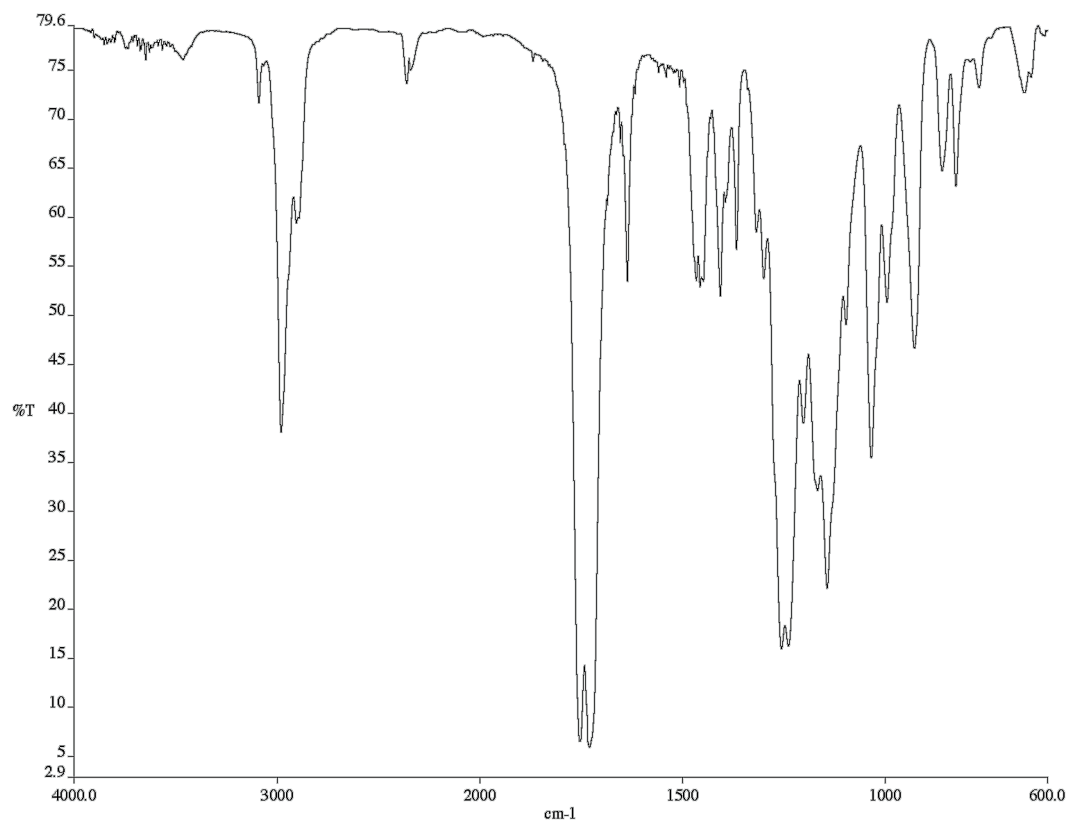


Figure A6.38 Infrared spectrum (Thin Film, NaCl) of compound **141a**.

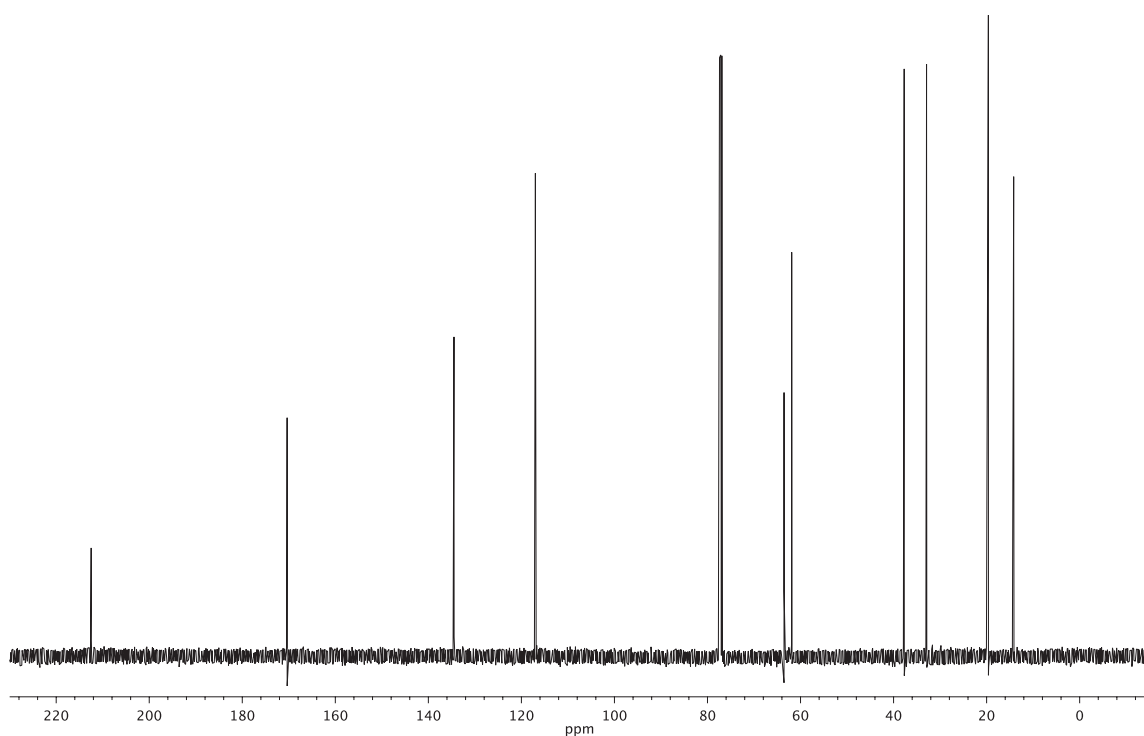


Figure A6.39 ¹³C NMR (126 MHz, CDCl₃) of compound **141a**.

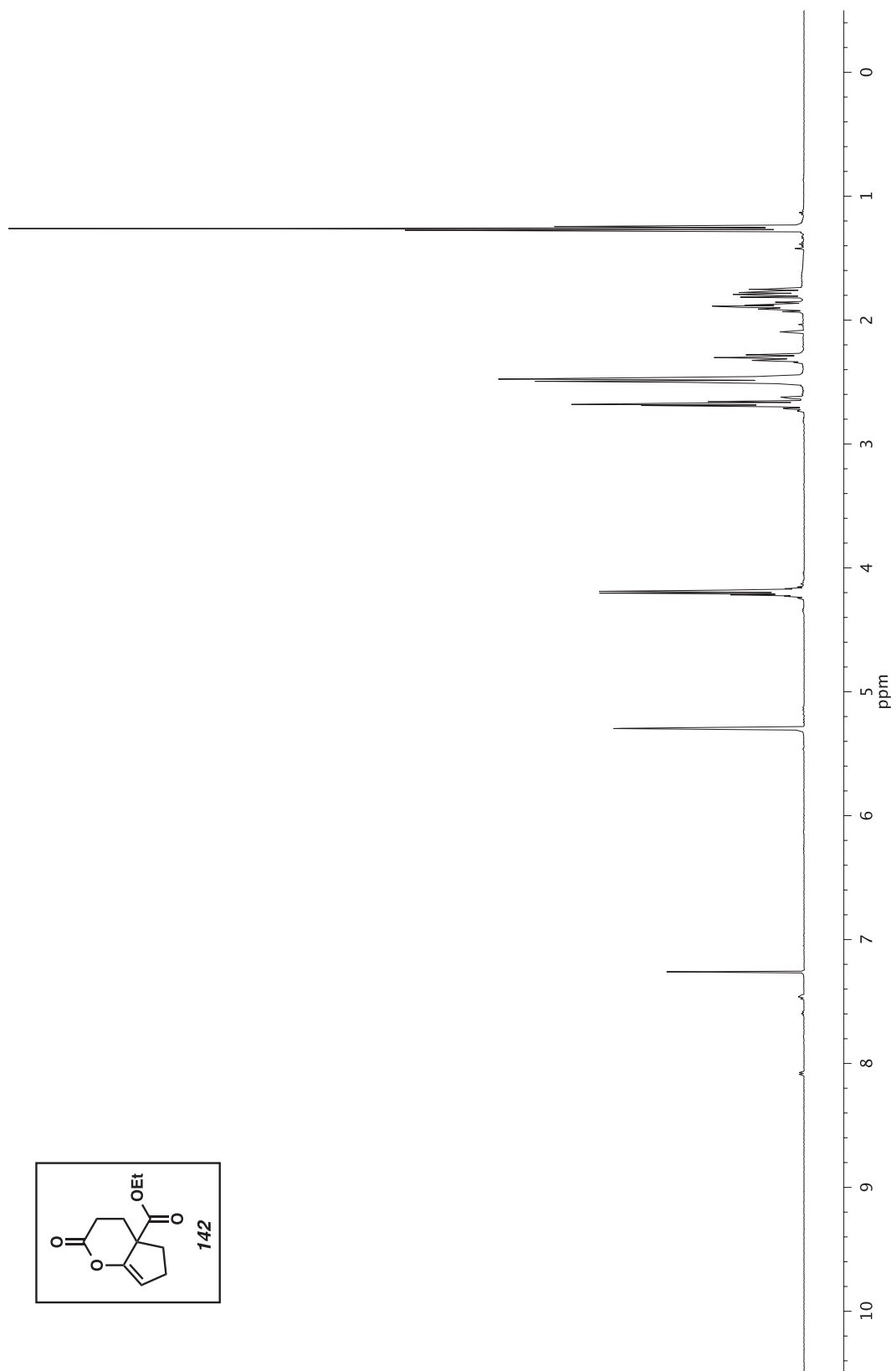


Figure A6.40 ^1H NMR (500 MHz, CDCl_3) of compound 142.

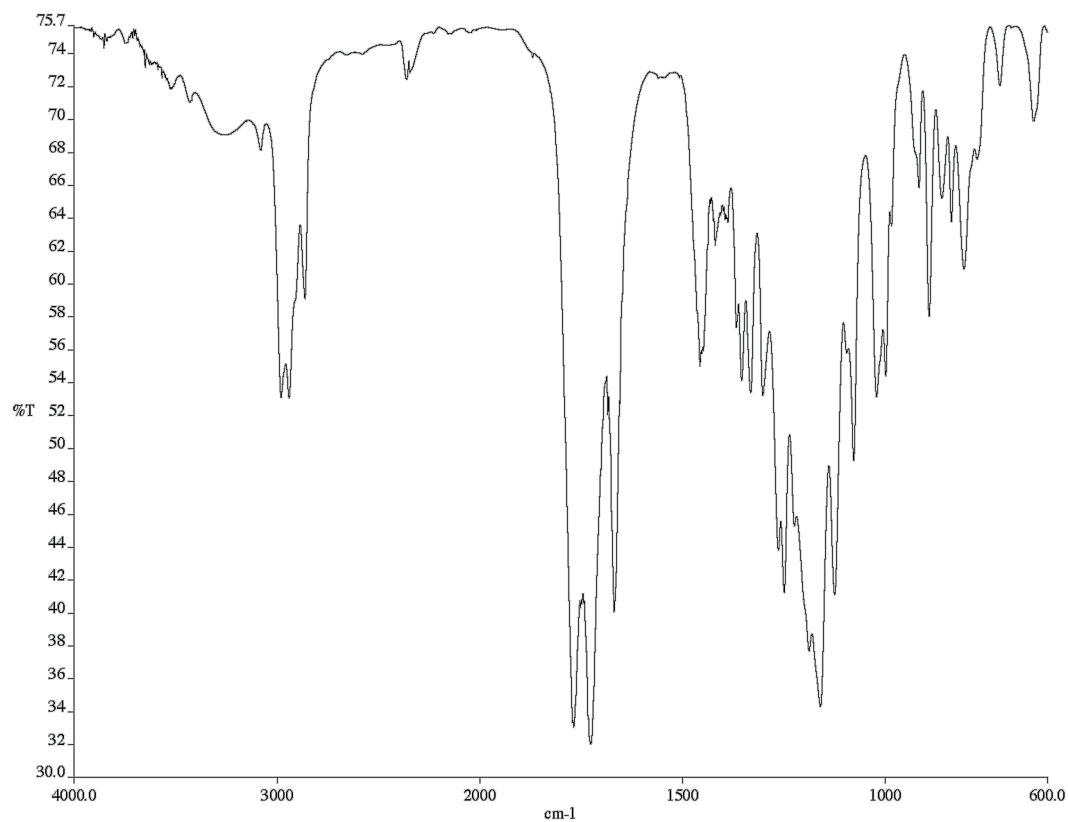


Figure A6.41 Infrared spectrum (Thin Film, NaCl) of compound **142**.

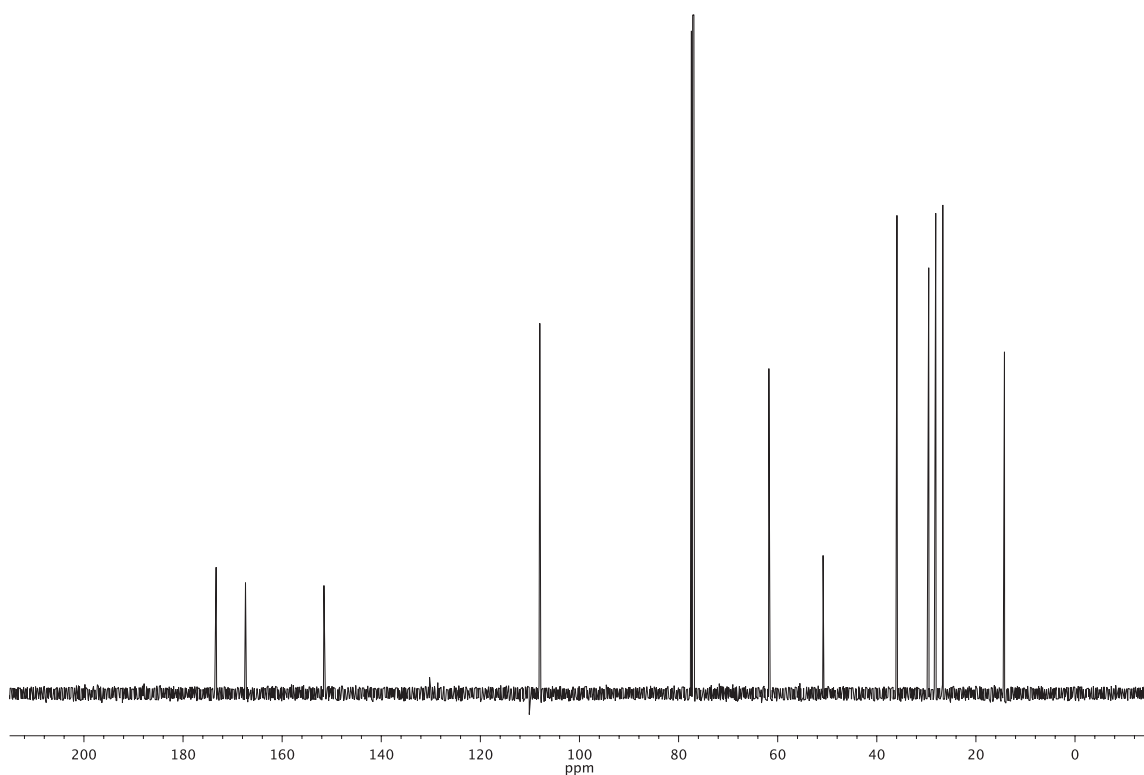


Figure A6.42 ¹³C NMR (126 MHz, CDCl₃) of compound **142**.

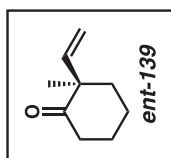
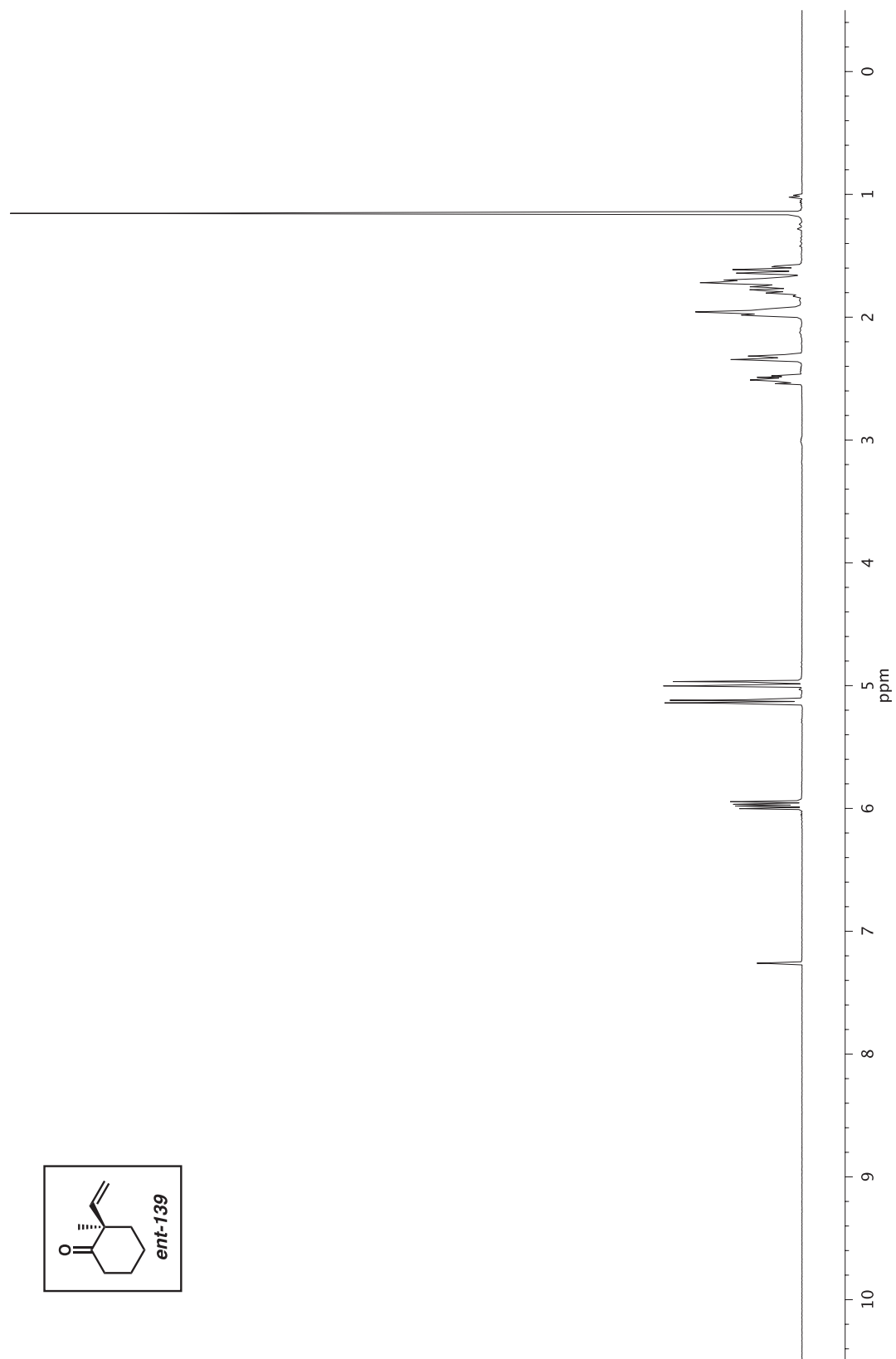


Figure A6.43 ^1H NMR (500 MHz, CDCl_3) of compound **139**.

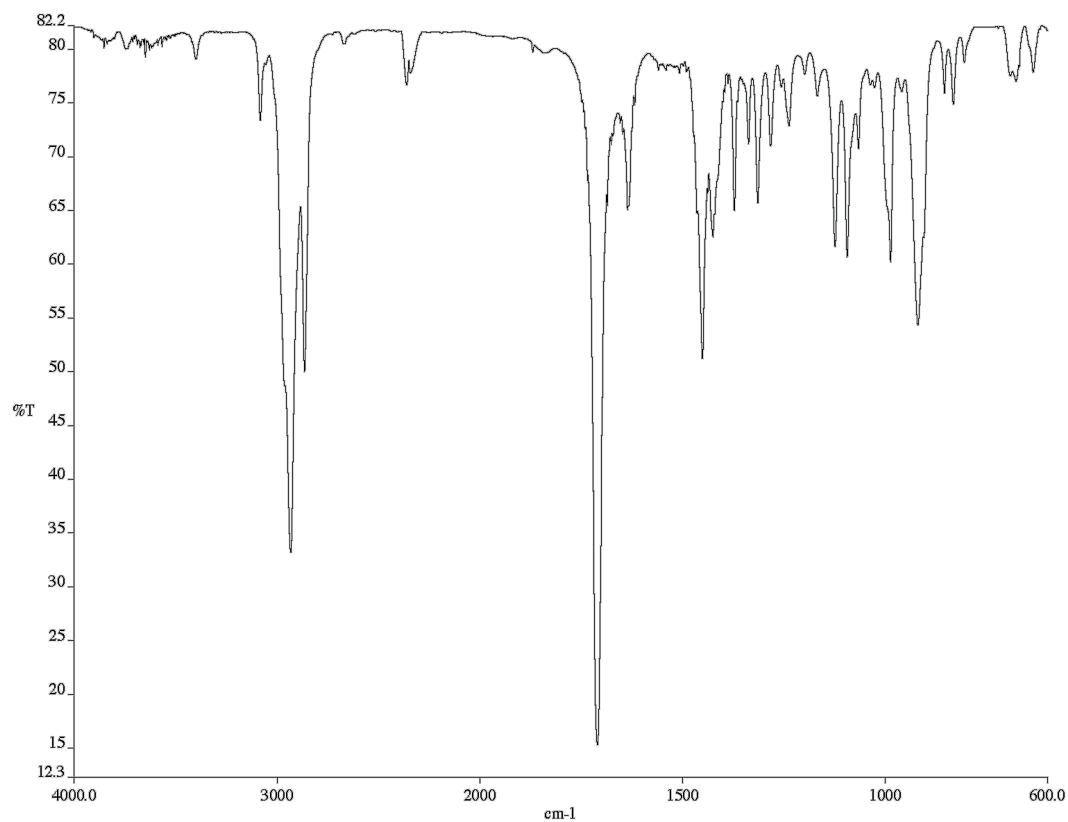


Figure A6.44 Infrared spectrum (Thin Film, NaCl) of compound **139**.

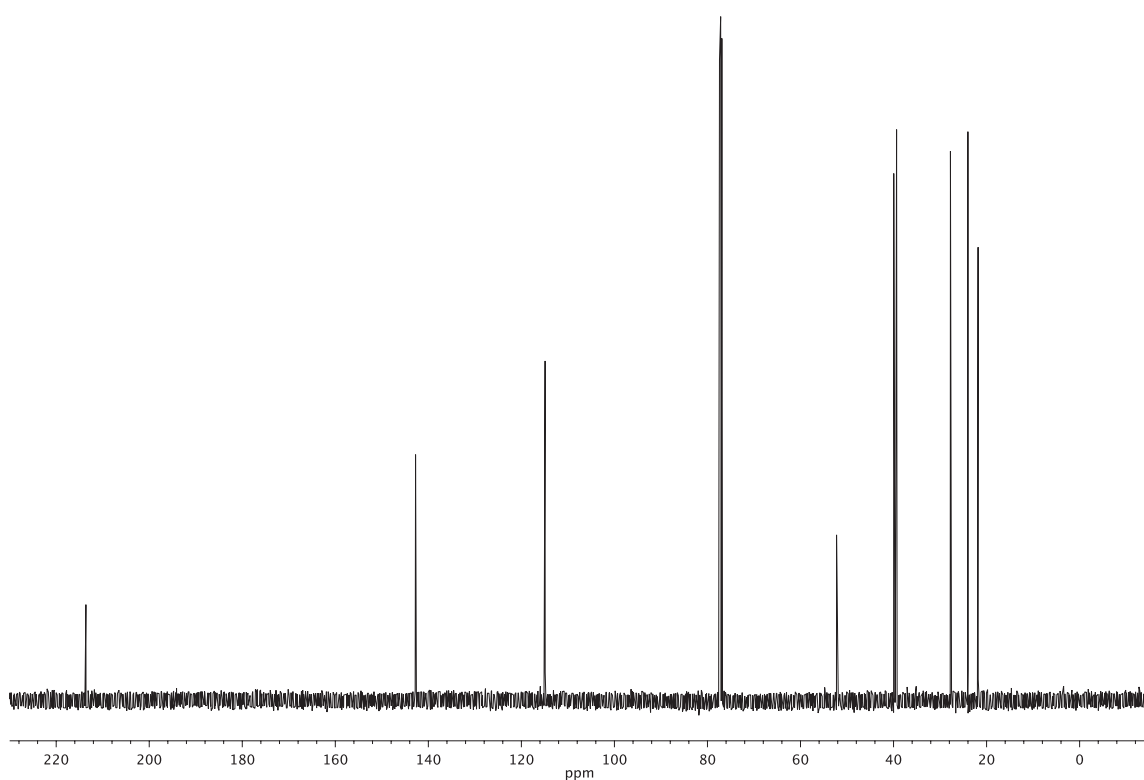


Figure A6.45 ¹³C NMR (126 MHz, CDCl₃) of compound **139**.

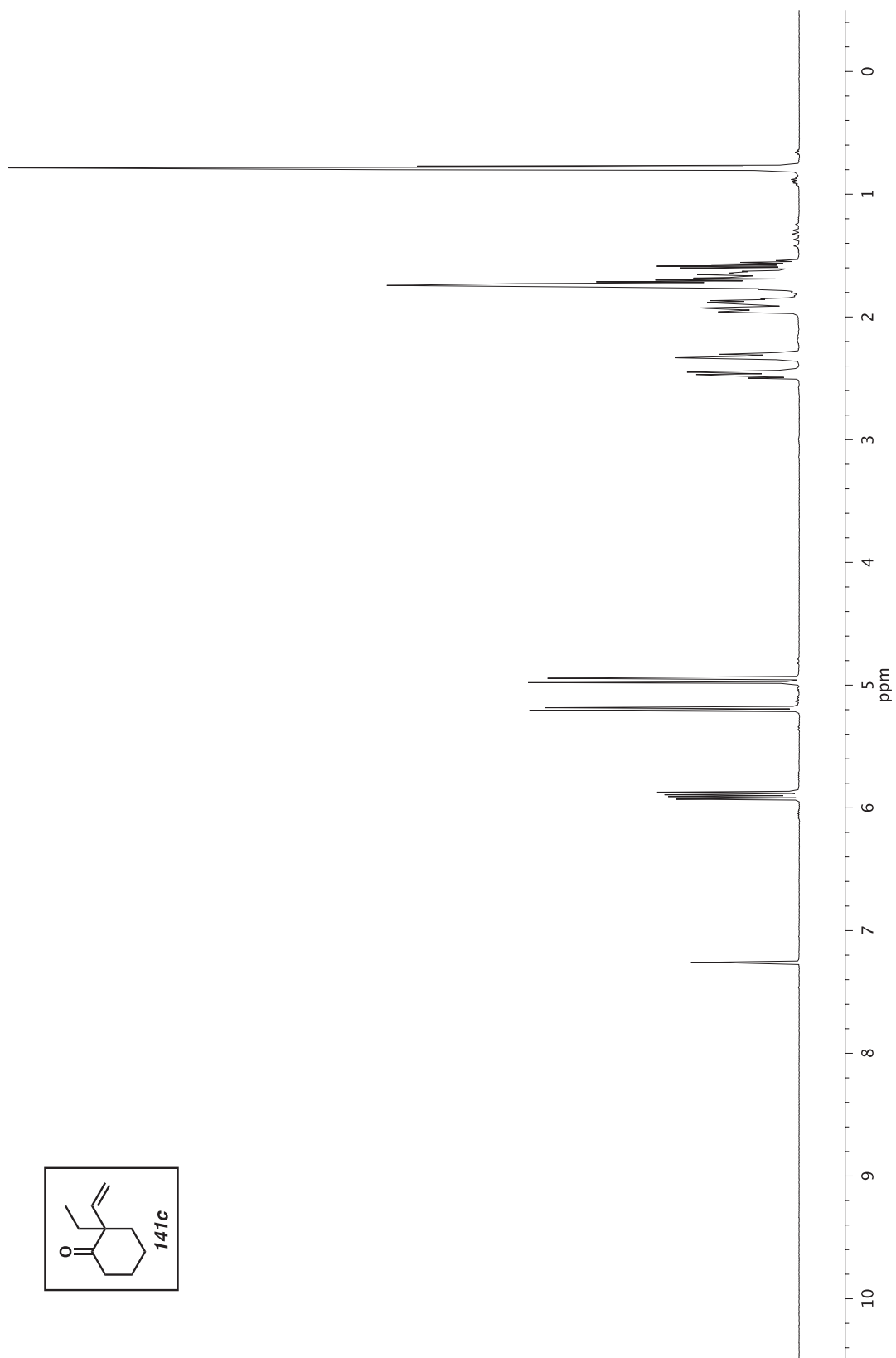


Figure A6.46 ^1H NMR (500 MHz, CDCl_3) of compound **141c**.

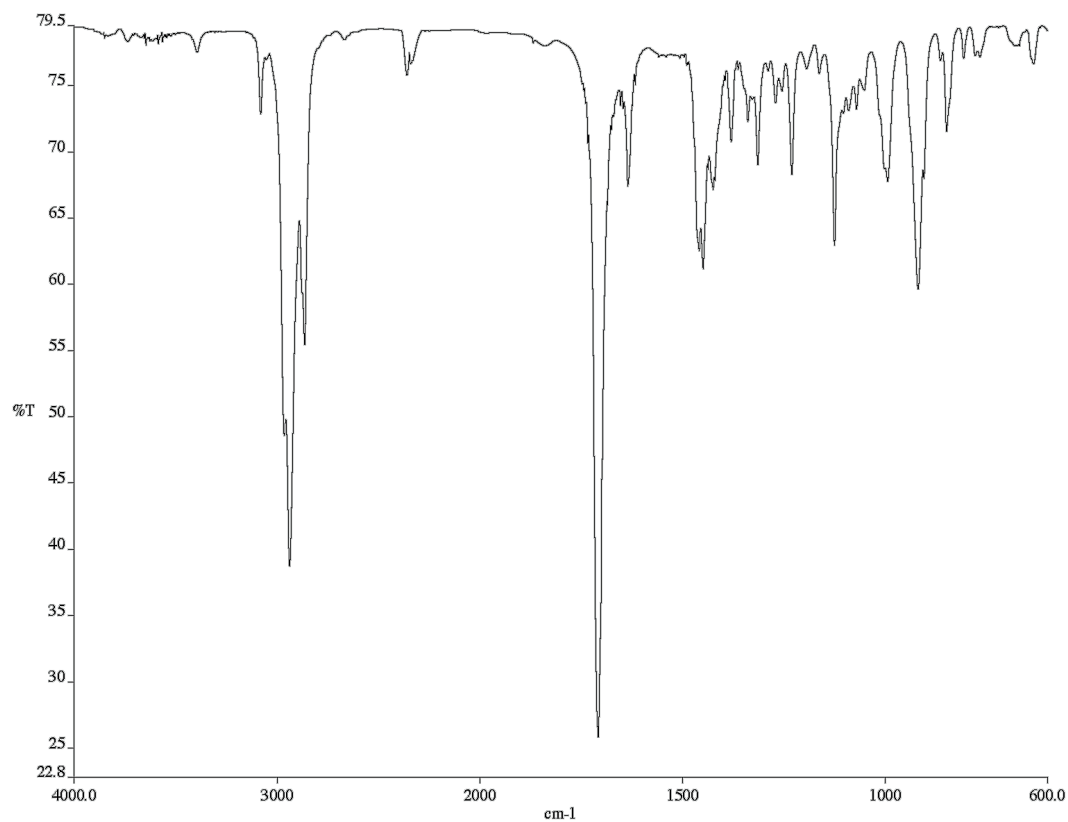


Figure A6.47 Infrared spectrum (Thin Film, NaCl) of compound **141c**.

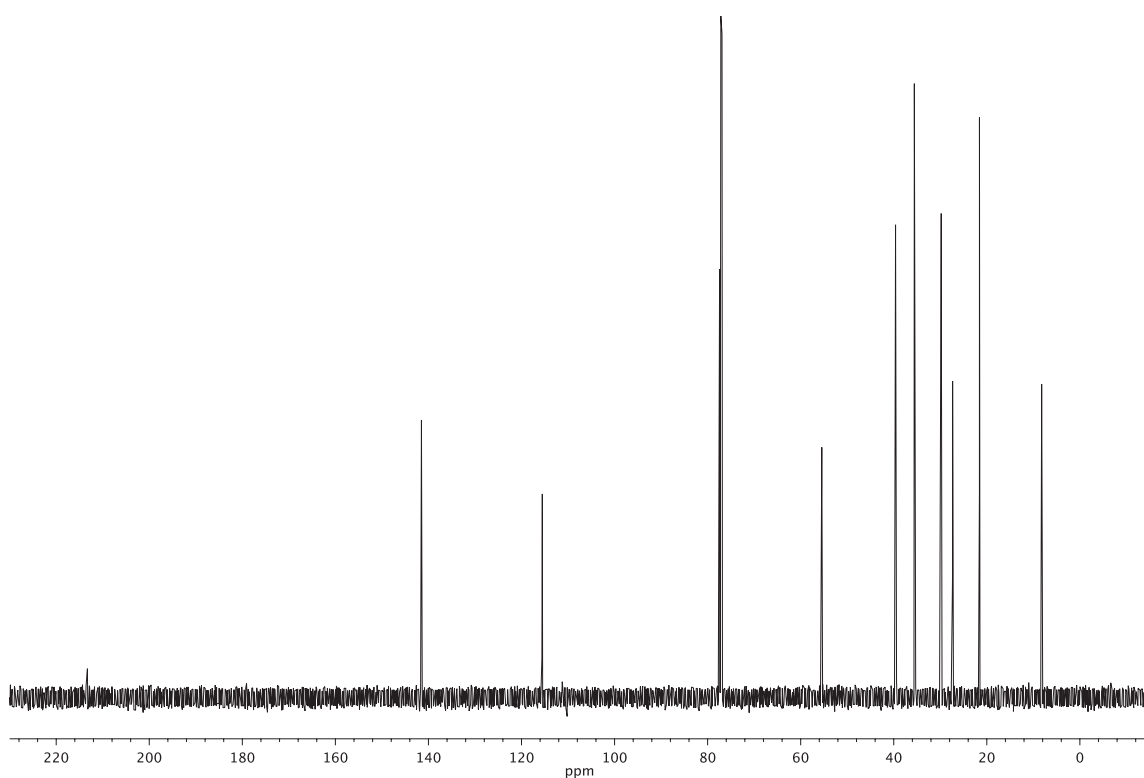


Figure A6.48 ¹³C NMR (126 MHz, CDCl₃) of compound **141c**.

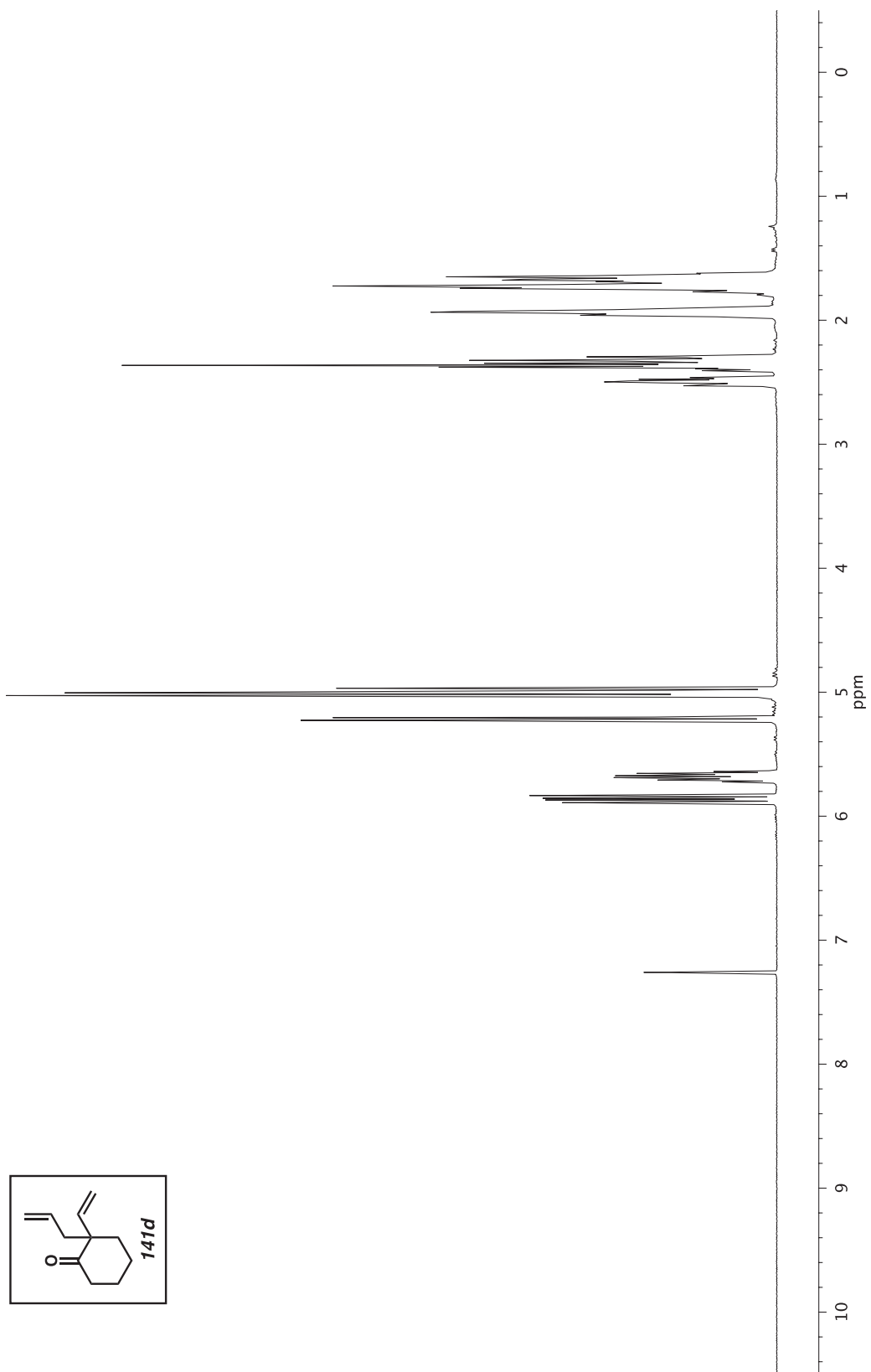


Figure A6.49 ^1H NMR (500 MHz, CDCl_3) of compound **141d**.

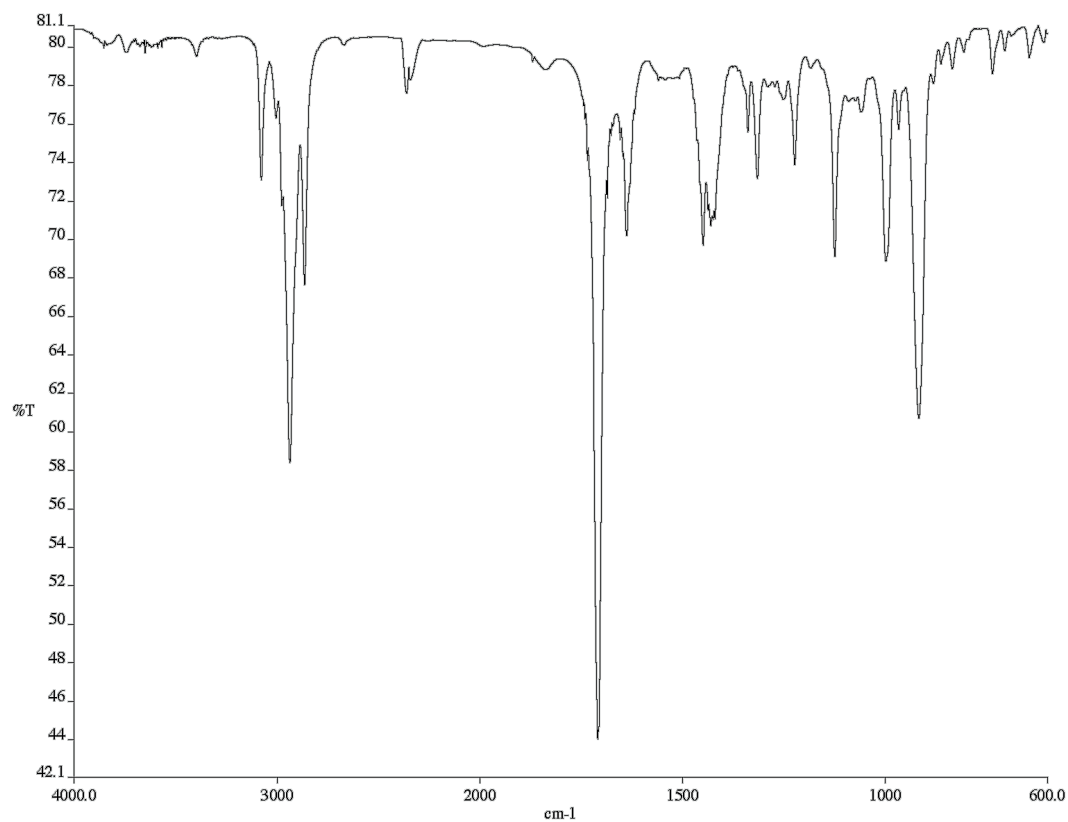


Figure A6.50 Infrared spectrum (Thin Film, NaCl) of compound **141d**.

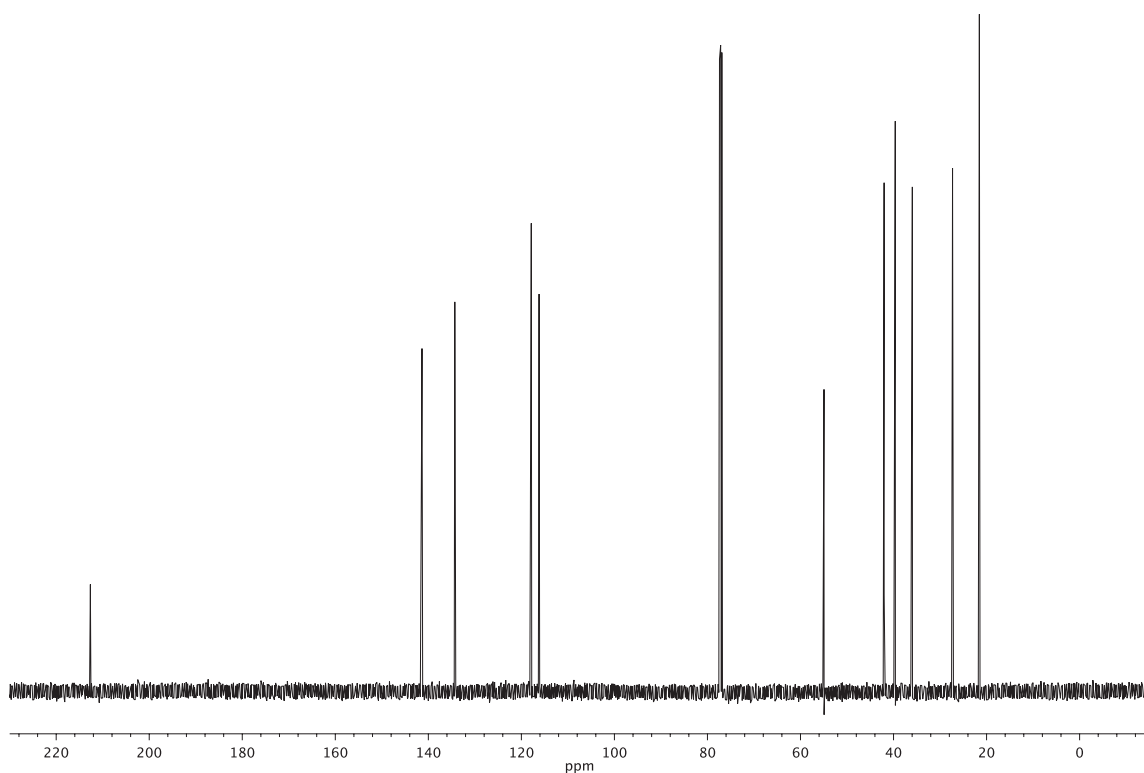


Figure A6.51 ¹³C NMR (126 MHz, CDCl₃) of compound **141d**.

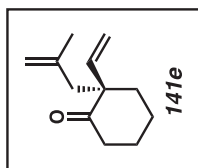
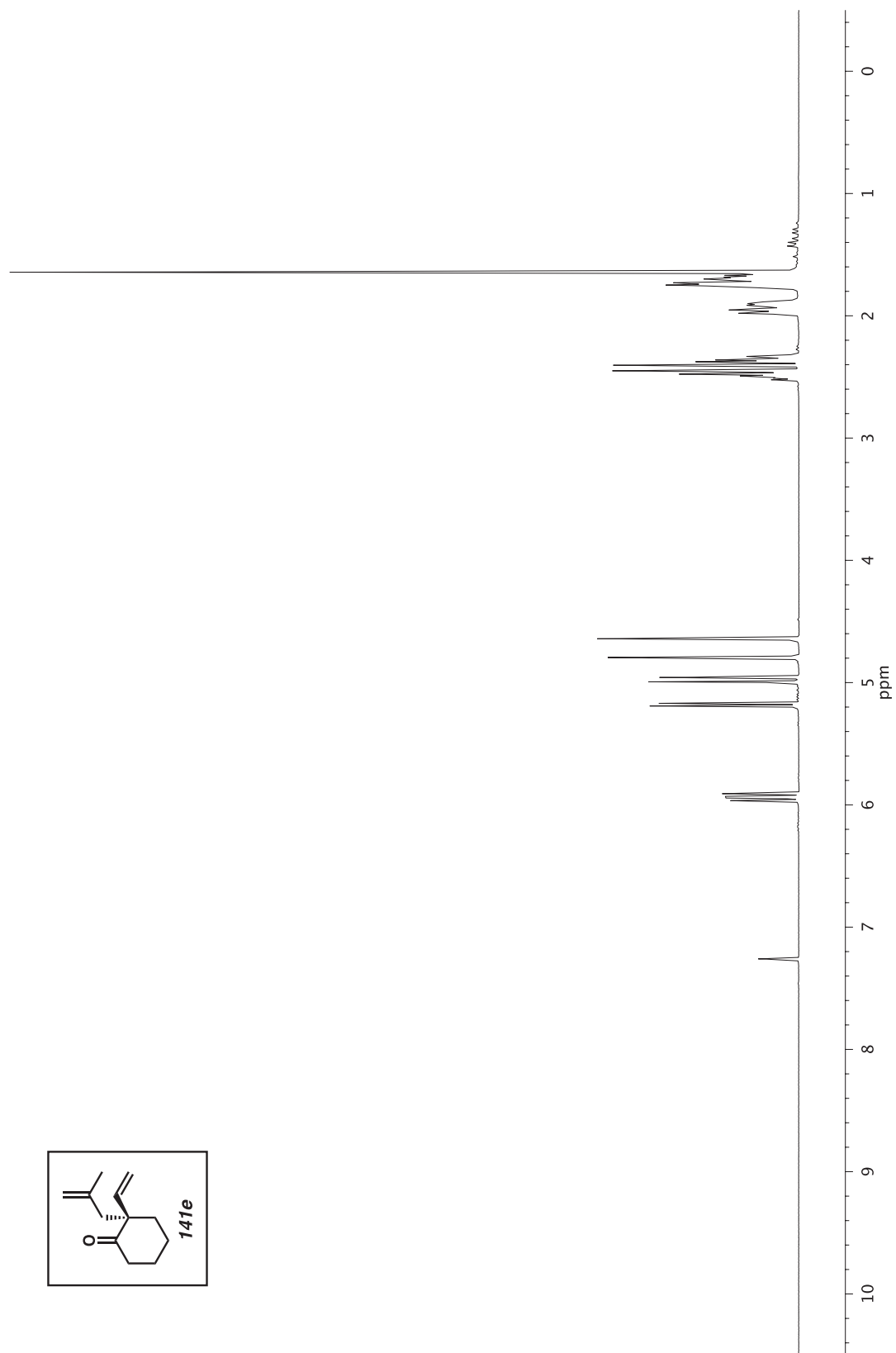


Figure A6.52 ^1H NMR (500 MHz, CDCl_3) of compound **141e**.

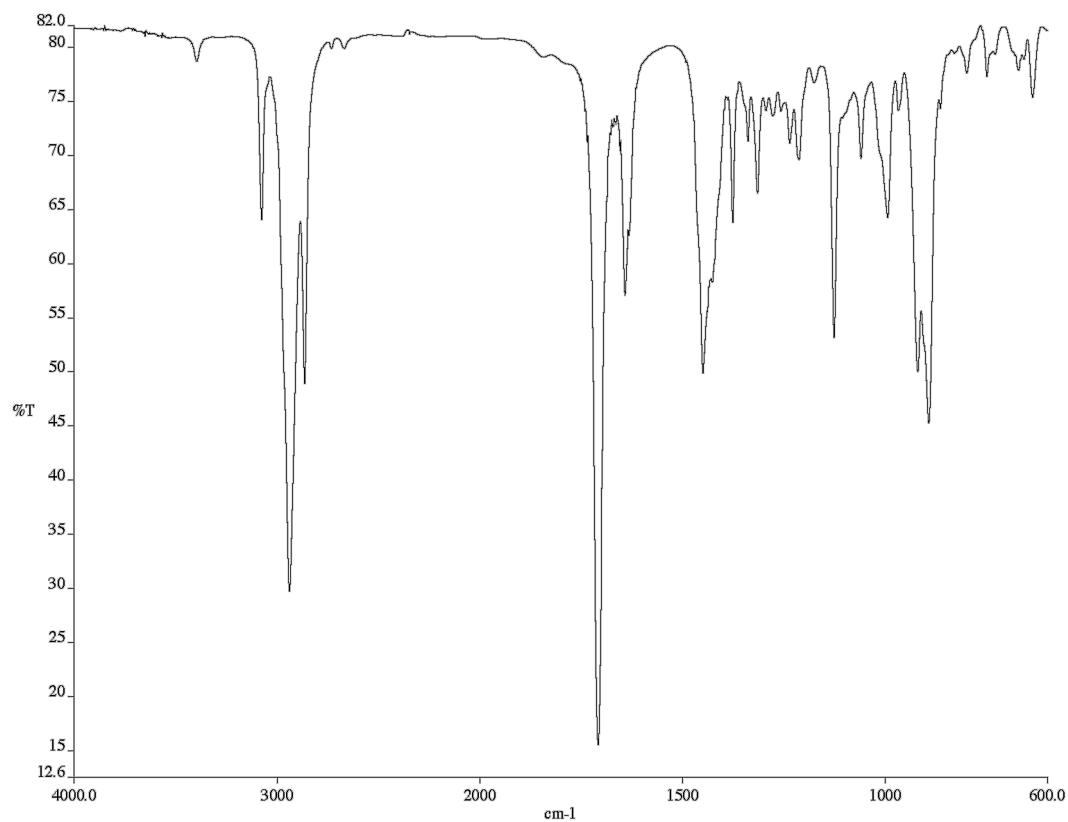


Figure A6.53 Infrared spectrum (Thin Film, NaCl) of compound **141e**.

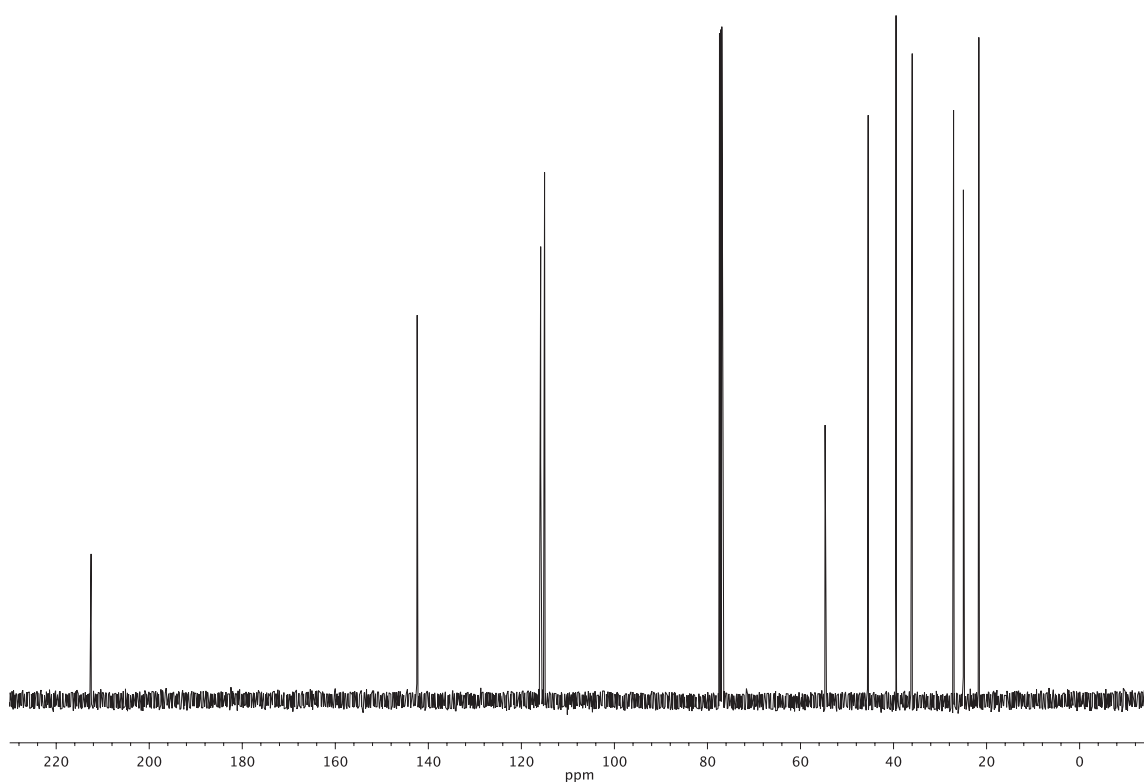


Figure A6.54 ¹³C NMR (126 MHz, CDCl₃) of compound **141e**.

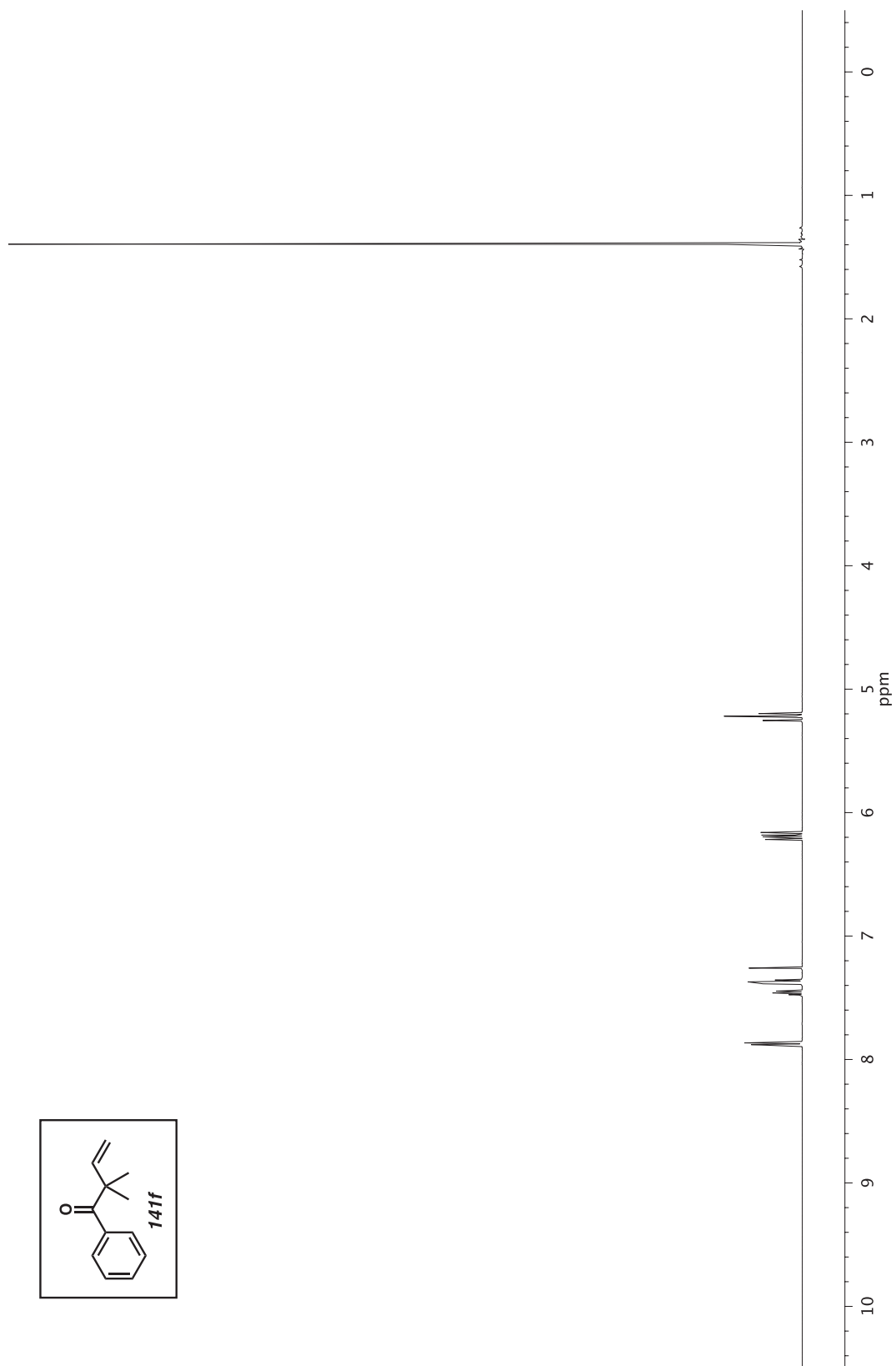


Figure A6.55 ^1H NMR (500 MHz, CDCl_3) of compound **141f**.

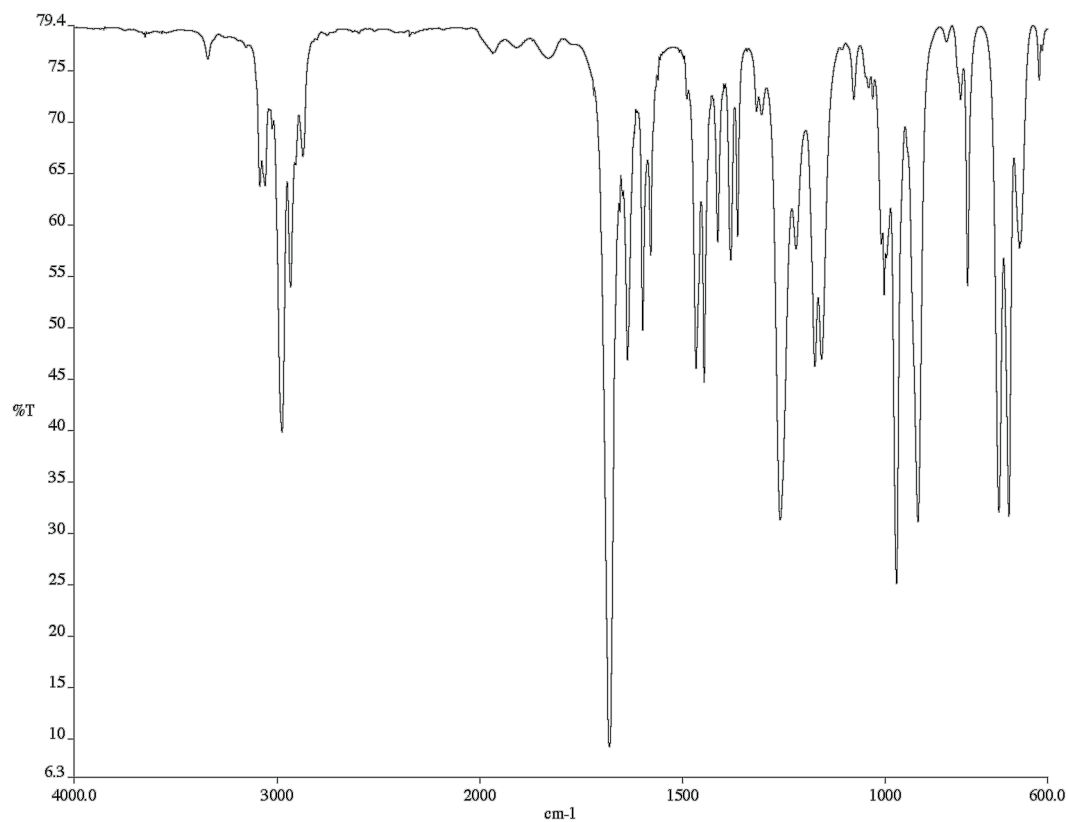


Figure A6.56 Infrared spectrum (Thin Film, NaCl) of compound **141f**.

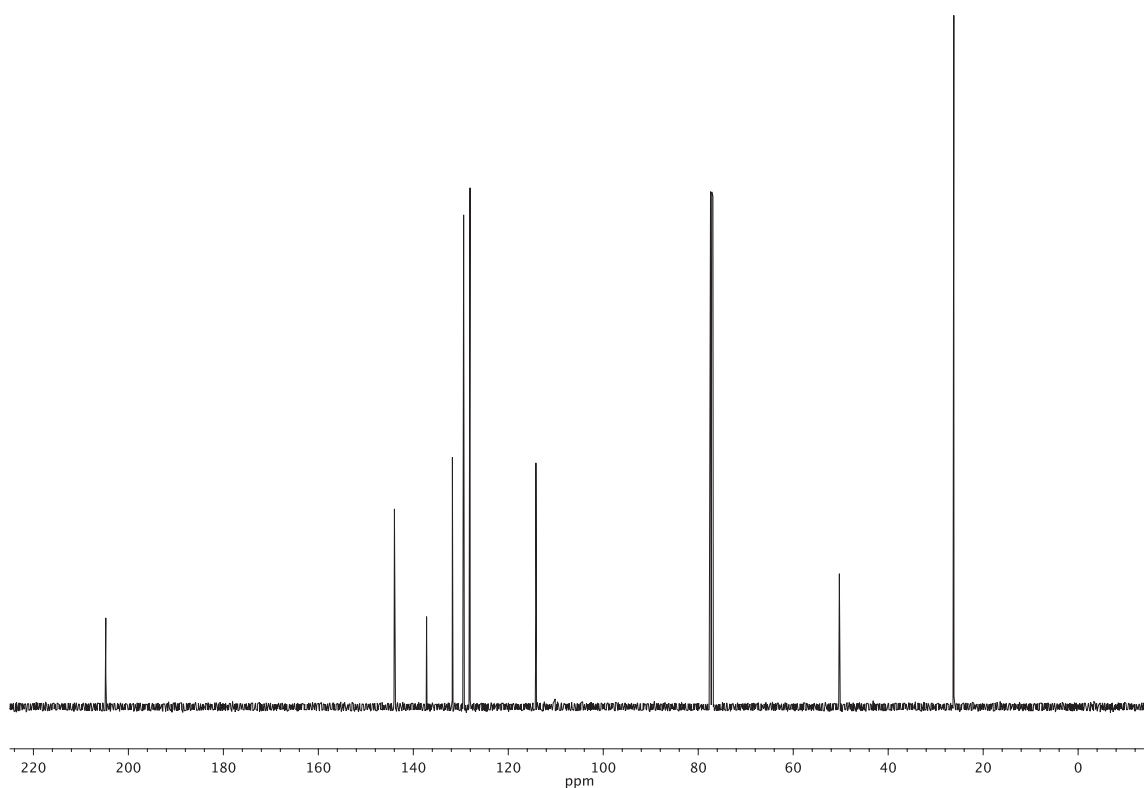


Figure A6.57 ¹³C NMR (126 MHz, CDCl₃) of compound **141f**.

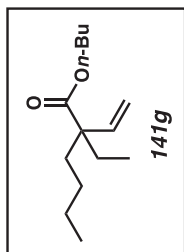
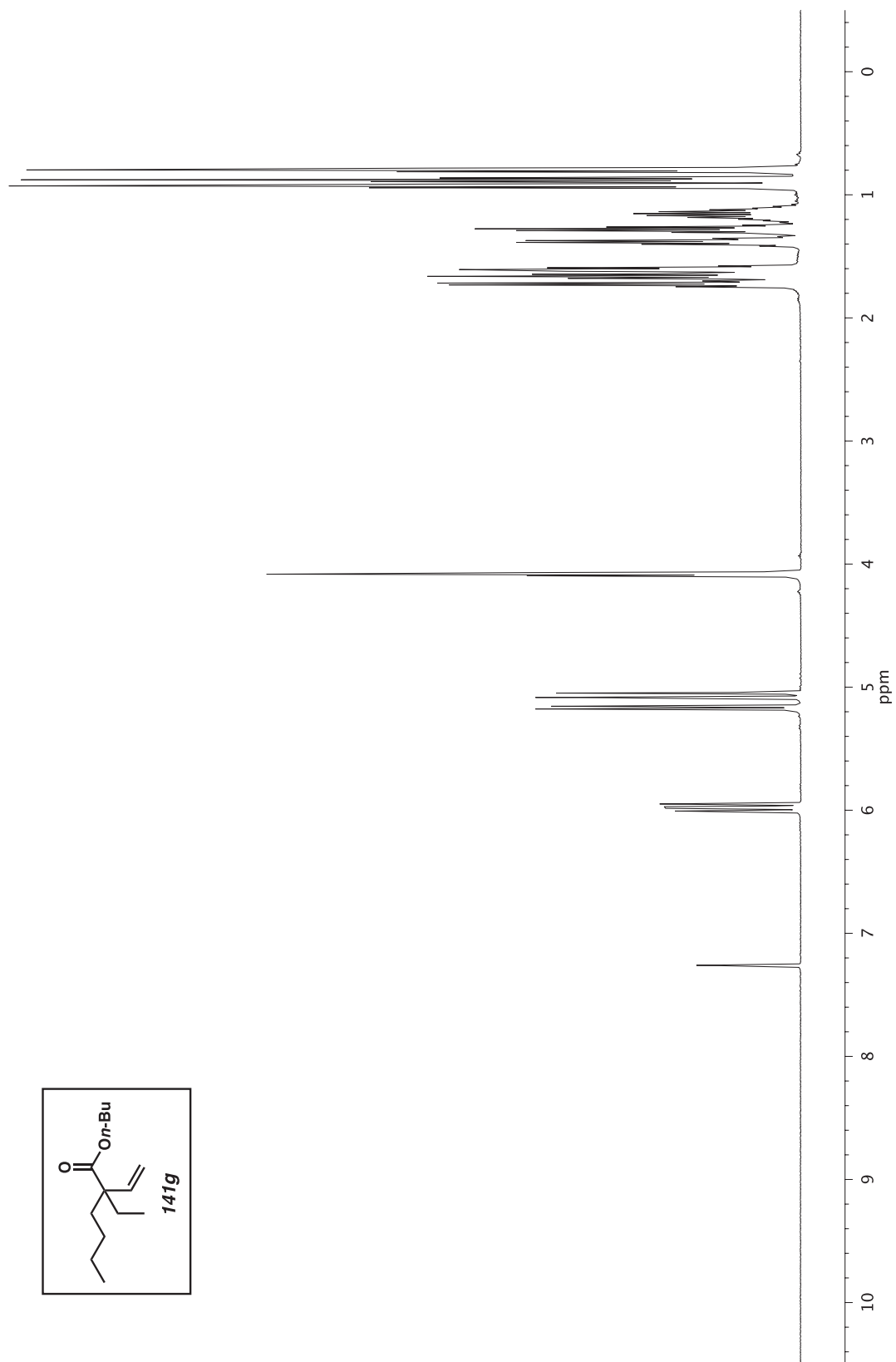


Figure A6.58 ^1H NMR (500 MHz, CDCl_3) of compound **141g**.

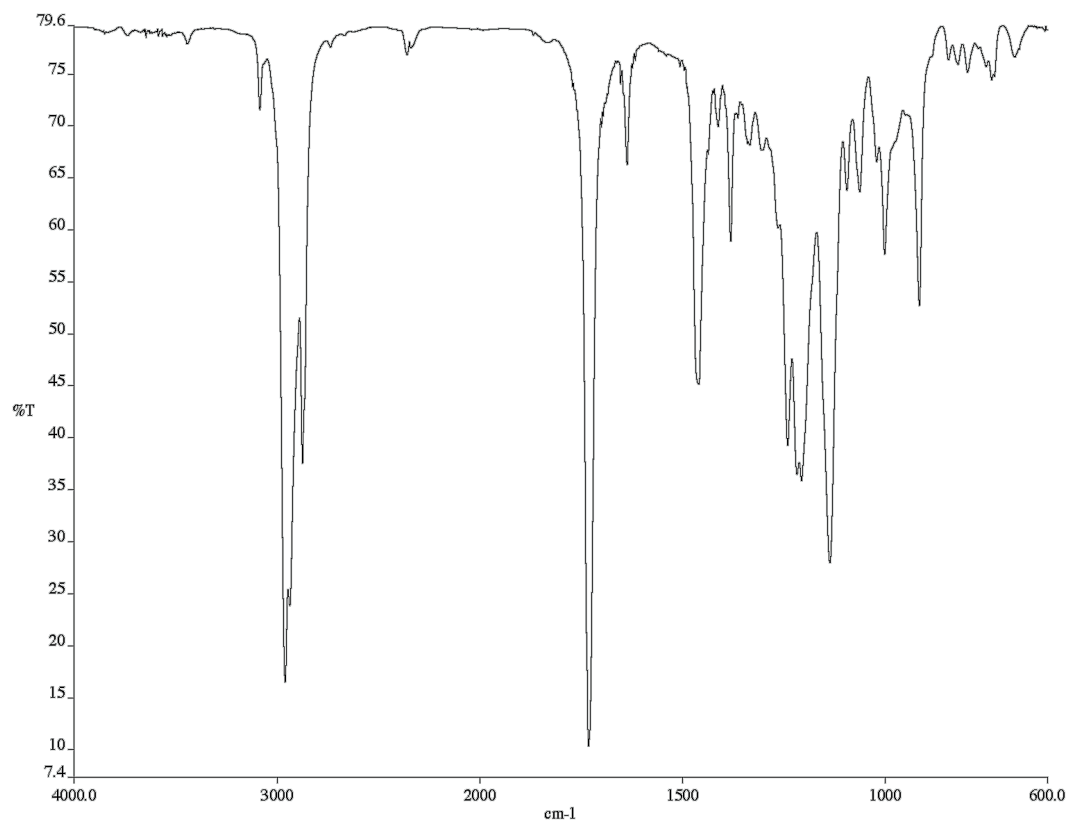


Figure A6.59 Infrared spectrum (Thin Film, NaCl) of compound **141g**.

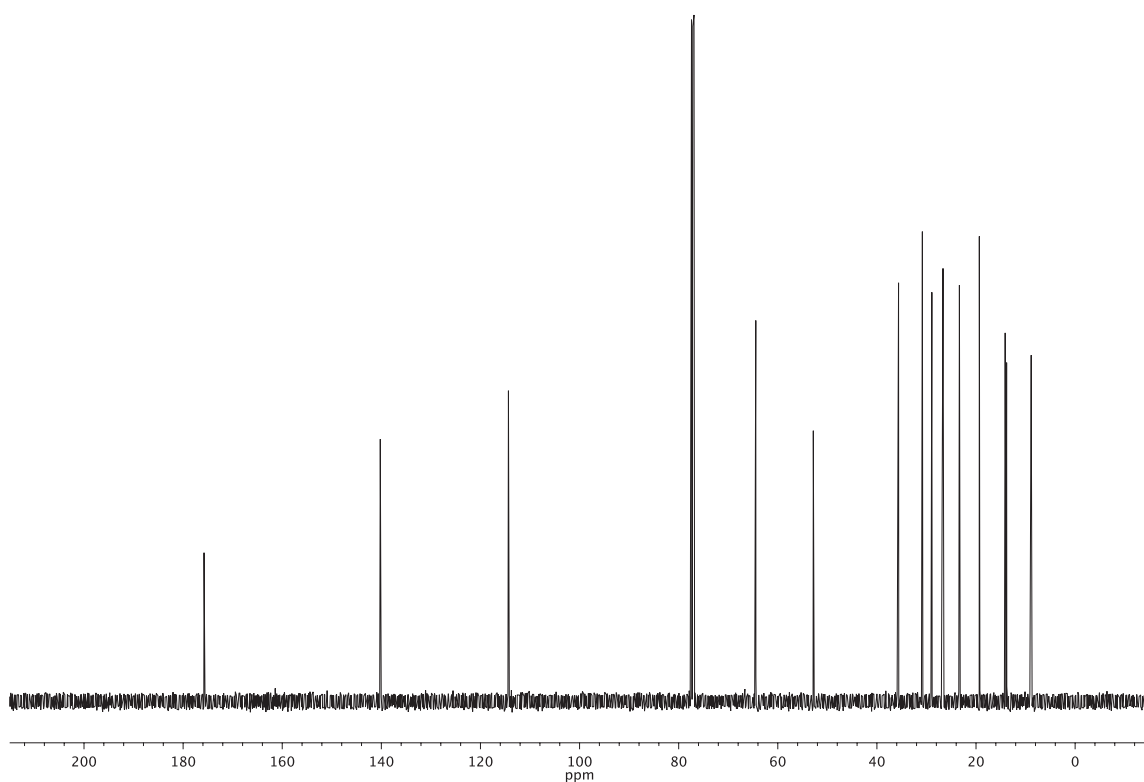


Figure A6.60 ¹³C NMR (126 MHz, CDCl₃) of compound **141g**.

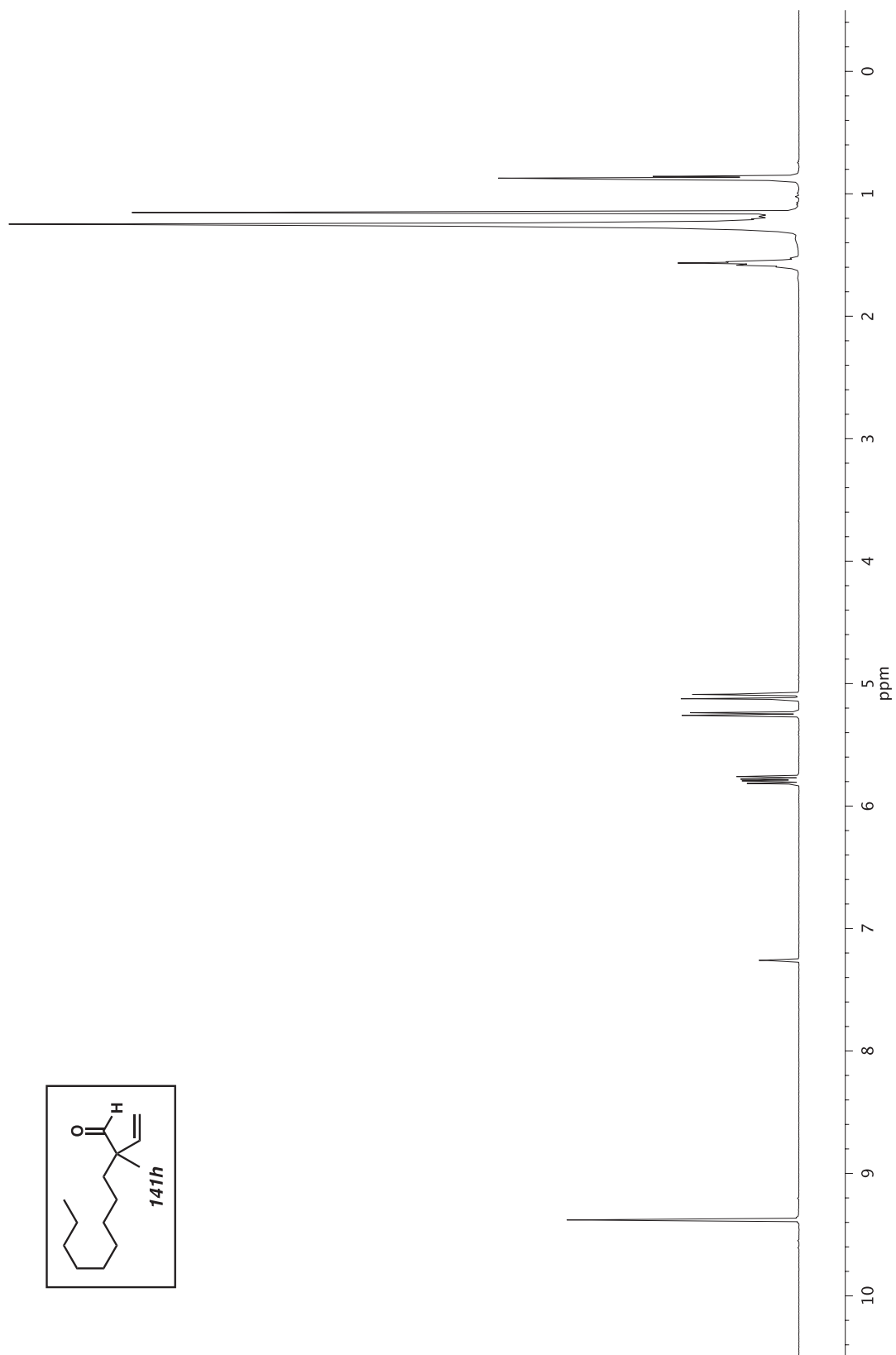


Figure A6.61 ^1H NMR (500 MHz, CDCl_3) of compound **141h**.

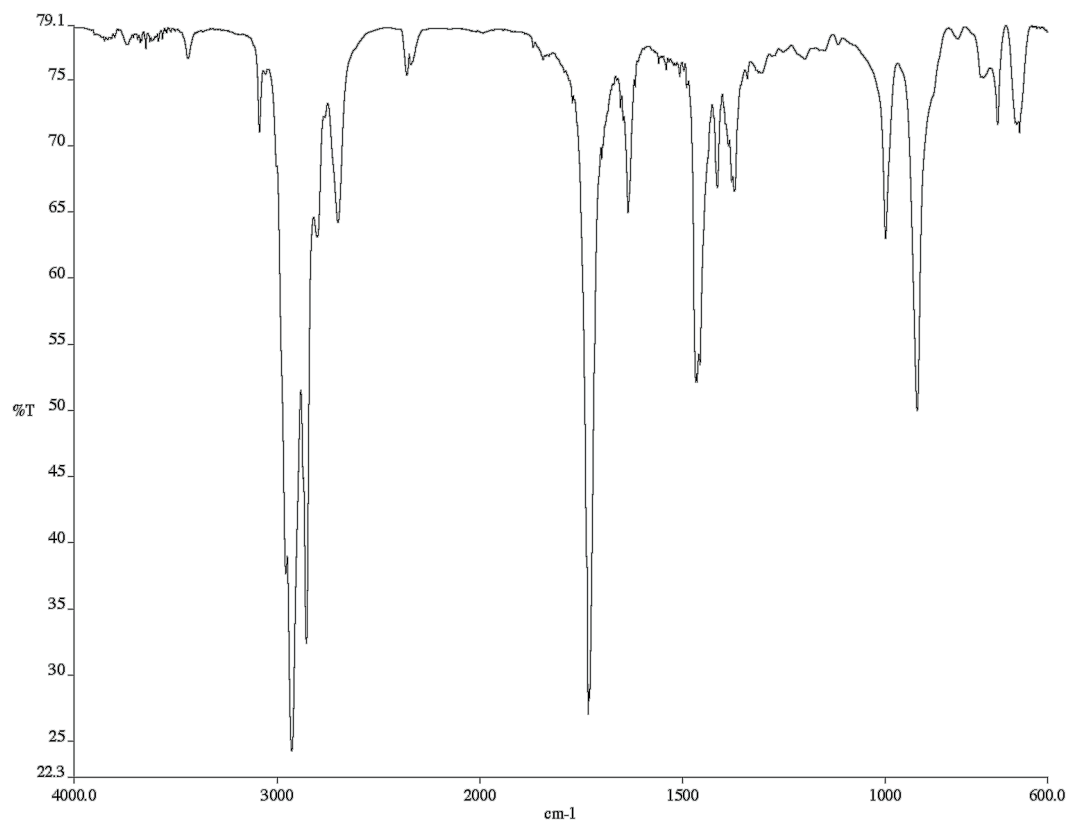


Figure A6.62 Infrared spectrum (Thin Film, NaCl) of compound **141h**.

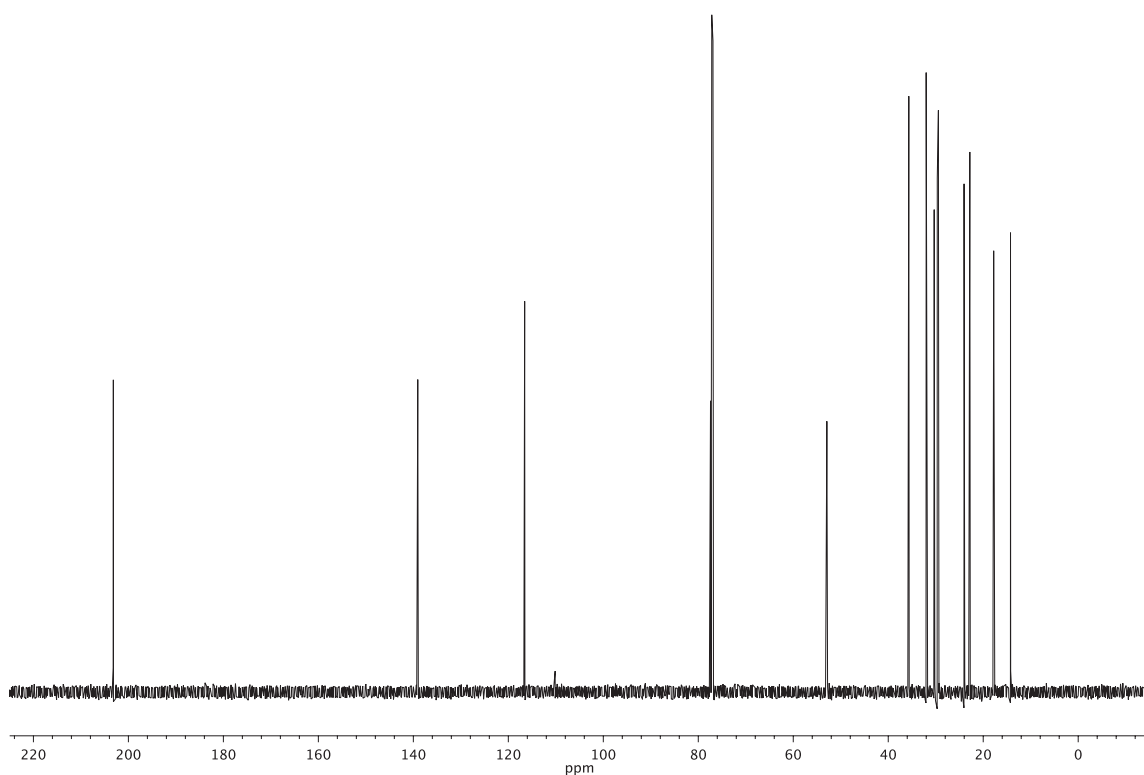


Figure A6.63 ¹³C NMR (126 MHz, CDCl₃) of compound **141h**.

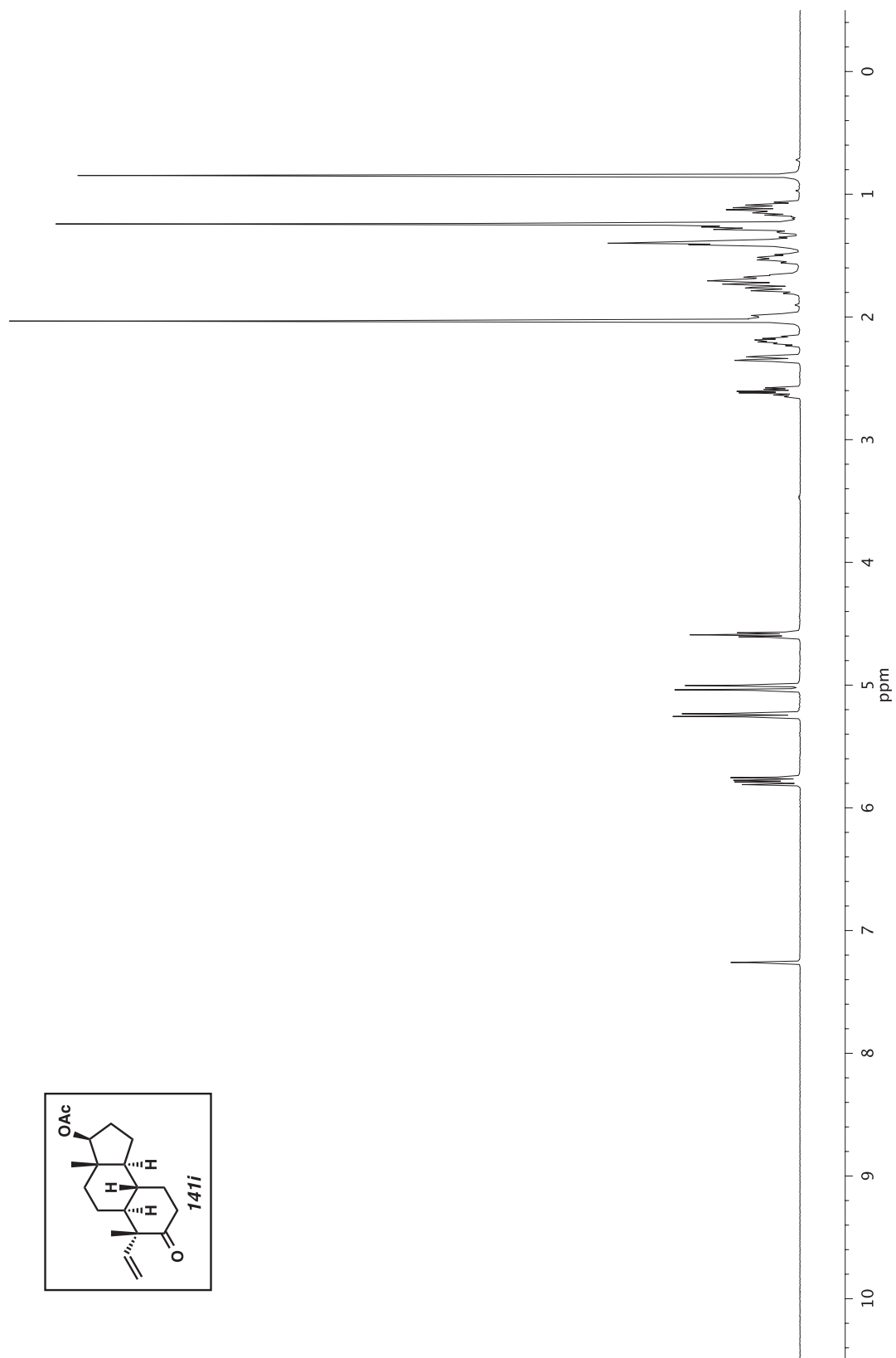


Figure A6.64 ^1H NMR (500 MHz, CDCl_3) of compound **141i**.

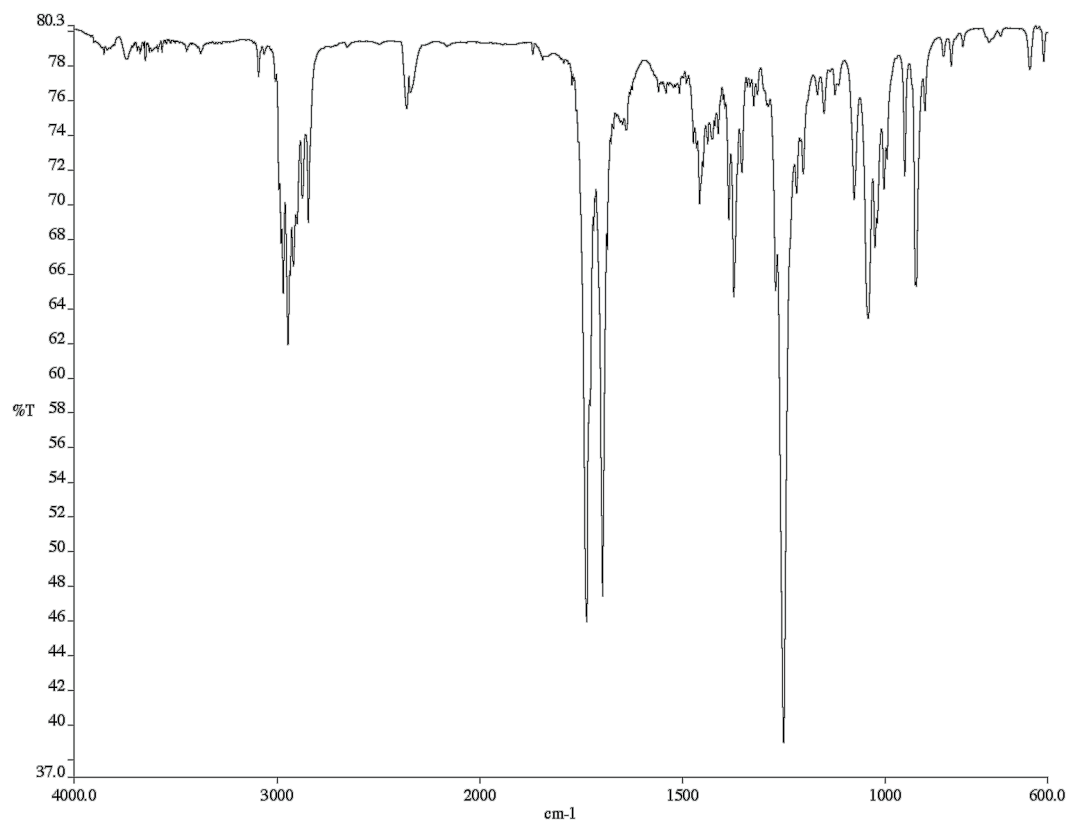


Figure A6.65 Infrared spectrum (Thin Film, NaCl) of compound **14i**.

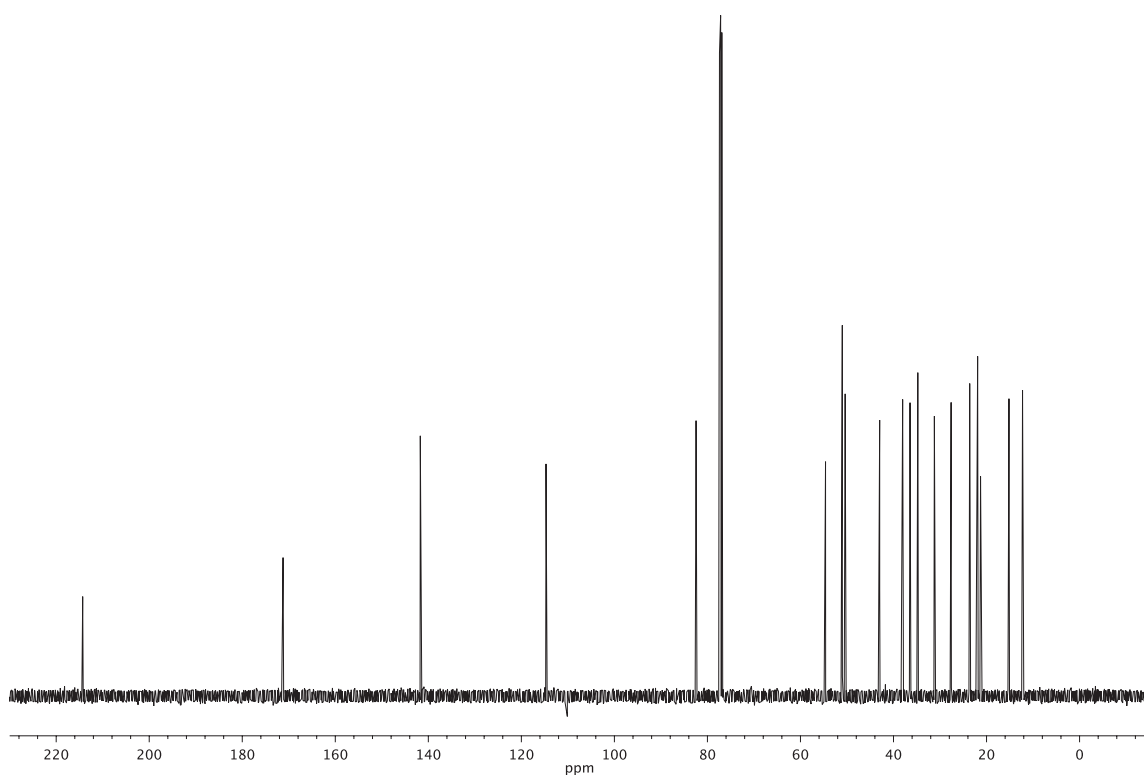


Figure A6.66 ¹³C NMR (126 MHz, CDCl₃) of compound **14i**.

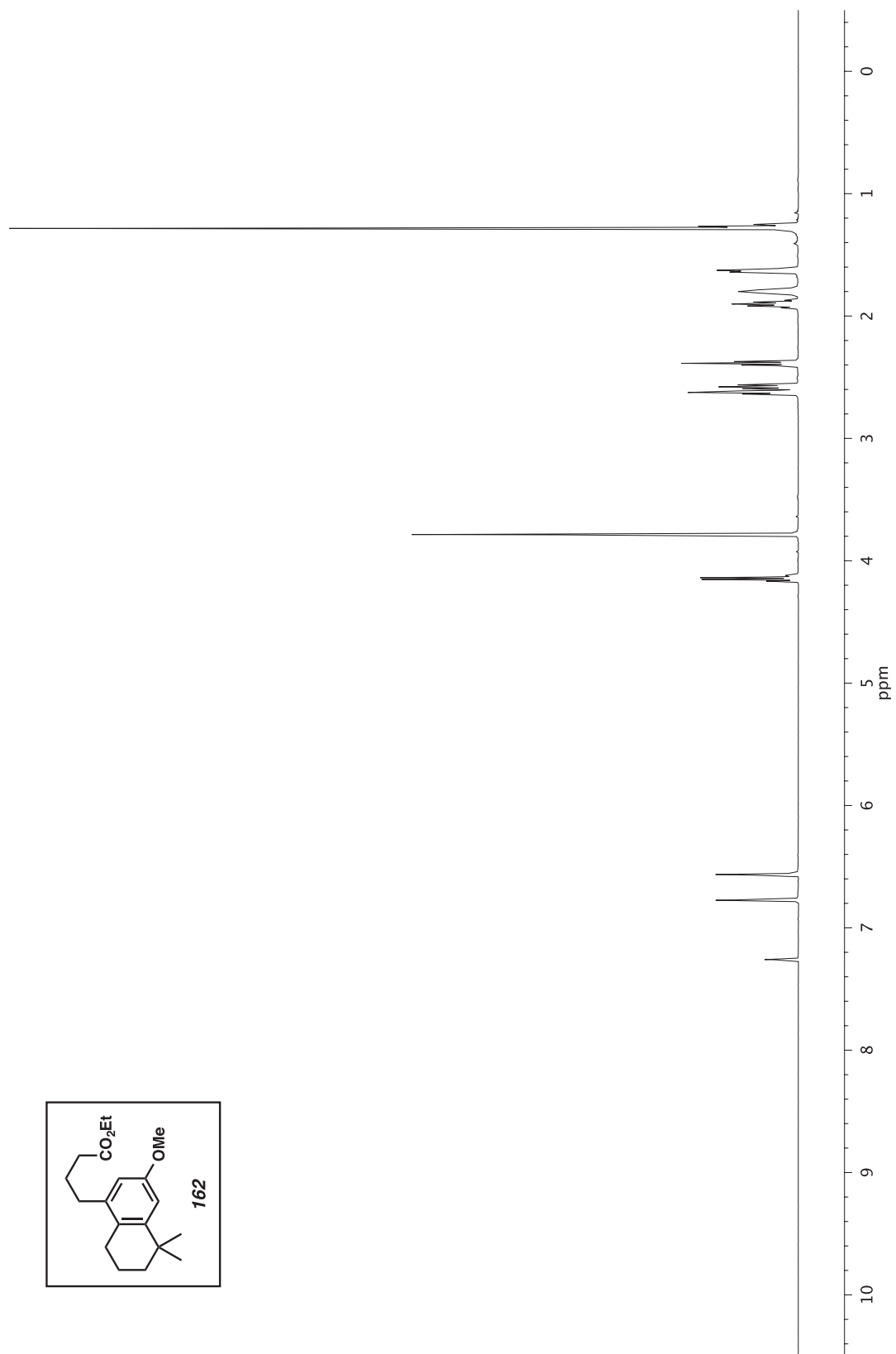


Figure A6.67 ^1H NMR (500 MHz, CDCl₃) of compound **162**.

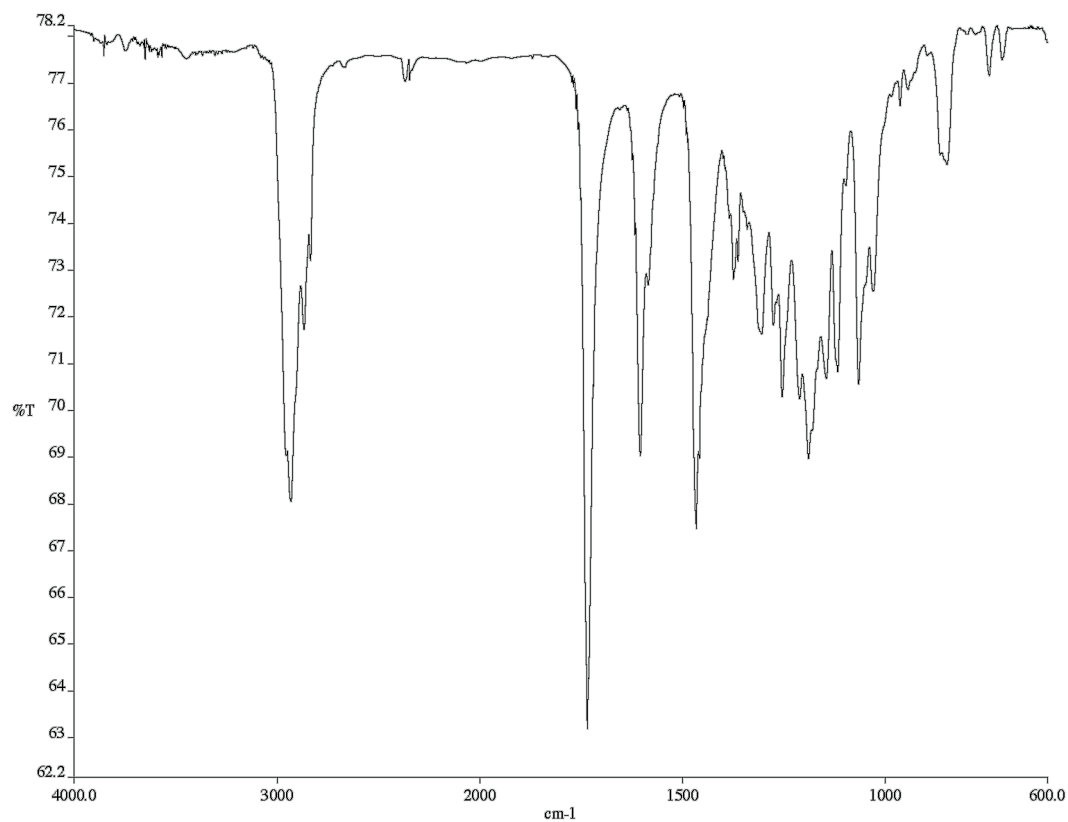


Figure A6.68 Infrared spectrum (Thin Film, NaCl) of compound **162**.

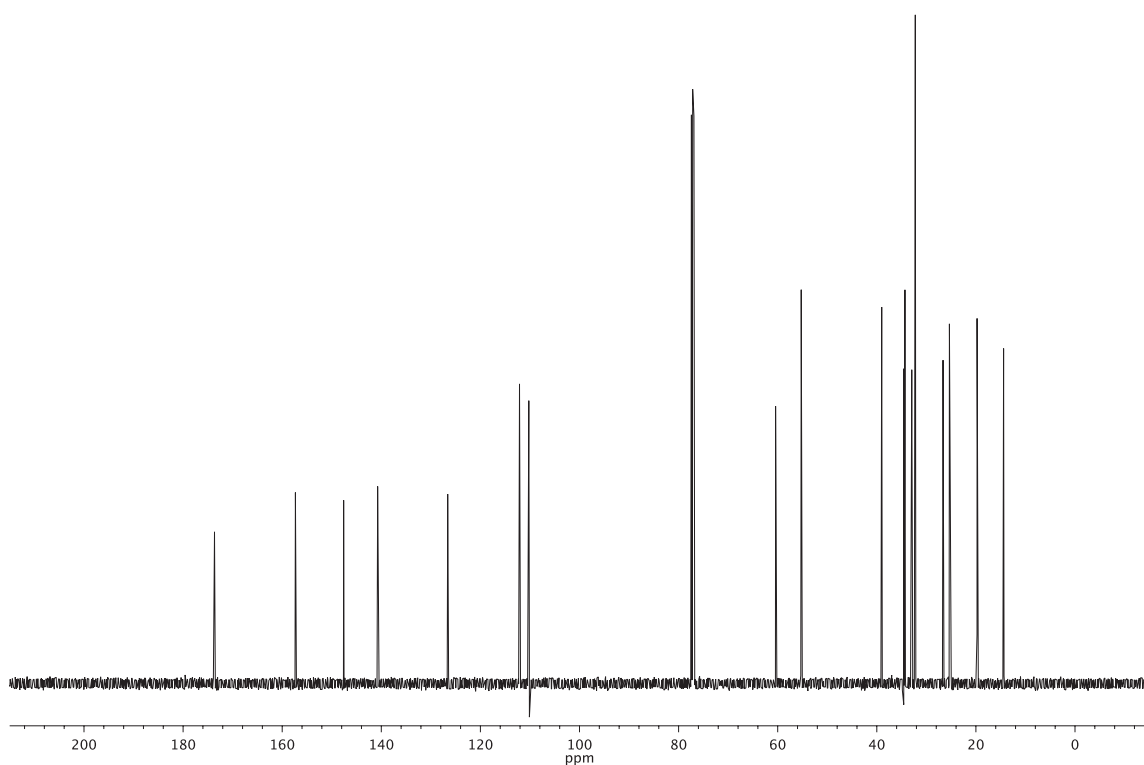


Figure A6.69 ¹³C NMR (126 MHz, CDCl₃) of compound **162**.

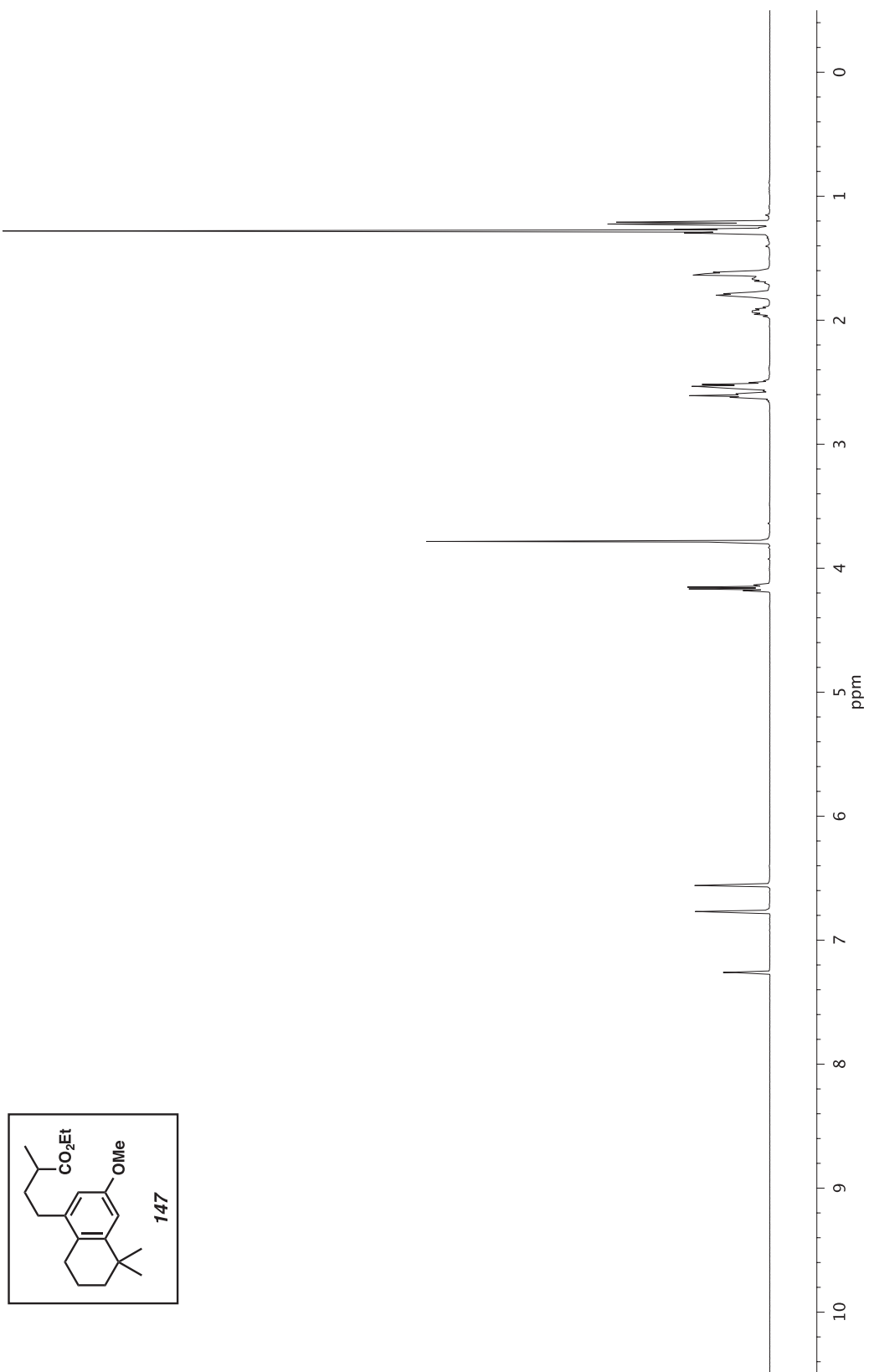


Figure A6.70 ^1H NMR (500 MHz, CDCl₃) of compound **147**.

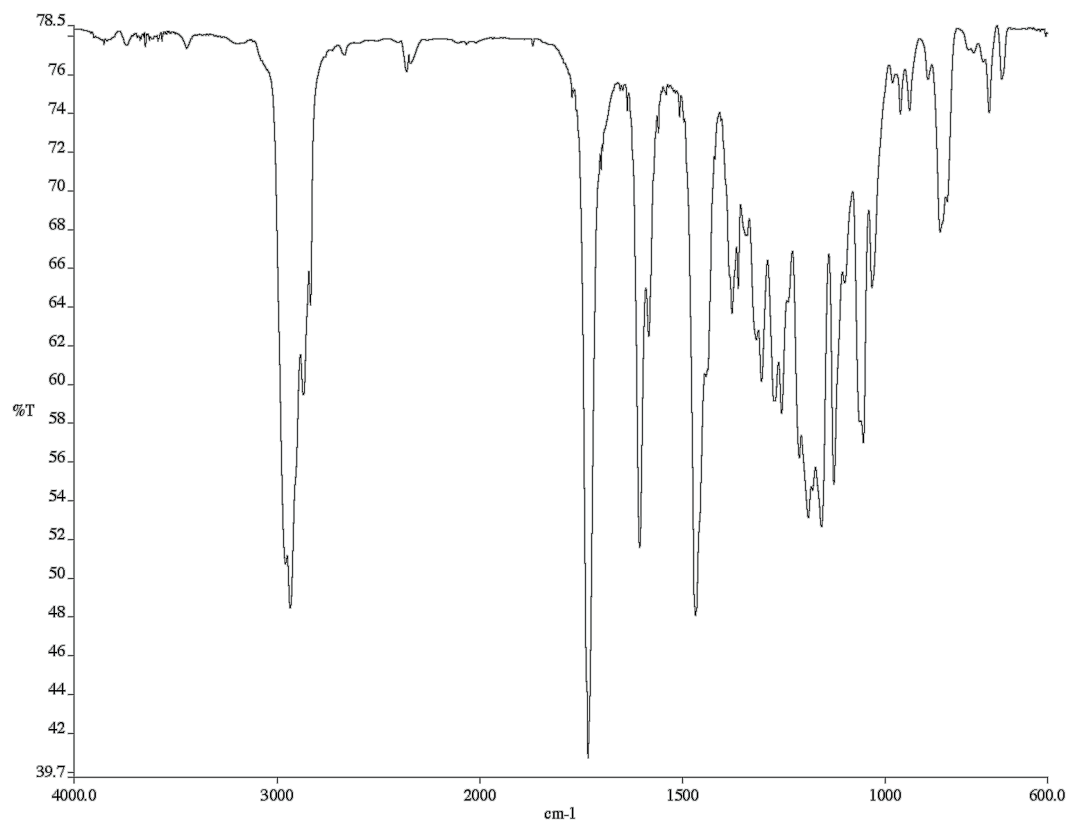


Figure A6.71 Infrared spectrum (Thin Film, NaCl) of compound **147**.

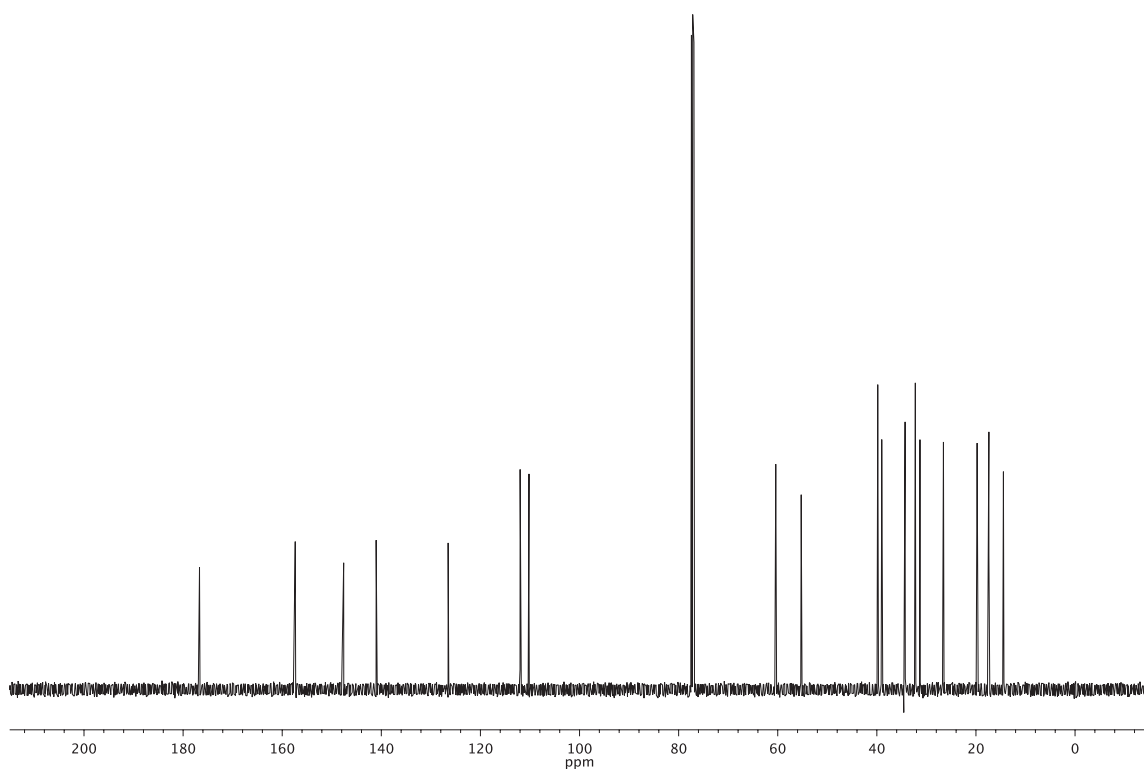


Figure A6.72 ¹³C NMR (126 MHz, CDCl₃) of compound **147**.

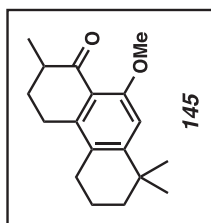
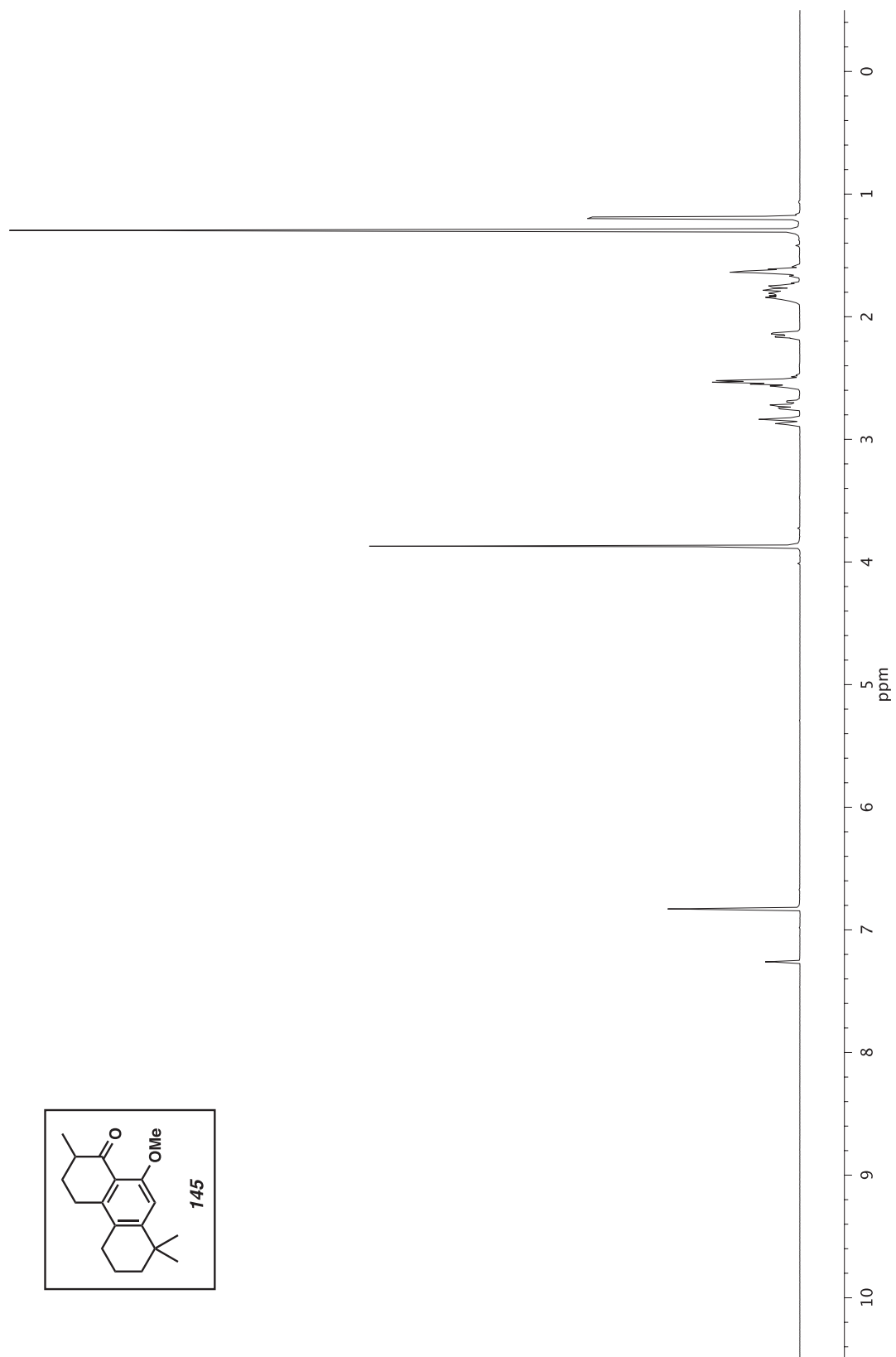


Figure A6.73 ^1H NMR (500 MHz, CDCl_3) of compound **145**.

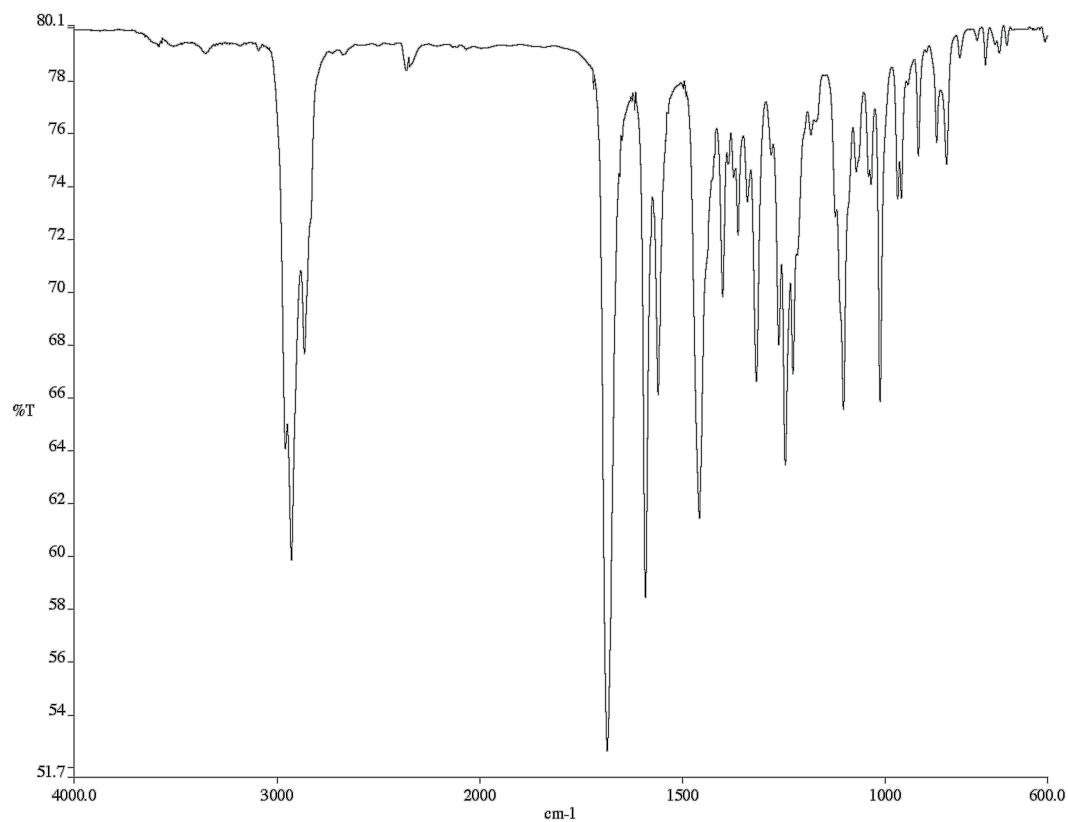


Figure A6.74 Infrared spectrum (Thin Film, NaCl) of compound **145**.

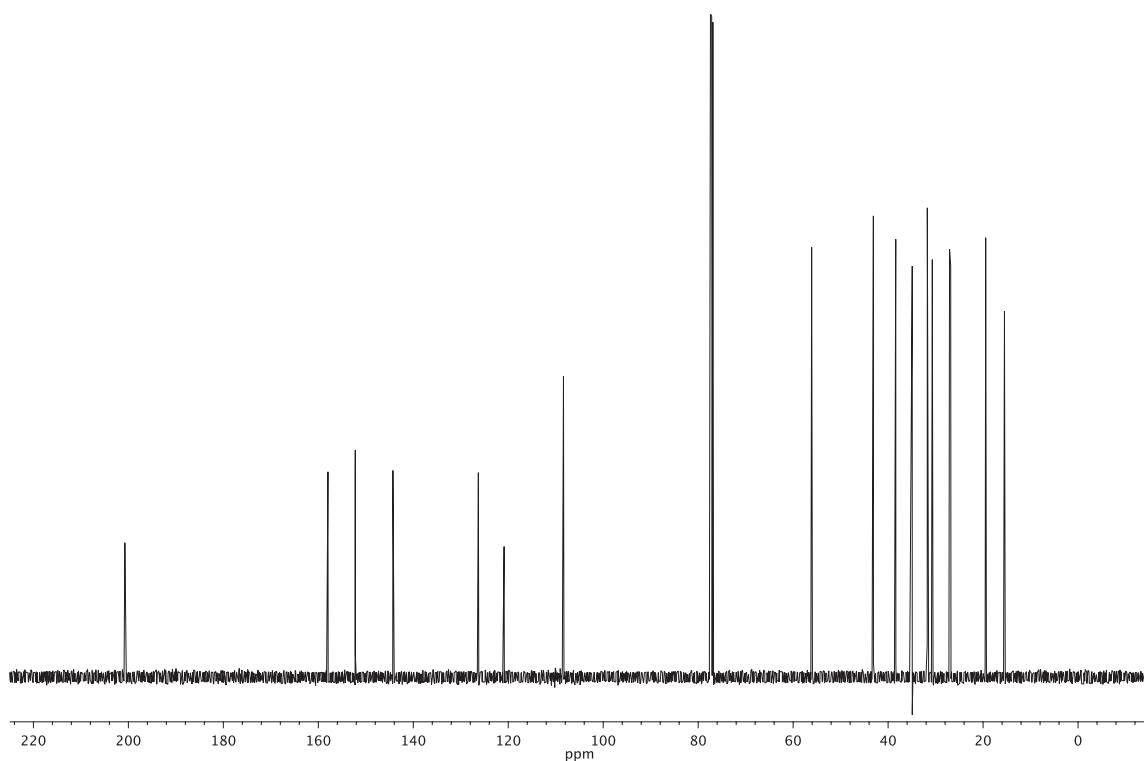


Figure A6.75 ¹³C NMR (126 MHz, CDCl₃) of compound **145**.

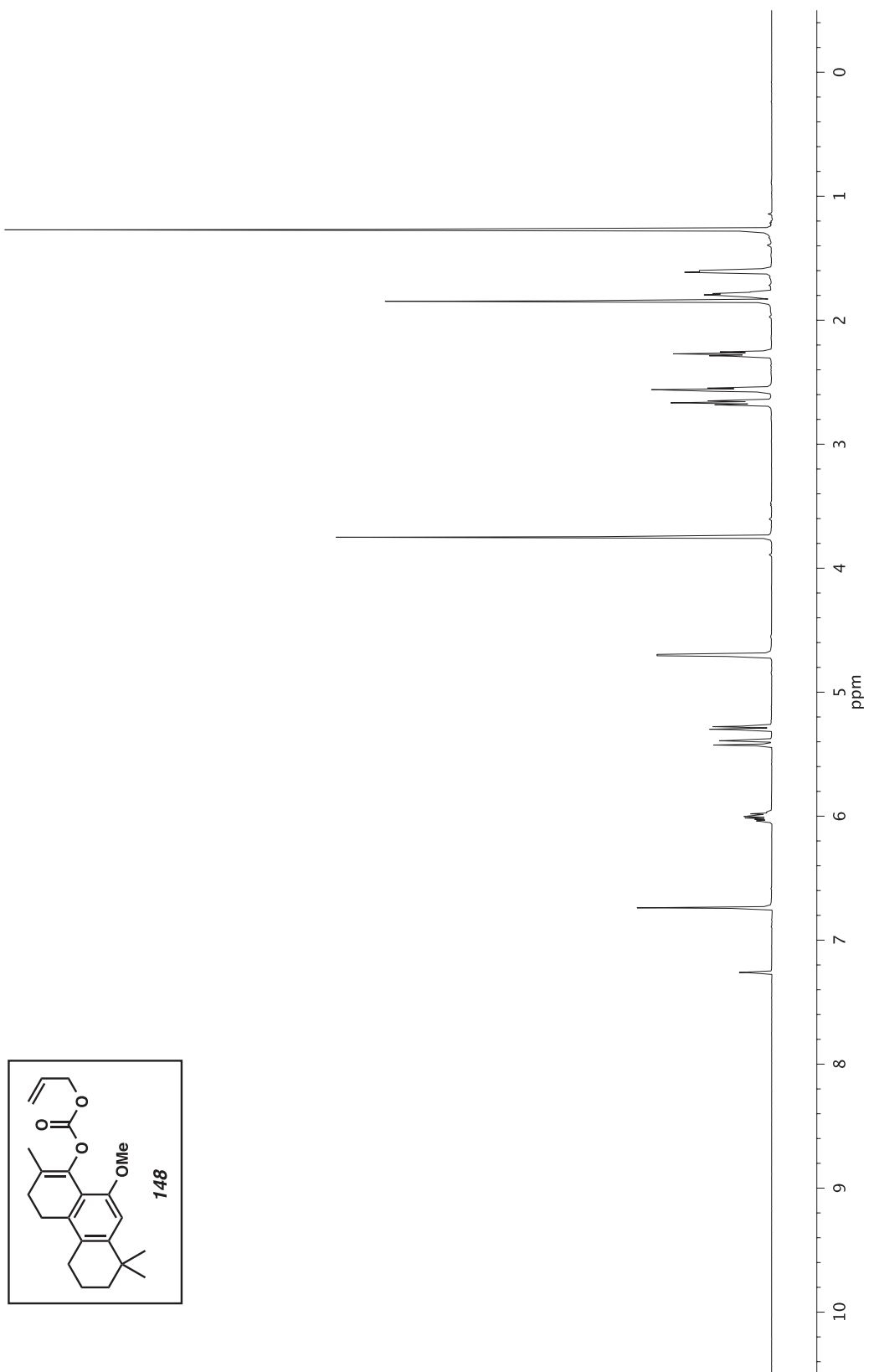


Figure A6.76 $^1\text{H NMR}$ (500 MHz, CDCl_3) of compound **148**.

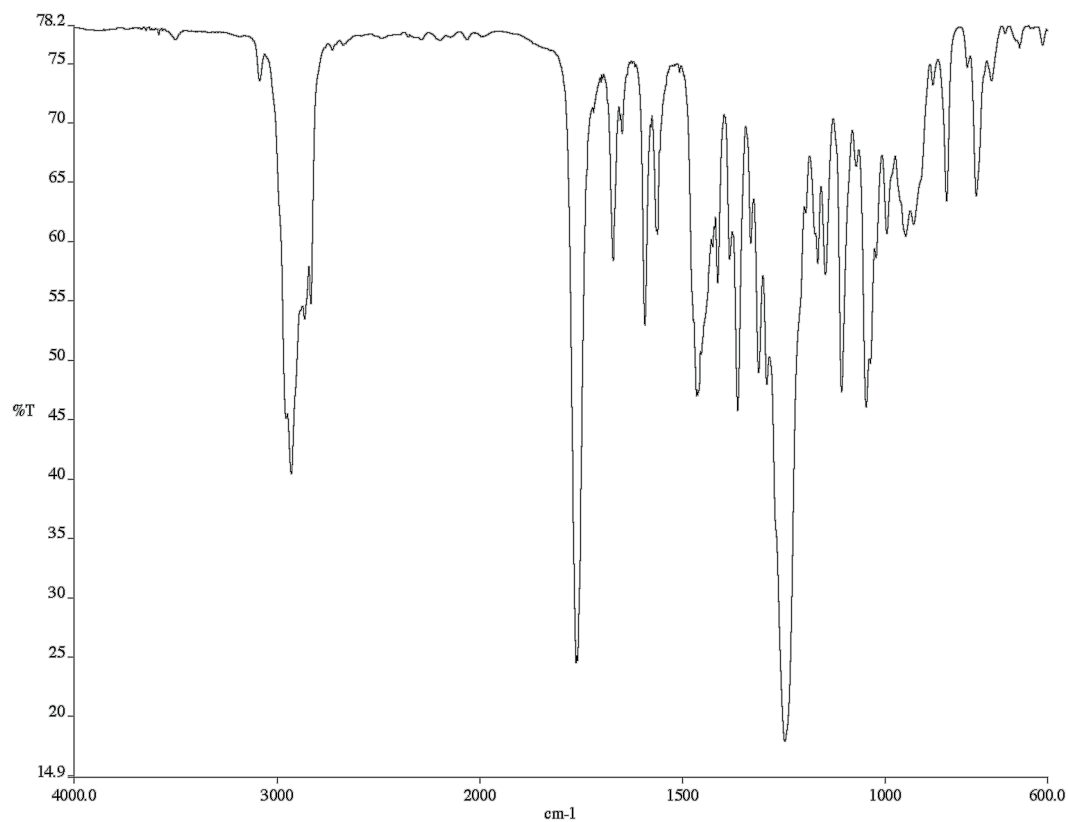


Figure A6.77 Infrared spectrum (Thin Film, NaCl) of compound **148**.

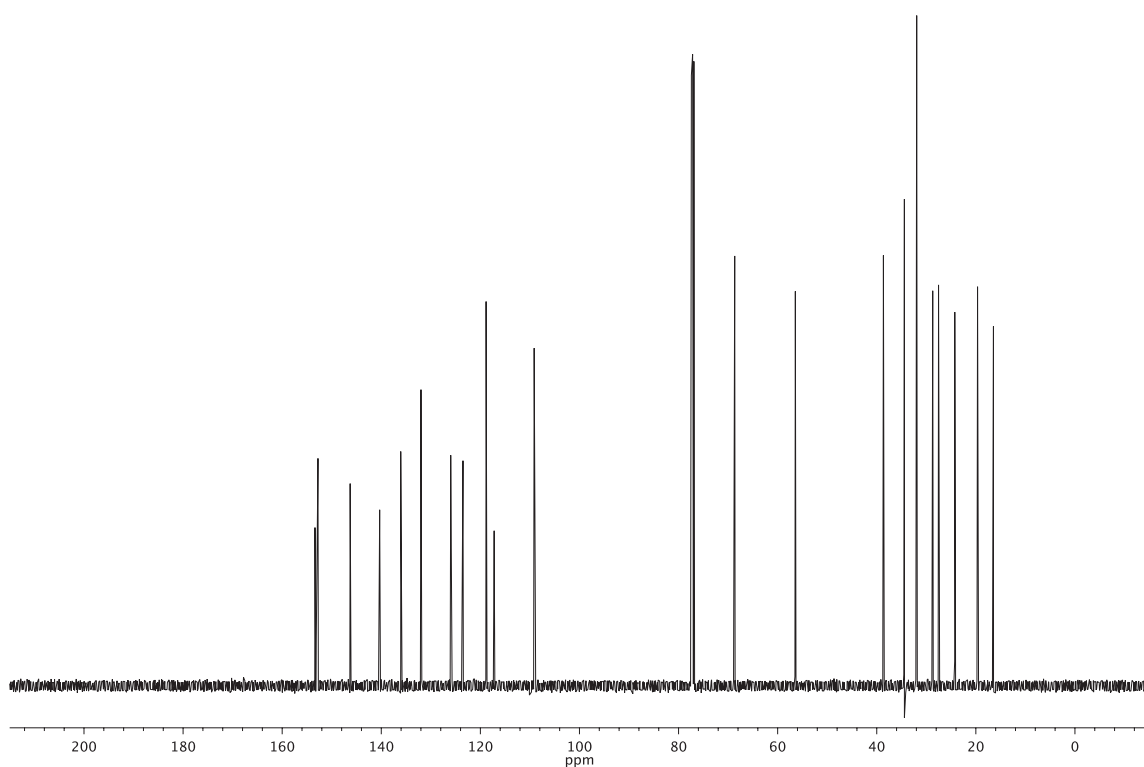


Figure A6.78 ¹³C NMR (126 MHz, CDCl₃) of compound **148**.

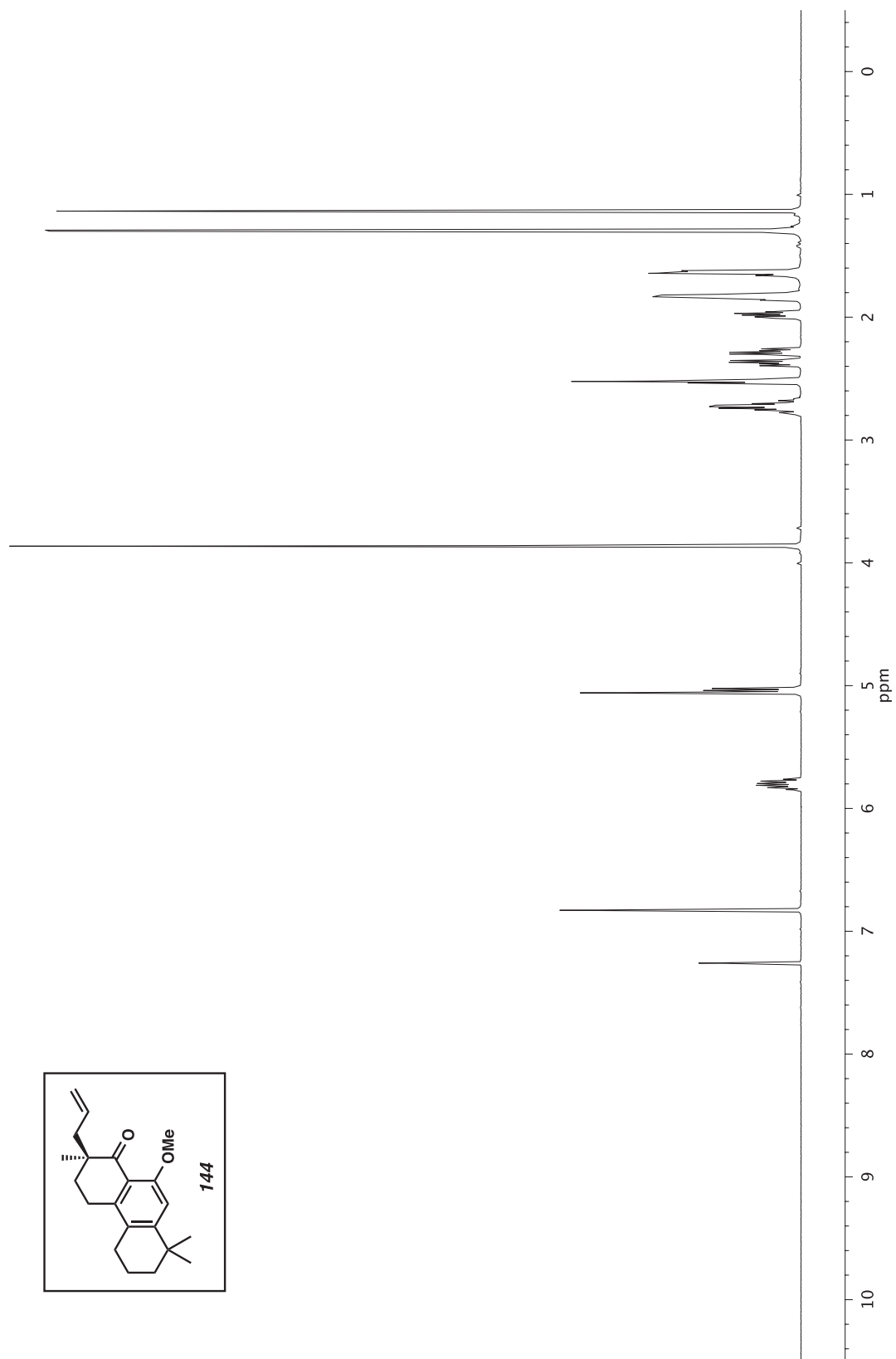


Figure A6.79 $^1\text{H NMR}$ (500 MHz, CDCl_3) of compound **144**.

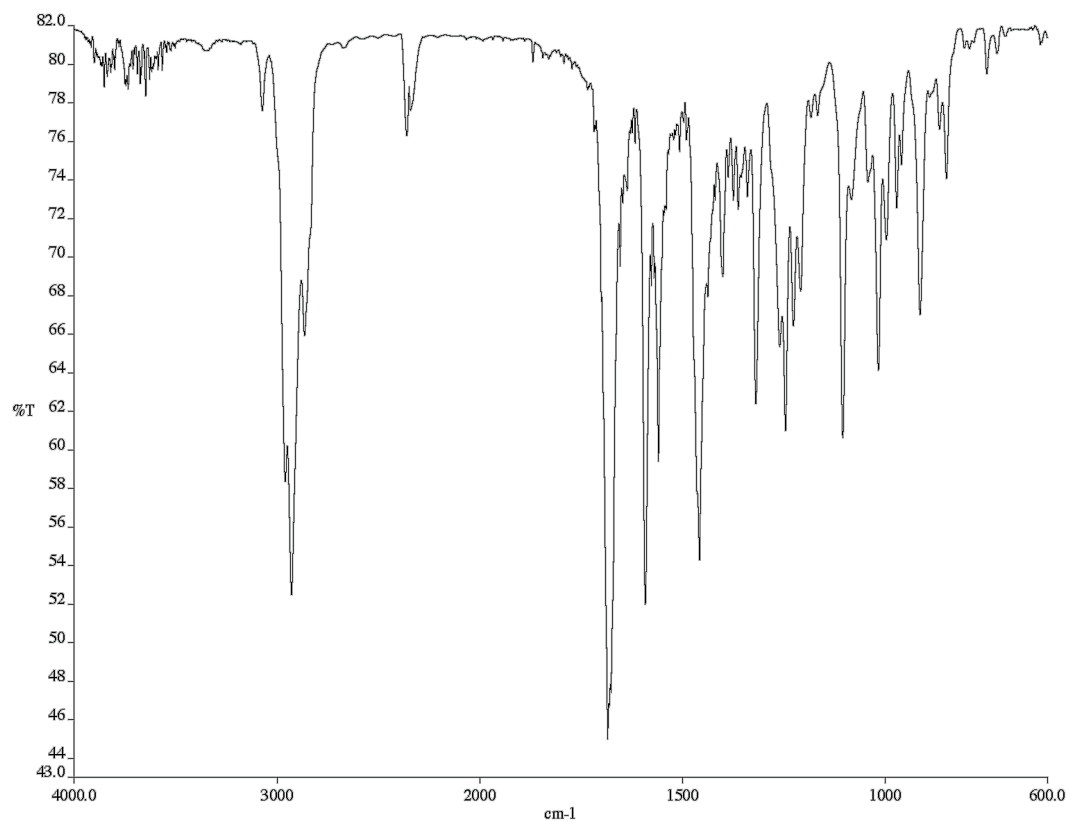


Figure A6.80 Infrared spectrum (Thin Film, NaCl) of compound **144**.

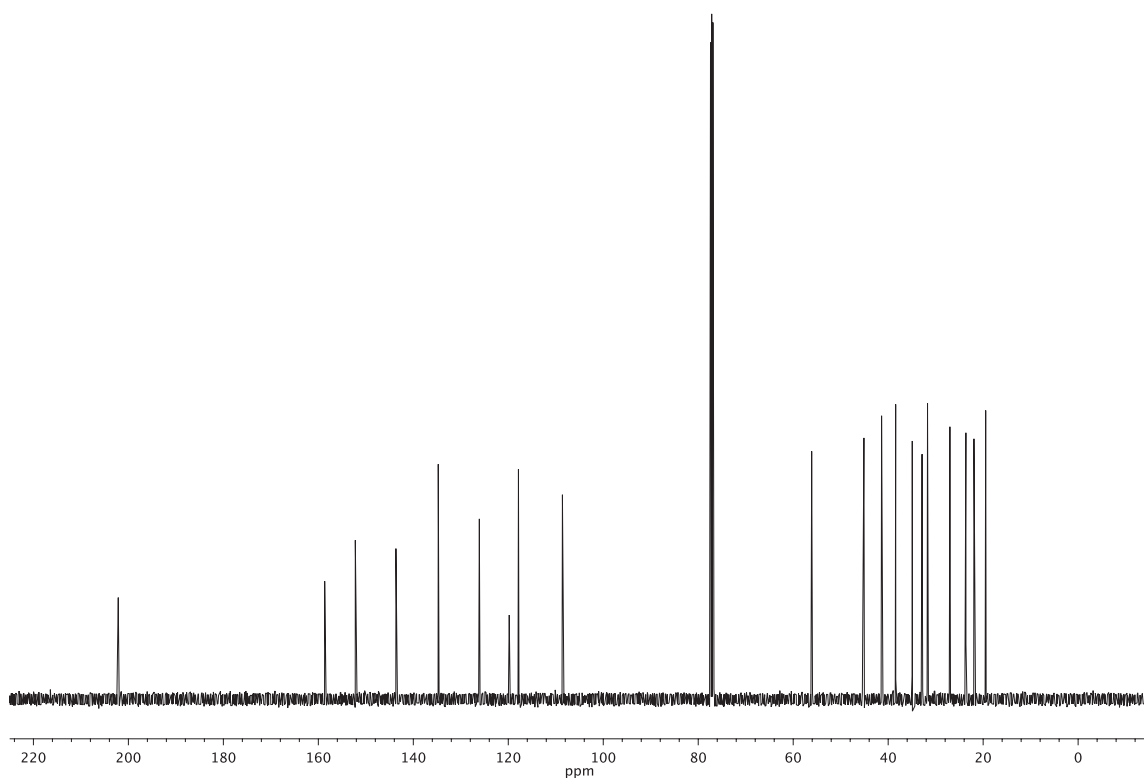


Figure A6.81 ¹³C NMR (126 MHz, CDCl₃) of compound **144**.

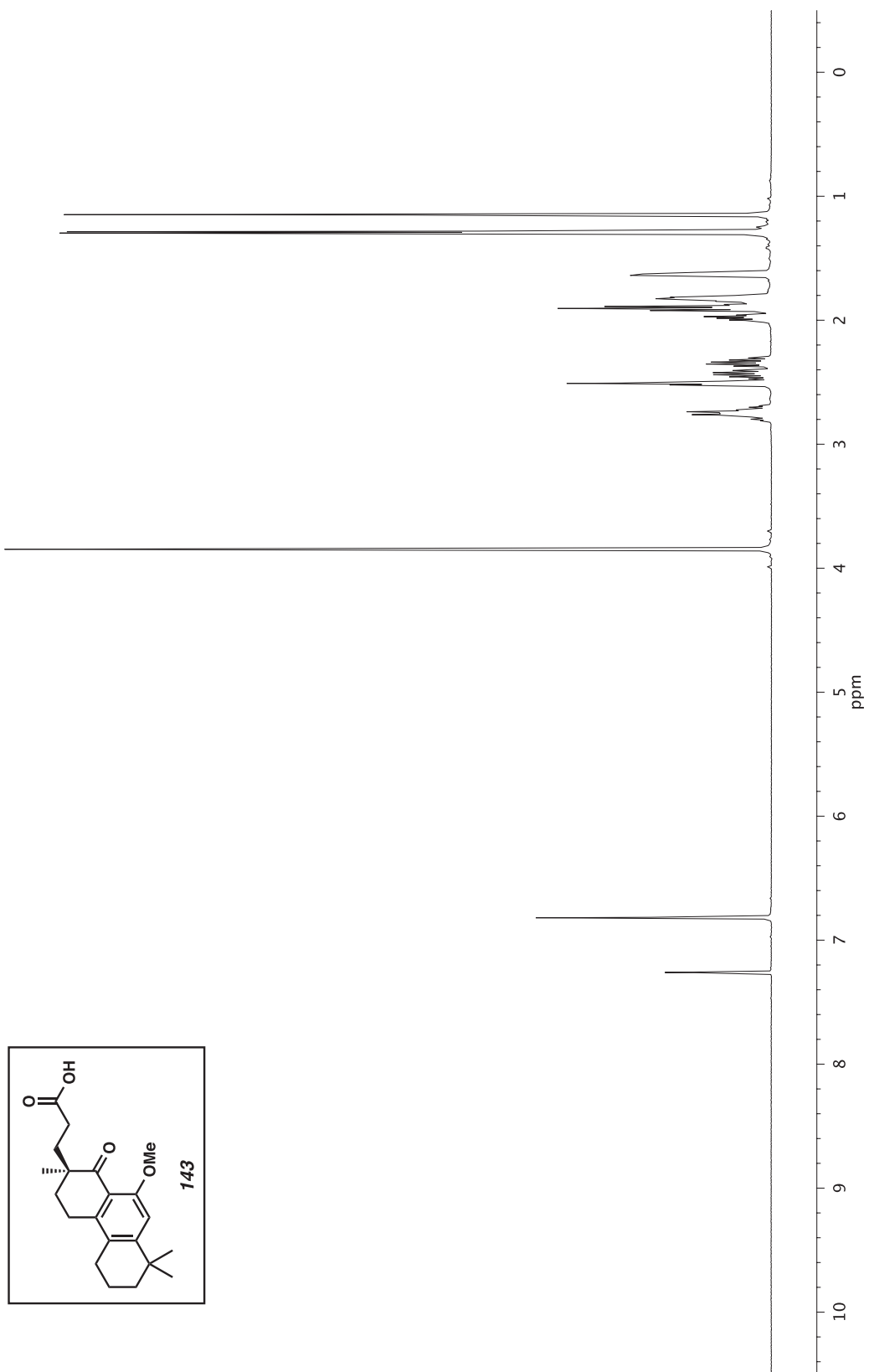


Figure A6.82 ^1H NMR (500 MHz, CDCl_3) of compound **143**.

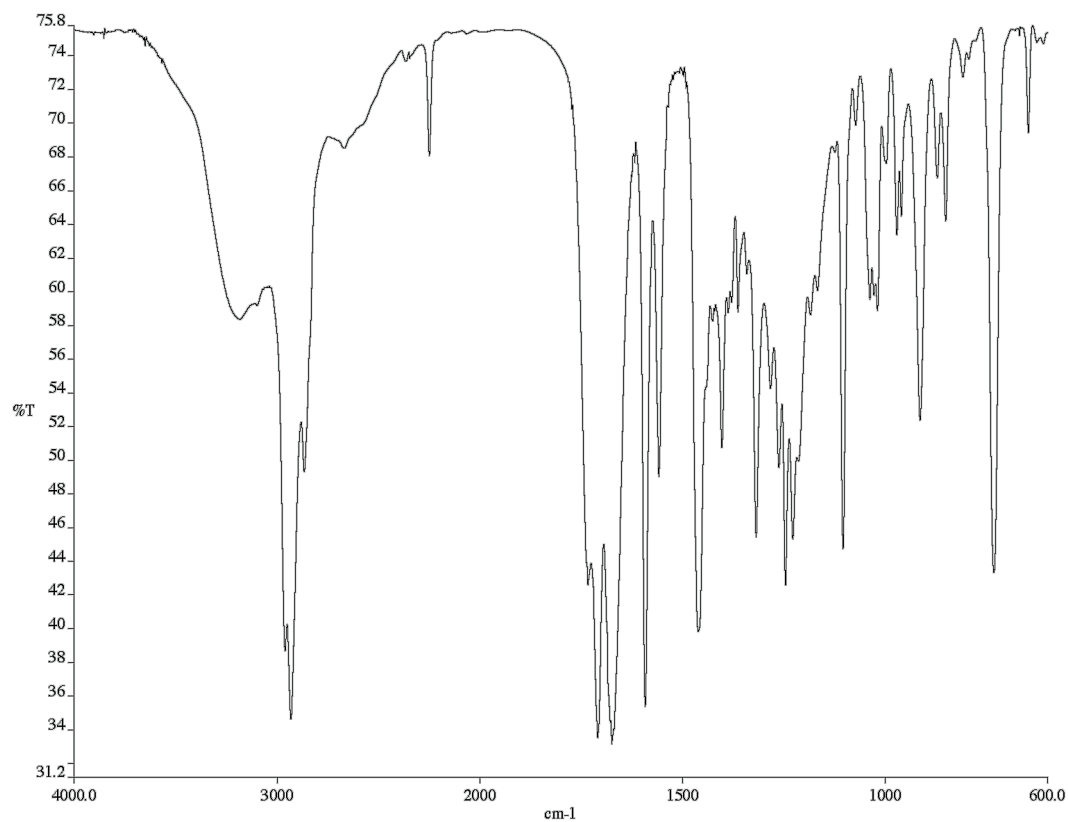


Figure A6.83 Infrared spectrum (Thin Film, NaCl) of compound **143**.

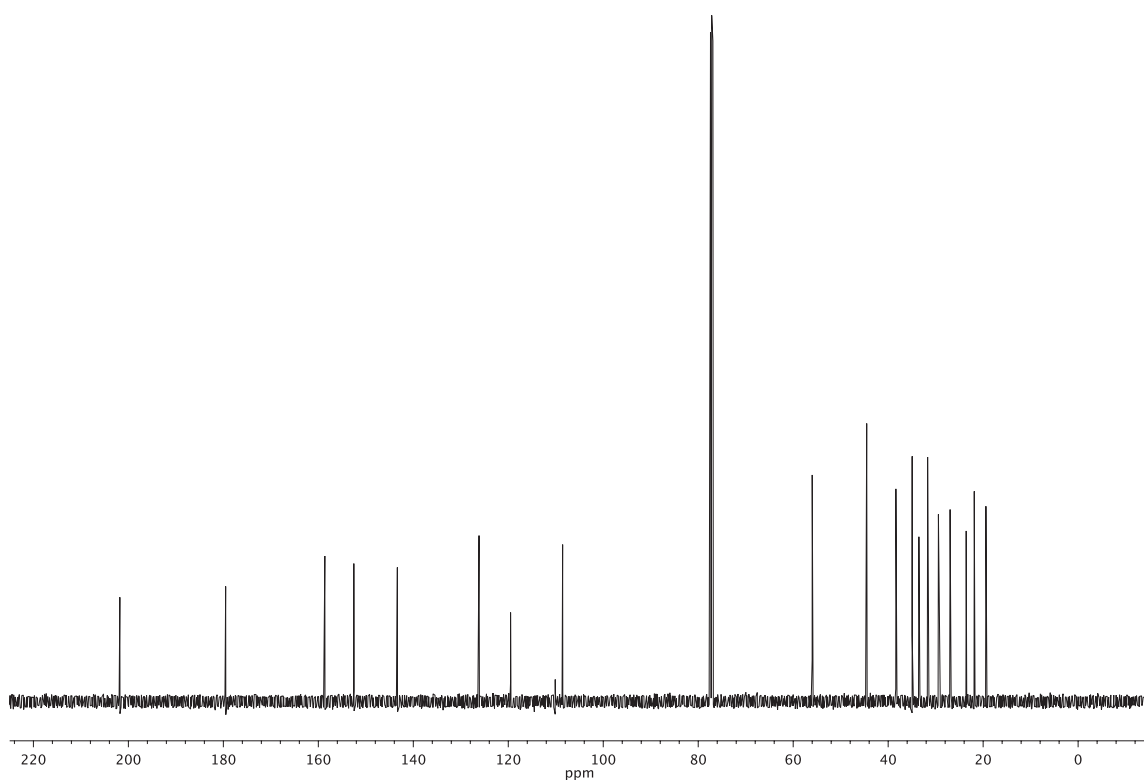


Figure A6.84 ¹³C NMR (126 MHz, CDCl₃) of compound **143**.

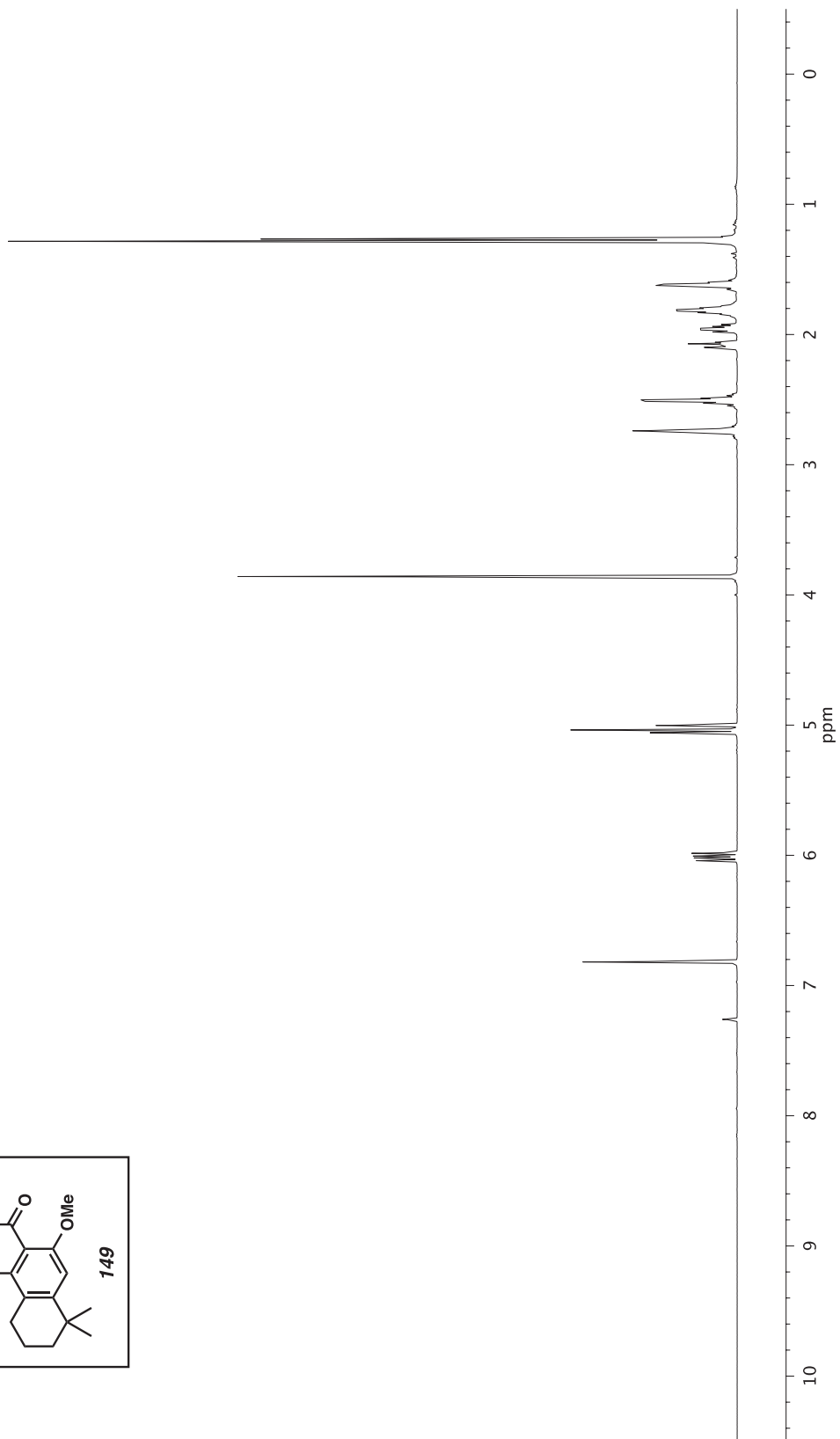
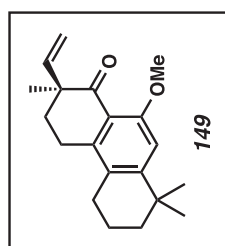


Figure A6.85 ¹H NMR (500 MHz, CDCl₃) of compound **149**.

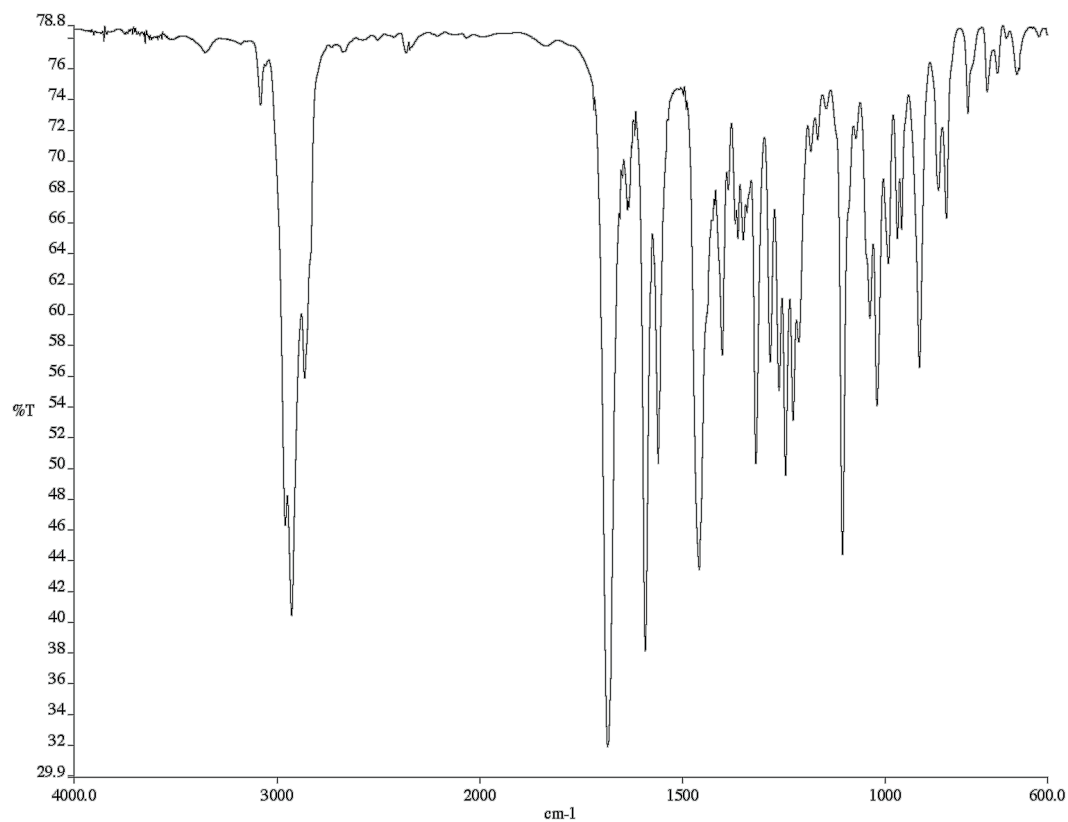


Figure A6.86 Infrared spectrum (Thin Film, NaCl) of compound **149**.

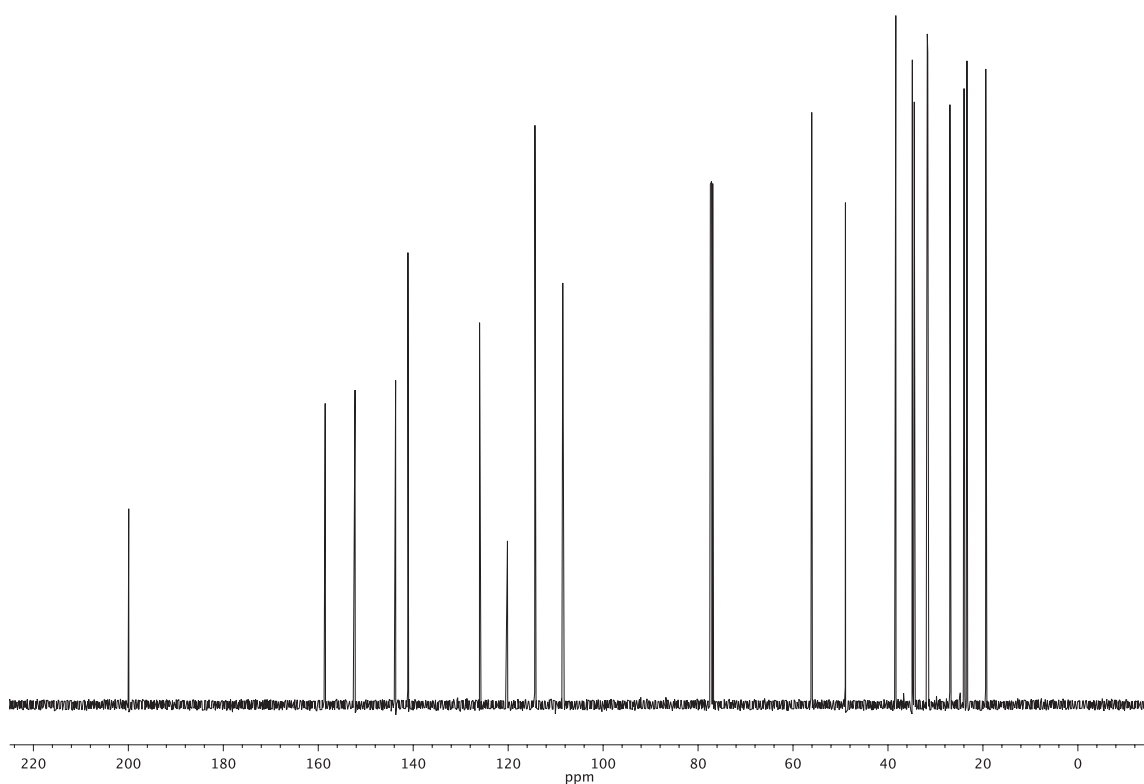


Figure A6.87 ¹³C NMR (126 MHz, CDCl₃) of compound **149**.

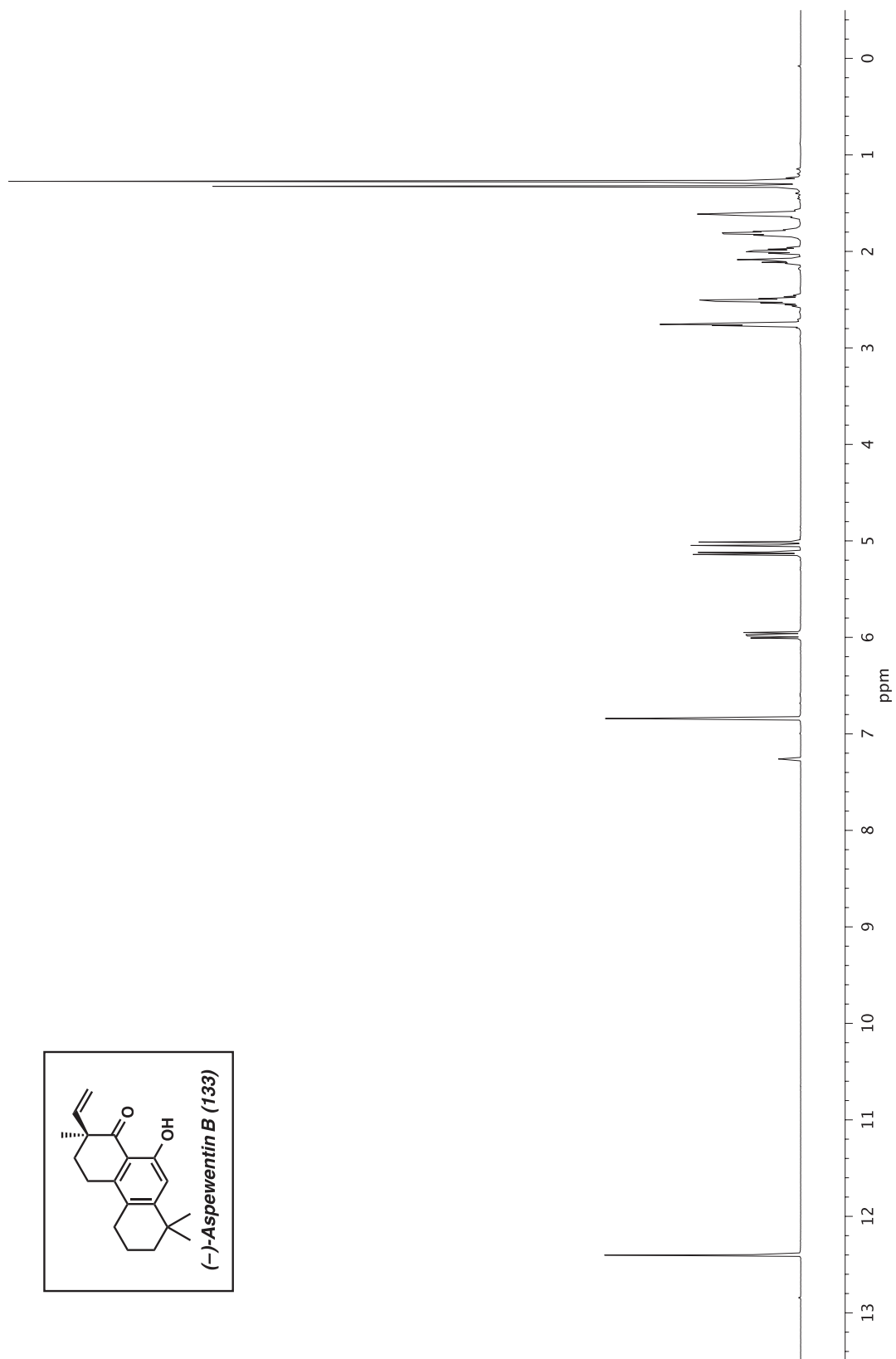
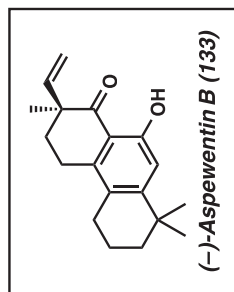


Figure A6.88 ^1H NMR (500 MHz, CDCl_3) of compound 133.

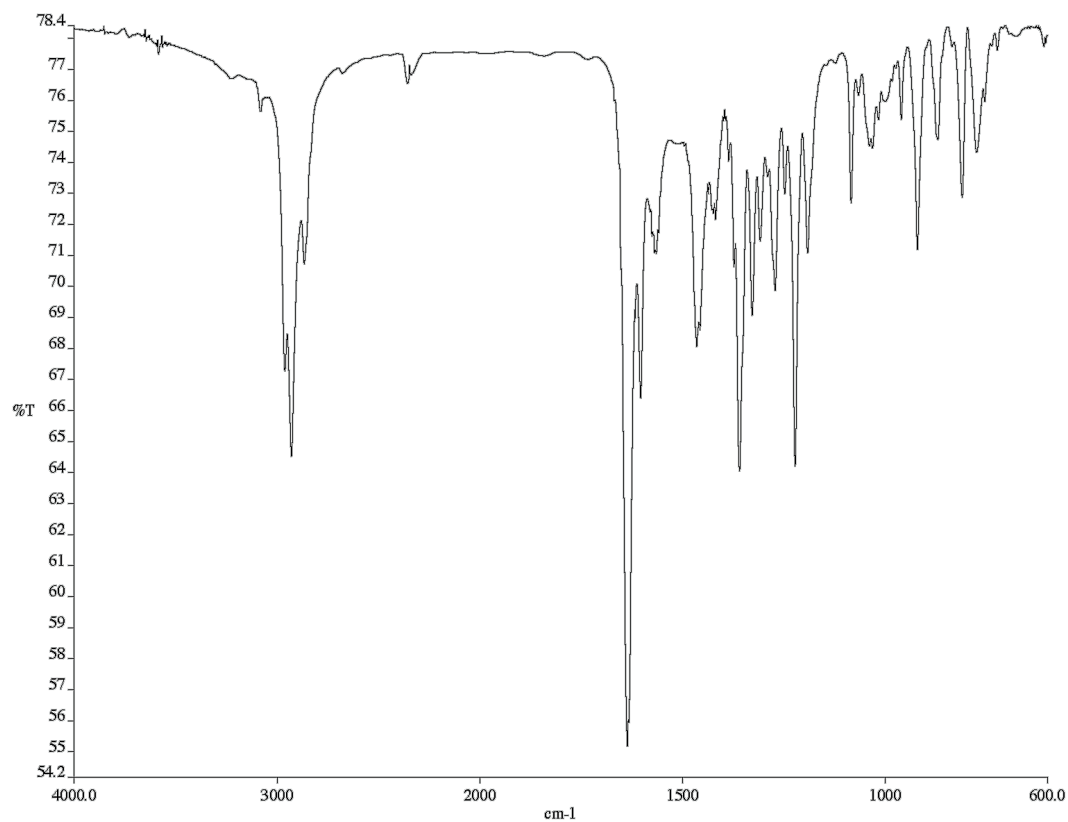


Figure A6.89 Infrared spectrum (Thin Film, NaCl) of compound **133**.

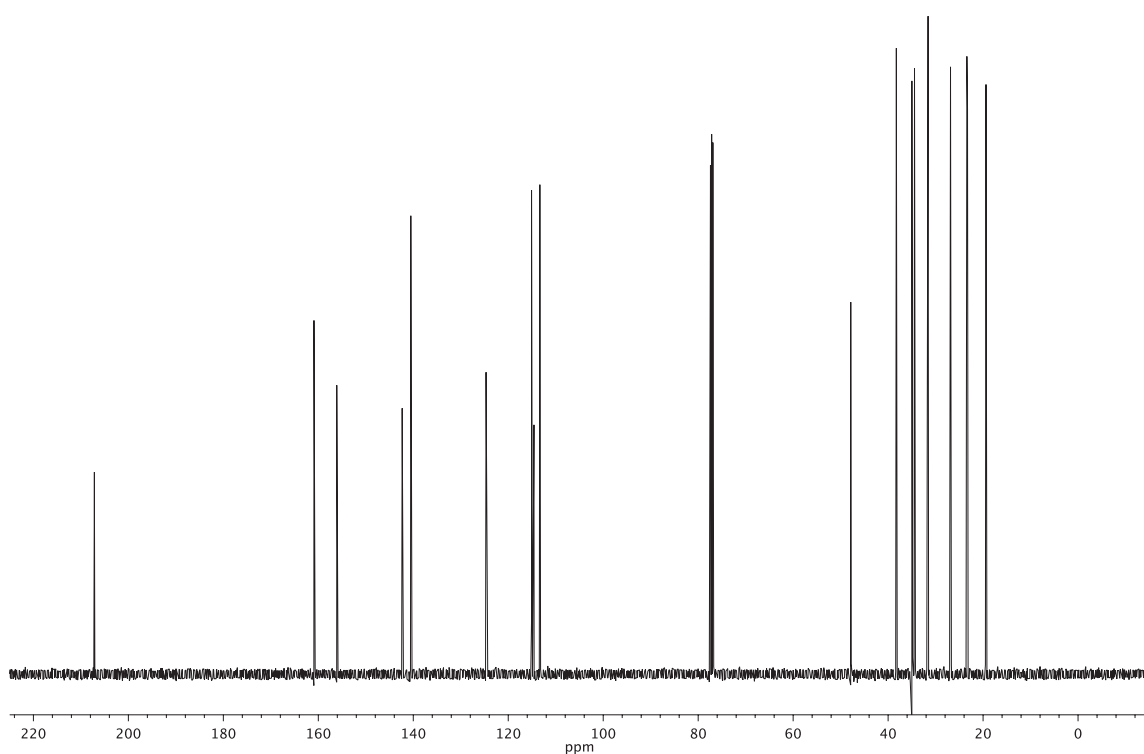
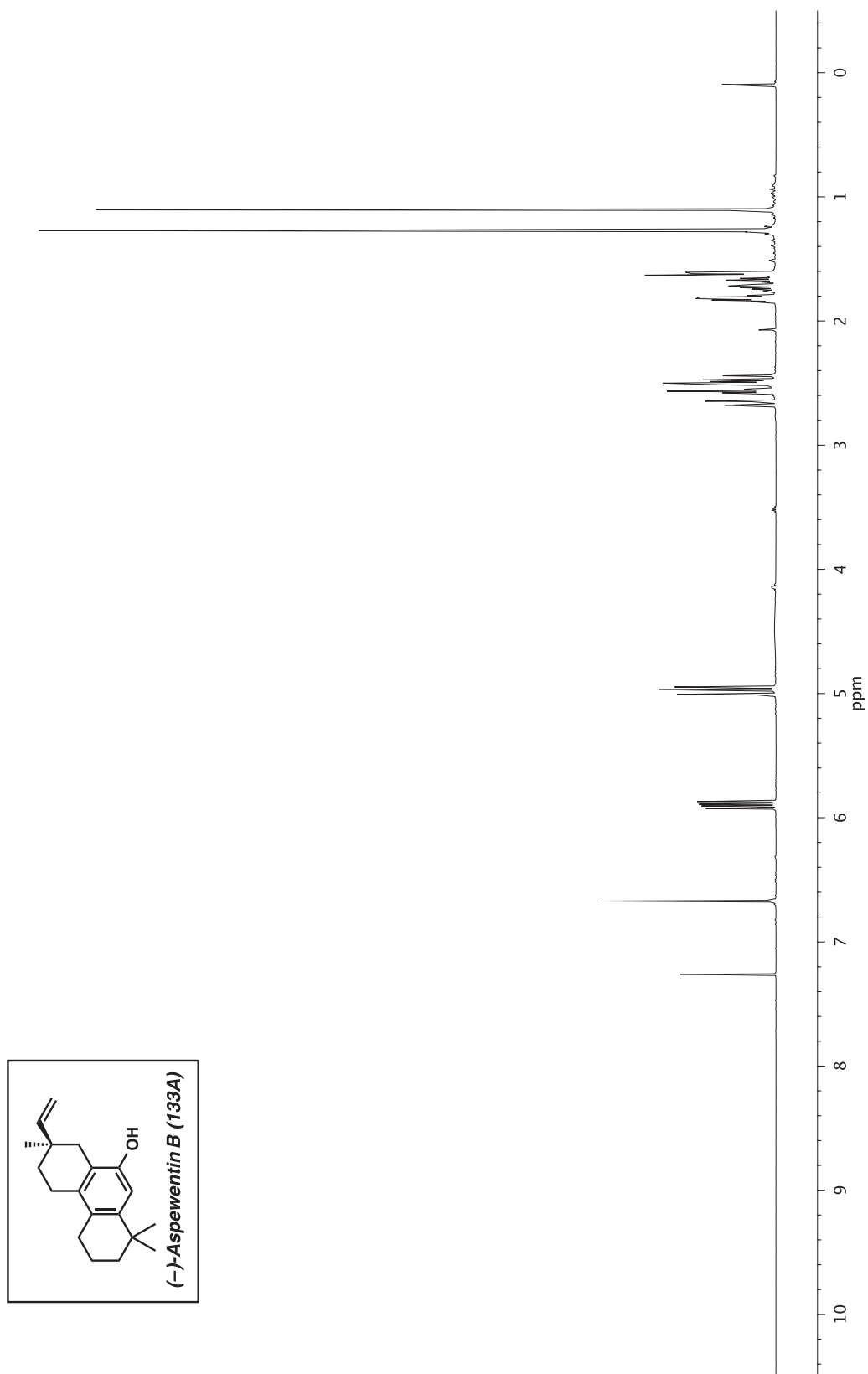


Figure A6.90 ¹³C NMR (126 MHz, CDCl₃) of compound **133**.



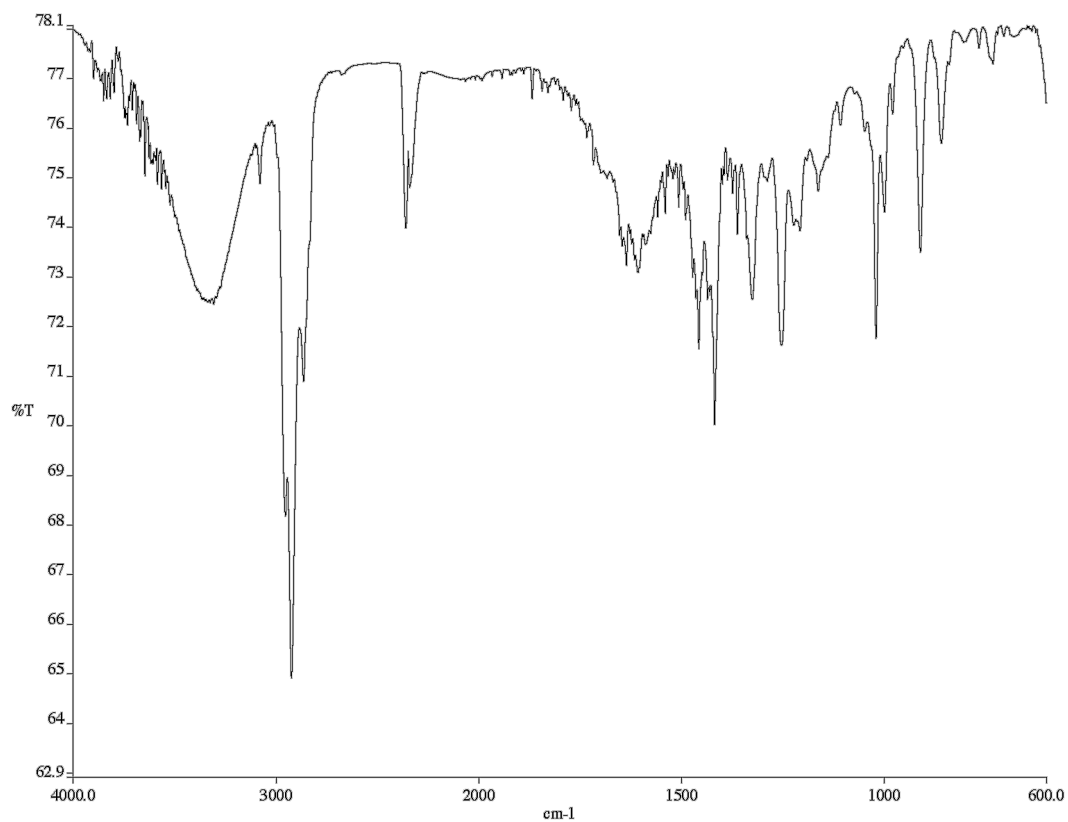


Figure A6.92 Infrared spectrum (Thin Film, NaCl) of compound **133A**.

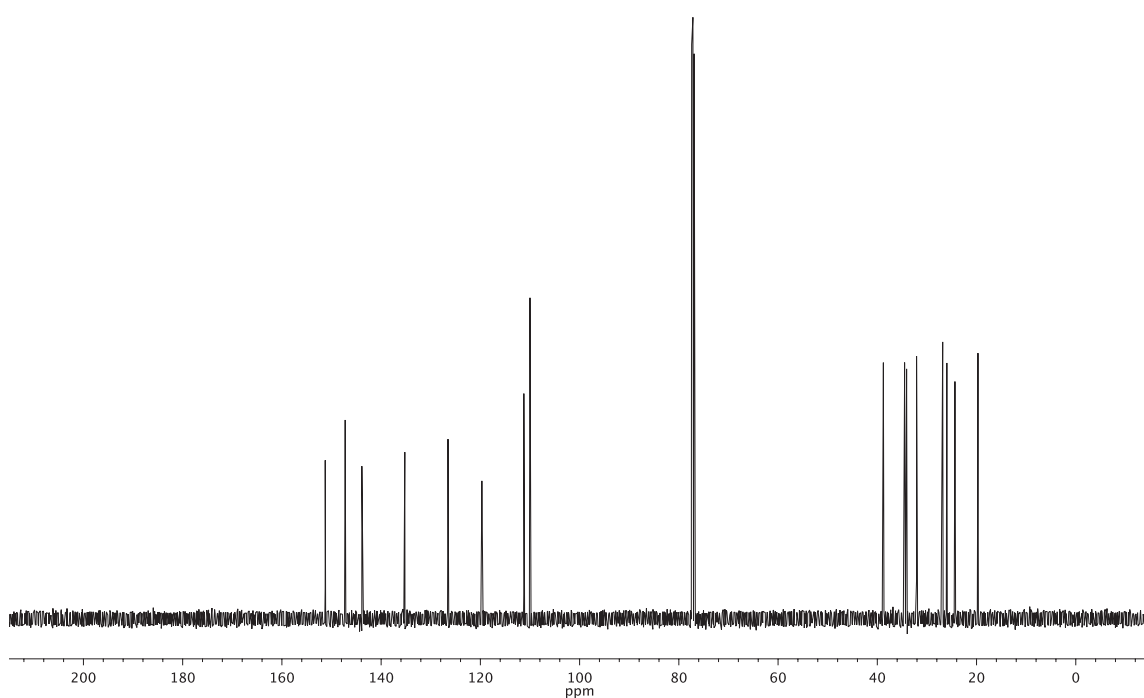


Figure A6.93 ¹³C NMR (126 MHz, CDCl₃) of compound **133A**.

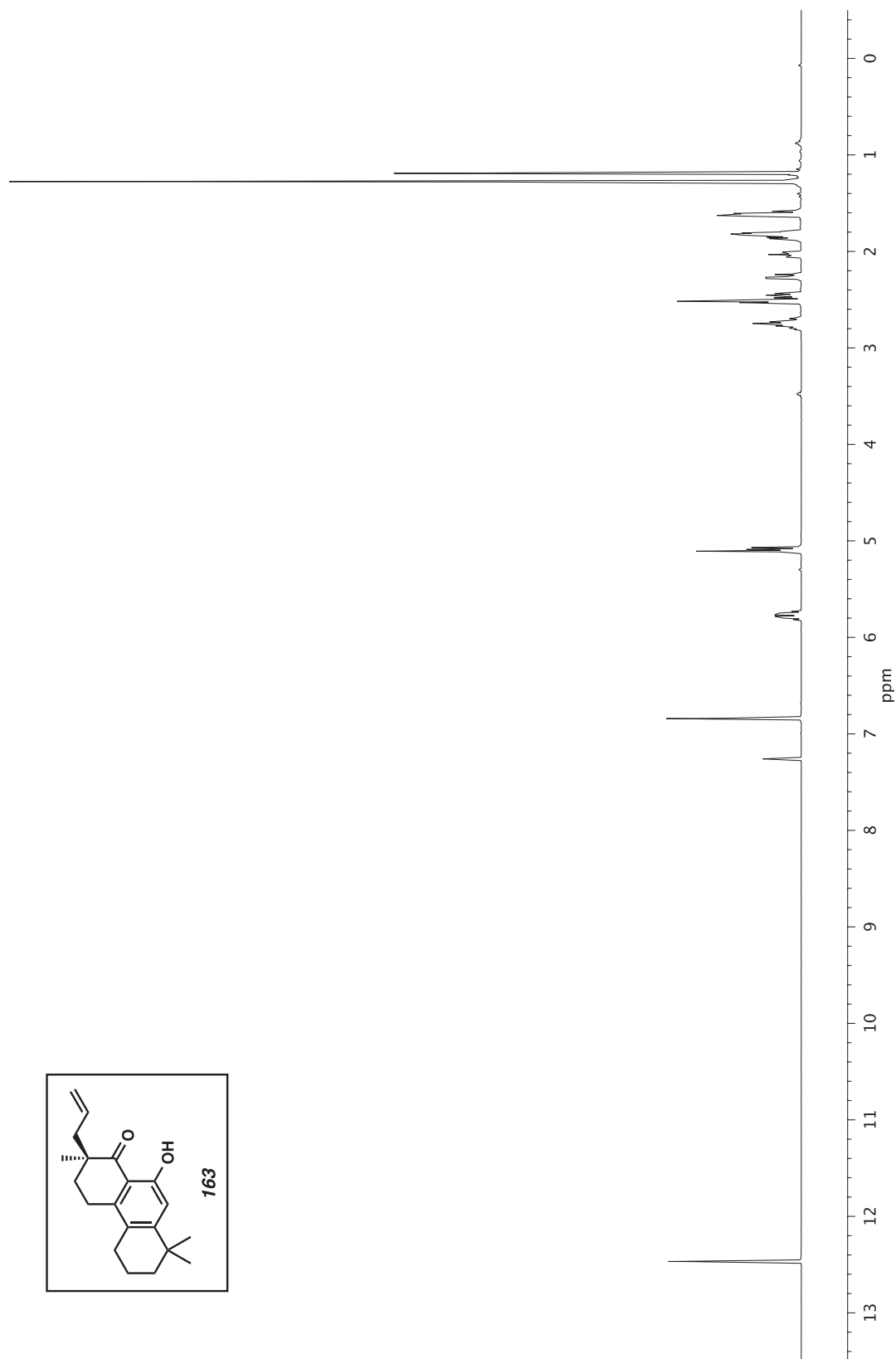


Figure A6.94 ^1H NMR (500 MHz, CDCl_3) of compound **163**.

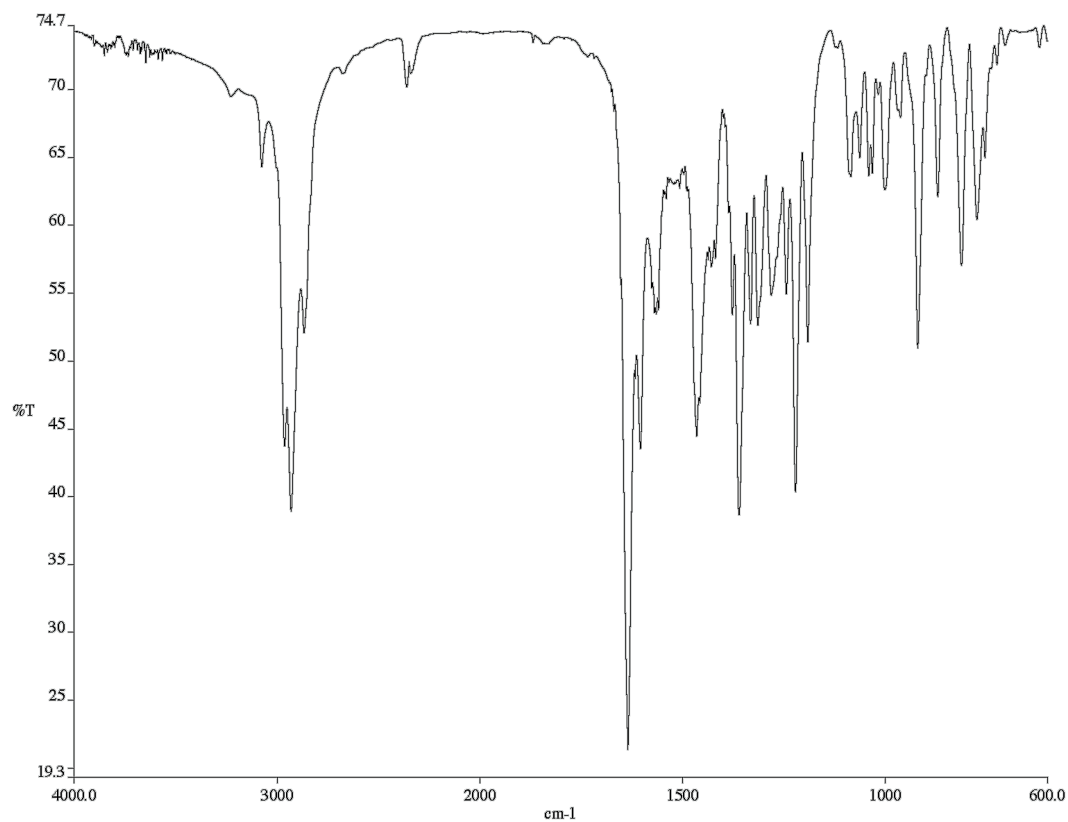


Figure A6.95 Infrared spectrum (Thin Film, NaCl) of compound **163**.

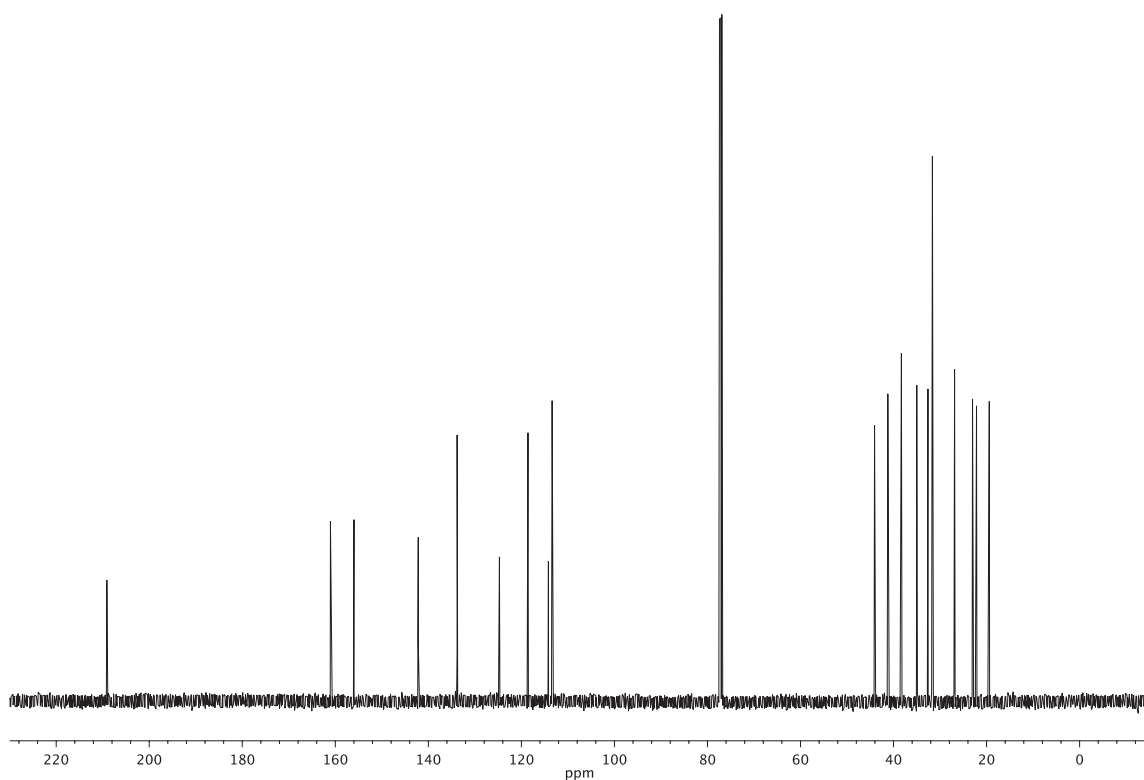


Figure A6.96 ¹³C NMR (126 MHz, CDCl₃) of compound **163**.

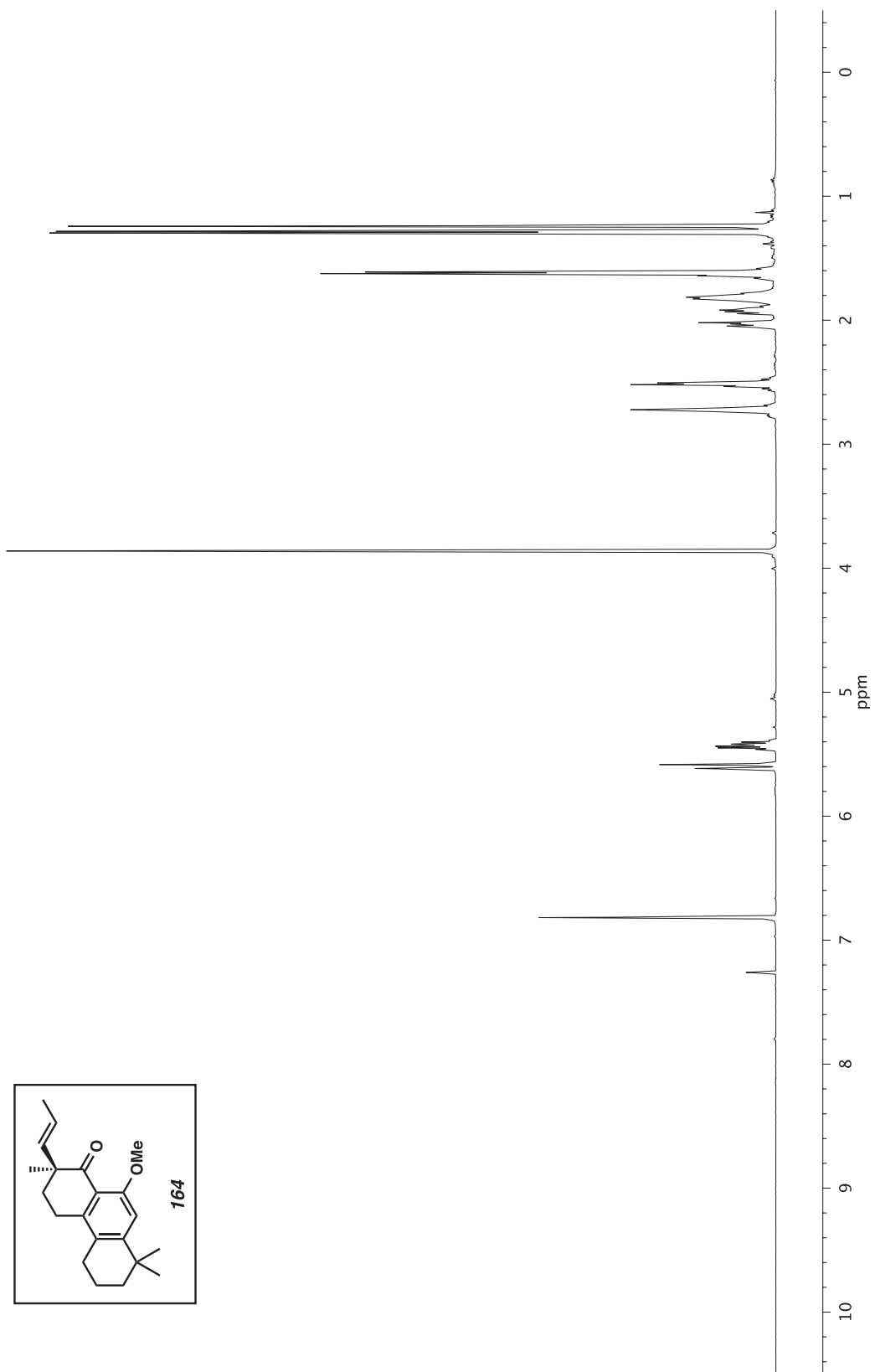


Figure A6.97 ^1H NMR (500 MHz, CDCl_3) of compound **164**.

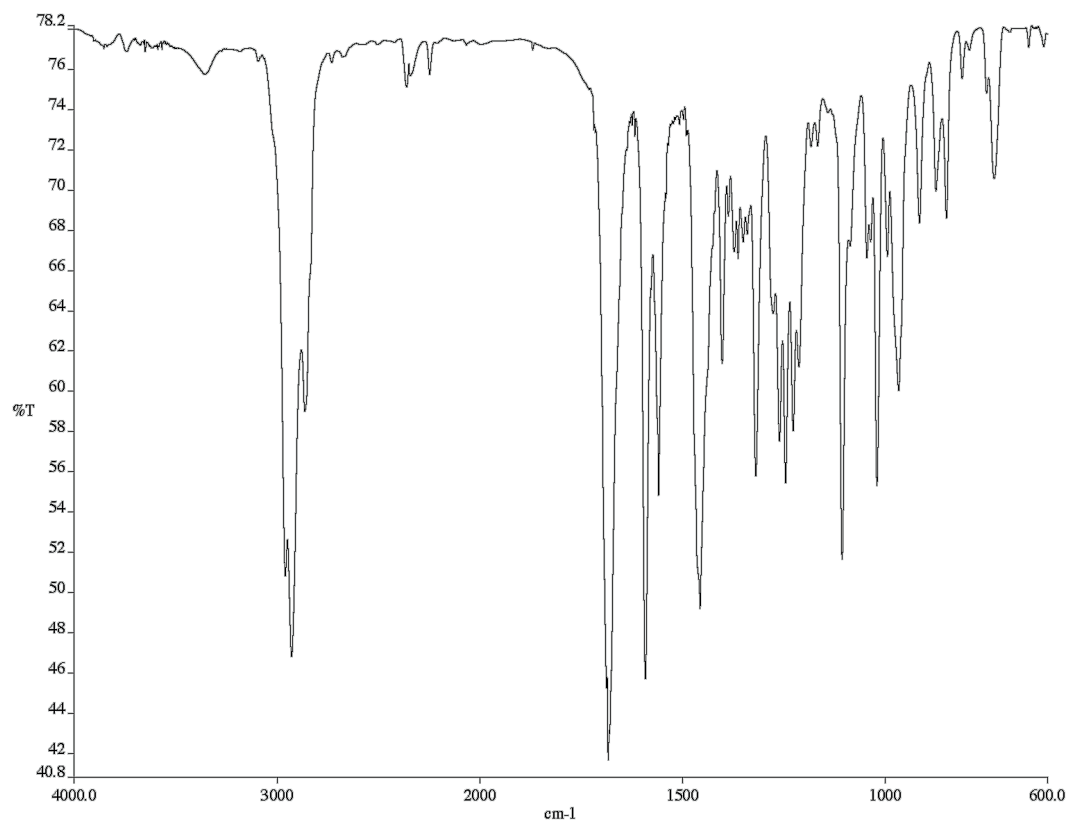


Figure A6.98 Infrared spectrum (Thin Film, NaCl) of compound **164**.

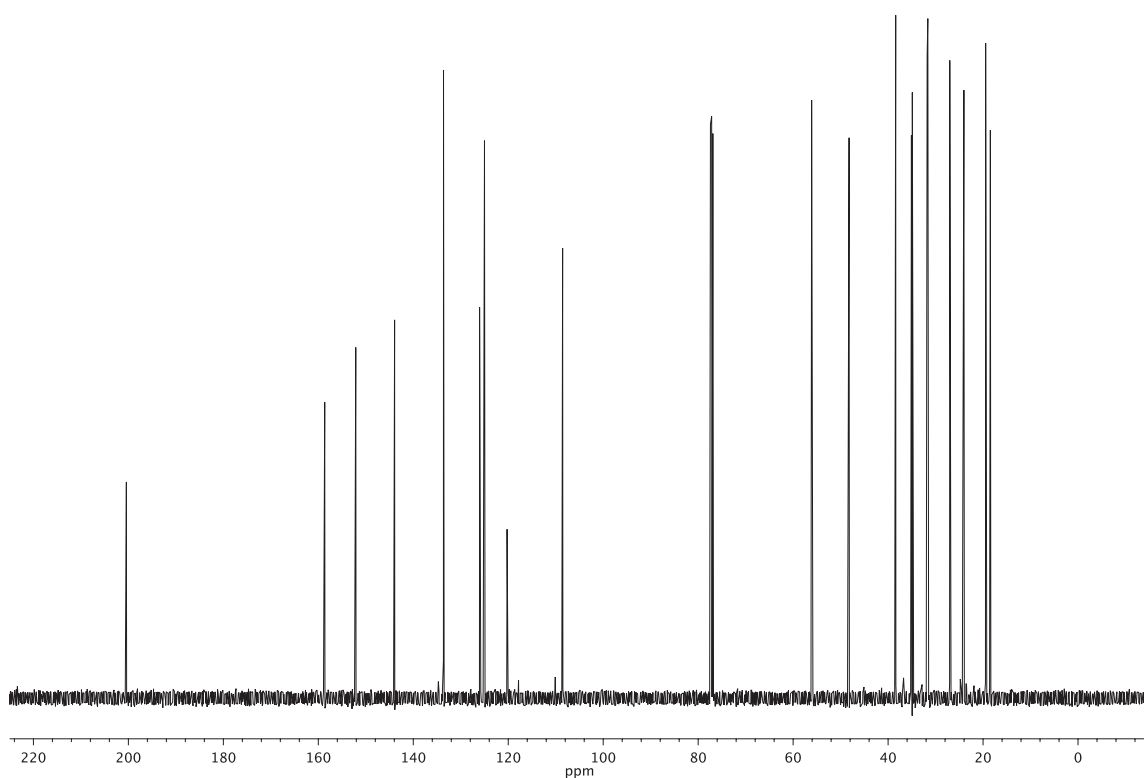


Figure A6.99 ¹³C NMR (126 MHz, CDCl₃) of compound **164**.

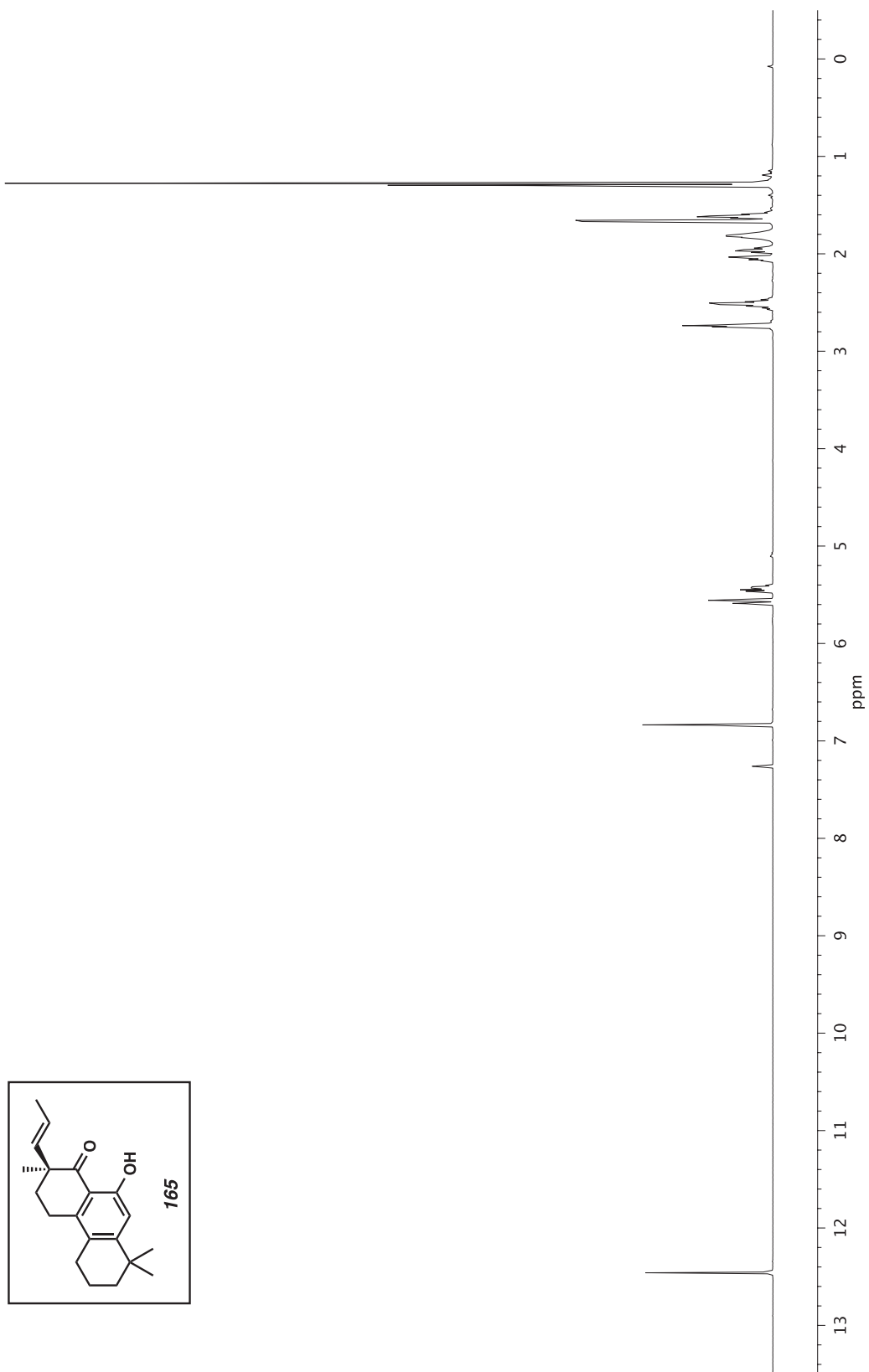


Figure A6.100 ^1H NMR (500 MHz, CDCl_3) of compound **165**.

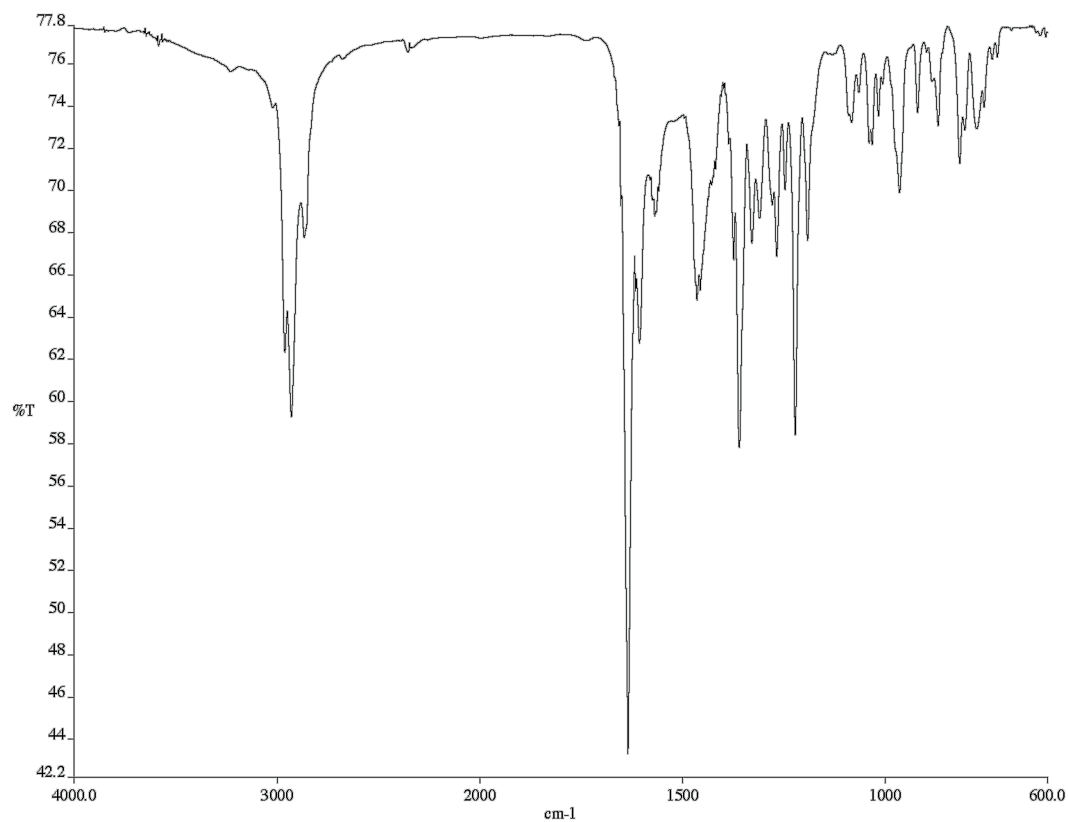


Figure A6.101 Infrared spectrum (Thin Film, NaCl) of compound **165**.

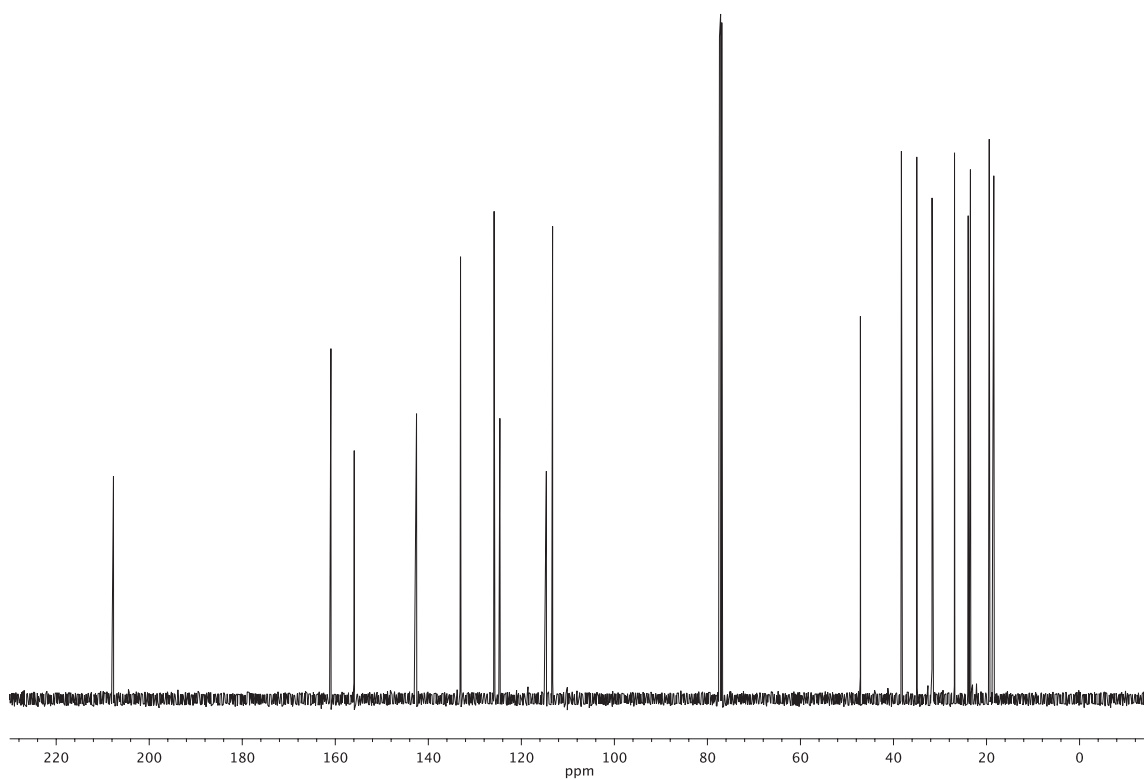


Figure A6.102 ¹³C NMR (126 MHz, CDCl₃) of compound **165**.

APPENDIX 7

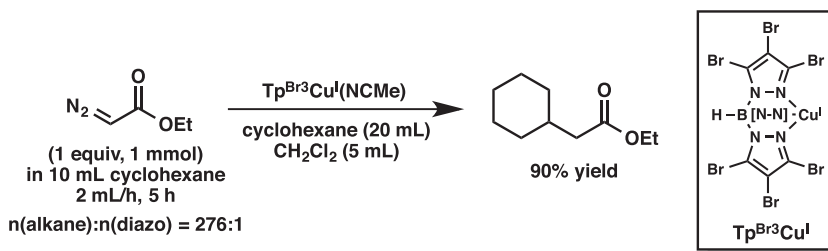
Copper-Catalyzed Insertion of Carbenoids into Unactivated C(sp³)-H Bonds

A7.1 Introduction

Direct functionalization of C–H bonds is a much desired goal in chemistry due to the ubiquity of C–H bonds and the potential to streamline the synthetic sequence.¹ However, C–H bonds are unreactive and often require transition metal complexes for activation and subsequent transformations.² Metal carbenoid insertion into C–H bonds, which forms a new C–C bond, is a viable approach and has witnessed rapid growth in the past few decades.³ The vast majority of examples rely on rhodium, a rare and expensive metal, as catalyst.⁴ From an economic perspective, it is more desirable to use earth-abundant first row transition metal catalysts. This area is much less developed. So far, the only successful system is based on copper-tris(pyrazolyl)borate complexes that catalyze the dediazotization of ethyl diazoacetate and insertion of the resulting copper

carbenoid into unactivated C(sp³)–H bonds of alkanes such as cyclohexane (Scheme A7.1).⁵

Scheme A7.1 Copper-tris(pyrazolyl)borate-catalyzed carbenoid C–H insertions



As a member of the NSF Center for Selective C–H Functionalization, our group became interested in developing new C–H functionalization chemistry using earth-abundant transition metals or main group metals. Although the aforementioned copper system partially addresses this challenge, it requires an exotic ligand and a huge excess of either the alkane substrate or the diazo reagent. We envisioned that a combinatorial screen of metals, ligands, and additives might allow us to spot a readily available catalyst system that performs the task more efficiently. We also wanted to explore C–H functionalization in a complex molecular setting and test the chemo-, regio-, and stereoselectivity of our new catalytic system.

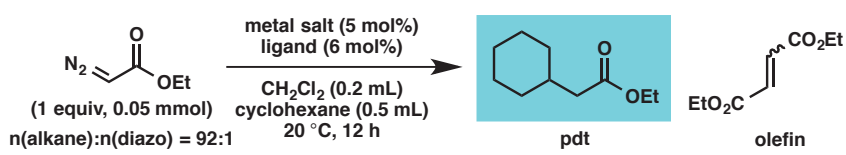
A7.2 Results and Discussions

At the outset of our investigation, we chose cyclohexane as the model alkane substrate and ethyl diazoacetate as the carbenoid precursor. The alkane was used in excess (92:1 molar ratio of alkane to diazo), but not as much as in the literature (276:1,

see Scheme A7.1). The desired product (ethyl cyclohexyl-acetate) and olefin side products (diethyl maleate/diethyl fumarate, resulting from carbenoid dimerization) are all commercially available. Thus, a simple GC assay enables quantitative measurement of yield and selectivity. Selectivity is defined as the ratio of desired product peak area to the total peak areas of both the desired product and olefin side products.

First, we surveyed a combination of first-row transition metal triflates and ligands for their ability to catalyze the carbenoid insertion reaction (Table A7.1). Manganese(II), iron(II), and nickel(II) triflates were all ineffective at dediazotization since neither the desired insertion product nor olefin byproducts were observed. Copper(II) triflate, on the other hand, catalyzed dediazotization efficiently. Unfortunately, the desired insertion product was formed in only trace amounts, while the vast majority of the diazo reagent went into the olefin side products.

Table A7.1 Screen of metal salts and ligands ^a



metal ligand	Mn ^{II} (OTf) ₂	Fe ^{II} (OTf) ₂	Ni ^{II} (OTf) ₂	Cu ^{II} (OTf) ₂	% selectivity ^b [for Cu ^{II} (OTf) ₂]
2,2'-bipy	0	0	0	0.9	4
1,10-phen	0	0	0	2.2	9
(S)- <i>t</i> -BuPHOX	0	0	0	1.2	4
PPh ₃	0	0	0	1.4	7
PCy ₃	0	0	0	1.9	7

^a Yield of desired insertion product determined by GC using tridecane as internal standard.

^b Selectivity = A(pdt)/[A(pdt)+A(olefin)].

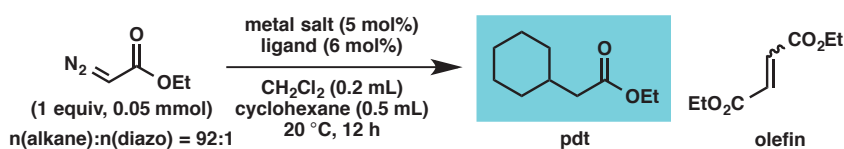
Having identified $\text{Cu}(\text{OTf})_2$ as a uniquely effective metal catalyst, we proceeded to investigate the effect of ligands (Table A7.2). Phosphine ligands (except bis(dicyclohexylphosphino)butane, entry 5) did not improve product yield but increased selectivity (entries 1–4, 6–8). In the absence of ligand, the reaction proceeded with slightly higher yield (entry 9).

Table A7.2 Screen of ligands with $\text{Cu}(\text{OTf})_2$ ^a

entry	ligand	% pdt yield	% selectivity ^b
1	dppm	2.3	12
2	dppe	2.7	16
3	dppp	1.9	8
4	dppb	2.3	13
5	dcypb	0	
6	dppf	2.2	13
7	(2-biph)P(<i>t</i> -Bu) ₂	2.0	17
8	Xantphos	2.2	12
9		3.9	15

^a Yield of desired insertion product determined by GC using tridecane as internal standard. ^b Selectivity = $A(\text{pdt})/[A(\text{pdt})+A(\text{olefin})]$.

Next, we investigated other metal salts (copper and non-copper) with or without ligand (Table A7.3). We found that $(\text{MeCN})_4\text{Cu}^+\text{PF}_6^-$ was a more effective catalyst in both yield and selectivity than any salt/ligand combination previously screened (entry 3). Lewis acidic main group metal salts, which are expected to be able to dediazotize ethyl diazoacetate, proved to be ineffective (entries 5 and 6).

Table A7.3 Screen of other metal salts ^a

entry	metal salt	ligand	% pdt yield	% selectivity ^b
1	Cu ^{II} Cl ₂	1,10-phen	0	
2	Cu ^{II} (<i>O</i> - <i>i</i> -Bu) ₂	1,10-phen	0	
3	(MeCN) ₄ Cu ^I PF ₆		7.8	37
4	(<i>R,R</i>)-Co ^{II} (<i>t</i> -Bu ₄ Salen)		0	
5	Ca ^{II} (<i>O</i> - <i>i</i> -Pr) ₂		0	
6	Mg ^{II} Br ₂ •OEt ₂		0	
7	Co ^{II} Cl ₂	1,10-phen	0	
8	Co ^{II} Br ₂	1,10-phen	0	
9	Cr ^{II} Cl ₂	1,10-phen	0	

^a Yield of desired insertion product determined by GC using tridecane as internal standard. ^b Selectivity = A(pdt)/[A(pdt)+A(olefin)].

Since Cu^I was found to be more effective than Cu^{II} salts, we next performed a screen of additives/ligands with (MeCN)₄Cu^IPF₆ (Figure A7.1) as well as with Cu^I(OTf)•toluene (Figure A7.2). The best results are summarized in Table A7.4. Generally, we found that additives bearing acidic protons promote the desired C–H insertion. In particular, carbanilide (entry 1) gave the highest selectivity for the desired insertion product (51%). However, the highest yield is only 11.6%, not much higher than that of the ligand-free conditions (8.7%, entry 6; see also Table A7.3, entry 3). These results demonstrate that the acidic additives could inhibit carbenoid dimerization, which forms the olefin side products, but could not significantly promote C–H insertion.

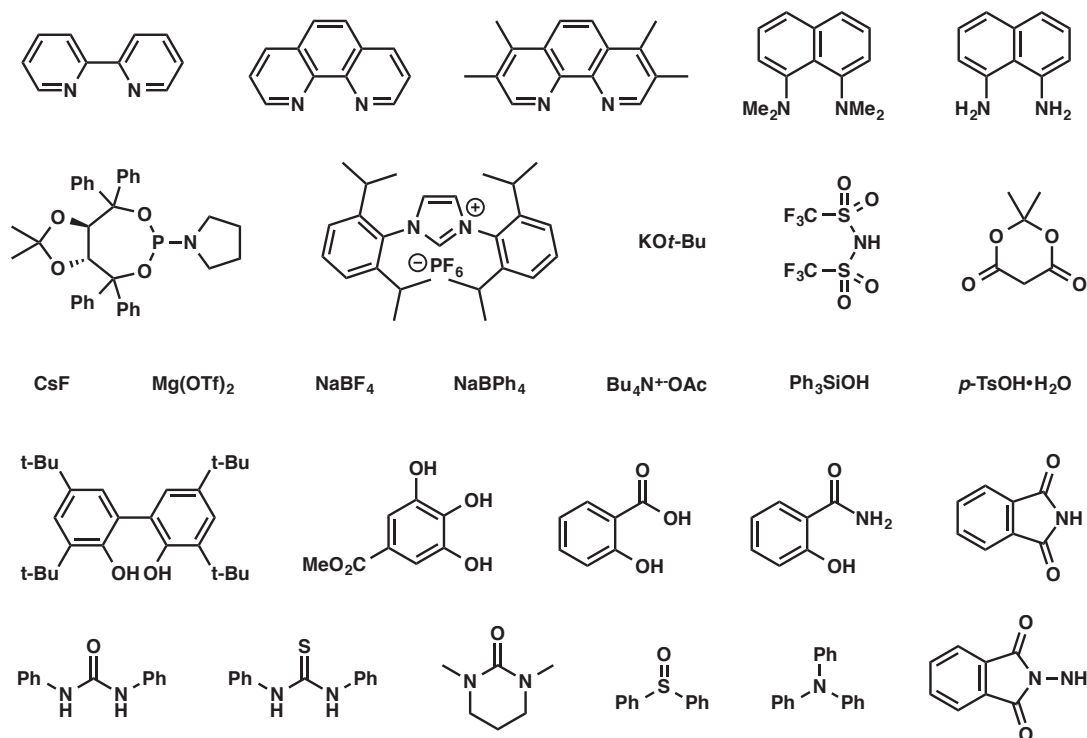
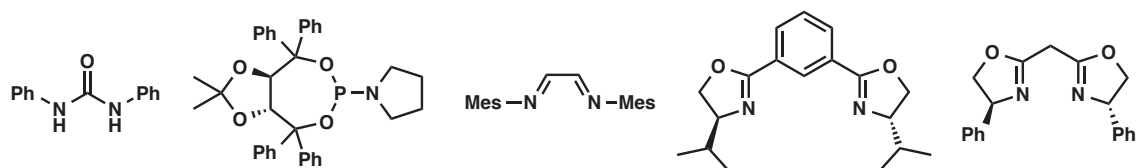
Figure A7.1 Additives/ligands with $(\text{MeCN})_4\text{Cu}^+\text{PF}_6^-$ Figure A7.2 Additives/ligands with $\text{Cu}^+(\text{OTf})\cdot\text{toluene}$ 

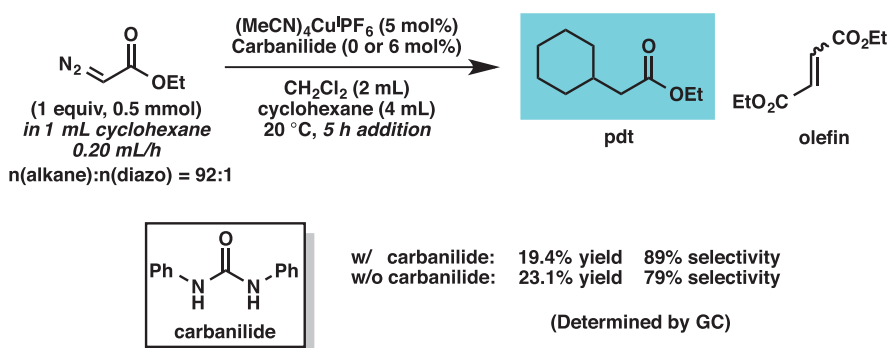
Table A7.4 Top results from the additive/ligand screen with Cu^I sources

entry	Cu ^I salt	ligand/additive	% pdt yield ^a	% selectivity ^b
1	(MeCN) ₄ Cu ^I PF ₆		11.6	51
2	(MeCN) ₄ Cu ^I PF ₆	Tf ₂ NH	11.6	47
3	(MeCN) ₄ Cu ^I PF ₆		10.5	50
4	Cu ^I (OTf)•toluene		10.0	41
5	(MeCN) ₄ Cu ^I PF ₆		9.8	38
6	(MeCN) ₄ Cu ^I PF ₆	none	8.7	39

^a Yield of desired insertion product determined by GC using tridecane as internal standard. ^b Selectivity = A(pdt)/[A(pdt)+A(olefin)].

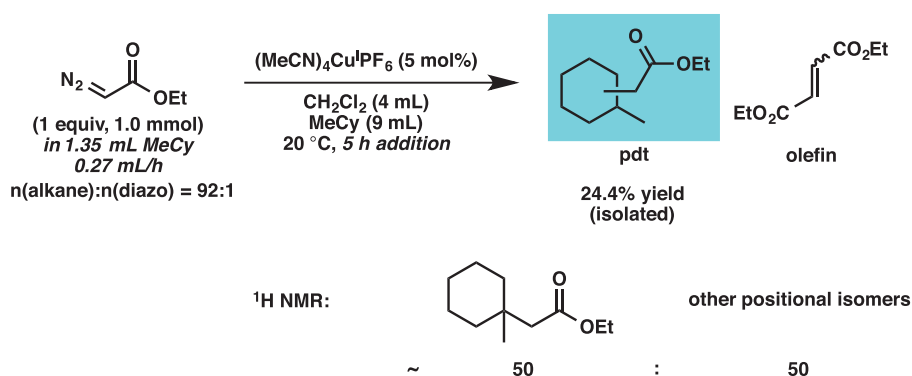
In all the screening reactions described above, the diazo reagent was added to the reaction mixture in one shot. Previous literature has suggested that slow addition of diazo reagent could minimize carbenoid dimerization. To test that hypothesis in our system, we performed slow-addition experiments using the optimal conditions identified so far (Scheme A7.2). We were delighted to observe that the yield indeed increased to ~20%, and selectivity rose to ~80%. Addition of carbanilide improved selectivity but decreased yield slightly.

Scheme A7.2 Slow-addition experiments



In addition to cyclohexane, we also explored methylcyclohexane as substrate because it contains all three types of alkyl C–H bonds (primary, secondary, and tertiary) and allows us to test the system’s chemoselectivity (Scheme A7.3). The insertion products were isolated in 24.4% yield. ^1H NMR analysis indicated the product to be a mixture of positional isomers, half of which is the tertiary C–H insertion product.

Scheme A7.3 Methylcyclohexane as substrate



A7.3 Concluding Remarks

We have investigated first-row transition metal-catalyzed carbenoid C–H insertion into simple alkanes. Extensive screen of metal salts, ligands, and additives led

to the identification of $(\text{MeCN})_4\text{Cu}^{\text{I}}\text{PF}_6$ as a uniquely effective catalyst. Additives such as carbanilide are capable of suppressing carbenoid dimerization but not improving product yield. While reactions using simple alkane substrates certainly need further improvement, we believe that future studies should focus on selective C–H functionalization of more complex substrates such as terpenes and steroids.

A7.4 Experimental Section

A7.4.1 Materials and Methods

All reactions were performed in flame-dried glassware under a nitrogen atmosphere using dry, deoxygenated solvents. Cyclohexane was distilled over CaH_2 under N_2 and transferred into the glove box. Ethyl diazoacetate was purchased from Sigma-Aldrich and used as received. Yield was determined using an Agilent 6850 GC (HP-1 column) with tridecane as internal standard.

A7.4.2 Procedure for Screening Reactions

In a nitrogen-filled glovebox, a 1-dram vial equipped with a magnetic stir bar was charged with ligand (0.003 mmol, 0.06 equiv) and metal salt (0.0025 mmol, 0.05 equiv). CH_2Cl_2 (0.2 mL) was added, and the mixture was stirred for 10 min. A stock solution of ethyl diazoacetate in cyclohexane (13.4 mg/mL, 0.5 mL, 0.05 mmol, 1.0 equiv) was added in one shot to the vial, which was then sealed with a PTFE screw cap. The reaction mixture was stirred at 20 °C for 10 h, and tridecane (12 μL , 0.05 mmol, 1.0 equiv) was added. The mixture was filtered through a small plug of silica (eluting with CH_2Cl_2), and the eluent was analyzed by GC.

A7.4.3 Procedure for Preparative Scale Reactions

In a nitrogen-filled glove box, a 25 mL round-bottom flask equipped with a magnetic stir bar was charged with $(\text{MeCN})_4\text{Cu}^{\text{I}}\text{PF}_6$ (9.3 mg, 0.025 mmol, 0.05 equiv), CH_2Cl_2 (2 mL), and cyclohexane (4 mL). The flask was sealed with a rubber septum, brought out of the glove box, and connected to a N_2 manifold. A solution of ethyl diazoacetate (67 mg, 0.5 mmol, 1.0 equiv) in cyclohexane (1 mL) was added slowly over 5 h using a syringe pump. After addition was complete, the reaction mixture was either analyzed by GC or concentrated and subjected to silica gel flash column chromatography (2% Et_2O in hexanes) to isolate the insertion product.

A7.5 Notes and References

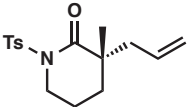
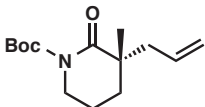
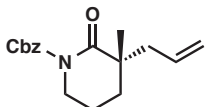
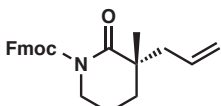
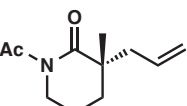
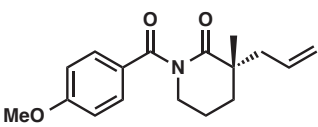
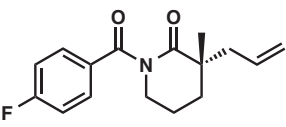
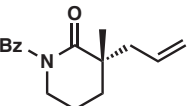
-
- (1) Godula, K.; Sames, D. *Science* **2006**, *312*, 67–72.
 - (2) (a) Bergman, R. G. *Nature* **2007**, *446*, 391–393. (b) Labinger, J. A.; Bercaw, J. E. *Nature* **2002**, *417*, 507–514.
 - (3) Davies, H. M. L.; Beckwith, R. E. J. *Chem. Rev.* **2003**, *103*, 2861–2903.
 - (4) Davies, H. M. L.; Manning, J. R. *Nature* **2008**, *451*, 417–424.
 - (5) (a) Diaz-Requejo, M. M.; Belderrain, T. R.; Nicasio, M. C.; Trofimenko, S.; Perez, P. J. *J. Am. Chem. Soc.* **2002**, *124*, 896–897. (b) Caballero, A.; Diaz-Requejo, M. M.; Belderrain, T. R.; Nicasio, M. C.; Trofimenko, S.; Perez, P. J. *J. Am. Chem. Soc.* **2003**, *125*, 1446–1447.

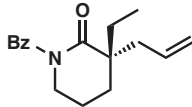
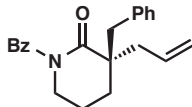
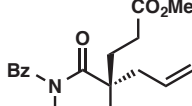
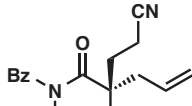
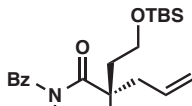
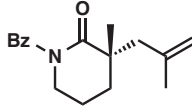
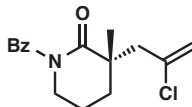
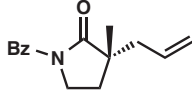
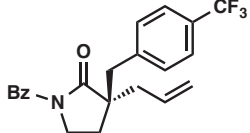
APPENDIX 8

Notebook Cross-Reference

Table A8.1 Compounds from Chapter 2

Compound	Structure	Notebook reference	NMR and IR data files
1a		YL-II-087	YL-II-87
1b		YL-II-073	YL-II-73
1c		TY-I-117	TY-Cbz
1d		YL-II-049	YL-II-49
1e		YL-II-045	YL-II-45
1f		YL-I-137	YL-I-137
1g		YL-I-143	YL-I-143
1h		YL-I-133 YL-I-211	YL-I-211
24		DCB-II-143	DCBII_143_char

Compound	Structure	Notebook reference	NMR and IR data files
2a		YL-III-089	YLIII_89 YLIII_89_C
2b		YL-II-077	YL-II-77
2c		YL-II-079	YL-II-79
2d		YL-II-065	YL-II-65
2e		YL-II-053	YL-II-53
2f		YL-I-263	YL-I-263
2g		YL-I-265	YL-I-265
2h		YL-I-205	YL-I-205-2

Compound	Structure	Notebook reference	NMR and IR data files
3		DCB-II-283	DCBII_283_H DCBII_283_C
4		DCB-II-263 DCB-II-269	DCBII_263_final DCBII_263 DCBII_269
5		DCB-II-281 DCB-II-285	DCBII_285 DCBII_281
6		DCB-II-287 DCB-II-291	DCBII_291 DCBII_287
7		DCB-III-113 DCB-III-115	DCBIII_115_25
8		YL-I-247	YL-I-247
9		YL-II-029	YL-II-29
10		DCB-II-265	DCBII_265
11		DCB-III-083	DCBIII_83_H DCBIII_83

Compound	Structure	Notebook reference	NMR and IR data files
12		DCB-III-045	DCBIII_45
13		YL-II-031	YL-II-31
14		DCB-III-085	DCBIII_85
15		DCB-II-293	DCBII_293_H DCBII_293
16		JK-III-289	JK-III-289
17		JK-IV-033	JK-IV-33
18		DCB-III-039 DCB-III-047	DCBIII_47
19		DCB-III-035	DCBIII_35
20		DCB-III-031 DCB-III-053	DCBIII_53-31

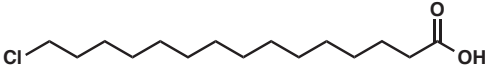
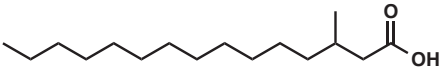
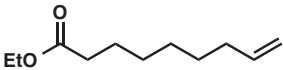
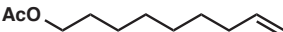
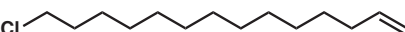
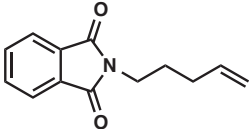
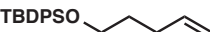
Compound	Structure	Notebook reference	NMR and IR data files
21		DCB-II-271 DCB-II-277	DCBII_277_H DCBII_277_C DCBII_271
22		DCB-III-019 DCB-III-033	DCBIII_33
23		DCB-III-081	DCBIII_81
25		DCB-III-073	DCBIII_73
26		DCB-III-147	DCBIII_147_2 DCBIII_147_2C DCBIII_147
28		YL-I-075	YL-I-75H YL-I-75
29		YL-I-079	YL-I-79-All YL-I-79-conc
30		YL-I-085	YL-I-85 YL-I-85C

Table A8.2 Compounds from Chapter 3

Compound	Structure	Notebook reference	NMR and IR data files
44		YL-X-187	13RMM3-0321215H 11RMM1-1003179CC13C 11RMM1-1003179CIRNaCD
45		YL-X-195	17RMM1-0617255CH1H 17RMM1-0617255C13C 11RMM1-1006193CIRNaCD
46A, 46B		YL-X-199	1-jm-062007-112H 1-jm-062007-112C13C jm-1-061907-111NaCD
47		YL-X-245	18RMM1-0820221H 18RMM1-0820221C13C 18RMM1-0820221NaCD
42		YL-X-247	18RMM1-0822229H 18RMM1-822229C13C 1jm-072707157NaCD
89		JLR-XV-203	JLR-XV-203a2 JLR-XV-203a3 MS-III-55a
53		JLR-XV-205	JLR-XV-205a4 JLR-XV-205a3 MS-III-79a
54		MS-III-101	MS-III-101a
55		MS-III-113	MS-III-113a
50		MS-III-143 JLR-XV-213	MS-III-143 JLR-XV-213b

Compound	Structure	Notebook reference	NMR and IR data files
61			17RMM1-0211109H 17RMM1-0211109C13C 17RMM1-0211109NaCD
62			17RMMc-0212115H 17RMMc-0212115C13C 17RMMc-0212115NaCD
59			17RMM1-0219139H 17RMM1-0219137C13C 17RMM1-0218137NaCD
69			17RMM2-0228151H 17RMM2-0228151C13C 17RMM2-0228151NaCD
70			18RMM1-0726157H 17RMM1-0312169C13C 17RMM1-0312169NaCD
65			18RMM1-0729161H 18RMM1-0729161C13C 18RMM1-0729161NaCD
80		DCB-III-131	DCBIII_131
77		DCB-III-137	DCBIII_137
87		ML-5-14	ML-5-14
88		ML-23-2	ML-23-2
84		ML-25-1	ML-25-1_2D

Table A8.3 Compounds from Chapter 4

Compound	Structure	Notebook reference	NMR and IR data files
128h		YL-VIII-151	YL-VIII-151
128o		YL-VIII-163	YL-VIII-163
129a		YL-VII-029 YL-VII-245 YL-VIII-223	YL-VIII-223
129b		YL-VII-073 YL-VII-213	YL-VII-213
129c		YL-VIII-207	YL-VIII-207
129d		YL-VIII-205	YL-VIII-205
129e		YL-VII-249	YL-VII-249
129f		YL-IX-019 YL-IX-039	YL-IX-039
129g		YL-VII-273	YL-VII-273
129h		YL-VIII-159	YL-VIII-159
129i		YL-VII-293	YL-VII-293
129j		YL-VIII-301	YL-VIII-301

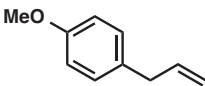
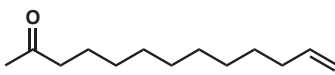
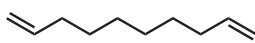
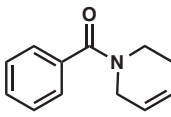
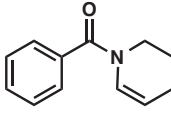
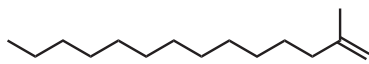
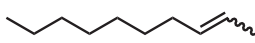
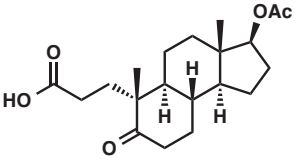
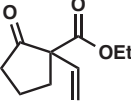
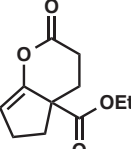
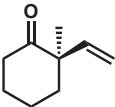
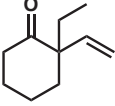
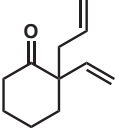
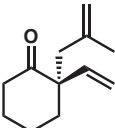
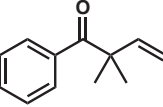
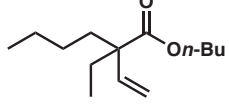
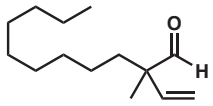
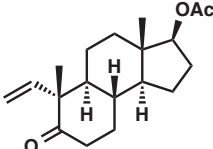
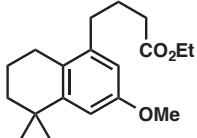
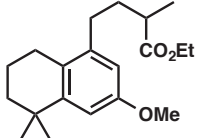
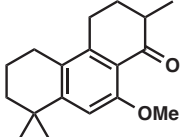
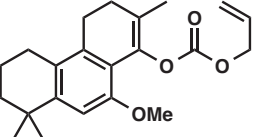
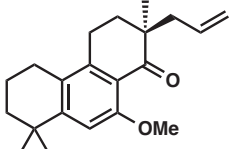
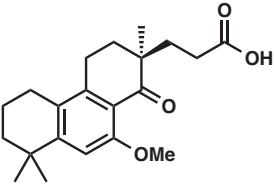
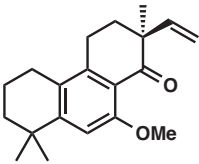
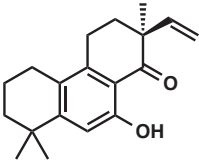
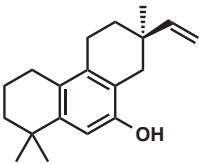
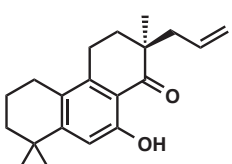
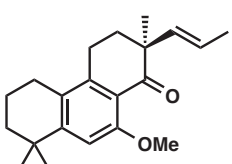
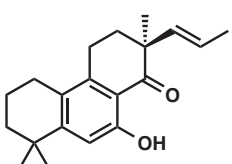
Compound	Structure	Notebook reference	NMR and IR data files
129k		YL-VIII-191 YL-VIII-197	YL-VIII-197
129l		YL-VIII-251	YL-VIII-251
129m		YL-VIII-247	YL-VIII-247
129n		YL-VII-247 YL-IX-015	YL-IX-015p2
130n		YL-IX-015	YL-IX-015p1
129o		YL-VIII-169	YL-VIII-169
130p		KK-2-303	KK-2-303-45-redo olefin indy no spin

Table A8.4 Compounds from Chapter 5

Compound	Structure	Notebook reference	NMR and IR data files
140a		YL-IX-143 YL-IX-183	YL-IX-143 YL-IX-183
152		YL-X-041 YL-XI-223B	YL-XI-223B
140b		YL-X-043	YL-X-043
140c		YL-X-215	YL-X-215
140d		YL-IX-167 YL-XI-149	YL-XI-149
156		YL-XI-169	YL-XI-169
157		YL-XI-177 YL-XI-219	YL-XI-219
140e		YL-X-209 YL-XI-227	YL-X-209
140f		YL-X-019 YL-XI-285	YL-XI-285
140h		YL-XI-145	YL-XI-145

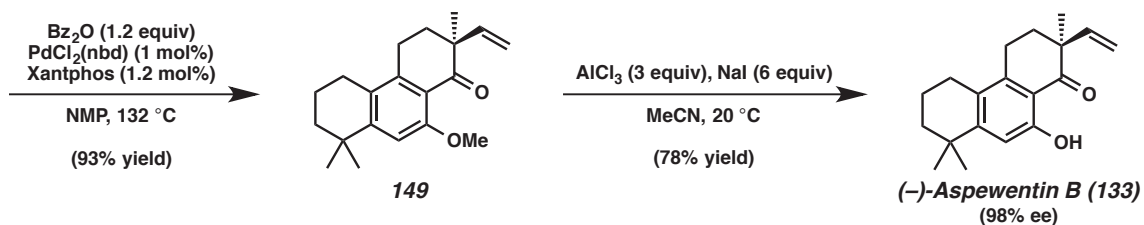
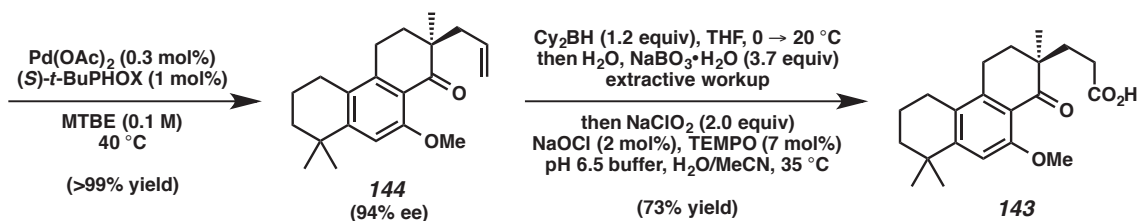
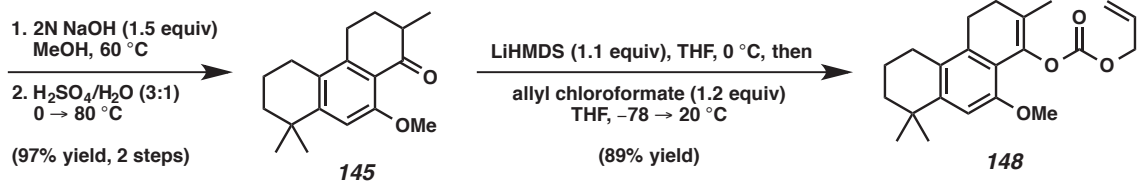
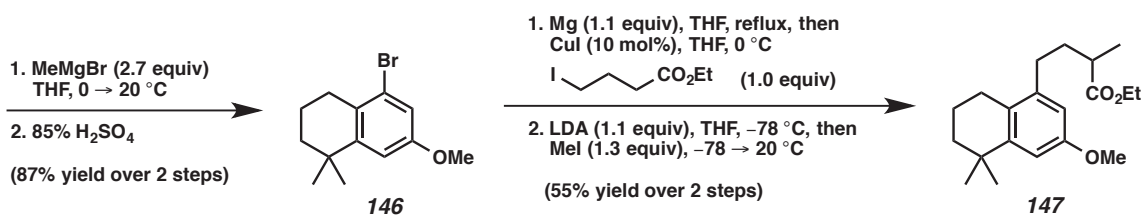
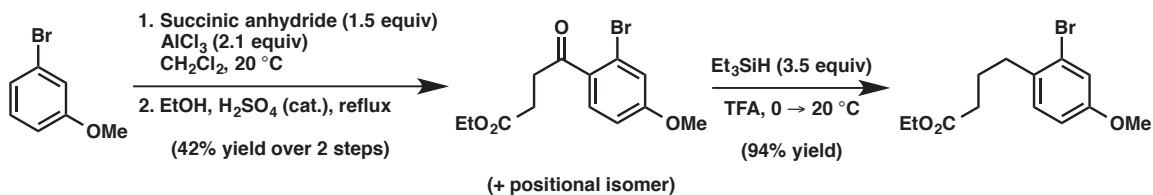
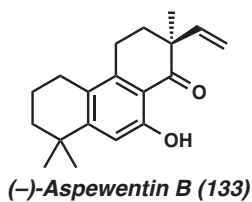
Compound	Structure	Notebook reference	NMR and IR data files
140i		YL-XI-121	YL-XI-121
141a		YL-IX-145	YL-IX-145f1
142		YL-IX-145	YL-IX-145f2
139		YL-X-045	YL-X-045
141c		YL-X-217	YL-X-217
141d		YL-IX-169	YL-IX-169
141e		YL-X-211 YL-XI-229	YL-XI-229 YL-X-211
141f		YL-X-027	YL-X-027
141g		YL-X-147 YL-XI-173	YL-XI-173
141h		YLXI-147	YLXI-147

Compound	Structure	Notebook reference	NMR and IR data files
141i		YL-XI-129	YL-XI-129
162		YL-XI-017 YL-XI-049 YL-XI-065	YL-XI-017
147		YL-XI-019 YL-XI-053 YL-XI-199	YL-XI-053
145		YL-XI-023 YL-XI-057 YL-XI-203	YL-XI-023
148		YL-XI-031 YL-XI-059 YL-XI-211	YL-XI-031
144		YL-XI-039 YL-XI-069 YL-XI-217	YL-XI-039

Compound	Structure	Notebook reference	NMR and IR data files
143		YL-XI-073 YL-XI-085 YL-XI-255	YL-XI-073
149		YL-XI-097 YL-XI-107	YL-XI-097
133		YL-XI-109 YL-XI-111	YL-XI-109
133A		YL-XII-127	YL-XII-127
163		YL-XI-119	YL-XI-119
164		YL-XI-123	YL-XI-123-2
165		YL-XI-127	YL-XI-127

APPENDIX 9

Synthetic Route for (-)-Aspewentin B



COMPREHENSIVE BIBLIOGRAPHY

Ackermann, L.; Kapdi, A. R.; Schulzke, C. *Org. Lett.* **2010**, *12*, 2298–2301.

Al-Jarallah, A. M.; Anabtawi, J. A.; Siddiqui, M. A. B.; Aitani, A. M.; Al-Sa'doun, A. W. *Catal. Today* **1992**, *14*, 1–121.

Allergan, Inc. Patent WO2005/58301 A1, 2005.

Amat, M.; Lozano, O.; Escolano, C.; Molins, E.; Bosch, J. *J. Org. Chem.* **2007**, *72*, 4431–4439.

Anderson, J. M.; Kochi, J. K. *J. Org. Chem.* **1969**, *35*, 986–989.

Andrus, M. B.; Liu, J.; Meredith, E. L.; Nartey, E. *Tetrahedron Lett.* **2003**, *44*, 4819–4822.

Anton, A.; Baird, B. R. *Polyamides, fibers. Kirk-Othmer Encyclopedia of Chemical Technology* (5th Ed.) **2006**, *19*, 739–772.

Arbain, D.; Dasman, N.; Ibrahim, S.; Sargent, M. V. *Aust. J. Chem.* **1990**, *43*, 1949–1952.

Arisawa, M.; Miyagawa, C.; Yoshimura, S.; Kido, Y.; Yamaguchi, M. *Chem. Lett.* **2001**, 1080–1081.

Arisawa, M.; Terada, Y.; Nakagawa, M.; Nishida, A. *Angew. Chem., Int. Ed.* **2002**, *41*, 4732–4734.

Bacha, J. D.; Kochi, J. K. *Tetrahedron* **1968**, *24*, 2215–2226.

Badillo, J. J.; Hanhan, N. V.; Franz, A. K. *Curr. Opin. Drug Disc. Dev.* **2010**, *13*, 758–776.

Baker, T. C.; Cardé, R. T.; Miller, J. R. *J. Chem. Ecol.* **1980**, *6*, 749–758.

Barton, D. H. R.; Boivin, J.; Crépon, E.; Sarma, J.; Togo, H.; Zard, S. Z. *Tetrahedron* **1991**, *47*, 7091–7108.

- Behenna, D. C.; Liu, Y.; Yurino, T.; Kim, J.; White, D. E.; Virgil, S. C.; Stoltz, B. M. *Nature Chem.* **2012**, *4*, 130–133.
- Behenna, D. C.; Stoltz, B. M. *J. Am. Chem. Soc.* **2004**, *126*, 15044–15045.
- Bernauer, K.; Englert, G.; Vetter, W.; Weiss, E. *Helv. Chim. Acta* **1969**, *52*, 1886–1905.
- Blaser, H.-U.; Spencer, A. *J. Organomet. Chem.* **1982**, *233*, 267–274.
- Borthakur, M.; Boruah, R. C. *Steroids* **2008**, *73*, 637–641.
- Burns, D. H.; Miller, J. D.; Chan, H.-K.; Delaney, M. O. *J. Am. Chem. Soc.* **1997**, *119*, 2125–2133.
- Chieffi, A.; Kamikawa, K.; Åhman, J.; Fox, J. M.; Buchwald, S. L. *Org. Lett.* **2001**, *3*, 1897–1900.
- Clive, D. L. J.; Russell, C. G.; Suri, S. C. *J. Org. Chem.* **1982**, *41*, 1632–1641.
- Cordell, G. A., Ed. *The Alkaloids: Chemistry And Biology*. In *Alkaloids*; Elsevier: San Diego, 2010; Vol. 69, p. 609.
- d'Angelo, J.; Desmaële, D.; Dumas, F.; Guingant, A. *Tetrahedron Asymmetry* **1992**, *3*, 459–505.
- Day, J. J.; McFadden, R. M.; Virgil, S. C.; Kolding, H.; Alleva, J. L.; Stoltz, B. M. *Angew. Chem., Int. Ed.* **2011**, *50*, 6814–6818.
- de Avellar, I. G. J.; Vierhapper, F. W. *Tetrahedron* **2000**, *56*, 9957–9965.
- Dias, D. A.; Kerr, M. A. *Org. Lett.* **2009**, *11*, 3694–3697.
- Edler, M. C.; Yang, G.; Jung, M. K.; Bai, R.; Bornmann, W. G.; Hamel, E. *Arch. Biochem. Biophys.* **2009**, *487*, 98–104.
- Enders, D.; Teschner, P.; Raabe, G.; Runsink, J. *Eur. J. Org. Chem.* **2001**, 4463–4477.
- Endo, K.; Hatakeyama, T.; Nakamura, M.; Nakamura, E. *J. Am. Chem. Soc.* **2007**, *129*, 5264–5271.
- Enquist, J. A., Jr.; Stoltz, B. M. *Nature* **2008**, *453*, 1228–1231.
- Finefield, J. M.; Sherman, D. H.; Kreitman, M.; Williams, R. M. *Angew. Chem., Int. Ed.* **2012**, *51*, 4802–4836.

- Foglia, T. A.; Barr, P. A. *J. Am. Oil Chem. Soc.* **1976**, *53*, 737–741.
- Franke, R.; Selent, D.; Börner, A. *Chem. Rev.* **2012**, *112*, 5675–5732.
- Fujimoto, T.; Endo, K.; Tsuji, H.; Nakamura, M.; Nakamura, E. *J. Am. Chem. Soc.* **2008**, *130*, 4492–4496.
- Garwood, R. F.; Naser-ud-Din; Scott, C. J.; Weedon, B. C. L. *J. Chem. Soc., Perkin Trans. 1* **1973**, 2714–2721.
- Gigant, N.; Chausset-Boissarie, L.; Belhomme, B.-C.; Poisson, T.; Pannecoucke, X.; Isabelle, G. *Org. Lett.* **2013**, *15*, 278–281.
- Gooßen, L. J.; Deng, G.; Levy, L. M. *Science* **2006**, *313*, 662–664.
- Gooßen, L. J.; Lange, P. P.; Rodríguez, N.; Linder, C. *Chem. Eur. J.* **2010**, *15*, 3906–3909.
- Gooßen, L. J.; Paetzold, J. *Angew. Chem., Int. Ed.* **2002**, *41*, 1237–1241.
- Gooßen, L. J.; Paetzold, J. *Angew. Chem., Int. Ed.* **2004**, *43*, 1095–1098.
- Gooßen, L. J.; Rodríguez, N. *Chem. Commun.* **2004**, 724–725.
- Groaning, M. D.; Meyers, A. I. *Tetrahedron* **2000**, *56*, 9843–9873.
- Guenin, E.; Monteil, M.; Bouchemal, N.; Prange, T.; Lecouvey, M. *Eur. J. Org. Chem.* **2007**, 3380–3391.
- Haley, C. K.; Gilmore, C. D.; Stoltz, B. M. *Tetrahedron* **2013**, *69*, 5732–5736.
- Helmchen, G.; Pfaltz, A. *Acc. Chem. Res.* **2000**, *33*, 336–345.
- Herbert, M. B.; Marx, V. M.; Pederson, R. L.; Grubbs, R. H. *Angew. Chem., Int. Ed.* **2013**, *52*, 310–314.
- Hosokawa, T.; Yamanaka, T.; Itotani, M.; Murahashi, S.-I. *J. Org. Chem.* **1995**, *60*, 6159–6167.
- Huang, J.; Bunel, E.; Faul, M. M. *Org. Lett.* **2007**, *9*, 4343–4346.
- Imao, D.; Itoi, A.; Yamazaki, A.; Shirakura, M.; Ohtoshi, R.; Ogata, K.; Ohmori, Y.; Ohta, T.; Ito, Y. *J. Org. Chem.* **2007**, *72*, 1652–1658.
- Ittel, S. D.; Johnson, L. K.; Brookhart, M. *Chem. Rev.* **2000**, *100*, 1169–1203.

Joule, J. A.; Mills, K. *Heterocycles in Medicine*. In *Heterocyclic Chemistry*, 5th Ed; Wiley: Chichester, 2010.

Kaiser, R.; Lamparsky, D. *Helv. Chim. Acta* **1978**, *61*, 2671–2680.

Kawashima, H.; Kaneko, Y.; Sakai, M.; Kobayashi, Y. *Chem. – Eur. J.* **2014**, *20*, 272–278.

Kazlauskas, R.; Murphy, P. T.; Wells, R. J.; Blackman, A. J. *Aust. J. Chem.* **1982**, *35*, 113–120.

Kohan, M. I., Ed. *Nylon*. In *Plastics*; Interscience: New York, 1973.

Kolbe, H. *Justus Liebigs Ann. Chem.* **1849**, *69*, 257–294.

Kowalski, C. J.; Dung, J.-S. *J. Am. Chem. Soc.* **1980**, *102*, 7950–7951.

Kraus, G. A.; Riley, S. *Synthesis* **2012**, *44*, 3003–3005.

Le Nôtre, J.; Scott, E. L.; Franssen, M. C. R.; Sanders, J. P. M. *Tetrahedron Lett.* **2010**, *51*, 3712–3715.

Lin, J.; Liu, F.; Wang, Y.; Liu, M. *Synth. Commun.* **1995**, *25*, 3457–3461.

Liu, Y.; Kim, K. E.; Herbert, M. B.; Fedorov, A.; Grubbs, R. H.; Stoltz, B. M. *Adv. Synth. Catal.* **2014**, *356*, 130–136.

Liu, Y.; Liniger, M.; McFadden, R. M.; Roizen, J. L.; Malette, J.; Reeves, C. M.; Behenna, D. C.; Seto, M.; Kim, J.; Mohr, J. T.; Virgil, S. C.; Stoltz, B. M. *Beilstein J. Org. Chem.* **2014**, *10*, 2501–2512.

Lu, Z.; Ma, S. *Angew. Chem., Int. Ed.* **2008**, *47*, 258–297.

Maetani, S.; Fukuyama, T.; Suzuki, N.; Ishihara, D.; Ryu, I. *Chem. Commun.* **2012**, *48*, 2552–2554.

Maetani, S.; Fukuyama, T.; Suzuki, N.; Ishihara, D.; Ryu, I. *Organometallics* **2011**, *30*, 1389–1394.

Magnus, P.; Rainey, T. *Tetrahedron* **2001**, *57*, 8647–8651.

Marquis, D. M.; Sharman, S. H.; House, R.; Sweeney, W. A. *J. Am. Oil Chem. Soc.* **1966**, *43*, 607–614.

Masuda, T.; Masuda, K.; Shiragami, S.; Jitoe, A.; Nakatani, N. *Tetrahedron* **1992**, *48*, 6787–6792.

- McDougal, N. T.; Streuff, J.; Mukherjee, H.; Virgil, S. C.; Stoltz, B. M. *Tetrahedron Lett.* **2010**, *51*, 5550–5554.
- McDougal, N. T.; Virgil, S. C.; Stoltz, B. M. *Synlett* **2010**, 1712–1716.
- McFadden, R. M.; Stoltz, B. M. *J. Am. Chem. Soc.* **2006**, *128*, 7738–7739.
- Melliou, E.; Chinou, I. *J. Agric. Food Chem.* **2005**, *53*, 8987–8992.
- Meyers, A. I.; Hanreich, R.; Wanner, K. T. *J. Am. Chem. Soc.* **1985**, *107*, 7776–7778.
- Miao, F.-P.; Liang, X.-R.; Liu, X.-H.; Ji, N.-Y. *J. Nat. Prod.* **2014**, *77*, 429–432.
- Miller, J. A.; Nelson, J. A.; Byrne, M. P. *J. Org. Chem.* **1993**, *58*, 18–20.
- Miranda, M. O.; Pietrangelo, A.; Hillmyer, M. A.; Tolman, W. B. *Green Chem.* **2012**, *14*, 490–494.
- Mohr, J. T.; Behenna, D. C.; Harned, A. M.; Stoltz, B. M. *Angew. Chem., Int. Ed.* **2005**, *44*, 6924–6927.
- Mohr, J. T.; Stoltz, B. M. *Chem. Asian J.* **2007**, *2*, 1476–1491.
- Moore, R. E.; Cheuk, C.; Patterson, G. M. L. *J. Am. Chem. Soc.* **1984**, *106*, 6456–6457.
- Mori, K. *Tetrahedron* **2009**, *65*, 3900–3909.
- Moss, T. A.; Alonso, B.; Fenwick, D. R.; Dixon, D. J. *Angew. Chem., Int. Ed.* **2010**, *49*, 568–571.
- Myers, A. G.; Tanaka, D.; Mannion, M. R. *J. Am. Chem. Soc.* **2002**, *124*, 11250–11251.
- Nakamura, M.; Endo, K.; Nakamura, E. *Org. Lett.* **2005**, *7*, 3279–3281.
- Nishimoto, Y.; Ueda, H.; Yasuda, M.; Baba, A. *Angew. Chem., Int. Ed.* **2012**, *51*, 8073–8076.
- Nozoye, T.; Shibamura, Y.; Nakai, T.; Hatori, Y. *Chem. Pharm. Bull.* **1988**, *36*, 4980–4985.
- Obora, Y.; Tsuji, Y.; Kawamura, T. *J. Am. Chem. Soc.* **1993**, *115*, 10414–10415.
- Ohishi, T.; Zhang, L.; Nishiura, M.; Hou, Z. *Angew. Chem., Int. Ed.* **2011**, *50*, 8114–8117.

- Olofson, R. A.; Abbott, D. E. *J. Org. Chem.* **1984**, *49*, 2795–2799.
- Oppolzer, W.; Radinov, R. N.; El-Sayed, E. *J. Org. Chem.* **2001**, *66*, 4766–4770.
- Ouyang, J.; Kong, F.; Su, G.; Hu, Y.; Song, Q. *Catal. Lett.* **2009**, *132*, 64–74.
- Pangborn, A. M.; Giardello, M. A.; Grubbs, R. H.; Rosen, R. K.; Timmers, F. J. *Organometallics* **1996**, *15*, 1518–1520.
- Pearlman, B. A.; Putt, S. R.; Fleming, J. A. *J. Org. Chem.* **1985**, *50*, 3625–3626.
- Peer, M.; de Jong, J. C.; Kiefer, M.; Langer, T.; Rieck, H.; Schell, H.; Sennhenn, P.; Sprinz, J.; Steinhagen, H.; Wiese, B.; Helmchen, G. *Tetrahedron* **1996**, *52*, 7547–7583.
- Pfau, M.; Revial, G.; Guingant, A.; d'Angelo, J. *J. Am. Chem. Soc.* **1985**, *107*, 273–274.
- Ravu, V. R.; Leung, G. Y. C.; Lim, C. S.; Ng, S. Y.; Sum, R. J.; Chen, D. Y.-K. *Eur. J. Org. Chem.* **2011**, 463–468.
- Rayabarapu, D. K.; Tunge, J. A. *J. Am. Chem. Soc.* **2005**, *127*, 13510–13511.
- Regourd, J.; Ali, A. A.; Thompson, A. *J. Med. Chem.* **2007**, *50*, 1528–1536.
- Rodríguez, N.; Gooßen, L. *J. Chem. Soc. Rev.* **2011**, *40*, 5030–5048.
- Rojas, G.; Wagener, K. B. *J. Org. Chem.* **2008**, *73*, 4962–4970.
- Rosebrugh, L. E.; Herbert, M. B.; Marx, V. M.; Keitz, B. K.; Grubbs, R. H. *J. Am. Chem. Soc.* **2013**, *135*, 1276–1279.
- Rubal, J. J.; Moreno-Dorado, F. J.; Guerra, F. M.; Jorge, Z. D.; Saouf, A.; Akssira, M.; Mellouki, F.; Romero-Garrido, R.; Massanet, G. M. *Phytochemistry* **2007**, *68*, 2480–2486.
- Schlack, P. *Pure Appl. Chem.* **1967**, *15*, 507–523.
- Seto, M.; Roizen, J. L.; Stoltz, B. M. *Angew. Chem., Int. Ed.* **2008**, *47*, 6873–6876.
- Shang, R.; Fu, Y.; Li, J.-B.; Zhang, S.-L.; Guo, Q.-X.; Liu, L. *J. Am. Chem. Soc.* **2009**, *131*, 5738–5739.
- Shimizu, I.; Yamada, T.; Tsuji, J. *Tetrahedron Lett.* **1980**, *21*, 3199–3202.
- Small, B. L.; Brookhart, M. *J. Am. Chem. Soc.* **1998**, *120*, 7143–7144.

Stephan, M. S.; Teunissen, A. J. J. M.; Verzijl, G. J. M.; de Vries, J. G. *Angew. Chem., Int. Ed.* **1998**, *37*, 662–664.

Straub, B. F.; Wrede, M.; Schmid, K.; Rominger, F. *Eur. J. Inorg. Chem.* **2010**, 1907–1911.

Streuff, J.; White, D. E.; Virgil, S. C.; Stoltz, B. M. *Nature Chem.* **2010**, *2*, 192–196.

Subchev, M.; Toth, M.; Wu, D.; Stanimirova, L.; Toshova, T.; Karpati, Z. *J. Appl. Ent.* **2000**, *124*, 197–199.

Tani, K.; Behenna, D. C.; McFadden, R. M.; Stoltz, B. M. *Org. Lett.* **2007**, *9*, 2529–2531.

Tanikaga, R.; Sugihara, H.; Tanaka, K.; Kaji, A. *Synthesis* **1977**, 299–301.

Taylor, A. M.; Altman, R. A.; Buchwald, S. L. *J. Am. Chem. Soc.* **2009**, *131*, 9900–9901.

Trost, B. M. *J. Org. Chem.* **2004**, *69*, 5813–5837.

Trost, B. M.; Brennan, M. K. *Synthesis* **2009**, 3003–3025.

Tsuda, T.; Chujo, Y.; Nishi, S.-i.; Tawara, K.; Saegusa, T. *J. Am. Chem. Soc.* **1980**, *102*, 6381–6384.

Tsuzuki, Y.; Chiba, K.; Mizuno, K.; Tomita, K.; Suzuki, K. *Tetrahedron: Asymmetry* **2001**, *12*, 2989–2997.

van der Klis, F.; van den Hoorn, M. H.; Blaauw, R.; van Haveren, J.; van Es, D. S. *Eur. J. Lipid Sci. Technol.* **2011**, *113*, 562–571.

Vijai Kumar Reddy, T.; Prabhavathi Devi, B. L. A.; Prasad, R. B. N.; Poornima, M.; Ganesh Kumar, C. *Bioorg. Med. Chem. Lett.* **2012**, *22*, 4678–4680.

Voutchkova, A.; Coplin, A.; Leadbeater, N. E.; Crabtree, R. H. *Chem. Commun.* **2008**, 6312–6314.

Wang, Z.; Ding, Q.; He, X.; Wu, J. *Org. Biomol. Chem.* **2009**, *7*, 863–865.

Wang, Z.; Zhu, L.; Yin, F.; Su, Z.; Li, Z.; Li, C. *J. Am. Chem. Soc.* **2012**, *134*, 4258–4263.

Weaver, J. D.; Recio, A., III.; Grenning, A. J.; Tunge, J. A. *Chem. Rev.* **2011**, *111*, 1846–1913.

White, D. E.; Stewart, I. C.; Grubbs, R. H.; Stoltz, B. M. *J. Am. Chem. Soc.* **2008**, *130*, 810–811.

Whittaker, A. M.; Lalic, G. *Org. Lett.* **2013**, *15*, 1112–1115.

Yamaguchi, M.; Tsukagoshi, T.; Arisawa, M. *J. Am. Chem. Soc.* **1999**, *121*, 4074–4075.

Yanagisawa, A.; Habaue, S.; Yasue, K.; Yamamoto, H. *J. Am. Chem. Soc.* **1994**, *116*, 6130–6141.

Yeung, P. Y.; Chung, K. H.; Kwong, F. Y. *Org. Lett.* **2011**, *13*, 2912–2915.

Zhang, W.-W.; Zhang, X.-G.; Li, J.-H. *J. Org. Chem.* **2010**, *75*, 5259–5264.

Zhao, M. M.; Li, J.; Mano, E.; Song, Z. J.; Tschaen, D. M. *Org. Syn.* **2005**, *81*, 195–203.

Zhou, F.; Liu, Y.-L.; Zhou, J. *Adv. Synth. Catal.* **2010**, *352*, 1381–1407.

INDEX**A**

alkaloid26, 163, 164, 165, 167, 168, 273
allyl enol carbonate285, 288, 357
allylic alkylation ..4, 7, 10, 11, 15, 16, 17, 19, 21, 22, 155, 159, 162, 166, 268, 273, 281, 282, 284, 285, 286,
287, 288, 289, 290, 291, 292, 293, 294, 352, 353, 356, 357
alpha olefin12, 13, 301, 303, 308, 309
alpha selectivity304, 306, 308
alpha-vinyl carbonyl compounds13, 14, 15, 351, 352, 358
amide165, 167
anhydride303, 304, 305, 307, 355
aspewentin A357
aspewentin B13, 15, 16, 351, 356, 357, 358, 359
aspidosperma26, 27, 163, 167, 168
aspidospermidine163
aspidospermine163, 164, 165, 170, 186
asymmetric 10, 12, 14, 20, 21, 26, 27, 155, 166, 167, 170, 269, 273, 274, 277, 279, 281, 282, 284, 285, 289,
290, 295, 351

B

beta-keto ester4, 285, 291, 294

C

caprolactam20
carbenoid470, 471, 474, 476, 477
carboxylic acid2, 4, 5, 6, 7, 8, 9, 14, 16, 17, 157, 158, 159, 160, 306, 309, 352, 353, 356
catalysis3, 6, 10, 12, 16, 20, 21, 26, 27, 155, 157, 162, 164, 170, 268, 273, 277, 280, 281, 282, 284, 285,
288, 294, 295, 301, 303, 351, 357, 470, 471, 477
chiral11, 20, 21, 22, 23, 25, 26, 159, 160, 161, 164, 169, 170, 274, 278, 281, 285
cyclic20, 24, 268, 273, 277, 279, 287, 290, 291, 292, 293, 353, 354

D

decarbonylation2, 3, 8, 9, 10, 16, 302, 303
decarbonylative dehydration .12, 13, 15, 16, 17, 301, 302, 303, 305, 308, 309, 351, 352, 353, 355, 356, 357,
358
decarboxylation2, 3, 5, 6, 8, 12, 16, 288, 301
decarboxylative1, 3, 4, 5, 6, 7, 10, 11, 16, 17, 19, 22, 25, 158, 166, 294, 351, 352, 357
dediazotization470, 471
diastereoselective159, 161
diastereoselectivity294
diazo471, 472, 476
distillation304, 306, 307, 308, 309, 352
dysidiolide161, 162, 163, 170

E

enantioenriched 11, 14, 26, 158, 159, 160, 166, 168, 278, 295, 354
enantioselective 4, 10, 11, 12, 15, 17, 19, 20, 21, 24, 26, 27, 155, 156, 157, 161, 162, 164, 165, 167, 168,
169, 170, 268, 273, 274, 276, 278, 281, 284, 285, 286, 287, 288, 289, 291, 351, 352, 353, 356, 357, 358
enolate 14, 20, 21, 27, 155, 269, 282, 284, 285, 288, 289, 290, 292
even-numbered 301

F

fatty acid 13, 16, 301, 305, 309, 352
formal synthesis 11, 12, 155, 157, 158, 159, 160, 161, 162, 163, 164, 165, 166, 167, 168, 169, 170
functional group 10, 13, 269, 274, 283, 306, 358
functionalization 470, 478

G

Grignard 16, 356

I

insertion 280, 469, 470, 471, 472, 473, 474, 476, 477
iridium 291, 294, 301
isomerization 169, 302, 303, 304, 306, 354

L

lactam 10, 19, 20, 21, 22, 23, 25, 26, 27, 166, 167, 169, 170, 288
large scale 280, 308, 309, 354
ligand ... 10, 21, 22, 23, 269, 276, 278, 281, 284, 285, 287, 289, 291, 292, 294, 302, 303, 304, 353, 471, 472,
473, 476

N

natural product . 11, 12, 14, 20, 21, 27, 155, 156, 157, 159, 161, 164, 170, 271, 273, 282, 309, 351, 356, 359

O

odd-numbered 301
oligomerization 12, 301

P

palladium 1, 3, 4, 5, 6, 7, 8, 9, 10, 11, 12, 13, 15, 16, 17, 19, 20, 22, 25, 26, 155, 157, 160, 162, 164, 166,
167, 169, 269, 277, 278, 279, 280, 281, 282, 284, 288, 289, 290, 294, 301, 302, 303, 309, 351, 352, 353,
356, 357, 358
petroleum 12, 301
pharmaceutical 12, 165, 269, 273
pheromone 308
piperidinone 20, 23, 165, 166, 169
protecting group 24
pyrrolidinone 20

Q

quaternary carbon 11, 15, 155, 161, 170, 358
quaternary stereocenter ... 13, 20, 157, 162, 164, 165, 167, 168, 268, 271, 272, 273, 277, 278, 281, 282, 286,
295, 351, 352, 353, 356
quebrachamine 26, 167, 168, 170
quinic acid 159, 160, 161, 170

R

racemic 11, 22, 26, 157, 161, 162, 165, 168, 170, 276, 278
rhazinilam 26, 165, 166, 170

rhodium277, 301, 470

S

silyl enol ether 159, 284, 285, 288

stearic acid.....303, 304, 308

stereoselective 20, 167, 351, 471

T

TEMPO357

terminal olefin 13, 169, 306, 352, 357

terpenoid.....271, 356

thujopsene 156, 157, 158, 170

transition metal.....6, 21, 277, 301, 470, 471, 477

V

vincadifformine 168, 169, 170

vinylation..... 14, 351, 352, 356

About the Author

Yiyang Liu was born on April 18, 1986 in Hefei, China. He is the only child of Yonglin Liu and Junling Yan. While in high school, Yiyang was given an opportunity to participate in the American Field Service (AFS) exchange program and spent his junior year in Twentynine Palms High School, California. His American experience at an early age made him excited about studying abroad in the future.

In the fall of 2005, Yiyang matriculated at Peking University in Beijing, China. He changed his major to chemistry after spending his first year at the School of Government. In the summer of 2008, Yiyang enrolled in the University of Michigan/Peking University (UM/PKU) undergraduate research exchange program and traveled to Ann Arbor, Michigan, where he worked in the laboratory of Professor Zhan Chen on the spectral analysis of polymer interfaces. During his brief stay in Michigan, a tour of the Pfizer site at Kalamazoo and introductory lectures aroused his interest in synthetic organic chemistry. Upon returning to Peking University, Yiyang joined the laboratory of Professors Jianbo Wang and Yan Zhang, where he studied migratory insertion reactions of palladium carbene species and their applications in β -lactam synthesis.

In the fall of 2010, Yiyang moved to Pasadena, California, where he began doctoral research with Professor Brian M. Stoltz at the California Institute of Technology. His research involves palladium-catalyzed decarboxylative and decarbonylative transformations and their applications in the synthesis of fine and commodity chemicals. During his graduate studies at Caltech, Yiyang became interested in chemical process design and development. He will move back to Ann Arbor, Michigan, in September 2015 and begin postdoctoral studies with Professor Adam J. Matzger in the field of crystal engineering.